31 March 2006 | $10

Science

AAAS

Believe it!

DNA Sequencing for $2.50 per reaction.

- Read length up to 900 bases.
- High quality electropherograms.
- Fast turnaround.
- Plasmid and PCR purification available.

$2.50 per reaction!

POLYMORPHIC
Polymorphic DNA Technologies, Inc.℠

Polymorphic exclusively uses ABI 3730XL sequencers.
Data delivered via secure FTP, email or CD.
No charge for standard sequencing primers.
384 sample minimum order.
96 well plates only—no tubes.

www.polymorphicdna.com
info@polymorphicdna.com

1125 Atlantic Ave., Ste. 102
Alameda, CA 94501

888.362.0888

For more information please visit
www.polymorphicdna.com

There's a new kit on the block.

Introducing StrataClone™ PCR Cloning Kits: A new, more affordable choice in Topoisomerase I technology

Our StrataClone™ PCR Cloning Kit* saves you time and money with topoisomerase-based PCR cloning priced lower than the competition. The simple, three step process, >95% efficiency guarantee, and affordable pricing make StrataClone™ PCR Cloning Kits your kit of choice for topoisomerase-based PCR cloning.

- **High-performance PCR cloning at a more affordable price**
- **Clone both long and short PCR amplicons with the same kit**
- **High efficiency results in >95% clones with insert**

Need More Information? Give Us A Call:

Stratagene USA and Canada
Order: (800) 424-5444 x3
Technical Services: (800) 894-1304 x2

Stratagene Europe
Order: 00800-7000-7000
Technical Services: 00800-7400-7400

Stratagene Japan K.K.
Order: 03-5159-2060
Technical Services: 03-5159-2070

www.stratagene.com

Ask Us About These Great Products:

StrataClone™ PCR Cloning Kit	**20 reactions**	**240205**
	10 reactions	**240206**

StrataClone™ is a trademark of Stratagene in the United States.
* Patent pending.

STRATAGENE®

GE Healthcare

Why do 100,000 scientists trust GE Healthcare for all their protein purification needs?

Here's Ä clue.

To 100,000 scientists worldwide, the name ÄKTA™ has always meant outstanding protein purification, and now it's brought to you by GE Healthcare. With the ability to purify virtually 100% of all biomolecules, the ÄKTAdesign™ platform can handle the toughest of challenges. Whatever the scale, from laboratory, to process development and manufacturing, there's an ÄKTAdesign system to meet every need. All systems in the ÄKTAdesign family work with the intelligent UNICORN™ software, which makes it easy to control every stage of your purification processes. Accurate, reproducible results just take a little pure imagination.

Visit www.amershambiosciences.com/aktadesign

imagination at work

YYePG Proudly Presents, Thx for Support

GE15-05

Volume 311, Issue 5769

COVER

Bundles of rice crop hanging on bamboo sticks in Japan. The earliest farmers unknowingly selected a single base pair mutation in a regulatory gene that substantially reduced grain shattering of the wild progenitor of rice. This led to domestication of the world's leading food crop. See page 1936.

Photo: Dex/Getty Images

DEPARTMENTS

EDITORIAL

NEWS OF THE WEEK

NEWS FOCUS

LETTERS

BOOKS *ET AL.*

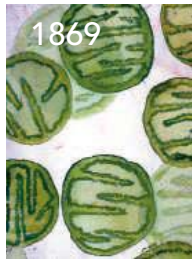

EDUCATION FORUM

PERSPECTIVES

CONTENTS continued >>

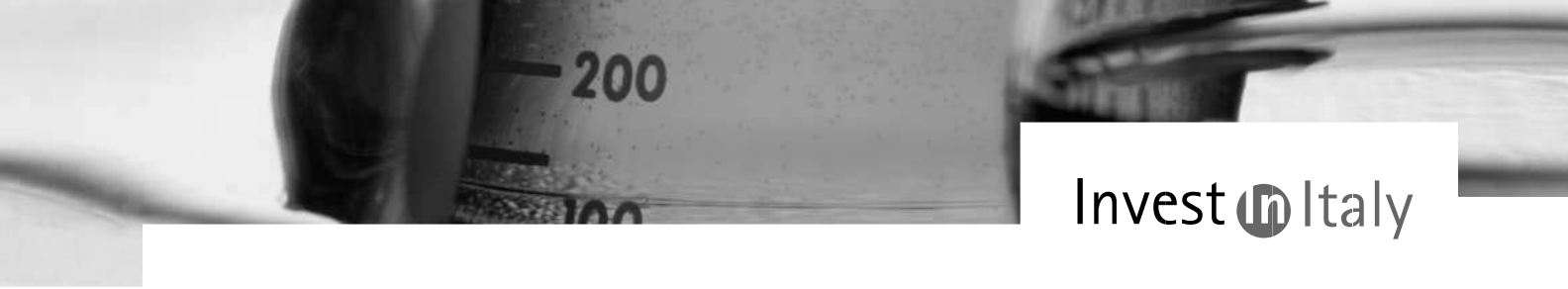

Invest in Italy

ITALY'S LIFE SCIENCES SECTOR IS GAINING MOMENTUM

A breeding ground for biotech companies

Italy's Life Sciences industry is becoming ever more appealing for multinational companies seeking to pursue biotechnology and pharmaceutical research. The sector is spurred on by the strong interaction between academia and business environment, a vibrant medical and hospital system, the capacity of world class scientists to produce leading-edge research as well as government support.

Italy's upsurge in the Life Sciences is also proved by a strong performance in the product pipeline with 21 drugs in clinical trials (particularly in Oncology and Neurosciences), which makes it rank ahead of some major European countries like France, Germany and Sweden, if we compare the number of companies with products in pipeline.

Performance Index of Biotech Companies

(Number of products/Number of companies)

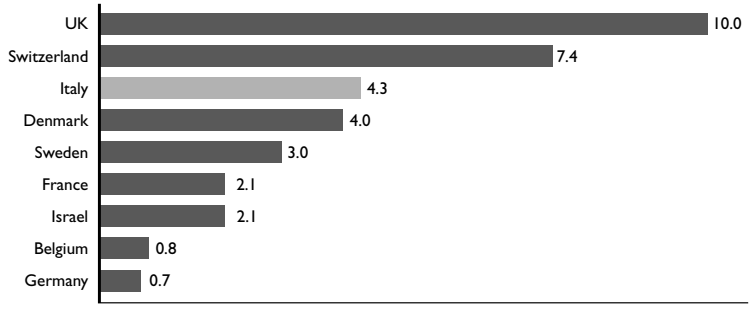

Source: InvestInItaly based on NES, Assobiotec – 2005

Competitive advantages for international investors

Italy's competitive advantage for international investors is also represented by the skilled workforce. Its R&D professionals – 6,000 researchers employed by businesses, a pool of 20,000 university researchers, 200,000 students and 35,000 graduates annually in Biotechnology, Pharmacy and Medicine – are extremely productive, with creativity second to no competitor country worldwide. As a proof, Italy ranks top in Europe for patent productivity and impact rate of publications.

Start-ups and new business initiatives can count on the support of a network of science parks specialized in life sciences, with a track record of excellence in Biotechnology, Biomedical technology, Diagnostics, Genomics. Besides, labor, business and clinical trials costs are internationally competitive with respect to USA, UK, France and Germany.

Innovation Spotlight

Italy to Launch Europe's First Institute for Regenerative Medicine

Modena – The University of Modena and the Eye Bank Foundation of Venice have joined forces to create a public/private partnership forming the Research Center for Regenerative Medicine. It will become the first such center in Europe focused on stem cell therapy for treating vision disorders caused by tissue/organ damage and genetic defects.

Italy Leads Development of Gene Expression Atlas

Naples – The Telethon Institute of Genetics and Medicine (TIGEM) is spearheading a team made up of 12 major European research institutes to develop the first comprehensive atlas of gene expressions with an estimated identification of 30,000 genes.

Italian and American Researchers Team Up on Heart Stem Cell Breakthrough

Rome – Researchers at La Sapienza University in Rome recently teamed up with John Hopkins University to conduct the first study using stem cells to repair the same type of organ from which they were derived. The promising results were presented at the American Cardiology Congress (ACC).

Come and visit us at BIO 2006

Italian Pavilion
McCormick Place, Chicago, IL
April 9th - 12th 2006

Italy Country Seminar
"From Strong Basic Research to Company Development"
Sunday, April 9th at 1:35 p.m.
room S405A

SviluppoItalia

Italian Trade Commission

InvestInItaly is the Italian organization for investment promotion created by Sviluppo Italia, the National Agency for Enterprise and Inward Investment Development and the Italian Trade Commission, the Government Agency which promotes the internationalization of Italian companies, mission to support a single and reliable national reference point to current and new foreign investors.

YoBDC Proudly Presents, Thx for Support

www.investinitaly.com info@investinitaly.com

Science

SCIENCE EXPRESS

www.sciencexpress.org

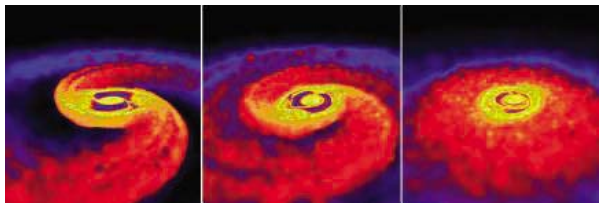

DEVELOPMENTAL BIOLOGY

Retinoid Signaling Determines Germ Cell Fate in Mice

J. Bowles et al.

After germ cells in the mouse gonad are directed by the hormone retinoic acid to enter meiosis and become oocytes, an enzyme in the testis degrades the hormone, allowing sperm production.

10.1126/science.1125691

EPIDEMIOLOGY

Synchrony, Waves, and Spatial Hierarchies in the Spread of Influenza

C. Viboud et al.

Examination of 30 years of data suggests that in the United States, seasonal flu epidemics often spread by adult-to-adult transfer during commuting on public transportation.

10.1126/science.1125237

ASTROPHYSICS

Producing Ultrastrong Magnetic Fields in Neutron Star Mergers

D. J. Price and S. Rosswog

Simulation of two neutron stars merging to form a black hole shows that their magnetic fields can strengthen rapidly and produce gamma rays.

10.1126/science.1125201

APPLIED PHYSICS

Spin Coupling in Engineered Atomic Structures

C. F. Hirjibehedin, C. P. Lutz, A. J. Heinrich

The spin interactions of chains of manganese atoms assembled on a thin insulating surface were measured and interpreted in terms of an open spin chain model.

10.1126/science.1125398

REVIEW

BREVIA

RESEARCH ARTICLES

REPORTS

CONTENTS continued **>>**

REPORTS *CONTINUED...*

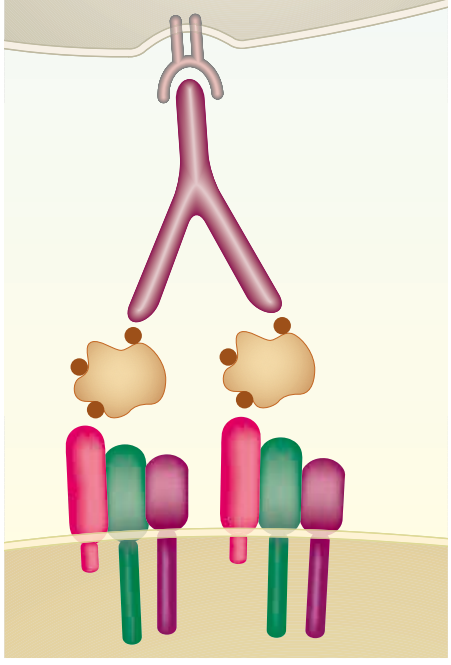

1875 & 1924

AAAS
ADVANCING SCIENCE, SERVING SOCIETY

SCIENCE (ISSN 0036-8075) is published weekly on Friday, except the last week in December, by the American Association for the Advancement of Science, 1200 New York Avenue, NW, Washington, DC 20005. Periodicals Mail postage (publication No. 484460) paid at Washington, DC, and additional mailing offices. Domestic individual membership and subscription (51 issues): $139 ($74 allocated to subscription). Domestic institutional subscription (51 issues): $650; Foreign postage extra: Mexico, Caribbean (surface mail) $55; other countries (air assist delivery) $85. First class, airmail, student, and emeritus rates on request. Canadian rates with GST available upon request, GST #1254 88122. Publications Mail Agreement Number 1069624. **Printed in the U.S.A.**

Change of address: Allow 4 weeks, giving old and new addresses and 8-digit account number. **Postmaster:** Send change of address to *Science*, P.O. Box 1811, Danbury, CT 06813–1811. **Single-copy sales:** $10.00 per issue prepaid includes surface postage; bulk rates on request. *Science* is indexed in the *Reader's Guide to Periodical Literature* and in several specialized indexes.

CONTENTS continued **>>**

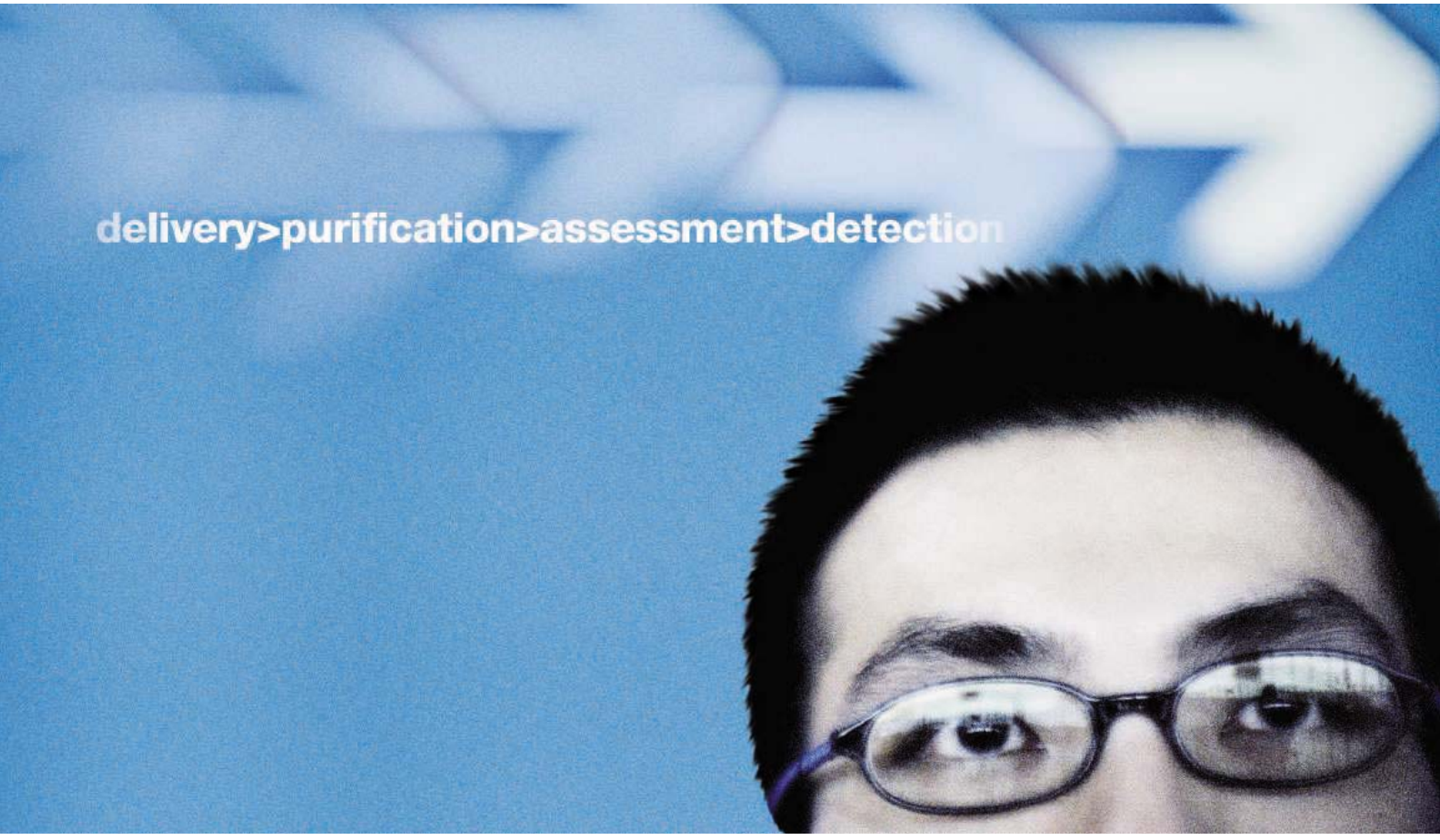

Bio-Rad and RNAi. Come have a look.

From delivery to detection, Bio-Rad supports your RNAi research.

With a broad range of proven delivery technologies, award-winning detection systems, and a suite of high-quality support products, it's clear that Bio-Rad has a vision for RNAi.

- Greatest choice of delivery technologies
- RNA and protein purification products
- Automated microfluidic RNA analysis
- Sensitive, optimized cDNA synthesis kits
- Systems for protein and mRNA detection

For a close look at Bio-Rad's tools for RNAi, visit us on the Web at **www.bio-rad.com/rnai/**

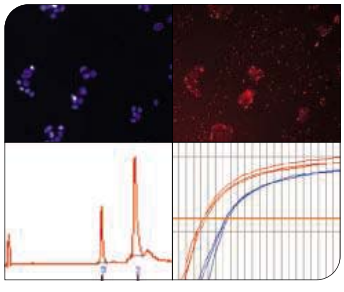

MCF-7 cells transfected using siLentFect™ reagent. RNA purified and analyzed using the Aurum™ total RNA kit and Experion™ system. Detection performed using iScript™ cDNA synthesis kit and the MyiQ™ system.

Visit us on the Web at **discover.bio-rad.com**
Call toll free at 1-800-4BIORAD (1-800-424-6723), outside the US, contact your local sales office.

BIO-RAD

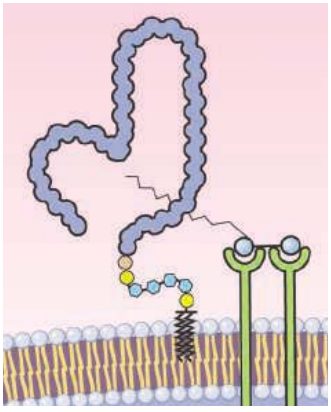

Glypicans as growth factor coreceptors.

SCIENCE'S **STKE**

www.stke.org SIGNAL TRANSDUCTION KNOWLEDGE ENVIRONMENT

PERSPECTIVE: Shedding Light on the Distinct Functions of Proteoglycans
S. B. Selleck
Growth factor–induced shedding of syndecans renders some cancer cells dependent on glypicans for their responses to mitogens.

CONNECTIONS MAPS
Browse for information about the more than 1400 components in this database of cell signaling.

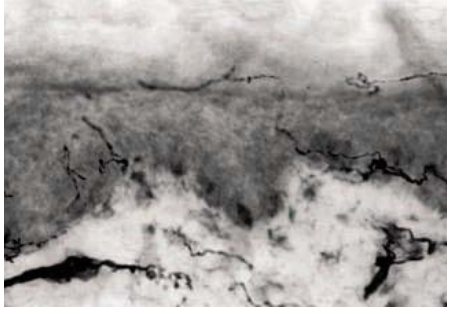

Paucity of nerve endings in neuropathy.

SCIENCE'S **SAGE KE**

www.sageke.org SCIENCE OF AGING KNOWLEDGE ENVIRONMENT

PERSPECTIVE: Small-Fiber Neuropathy—Answering the Burning Questions
E. Fink and A. L. Oaklander
New techniques offer promise for diagnosing peripheral nerve disease.

TEACHING RESOURCES
Check out the figures, outlines, and other teaching materials suitable for courses on the science of aging.

SCIENCE**NOW**

www.sciencenow.org DAILY NEWS COVERAGE

Mmmm... Healthy Bacon
Researchers create transgenic pig that makes high levels of omega-3 fatty acids.

Have No Fear, Cortisol's Here
New study suggests stress hormone may reduce social and spider phobias.

Hidden Comets Tell Icy Tale
New discovery in asteroid belt may give clues to origin of Earth's oceans.

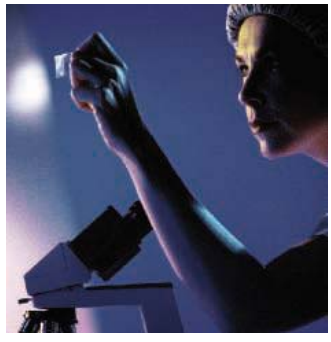

What do you do outside the lab?

SCIENCE **CAREERS**

www.sciencecareers.org CAREER RESOURCES FOR SCIENTISTS

GLOBAL: Mind Matters—Secret Passions
I. S. Levine
Our Mind Matters expert looks into the off-hours activities of successful scientists.

GLOBAL: Scientists as Schoolteachers—Part 2
R. Arnette
Get more stories and guidance about making the leap from the bench to the blackboard.

US: Switching Gears
R. Arnette
Three former scientists find professional fulfillment after leaving their research careers to teach.

EUROPE: Scientists Step into the Classroom
A. Forde
Scientists across Northern Europe explain why they picked teaching as an alternative career.

EUROPE: Canadian Teaching and Cross-Border Training
A. Fazekas
An educational consultant offers her perspectives on becoming a schoolteacher in Canada.

EDITED BY STELLA HURTLEY AND PHIL SZUROMI

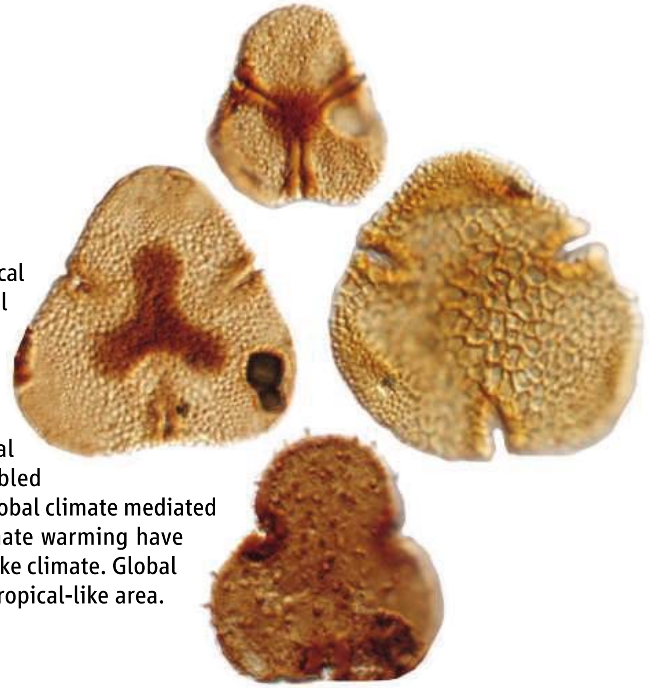

Ancient Tropical Forest Diversity

Understanding how the high plant species diversity of tropical forests arose has been hampered by the scant fossil evidence of lowland tropical rainforest species diversity in the geological record. **Jaramillo *et al.*** (p. 1893) now present a 45-million-year time series of plant diversity in the Neotropics with an unparalleled resolution. Changes in tropical-biome area were the main factor driving local tropical diversity. The observed diversity pattern resembled reconstructed global temperatures, which suggests that global climate mediated the change in tropical-biome area. Past episodes of climate warming have driven local speciation by increasing the area of tropical-like climate. Global cooling, however, drove local extinction by reducing the tropical-like area.

Fast Spinning

Pulsars are fast-spinning neutron stars that emit flashing twin radio beams. For the last 23 years, the speed limit was set by the first such pulsar discovered, which rotates at 642 hertz. **Hessels *et al.*** (p. 1901, published online 12 January; see the Perspective by **Grindlay**) have now found an even faster pulsar that spins 716 times a second. This extreme pulsar was found with the giant Green Bank Telescope during a survey of the globular cluster Terzan 5. From the pulsar's rotation speed, the star's diameter is calculated to be less than 16 kilometers, and limits can be placed on mechanisms for braking of the system by gravitation radiation. The faintness of this pulsar suggests that even faster ones await discovery.

Up in the Middle

Meteorological observations show that surface temperature of the western side of the Antarctic Peninsula has increased at a rate faster than that of any other region on Earth in the last 50 years. However, there have been few statistically significant surface temperature changes across the rest of Antarctica, which may even have cooled slightly in some places during recent decades. In order to help provide a more complete picture of how temperatures in the Antarctic troposphere have changed, **Turner *et al.*** (p. 1914) examined recently released radiosonde data from 1971 to 2003. The Antarctic middle troposphere has warmed by 0.5°C or more per decade during the winters during that time. Although this rise has been detected, its cause is still unknown.

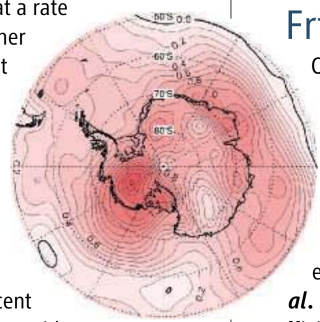

Uplifting Off Sumatra

Rupture of the Sunda megathrust during the giant earthquake of 28th March 2005 with a moment magnitude of 8.7 produced spectacular tectonic deformation along a 400-kilometer strip of the western Sumatran archipelago. **Briggs *et al.*** (p. 1897; see the Perspective by **Bilham**) combine measurements of uplifted coral and continuous satellite records to map the pattern of deformation in the region. They reveal belts of uplift as high as 2.9 meters parallel to the trench and a 1-meter-deep subsidence trough between the islands and main Sumatran coast. Two barriers to the propagation of this earthquake are identified.

Frictionless Spinning

One of the principal changes in moving a chemical system from the gas to solution phase is a huge increase in collision frequency. Constant bombardment by solvent molecules tends to quickly equilibrate any excess energy that a solute may acquire, for example, by photoexcitation. **Moskun *et al.*** (p. 1907) show that if a solute is given a sufficient burst of angular momentum, it can transiently push aside the surrounding solvent and rotate for picoseconds as if it were in a collisionless gas phase environment. Rapidly spinning CN fragments were generated with specific energies by photoexcitation of ICN in alcohol or aqueous solution. The persistent coherent rotation was well reproduced by simulating CN rotors in liquid argon, which suggests that solvent structure had little impact on the initial phase of nearly frictionless spinning.

High-Performance Superconducting Wires

Potential applications of high-temperature superconductors have included high-efficiency power transmission and levitating trains. However, these applications require wires that can carry huge currents and still remain superconducting in high magnetic fields. **Kang *et al.*** (p. 1911; see the news story by **Service**) have fabricated so-called second-generation superconducting wires, flexible metal substrates coated with thick high-temperature superconducting material, and show that they can meet the performance targets that have been set by industry for many applications.

Drying Streams

Africa is particularly vulnerable to the tragic consequences of drought, and climate models project that the mean annual rainfall in the northern and southern sections of the continent will decrease significantly during this century. **De Wit and Stankiewicz** (p. 1917, published online 2 March) examine what effects these expected changes in precipitation will have on perennial stream flow using a continent-wide database of all of the rivers and lakes in Africa and the fields of precipitation projected by a collection of climate

CREDITS (TOP TO BOTTOM): JARAMILLO AND RUEDA, 2006; TURNER ET AL.

change models. Perennial drainage could be significantly reduced in 25% of Africa by the end of the century, which would place an even greater burden on already struggling populations.

Highlighting the Niche

Replenishment of hair, skin, mucosal surfaces, and blood all depend on a steady supply of replacement cells that are generated by a small population of quiet but dedicated stem cells. These sorts of stem cells seem to reside in particular physical locations, or niches, within the organism. **Moore and Lemischka** (p. 1800) now review stem cell niches, including what they look like and how they direct the function of the stem cells, and also explore some of the questions about them that remain open.

Kaposi's Virus Entry Receptor

Kaposi's sarcoma–associated herpes virus (KSHV) is responsible for causing the debilitating life-threatening lesions often observed in patients with HIV/AIDS. **Kaleeba and Berger** (p. 1921) now identify human xCT, the light chain of human cystine/glutamate transporter as a receptor for the virus necessary and sufficient for its entry into target cells. Recombinant xCT rendered otherwise nonpermissive target cells susceptible to KSHV glycoprotein–mediated cell fusion and to KSHV virion entry, and antibodies to CT blocked KSHV fusion and entry with naturally permissive target cells.

A Mitotic Function for Lamin B

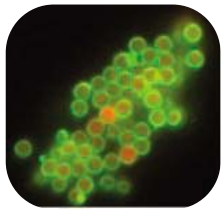

Nuclear lamins line the nuclear envelope to make up the nuclear lamina, which helps to maintain the structure and function of the nucleus. During cell division, the nuclear lamina disassembles, and the role for the lamins, if any, in mitosis is unclear. **Tsai *et al.*** (p. 1887, published online 16 March) now show that lamin B is required for the formation of the mitotic spindle. In cell extracts, lamin B formed a matrix with which spindle-assembly factors (which promote assembly of microtubules) were associated. Thus, lamin B is a key part of the so-called "spindle matrix," a structure known to be associated with assembly of the spindle but whose molecular constituents have not been described.

Accentuate the Positive

The cytokine interleukin-2 (IL-2) facilitates proliferation of naïve T cells, but several studies have shown that antibodies that bind IL-2, which at first glance should be inhibitory, can promote the expansion of subsets of memory $CD8^+$ T cells. Thus, IL-2 somehow might inhibit suppressive T cell populations that would otherwise prevent memory $CD8^+$ T cell expansion. **Boyman *et al.*** (p. 1924, published online 16 February; see the Perspective by **Prlic and Bevan**) now show that instead, binding of antibodies to IL-2 augments the direct activity of the cytokine on memory $CD8^+$ T cells themselves. Immune complexes form that focus local levels of IL-2 through presentation by Fc receptors. These observations could be important to consider in therapies that involve the manipulation of IL-2 and other cytokines, such as bone marrow transplantation and tumor immunotherapy.

Keeping the Wheat Near the Chaff

Wild grasses tend to release their mature seed fairly easily to facilitate widespread propagation. Domesticated grasses, such as wheat, rice, maize, and oat crops, do not release their grain as easily, and indeed would be of little value if the grain were to fall willy-nilly to the ground. **Li *et al.*** (p. 1936; see the cover and the Brevia by **Tanno and Willcox**) describe a one-nucleotide substitution in a rice gene that encodes a putative transcription factor that appears to account for this difference. The gene is expressed late in grain development at the junction between the seed and the mother plant.

The Making of Complex Carbohydrates

The cell walls of grasses differ from those of other plants in that they contain a particular type of polysaccharide, glucan. **Burton *et al.*** (p. 1940; see the Perspective by **Keegstra and Walton**) have now identified the (1,3;1,4)-β-D-glucan synthase genes of rice, which are critical for production of the grain-specific glucan. The rice gene was identified by comparison with quantitative trait loci of barley that affect its malt quality. Improved understanding of the complex carbohydrate biochemistry behind cell walls could lead to modifications tailored for specific purposes, whether as fuel, food, or fiber.

CREDIT: TSAI *ET AL.*

We gratefully acknowledge the following for their support

Fast, efficient and contamination-free cutting of cells saves time of entire experiments.

“Single-cell gene expression analysis is crucial for our research.”

Prof. Liss is using the Leica LMD6000 Laser Microdissection system.
Contamination-free, fully automated laser microdissection system for targeted cell isolation using a UV diode laser. Single cells or groups of cells can be microdissected from tissue sections, biopsies, smears, cytospins, and cell cultures. The laser can be also applied for intracellular and cellular ablation. Nuclei acids and proteins isolated from the dissected specimens can be directed to molecular analyses such like: sequencing, genotyping, PCR, real-time PCR, 2D gel electrophoresis or MALDI.

Prof. Dr. Birgit Liss, Department of Molecular Neurobiology, Institute of Normal and Pathological Physiology
Philipps University Marburg, Germany

Leica
MICROSYSTEMS

www.leica-microsystems.com/LMD6000

In Search of Biosecurity

David A. Relman is associate professor of Microbiology and Immunology and of Medicine at Stanford University, Stanford, CA. His research interests include human microbial ecology and pathogen biology.

Eileen Choffnes is director of the Forum on Microbial Threats at the U.S. Institute of Medicine, Washington, DC.

Stanley M. Lemon is director of the Institute for Human Infections and Immunity at the University of Texas, Galveston, TX, and chair of the Forum on Microbial Threats at the U.S. Institute of Medicine, Washington, DC.

The changing nature of biological threats, both natural and human-made, has made these challenging and unsettling times. As progress in life sciences research accelerates, it expands the scope of potential biological weapons, whose use for political purposes seems increasingly likely in a post-9/11 world. A recent report from the U.S. National Research Council and Institute of Medicine, *Globalization, Biosecurity, and the Future of the Life Sciences* (http://fermat.nap.edu/books/0309100321/html),* concludes that the breadth of potential biological threats is far wider than is commonly appreciated and will continue to expand in the future.

In the face of these challenges, the United States has made efforts to control, contain, and regulate research that involves certain biological agents and toxins that pose a special threat to public health and safety: the so-called "select agents." Proposals by several federal agencies call for more stringent measures, such as strict interpretation of the "deemed export" rule. These efforts are intended to limit the risk of research by restricting the involvement of foreign nationals and the communication of scientific information. However, they are impractical, counterproductive, and even dangerous.

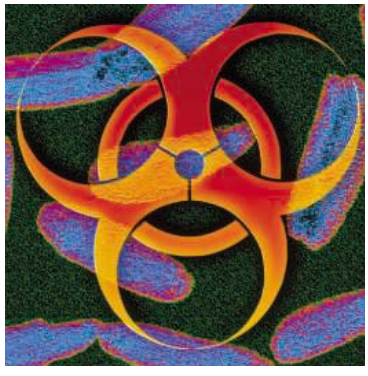

Research on select agents now requires rigorous security safeguards, including background checks of personnel by the Department of Justice, restricted access to laboratories, and even armed guards at some institutions. Regardless of their merits, such measures segregate scientists from their peers and complicate efforts to recruit the best and brightest to important research. More troublesome is the mandate to extend such rules to collaborating labs abroad that receive U.S. federal funds. In such foreign settings, the select agents that these rules seek to control may be endemic and otherwise readily available, making these measures impractical and politically unpalatable. The result is an unfortunate loss of foreign collaboration in critically needed surveillance of newly emerging infectious diseases.

Of even greater concern are potential constraints on the flow of scientific information stemming from fundamental research on dangerous pathogens. In a world concerned with the threat of terrorism, it is understandable that politicians and their constituents might feel safer if pathogens were locked up, tight regulations imposed on research, and strict controls placed on the dissemination of research results. Unfortunately, such measures won't reduce risks and may cause a false illusion of security. The risk of malevolent dual use goes far beyond infectious agents, let alone a select subset, and extends into virtually every aspect of the life sciences. Moreover, U.S. regulations will have no effect on a large and increasingly successful global life science enterprise. Stricter regulations will simply make it more difficult to exploit the benefits of the life sciences, threaten the vitality of biodefense research, and ultimately weaken our national security. Society has gained from the open exchange of scientific advances, and this tradition should not be lost.

In the early 1980s, the Reagan administration sought to restrict scientific communication in some fields. In the face of subsequent controversy, Reagan issued National Security Decision Directive 189 (NSDD-189). The directive states that "no restrictions may be placed upon the conduct or reporting of fundamental research that has not received national security classification, except as provided in applicable U.S. statutes." Where restriction is deemed necessary in the interest of national security, the proper control mechanism is classification. Although NSDD-189 remains in effect today, it is now being eroded by pervasive efforts to promote a class of information called "sensitive but unclassified."

The societal concerns that are driving these changes cannot be ignored. The risk that knowledge emerging from life sciences research could be misused, either intentionally or otherwise, needs responsible attention. Some life scientists argue that the benefits of dual-use research always outweigh the risks; others don't stop to consider the issue. Neither position is in the public interest. The scientific community needs to show that it can assume greater responsibility for research that presents potential security concerns. Those working in the life sciences must gain a greater awareness of the potential threats and learn to recognize, discourage, and report misuse or irresponsible behavior. Unless we adopt a shared culture of awareness and responsibility, we will face increasing restrictions on research and stricter controls on information. In this undesirable scenario, we will have gained little protection but done great harm to the research enterprise and threatened scientific progress.

– David A. Relman, Eileen Choffnes, Stanley M. Lemon

10.1126/science.1127725

*The authors participated in the U.S. National Research Council/Institute of Medicine study described here.

CREDIT: ALFRED PASIEKA/PHOTO RESEARCHERS, INC

EDITED BY GILBERT CHIN AND JAKE YESTON

HIGHLIGHTS OF THE RECENT LITERATURE

EVOLUTION

Three into One Makes Three

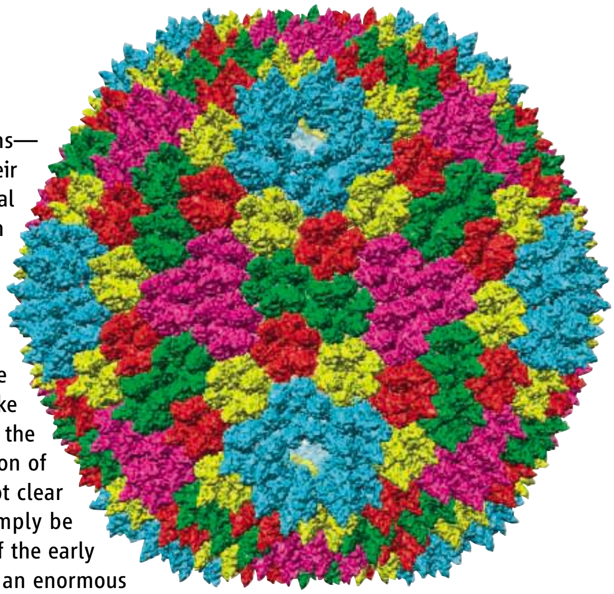

The MCP shell of STIV.

Molecular explorations into the origins of the three major cellular domains—Archaea, Bacteria, and Eukarya—have generated warring interpretations of their differences and similarities. For instance, the components of the translational machinery (ribosomal RNAs and proteins) serve as a distinctive identifier for each domain, whereas some of the enzymes involved in DNA replication (as well as recombination and repair) are shared (in the sense of being homologs) between two domains, though not consistently the same two.

Forterre discusses a scenario in which the initiating events for converting a primordial common ancestor (a cell containing an RNA genome) into the modern-day triumvirate were infection and transformation (via a plasmid-like intermediate stage) by three DNA viruses. The substitution of DNA for RNA as the cellular genetic repository is postulated to have reduced the rate of evolution of proteins and to have established a barrier to subsequent takeovers. It is not clear whether the long-standing problems that this proposal addresses will simply be replaced by new ones, but the reminder that viral lineages are also a part of the early landscape is welcome. Indeed, structural analyses have placed viruses with an enormous range of host specificity (bacteriophage PRD1, *Paramecium bursaria Chlorella* algal virus, and mammalian adenovirus) in the same family on the basis of their major capsid protein (MCP) architectures, as revealed most recently by Khayat *et al.* for the *Sulfolobus* turreted icosahedral virus (STIV) and by Laurinmäki *et al.* for bacteriophage Bam35. – GJC

Proc. Natl. Acad. Sci. U.S.A. **103**, 3669 (2006); **102**, 18944 (2005); *Structure* **13**, 1819 (2005).

CELL BIOLOGY

A Conserved Complement Collector

The complement system is important in the clearance of circulating pathogens; component C3 reacts with bacterial surfaces and promotes their binding to phagocytic cells that then internalize and destroy the bacteria. Some of the key players in clearing complement-coated pathogens are the Kupffer cells, a class of macrophages that reside in the liver.

Helmy *et al.* have identified a receptor present in Kupffer cells, the complement receptor of the immunoglobulin family (CRIg), which is required for the efficient binding and phagocytosis of complement-coated pathogens. Mice lacking CRIg were unable to clear complement-coated pathogens from the circulation and were more likely to succumb to infection. Thus, CRIg, which is conserved in mice and humans, represents a critical component of the innate immune system allowing the liver to act as a sentinel to invasion by pathogens. – SMH

Cell **124**, 915 (2006).

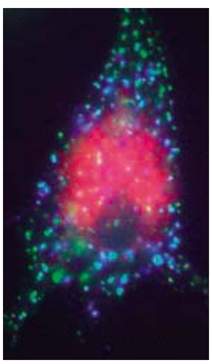

CRIg (green) localizes to cycling endosomes (blue) and does not enter lysosomes (red).

BIOMEDICINE

A Colorectal Catalog

Global surveys, inaugurated by almost complete compendiums of the genes of various organisms, have been expanded to cover proteins and, more recently, microRNAs (miRNAs), which are roughly 25-nucleotide–long RNA molecules that function to block the production of proteins from mRNAs. Cummins *et al.* describe a protocol—the miRNA serial analysis of gene expression (miRAGE)—and its application to assessing the miRNA composition of human colorectal cancer cells. Their approach meets the technical challenge of recovering short RNA pieces, present in vanishingly small quantities; analyzing an enormous number of parallel amplification reactions resulted in the identification of 200 miRNAs known within these cells (with one-quarter differentially expressed in comparison to normal colonic epithelial cells) and of 68 candidate miRNAs, of which one-fifth were independently identified and deposited by other groups during the course of their study. – GJC

Proc. Natl. Acad. Sci. U.S.A. **103**, 3687 (2006).

CHEMISTRY

Crystal Tuning

Chemists can rationally tune the extended structure of thin films by choosing the substrate on which the films are grown. However, the growth conditions that yield specific morphologies of three-dimensional crystals are still largely determined by trial and error, without a clear understanding of the factors that promote specific structural outcomes.

Grzesiak *et al.* sought to influence the structure of a metal organic framework solid by adding insoluble polymers to the crystallization solutions, for the purpose of guiding the nucleation process and thereby producing unusual bulk morphologies. The suspended polymers contained either acidic (methacrylic acid) or basic (4-vinylpyridine) components in varied proportion to a hydrophobic cross-linker (divinylbenzene). In the absence of polymer, two crystal phases were known to form from the Zn^{2+} and benzenedicarboxylate building blocks. A distinct third phase emerged when

CREDITS (TOP TO BOTTOM): KHAYAT *ET AL.*, *PROC. NATL. ACAD. SCI. U.S.A.* **102**, 18944 (2005); HELMY *ET AL.*, *CELL* **124**, 915 (2006)

predominantly nonpolar polymers were added (>70 % divinylbenzene), and the authors characterized its plate-like structure by powder and single-crystal x-ray diffraction, as well as Raman spectroscopy. This heterogeneous nucleation strategy produced additional phases when the benzenedicarboxylate bridges were functionalized with either Br or NH_2 groups. – JSY

Angew. Chem. Int. Ed. **45**, 10.1002/anie.200504312 (2006).

CHEMISTRY

On the Face of It

Varying the size of a nanometer-scale metal cluster can alter its catalytic activity. This phenomenon is usually attributed either to geometrical effects (such as the distribution of defect atoms or step sites) or to electronic effects (such as the scaling of metallic character with particle size) but has rarely been quantified for very small catalyst particles. Wilson *et al.* have systematically measured the size-dependent activity of cuboctahedral Pd clusters toward the catalysis of allyl alcohol hydrogenation. Clusters of precise size were synthesized using dendrimer templates and ranged in diameter from 1.3 to 1.9 nm (or ~50 to ~250 atoms). For clusters larger than 1.5 nm, the observed increase in reaction rate with increasing diameter was best fit by positing preferential reaction on facial sites, thus suggesting a geometrical origin for the activity change. For smaller clusters, reactivity did not correlate with physical properties such as the number of defect atoms or surface area, and activity changes were therefore attributed to electronic effects. – PDS

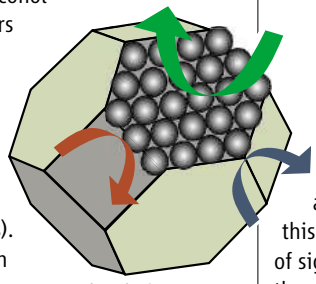

Reaction is faster at facial sites (green) than at edges (red) or vertices (blue) of Pd catalysts.

J. Am. Chem. Soc. **128**, 10.1021/ja058217m (2006).

CREDIT: ADAPTED FROM WILSON *ET AL.*, *J. AM. CHEM. SOC.* **128**, 10.1021/JA058217M (2006)

COMPUTER SCIENCE

Biologically Inspired Networking

Biological systems are typically better at adapting to new situations than computers because their design emphasizes robustness and sustainability even though the proximal response may not be the optimal one. In an information network such as the Internet, data are broken up into packets before being transmitted, and each packet can take a different path across the nodes of the network. How might a method for data transmission over multiple paths be redesigned whereby the network can itself adapt to an unpredictable and fluctuating environment?

Leibnitz *et al.* based their biologically inspired network routing scheme on a model developed to account for the response of *Escherichia coli* bacteria to variations in nutrient availability. The model uses stable attractors: equilibrium states into which the system settles until disrupted by a change in the environment, at which point the system converges to a new attractor. For network switching, information about the data paths (available bandwidth or transit time) is collected to find a stable attractor. When conditions change (for example, if a link breaks), a new attractor is selected, and the packets are switched to a new path. Because randomness is an intrinsic feature of the optimization method, the system is highly stable in noisy environments. – DV

Commun. Assoc. Comput. Mach. **49**, 63 (2006).

IMMUNOLOGY

Strength in Numbers

The autoimmune condition myasthenia gravis results from the production of self-reactive antibodies to the nicotinic acetylcholine receptor (AChR). Because this receptor is required for the transmission of signals at the neuromuscular junction, the aberrant nerve-muscle communication that results from an antibody-mediated inhibition of AChR clustering leads to muscular weakness at a range of anatomic locations.

A small proportion of myasthenic patients do not carry detectable levels of AChR antibodies, and most of these present instead with antibodies directed against muscle-specific kinase (MuSK). Using an experimental model for myasthenia, Shigemoto *et al.* show that such self-reactive antibodies may mediate pathogenesis, too. After the induction of antibodies to MuSK by vaccination with a chimeric protein, rabbits developed progressive muscular weakness. Reduced AChR clustering was detected at neuromuscular junctions in tissue sections taken from these animals; and in cell culture, antibodies to MuSK diminished experimentally induced AChR clustering. It will be important to establish whether antibodies to MuSK or other neuromuscular targets have an equivalent influence on myasthenia gravis in humans; if this is the case, then improved mechanistic understanding of the disease and new therapeutic options may follow. – SJS

J. Clin. Invest. **116**, 10.1172/JCI27545 (2006).

www.sciencemag.org

Science

1200 New York Avenue, NW
Washington, DC 20005
Editorial: 202-326-6550, FAX 202-289-7562
News: 202-326-6500, FAX 202-371-9227

Bateman House, 82-88 Hills Road
Cambridge, UK CB2 1LQ
+44 (0) 1223 326500, FAX +44 (0) 1223 326501

Subscription Services For change of address, missing issues, new orders and renewals, and payment questions: 800-731-4939 or 202-326-6417, FAX 202-842-1065. Mailing addresses: AAAS, P.O. Box 1811, Danbury, CT 06813 or AAAS Member Services, 1200 New York Avenue, NW, Washington, DC 20005

Institutional Site Licences please call 202-326-6755 for any questions or information

Reprints: Author Inquiries 800-635-7181
Commercial Inquiries 803-359-4578
Corrections 202-326-6501

Permissions 202-326-7074, FAX 202-682-0816

Member Benefits Bookstore: AAAS/BarnesandNoble.com bookstore www.aaas.org/bn; Car purchase discount: Subaru VIP Program 202-326-6417; Credit Card: MBNA 800-847-7378; Car Rentals: Hertz 800-654-2200 CDP#343457, Dollar 800-800-4000 #AA1115; AAAS Travels: Betchart Expeditions 800-252-4910; Life Insurance: Seabury & Smith 800-424-9883; Other Benefits: AAAS Member Services 202-326-6417 or www.aaasmember.org.

science_editors@aaas.org	(for general editorial queries)
science_letters@aaas.org	(for queries about letters)
science_reviews@aaas.org	(for returning manuscript reviews)
science_bookrevs@aaas.org	(for book review queries)

Published by the American Association for the Advancement of Science (AAAS), *Science* serves its readers as a forum for the presentation and discussion of important issues related to the advancement of science, including the presentation of minority or conflicting points of view, rather than by publishing only material on which a consensus has been reached. Accordingly, all articles published in *Science*—including editorials, news and comment, and book reviews—are signed and reflect the individual views of the authors and not official points of view adopted by the AAAS or the institutions with which the authors are affiliated.

AAAS was founded in 1848 and incorporated in 1874. Its mission is to advance science and innovation throughout the world for the benefit of all people. The goals of the association are to: foster communication among scientists, engineers and the public; enhance international cooperation in science and its applications; promote the responsible conduct and use of science and technology; foster education in science and technology for everyone; enhance the science and technology workforce and infrastructure; increase public understanding and appreciation of science and technology; and strengthen support for the science and technology enterprise.

Information for Contributors

See pages 102 and 103 of the 6 January 2006 issue or access www.sciencemag.org/feature/contribinfo/home.shtml

EDITOR-IN-CHIEF **Donald Kennedy**
EXECUTIVE EDITOR **Monica M. Bradford**
DEPUTY EDITORS **R. Brooks Hanson, Katrina L. Kelner**
NEWS EDITOR **Colin Norman**

Editorial supervisory senior editors Barbara Jasny, Phillip D. Szuromi; **senior editor/perspectives** Lisa D. Chong; **senior editors** Gilbert J. Chin, Pamela J. Hines, Paula A. Kiberstis (Boston), Beverly A. Purnell, L. Bryan Ray, Guy Riddihough (Manila), H. Jesse Smith, Valda Vinson, David Voss; **associate editors** Marc S. Lavine (Toronto), Jake S. Yeston; **online editor** Stewart Wills; **associate online editor** Tara S. Marathe; **book review editor** Sherman J. Suter; **associate letters editor** Etta Kavanagh; **information specialist** Janet Kegg; **editorial manager** Cara Tate; **senior copy editors** Jeffrey E. Cook, Harry Jach, Barbara P. Ordway; **copy editors** Cynthia Howe, Alexis Wynne Mogul, Jennifer Sills, Trista Wagoner; **editorial coordinators** Carolyn Kyle, Beverly Shields; **publication assistants** Ramatoulaye Diop, Chris Filiatreau, Joi S. Granger, Jeffrey Hearn, Lisa Johnson, Scott Miller, Jerry Richardson, Brian White, Anita Wynn; **editorial assistants** Lauren Kmec, Patricia M. Moore, Brendan Nardozzi, Michael Rodewald; **executive assistant** Sylvia S. Kihara

News senior correspondent Jean Marx; **deputy news editors** Robert Coontz, Jeffrey Mervis, Leslie Roberts, John Travis; **contributing editors** Elizabeth Culotta, Polly Shulman; **news writers** Yudhijit Bhattacharjee, Adrian Cho, Jennifer Couzin, David Grimm, Constance Holden, Jocelyn Kaiser, Richard A. Kerr, Eli Kintisch, Andrew Lawler (New England), Greg Miller, Elizabeth Pennisi, Robert F. Service (Pacific NW), Erik Stokstad; Katherine Unger (intern); **contributing correspondents** Barry A. Cipra, Jon Cohen (San Diego, CA), Daniel Ferber, Ann Gibbons, Robert Irion, Mitch Leslie (NetWatch), Charles C. Mann, Evelyn Strauss, Gary Taubes, Ingrid Wickelgren; **copy editors** Linda B. Felaco, Rachel Curran, Sean Richardson; **administrative support** Scherraine Mack, Fannie Groom **bureaus:** Berkeley, CA: 510-652-0302, FAX 510-652-1867, New England: 207-549-7755, San Diego, CA: 760-942-3252, FAX 760-942-4979, Pacific Northwest: 503-963-1940

Production director James Landry; **senior manager** Wendy K. Shank; **assistant manager** Rebecca Doshi; **senior specialists** Jay Covert, Chris Redwood; **specialist** Steve Forrester **Preflight director** David M. Tompkins; **manager** Marcus Spiegler; **specialist** Jessie Mudjitaba

Art director Joshua Moglia; **associate art director** Kelly Buckheit; **illustrators** Chris Bickel, Katharine Sutliff; **senior art associates** Holly Bishop, Laura Creveling, Preston Huey; **associate** Nayomi Kevitiyagala; **photo editor** Leslie Blizard

***Science* International**

Europe (science@science-int.co.uk) **editorial: international managing editor** Andrew M. Sugden; **senior editor/perspectives** Julia Fahrenkamp-Uppenbrink; **senior editors** Caroline Ash (Geneva: +41 (0) 222 346 3106), Stella M. Hurtley, Ian S. Osborne, Stephen J. Simpson, Peter Stern; **associate editor** Joanne Baker **editorial support** Alice Whaley; Deborah Dennison **administrative support** Janet Clements, Phil Marlow, Jill White; **news: international news editor** Eliot Marshall **deputy news editor** Daniel Clery; **correspondent** Gretchen Vogel (Berlin: +49 (0) 30 2809 3902, FAX +49 (0) 30 2809 8365); **contributing correspondents** Michael Balter (Paris), Martin Enserink (Amsterdam and Paris), John Bohannon (Berlin); **intern** Michael Schirber

Asia Japan Office: Asca Corporation, Eiko Ishioka, Fusako Tamura, 1-8-13, Hirano-cho, Chuo-ku, Osaka-shi, Osaka, 541-0046 Japan; +81 (0) 6 6202 6272, FAX +81 (0) 6 6202 6271; asca@os.gulf.or.jp; **asia news editor** Richard Stone +66 2 662 5818 (rstone@aaas.org) **japan news bureau** Dennis Normile (contributing correspondent, +81 (0) 3 3391 0630, FAX 81 (0) 3 5936 3531; dnormile@gol.com); **china representative** Hao Xin, + 86 (0) 10 6307 4439 or 6307 3676, FAX +86 (0) 10 6307 4358; haoxin@earthlink.net; **south asia** Pallava Bagla (contributing correspondent +91 (0) 11 2271 2896; pbagla@vsnl.com)

EXECUTIVE PUBLISHER **Alan I. Leshner**
PUBLISHER **Beth Rosner**

Fulfillment & Membership Services (membership@aaas.org) **director** Marlene Zendell; **manager** Waylon Butler; **systems specialist** Andrew Vargo; **specialists** Pat Butler, Laurie Baker, Tamara Alfson, Karena Smith, Vicki Linton; **circulation associate** Christopher Refice

Business Operations and Administration director Deborah Rivera-Wienhold; **business manager** Randy Yi; **senior business analyst** Lisa Donovan; **business analyst** Jessica Tierney; **financial analyst** Michael LoBue, Farida Yeasmin; **rights and permissions: administrator** Emilie David; **associate** Elizabeth Sandler; **marketing: director** John Meyers; **marketing managers** Darryl Walter, Allison Pritchard; **marketing associates** Julianne Wielga, Mary Ellen Crowley, Catherine Featherston, Alison Chandler; **director of international marketing and recruitment advertising** Deborah Harris; **international marketing manager** Wendy Sturley; **marketing/member services executive:** Linda Rusk; **japan sales** Jason Hannaford; **site license sales: director** Tom Ryan; **sales and customer service** Mehan Dossani, Kiki Forsythe, Catherine Holland, Wendy Wise; **electronic media: manager** Lizabeth Harman; **production associates** Sheila Mackall, Amanda K. Skelton, Lisa Stanford, Nichele Johnston; **applications developer** Carl Saffell

Advertising director worldwide ad sales Bill Moran

Product (science_advertising@aaas.org); **midwest/west coast/w. canada** Rick Bongiovanni: 330-405-7080, FAX 330-405-7081 • **east coast/e. canada** Christopher Breslin: 443-512-0330, FAX 443-512-0331 • **uk/europe/asia** Tracey Peers (Associate Director): +44 (0) 1782 752530, FAX +44 (0) 1782 752531 **japan** Mashy Yoshikawa: +81 (0) 33235 5961, FAX +81 (0) 33235 5852 **traffic manager** Carol Maddox; **sales coordinator** Deiandra Simms

Classified (advertise@sciencecareers.org); **u.s.: sales director** Gabrielle Boguslawski: 718-491-1607, FAX 202-289-6742; **inside sales manager** Daryl Anderson: 202-326-6543; **west coast/midwest** Kristine von Zedlitz: 415-956-2531; **east coast** Jill Downing: 631-580-2445; **canada, meetings and announcements** Kathleen Clark: 510-271-8349; **line ad sales** Emnet Tesfaye: 202-326-6740; **sales coordinators** Erika Bryant; Rohan Edmonson Christopher Normile, Joyce Scott, Shirley Young; **international: sales manager** Tracy Holmes: +44 (0) 1223 326525, FAX +44 (0) 1223 326532; **sales** Christina Harrison, Svitlana Barnes; **sales assistant** Helen Moroney; **japan:** Jason Hannaford: +81 (0) 52 789 1860, FAX +81 (0) 52 789 1861; **production: manager** Jennifer Rankin; **assistant manager** Deborah Tompkins; **associates** Christine Hall; Amy Hardcastle; **publications assistants** Robert Buck; Natasha Pinol

AAAS Board of Directors retiring president, chair Gilbert S. Omenn; **president** John P. Holdren; **president-elect** David Baltimore; **treasurer** David E. Shaw; **chief executive officer** Alan I. Leshner; **board** Rosina M. Bierbaum; John E. Dowling; Lynn W. Enquist; Susan M. Fitzpatrick; Alice Gast; Thomas Pollard; Peter J. Stang; Kathryn D. Sullivan

AAAS
ADVANCING SCIENCE, SERVING SOCIETY

val´i·da´tion

It's a synonym for TaqMan® Gene Expression Assays.

Your single easiest solution
TaqMan® Gene Expression Assays deliver accurate real-time PCR results to validate your microarray discoveries. TaqMan® Assays are designed to run under universal thermal cycling conditions and are formulated into a single 20X solution—less pipetting means less chance of error.

NOW AVAILABLE
Arabidopsis and Drosophila Assays!

>600,000 assays, and all very affordable
Virtually every gene and every transcript for human, mouse, rat, Arabidopsis and Drosophila is covered—with no time, reagents or effort spent on design and optimization, you save money on every experiment.

The gold standard in quantitative gene expression analysis
TaqMan Assays provide unmatched sensitivity, specificity and reliability for true gene expression validation—you can publish your data with confidence.

To learn more about TaqMan Gene Expression Assays and how they can help you validate your research, visit **www.allgenes.com**.

Applied Biosystems

25 YEARS ADVANCING SCIENCE

“THE FASTEST GROWING CROP IN IOWA IS NOT WHAT YOU EXPECT.”

MORE AND MORE BIOSCIENCE COMPANIES PLANNING TO EXPAND ARE TAKING A LOOK AT IOWA. And for good reason. Iowa leads the nation in the production of raw biomass at roughly 2.75 billion bushels. The state is home to three public universities that are world-renowned for their research in plant, animal and human bioscience. And to date there are more than 1,800 Iowa establishments already involved in the bioscience industry. To learn more about expanding your business in Iowa, visit iowalifechanging.com. Because the closer you look, the more Iowa grows on you.

www.iowalifechanging.com

IOWA
life | changing™

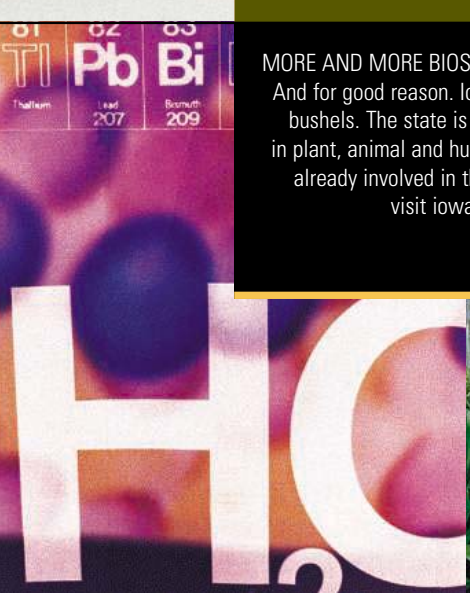

EXHIBIT

WHEN THE BIG ONE HIT

San Francisco residents woke early on the morning of 18 April 1906 to find their city collapsing around them. A rupture in the San Andreas fault split this street (above) and, combined with subsequent fires, razed some 28,000 buildings. At these two sites that commemorate the quake's centennial, visitors can relive the calamity, which killed more than 3000 people and left more than half of the city's inhabitants homeless.

Nearly 14,000 period photos and other visuals crowd this collection* from the Bancroft Library at the University of California, Berkeley. One highlight is footage of a pulverized downtown shot just a few days after the disaster. FaultLine† from the Exploratorium in San Francisco recounts the quake's history and delves into the science of earth movement. Backgrounders explain earthquake essentials and examine subsequent changes in building design intended to reduce damage. Fun graphics include video of a Jell-O model of the city, which shows how today's buildings would respond to a temblor. >>

* bancroft.berkeley.edu/collections/earthquakeandfire
† www.exploratorium.edu/faultline/index.html

DIRECTORY

They Know Aliens

With introduced cane toads hopping across Australia, Chinese silver grass sprouting along U.S. highways, and the raccoon dog, a native of northern Europe and Asia, showing up in Italy, invasive species are a worldwide issue. To track down experts on particular invaders, click over to this new global registry. Sponsored by a consortium of European institutions, the site lists more than 800 researchers, organized by country, type of organism, and field. >> daisie.ckff.si

LINKS

Economics Lab

Economists don't use test tubes or gene-sequencing machines, but they can run experiments on questions such as how we make choices when there's uncertainty about the outcome. Hosted by Georgia State University in Atlanta, EconPort brims with resources for researchers and teachers interested in economic experiments. A virtual textbook explains basics such as game theory and decision-making. Visitors can also consult a glossary and prowl a links catalog loaded with software, papers, tutorials, and other resources. The site also includes a feature to help users set up and run online experiments such as auctions. >> www.econport.org

DATABASE

To Build a Tooth >>

A tooth starts out as a thick patch in the lining of an embryo's mouth. To find out which genes morph these cells into a pearly white, bite into this database from the University of Helsinki in Finland. The site houses qualitative data pulled from the literature on gene activity during tooth development. You can sort through gene lists to discover when and where a specific one is active. Orange in this diagram (right) marks where the *sonic hedgehog* gene is working in the first molar of an embryonic mouse. >> bite-it.helsinki.fi

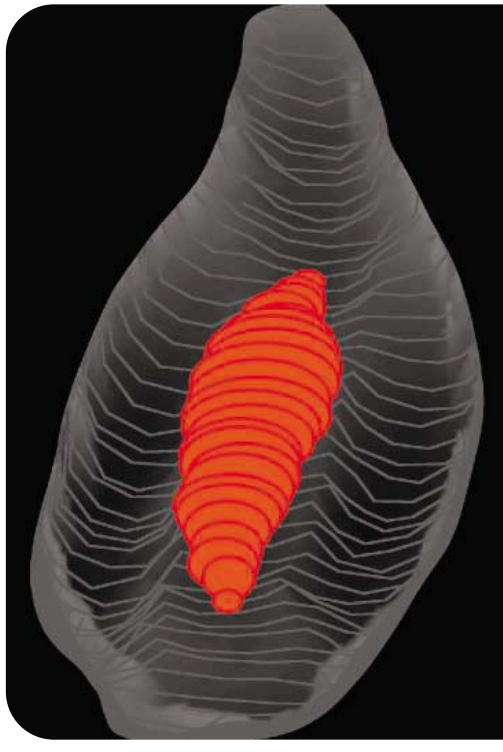

WEB LOG

Astronomy Daily

At his popular Bad Astronomy Web site, Phil Plait has long corrected misconceptions about the universe, skewered crackpots, and chastised the news media for purveying pseudoscience (NetWatch, 2 June 2000, p. 1543). The Sonoma State University astronomer offers a daily dose of his insights and opinions at the year-old Bad Astronomy Blog. Plait actually highlights plenty of good science, such as a recent study showing that the bright star Vega (left) twirls much faster than researchers imagined. But he also continues to attack ignorance, antiscience, and dubious schemes. Recent targets include a plan to have a cosmonaut belt a golf ball off the international space station. Plait notes that this will leave behind another piece of speeding junk that is "the equivalent of an invisible mine" for other spacecraft. >> www.badastronomy.com/bablog

Send site suggestions to >> netwatch@aaas.org
Archive: www.sciencemag.org/netwatch

CREDITS (TOP TO BOTTOM): NATIONAL INFORMATION SERVICE FOR EARTHQUAKE ENGINEERING/UC BERKELEY; JUKKA JERNVALL, PÄIVI KETTUNEN, AND SOILE KERÄNEN; NASA

Houston

live. work. play. stay.

Houston has it all! With over 5,000 restaurants,
teams in every major professional sport, golf 365 days a year,
world-class shopping, nationally renowned museum and theater districts,
cruising and the beach just a short drive, there's something fun for everyone!

Click: **www.visithoustontexas.com** Call: **1-800-4HOUSTON**

NEW SAUROPOD IS A STRETCH

Scientists have unveiled a new dinosaur species, a sauropod, with a neck about 8 meters long. These giant dinosaurs are famous for their long necks, some of which reached almost 9 meters, that helped them forage for greenery. But the new species, excavated in Mongolia in 2002, had a remarkably long neck given its medium-sized body—judging from the six very elongated neck vertebrae that were preserved.

The adult skeleton of the newly named *Erketu ellisoni*, on loan to the American Museum of Natural History in New York City, also includes most of the right rear leg, which suggests the beast stood only some 3 meters high at the hip. Daniel Ksepka, a grad student at Columbia University, who with the museum's Mark Norell describes the fossil in the current issue of *American Museum Novitates*, speculates that the species' long necks "helped them exploit different resources." But these were not treetop resources; scientists say that sauropods couldn't walk around like giraffes, as their neck vertebrae would have been dislocated. Ksepka says the new sauropod may help clear up the evolutionary relationships of early forms of this group of sauropods, the Titanosauriformes.

Undeterred by Dover

"This is an innovative effort by the Lancaster School District to propel science education out of the 19th century and into the 21st century."

—Alex Branning, president of a group called Integrity in Academics, after the board of the Lancaster School District, in suburban Los Angeles, voted last week to adopt a policy stating that evolution should not be taught as an "unalterable fact."

Missing Link

Archaeologists working in the Ethiopian desert last month found a hominid skull they believe to be some half-million years old. Sileshi Semaw of Indiana University, Bloomington, who is director of excavations at a site called Gona, announced the find last week in Addis Ababa. The skull, which is missing a jaw, could be tremendously important because fossils from this era—the Middle Pleistocene—are exceedingly rare. Yet this is the crucial time when modern *Homo sapiens* emerged from *Homo erectus*.

Paleoanthropologist Tim White of the University of California, Berkeley, says the closest hominid skull in time and place is from another Ethiopian site, the Middle Awash. Known as Bodo, it was found in 1976. But White says the Bodo skull had a more massive face and brow ridge than the current find. "Once again, the Afar [region] has yielded a very important fossil that is going to figure prominently in our ability to understand human evolution when it's been dated and studied," he adds. Semaw and his team say they are optimistic about getting a secure age for the fossil because of the many distinct layers of volcanic ash in the area.

TYPING DEPRESSION

Only about two-thirds of depressed people feel better after taking antidepressants, and currently, doctors have no way of knowing who is likely to benefit. Now a team led by psychiatrist Francis McMahon of the National Institute of Mental Health in Bethesda, Maryland, has identified a gene variant that appears to enhance a person's odds of responding to Prozac and other selective serotonin reuptake inhibitors (SSRIs).

McMahon and colleagues analyzed DNA samples from 1953 patients with major depressive disorder who were being treated with the SSRI citalopram (Celexa). Looking at 768 markers within 68 candidate genes, they found only one marker—in a gene coding for the 2A serotonin receptor—that was significantly associated with response to the drug. Everyone has two copies, or alleles, of the gene, which comes in two versions, A and G. The researchers found that 80% of patients with two A alleles got better on the drug, compared to 62% of those with two G's.

The finding could help explain why blacks appear to have a poorer response than whites to antidepressants, the authors say in a report to be published in May in the *American Journal of Human Genetics*. Of the 313 blacks in the study, only 6% had at least one A allele, whereas 42% of the whites did. And people with two A's (14% of whites and 1% of blacks) did much better than those with only one, says co-author Dennis Charney, a psychiatrist at Mount Sinai Medical Center in New York City.

"This work presages a revolutionary future for psychiatry where choice of antidepressant treatment will be determined in part on an individual patient's genotype," says psychiatrist Eric Nestler of the University of Texas Southwestern Medical Center in Dallas. McMahon adds that future research will look at the entire genome, including genes involved in drug metabolism.

IVY PCG Proudly Presents Thanks for Support

CREDITS (TOP TO BOTTOM): JASON BROUGHAM, WWW.JASONBROUGHAM.COM; SILESHI SEMAW; PHOTODISC GREEN

Gaps in a cancer test
1847

The U.K. budget shuffle
1848

DISASTER RELIEF

Too Late, Earth Scans Reveal the Power of a Killer Landslide

MANILA—New insights into the physics of the landslide that entombed a mountain village in the southern Philippines last month offer a bleak epilogue to the tragedy. Five days after a massive landslide buried Barangay Guinsaugon, in Southern Leyte Province, on 17 February, geologists and physicists dispatched to the scene came to a disturbing conclusion: Search teams were probing for survivors in the wrong place. The village, the scientists discovered, had been swept, en masse, downhill. "The rescuers were stunned," says Mark Lapus, a geologist with Manila-based Earth Probe Inc., whose ground-penetrating radar equipment was used to survey the site. "One shouted at me, 'When did you learn of this!' He thought I was withholding information."

This wasn't the only grim revelation in the disaster's aftermath. Ongoing analyses may explain why the rain-drenched scarp gave way, whether there were warning signs of an imminent landslide, and how rescuers might have been better guided to victims in air pockets. Although studies are still under way, one lesson is inescapable. "More scientists and more instruments should have been there from day one," says Alfredo Mahar Lagmay, a volcanotectonic specialist at the University of the Philippines, Diliman.

At about 10:30 a.m. on Friday, 17 February, a cliff face of a ridge straddling the Philippine fault, a tectonic zone running the length of the archipelago, disintegrated. Residents of Barangay Guinsaugon had no chance to escape: An estimated 15 million to 20 million cubic meters of rock and soil hurtled down the slope, reaching a top speed pegged at 140 kilometers per hour. Within 3 or 4 minutes, the landslide had rumbled to a halt, and the village was gone.

Rescuers were confronted with a moonscape dotted with hummocks, later determined to be debris-covered boulders. Miraculously, nearly two dozen people were pulled alive from just under the surface of the viscous debris. Meanwhile, victims trapped in air pockets were firing off cell phone text messages that grew more frantic as the hours passed. One sent on Sunday, 19 February, said simply, "Hurry, the waters are rising."

Desperate hours. Rescue workers from Taiwan set up seismic equipment in an unsuccessful attempt to locate survivors.

That day, the governor of Southern Leyte called Lagmay, asking if his team could carry out a ground-penetrating radar survey. Lagmay, Lapus, and colleagues at the University of the Philippines and Ateneo de Manila University flew down and started work on the morning of Tuesday, 21 February. By then, no survivors had been found or text messages received for more than 24 hours.

Initial news reports failed to capture the enormity of what had transpired, Lagmay says: "We didn't know the scale of the landslide until we got there. The whole side of the mountain had collapsed." His study set out to confirm that radar scans and creating an inventory map of where victims and belongings had been found. By the end of the day, the researchers had concluded that the rubble was 30 meters thick and that the water table lay 14 meters below the surface—dashing hopes of finding deeply buried survivors. Radar readings coupled with the debris inventory map suggested that Barangay Guinsaugon had been displaced 550 to 600 meters southeast of its original location. Many buildings were largely intact, and neighboring houses remained adjacent to each other, Lagmay's team reported in the 21 March issue of *Eos*.

Lagmay briefed the leader of the rescue operation, a Philippine army general, on the evening of 21 February. At first, Lagmay says, "he resisted the idea" that the search had been off target, citing insufficient evidence. The researchers redoubled their efforts the next day. "We took new measurements and plotted everything to demonstrate that the town did indeed move," he says. Their findings persuaded the general to search in several priority areas the team had identified. It rained all day, though, and an aerial survey using Chinook helicopters lent by the U.S. military revealed that the water table at the foot of the slide, near where the village now lay, had risen to the surface of the muddy debris. That made rescue efforts more treacherous and suggested that any air pockets had been submerged. The rains continued, and by the evening of 24 February, the governor called off the search. The rescuers had saved 20 people—all in the 48 hours following the disaster—and recovered 122 bodies; more than 1300 villagers are listed as missing. An embankment is being built around the foot of the slide to preserve it as a mass grave.

Precisely what triggered the deadly landslide remains a mystery. At first, researchers fingered an earthquake that occurred 25 kilometers west of Barangay Guinsaugon around the time of the slide. But time records of victims' cell phone calls have since confirmed that the magnitude-2.6 temblor struck several minutes after the landslide. Any other faint tremor registered that day "alone would not be enough to trigger the landslide," says Renato Solidum Jr., director of the Philippine Institute of Volcanology and Seismology (PHIVOLCS). Kyoji Sassa of the University of Kyoto's Disaster Prevention Research Institute, who led a Japanese-Philippine team that carried out geophysical measurements last week at the site, including ground-based laser scanning of the topography, believes that a small earthquake, if near enough, could have been sufficient if the hill was primed to fall.

A precipitating factor, experts agree, is

CREDIT: REUTERS

From bench to bedside
1852

Battling over a fundamental patent
1855

Several Major Debris Avalanches

Year	Country	Triggering process	Volume of material*	Impact
1962	Peru (Ancash)	Unknown	13	4000 to 5000 killed
1970	Peru (Ancash)	Earthquake	30–50	18,000 killed
1980	U.S. (Washington)	Volcanic eruption	1600	World's largest historic landslide; 5 to 10 killed
1997	Montserrat	Lava dome collapse	64	Evacuation in 1996 prevented loss of life
2002	U.S. (Alaska)	Earthquake	10–70	Occurred in isolated national park
2006	Philippines (Leyte)	Rainfall/ earthquake?	15–20	122 killed; 1328 missing and presumed dead

* m^3, in millions.

that the scarp had been saturated by 10 days of heavy rain in the Leyte region in early February. To test the rainfall-earthquake scenario, Sassa is putting debris through the rigors of a new simulator of landslide shearing forces that his group has developed, accompanied by computer modeling. Preliminary results should be available in April, he says. Intriguingly, survivors from Barangay Guinsaugon told Lagmay's team that a river between the base of the scarp and the village dried up 2 days before the landslide. (Solidum calls the observation of the lost river "unverified.") And mountain dwellers "reported having felt an earthquake 2 months prior to the disaster and noticed cracks in the ground," Lagmay's team reported in *Eos*. River water and rain "may have seeped into these fractures and lubricated the slip planes," they wrote.

Lubrication, coupled with the type of landslide that occurred—a deep-seated rockslide-debris avalanche that is "less turbulent" than shallower kinds of slides—explains how a whole village could be transported down the slope, Lagmay says. The Philippine disaster is the deadliest debris avalanche since the Nevados Huascarán event in Peru that killed 18,000 in 1970 (see table).

The Leyte disaster's consequences are still sinking in. Lagmay notes that it's impossible to say whether rescuers, even if they had known exactly where to dig from the get-go, could have reached victims who initially survived before succumbing to rising water levels. Thus much of the scientific postmortem has shifted to what can be done to prevent future such disasters. A key task is refining risk models of rare, deep-seated landslides. "We need to evaluate this better," Solidum says.

Lagmay and others hope that more-precise hazard maps and better community outreach—for instance, prompting people to quickly report potential warning signs, such as rivers suddenly drying up—will enable officials to react more nimbly to disasters and perhaps even prevent casualties. And there's one message that governments around the world should heed. In the event of a future calamity, Lagmay says, any rescue operation "should be scientific from the start."

–RICHARD STONE

U.S. HIGHER EDUCATION

Foreign Grad Students Show Renewed Interest

Foreign students flooded U.S. graduate schools with applications this winter, reversing a 2-year decline and allaying fears that U.S. government policies were turning off talented Asian students.

The latest results from an annual survey by the Council of Graduate Schools (CGS) released last week found that international graduate applications for the 2006–'07 academic year rose by 11% over the previous year, with particularly significant upticks in Chinese and Indian applicants. All fields enjoyed a boost, although life sciences and engineering led the way with 16% and 17% increases, respectively (see graph). Although only one-third of the 450 universities queried responded to the survey, they included 80% of the 25 institutions with the largest international student enrollments.

Applications are the first of three points along the matriculation route for prospective students, and the other two metrics—admissions and enrollments—have presented a brighter picture. In fact, enrollments actually increased by 1% last year for the first time since 2001 (*Science*, 11 November 2005, p. 957). Peggy Blumenthal, executive vice president of the Institute of International Education, says the rise in applications suggests "we've turned the corner." The renewed interest among Chinese and Indian students is especially welcome because those countries have consistently provided the two largest pools of international students for U.S. universities.

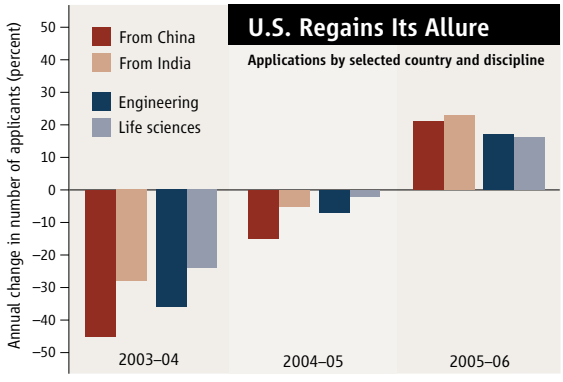

Friendlier shores. U.S. graduate schools received a surge of applications this year from Chinese and Indian students, and those in engineering led the way.

SOURCES (TOP TO BOTTOM): ADAPTED FROM A. M. LAGMAY *ET AL. EOS*, 214 (21 MARCH 2006); COUNCIL OF GRADUATE SCHOOLS

University administrators have blamed the 2003–'05 downturn in large part on tighter immigration policies following the September 2001 terrorist attacks and perceptions that the United States was less welcoming of foreigners. CGS President Debra Stewart believes that the government's willingness to address those concerns, including speeding up the visa application process, has helped remove those obstacles. Interestingly, applications from Middle Eastern students, arguably the most likely to be deterred by post–9/11 policies, have risen steadily for the past 3 years, by 4%, 7%, and 4%.

Many institutions have also strengthened their recruiting efforts. Washington State University (WSU) in Pullman, for example, has held focus groups among its international students to find out "things that they were drawn to, things we could play up" in recruiting, says associate graduate dean Lori Wiest. WSU now provides potential applicants from abroad with information specifically geared to their needs, she says. The approach seems to be paying off: Applications from foreign graduate students were up 37%, outpacing the national average.

–KATHERINE UNGER

HIGHER EDUCATION

$200 Million Gift for Ancient World Institute Triggers Backlash

When New York University (NYU) officials announced last week the creation of the Institute for the Study of the Ancient World, it was widely seen as a major coup. The new Ph.D.-granting research institute, devoted to the art, archaeology, history, literature, and geography of ancient societies, was made possible by a private gift of $200 million in cash and real estate, one of the largest donations the university has ever landed. Yet some NYU faculty members, along with outside archaeologists, are aghast that the school accepted the money. One leading NYU archaeologist has already resigned from the university's existing ancient studies center to protest the decision.

The fracas stems from the source of the new institute's funds: The Leon Levy Foundation, named after the late Wall Street investor and philanthropist. Levy and his widow Shelby White, the foundation's trustee, have for years been at the center of controversies surrounding their antiquities collection, which some archaeologists believe includes objects that had been looted and illicitly traded. Indeed, several institutions, including Bryn Mawr College in Pennsylvania and the University of Cincinnati in Ohio, have adopted explicit policies against accepting funds from the foundation. "If we or our students accepted these kinds of funds, it would simply be giving credibility to the longstanding Levy-White practice of buying objects of questionable provenance," says James Wright, chair of Bryn Mawr's department of classical and Near Eastern archaeology. Archaeologist Colin Renfrew of Cambridge University in the United Kingdom is more outspoken: "I wouldn't touch a gift from Shelby White with a barge pole," he says.

But other scholars argue that the Levy Foundation has been a positive force, spending millions for archaeological digs, such as a major excavation at the Philistine site of Ashkelon in Israel (*Science*, 2 July 1999, p. 36). It also funds a program based at Harvard University that supports the publication of archaeological findings. "The foundation has done a power of good," says Baruch Halpern, an expert in ancient history at Pennsylvania State University in State College. And Christopher Ratté, a classical archaeologist at NYU, whose publications have received Levy-White support, says that "it is very difficult to argue with this kind of generosity." Ratté adds that the Levy-White collection "is not coming to NYU, and there will be no direct association between the collection and the university."

Levy and White have generated debate among many archaeologists since at least 1990, when the Metropolitan Museum of Art in New York City mounted a major exhibition of some 200 of their artifacts from the Near East, Greece, and Rome. A study published later in the *American Journal of Archaeology* concluded that more than 90% of those artifacts had no known provenance.

More recently, publications including *The New York Times* and *The New York Observer* have reported accusations by Italian authorities that objects in the Levy-White collection, including some that are still on view at the Metropolitan Museum, can be traced to illicit trade. White takes strong issue with these criticisms. "We have been involved in the field of archaeology for many years," she told *Science*, referring to herself and her late husband. "We have always collected in good faith, and we have always exhibited our collection publicly." White adds that the items in the collection were not purchased in "obscure places" but at public auctions and from leading dealers: "If it turns out that there are objects that I should not have bought, then I will deal with them."

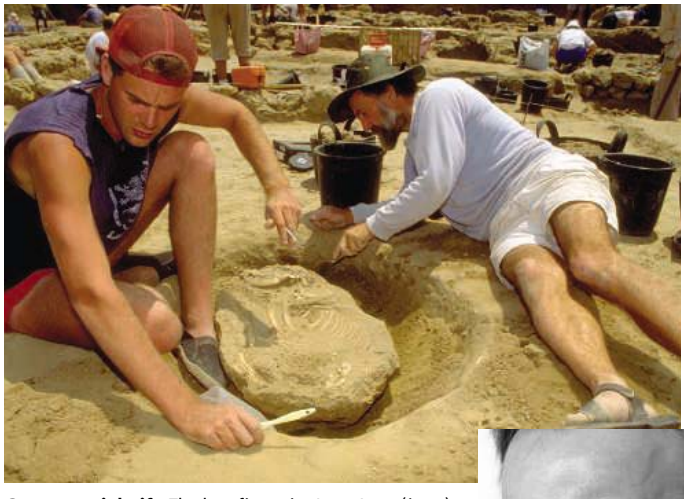

Controversial gift. The late financier Leon Levy (*inset*) and his wife Shelby White have funded archaeological digs in Ashkelon, Israel (*above*), and elsewhere, but controversy surrounding their antiquities collection has cast a shadow over their $200 million donation to New York University.

Some NYU faculty members began questioning the wisdom of accepting the donation in January, when Matthew Santirocco, director of the university's existing Center for Ancient Studies, called a meeting of the center's advisory committee—the first of three committee meetings devoted to discussing the proposed institute. At least five of 13 members of the center's advisory committee expressed varying degrees of concern about accepting money from the foundation during the meetings. Some members also worried that White would have considerable input into the naming of the institute's director and faculty. "We wanted to be sure that NYU administrators were aware of concerns in the archaeological community about the problem of safeguarding cultural property," says NYU classicist and advisory committee member Laura Slatkin.

Members of the committee say the decision was very close to being finalized by the time they were consulted. "The people in the administration and [Shelby] White had gone a long way down the road," says Michael Peachin, chair of the university's classics department. Another member, who asked not to be identified, agrees: "It was a fait accompli."

Santirocco counters that the committee "was not at all opposed to pursuing this opportunity" and that there was a "majority consensus" in favor of accepting the donation. Santirocco adds that the funds to create an interdisciplinary institute are a "truly transformative gift" that will "lead to a more holistic understanding of the ancient world." University officials also say that although White will be on the search committee for the new institute's director, NYU's provost and president will have the final say.

But those assurances did not satisfy archaeologist Randall White. In a letter last week to Santirocco, White resigned his membership in the school's ancient studies center, arguing that accepting money from the Levy Foundation could have negative consequences for NYU scholars. Countries victimized by antiquities looters could shut down digs associated with the new institute, he suggests. "The gift will promote suspicion that objects would be ripped from their archaeological context by looters," Randall White says.

Most opponents of the donation assume, however, that the institute will go ahead. Says NYU archaeologist and center member Rita Wright: "It remains to be seen whether this donation, and the institute it will create, will be in the best interests of research into ancient cultures."

–MICHAEL BALTER

CREDITS (TOP TO BOTTOM): RICHARD T. NOWITZ/CORBIS; COURTESY OF THE LEON LEVY FOUNDATION

DNA TESTING

Genetic Screen Misses Mutations in Women at High Risk of Breast Cancer

For women trying to learn more about their risk of developing breast or ovarian cancer, genetic tests can have a cruel twist. The bad news—that a woman carries a mutation known to raise the odds of such cancers—is definitive. But for some women, the good news that they don't have such a mutation doesn't remove the worry. That's because the only commercially available test in the United States doesn't detect many mutations that can occur in the two genes most frequently associated with breast cancer risk, *BRCA1* and *BRCA2*.

Now a study, published in the 22/29 March issue of the *Journal of the American Medical Association*, has measured the frequency of such false negatives for women with a particularly high risk of breast cancer. The number "is not trivial," says Stephen Gruber of the University of Michigan, Ann Arbor. "People who have a very high risk of having a mutation should be offered the chance to have [more complete] testing." Critics charge that Myriad Genetics's broad patent has slowed research into alternative tests, a claim Myriad denies.

The test, called BRCAnalysis, has been controversial from the start. In 1997, Myriad Genetics in Salt Lake City, Utah, was awarded a broad patent that gave it the rights to test for mutations in *BRCA1*, and, later, *BRCA2*. Some researchers claimed the patent was essentially a monopoly that would limit innovation. After an uncertain beginning (*Science*, 7 February 1997, p. 782), the company says it now tests tens of thousands of women a year. The $3000 assay involves sequencing DNA to look for point mutations or small insertions or deletions in the two genes, then checking for five larger flaws known as rearrangements. It has won high marks for accurately detecting these mutations.

Clinicians order the test for women at high risk of familial breast or ovarian cancer. If the test turns up one of these mutations, women might opt to begin having regular mammograms at a younger age, for example; some undergo preventive surgery to remove their breasts or ovaries. It's been known from the start, however, that Myriad's test won't detect all the possible mutations. So a "no mutation found" result does not necessarily mean a woman is not at risk.

Mary-Claire King of the University of Washington, Seattle—who in 1990 proved the existence of and mapped *BRCA1* but was beaten by Myriad in cloning the gene—and her colleagues wanted to know the exact rate of such "false negatives." The researchers sampled DNA from 300 people from very high-risk families in which four or more members had been diagnosed with breast or ovarian cancer. All 300 had received negative test results from Myriad. King's team searched the DNA using six methods, including one called multiplex ligation-dependent probe amplification (MLPA), a technique that's widely used in European labs. King and her colleagues found that 12% of the patients carried rearrangements on *BRCA1* or *BRCA2* that were not included in Myriad's array. The MLPA test, which is relatively inexpensive and indicates the presence of any rearrangement, is not used clinically for testing *BRCA* genes in the United States. Myriad says "that would probably infringe on our patents."

Under the gun? Myriad Genetics tests breast cancer susceptibility genes, but a new study suggests the assay doesn't detect mutations in 12% of high-risk subjects.

CREDIT: DOUGLAS C. PIZAC/AP

Myriad defends the sensitivity of its test. Only a few percent of women who take the test have as high a risk as the group King tested, says president Gregory Critchfield. Overall, it claims, less than 0.5% of women tested have mutations that go undetected. King thinks the percentage is higher, as people who seem to be at lower risk may also have undetected genomic rearrangements. The company anticipates implementing an additional array, which it says is similar to MLPA but more accurate, for high-risk people by the end of the year.

–ERIK STOKSTAD

A New Dawn for NASA, and Some Help for Astrobiologists

NASA has eased the pain to researchers bloodied by cuts in its planetary science and astrobiology programs.

This week, NASA reinstated the $440 million Dawn mission to two giant asteroids that it had canceled 3 weeks earlier. Mission managers at NASA's Jet Propulsion Laboratory in Pasadena, California, convinced an appeal panel that they have conquered formidable fiscal and technical problems. NASA expects to launch Dawn next summer, a year late, for its rendezvous beyond Mars.

NASA officials have also softened the blow of a 25% cut to the agency's $65 million astrobiology program. They will add back $30 million to allow funding this year of half the usual number of 3-year proposals. But President George W. Bush's 2007 request for the agency includes a 50% cut to the program from 2005 levels, and as one researcher noted, "we still have a pretty significant problem."

–RICHARD A. KERR

DOE Takes Fresh Look At a Delayed Accelerator

It's back to the drawing board for physicists developing an accelerator to generate beams of exotic nuclei. Last month, the Department of Energy (DOE) put a 5-year hold on the proposed $1 billion Rare Isotope Accelerator (RIA), which promises to unlock the secrets of stellar explosions (*Science*, 24 February, p. 1082). Now DOE has scrapped the RIA design and asked the community to devise a cheaper machine that can make a unique contribution.

RIA would have generated exotic nuclei in three ways: by bombarding a target of heavy atoms with protons; by shooting a beam of heavier nuclei through a target of light atoms, causing nuclei in the beam to fragment in flight; and by capturing the fragments in such a beam in a tank of gas and then "reaccelerating" them. DOE would like researchers to focus on reacceleration because it's a novel approach, says Konrad Gelbke, director of the National Superconducting Cyclotron Laboratory (NSCL) at Michigan State University in East Lansing.

But reacceleration is an unproven technology, Gelbke says, and NSCL leads the world in the "fast fragmentation" technique. "Build on your strengths," he says. "That's my motto."

–ADRIAN CHO

U.K. BUDGET

Government Aids Science Teaching, Streamlines Research Funding

CAMBRIDGE, U.K.—In what has been deemed by many as a cautious 2006–'07 budget for the United Kingdom, there is much shuffling of responsibilities for science and technology funding but little new cash. In his 22 March budget statement, Chancellor Gordon Brown said the government will spend more on secondary school science education, restructure funding councils that oversee biomedical and physical sciences, and create a "radically simplified" method of allocating research overheads to universities. Brown also promised to foot half the bill for a new "virtual institute" to develop technologies that can help lower carbon emissions; five major energy companies have agreed to cofund it. Researchers are generally pleased by the changes, but many say they want to see the details, which should be made public in the next few weeks.

As part of a generous package for state secondary schools, Brown is proposing to spend $53 million training 3000 new science teachers who actually have degrees in the subjects they will teach—chemistry, physics, and biology. Unions are enthusiastic: Steve Sinnott, general secretary of the National Union of Teachers, said the government is to be "congratulated" for "exactly the kind of vision we want."

Inside the box. A budget prepared by U.K. Chancellor Gordon Brown highlights the value of science but hews to steady-state funding.

But Brown's rearranging of the science funding furniture has met with a mixed response. For example, he outlined a scheme to take the funding of the Medical Research Council and the research managed by the Department of Health and merge it into a single fund of "at least" $1.74 billion per year. This tidying-up effort is "good news," according to a statement by Mark Walport, director of the giant biomedical foundation the Wellcome Trust. But Walport is "concerned that the figure mentioned … is considerably less" than the current total of the two agencies' research budgets. A Treasury Department spokesperson says this number isn't meant to be a cap but a general indicator of size, and that scientists will have a chance to debate it all before a decision is made later this year.

University of Edinburgh physicist Ian Halliday, president of the European Science Foundation, says he sees in this proposed merger a hint of the "British disease: Let's take something that works and see if we can't make it better." It might be wiser to follow an American adage, he suggests: "If it ain't broke, don't fix it." For the same reason, Halliday is wary of another proposal that would split the Particle Physics and Astronomy Research Council—a body he formerly headed—and merge the parts with two other councils. The aim is to give one research council responsibility for all spending on big research facilities, such as telescopes, particle accelerators, and neutron sources.

University leaders, however, seem ▶

PROFESSIONAL SOCIETIES

Physics Institute Settles Suit, Takes Steps to Increase Diversity

"This book is stolen. Written in part on stolen time, that is." When science journalist Jeff Schmidt penned those words, he inadvertently began a 6-year legal tale that even he didn't see coming. The yarn ended last month, as Schmidt settled a lawsuit against his former employer, the American Institute of Physics (AIP), which represents 10 professional societies.

In the suit, Schmidt claimed that AIP, based in College Park, Maryland, fired him in 2000 for protesting the lack of racial diversity on the editorial staff of AIP's magazine *Physics Today*. AIP says it was responding to his claim that he used company time to write his book *Disciplined Minds: A Critical Look at Salaried Professionals and the Soul-Battering System That Shapes Their Lives*. The book's first line says as much, although Schmidt says he was engaging in hyperbole.

Under the settlement, most of which is public, AIP admits no wrongdoing. Schmidt, who was an editor at *Physics Today* for 19 years, receives compensation for lost wages and benefits, pain and suffering, and legal fees. He also got his job back—just long enough to resign—and a recommendation that says his work consistently met or exceeded requirements. "Getting any one of these terms would have surprised me," Schmidt says. "Getting all of them is amazing."

The Washington Lawyers Committee for Civil Rights and Urban Affairs, which helped represent Schmidt, reports in a press release that AIP also agreed in the settlement to support efforts by the National Society of Black Physicists (NSBP) and the National Society of Hispanic Physicists (NSHP) to become nonvoting members. If invited, AIP will also conduct a science writing course at the next NSBP annual conference, according to the release. AIP would not comment on the settlement.

"Historically, AIP has always worked with the NSBP and NSHP to promote diversity," says Marc Brodsky, AIP executive director and CEO. Brodsky says *Physics Today* now has at least one minority editor but that he doesn't generally ask employees about their ethnicity.

As the dispute went on, Schmidt, 59, became a minor cause célèbre among some physicists. Hundreds signed a statement accusing AIP of squelching free expression.

Jean Kumagai, an editor at *Physics Today* from 1989 to 1999, says she and Schmidt raised the issue of workplace diversity with higher-ups. "We suggested that they actually practice what they had on paper as a policy," says Kumagai, now an editor at *IEEE Spectrum* magazine. "And that didn't go over too well."

However, Graham Collins, an editor at *Scientific American* who worked at *Physics Today* from 1991 to 1998, says Schmidt deserves some of the blame for the conflict. "There were serious problems at the magazine, but he was one who tended to exacerbate the situation."

Schmidt, who has not been employed since he was fired, credits researchers for speaking out. "I think physicists protested my firing because it made the institution of physics look as political as other fields," he says. But, he adds, few voiced concern about racial diversity.

–ADRIAN CHO

CREDIT: KIRSTY WIGGLESWORTH/AP

delighted with another announcement—Brown's promise to overhaul the Research Assessment Exercise (RAE), a process that ranks departments by merit every 4 to 5 years and allocates funding for overhead costs of research. Critics say it has concentrated wealth in elite universities and destroyed some good departments elsewhere (*Science*, 4 February 2005, p. 668). Peter Cotgreave, head of the advocacy group Campaign for Science and Engineering in the U.K., says, "abolishing the RAE is the best thing they could do." Brown hasn't provided details of what might replace the RAE. But few will mourn its demise.

–ELIOT MARSHALL

ITALY

CNR Reform Moves Ahead, But Critics Cry Foul

TRIESTE, ITALY—Italy has begun to reform its National Research Council (CNR). But some scientists are worried that the changes are damaging and unlikely to improve the productivity of its 110 national institutes.

One goal is to make the institutes more attuned to national needs. By managing its projects and allocating funding through 11 new departments, says CNR governing board member and former president Luigi Rossi-Bernardi, the council will be transformed "from a traditional disciplinary structure to a mission-oriented organization, similar to that of the French CNRS and the Max Plank Society." Earlier this month, CNR President Fabio Pistella nominated directors for the new departments and announced that 67 existing institutes satisfy criteria of size and funds and will now move on to be scientifically assessed.

But the selection of the first batch of institutes has been criticized by scientists, including some members of Pistella's own scientific council. In an open letter to Pistella, 39 of Italy's top scientists called for greater transparency and consultation in the selection process, which took no account of scientific achievement. Some scientists see Pistella's move as an attempt to push through CNR reform before the country's general elections in early April. Pistella defended his actions and their timing, saying that he is adhering to a reform plan whereby institutes with adequate "concentration of resources" and "critical mass" move forward for assessment of activities. But Luciano Pietronero, head of the Complex Systems Institute in Rome, says that directors' internal evaluations were ignored in the selection, wasting 2 years of reporting to management.

Under the new structure, the funds from the research ministry are earmarked for particular departments: for example, 19% for the new materials and devices department, 5% for energy and transport. Then institutes apply to work on 76 projects run by the departments, through some 700 parcels of work known as *commesse*. However, the value of the *commesse* barely covers fixed costs, says Franco Miglietta, research manager at CNR's Biometeorology Institute in Florence, and institutes must find cash for research elsewhere.

The restructuring follows the CNR reform law passed by the Italian parliament in 2003 and will transform the $1.2-billion-a-year council into a resource "for the social and economic development of the country," says Pistella. Although 15% of the budget will be allocated to "curiosity-driven research," Pistella suggests that CNR's role is not basic science. "Universities are the place for research not directly targeting goals of competitiveness in manufacturing or meeting individual and collective needs," he told *Science*.

The fate of the rest of the CNR institutes will be decided within 3 months "after further considerations," says Rossi-Bernardi. CNR may be planning some clustering and networking of institutes, according to documents circulated last month.

Many researchers believe that much of the change is simply adding unnecessary bureaucracy, and doubters have their eyes set on next month's general elections. Molecular biologist Arturo Falaschi of the Scuola Normale university center in Pisa says that only a change of government will allow the creation of "a CNR on a par with organizations like the German Max Planck Society or the U.K. research councils."

–SUSAN BIGGIN

CREDIT: CNR

Top down. CNR President Fabio Pistella wants the council to follow national goals.

Nuclear Neighbors Talk Science

NEW DELHI—A devastating act of nature has led to the first-ever official talks on possible scientific collaborations between India and Pakistan. Last week, three senior Indian science administrators met in Islamabad with seven of their Pakistani counterparts to explore mitigation strategies in the wake of last fall's deadly earthquake in Kashmir. Seismology has long been a touchy subject for these rival nuclear powers. Joint research projects in weather, climate, and agricultural sciences were also discussed.

India is expected to host a second meeting later this year and has offered Pakistan its touring "science train" exhibit touting the country's accomplishments. **–PALLAVA BAGLA**

Spain Says Sí on Stem Cells

BARCELONA—The Spanish government has decided to authorize and fund the use of human embryos in somatic cell nuclear transfer experiments. The proposed legislation would allow this particular use of human embryos, also known as therapeutic cloning, for the first time. It updates a 2004 law that authorized studies on unused embryos from fertility clinics—but not nuclear transfer. Francisco Gracia, director of the Ministry of Health research funding agency, says that calling the nucleated egg an "activated egg" rather than an embryo will help skirt sensitive issues in a Catholic country.

Approval is expected before the end of the year, making Spain the fourth European country to fund such work. **–XAVIER BOSCH**

New School Science Journal

Help is on the way for Europe's secondary school science teachers. A new print and online journal, *Science in School* (scienceinschool.org), made its debut this week with the ambitious goal of providing teachers with news about research, teaching practices, and policy developments that affect the profession. "Our focus will be on secondary school teachers, but we hope to reach an international audience," explains Eleanor Hayes, the journal's editor and only full-time staffer.

The quarterly journal is being published by a consortium of Europe's seven largest intergovernmental research organizations and is based at the European Molecular Biology Laboratory in Heidelberg, Germany. A Ph.D. insect biologist, Hayes relies on volunteers to write and review articles for the magazine, which is making its 20,000 print copies available upon request. **–JEFFREY MERVIS**

APPLIED PHYSICS

Nanocolumns Give YBCO Wires a Big Boost

As high-temperature superconducting wires inch ever closer to market, a couple of shortcomings have continued to hold them back. Now, on page 1911, researchers at Oak Ridge National Laboratory in Tennessee report that they have surmounted those hurdles, at least for short lengths of wire made in the lab. If the work can be scaled up to make kilometers of wire, the advances could finally propel high-temperature superconducting wire into the myriad applications technologists have dreamed of ever since "high-T_c" materials were discovered 2 decades ago.

"It's very promising," says David Larbalestier, a superconductivity expert at the University of Wisconsin, Madison. "It puts a mark in the sand that is well ahead of where we are now."

At present, the performance of high-T_c wires—those that carry electricity without resistance at temperatures well above absolute zero (although still hundreds of degrees below room temperature)—is decidedly mixed. Companies have already commercialized high-current-carrying wires made from a mix of bismuth, strontium, calcium, copper, and oxygen. But the market for such wires is limited because they are expensive and lose their superconducting capabilities in the presence of strong magnetic fields, such as those routinely generated in motors and power-transmission cables. The ability to withstand such fields is considered a sine qua non for a wide range of practical applications.

A second generation of more field-resistant wires made from yttrium, barium, copper, and oxygen (YBCO) has been making steady progress in recent years (*Science*, 15 April 2005, p. 348). But it has been difficult to grow the superconductors in these wires thick enough to carry enough resistance-free current for applications. Typically, when YBCO is grown more than 1.5 micrometers thick, imperfections creep into the lattice and destroy its superconducting abilities. YBCO wires also aren't completely immune to magnetic fields; very strong fields cause tiny whirlpools of magnetic flux to move through the superconductors, snuffing out their ability to carry current without resistance.

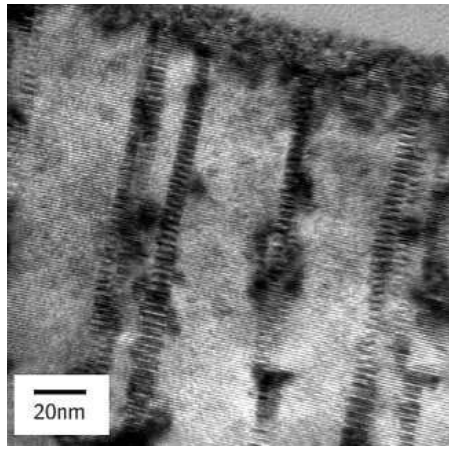

Power towers. Insulating ceramic columns inside a high-T_c superconductor keep magnetic vortices from sapping its ability to carry currents.

Other teams have made some progress on both fronts. Fifteen years ago, for example, a group from the United States showed that ▶

STEM CELLS

Versatile Sperm Cells May Offer Alternative to Embryos

Scientists in Germany reported last week that, in mice, they have succeeded in turning sperm precursor cells into cells with many of the characteristics of embryonic stem (ES) cells. If the same feat can be done with human sperm precursors, scientists say the technique could offer a much-sought alternative to human ES cells. ES cells are highly prized for their ability to differentiate into any type of bodily tissue.

Researchers have long suspected that spermatogonial stem cells, which males need for continuous sperm production, might have further potential. But only in 2004 did scientists finally succeed in growing such cells in culture from mice.

Now a team led by heart researcher Gerd Hasenfuss and Wolfgang Engel of Georg August University of Göttingen in Germany has taken the next step. After experimenting with various culture conditions, the researchers produced cell colonies that exhibit markers like those of ES cells. The cells, which the scientists labeled multipotent adult germ line stem cells (maGSC), differentiated into many types of body cells in all three germ layers: ectoderm (such as nerve cells), mesoderm (muscle and blood vessel cells), and endoderm (liver cells).

To see if the precursor cells would differentiate in live animals, the researchers injected maGSCs into mice whose immune systems had been knocked out. The mice produced teratomas, a kind of tumor that grows from germ line cells and that contains many types of tissues. The scientists also injected dye-tagged cells into blastocysts, very early embryos, that they inserted into female mice. When the embryos developed, the introduced cells contributed to multiple tissues in the offspring, the team reported online 24 March in *Nature*.

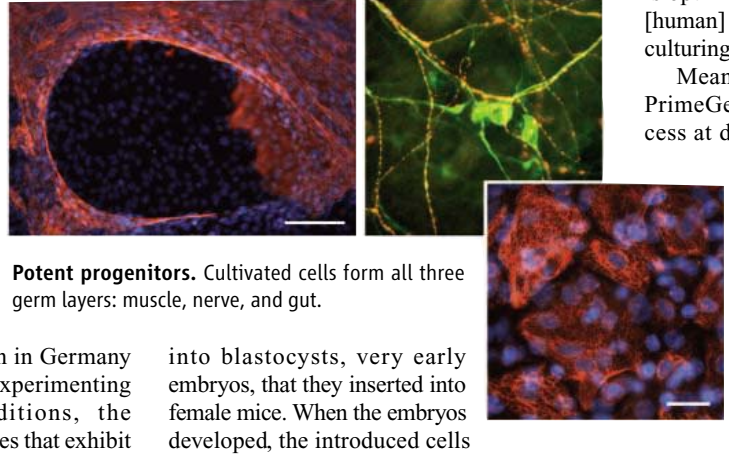

Potent progenitors. Cultivated cells form all three germ layers: muscle, nerve, and gut.

"I would consider this a major breakthrough," says David Garbers of the University of Texas Southwestern Medical Center in Dallas, who has been working on sperm

pluripotent cells from both murine and human testes. "If one can obtain ES-like cells from adult mice, then no doubt it will be possible in the human as well."

Other researchers are not as certain. Stephen Minger of King's College London notes that the success "doesn't necessarily mean it will also work in people." But Hasenfuss is optimistic. "Right now, we are looking at [human] testicular biopsies and trying to adapt culturing conditions," he says.

Meanwhile, California biotech company PrimeGen in Irvine this week claimed success at deriving pluripotent cells from both mouse and human testes, but the work has not been published.

John Gearhart, a stem cell researcher at Johns Hopkins University in Baltimore, Maryland, says the German study "appears to be the best so far" at offering a potential alternative source of cells that would bypass the ethical dilemmas surrounding human ES cells, as no embryo would be involved. And for the male half of the population, they raise the possibility of treatment with genetically matched tissues cultivated with cells from a simple testicular biopsy, without resort to the controversial procedure of therapeutic cloning.

–CONSTANCE HOLDEN

CREDITS (TOP TO BOTTOM): S. KANG *ET AL.*; K. GUAN ET AL., *NATURE* (DOI:10.1038/NATURE04697)

by shooting heavy ions through a high-temperature superconductor, they could riddle the crystalline lattice of YBCO with defects that snagged passing magnetic vortices, allowing the material to superconduct in higher magnetic fields. More recently, researchers at Los Alamos National Laboratory in New Mexico discovered a way to increase the effective thickness and current-carrying capacity by laying down several 1-micrometer-thick layers of YBCO separated by thin layers of cerium oxide. Unfortunately, both advances require complex, expensive synthetic procedures that limit their usefulness, says Oak Ridge materials scientist Amit Goyal.

So Goyal and colleagues led by postdoctoral assistant Sukill Kang decided to seek other approaches. The Oak Ridge team has long used a technique called pulsed laser deposition (PLD) to lay down YBCO atop a metal substrate. And Goyal says there was no one trick in particular in getting the technique to lay down thick superconducting films successfully. Rather, he says it was just a matter of systematically testing a wide range of deposition conditions until they found a combination that did the job.

The group did turn a new page, however, when it came to halting or "pinning" the magnetic vortices. They crushed a ceramic called barium zirconate (BZO) into nanometer-sized bits and then mixed it in with their YBCO starting material. As the researchers laid down their films, they bombarded a YBCO-BZO "target" with pulses from a laser. Under fire, the group reports, YBCO vaporized and condensed atop the metal substrate, while nanosized dots of BZO fell alongside. But because BZO has a somewhat larger spacing in its crystalline lattice than YBCO does, the two materials were energetically unhappy next to one another, creating a strain where their lattices met. The researchers found that the lattices minimized that strain by layering successive BZO nanodots right on top of one another. The result was BZO columns that ran vertically through YBCO and efficiently pinned magnetic vortices, thereby dramatically increasing the ability of the YBCO wires to withstand high magnetic fields.

The performance of the new wires is so good, in fact, that for the first time it surpasses the requirements for a wide range of electrical applications, including motors, high-field magnets, and power cables. So far, the wires are only 1.5 centimeters long. Two Japanese companies, however, are working on making long YBCO wires using PLD, while companies in the United States are racing to commercialize cheaper synthetic approaches in hopes of being the first to toe the latest line in the sand.

–ROBERT F. SERVICE

CREDIT: SHAW *ET AL.*, *NATURE* **440**, 676 (2006)

NEUROSCIENCE

The Thick and Thin of Brainpower: Developmental Timing Linked to IQ

Having a big brain probably won't ensure your eligibility for Mensa, but many studies have found modest correlations between the size of a person's brain and various measures of mental ability. Now, a study in the 30 March issue of *Nature* suggests that how the brain develops may be even more important to one's intellect than its final dimensions.

Using magnetic resonance imaging, Philip Shaw, a psychiatrist at the National Institute of Mental Health (NIMH) in Bethesda, Maryland, and colleagues scanned the brains of more than 300 healthy children at different ages and gave them standard IQ tests. They found that the highest-scoring children had a delayed but prolonged growth spurt in the cerebral cortex. "The idea that we can study the development of the brain and relate it to intelligence is really striking and gives us lots of ideas for future research," says Richard Haier, a neuroscientist at the University of California, Irvine.

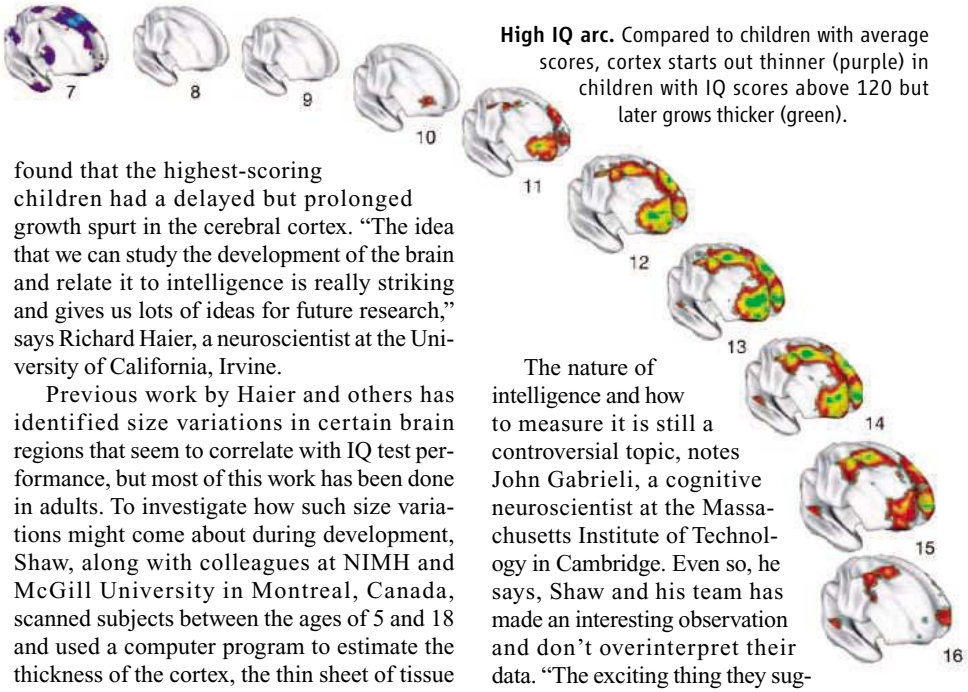

High IQ arc. Compared to children with average scores, cortex starts out thinner (purple) in children with IQ scores above 120 but later grows thicker (green).

Previous work by Haier and others has identified size variations in certain brain regions that seem to correlate with IQ test performance, but most of this work has been done in adults. To investigate how such size variations might come about during development, Shaw, along with colleagues at NIMH and McGill University in Montreal, Canada, scanned subjects between the ages of 5 and 18 and used a computer program to estimate the thickness of the cortex, the thin sheet of tissue on the surface of the brain. Most children were scanned two or more times, typically separated by 2 years. The researchers divided the children into three groups based on their IQ scores: average (83 to 108), high (109 to 120), and superior (121 or higher) intelligence.

The overall sequence of cortical development was similar in all three groups, Shaw says. "The cortex gets thicker during childhood and reaches a peak and then gets thinner." But the timing of these events was dramatically different in the "superior" group. Surprisingly, Shaw says, the cortex in these children started out thinner, on average, than in the other groups. Then it grew rapidly, starting around age 7, and peaked in thickness around 11 years. By early adulthood, the cortex in all three groups was roughly the same thickness.

The most pronounced disparity in cortical development between the superior-IQ group and the two lower-scoring groups occurred near the front of the brain. "The regions where the differences were most striking were in prefrontal cortex, which is interesting because that's the seat of the most complex and uniquely human activities like planning and abstract thought," Shaw says.

The nature of intelligence and how to measure it is still a controversial topic, notes John Gabrieli, a cognitive neuroscientist at the Massachusetts Institute of Technology in Cambridge. Even so, he says, Shaw and his team has made an interesting observation and don't overinterpret their data. "The exciting thing they suggest is that prolonged maturation is a good thing for intellectual development," Gabrieli says. Whether that extended process in the highest IQ children is determined by genetics or is susceptible to environmental influences—parenting or teaching styles, for example—is an open question, says Richard Passingham, a cognitive neuroscientist at Oxford University in the U.K.

Another fascinating question raised by the study is what cellular events cause the cortex to swell and shrink, says Haier. He speculates that the changes may reflect the growth and subsequent pruning of connections between neurons. If these two processes are well-timed, the adult brain may be more efficient, he suggests.

–GREG MILLER

MRC Cognition and Brain Sciences Unit, Cambridge, U.K. Thanks for support.

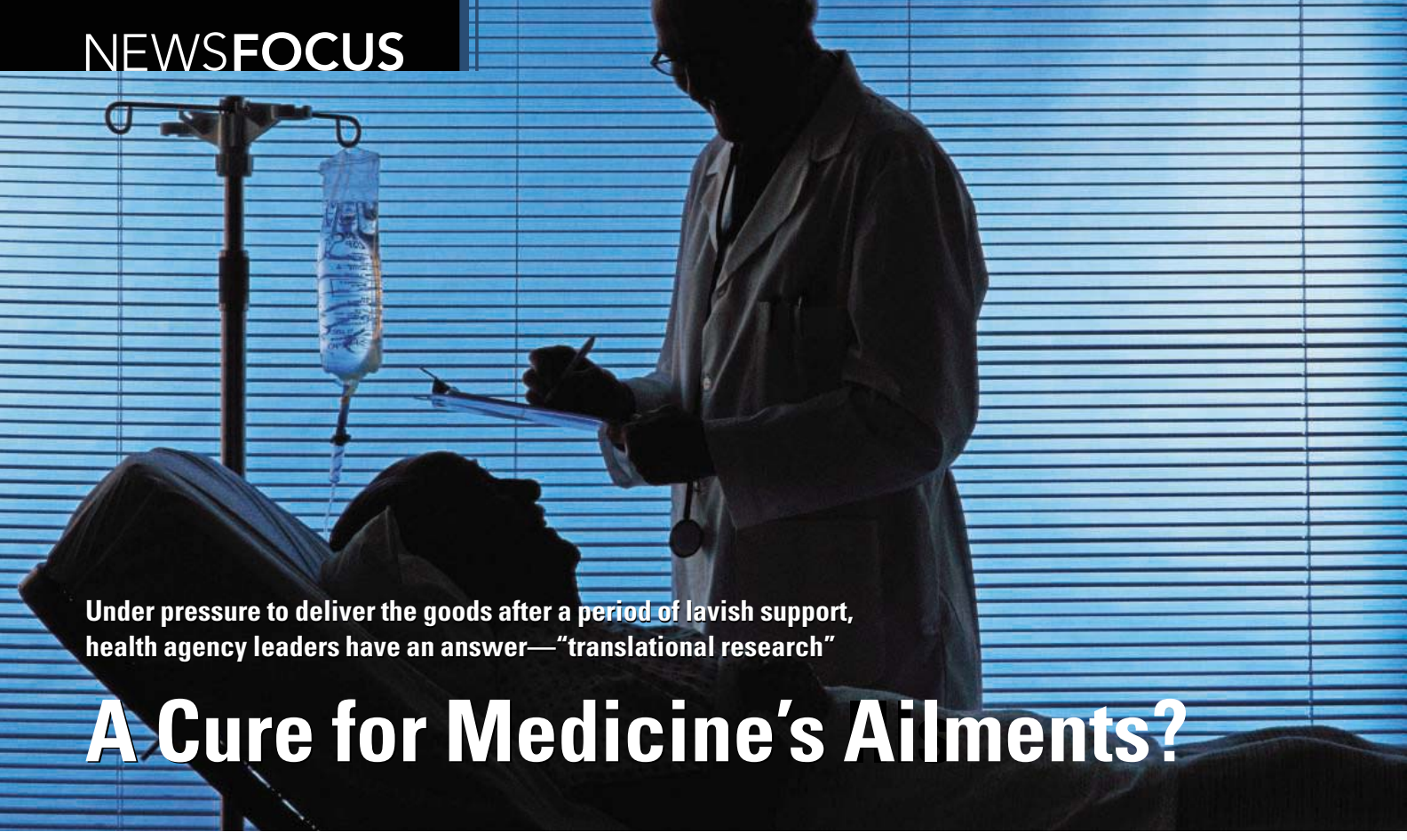

Under pressure to deliver the goods after a period of lavish support, health agency leaders have an answer—"translational research"

A Cure for Medicine's Ailments?

TWELVE YEARS AGO, WHEN IMMUNOLOGIST Elizabeth Jaffee was developing vaccines that could shrink tumors in mice, she decided to pursue a bold experiment: testing the new vaccines on patients with pancreatic cancer. This disease, which had killed a beloved uncle at age 51, is notoriously hard to treat and usually fatal within a year.

The project was risky, and so was her career move: from bench science to clinical medicine. While co-workers in the lab kept churning out papers, Jaffee's publications lagged. It took her 3 years to negotiate procedural hurdles and secure approvals to launch an initial human safety study. She also had to learn how to write a human trial protocol on her own. "There was nothing available to help you," she says.

In the end, says the Johns Hopkins University physician-researcher, "I was lucky. Things went well." Indeed, 8 years after her first trial with higher doses began, three of 14 patients are still alive, and 38 of 60 people in a second trial have survived 2 years compared to less than half of a control group. A bigger study of 600 patients is planned.

Jaffee's efforts to move a basic discovery into patients are a success story for "translational research," the new buzzword in biomedicine. This kind of research has suffered, she and others say, because few young investigators are attracted to the field. "We don't get as much respect for what we do," says Jaffee. People tend to dismiss it as "not as basic, as creative." But that may be changing.

Public and congressional pressure on the National Institutes of Health is growing to find "cures" after a 5-year doubling of the NIH budget that ended in 2003. Translational research is being offered as the way to move basic findings from the bench to the clinic. And it is hot: Everywhere you look, academic health centers are naming deans of translational research and creating centers that bring basic and clinical researchers together. NIH Director Elias Zerhouni has made speeding basic discoveries into diagnostics and treatments one of his top priorities, and to this end he is urging universities to create administrative "homes" to nurture investigators like Jaffee. Translational research "is an intellectual discipline in itself now," Zerhouni says.

> "There aren't many people who want to do this. It's not lucrative, it's not supported, **and there's a culture that looks down on it."**
>
> —Nina Bhardwaj, New York University

This declaration pleases some. "Without sounding pollyannaish about it, I am very optimistic" that new programs will rejuvenate the field, says Alan Schechter, an NIH intramural researcher and longtime champion of clinical research. Even some basic researchers who have never gotten grants are applying for support-

ies to patients are beginning to change their thinking. But others worry that if the objectives aren't defined carefully, translational medicine could be perceived as little more than a new label for familiar work. Worse, in a time of budget cutbacks, it could be seen as a threat to basic science programs funded from the same NIH pot.

Whether the available funding will be enough to build this new discipline—and spur the culture change that many say is needed—isn't yet clear. The "signals are good, but it's going to require quite a lot of thought from the government and institutions," says Bert Vogelstein of Johns Hopkins. "It's definitely a change from how research has been done."

In the trenches

People on the front lines attest to how hard it is to do the kind of work NIH now calls "translational." One frustration, says M.D. microbiologist Jane Koehler of the University of California (UC), San Francisco, is that reviewers tend to find applied grant proposals less compelling. Koehler has spent nearly 15 years studying the natural history and pathogenesis of diseases from bacteria called *Bartonella.* The microbes cause devastating lesions in AIDS patients as well as trench fever and cat scratch disease. Koehler has published her work in high-profile journals such as *The New England Journal of Medicine* (*NEJM*), but sometimes

CREDIT: WALTER HODGES/CORBIS

has found it difficult to convince grant reviewers in the basic sciences that work directly relevant to patient care is as important as mechanistic studies, she says.

Especially daunting, many say, is moving a basic discovery into early clinical trials. Jaffee ticks off a list of obstacles to her pancreatic cancer vaccine trials: obtaining grant support, problems with having a small biotech company produce clinical-grade vaccine ("they screwed up each time"), and moving her protocols through five university committees and two federal reviews. "Getting all that to happen at the same time is not simple," she says.

Although she still does lab work and mentors students, Jaffee and the clinician she now works with, Daniel Laheru, spend much of their time in meetings with data managers and nurses, hashing out glitches and paperwork that come with even a small trial. "This is translation," she whispers in a meeting at which the topic is what to do about a drop in blood pressure in one patient—probably unrelated to the trial—and the discovery that a solvent used to make the vaccine was 6 months past its expiration date.

New York University M.D.-Ph.D. immunologist Nina Bhardwaj, who has developed dendritic cell vaccines for patients with HIV or melanoma, tells of similar struggles to get her first trials under way and build a translational team. "It's a lot of groundwork and paperwork," she says. "There aren't many people who want to do this. It's not lucrative, it's not supported, and there's a culture that looks down on it."

Cutting your teeth on phase I trials is a tough way to advance in research because it's hard to accumulate high-impact publications. Early trials are building on a basic discovery, so they don't make it into journals such as *Science*, *Nature*, or *Cell*. Working with very sick cancer patients is difficult for many reasons; not only will most of them not be helped by the treatment, but the low probability of success means "you're not going to publish that in the [*NEJM*]," says NIH cancer immunologist Francesco Marincola, editor of the 3-year-old *Journal of Translational Medicine*. Plus, the pace is much slower than basic research: It might take 4 years to get enough test drug to begin treatment, accrue patients, write a paper, and get published in that specialty journal, notes Lee Nadler, who heads experimental medicine at the Dana-Farber Cancer Institute in Boston. "What happens if it didn't work? You're out of a job," says Nadler.

These challenges come on top of other deterrents to a career in clinical research: meager salaries compared to practicing medicine; growing medical school debts; lowered chances of NIH funding (see graph, p. 1854); and demands on medical centers for clinical income, leaving them unable to give budding physician-scientists sufficient "protected time" for research. Various panels have tried to address these issues, from a clinical research panel that reported to then–NIH director Harold Varmus in 1997, to an Institute of Medicine roundtable that met for the past 5 years.

Varmus responded by creating new training and early-career grants for clinical research; NIH later added debt-relief programs. Foundations have also stepped into the breach: The Doris Duke Charitable Foundation and Burroughs Wellcome Fund have supported early and midcareer translational researchers since 1998, and the Howard Hughes Medical Institute (HHMI) selected for its 2002 class of investigators only patient-oriented researchers. Such support can be crucial, say recipients. "It enabled me to do trailing-edge science," says HHMI geneticist Matthew Warman of Case Western Reserve University in Cleveland, Ohio, of his Burroughs grant, which he used to develop a mouse model for an inherited skeletal disease that affects only 200 people in the world.

These programs appear to be attracting more young physicians to research, according to an analysis of indicators last September in the *Journal of the American Medical Association*. An annual survey by the Association of American Medical Colleges has found that growing numbers of medical students say they're interested in research, for example, and applications are rising for NIH clinical support grants.

Some institutions have revived an old educational practice, introducing Ph.D. students and postdocs to disease research. Varmus, now at the Memorial Sloan-Kettering Cancer Center in New York City, has started a graduate program in cancer biology that will include exposure to clinical research; Stanford just announced a master's program in medicine for Ph.D. students; and HHMI last month announced $10 million in awards for similar programs at 13 institutions. Brian Druker of Oregon Health & Science University in Portland, an M.D. who spent a dozen years in the lab before conducting clinical trials with Gleevec, the widely heralded new drug for chronic myeloid leukemia, is all for it: "We need to bring Ph.D.s to clinical trials," he says.

Boom times

But focusing on individuals is not enough, some argue; they think more resources must go to building teams. Many observers agree that a single physician-scientist can no longer carry the burden of bridging basic and clinical research: "You can't do both well at the same time," says Druker. While some NIH institutes have been funding translational centers or collaborations such as the Immune Tolerance Network, a new crop of projects has taken root in the last few years funded by NIH, foundations, and others.

At Yale University, for example, pathologist and immunologist Jordan Pober realized 6 years ago that his group's cell and mouse studies on the role of inflammation in cardiovascular disease had reached the point at which they needed to see whether the same mechanisms were relevant in human disease. After much "cajoling," he raised seed money from Yale and later an industry sponsor, Boehringer Ingelheim, and started a translational program in vascular biology and

Clinical complexity. Elizabeth Jaffee of Johns Hopkins University, with colleague Daniel Laheru, faced a steep learning curve when she moved from basic research to testing pancreatic cancer vaccines in patients.

CREDIT: JOHNS HOPKINS UNIVERSITY

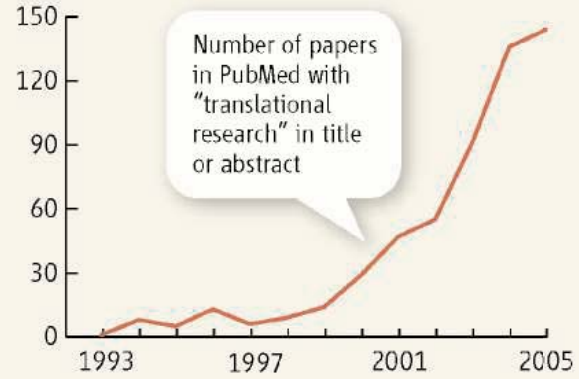

Ups and downs. Despite the growing popularity of the term "translational research" (*left*), researchers in this area still face lower success rates for clinical grants compared to nonclinical proposals (*below*). The study, published in the January issue of the *Journal of Investigative Medicine*, found the discrepancies held even in study sections with more clinical investigators.

	1994		2004	
	Clinical	Nonclinical	Clinical	Nonclinical
No. of NIH R01 grant applications	4126	10,743	5813	10,652
Median priority score*	232	205	264	234
% Funded	17.8	22	18.3	23.5

** A lower score means higher priority.*

transplantation. Now 35 faculty members are involved, including cardiologists and surgeons, and some are conducting observational trials. And basic researchers will "no longer have to read about someone else seeing if what works in the mouse is relevant in humans," Pober says.

A similar desire to bring together a critical mass of researchers inspired pharmacologist Garret FitzGerald to create the Institute for Translational Medicine and Therapeutics at the University of Pennsylvania. FitzGerald says he was concerned that "the intellectual resource was fragmented" at Penn. Taking a page from the drug company GlaxoSmithKline, which has reorganized its scientific staff into teams focused on a single disease, FitzGerald's 1-year-old center brings together three teams focused on neurotherapeutics, targeted drug delivery, and systems biology. He is assembling vast resources: 2140 square meters of dedicated lab space; study coordinators and research nurses; a "freezer farm" for biological samples; a drug-screening component; seed grants of up to $150,000; and links with Pennsylvania companies. He aims to train grad students and postdocs as well. "Growing your own is where we are with the bulk of staff," he says.

Comparable efforts are under way across the country. The University of Minnesota last year opened an 8825-square-meter building devoted to translational research on stem cells, orphan drugs, and infectious diseases. UC San Diego has a new "clinical investigation" institute that will focus partly on early drug trials. The University of Cincinnati in Ohio created an Office of Translational Research 5 years ago that offers seed grants for gathering preliminary data and helps investigators work up protocols and get them through Food and Drug Administration approval. The office has spurred 26 patient studies, including 15 new drug investigations and three gene-therapy trials, researchers there report.

Even basic labs are getting interested in applying discoveries. Vogelstein, a pioneering cancer genetics researcher, for example, says about half of his 20-person lab is now working on translational projects, compared to none a decade ago. The projects include developing cancer diagnostics based on detecting abnormal DNA in blood and stool samples, drug discovery, and engineering anaerobic bacteria to treat tumors. These applied projects attract a different kind of student or postdoc, Vogelstein says—often someone who had cancer in their family or even survived it herself or himself. "They are driven to do something," he says, even though they recognize that it may be harder than it would be for a basic researcher to get a faculty position down the road.

> "Measuring individual contributions **will be fuzzy wuzzy.**"
>
> —Garret FitzGerald, University of Pennsylvania

New translational programs at NIH institutes are also encouraging basic researchers to add applied projects. "A lot of these investigators say, 'I want to make a difference, I really want to develop a therapy before I retire,' " says Thomas Miller, who heads one such program at the National Institute of Neurological Disorders and Stroke.

Inertia

Zerhouni is trying to spur such changes across all of U.S. academic medicine, but he faces some challenges along the way. Persuading academic centers to buy into his plan to create campuswide "homes" for translational researchers could be tricky. Leading academics are anxious about the numbers they see in a new program, called Clinical and Translational Science Awards, that is part of Zerhouni's "Roadmap" of trans-NIH initiatives. Institutes that now have one of NIH's blue-ribbon general clinical research centers will have to compete for one of the new awards, which requires putting all clinical research and training under one administrative roof (*Science*, 21 October 2005, p. 422). This should give all clinical research the prestige now enjoyed by studies conducted by the National Cancer Institute's cancer centers, says Schechter. But there's a catch: Whereas there are 78 general clinical research centers today, Zerhouni's plan calls for only 60 of the new clinical and translational research awards.

Some researchers, including Jaffee, also worry that the new awards won't be large enough both to pay salaries and fund new translational studies. Druker would like to see NIH set aside more money for quick turnaround, early-stage clinical trials.

Another challenge will be getting institutions to create a clear promotion path for translational researchers. Because much of this work is done by teams, "measuring individual contributions will be fuzzy wuzzy," FitzGerald says. Counting publications as a measure of achievement is also a problem because translational researchers publish fewer papers in high-profile journals. Pober says Yale is talking about giving credit for designing successful protocols, not just publications.

Perhaps the biggest concern is that the translational research push could be coming at the wrong moment. Growth in NIH's budget is being held down, basic research may be headed for a funding slump, and grant success rates are in decline. "I think there's beginning to be a backlash to this" from basic researchers who feel their funding is threatened, says Pober. He cites a recent editorial by Gerald Weissman, editor-in-chief of the *FASEB Journal*, arguing that biomedical breakthroughs come from "childish curiosity" and not an "empire of translational research centers."

Whether NIH sticks to its plan to bolster bench-to-bedside research may also depend on how long Zerhouni, who has now been at NIH 4 years, stays in the job, researchers say. Richard Rettig, a former RAND researcher and longtime NIH observer, says, "The next director could shut it down or turn the spigot slowly." Yet if there's anything translational research needs, it's a sense that the field has a stable future.

–JOCELYN KAISER

SOURCES: (GRAPH) PUBMED/NATIONAL LIBRARY OF MEDICINE; (TABLE) T. KOTCHEN *ET AL.*, *JOURNAL OF INVESTIGATIVE MEDICINE* **54**, 14 (2006)

BIOMEDICAL PATENTS

Broad Patent Faces Narrow Odds in Court Battle

Upstream biotech patents face a crucial test in April in a trial with implications for future drug development

This year marks the 20th anniversary of the discovery of NF-κB, arguably one of the most prolific molecules in biology. But celebration is overshadowed by litigation, as a high-stakes legal battle approaches its climax.

In 2002, Ariad Pharmaceuticals, Harvard University, the Massachusetts Institute of Technology (MIT), and the Whitehead Institute sued Eli Lilly & Co. for patent infringement. Because the Lilly osteoporosis drug Evista and sepsis drug Xigris work by affecting NF-κB, the plaintiffs argued, they infringe a patent issued to the three research institutions and exclusively licensed to Ariad. After years of contentious legal maneuvering, the case is scheduled to go to trial on 10 April before a Boston jury.

The lawsuit has financial and legal implications well beyond the two drugs in question. NF-κB, a powerful transcription factor, controls whether cells live or die in response to outside stresses, and its inappropriate activation has been linked to cancer, arthritis, atherosclerosis, diabetes, and stroke. The patent covers methods for reducing NF-κB activity in cells—a strategy that could prove effective against at least some of these common diseases.

Closely watched. In addition to Lilly's Evista and Xigris, many existing drugs and some in development affect NF-κB and so may infringe Ariad's patent.

In addition, many other drugs on the market, besides Lilly's, affect NF-κB and so may already infringe the patent. One recent review paper listed more than 200 compounds known to inhibit NF-κB, including aspirin and several top-selling prescription drugs. The same day it sued Lilly, Ariad sent letters to about 50 companies with products either on the market or in development that work via NF-κB, asking them to license its methods, according to *The Wall Street Journal*. (Ariad declined to comment for this story.) An Ariad legal victory over Lilly could force these companies—and others developing drugs that affect NF-κB—to pay royalties to Ariad. "It is a pretty broad patent that would cover a huge number of compounds," says Arti Rai, a law professor at Duke University in Durham, North Carolina.

Patent experts worry that an Ariad victory could set a new legal precedent for patents with broad claims on biological processes far "upstream" of actual drugs. Because of their potential to discourage new drug development, "upstream patents are something to be worried about," says Rai, who adds that "thus far the federal circuit [court] has tended not to uphold these broad claims." Ariad, on the other hand, has argued that there's nothing unusual about the patent, and that it's similar to many Lilly itself has filed.

Ariad's chances of winning, at first glance, appear small. "It's probably somewhat less than 20%," says Philip Nadeau, a biotech analyst at investment bank Cowen & Co., which counts Ariad among its clients. "These broad patents in general seem to be tough to defend when brought to court." But among the inventors on the NF-κB patent are David Baltimore, now president of the California Institute of Technology in Pasadena, fellow Nobel laureate Phillip Sharp of MIT, and well-known Harvard molecular biologist Thomas Maniatis. Their very presence on the patent, and possibly in court, could be decisive. "You've got very prominent scientists who are the inventors," notes Rochelle Seide, a patent attorney with Arent Fox in New York. "That sells very well before a jury." (These inventors have not commented publicly on the patent or lawsuit and declined to do so for this story.)

Multitalented

Ironically, NF-κB's debut 20 years ago attracted little attention. No one then, including Baltimore, suspected that NF-κB played a wide role in biology. He found the protein while studying how the immune system's B cells make antibodies and other immunoglobulins in response to foreign invaders. (Sharp contributed the key technology.) Baltimore named the protein "nuclear factor kappa B" because it bound to the "B" site of the kappa subunit of the immunoglobulin gene and was, he thought, confined to the nucleus.

That turned out not to be the case. NF-κB, except in B cells and a few others, is kept biologically inert in the cytoplasm by an inhibitor molecule, IκB, that must be degraded for NF-κB to be activated. Baltimore first described IκB in 1988. (Preventing IκB degradation is now a promising anti–NF-κB drug strategy.) Another piece of the puzzle fell into place in 1989, when Maniatis isolated a protein that bound to the gene for interferon, which is produced by cells under viral attack. The binding protein resembled NF-κB, Baltimore recalls. "Tom and I were talking about the induction of interferon, and the factor that he was describing sounded so much like the factor we had found. I said, 'Well, why don't we just look and see if it's the same thing?' " says Baltimore. It was. Because the interferon response is general, it was clear that NF-κB plays an important role throughout the body. Suddenly other researchers wanted to study NF-κB, and its many roles gradually emerged.

The NF-κB pathway, we now know, is amazingly multifunctional, activating or deactivating more than 175 genes in response to a wide range of substances, organisms, and conditions. "Evolution has utilized this system over and over again, in different circumstances," says Baltimore. From its location in the cell cytoplasm, NF-κB acts as a messenger, carrying outside signals to the nucleus and orchestrating the cell's response. NF-κB, by

CREDITS (TOP TO BOTTOM): DARRON CUMMINGS/AP; ELI LILLY (INSET)

stimulating the immune system, is central to inflammation, which in turn is an important contributor to atherosclerosis, arthritis, and cancer. By shutting off death pathways in cancer cells, NF-κB plays a key role in tumor progression. All that makes NF-κB a tempting but problematic drug target, because so many normal processes depend on it.

And given its many roles, it's not surprising that so many drugs affect NF-κB. Even before NF-κB was discovered, Lilly was developing raloxifene hydrochloride and activated protein C, the drugs later named Evista and Xigris. According to Lilly, the company made both "in the early '80s, … well before the discovery of NF-κB." Initially, it evaluated raloxifene because it works through the estrogen receptor to prevent bone loss, and protein C for its blood-thinning properties. Only much later, in a 1996 patent application and at a 2000 scientific meeting, respectively, did Lilly report that the drugs lowered NF-κB levels. But "we do not concede that Evista and Xigris work through an effect on NF-κB," the company writes.

The Food and Drug Administration approved Evista in 1997, and Xigris in 2001. When the NF-κB patent was issued in 2002, after a 16-year patent office review, Ariad sued. According to an Ariad press release, Lilly ignored Ariad's offer of a patent license. "Consequently, we were left with no option other than initiating this litigation," the release reads. Counters Lilly: "No license is needed. … The claims in [the] suit are invalid, not infringed, and unenforceable."

Courtroom confrontation now looms. Lilly would not comment on its defense strategy, but court records show that the company is challenging the validity of the patent on at least two grounds. Lilly argues that earlier drugs that lower NF-κB levels—antibiotics, for example—predate the patent and thus invalidate it, because one cannot patent an already-discovered method. Lilly also argues that the patent does not describe methods that "enable any person skilled in the art" to make an NF-κB inhibitor "without undue experimentation"—a key requirement of U.S. patent law.

This "enablement" clause that Lilly invokes has been used to defeat other broad patent claims. Three years ago, a New York judge denied the University of Rochester's patent claims over COX-2 inhibitors, a class of drugs that includes Pfizer's Celebrex (*Science*, 14 March 2003, p. 1638). The judge ruled the Rochester patent invalid because it did not show how to specifically inhibit COX-2. The same judge also concluded that the COX-2 patent did not meet the law's standard for "written description" of the invention, because the patent did not describe a COX-2 inhibitor.

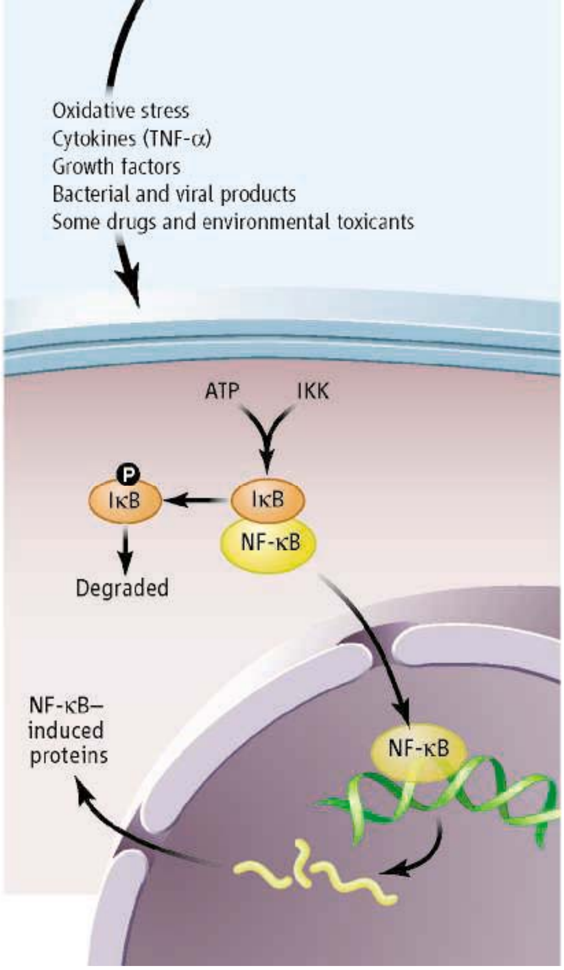

Center of contention. Many substances, organisms, and conditions activate NF-κB, which turns on protective proteins that promote inflammation and resist cell death. That makes it a tempting but problematic drug target; it is also the center of a patent fight.

ILLUSTRATION: K. SUTLIFF/SCIENCE

Barrier to entry?

Regardless of the lawsuit outcome, the very existence of an exclusively licensed patent on an important drug target raises questions of the greater public good. "NF-κB ought to be available to anybody who wants to make a drug against it, and the terms should not be unreasonable," says Roger Brent, president of the Molecular Sciences Institute, a nonprofit genomics research laboratory in Berkeley, California. Brent notes that a proliferation of broadly enforced upstream patents would constitute a "barrier to entry" for smaller companies contemplating new drug projects, because of legal and financial hurdles. Faced with many such patents to identify and license separately, "you cannot even begin," he says. "Do not bother to pick up the phone." Instead, Brent favors compulsory, nonexclusive licensing of drug-target patents, or eliminating them altogether.

Rai points out that publicly funded research should promote innovation, not put barriers in its way. "The only reason for having patents on publicly funded information is to promote technology development, not to impede it," she says. "If anything, this particular patent is impeding development." Seide, though, points to a new report by the National Academy of Sciences that concludes that "support to patented inventions … rarely imposes a significant burden for biomedical researchers." The academy report encompassed patents on the NF-κB pathway, among others.

Ariad, a research-based pharmaceutical company in Cambridge, Massachusetts, says licensing proceeds will be used to advance its cancer programs and that, as exclusive licensee, it must "create value" for the inventors and their institutions. "There's nothing unusual about this patent," Ariad CEO Harvey Berger told the *Boston Globe* in 2002. Berger, in a 2002 press release, said that "Lilly has filed hundreds of patent applications on treatment methods similar to our newly issued patent on NF-κB" and that "such patents are one of the cornerstones of pharmaceutical R&D and that they represent a recognized way of rewarding innovation." (Lilly disagrees, saying its patents are much more specific.)

Broad upstream patents like Ariad's are actually not unusual, says Chris Holman, a law professor at the University of Missouri, Kansas City. But enforcing them on marketed drugs is. "There are a lot of patents like this out there," he says. "[But] off the top of my head, I don't know of any case where one's successfully been asserted."

Ariad's lawsuit will directly affect the companies that Ariad contacted in 2002. Ariad has revealed only two that have so far agreed to terms. "If Ariad wins on this, there will probably be other lawsuits, or lots of settlements," says Seide. As *Science* went to press, U.S. District Judge Rya Zobel was considering two Lilly motions to invalidate the patent. If she rules against Lilly and the trial proceeds, Ariad seems prepared to see it through, despite the apparently long odds.

Meanwhile, several companies are working on drugs that directly target NF-κB. Among them are Millennium Pharmaceuticals and Nereus Pharmaceuticals, both of which declined to comment for this story. Baltimore says such drugs are well worth pursuing, but their success in any given disease can't be predicted. "Anybody who's developing a drug against NF-κB would have to be very conscious of side effects … because NF-κB is involved in the whole organism," Baltimore says. "It doesn't mean you can't develop drugs; it means that you've got to be very careful." If Ariad defeats Lilly in court, that warning will take on new meaning.

–KEN GARBER

Ken Garber is a science writer in Ann Arbor, Michigan.

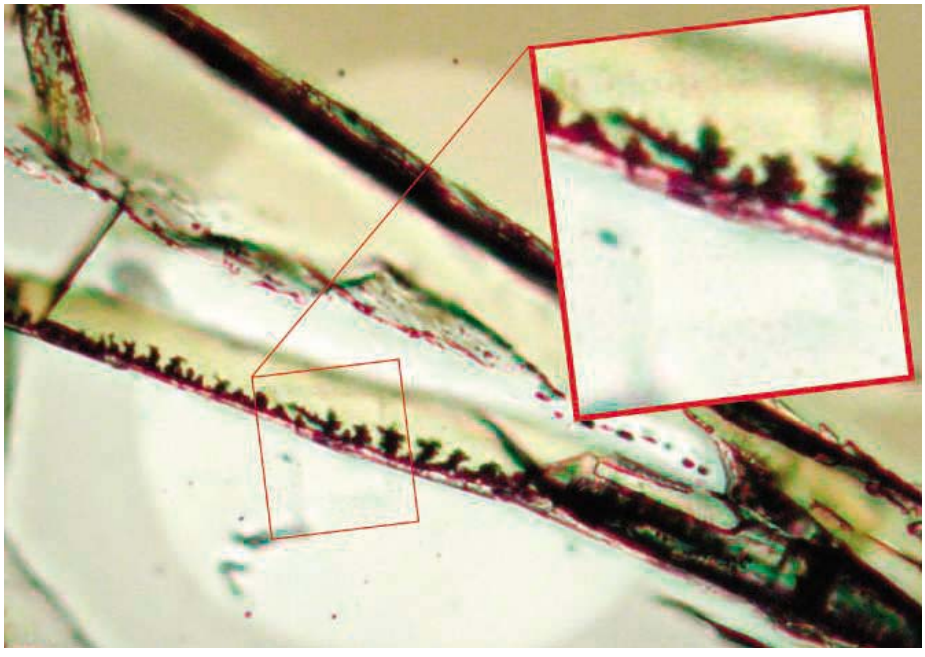

Nibblings? Martian microbes may have bored these 5-micrometer-long tunnels in olivine.

New Signs of Ancient Life in Another Martian Meteorite?

They're back. Ten years ago, astrobiologist David McKay of the Johnson Space Center (JSC) in Houston, Texas, and colleagues found potentially life-generated minerals, organic matter, and even wormy-looking relics in martian meteorite ALH84001. Now the mini-Martians have returned with a twist. At the meeting, much the same group presented new evidence of organic remains of life in another martian meteorite. And they're not alone. This week, another group published entirely independent, inorganic evidence of microbial life in the same meteorite. The combination intrigues but hardly convinces an astrobiological community still smarting from its first encounter with a martian meteorite.

McKay's 1996 *Science* paper (16 August 1996, p. 924) on ALH84001, written with several of the same colleagues as the new report, launched the modern field of astrobiology nearly single-handedly. In the end, their numerous critics picked apart their half-dozen lines of evidence. Intriguing minerals could have formed without the help of living organisms, they found, and the wormy shapes were purely mineralogical creations, not microfossils. But one bit of evidence—the presence of complex, high-molecular-weight organic matter somewhere in martian meteorites—stood up to criticism better than the rest.

McKay and colleagues now believe they can see exactly where complex organic matter is stuffed into microscopic veins and pockets in a second martian meteorite, called Nakhla. Bringing a half-dozen microanalytical techniques to bear on a transparently thin sliver of Nakhla, they find vein-filling organic matter with a carbon isotopic composition that others have also found in large bits of Nakhla. The McKay group is convinced their organic matter is not just the vein-filling epoxy used to hold such "thin section" samples together and that the organic matter entered the rock on Mars, not Earth. It may have come from an organic-rich meteorite that hit Mars, they say. Or groundwater on Mars may have carried the organic matter from organisms into rock that became the meteorite.

Even more eye-catching than what the JSC researchers think they found is where they think they found it. The putative organics are in veins whose walls are peppered by tiny tubules extending into the adjacent mineral, olivine. These tubules bear a striking resemblance to ones found in the basaltic glass of modern ocean crustal rock (*Science*, 23 April 2004, p. 503). Several groups have found organic matter and even DNA in these terrestrial tubules. They have argued that microbes acid-etched the tunnels in the hunt for nutrients. Similar tubules show up in ocean crustal rocks that are billions of years old.

Now, petrologist Martin Fisk of Oregon State University in Corvallis and his colleagues report in the April issue of *Astrobiology* that

Snapshots From the Meeting >>

Dust gets in your eyes. Deep Impact scientists have figured out why they couldn't see the crater formed last July when they smashed a nearly half-ton "bullet" into comet Tempel 1. Team members compared the plumes of debris blown off Tempel 1 with ejecta from laboratory impact experiments, and they simulated debris trajectories under a comet's feeble gravity. Both approaches indicate that the dirty snowball at the heart of Tempel 1 is mostly empty space. Surface materials especially have all the heft of fluffy snow or photocopier toner. A low-angle collision into such porous material sends a cloud of fine dust straight up, blocking the view from above.

Not to worry. Planetary scientist Joseph Veverka of Cornell University announced at the meeting that he and colleagues will soon be proposing to NASA that they fly a "Stardust Next" mission. They would send the now-hibernating Stardust spacecraft—which just returned comet material to Earth (*Science*, 17 March, p. 1536)—on to Tempel 1 on Valentine's Day 2011. Then it could take a look at the comet's fresh and by-then-unobscured crater.

Martian ring of fire. Most Mars rover scientists have concluded that the cryptic "Home Plate" that the Spirit rover spent 3 months reaching is the remains of a little ash-spewing volcano. The 90-meter-wide, 2-meter-high platform of layered ash has a distinctive chemical composition linking it to nearby lavas on the floor of Gusev impact crater and to rocks on the adjacent Columbia Hills, says team member Harry McSween of the University of Tennessee, Knoxville. He thinks volcanism driven from beneath Gusev blanketed any lake sediments mission planners expected to find on the floor of Gusev.

Hobbled by a broken right-front drive wheel, Spirit is now on a "drive or die" mission to a nearby hillside. It must tilt its dust-laden solar panels toward the sinking sun to boost power production and survive the coming winter, or hibernation. **–R.A.K.**

CREDIT: D. MCKAY *ET AL.*, LUNAR AND PLANETARY SCIENCE XXXVII (2006)

they have found the same boreholelike tubules in the mineral olivine in terrestrial basalts and in Nakhla. Fisk's Nakhla tubules are indistinguishable from McKay's organic-rich Nakhla tubules.

Could the organic matter be the remains of tubule-boring microbes? "I think they have something interesting, [but] I'm not convinced," says astrobiologist Andrew Steele of the Carnegie Institution of Washington's Geophysical Laboratory in Washington, D.C. McKay "has so many contaminants he has to eliminate. We do know Nakhla is contaminated with a lot of organics." They include organic matter produced by abiotic means on Mars, organisms that invaded Nakhla after it fell to Earth in Egypt in 1911 killing a dog, and organic agents used in the preparation of thin sections. Steele would take another tack: "In Nakhla, I assume it's contamination. Prove me wrong."

Tumbling Icy Moons

In all their excitement over a watery geyser on Saturn's little satellite Enceladus, the media overlooked a geophysical oddity. What's the geysering doing at the south pole, of all places? At the meeting, two planetary scientists suggested an answer: An imbalance in Enceladus's innards may have rolled the moon over to bring the geysering down there. If so, they may have found a solution to a 25-year mystery on Uranus as well.

Rollerball. Internal churnings may have repeatedly tumbled the uranian moon Miranda.

Contrary to intuition, spinning planetary bodies need not spin like a perfect top forever. Move some weight around, and they can go topsy-turvy. Pile too much ice on one pole, for example, and the ice mass will drag the former pole down to the equator, the stable position for the excess mass to rotate. Robert Pappalardo of the University of Colorado, Boulder, and Francis Nimmo of the University of California, Santa Cruz, wondered if something like that might have happened to Enceladus, but in the opposite sense. What if a warmer, less-dense, and therefore buoyant plume rose through an icy interior? In principle, that would roll the moon until the lower-density plume was at a pole, where it could deliver its heat to a geyser. In detailed calculations, a plume did just that, at least under favorable conditions. Those included a particularly buoyant plume rising through a thick, icy mantle overlying a liquid ocean.

If a rolling moon could explain a curiosity at Enceladus, it may resolve a deep mystery at Uranus. The planet's moon Miranda is dominated by not one but three huge "coronae" imprinted on the surface. Apparently, three rising plumes shoved the surface upward at those spots and spewed icy lavas. But one corona sits at the south pole, whereas the other two face off at east-west antipodes on the equator. Pappalardo and Nimmo suggest that three rising plumes in sequence could have repeatedly rolled Miranda around, thinning the ice at the south pole.

Tumbling moons "is an interesting hypothesis," says planetary physicist William McKinnon of Washington University in St. Louis, Missouri. "It's possible, but I'm waiting for more information" on the interior of Enceladus. That could be coming after June 2008, when the Cassini spacecraft orbiting Saturn may extend its mission and fly by Enceladus. A close pass would refine the picture of the saturnian moon's gravity field and therefore its internal structure.

–RICHARD A. KERR

Roughed Up and Far From Home

Japan's Hayabusa spacecraft is in a sad state. Battered and drained of its life's blood, it lies 190 million kilometers from Earth, and no one knows whether it carries a precious sample of asteroid Itokawa intended for return home. But the asteroid looks to have a sadder tale to tell. Hayabusa team members reported at the meeting that half-kilometer Itokawa shows every sign of having been smashed into a zillion bits and pieces over the eons and reassembled into a bloated, misshapen version of its former self. That now appears to be the likely fate of all small asteroids.

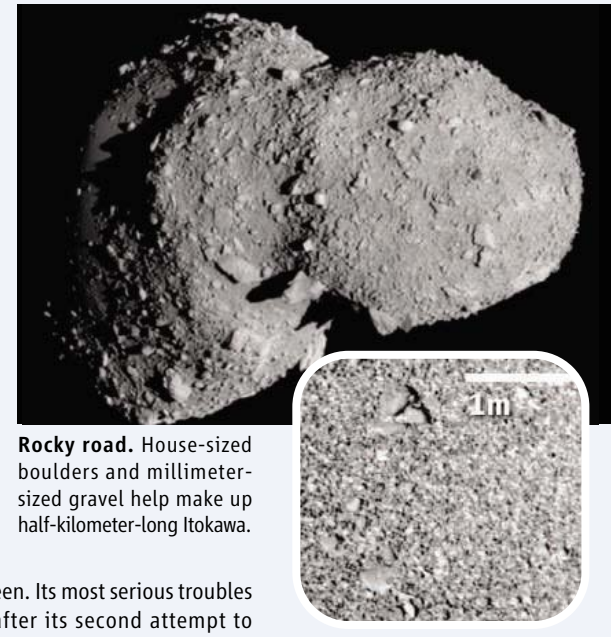

Rocky road. House-sized boulders and millimeter-sized gravel help make up half-kilometer-long Itokawa.

Mission chief scientist Akira Fujiwara of the Japan Aerospace Exploration Agency (JAXA) ticked off the signs that Itokawa is nothing more than a pile of rubble: boulders protruding tens of meters everywhere; an overall low density, implying a porous interior; rounded ends; and broad facets that hint at 100-meter boulders beneath. In its most recent reassembly, a small, roundish "head" evidently merged gently with an oblong "body." Team members have dubbed the result "the sea otter."

Whether Hayabusa can pull itself together as well and return to Earth remains to be seen. Its most serious troubles began last November right after its second attempt to touch down on Itokawa and pick up a rock sample (*Science*, 2 December 2005, p. 1409). Once it sprang a leak and began gushing the chemical fuel for its attitude-control thrusters, things went downhill rapidly. Hayabusa lost its proper orientation, breaking off communications and losing solar power. It short-circuited its batteries and sank into a deep freeze. Engineers have managed to recover some control, project manager Jun'ichiro Kawaguchi of JAXA reported. They jury-rigged an attitude-control system by commandeering the xenon-gas jets of the ion-drive main engine to counter any unwanted spinning. Hayabusa still has enough main-engine fuel onboard for both attitude control and propulsion on the homeward voyage, Kawaguchi said.

If deep-frozen components still work, Hayabusa may be able to leave the vicinity of Itokawa in spring of 2007, Kawaguchi said, and return to Earth in June 2010, 3 years behind schedule. Whether it will bring any of Itokawa with it is unknown. No one is sure whether contact with the surface ever triggered the sample-collection system. The craft did make contact on its first try, however, so hope remains for some sort of sample. "It would be extraordinary" if wounded Hayabusa made it back with a sample, says asteroid specialist Clark Chapman of the Southwest Research Institute in Boulder, Colorado, "but I'm not betting against them."

–R.A.K.

CREDITS: NASA/JPL (BOTH)

Semiconductor Advance May Help Reclaim Energy From 'Lost' Heat

Harnessing even a fraction of the waste heat given off by engines, boilers, and other high-temperature machines could save billions of dollars a year in energy costs. Researchers are counting on thermoelectrics—semiconductor devices that turn heat into electricity—to perform that trick. First, however, these devices must do their job much more efficiently.

Two years ago, a group led by Mercouri Kanatzidis, a chemist at Michigan State University (MSU) in East Lansing, took a huge stride in that direction by unveiling a thermoelectric semiconductor with higher energy-conversion properties than any such bulk material ever invented. It was a so-called n-type material that conducts electrons. But to make real-world devices, researchers need to marry an n-type material with a p-type partner that conducts positive charges called holes. At the Baltimore, Maryland, meeting, Kanatzidis reported that his team had found just the thing—two of them, in fact.

"It's a really important piece of work," says Terry Tritt, a physicist and bulk thermoelectrics expert at Clemson University in South Carolina. Having both the n-type and p-type materials opens the door to making energy conversion devices about 50% more efficient than those on the market today. Kanatzidis has already licensed the technology to a company called Tellurex that hopes to recover waste heat from diesel truck exhausts. But because turning thermoelectrics into high-efficiency devices can require complex engineering, it's still too early to say whether they will make it to market, Tritt says.

Materials that convert heat to electricity and vice versa have been known for nearly 200 years. They work because when a semiconductor spans two different temperatures, it will move heat—and typically electrical charges—from the warm side to the cold side. Researchers harness that movement of charges to create a tiny voltage difference between electrical contacts on opposite sides. To get enough current for practical purposes, however, they must wire many such devices in a series. A simple approach is to alternate devices incorporating n-type and p-type materials so that they form a continuous path for electrons to flow along.

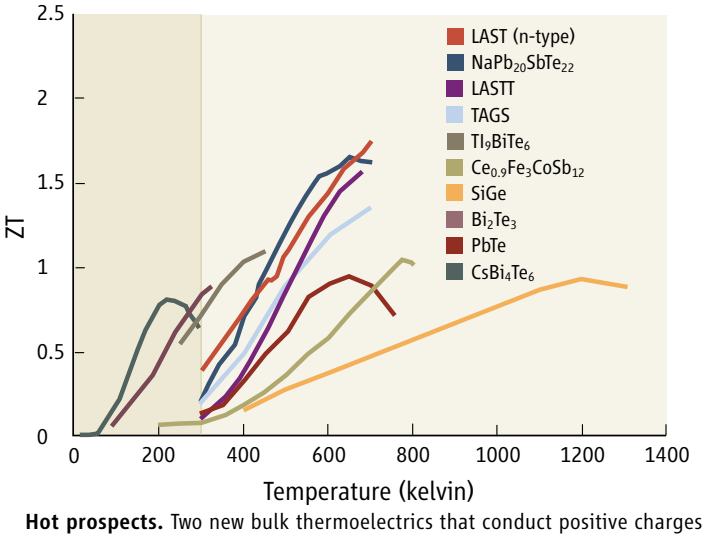

Hot prospects. Two new bulk thermoelectrics that conduct positive charges (dark blue and purple lines) rate among the best developed so far.

Researchers compare thermoelectrics by measuring a property known as ZT. Today's best thermoelectrics, thin films just a few dozen atomic layers thick, have a ZT of 2.5 to 3. But such devices are costly to make and too slender to maintain the large temperature differences needed for large-scale applications, Tritt says. As a result, researchers are trying to chemically synthesize bulk quantities of thermoelectrics with high ZTs.

Kanatzidis made his record-setting n-type semiconductor from lead, antimony, silver, and tellurium; it was abbreviated LAST. That material excels thanks to a series of tiny nano-sized inclusions that form during synthesis. The inclusions, Kanatzidis explains, scatter heat-carrying phonons—vibrations of the crystal lattice—as they try to pass through the material. The result is that electrons careen swiftly through while stifled phonons maintain the heat differential between the two sides of the material.

To create a p-type material, Kanatzidis and MSU colleague Timothy Hogan and S. D. Mahanti synthesized dozens of different compounds, systematically altering the composition of silver and antimony to change the number of electrons in the mix. Doing so provided a matrix with electrical vacancies that make it p-type. And in two cases—one in which they spiked LAST with tin, and another made from silver, antimony, lead, and tellurium, which they dubbed SALT—the researchers produced thermoelectrics with ZTs of about 1.6, the highest ever for bulk p-type materials.

Kanatzidis says he and his colleagues are now trying to incorporate their n-type and p-type materials into working devices. If they and other researchers can pull it off, thermoelectrics could soon usher in a whole new scheme for increasing energy efficiency.

–ROBERT F. SERVICE

In a Jumble of Grains, A Good Hard Shake Restores Order

Whether they're chess pieces on a board or nuts in a jar, things usually move and mix when shaken. But vibrations can cause flowing beads to "freeze" into an orderly pattern like atoms in a crystal, a pair of physicists reports. The surprising observation could lead to deeper insights into disorderly solids such as glasses, in which the atoms or molecules are locked or "jammed" into a random state because they lack the energy to reach a more orderly one.

In keeping with the second law of thermodynamics, pumping energy into something usually raises its temperature and jumbles its insides. For example, heating a crystalline solid such as ice scrambles the regular pattern of atoms or molecules within it, eventually causing it to melt into a disorganized liquid. So "if you think of shaking as raising the temperature, then [the result] creates a cognitive paradox," says Jerry Gollub of Haverford College and the University of Pennsylvania.

But granular materials—in which grains, marbles, or other macroscopic objects play the role of the atoms or molecules—often defy common sense. For example, shaking beads in a can doesn't always mix them. If the beads vary in size and density, the shaking may drive the larger ones to the top (the so-called Brazil-nut effect) or the bottom (the reverse Brazil-nut effect) depending on the details of the shaking and the precise sizes and masses of the beads. Lacking a

SOURCE: M. KANATZIDIS/MICHIGAN STATE UNIVERSITY

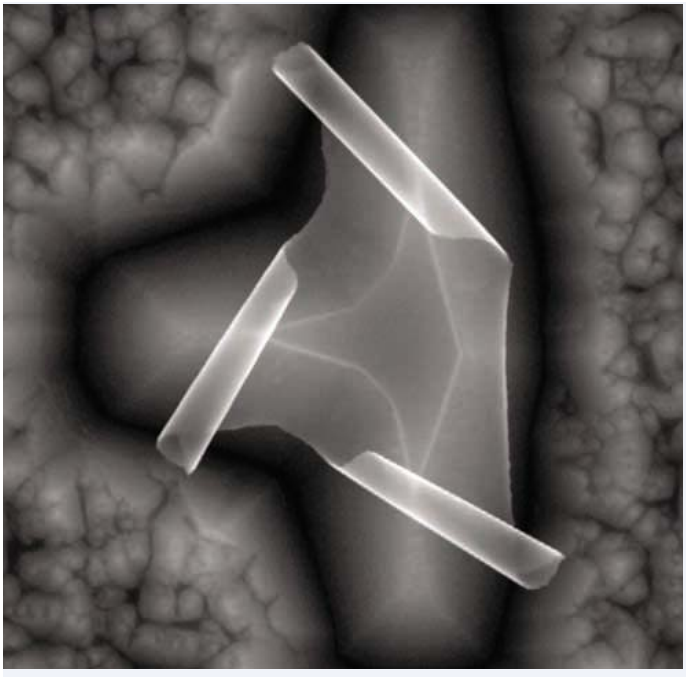

Tubular. Rolled-up films could marry nanotechnology and traditional microchip technology.

New Trick With Silicon Film Could Herald a Bright Future for Rolled-Up Nanotubes

Rolling a carpet may not seem high-tech, but doing it on a nanoscale with a single material is quite a feat. Researchers reported at the meeting that they have coaxed a layer of silicon—the material of choice for microchips—to roll up into nanotubes, and that similar tubes can guide and generate light. The advances might lead to devices that can be built into ordinary electronic microchips.

Widespread applications may be years away, but the ease and control with which the structures can be made gives them great promise, says Max Lagally, a materials physicist at the University of Wisconsin, Madison. "The whole idea that you do this with ordinary electronics and put [the structures] where you want them is potentially paradigm-shifting," Lagally says.

To make rolled-up nanotubes, researchers use lithography—the etching of materials that's key to making microchips—to lift the films off a surface, dissolving the underlying substrate. At the same time, they exploit the penchant of films to bow and curl when stresses build up inside them. Researchers typically start by depositing one semiconductor on top of another, such as silicon on top of germanium, in layers as thin as a single plane of atoms. In such a film, the silicon atoms are stretched a bit farther apart than normal, and the germanium atoms are slightly squeezed together. So if the underlying substrate is etched away, the silicon atoms pull together, and the germanium atoms push apart, causing the film to curl.

If done correctly, the films coil into tight rolls as narrow as a few nanometers, says physicist Victor Prinz of the Siberian Branch of the Russian Academy of Sciences in Novosibirsk, who pioneered the technique in the late 1990s. "Nobody around us thought that it would be possible to make such a thing," Prinz says. "Our experiments disproved all these theoretical predictions." In recent years, Prinz and colleagues have curled films into elaborate structures, including spiraling "nanodrills" and needles small enough to puncture a single cell.

Now, physicists Oliver Schmidt and Rudeesun Songmuang of the Max Planck Institute for Solid State Research in Stuttgart, Germany, and colleagues have taken the budding technology a step further. First, the researchers found a way to roll up a film of a single material. The key, Schmidt said at the meeting, is to grow the film thick enough that the atoms are stretched together or pulled apart on the bottom, but spaced normally on the top. "That's really surprising," Lagally says. "I don't really understand how it works, and he didn't really explain it." Still, he says, the advance opens the way to all-silicon nanotubes on silicon chips.

Schmidt also reported that nanotubes of silicon and silicon oxide can emit light when zapped with a laser. That advance is also exciting, Lagally says, because it could lead to tiny silicon lasers and all-silicon optoelectronic circuits that manipulate both electricity and light.

Those goals may be a way off, but Lagally and others say they see no fundamental problems to be overcome. Wound-up films, it seems, are nanotech on a roll.

–A.C.

CREDITS (TOP TO BOTTOM): O. SCHMIDT/MAX PLANCK INSTITUTE; K. DANIELS/NORTH CAROLINA STATE UNIVERSITY

comprehensive theory of granular materials, physicists and engineers continue to puzzle over such phenomena, which can affect materials as diverse as sand, gravel, foods, and powdered medicines.

When Karen Daniels of North Carolina State University in Raleigh and Robert Behringer of Duke University in nearby Durham observed that shaking can freeze flowing spherical beads into an orderly pattern, the finding took them by surprise. The researchers filled a can 50 centimeters wide and 10 centimeters deep with plastic beads measuring 2.5 millimeters in diameter. The bottom of the can was spring-loaded to gently squeeze the beads, and the top of the can rotated, causing the beads near the top to flow randomly over those below. At the same time, the researchers shook the can up and down and used a high-speed camera to film the motion of the beads.

They had hoped to study the details of the flow of the beads over one another, Daniels says. But when the shaking was sufficiently vigorous, the flow stopped and the beads locked into a regular three-dimensional array like the atoms in a crystal. "My initial reaction was frustration," Daniels says. "The thing kept freezing on me."

Sidney Nagel of the University of Chicago in Illinois says that the extra energy of the shaking may let the jumbled grains seek out an orderly state from which they'd otherwise be cut off. Because the disorderly atoms in glass are similarly cut off from reaching a more organized arrangement, the surprisingly orderly grains could lead to insights into the puzzling physics of glass. "What's nice is the control you can have over some of these experiments" with granular materials, Nagel says.

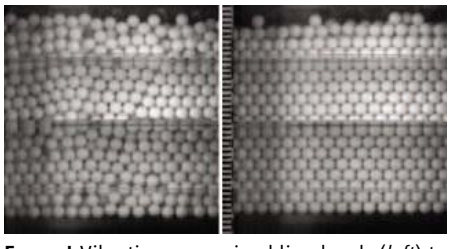

Freeze! Vibrations cause jumbling beads (*left*) to lock into crystallike order.

As for the paradox that shaking causes the beads to freeze into place, the resolution may come in finding the right definition of the effective temperature of the beads, Daniels says. The actual temperature describes only how hot each grain is and reveals nothing about the organization and motion of the grains. With the right definition, Daniels says, it might turn out that shaking actually causes the effective temperature of the beads to decrease.

–ADRIAN CHO

EDITED BY KELLI WHITLOCK BURTON

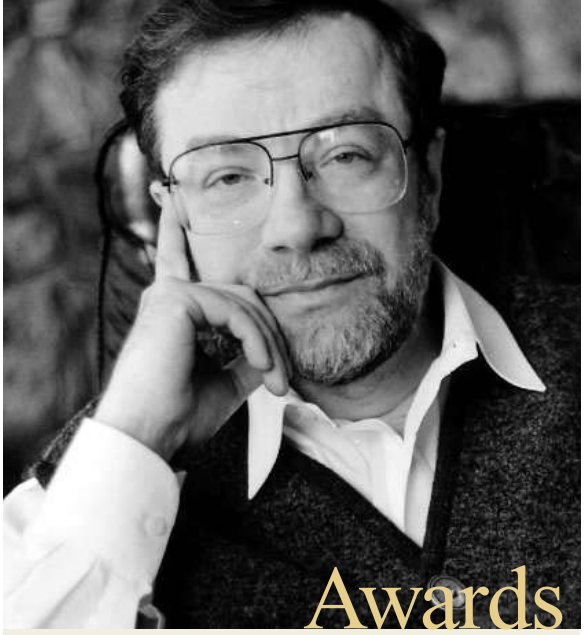

Awards

PROTEIN PRIZE. Biologist Alexander Varshavsky of the California Institute of Technology in Pasadena has been awarded the March of Dimes Prize in Developmental Biology for his research on the protein ubiquitin. Varshavsky, 59, is widely credited for first explaining how ubiquitin works in living cells, and some felt he should have been among the laureates when the discoverers of ubiquitin received the 2004 Nobel Prize in chemistry. "Alex's pioneering work catapulted the ubiquitin field into one of the hottest in modern biology," says biochemist Stefan Jentsch of the Max Planck Institute for Biochemistry in Martinsried, Germany. But he and others say Varshavsky's work is more appropriate for a physiology or medicine award, and they have called for a second ubiquitin-related Nobel.

The March of Dimes awards its $250,000 prize each year for research that expands scientists' understanding of birth defects.

FIRST FOR FRANCE. Geneticist Antoine Kremer is the first French scientist to win the Marcus Wallenberg Prize for forestry research. He will receive $250,000 from Sweden's Wallenberg Foundation for a genetic inventory of European oak trees in 2600 forests from Spain to the Urals.

Kremer led a network of 30 labs in 15 countries tracing European oak migration since the last ice age 17,000 years ago. The data will improve tree conservation and forest management. "The trees' diversity enabled them to adapt to the changing climate and should continue to do so as global warming progresses," says Kremer, 54, who is research director at L'Institut National de la Recherche Agronomique in Bordeaux.

Kremer will receive the award in Stockholm in September. The Wallenberg Foundation was created in 1980 to recognize advances in forestry research.

CREDITS (TOP TO BOTTOM): CALIFORNIA INSTITUTE OF TECHNOLOGY; LLNL; ASK.COM; LADISLAV PAULE/INRA

MOVERS

NUCLEAR OPTIONS. Weapons designer George Miller sees his new post as interim director of the Department of Energy's (DOE's) Lawrence Livermore National Laboratory as a "special responsibility" to protect and study the nation's nuclear arsenal. A Livermore employee for more than 2 decades, Miller, 61, replaces Michael Anastasio, who is leaving to run Los Alamos National Laboratory in New Mexico.

Livermore, a $1.6 billion facility east of San Francisco currently managed by the University of California (UC), is one of three main government nuclear weapons laboratories. Insiders say hiring a weapons designer such as Miller suggests the focus at Livermore will remain development and studies of the nuclear stockpile, despite the lab's recent forays into biodefense and computing.

Miller says he wants the lab to compete aggressively for a DOE-funded initiative to design new nuclear weapons. He's also "working vigorously" to address recent findings by a DOE investigation into two contained leaks of radioactive material.

Miller will serve as interim director until September 2007, when Livermore's contract expires. UC hasn't decided whether it will try to retain the contract, or whether Miller would play a role.

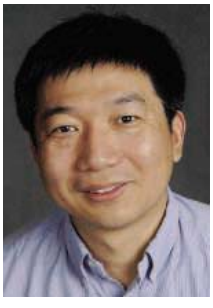

ANSWER MAN. As the recently appointed chief scientist for Ask.com, Tao Yang has a lot of questions on his mind. The company he works for, the Web search engine formerly known as Ask Jeeves, receives more than 130,000 queries per month.

In addition to day-to-day troubleshooting, Yang will oversee development of technology to improve the speed and accuracy of responses to submitted questions. The work "is extremely challenging because it touches on all aspects of computer science," he says.

Yang joined Ask.com 5 years ago after he and his colleagues invented the ExpertRank search algorithm, which identifies "expert" Web pages on a certain topic and uses their links as a way to rank other sites, as opposed to other engines that treat all links equally. The algorithm has powered Ask.com since 2001, says Yang, who is also a computer science professor at the University of California, Santa Barbara. With billions of Web pages to sift through, Yang says his goal is to "order the information so people can digest it."

ON CAMPUS

RECORD GIFT. Columbia University plans to use a $200 million gift from a longtime benefactor to build a neuroscience research center at its new Manhattanville campus in West Harlem. The largest donation in Columbia's history comes from the Jerome L. Greene Foundation and was announced last week by the New York lawyer's widow, Dawn Greene.

The center, to be named after Greene, will be headed by neurobiologist Thomas Jessell and Nobel laureates Richard Axel and Eric Kandel and will be the hub of Columbia's new Mind, Brain, and Behavior initiative launched in 2004. "Mixing physics, chemistry, and engineering with a core of neuroscience is the way to go," Jessell says.

Construction of the new 37,000-square-meter center will begin "as soon as possible," Jessell says.

San Francisco, CA 2006 MRS Spring Meeting April 17 - April 21

2006 MRS SPRING MEETING

www.mrs.org/meetings/spring2006/

MEETING CHAIRS

J. Charles Barbour
Sandia National Laboratories
jcbarbo@sandia.gov

Paul S. Drzaic
Alien Technology Corporation
pdrzaic@alientechnology.com

Gregg S. Higashi
Applied Materials
gregg_s_higashi@amat.com

Viola Vogel
Swiss Federal Institute of Technology, ETH
viola.vogel@mat.ethz.ch

For additional meeting information, visit the MRS Web site at

www.mrs.org/meetings/

or contact:

MRS

Member Services
Materials Research Society

506 Keystone Drive
Warrendale, PA 15086-7573
Tel 724-779-3003
Fax 724-779-8313
E-mail: info@mrs.org
www.mrs.org

SYMPOSIA

MICROELECTRONIC DEVICE PROCESSING AND FABRICATION

- A: Amorphous and Polycrystalline Thin-Film Silicon Science and Technology
- B: Silicon Carbide—Materials, Processing, and Devices
- C: Sub-Second Rapid Thermal Processing for Device Fabrication
- D: Transistor Scaling—Methods, Materials, and Modeling
- E: Gate Stack Scaling—Materials Selection, Role of Interfaces, and Reliability Implications
- F: Materials, Technology, and Reliability of Low-*k* Dielectrics and Copper Interconnects
- G: Science and Technology of Nonvolatile Memories
- H: Chalcogenide-Based Phase-Change Materials for Reconfigurable Electronics

PHOTONICS, ELECTRONICS, MAGNETICS, AND SENSORS

- I: Silicon-Based Microphotonics
- J: Negative Index Materials—From Microwave to Optical
- K: Materials Research for THz Applications
- L: Materials for Next-Generation Display Systems
- M: Conjugated Organic Materials—Synthesis, Structure, Device, and Applications
- N: Molecular-Scale Electronics
- O: Hybrid Organic/Inorganic/Metallic Electronic and Optical Devices
- P: Semiconductor Nanowires—Fabrication, Physical Properties, and Applications
- Q: Magnetic Thin Films, Heterostructures, and Device Materials
- R: Nanostructured Materials and Hybrid Composites for Gas Sensors and Biomedical Applications
- S: Smart Nanotextiles

COMPLEX AND BIOLOGICAL NANOSCALE MATERIALS AND SYSTEMS

- T: Nanomanufacturing
- U: Organic and Inorganic Nanotubes—From Molecular to Submicron Structures
- V: Structure and Dynamics of Charged Macromolecules at Solid-Liquid Interfaces
- W: Colloidal Materials—Synthesis, Structure, and Applications
- Y: Nanostructured Probes for Molecular Bio-Imaging
- Z: Mechanics of Nanoscale Materials and Devices
- AA: Molecular Motors, Nanomachines, and Engineered Bio-Hybrid Systems
- BB: Mechanotransduction and Engineered Cell-Surface Interactions
- CC: Electrobiological Interfaces on Soft Substrates

ENERGY AND ENVIRONMENT

- DD: Solid-State Lighting Materials and Devices
- EE: Hydrogen Storage Materials
- FF: Materials and Basic Research Needs for Solar Energy Conversion
- GG: Current and Future Trends of Functional Oxide Films
- HH: Recent Advances in Superconductivity
- II: Materials in Extreme Environments
- JJ: Materials Science of Water Purification

FORUM

- KK: Education in Nanoscience and Engineering

GENERAL

- X: Frontiers of Materials Research

MEETING HIGHLIGHTS

SYMPOSIUM TUTORIAL PROGRAM

Available only to meeting registrants, the symposium tutorials will concentrate on new, rapidly breaking areas of research and are designed to encourage the exchange of information by meeting attendees during the symposium.

EXHIBIT

A major exhibit encompassing the full spectrum of equipment, instrumentation, products, software, publications, and services is scheduled for April 18-20 in Moscone West, convenient to the technical session rooms.

SYMPOSIUM ASSISTANT OPPORTUNITIES

Graduate students who are interested in assisting in the symposium rooms during the 2006 MRS Spring Meeting are encouraged to apply for a Symposium Assistant position. By assisting in a minimum of four half-day sessions, students will receive a complimentary student registration, a one-year MRS student membership commencing July 1, 2006, and a stipend to help defray expenses. Applications will be available on our Web site by November 1.

CAREER CENTER

A Career Center for MRS members and meeting attendees will be offered in Moscone West during the 2006 MRS Spring Meeting.

PUBLICATIONS DESK

A full display of over 885 books will be available at the MRS Publications Desk. Symposium Proceedings from both the 2005 MRS Spring and Fall Meetings will be featured.

GRADUATE STUDENT AWARDS

The Materials Research Society announces the availability of Gold and Silver Awards for graduate students conducting research on a topic to be addressed in the 2006 MRS Spring Meeting symposia. Applications will be available on our Web site by October 1 and must be received at MRS headquarters by January 6, 2006.

LETTERS

edited by Etta Kavanagh

Invasive Plants

THE PERSPECTIVE "INTERRELATED CAUSES OF PLANT INVASION" BY D. BLUMENTHAL (14 Oct. 2005, p. 243) presents a framework for uniting hypotheses used to explain the invasive success of exotic plants. The escape-from-natural-enemies (pathogens and herbivores) and the "resource" hypotheses were united into the resource–enemy release hypothesis (R-ERH). The R-ERH proposes that plants adapted to high-resource environments are more successful invaders than species adapted to low-resource environments because they benefit more from escaping their natural enemies than plants in low-resource environments.

There are some problems with Blumenthal's R-ERH. First, the role of escape from natural enemies in invasions remains unclear (*1*), and R-ERH does not distinguish between specialist and generalist enemies, which is central to the escape-from-natural-enemies hypothesis (*2*). Blumenthal assumes that "poorly defended, nutritious, high-resource species tend to be preferred by herbivores" and that "high-resource plant species are more strongly affected by enemies than are low-resource species." R-ERH predicts that exotic plants with high nutritional content and poor defenses are most likely to benefit from escaping their natural enemies; however, generalist herbivores in exotic ranges are likely to prey on these displaced exotic plants and resist their invasion (*3*, *4*). In addition, chance colonization events may produce situations where plant colonizers are not impacted by resident enemies (e.g., generalist herbivorous enemies are too naïve to prey upon a new potential food source). Furthermore, many of the most invasive exotic plants are not found in resource-rich systems and/or are not palatable to herbivores (e.g., arid grassland invaders) and therefore do not support the assumptions of R-ERH.

Biological control of exotic plants relies on host-specific enemies from the exotic plants' native ranges to selectively control the pest plants in their exotic ranges while not affecting local plants (*5*). It is incorrect to advise that "biological control may be most effective against high-resource invaders." For a "poorly defended, nutritious, high resource" exotic plant, enemies from its native range are not likely to be selective enough to make good biological controls and may add insult to injury by preying on local plants that are already being negatively affected by the exotic plant.

KURT O. REINHART

Department of Biology, Indiana University, Bloomington, IN 47405–3700, USA.

References

1. R. I. Colautti, A. Ricciardi, A. Grigorovich, H. J. Maclsaac, *Ecol. Lett.* **7**, 721 (2004).
2. R. M. Keane, M. J. Crawley, *Trends Ecol. Evol.* **17**, 164 (2002).
3. J. D. Parker, M. E. Hay, *Ecol. Lett.* **8**, 959 (2005).
4. A. A. Agrawal, P. M. Kotanen, *Ecol. Lett.* **6**, 712 (2003).
5. D. Simberloff, P. Stiling, *Ecology* **77**, 1965 (1996).

Response

AS SUGGESTED BY REINHART, THE DISTINCTION BETWEEN specialist and generalist plant enemies is important to the predictions of the resource–enemy release hypothesis (R-ERH). The R-ERH applies most clearly to specialist enemies, not only because release is more likely from specialist enemies (*1*) but also because high-resource species are predicted to be less well defended against specialists than generalists (*2, 3*). However, to the degree that generalist enemies prefer high- to low-resource plant species (*3, 4*), both release and biotic resistance (regulation of exotic plant populations by native enemies) from generalist enemies may be related to resource availability. If naïve generalists avoid exotic plant species (*5*, *6*), then the high-resource exotic species most consumed by generalists in their native range may be most released. Conversely, if generalists preferentially consume exotic plant species (*7*), this biotic resistance could also be strongest for high-resource exotic species, the opposite of the pattern suggested by the R-ERH.

Reinhart also notes that unproductive ecosystems can be highly invaded, which appears to contradict the R-ERH prediction that high resource availability may favor exotic species over native species. Within such ecosystems, however, exotic species often occupy disturbed and relatively resource-rich sites (*8*). Moreover, both observational and experimental studies suggest that exotic species tend to outcompete native species primarily in resource-rich environments (*9*, *10*).

Finally, although prudent biological control certainly requires the use of enemies with high host specificity, such enemies can often be found on high-resource plant species. In fact, numerous specialist enemies have been released against fast-growing, high-resource species (*11*). Furthermore, if high-resource species are poorly defended, particularly against specialists, as predicted (*2*), they may also be particularly susceptible to biological control.

DANA BLUMENTHAL

USDA-ARS Rangeland Resources, Crops Research Laboratory, Fort Collins, CO 80526, USA.

References

1. R. M. Keane, M. J. Crawley, *Trends Ecol. Evol.* **17**, 164 (2002).
2. P. D. Coley, J. P. Bryant, F. S. Chapin, *Science* **230**, 895 (1985).
3. D. M. Blumenthal, *Ecol. Lett.*, in press.
4. L. H. Fraser, J. P. Grime, *J. Ecol.* **87**, 514 (1999).
5. H. V. Cornell, B. A. Hawkins, *Am. Nat.* **141**, 847 (1993).
6. R. A. Lankau, W. E. Rogers, E. Siemann, *Ecol. Entomol.* **29**, 66 (2004).
7. J. D. Parker, M. E. Hay, *Ecol. Lett.* **8**, 959 (2005).
8. T. J. Stohlgren, K. A. Bull, Y. Otsuki, C. A. Villa, M. Lee, *Plant Ecol.* **138**, 113 (1998).
9. M. J. Crawley, in *Colonization, Succession and Stability*, M. J. Crawley, P. J. Edwards, A. J. Gray, Eds. (Blackwell Scientific, Oxford, UK, 1987), chap. 21.
10. C. C. Daehler, *Annu. Rev. Ecol. Syst.* **34**, 183 (2003).
11. M. H. Julian, M. W. Griffiths, Eds., *Biological Control of Weeds: A World Catalogue of Agents and Their Target Weeds* (CABI Publishing, New York, ed. 4, 1998).

Save the Lab in Montemar, Chile

THE UNIVERSITY OF CHILE IN SANTIAGO HAS decided to sell the laboratory in Montemar to build apartments for tourists. We believe that the Montemar laboratory should be preserved as a landmark to commemorate an important period in the history of Chilean biological science.

In the early 1960s, a group of Chilean scientists led by Mario Luxoro opened the biophysics laboratory in Montemar, on the Pacific coast near Valparaíso, to study the giant axons of the squid species *Dosidicus gigas*. In the early 1970s, they extended their research to the *Megabalanus psittacus*, a large barnacle whose giant muscle fibers provide an excellent model for studying muscle electrophysiology. The several dozen researchers who lived and worked for months at a time in the Montemar laboratory performed breakthrough science there for three decades.

When the laboratory was set up, there was limited funding to support science in Chile. Indeed, the laboratory is indistinguishable from the humble houses of the local fishermen. Researchers built much of the equipment with their own hands and had to contend with indifference and a lack of critical scientific mass in Chile. Despite the obstacles, the investigators at Montemar consistently published excellent work [such as (*1*, *2*)]. Although the Pinochet dictatorial regime resulted in a massive emigration of Chilean scientists, Montemar remained active until the end of the 1980s. Today, José Soto, the former squid fisherman for the lab, maintains the building and gives passionate tours of the house to visitors.

Chile should display Montemar with great pride. The laboratory could be a museum displaying the seminal research that was conducted under the most unfavorable conditions and a venue for courses and seminars. Please, don't condemn this valuable piece of Chilean history to demolition.

RICARDO BORGES,[1]* O. HUMBERTO VIVEROS,[1] RAMÓN LATORRE[2]

[1]Unidad de Farmacología, Facultad de Medicina, Universidad de La Laguna, 38071 La Laguna, Spain. [2]Centro de Estudios Científicos, Valdivia, Chile.

*To whom correspondence should be addressed. E-mail: rborges@ull.es

References

1. E. Rojas, M. Luxoro, *Nature* **199**, 78 (1963).
2. C. Armstrong, F. Bezanilla, E. Rojas, *J. Gen. Physiol.* **62**, 374 (1973).

Letters to the Editor

Letters (~300 words) discuss material published in *Science* in the previous 6 months or issues of general interest. They can be submitted through the Web (www.submit2science.org) or by regular mail (1200 New York Ave., NW, Washington, DC 20005, USA). Letters are not acknowledged upon receipt, nor are authors generally consulted before publication. Whether published in full or in part, letters are subject to editing for clarity and space.

Scrapie and the Origin of the Chinese "Itchy"

I READ THE LETTER "SCRAPIE IN ANCIENT CHINA?" by R. B. Wickner (5 Aug. 2005, p. 874) with interest. Wickner proposes that scrapie, the transmissible spongiform encephalopathy found in sheep, was known in ancient China, and as evidence he offers that the Chinese character "itchy" (痒) is composed of "disease" (疒) and "sheep" (羊).

However, according to the *Kangxi Dictionary* (*1*), which includes 47,035 Chinese characters and provides the meaning of each character in detail, the oldest recorded meaning of 痒 is not "itchy" or "pruritis," but "disease" (with 疒 indicating the meaning and 羊 acting as a phonetic cue). In comparison, "itchy" or "pruritis" was represented by 癢. Because both 癢 and 痒 are pronounced "yang," the former character was usually

simplified as the latter. Therefore, the composition of 痒 does not mean that scrapie was known in ancient China. Of course, this analysis does not exclude the possibility that ancient Chinese observed scrapie.

HONG-YU ZHANG

Shandong Provincial Research Center for Bioinformatic Engineering and Technique, Center for Advanced Study, Shandong University of Technology, Zibo 255049, China. E-mail: zhanghy@sdut.edu.cn

Reference

1. T.-J. Chen, Ed., *Kangxi Dictionary* (World Press, Shanghai, China, 1936).

Disease but No Sheep

IN HIS LETTER "SCRAPIE IN ANCIENT CHINA?" (5 Aug. 2005, p. 874), R. B. Wickner analyzes the orthographic features of several Chinese characters and concludes that scrapie, the transmissible spongiform encephalopathy found in sheep, may have existed more than 2000 years ago. Unfortunately, Wickner's analyses ignore the fact that Chinese characters evolve, not only in form, but also in meaning. The same character may refer to totally different things across time and geographical location. Such is the case for Wickner's crucial evidence, the character 痒 for "itchy," which he interprets as consisting of components for "disease" and "sheep" and as having the meaning "pruritis." According to the ancient dictionary compiled by the Later Han scholar Xu Shen (who lived roughly between 54 and 149 A.D.), the original meaning of the character 痒 was "head injury" or "disease" (*1*). Xu wrote that 羊, the sheep component of the character, simply indicated the method of pronunciation and was unrelated to the meaning of the word sheep.

Wickner's analyses of other characters are similarly flawed. For example, 包, the character for "packet," was originally used to mean "pregnancy" (*2*) and 養, the character for nutrition, was originally used to mean "support" (the sheep component again refers to the sound of the character). In fact, this character, 養, and not 羊 for "sheep" (as Wickner proposed), was part of the character 癢 for "itchy" just 50 years ago, before the traditional forms of Chinese characters were simplified in mainland China as 痒 (the traditional form 癢 is still widely used in Hong Kong, Malaysia, and Taiwan). The same holds true for 痴, whose traditional form was 癡, which combined the sound component 疑 "doubt" (rather than 知 as in Wickner's letter) with the meaning component 疒 that indicates disease. Finally, the character 瘙 does not exist in Chinese; the true character for "itchy" is 瘙, which uses 叉 ("fingernails" or "toenails") and not 又 ("hand").

All of these examples contain the so-called phonograms that emerged during the Han Dynasty (206 B.C. to 220 A.D.)—characters that have a component indicating the sound and one indicating the meaning. Such phonograms make up nearly 90% of all Chinese characters used today (*3*). Wickner mistakenly interprets these phonograms as ideograms (characters that are picture-like and symbolize objects and ideas), which were popular before the Han Dynasty but are uncommon today (*4*).

PING LI[1]* AND HONGBING XING[2]

[1]Cognitive Science Laboratory, Department of Psychology, University of Richmond, Richmond, VA 23173, USA. [2]Center for the Study of Chinese as a Second Language, Department of Language Information Processing, Beijing Language and Culture University, Beijing 100083, China.

*To whom correspondence should be addressed. E-mail: pli@richmond.edu

References

1. S. Xu, *Shuo Wen Jie Zi* (121 A.D.) (reprinted by Commercial Press, Beijing, 1979).
2. Z. Xu, Ed., *Hanyu Da Zidian* [A Comprehensive Dictionary of Chinese Characters] (Sichuan Dictionary Press, Chongqing, China, 1993).
3. D. Honorof, L. Feldman, in *Handbook of East Asian Psycholinguistics*, P. Li, E. Bates, L.-H. Tan, O. Tzeng, Eds. (Cambridge Univ. Press, Cambridge, UK, 2006), vol. 1, pp. 195–208.
4. W. S.-Y. Wang, *Sci. Am.* **228**, 50 (1973).

PALEONTOLOGY

Crime Scene Investigation—Permian

Andrew M. Bush

Mass extinctions sometimes seem to have their own third law. For every proposed explanation there is an equal and opposite explanation: global warming versus global cooling, sea level rise versus sea level fall, or explosive ejection of material from the depths of the earth versus explosive impact of material from the depths of space. As Douglas Erwin puts it in *Extinction: How Life on Earth Nearly Ended 250 Million Years Ago*, "Geologists are endlessly creative so there is no lack of [causal] suggestions, some of which are even plausible. Not wanting to feel left out of the mother of mass extinctions, physicists, evolutionary biologists, and complexity theorists have all offered their solutions to the mystery. And it is a mystery." Thankfully, theories and mysteries can be dispelled with good data from the geologic record, and Erwin (a paleobiologist at the Smithsonian Institution's National Museum of Natural History) offers an authoritative account of the search for these data and for the cause of the extinction.

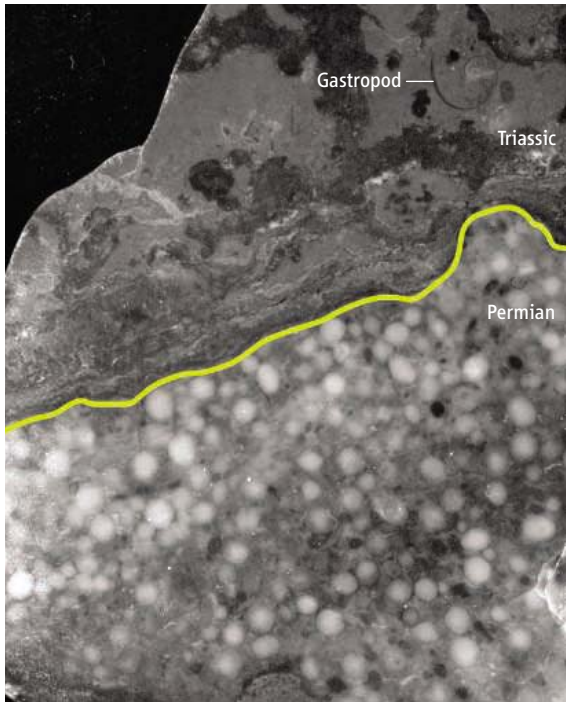

Boundary in a slab. Fusulinid foraminifera (2 mm in size) thrived in the Permian but disappeared at the Triassic boundary. After the extinction, microbial growths covered the sea floor, and a lone gastropod represents the survivor fauna that later rose to dominance. (The sample is from Guizhou Province, China.)

The analogy of the end-Permian extinction as a murder mystery is irresistible—251 million years ago, about 90% of all the species in the world's oceans perished in the deadliest mass extinction of all time, and terrestrial ecosystems suffered heavily as well. Since Erwin's earlier book on the topic (*1*), and thanks in no small part to his own efforts, our view of the Permian extinction has been transformed by advances in geochronology, analytical paleontology, geochemistry, computer modeling, and good old-fashioned field work. What was initially perceived as a slow, protracted loss of diversity is now viewed as a (geologically) sudden crisis lasting less than a couple hundred thousand years, perhaps even less than tens of thousands of years. Erwin evaluates such currently discussed extinction triggers as an extraterrestrial impact, climate change associated with the eruption of the great Siberian flood basalts, anoxia, and hypercapnia (carbon dioxide poisoning).

Erwin hesitates to put his stamp of approval on any of these theories. Early in the book he comments, "None of the extinction models fits all the evidence and some hypotheses require data that despite every effort have not been found." In the end, he pencils a tentative check mark next to the Siberian flood basalts, citing their temporal coincidence with the extinction and the lack of convincing support for alternative scenarios. At the same time, Erwin notes that we are far from understanding how the eruptions might have caused the extinction. Although some readers might hope for a tidier conclusion, they shouldn't overlook the strengths of the book: Erwin's honest appraisal that the data do not yet unambiguously support one hypothesis or another, and his clear, droll depiction of modern paleontology at its finest. The search for the trigger of the end-Permian extinction has succeeded (up to the point that it has been an impressive effort, integrating cutting-edge techniques from across the earth sciences and data from across the globe.

The end-Cretaceous extinction, which coincides with definitive evidence for an extraterrestrial impact (*2*), has been the gold standard against which all other mass extinctions are measured. Given the absence of similar definitive evidence for the Permian extinction's cause, some of the more interesting passages in the book are those in which Erwin contemplates the nature of inference in historical science. For example, he remarks

> Our difficulties in understanding this event may lie more within how we tend to define a satisfactory answer than in the event itself. In the wake of the apparent success of the Alvarez-impact hypothesis [for the Cretaceous extinction] many of us seem to prefer a single dramatic cause as an explanation for such events. Our knowledge of recorded history provides precious little support for such a view, and I see little reason, a priori to expect such a neat and tidy resolution to this riddle.

In addition, Erwin points out, there was a lot going on near the end of the Permian, and it isn't always clear which events were causes and which were effects. When a causal relationship is suspected, as between the Siberian volcanism and the mass extinction, the relevant mechanistic links often remain poorly understood. Such difficulties are not unique to the Permian extinction—they are part of historical research. Sometimes we get lucky and find the smoking gun, but sometimes we do not. The author's account presses home how a concerted, multidisciplinary effort is every bit as important in unraveling the intertwined histories of Earth and its inhabitants.

Although the cause of the Permian extinction remains shrouded and controversial, its effects were clear and devastating. In its aftermath, "in that virtually complete desolation," microbial mounds thrived on the sea floor as they had not since the early days of animal evolution and a few small, weedy species proliferated. The extinction swept away forever the Paleozoic ecosystems that had flourished for hundreds of millions of years and with them such groups as trilobites and fusulinid foraminifera (see the figure). The depauperate ecosystems that remained would become the forebears of the modern world. Erwin compellingly argues that the dynamics of the Triassic recovery interval deserve further study. What exactly controlled ecology and evolution in such an alien world?

Extinction
How Life on Earth Nearly Ended 250 Million Years Ago
by Douglas H. Erwin
Princeton University Press, Princeton, NJ, 2006. 306 pp. $24.95, £15.95. ISBN 0-691-00524-9.

The reviewer is at the Department of Ecology and Evolutionary Biology, University of Connecticut, 75 North Eagleville Road, Unit 3043, Storrs, CT 06269–3043, USA. E-mail: andrew.bush@uconn.edu

CREDIT: D. J. LEHRMANN AND J. L. PAYNE

Research on the Permian extinction continues. Given the progress of the past ten years, who knows what the next decade will bring? For now, *Extinction* provides a great reference for researchers and the interested lay reader alike.

References

1. D. H. Erwin, *The Great Paleozoic Crisis: Life and Death in the Permian* (Columbia Univ. Press, New York, 1993).
2. W. Alvarez, *T. Rex and the Crater of Doom* (Princeton Univ. Press, Princeton, NJ, 1997).

10.1126/science.1125756

CELL BIOLOGY

Energizing Eukaryotes

David G. Nicholls

Despite (or perhaps because of) a title that might have come from a Monty Python sketch, *Power, Sex, Suicide* is an enjoyable and readable book. Research on mitochondria has flourished during the past ten years because of the organelle's apparently ubiquitous involvement in the life and death of the cell, and Nick Lane has achieved the difficult goal of taking selected aspects of a complex field and making them intelligible—if not to the general reader, at least to the life scientist with a basic understanding of metabolic reactions and genetics. To do so, he employs some felicitous turns of phrase (for example, in likening the contrast between DNA and RNA to that between library books and disposable photocopies made from them).

Power, Sex, Suicide
Mitochondria and the Meaning of Life

by Nick Lane

Oxford University Press, Oxford, 2005. 368 pp. $30, £18.99. ISBN 0-19-280481-2.

Lane [a science writer whose previous book *Oxygen* (*1*) was well received and whose doctoral research involved free radicals and mitochondrial function in organ transplants] is clearly fascinated with the origin of the eukaryotic cell. He devotes considerable attention to (frequently controversial) theories for that origin as well as to the beginnings of life itself and to the ways in which mitochondria have subsequently evolved within the cell. He supports the "hydrogen hypothesis" of William Martin and Miklós Müller (2), who proposed that the original symbiosis occurred not between an invading bacterium and a nonrespiring eukaryote but rather between a primitive purple bacterium that emitted hydrogen and carbon dioxide and a methanogen that could use these end products to generate energy. Lane goes on to discuss the subsequent transfer of genes from mitochondrion to nucleus along with the idea that the residual mitochondrial-encoded proteins serve as scaffolding for the assembly of the respiratory chain complexes from nuclear genes.

The author is less convincing when he turns to the origin of life (at least he is not afraid to deal with big topics). Citing the work of Mike Russell and Alan Hall (*3*), Lane states that in order to generate a primitive cell from an iron sulphide vesicle "all that the cells need to do to generate ATP is to plug an [proton translocating] ATPase through the membrane." Any bioenergeticist who has followed the elucidation of the extraordinary structure and mechanism of the mitochondrial ATP synthase over the past decade will pause at the word "all," because the ATP synthase—with its spinning rotor massaging the surrounding subunits to generate ATP—is without doubt the most amazingly complex molecular structure in the cell.

Nonetheless, Lane does a good job of describing the historical development of mitochondriology from Charles MacMunn's pigments in the 19th century through David Keilin's cytochromes to Peter Mitchell's chemiosmotic coupling. He avoids the heresy that many undergraduate textbooks still fall into (the claim that ATP has a "high-energy bond") and instead emphasizes the displacement of the ATPase reaction from equilibrium. His discussion of the Mitchellian revolution of the 1960s and 1970s is accurate but rather brief, which is surprising in view of the fierce intellectual battles that were fought over the acceptance of the basic concepts.

Some of the chapters (for example, those on power-law scaling in biology and on endotherms) are not particularly well integrated with the rest of the book, and their connections to mitochondria seem a little forced. On the other hand, the actively developing field of apoptosis is well described with such flamboyant phrases as "mitochondria, angels of death" and "caspases [cysteine proteases that are key mediators of programmed cell death] … hang poised over the cell like the sword of Damocles." Eager readers drawn by the "sex" in the title will at least be rewarded with an engaging review of maternal inheritance of mitochondrial genes and the mitochondrial bottleneck of the oocyte.

The book's final section provides a good introduction to mitochondrial aging, mutations, and disease. I cannot, however, support basic principles of mitochondria theories of aging together with the roles of free radicals. But, in a major omission, he fails to provide any detailed discussion of mitochondria and disease other than specifically mitochondrial mutations. Although diabetes, stroke, heart attack, Huntington's disease, and Parkinson's disease all have mitochondrial components that are being actively researched, they are scarcely mentioned.

In summary, *Power, Sex, Suicide* focuses strongly on theories relating to evolutionary aspects of the mitochondrion. Lane is evidently more interested in why than how. This is a legitimate approach, but one result is that his account skips over much of the detail of how mitochondria actually work (the topic is covered in a little over 20 pages). The how could perhaps be the subject of an equally fascinating book. Inevitably, in view of the breadth of his coverage, the author has been selective in the sources that he quotes. Mitochondriologists may find some of his preferred hypotheses too controversial (or, at best, still unproven). But they, and anyone interested in the broader and more philosophical aspects of their discipline, will profit from reading the book.

The more the merrier. Lane argues that more mitochondria means more power and greater metabolic efficiency.

CREDIT: INA SCHUPPE-KOISTINEN

The reviewer is at the Buck Institute for Age Research, 8001 Redwood Boulevard, Novato, CA 94945, USA. E-mail: dnicholls@buckinstitute.org

References

1. N. Lane, *Oxygen: The Molecule That Made the World* (Oxford Univ. Press, Oxford, 2002).
2. W. Martin, M. Müller, *Nature* **392**, 37 (1998).
3. M. J. Russell, A. J. Hall, *J. Geol. Soc. London* **154**, 377 (1997).

10.1126/science.1126251

DIVERSITY

Preparing Minority Scientists and Engineers

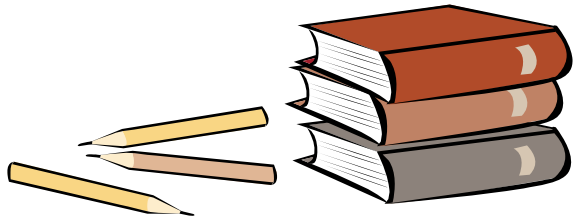

Michael F. Summers[1]* and Freeman A. Hrabowski III[2]

An undergraduate program involving mentorship, summer and other workshops, and targeting high-achieving high school students improves participation of underrepresented minorities in science.

As international participation in advanced science and engineering (S&E) increases, and as national populations become more diverse (*1*–*3*) it becomes even more important to provide quality science education to all children, including those from racially diverse groups (*2*, *3*). Despite several decades of federally supported programs, Americans from these groups continue to be underrepresented among Ph.D. recipients and in the S&E workforce (*4*–*6*).

Enhanced online at www.sciencemag.org/cgi/content/full/311/5768/1870

Contrary to popular belief (*7*), many well-prepared underrepresented minority students (URMs)—including men and women of Latino, Native-American, Pacific Island, and African-American descent—are interested in pursuing scientific or engineering careers. In 2005, the same percentage (44%) of African-American and Caucasian college-bound high school students indicated their intent to major in S&E fields (*8*). Many students with strong SAT scores, impressive grades, and success in high school honors math and science courses leave the college science pipeline, but the loss is disproportionately among women and minorities (*9*, *10*). Thus, factors other than school preparation, science aptitude, and interest must be responsible for the low achievement and low persistence in these subgroups of undergraduate and graduate S&E students. Identifying these negative factors and retaining well-educated students with S&E interests would improve the United States' ability to compete in today's global scientific community.

Factors that keep URMs from persisting with science include academic and cultural isolation, motivation and performance vulnerability in the face of low expectations, peers who are not supportive of academic success, and discrimination, whether perceived or actual (*10*–*15*). These factors can have a stronger effect at institutions with predominantly majority populations. Such institutions award about 75% of all bachelor's degrees earned by African Americans (*16*). To address these particular factors, we developed the Meyerhoff Scholars Program in 1989 at the University of Maryland, Baltimore County (UMBC). At that time, the university was graduating fewer than 18 African-American S&E majors per year (see graph below). Typically, fewer than five of these students graduated with a grade point average above 3.0 (on a 1 to 4 scale), consistent with achievement levels observed at other institutions (*17*, *18*).

The Meyerhoff Scholars Program (named after its founders, Baltimore philanthropists Robert and Jane Meyerhoff) focuses on producing bachelor's degree recipients, particularly African Americans, who go on to doctoral programs in science and engineering. Since 2000, an average of 1900 candidates have been nominated each year by high school teachers and counselors. Of those nominated, the 80% who are from Maryland (~1500) represent about 2% of graduating high school students in Maryland. We typically invite about 180 students and their parents to UMBC for interviews, and offer 4-year scholarships to about 100 of them. About half accept. Most students who decline the Meyerhoff program accept other scholarships at UMBC or other institutions. Transfer students, typically not more than two per year, can join the program later.

The program has supported 768 students, 260 of whom are currently undergraduates. Most of the Meyerhoff graduates (435 of 508 students, 86%) earned science or engineering bachelor's degrees (students in good academic standing who leave S&E fields before graduation become supported by other UMBC scholarship programs). Most of the S&E graduates (379 students, 87%) went on to graduate studies (60% to Ph.D. or M.D.-Ph.D., 22% to master's, 24% to medical or other professional programs, and 13% employed). Meyerhoff students with completed advanced degrees now number 44 with Ph.D.'s or M.D.-Ph.D.'s (most earned in the past 2 years), 72 with master's degrees, and 32 with medical degrees.

The effectiveness of the Meyerhoff program is highlighted by comparing students who entered the Meyerhoff program with those who were invited but declined and attended other institutions (*9*, *19*, *20*). Both groups earned similar grades and graduated at similar rates. But students who entered the Meyerhoff program were twice as likely to earn a science or engineering bachelor's degree (*9*) and 5.3 times more likely to enroll in post-college graduate study (*19*, *20*). In addition, Meyerhoff students were about twice as likely to earn S&E B.S. degrees as Asian, Caucasian, and non-Meyerhoff African-American students with similar preparation and interests (*9*).

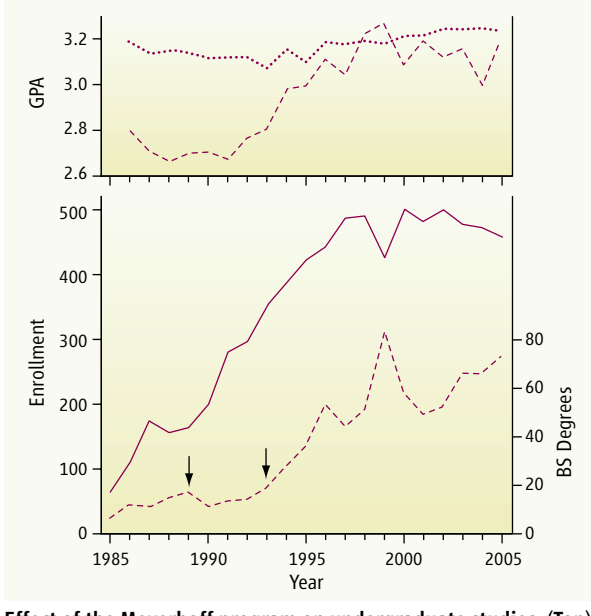

Effect of the Meyerhoff program on undergraduate studies. (Top) Average grades of Caucasian (dotted line) and African-American (dashed line) students at graduation in S&E fields (biology, biochemistry, chemistry, computer science, engineering, mathematics, and physics). **(Bottom)** African-American enrollment (solid line) and graduations (dashed line) at UMBC for S&E undergraduates. The Meyerhoff undergraduate program was initiated in 1989 and began [illegible] students in 1993 (arrows).

[1]Howard Hughes Medical Institute (HHMI) and Department of Chemistry and Biochemistry, [2]Office of the President, University of Maryland, Baltimore County, 1000 Hilltop Circle, Baltimore, MD 21250, USA.

*To whom correspondence should be addressed. E-mail: summers@hhmi.umbc.edu

The Meyerhoff model has four overarching objectives: (a) academic and social integration, (b) knowledge and skill development, (c) support and motivation, and (d) monitoring and advising (*9*, *19*, *20*). Our ongoing evaluation of outcomes leads us to identify five elements as most important for achieving these objectives: (i) recruiting a substantial pool of high-achieving minority students with interests in math and science who are most likely to be retained in the scientific pipeline, (ii) offering merit-based financial support, (iii) providing an orientation program for incoming freshmen, (iv) recruiting the most active research faculty to work with the students (our philosophy is that it takes a scientist to train a scientist), and (v) involving the students in scientific research projects as early as possible, so that they can engage in the excitement of discovery. Encouraging high academic performance in the first 2 years is critical. Students are encouraged to retake courses in which they earn a C in order to strengthen foundation knowledge before advancing to other courses.

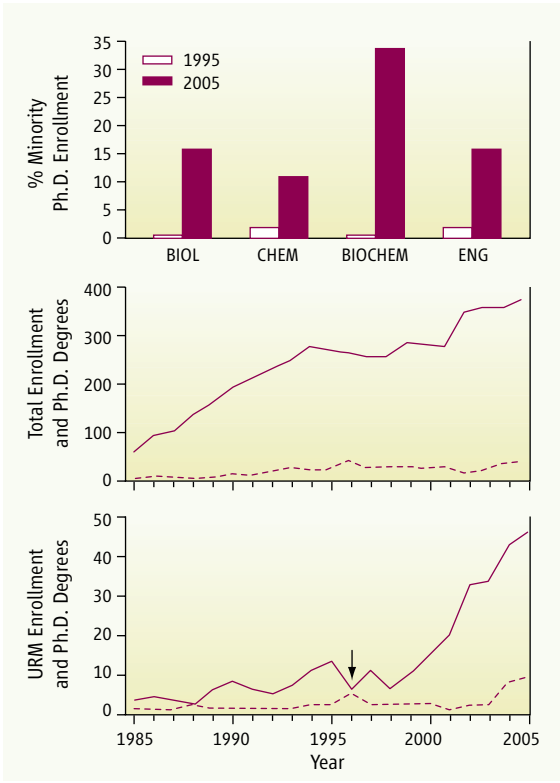

Effect of the Meyerhoff program on graduate studies. (**Top**) Effect of diversity efforts on minority S&E Ph.D. enrollment. (**Middle**) Total S&E Ph.D. enrollment (solid line) and degrees awarded (dashed line) at UMBC. (**Bottom**) Total African-American and Latino S&E Ph.D. enrollment (solid line) and degrees awarded (dashed line). The Meyerhoff graduate program was initiated in 1996 (arrow).

The program encourages students to pursue academic goals, earn top grades, and prepare for graduate school. Students participate in study groups and use university resources for tutoring and counseling. Students also mentor and tutor other students on campus as well as children in inner city schools. Group activities such as monthly focus groups to discuss class and research experiences, receptions with mentors and parents, competitive team building events, and group travel and participation at scientific conferences encourage a sense of community among the students, faculty, and staff.

As participation in the Meyerhoff program has grown, we have observed a simultaneous increase in S&E participation among UMBC minority students who are not in the Meyerhoff program. The number of African-American undergraduates majoring in science and engineering has increased more than sevenfold since 1985 (see graph, bottom panel, on page 1870) whereas overall African-American enrollment increased 1.4-fold. Overall and S&E enrollments among Latino students have also grown (three- and fivefold, respectively) since 1985. The number of Caucasian S&E majors also increased during this time period (from 710 to 1287 students, 1.8-fold) at a rate greater than that of total undergraduate enrollment (from 7914 to 9406 students, 1.2-fold). The average GPA of all African-American S&E graduates has increased from 2.70 in 1989 to 3.21 in 2005, due primarily to the high achievement of the Meyerhoff Scholars (average graduating GPA = 3.42 ± 0.12). The average GPA of Caucasian S&E graduates has remained relatively unchanged (3.17 ± 0.05) (see graph, top panel, on page 1870).

In the 1990s, participation of URMs in graduate studies at UMBC continued to reflect low national averages (Meyerhoff undergraduates are encouraged to pursue graduate studies elsewhere). To address this, we began the Meyerhoff Graduate Biomedical Fellows Program in 1996. The program includes (i) a prematriculation orientation program; (ii) group social activities, including annual weekend retreats and picnics (with white-water rafting and hiking); (iii) monthly student seminars; (iv) instruction on technical writing and grantsmanship; and (v) financial support for student travel and minority-scientist seminars. Efforts to encourage student applications focused on predominantly minority-serving campuses. Research opportunities for summer students and undergraduate research symposia were available. Applications from African-American and Latino students went from about 2 per year in 1998 to about 50 per year since 2002, and URM participation has increased by an average of 18% (see graphs above).

Sustaining this research, scientific support is every bit as important in producing the scientific workforce as is generating the interest and knowledge in the first place. Retention of both undergraduate and graduate students can focus on specific populations. Success depends on addressing both academic and community issues. At the undergraduate level, administrative efforts and resources are needed to attract high-achieving minority S&E students and prepare them for the rigors of college courses. Research faculty are usually eager to mentor minority students who are academically successful. At the graduate level, departmental leadership is critical, since this is where admissions, mentoring, and candidacy decisions are made.

References and Notes

1. National Academy of Sciences, *Rising Above the Gathering Storm: Energizing and Employing America for a Brighter Economic Future* (The National Academies Press, Washington, DC, 2005).
2. U.S. Census Bureau, "U.S. Census Bureau news: Texas becomes nation's newest 'majority-minority' state," August, 2005.
3. U.S. Census Bureau, "U.S. interim projections by age, sex, race, and Hispanic origin," March, 2004.
4. "Doctorate recipients from United States universities: Summary report 2003" [National Science Foundation, (NSF) Washington, DC, 2004].
5. "Women, minorities, and persons with disabilities in science and engineering: 2002" (NSF, Washington, DC, 2003).
6. For examples of existing federal S&E diversity programs see the National Institutes of Health (NIH) Web site (www.nigms.nih.gov/Minority), or search for "minority programs" on the NSF Web site (www.nsf.gov) or the Department of Energy Web site (www.doe.gov).
7. H. Schuman, C. Steeh, L. Bobo, M. Krysan, *Racial Attitudes in America: Trends and Interpretations* (Harvard Univ. Press, Cambridge, MA, 1997).
8. "2005 College-Bound Seniors: College Plans" (College Board, in preparation).
9. K. Maton *et al.*, *J. Res. Sci. Teach.* **37**, 7 (2000).
10. E. Seymour, N. Hewitt, *Talking About Leaving: Why Undergraduates Leave the Sciences* (Westview Press, Boulder, CO, 1997).
11. H. H. Garrison, in *Minorities: Their Underrepresentation and Career Differentials in Science and Engineering*, L. S. Dix, Ed. (National Academy Press, Washington, DC, 1987).
12. M. T. Nettles, Ed., *Toward Black Undergraduate Student Equality in American Higher Education* (Greenwood Press, New York, 1988).
13. W. R. Allen, *Harvard Ed. Rev.* **62**, 26 (1992).
14. C. M. Steele, J. Aronson, *J. Personality Soc. Psych.* **69**, 797 (1995).
15. P. Gandara, J. Maxwell-Jolly, "Priming the pump: A review of programs that aim to increase the achievement of underrepresented minority undergraduates" (College Board, New York, 1999).
16. American Council on Education, *Minorities in Higher Education 2003–2004: Twenty-First Annual Status Report* (American Council on Education, Washington, DC, 2005).
17. A. M. Garibaldi, *J. Negro Ed.* **66**, 105 (1997).
18. G. Mannan *et al.*, *J. Negro Ed.* **55**, 155 (1986).
19. F. A. Hrabowski III, K. Maton, *School Sci. Math.* **95**, 18 (1995).
20. K. Maton, F. A. Hrabowski III, *Am. Psych.* **59**, 547 (2004).

21. We thank the Meyerhoff Foundation, NSF, NIH, HHMI, and a variety of other agencies, companies, foundations, and individual donors for financial support.

10.1126/science.1125257

PLANT SCIENCE

β-Glucans—Brewer's Bane, Dietician's Delight

Identification of the enzyme that synthesizes a polysaccharide in plant cell walls will allow manipulation of grasses to enhance their utility as food, feed, and fuel.

Kenneth Keegstra and Jonathan Walton

According to *Brewers Digest* (*1*), a beer maker's biggest biochemical headache lies in the cell wall of barley grains. β-Glucan, otherwise known as (1,3;1,4)-β-glucan, is the notorious cell wall polymer. It is a major cell wall component in grains, including the barleys used in brewing. Its presence can not only negatively affect fermentation, but can also inhibit the filtration process, leaving beer with an unappealing haze. Thus, it is not surprising that plant breeders have sought to identify the genes that determine how much β-glucan is produced in barley. A region of genomic DNA that controls the production of this polysaccharide in barley grains has been mapped to chromosome 2 (*2*). To identify the genes and proteins responsible for β-glucan biosynthesis, Burton *et al.* (*3*) have taken advantage of this information and the conserved genome structure between barley and rice, whose genome has been completely sequenced. On page 1940 of this issue, they show that the corresponding locus in the rice genome contains six *CslF* genes, making them strong candidates for involvement in β-glucan biosynthesis.

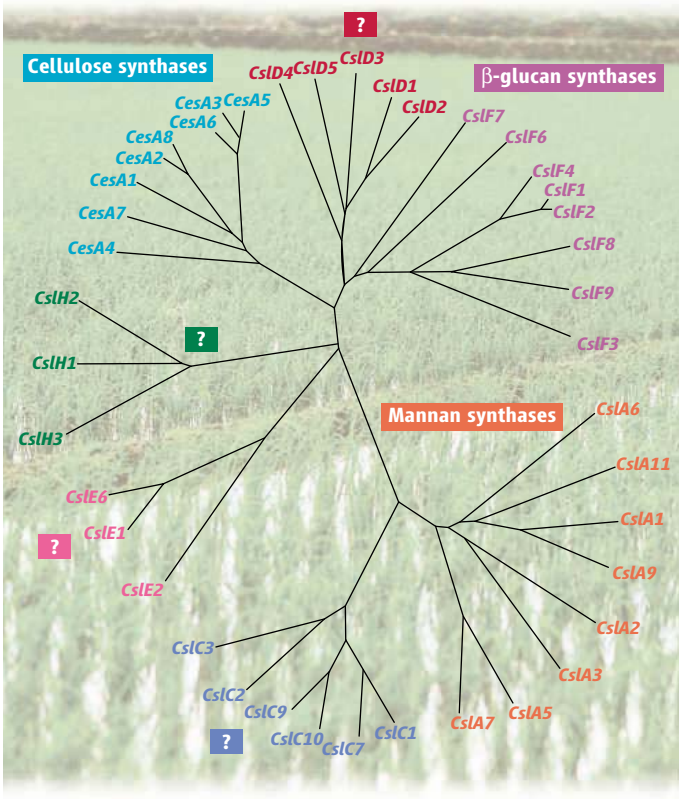

The cellulose synthase superfamily in rice. The *CesA* genes, *CslA* genes, and cereal-specific *CslF* genes encode enzymes (as indicated) that are required for the synthesis of cell wall constituents. Functions of other superfamily members are presently unknown. The alignment of deduced protein sequences was constructed with CLUSTAL W and the unrooted tree figure was drawn with TreeView (*11*). [Figure based on the completed genome sequence of rice (www.prl.msu.edu/walton/CSL_updates.htm)]

The *Csl* (cellulose synthase–like) genes were first identified in the model plant *Arabidopsis thaliana* (*4*) and rice (*5*) genomes. Sequence analyses indicate that the cellulose synthase superfamily contains multiple subfamilies (see the figure). Although some subfamilies of genes—*CesA*, *CslA*, *CslC*, and *CslD*—are found in all land plants examined to date, other subfamilies are found only in certain plants. For example, *CslF* and *CslH* are found only in grasses, including barley and rice; *CslB* and *CslG* are found in *Arabidopsis* but not in rice.

Abundant evidence indicates that the *CesA* genes, the archetypal members of this superfamily, encode proteins that synthesize cellulose, the major structural component in plant cell walls (*6*).

The authors are with the U.S. Department of Energy Plant Research Laboratory, Michigan State University, Plant Biology Building, East Lansing, MI 48824, USA. E-mail: keegstra@msu.edu; walton@msu.edu

Although the functions of most of the Csl proteins remain uncertain, it has been suggested that they may synthesize hemicellulosic polysaccharides (*4*). The walls of all plant cells contain both cellulose and hemicellulose, but unlike cellulose, the hemicelluloses are highly diverse in composition of the major sugar backbone and most of them have additional sugars attached as side chains. Different hemicellulosic polysaccharides are found in different plant species and even in different cell types within a plant. Land plants contain four major hemicellulosic polysaccharides: xyloglucans with a β-1,4-glucan backbone; arabinoxylans with a β-1,4-xylan backbone; galactomannans with a β-1,4-mannan backbone; and (1,3;1,4)-β-glucan, a polymer found only in grasses (a group that includes our most important food crops). The structures of hemicellulosic polysaccharides have been well studied and their biological roles and practical applications are becoming clearer, yet their biosynthesis has remained poorly characterized. The hypothesis that *Csl* genes might encode the elusive hemicellulose synthases is supported by two recent reports demonstrating that *CslA* genes encode mannan synthases, enzymes that synthesize the β-1,4-mannan backbone of galactomannans found in cell walls (*7*, *8*).

To determine whether *CslF* genes encode enzymes involved in β-glucan biosynthesis, Burton *et al.* expressed rice *CslF* genes in *Arabidopsis*, which lacks both β-glucan and the *CslF* genes thought to produce it. They detected β-glucan in the transgenic *Arabidopsis* plants, confirming that CslF proteins are involved in β-glucan biosynthesis.

Understanding β-glucan biosynthesis extends far beyond the brewer's world. As a major component of soluble fiber in the human diet, β-glucan has been implicated in reducing the risk of colorectal cancer and lowering serum cholesterol and glucose levels (*9*). Many grains consumed by humans, such as wheat, have relatively low amounts of β-glucan as compared with barley. Knowledge of the pathway of β-glucan biosynthesis could be used to enhance β-glucan content of wheat, either by traditional plant-breeding programs or by creating transgenic plants with enhanced expression of *CslF* genes.

In addition to its effects on health, understanding the biosynthesis of plant cell wall components has other important practical applications. Recently, considerable emphasis has been placed on converting cell wall components (lignocellulose) into sugars that can be fermented into ethanol for use as fuel (*10*). An important part of making this process economically feasible is to improve the quality and quantity of the plant materials that are used as feedstocks. Understanding the biosynthesis of wall components, including parameters that regulate when

and where various polysaccharides are deposited, will likely be important in creating improved raw materials for biofuels.

The major conclusion reached by Burton *et al.* is that CslF proteins are involved in β-glucan biosynthesis. However, as is often the case, this important advance raises many additional questions. For example, the amounts of β-glucan were low in the transgenic plants and the polysaccharide could be detected only in selected cells, even though expression was driven by a strong constitutive genetic promoter. Burton *et al.* speculate that β-glucan biosynthesis may also require "ancillary factors." If so, we need to find out what these factors are and determine their biochemical functions. Do CslF proteins synthesize both sugar linkages of β-glucan? Or does CslF make one linkage while an "ancillary factor" makes the other? The work of Burton *et al*. opens up many opportunities for studying β-glucan biosynthesis and adds CslF to the list of Csl proteins with known functions. Still, the roles of the many other cellulose-like synthase gene products remain a mystery. Indeed, why are there so many? More food for thought.

References

1. C. W. Bamforth, *Brewers Digest* **69**, 12 (1994).
2. F. Han *et al*., *Theor. Appl. Genet.* **91**, 921 (1995).
3. R. A Burton *et al*., *Science* **311**, 1940 (2006).
4. T. A. Richmond, C. R. Somerville, *Plant Physiol*. **124**, 495 (2000).
5. S. P. Hazen *et al*., *Plant Physiol.* **128**, 336 (2002).
6. C. Somerville *et al*., *Science* **306**, 2206 (2004).
7. K. S. Dhugga *et al*., *Science* **303**, 363 (2004).
8. A. H. Liepman *et al*., *Proc. Natl. Acad. Sci. U.S.A.* **102**, 2221 (2005).
9. C. S. Brennan, L. J. Cleary, *J. Cereal Sci.* **42**, 1 (2005).
10. A. J. Ragauskas *et al*., *Science* **311**, 484 (2006).
11. R. D. M. Page, *Comput. Appl. Biosci*. **12**, 357 (1996).

10.1126/science.1125938

GEOPHYSICS

Dangerous Tectonics, Fragile Buildings, and Tough Decisions

The occurrence of four fatal earthquakes within and around the Indian plate in the last 5 years, including two great ones, highlights the need for earthquake-resistant construction and replacement throughout the region.

Roger Bilham

When the going gets tough, it is merely a matter of time before rupture on a plate boundary gets going—again. Stresses from Indonesia's December 2004 moment magnitude (M_w) = 9.2 earthquake took 92 days to reach across the island of Simeulue before they propelled a second great earthquake, this time to the south. Deformation in this 28 March M_w = 8.7 Nias earthquake was captured in unprecedented detail, as reported on page 1897 of this issue by Briggs and his colleagues (*1*). At that time, the authors were documenting the effects of its December predecessor, which, at M_w = 9.2, was the largest earthquake in 40 years.

Had the March Nias quake with its rupture length of 400 km occurred simultaneously with that of the earlier 1600-km-long neighbor, the total energy release would have been equivalent to a M_w = 9.3 earthquake. But it didn't, and the reasons for its hesitation now pose interesting questions, the answers to which have important consequences for nations in the path of plate collisions in Southeast Asia. Each end of this new 2000-km-long rip along the northeast edge of the Indo-Australian plate now points suggestively at adjoining segments of the plate boundary that are themselves considered overdue for rupture (*2*, *3*). Why did the rupture stop where it did, and could the plate boundary conceivably rip further?

Simeulue, an island similar in size and shape to Long Island, New York, lies above a wrinkle in the plate boundary—ground zero to both the December and March earthquakes, and, apparently, a barrier tough enough to prevent through-going slip. Such barriers pin the ends of earthquake ruptures, yet no one is certain how they do it (*3*–*5*). Slip often nucleates from them and/or to them, and occasionally straight through them, as was the case in contiguous great Japanese earthquakes that sometimes rupture individually and at other times simultaneously (*6*). Dual behavior is vexing because it implies that barriers cannot always be relied on to arrest rupture, adding a chaotic element to forecasting the locations of likely future events. Barriers prevent small earthquakes from becoming big earthquakes at all scales, and many problems in seismology would benefit from a better understanding of their physics (*7*). Serendipitously, the Simeulue barrier afforded a veiled view of some of its secrets during the flurry of postseismic deformation studies that followed December's earthquake.

The time history of vertical deformation there is recorded in the growth and kill fields of a million tiny corals (*8*). In December the northern end of the island rose 1.4 m. Near-shore corals responded to the twisting and bending of their island, dying where exposed to the tropical sun, but establishing new thriving colonies safely below the lowest tides. On 28 March 1.6-m uplift of the southern end of the island again checked their growth, establishing yet lower, optimum growth levels from which Briggs and co-workers have pieced together an elegant four-dimensional time history of distortion of the island's shorelines. The complex deformation of Simeulue and its neighboring islands was confirmed by data from Global Positioning System receivers placed throughout the islands (and mainland) monitoring the aftermath of the December event.

The measurements indicated clearly why the March earthquake, [illegible] catastrophe, produced no substantial tsunami—energy release was one-fifth, rupture length one-quarter, and maximum uplift one-half that of the December earthquake, and most of the uplift occurred on land rather than beneath the sea.

But the measurements also captured Simeulue in the act of impeding, or seeding, rupture. The corals tell of a 20-cm uplift of the foundations to their watery homes in 2003 during a M_w = 7.3 earthquake. This modest ancestor to the two great earthquakes separated their slip areas but failed to trigger either event. Briggs and co-authors speculate that most probably the barrier corresponds to a scissors-like tear in the descending plate. Certainly, elucidation of its structure and rheological properties are now of great importance to understanding how it permitted earthquakes to nucleate to north and south, and may provide important clues applicable to earthquakes elsewhere.

These clues are more than of esoteric interest because numerous segments of Southeast Asia's plate boundaries are today sufficiently mature to slip in massive earthquakes. They include not only segments of the Sunda arc east of the March earthquake that are clearly ripe for failure (*2*, *3*), but also the region of the Indo-Burman ranges north of the December rupture, which has no recent history of significant slip, and where such slip must now be considered quite possible. They also include parts of the Himalaya and India's western plate boundary.

The Indian plate has been cornered by four killer quakes in the past 5 years: the M_w = 7.6 Bhuj (≈18,500 dead), the M_w = 9.2 Sumatra-Andaman rupture (≈300,000 dead), the 28 March earthquake (>700 dead) and most recently the M_w = 7.6 Kashmir earthquake (73,338 dead as of January 2006). This fatal

The author is in the Department of Geological Sciences, University of Colorado, Boulder, CO 80309, USA. E-mail: roger.bilham@colorado.edu

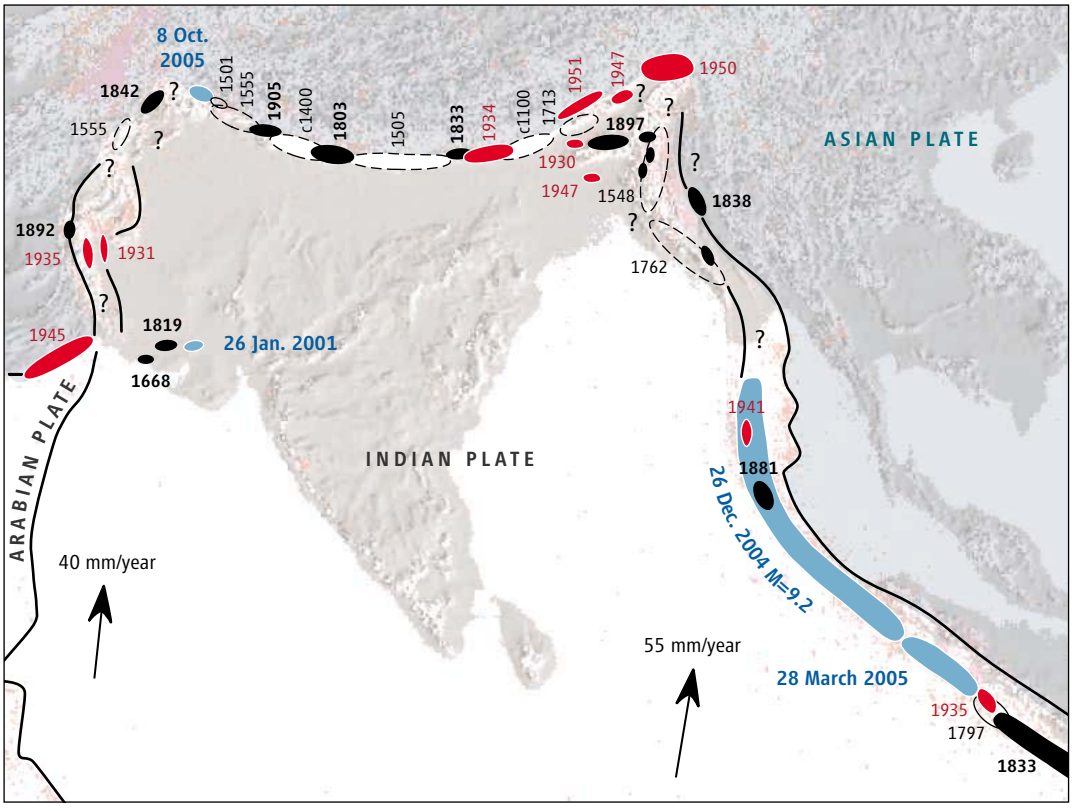

Disaster zone. Earthquakes surround the northern edge of the Indian plate in response to its northward motion toward Asia. The most recent destructive ($M > 7.5$) earthquakes are shown in black (1800 to 1905), red (1930 to 1951), or blue (since 2001). Historical earthquakes where known are shown in white (evidence from trenching or historical accounts), in dashed lines (incomplete data), or with a question mark (no data). In the millennium before 2000, the cumulative death toll in Indian plate boundary earthquakes amounted to fewer than 80,000 of which 50,000 occurred between 1930 and 1950. Earthquakes in the first 5 years of the new millennium have already claimed more than 380,000 lives.

sequence has no precise historical precedent in the Indo-Asian collision zone, and therefore, no easy answer can be offered to the most obvious of questions—is this the end, or are more catastrophic earthquakes poised to occur?

The conservative answer to this question is that we are witnessing a coincidence, a random fluctuation in the timing of earthquakes that occur at intervals of hundreds of years. History reveals numerous of these coincidences, however, which suggests that these clusters may be more common than can be explained by chance: in Mongolia (*9*), in the northern United States (*10*), and in the Pacific (*11*). Even in India a cluster of seven fatal earthquakes bracketed World War II, leaving 50,000 dead in their wake (see the figure). The comparative lull following this sequence has led to complacency in the rigorous application of earthquake-resistant building codes in India, despite the definition of a code in 1931 following the $M_w = 7.3$ Mach earthquake near the start of this sequence.

The nonconservative answer is that several mature seismic gaps are known (*12*), and that the past 5 years have nudged these and neighboring regions toward failure (see the figure). The 1819 Allah Bund and 2001 Bhuj earthquakes have stressed regions within striking distance of populations exceeding 20 million (Karachi and Ahmedabad). The 8 October Kashmir earthquake has stressed adjoining Himalayan regions, where no great earthquake has occurred since the 16th century (*13*). A 600-km-long region of the central Himalaya has apparently not slipped since 1505 (*14*). The more ancient the predecessor, the larger will be the future earthquake, and the recurrence of these Himalayan $M > 8$ earthquakes would now threaten a dozen megacities in Pakistan and India. No $M > 8$ earthquakes are known on the Chaman fault system that separates the western edge of the Indian plate from the Asian plate, and although it is possible that earthquakes here cannot exceed $M_w = 7.7$, similar to that suffered by Quetta in 1935, this earthquake is infamous for holding the previous record number of fatalities (35,000) for an Indian subcontinent earthquake before last October's Kashmir earthquake.

The question of why these recent earthquakes stopped where they did, and whether the increased stresses that now lay siege to their rupture termination points will succumb to failure sooner rather than later, is one that regrettably cannot be answered. Why do contiguous ruptures tarry? Coulomb failure models can tell us clearly where to expect failure (*3*, *15*), but we remain unable to predict the storm gaps for the delayed-action fuses that have now been lit.

Tough decisions now face the politicians and urban planners of Sumatra, India, Pakistan, Nepal, and Bangladesh. The simple solution, to toss money at seismic-monitoring technologies, is laudable but may be less effective in saving lives than community education. The proposed Indian Ocean tsunami warning system will cost far more than telling schoolchildren and their parents about the causes and effects of tsunamis. The half-million dwellings and 7600 schools that collapsed in Kashmir last October were almost entirely constructed in the past 20 years. They collapsed more from poor assembly than from severity in shaking. Correctly assembled buildings survived intact as beacons to education. The 26 January Bhuj 2001 earthquake occurred in a region long designated at high risk from future shocks, yet the earthquake-resistant code here was so unevenly applied that the same percentage of the population was killed by building collapse as occurred in 1819 when earthquake-resistant construction was unknown (*16*).

Most troubling is that although these three recent Indian plate earthquakes have raised public awareness of the precarious state of dwellings in their region, these earthquakes could have occurred in any of a dozen other locations surrounding the Indian plate with similar or worse effects. None of the recent earthquakes were direct hits on any of the numerous megacities that populate the plate. A death toll of more than 30% is typical of a direct hit from a quite modest earthquake beneath a city like Tangshan, Muzzafarabad, or Balakot. Such an event beneath Karachi, Lahore, Lucknow, Benares, Dacca, or Bombay would result in a disaster of unprecedented magnitude were it to occur, and it seems only a matter of time before it does (*17*). The well-intentioned frenzy of earthquake-resistant reconstruction that is now essential in the epicentral regions in response to the past 5 years of earthquake-induced collapse has not been attended by any similar frenzy of attention to reconstruction and retrofitting of the next dozen potential earthquake targets. That is not to say that urban planners are being complacent. New Delhi and other cities have started a retrofit campaign (*18*), but the costs are daunting and almost unimaginably expensive.

The diversion of funds to a project as simple and fundamental as safe dwellings for citizens of the Indian plate surely poses tough decisions for leaders of nations in the collision zone. It's tough luck for citizens of these nations if their leaders decide, through indifference, to ignore this early-millennium quadruple wake-up call. Unwavering common sense, rather than a knee-jerk reaction designed to score political points, appears to be the only solution to the world's earthquake-vulnerable populations. It is essential that the replacement of the ancient building stock of cities, be it a 20-year or 50-year turnover, be undertaken with mandatory earthquake-resistant code. This won't stop the carnage immediately, but it will substantially reduce it, and it will make politicians and urban planners look less culpable than they do now.

References

1. R. W. Briggs *et al*., *Science* **311**, 1897 (2006).
2. K. Sieh, *Nature* **434**, 573 (2005).
3. J. McCloskey, S. S. Nalbant, S. Steacy, *Nature* **434**, 291 (2005).
4. R. A. Harris, R. J. Archuleta, S. M. Day, *Geophys. Res. Lett.* **18**, 893 (1991).
5. G. King, J. Nabelek, *Science* **228**, 984 (1985).
6. M. Ando, *Tectonophysics* **27**, 119 (1975).
7. N. Sleep, *Geochem. Geophys. Geosyst.* **6**, Q11008 (2005).
8. J. Zachariasen, K. Sieh, F. Taylor, W. Hantoro, *Seismol. Soc. Am. Bull.* **90**, 897 (2000).
9. J. Chery, S. Carretier, J.-F. Riz, *Earth Planet. Sci. Lett.* **194**, 277 (2001).
10. S. E. Hough, *Bull. Seismol. Soc. Am.* **91**, 1574 (2001).
11. H. Kanamori, *Nature* **271**, 411 (1978).
12. R. Bilham, K. Wallace, *Geol. Surv. India Spec. Publ.* **85**, 1 (2005).
13. R. N. Iyengar, S. D. Sharma, *Earthquake History of India in Medieval Times* (Central Building Research Institute, Roorkee, India, 1998).
14. N. Ambraseys, D. Jackson, *Curr. Sci.* **84**, 570 (2003).
15. R. S. Stein, *Nature* **402**, 605 (1999).
16. R. Bendick *et al*., *Seismol. Res. Lett.* **72**, 328 (2001).
17. S. Hough, R. Bilham, *After the Earth Quakes* (Oxford Univ. Press, New York, 2005).
18. www.quakesafedelhi.net/rollout/projectbrief.pdf

10.1126/science.1125176

IMMUNOLOGY

An Antibody Paradox, Resolved

Martin Prlic and Michael J. Bevan

The immune effect of a cytokine bound to an antibody is paradoxically much stronger than that of the cytokine alone, suggesting a way to lower therapeutic doses and thereby reduce side effects.

Lymphocytes are the epitome of migrant cells in the body, coursing through blood and lymphatic vessels, trafficking through lymphoid organs such as spleen and lymph nodes, and entering any tissue upon activation. Yet the numbers of these highly mobile populations of immune cells—B and T lymphocytes and natural killer cells—must be balanced and maintained to sustain lymphoid homeostasis. In the absence of such balance, autoimmunity or the failure to respond to an infection may result. Cytokines, soluble factors produced by lymphoid and nonlymphoid cells, provide signals for the survival, proliferation, and turnover of many subpopulations of lymphocytes. A report by Boyman *et al*. (*1*) on page 1924 of this issue shows that the balance of lymphocyte subpopulations can be dramatically skewed by the injection of monoclonal antibodies previously designated as cytokine-neutralizing antibodies. As it turns out, these antibodies paradoxically enhance the potency of the cytokine in vivo and disrupt lymphoid homeostasis.

Many of the cytokines involved in lymphoid homeostasis are members of the "common gamma chain" family of cytokines, so called because they all activate lymphocyte receptors that include a subunit called the γc chain. Interleukin-2 (IL-2) is the founder member of this family of cytokines, and is historically thought of as an acute cytokine—that is, one that is made and secreted in large quantities only by T cells (CD4 T cell subtype) that have been recently activated by antigen. Acute cytokines are also consumed by activated CD8 T cells.

The high-affinity receptor for IL-2 is a trimeric structure composed of an α chain (CD25), whose expression increases in T cells shortly after antigen exposure, plus a β chain (CD122), and γc chain. In this way, activated T cells expressing the high-affinity receptor can respond to secreted IL-2 as a growth and differentiation signal. Nonactivated, "resting" T cells that do not express CD25 may express the two-chain intermediate-affinity receptor for IL-2 composed of CD122 plus γc. In addition to its acute role in the immune response to antigen, IL-2 is also a maintenance cytokine for regulatory T cells, another T cell subset (*2*). Regulatory T cells constitutively express the high-affinity, trimeric IL-2 receptor. To complicate things further, the cytokine interleukin-15 (IL-15) is necessary for the maintenance of memory CD8 T cells and

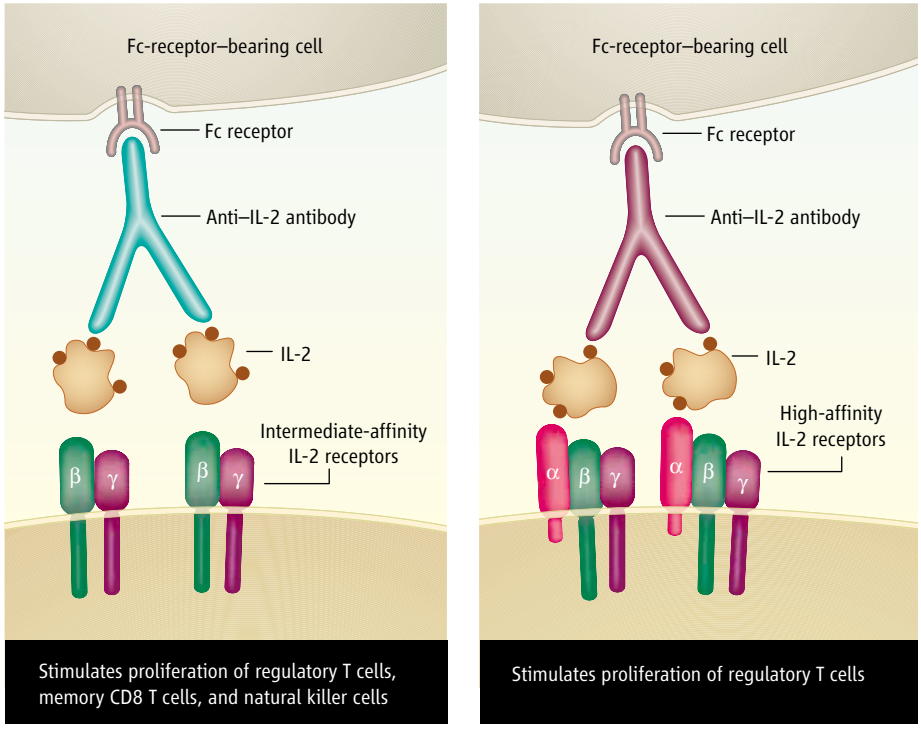

Antibodies determine which lymphocytes get stimulated. Monoclonal antibodies that bind to different sites on IL-2 can enhance, rather than neutralize, the potency of the cytokine in vivo and stimulate the proliferation of different subpopulations of lymphocytes. Possibly, polymerization of the IL-2 on the surface of cells bearing Fc receptors, as for some of IL-2 and causes these cells to proliferate.

The authors are in the Department of Immunology and the Howard Hughes Medical Institute, University of Washington, Seattle, WA 98195–7370, USA. E-mail: mprlic@u.washington.edu, mbevan@u.washington.edu

natural killer cells (*3*, *4*). The receptor on these cells that is thought to receive tonic IL-15 signals is composed of CD122 plus γc, the same two chains that make up the intermediate-affinity receptor for IL-2. In sharp contrast to IL-2, it is thought that IL-15 remains bound to the surface of the cell that produces it (*5*, *6*). Thus, memory CD8 T cells and natural killer cells receive an IL-15 signal via their two-chain receptors as they journey through lymphoid organs.

Boyman and colleagues found that when they injected mice with a "neutralizing" monoclonal antibody against IL-2, memory CD8 T cells and natural killer cells that express only the two-chain intermediate-affinity receptor for IL-2 proliferated. This effect depended on the presence of endogenous IL-2. The stimulating effect on memory CD8 T cells of injected anti-IL-2 antibody as reported previously, though how this occurred remained a mystery (*7*). Daily injections of small amounts of IL-2 in complex with IL-2–specific antibodies (anti–IL-2) led to a dramatic 20- to 100-fold increase in the number of these cells within 7 days. Because the Fc portion of the antibody was required for this huge expansion in cell number, the authors propose that the antibody–IL-2 complexes become fixed on the surface of cells expressing receptors for the Fc portion of the antibody. These Fc-receptor–bearing cells thus present the cytokine to lymphocytes that express the intermediate-affinity IL-2 receptor. In other words, soluble IL-2 has become membrane bound and might now be acting like IL-15 on memory CD8 T cells and natural killer cells (see the figure). It remains uncertain whether antibody-bound IL-2 delivers a qualitatively different signal from that delivered by IL-2 or IL-15 alone, or whether the difference is one of magnitude only, such that cells simply receive a longer lasting or stronger signal.

Interestingly, the outcome of treatment with the antibody–IL-2 complex depends heavily on the type of anti–IL-2 antibody that is used. The IL-2–specific monoclonal antibody with the properties described above binds to a site on the cytokine without blocking the interaction of IL-2 with the intermediate-affinity receptor. However, this antibody prevents IL-2 from binding to the CD25 subunit of the high-affinity trimeric receptor. Remarkably, another monoclonal antibody that binds to a different site on IL-2 prevents the stimulation of natural killer cells and memory CD8 T cells, presumably by blocking interaction with the intermediate-affinity receptor. However, this antibody–IL-2 complex still triggers the expansion of regulatory T cells by engaging CD25 in the high-affinity receptor (see the figure). Only when these two antibodies are used in combination is IL-2 truly neutralized, and proliferation of all previously affected lymphocyte subpopulations is ablated.

Further elucidating the effects of the different antibody–IL-2 complexes on the signaling cascade downstream of the IL-2 receptor might be of therapeutic interest, especially given the potential to increase the number of regulatory T cells alone or in conjunction with other lymphocyte subpopulations.

Currently, IL-2 injection is used for antitumor therapy in renal cell carcinoma and melanoma patients and as a restorative therapy in patients infected with HIV. Administration of high doses of IL-2 intravenously is accompanied by severe side effects such as hypotension and vascular leak. It is unclear if antibody–IL-2 complexes can mimic the therapeutic effects of IL-2 alone, but the increased potency of these complexes compared to that of the cytokine alone could result in a reduction of dosage and the number of treatment cycles required during IL-2 therapy. It is therefore of great interest to follow up on the discovery of the potent nature of antibody–IL-2 complexes in mice, and to figure out which antibody to use to target specific lymphocyte subpopulations. Only then can effective clinical applications be rationally devised.

References

1. O. Boyman, M. Kovar, M. P. Rubinstein, C. D. Surh, J. Sprent, *Science* **311**, 1924 (2006); published online 16 February 2006 (10.1126/science.1122927).
2. J. D. Fontenot, J. P. Rasmussen, M. A. Gavin, A. Y. Rudensky, *Nat. Immunol.* **6**, 1142 (2005).
3. K. S. Schluns, L. Lefrancois, *Nat. Rev. Immunol.* **3**, 269 (2003).
4. W. M. Yokoyama, S. Kim, A. R. French, *Annu. Rev. Immunol.* **22**, 405 (2004).
5. M. M. Sandau, K. S. Schluns, L. Lefrancois, S. C. Jameson, *J. Immunol.* **173**, 6537 (2004).
6. P. R. Burkett *et al.*, *J. Exp. Med.* **200**, 825 (2004).
7. C.C. Ku, M. Murakami, A. Sakamoto, J. Kappler, P. Marrack, *Science* **288**, 675 (2000).

10.1126/science.1126030

ASTRONOMY

A Neutron Star in F-sharp

Discovery of the fastest spinning pulsar gives new constraints on the size of a neutron star and matter under extreme conditions and decreases the need for gravitational waves to impose a limiting maximum spin.

Jonathan E. Grindlay

Millisecond pulsars are extreme examples of what can happen when stars evolve into neutron stars in compact binary systems. These rotating objects are spun up by accretion of matter from their binary companions, producing luminous x-ray emission, and later become detectable as pulsars with periods of a few milliseconds (*1*). As a result, these "fast pulsars" may offer some of the best probes to study matter and space in the relativistic regime of strong gravity. On page 1901, Hessels *et al*. (*2*) report the discovery of pulsar PSR J1748-2446ad in the dense globular cluster Terzan 5 (Ter5-ad). This object, detected with the Green Bank radio telescope, holds the new record for the fastest spinning neutron star (or, indeed, any object of stellar mass or larger). Its spin period is only 1.396 ms, even shorter than that of B1937+21 [the first millisecond pulsar discovered (*3*)] at 1.558 ms. With a rotation frequency of 716 Hz, Ter5-ad reaches a new high note for the music of the celestial spheres—between F and F-sharp, whereas B1937+21 (at 642 Hz) can only hit a note between D-sharp and E.

Since their discovery in 1967, pulsars have been the gateway to the study of matter and energy at the extremes found only in neutron stars (*4*). Such stars are nature's last stable outposts of matter and are only a factor of ~3 larger in radius than an object that would collapse to a black hole. With ~1.4 to 2 solar masses ($M_\odot$) packed into a radius of ~10 to 15 km, neutron stars are the ultimate laboratories for the astrophysics and physics of the extreme. Neutron stars can exhibit magnetic fields about 10^{15} times stronger, as toward the giant flares from magnetars. And neutron star–binary pairs merge to produce extremely energetic events as revealed in short gamma-ray bursts. However, it is the oldest and fastest pulsars, the millisecond pulsars, that may allow the most direct measures of the ultimate prize: the mass M and radius R of the neutron star itself, which would fix the equation of state and the composition of matter at hypernuclear density. The Ter5-ad system is a new stepping stone on the quest for M and R as well as a constraint on the ultimate rotational limits that may yet be revealed by gravitational waves.

A point on the rotation equator of Ter5-ad has velocity nearly one-fourth the speed of light, assuming R = 15 km. The constraint that the maximum spin frequency ν_s not exceed the Keplerian orbital frequency ν_k at the neutron star surface gives the simple constraint that $\nu_s \leq 1833(M/M_\odot)R_{10}^{-3/2}$ where M is the neutron star

The author is at the Harvard-Smithsonian Center for Astrophysics, 60 Garden Street, Cambridge, MA 02138, USA. E-mail: josh@cfa.harvard.edu

mass and R_{10} is the radius in units of 10 km. Taking into account general relativistic effects, Lattimer and Prakash (*5*) derived a value of 1045 Hz as the maximum spin frequency for a neutron star with (nonrotating) radius R and with a mass M less than the maximum mass allowed by its equation of state. A measured value of ν_s then sets an upper bound on the neutron star radius. For Ter5-ad with ν_s = 716 Hz, R is restricted to be ≤14.4 to 16.7 km when M is ≤ 1.4 to 2.2 $M_\odot$, which is the approximate range encompassed by recent neutron star mass measurements with quoted uncertainties of ≤10% (*5*). As Hessels *et al*. point out, a mass measurement—and thus a constraint on the equation of state—for the neutron star in Ter5-ad is conceivable given its eclipsing geometry if the radial velocity of the ≥0.14 $M_\odot$ main-sequence binary companion can be measured. Given likely stellar crowding, this will be difficult, however: With the ~7 magnitudes of optical extinction to Terzan 5, the companion must be sought in the near-infrared with an expected infrared magnitude as faint as ~25.

X-ray observations allow complementary constraints on M and R for the neutron stars in quiescent low-mass x-ray binaries (qLMXBs) as well as their millisecond pulsar descendants. The first Chandra x-ray survey of the globular cluster 47Tuc revealed that source X7 was one of several qLMXBs (*6*). Analysis of deeper Chandra observations of X7 with fits of neutron star atmosphere models (including surface gravities) to its purely thermal x-ray emission spectrum can be made. These fits yield 90% confidence limits ranging from R = 12.7 to 16.7 km (for M = 1.4 $M_\odot$) to R = 10.0 to 15.0 km (for M = 2.2 $M_\odot$) (*7*), which are consistent with those for Ter5-ad. Even more accurate constraints on the gravitational redshift factor M/R (which in turn constrains the equation of state given measures of M) for neutron stars are possible from studies of the pulsed profiles of thermal x-ray emission from millisecond pulsars, provided the pulsar distance and inclination angles are known (*8*). Unfortunately, Ter5-ad may not allow this, because its x-ray emission is likely dominated by unpulsed nonthermal emission caused by the shock where its pulsar wind encounters gas from its main-sequence binary companion, as recently identified (*9*) in the similar millisecond pulsar 47Tuc-W.

Hessels *et al*. suggest that even faster millisecond pulsars exist but may be hidden by the increased likelihood of radio eclipses, because their increased spin-down energy loss rate and resulting pulsar wind more readily drives matter off their binary companions. Indeed, the distribution (see the figure) of the energy flux from spin-down energy loss incident on the binary companion for the 12 fastest millisecond pulsars with binary companions (*10*) shows that the eclipsing (radio) systems are generally those with the largest incident flux. Still faster millisecond pulsars are preferentially hidden (if in binaries) from radio surveys but could be detectable as relatively hard x-ray sources (unpulsed) from their pulsar wind shocks.

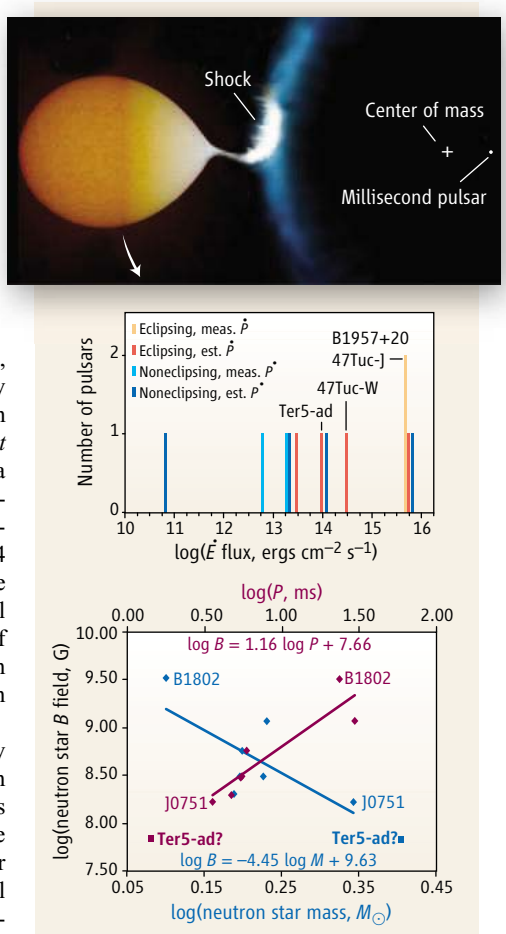

Pulsar properties. (**Top**) Gas from the normal star in the binary system is prevented from accreting onto the neutron star at the shock formed where it meets the pulsar's "wind" of relativistic particles. This shocked gas eclipses the pulsar for much of the time so that pulsars with the shortest spins (strongest wind) and closest companions may be permanently hidden at radio frequencies, although unpulsed x-rays are expected. [Adapted from (*9*)] (**Center**) Pulsar wind energy flux of the 12 fastest spinning millisecond pulsars in binary systems that would be incident on their binary companion stars [parameters from (*2*) and (*10*)]. For pulsars without measured period derivatives (including Ter5-ad), an estimated fixed value of 2×10^{-20} s s^{-1} is used. The eclipsing systems generally do have higher pulsar wind flux values, although Ter5-ad is not extreme, which implies that still faster systems could be found. The second fastest millisecond pulsar, B1937+21, cannot be plotted because it has no binary companion. The other pulsars marked are B1957+20 (Black Widow), 47Tuc-J, and 47Tuc-W, which are numbers 3, 10, and 12 in order of increasing spin period (*10*). The two highest pulsar wind flux pulsars are the eclipsing system Ter5-O and the noneclipsing system M62-C. (**Bottom**) Correlations for millisecond pulsars with neutron star mass [values from (*5*)]. Correlation between mass and neutron star magnetic field B [blue, from (*10*)], and between B and spin period P (purple). Extrapolated values are predicted for Ter5-ad; two other millisecond pulsars [see (*9*)] are marked for comparison.

A maximum neutron star spin frequency, ν_{max} ~ 760 Hz, was suggested (*11*) given the spin distribution for accretion-powered as well as radio millisecond pulsars. A value for ν_{max} much less than 1045 Hz, the maximum allowed value independent of the equation of state (*5*), could require a source of angular momentum loss such as gravitational radiation from an *r*-mode instability in the neutron star core (*12*). Another mechanism may be at work: If the accreting matter spinning up the neutron star is burying its primordial magnetic field—as is generally believed (*1*) to account for the $B \leq 10^9$ G fields inferred for qLMXBs and millisecond pulsars—then the increased accretion and final spin ν_s imply a lower B field emerging from the neutron star when accretion stops. The millisecond pulsars that spin fastest would then have the lowest B fields (above threshold for pulsations) and the largest neutron star mass; neutron stars with larger values of ν_s and mass have smaller B and do not pulse. For those millisecond pulsars with neutron star mass estimates (*5*), including the 2.2 ± 0.2 $M_\odot$ value for the neutron star in the millisecond pulsar J0751+1807 (*13*), possible correlations between B and M and between B and the pulsar spin period P are evident (see the figure). The implied values for Ter5-ad are ~2.5 $M_\odot$ and ~7×10^7 G and thus a predicted change in spin period $\dot{P}$ ~3×10^{-21} s^{-1}, which can be tested when a final timing solution is found. If this were the case, then Ter5-ad would have a mass approaching the maximum (*5*) for neutron stars, and it could be singing nearly the highest note without having made gravitational waves.

YYDG Proudly Presents | Thx for Support

References

1. D. Bhattacharya, E. P. J. van den Heuvel, *Phys. Rep*. **203**, 1 (1991).
2. J. W. T. Hessels *et al*., *Science* **311**, 1901 (2006); published online 12 January 2006 (10.1126/science.1123430).
3. D. C. Backer, S. R. Kulkarni, C. Heiles, M. M. Davis, W. M. Goss, *Nature* **300**, 615 (1982).
4. Special issue on pulsars, *Science* **304** (23 April 2004).
5. J. M. Lattimer, M. Prakash, *Science* **304**, 536 (2004).
6. J. E. Grindlay, C. Heinke, P. D. Edmonds, S. S. Murray, *Science* **292**, 2290 (2001); published online 17 May 2001 (10.1126/science.1061135).
7. C. O. Heinke, G. B. Rybicki, R. Narayan, J. E. Grindlay, *Astrophys. J*., in press.
8. G. G. Pavlov, V. E. Zavlin, *Astrophys. J.* **490**, L91 (1997).
9. S. Bogdanov, J. E. Grindlay, M. van den Berg, *Astrophys. J*. **630**, 1029 (2005).
10. Australia Telescope National Facility Pulsar Catalogue (www.atnf.csiro.au/research/pulsar/psrcat).
11. D. Chakrabarty *et al*., *Nature* **424**, 42 (2003).
12. R. V. Wagoner, *Astrophys. J.* **278**, 345 (1984).
13. D. J. Nice *et al*., *Astrophys. J*. **634**, 1242 (2005).

10.1126/science.1125125

SCIENCE AND EDUCATION

Education, Religion, and Science Come Together at Evolution Event

As a long-time chemistry teacher and chair of her high school Science Department, Bertha Spahr knew of AAAS's broad interest in science and policy. She hadn't realized, though, that its involvement extended to her classroom in Dover, Pennsylvania.

But at a special evolution event organized by AAAS, Spahr realized that the U.S. science and technology communities are rallying to aid teachers like herself in schools nationwide who are subject to mounting pressure by antievolution groups to inject religion into public school science classrooms.

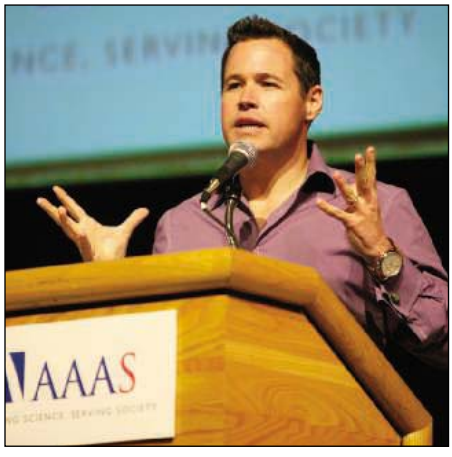

Naturalist Jeff Corwin, the Emmy Award–winning host of *Corwin's Quest* on the Animal Planet cable television channel.

"It was a great encouragement," Spahr said in an interview after the event. "It gave us additional strength to stand up and fight for what we believe to be science.…It gave us even greater courage to go out and do what we can to assist other people."

Spahr was among nearly 500 educators, students, and others who attended a special half-day session, "Evolution on the Front Line," held during the AAAS Annual Meeting in St. Louis. Spahr and seven other educators from Dover and Cobb County, Georgia, received travel awards from the Geological Society of America to participate in the event, where they received a standing ovation for their efforts to preserve the integrity of science education.

The 19 February event featured a remarkable roster of speakers—influential educators, clergy, scientists, and others—who exchanged ideas on building a broad social consensus in support of science education. The audience heard both elegant discourse on the origins of life and practical advice on how to respond when students, parents, or local school officials pressure teachers to avoid evolution or to introduce faith-based doctrine into classes.

Among those who spoke at the event were the Rev. George Coyne, a Jesuit priest and director of the Vatican Observatory; U.S. Representative Russ Carnahan (D–Mo.); Linda Froschauer, president-elect of the National Science Teachers Association; and biologist Kenneth R. Miller, the author of *Finding Darwin's God: A Scientist's Search for Common Ground Between God and Evolution.*

Miller and Spahr were witnesses in the 2005 trial that led a federal judge to strike down the Dover school board's policy of introducing intelligent design in the community's ninth-grade biology classes.

"As a legal strategy, intelligent design is dead," Eugenie Scott, executive director of the National Center for Science Education, told reporters at a news conference before the event. "That doesn't mean intelligent design is dead as a very popular social movement. This is an idea that has got legs ... It will continue to evolve."

"If you want to believe in intelligent design, you absolutely may," said naturalist Jeff Corwin, the Emmy Award–winning host of *Corwin's Quest* on the Animal Planet cable television channel. "But just because you aspire to a particular philosophy does not necessarily give you the right to take that information and integrate it into curriculum.

"I look out and I see all these teachers who have come together at this critical time in our lives.…Make no mistake—what you are doing is important."

Just before the event began, the AAAS Board of Directors issued a new statement expressing deep concern about antievolution efforts in a number of states "that would undermine the teaching of evolution and deprive students of the education they need to be informed and productive citizens in an increasingly technological, global community."

"Evolution on the Front Line" generated extensive coverage by Reuters, the *Chronicle of Higher Education,* and many other news media outlets. The event was moderated by AAAS Board Chair Gilbert S. Omenn, professor of medicine, genetics, and public health at the University of Michigan. It was made possible by the William T. Golden Endowment Fund for Program Innovation, and was planned in collaboration with three dozen prominent science and education organizations, including the National Academy of Sciences, the American Federation of Teachers, the National Education Association, and the Missouri Botanical Garden.

An introductory video, a new guide to teaching evolution from Project 2061 at AAAS, speaker presentations, and other resources are available online at www.aaas.org/evoevent.

BUDGET AND POLICY

AAAS Worries U.S. R&D Cuts Will Hinder Innovation

Most U.S. agencies could face deep cuts in their research and development budgets over the next 5 years, the director of AAAS's R&D Budget and Policy Program told a Capitol Hill briefing. Kei Koizumi said the projected cuts, outlined in President George W. Bush's 2007 budget proposal, range from 10 to 30% for most nondefense R&D agencies.

If the Administration's proposal were approved, the R&D budget for the National Institutes of Health (NIH) would decline every year to 2010 before rebounding slightly in 2011, according to Koizumi. NIH R&D would fall 12.1% in real terms between 2006 and 2011. Pentagon R&D would fall 11.6% below the current budget, after inflation.

Koizumi presented his analysis at a 9 March briefing attended by about 130 congressional staffers and others. There are some winners in the budget, he told them. Bush's proposed "American Competitiveness Initiative" would double funding over the next decade for three agencies—the National Science Foundation (NSF), the Department of Energy's Office of Science, and the National Institute of Standards and Technology (NIST)—that support basic research programs in the physical sciences.

But Koizumi projected that even the physical sciences could take a hit overall in 2007 as cuts in three other major sponsors of the physical

CREDIT: MICHAEL J. COLELLA


Kei Koizumi

sciences—the Defense Department, NASA, and NIH—offset the requested increases at NSF, the Department of Energy, and NIST.

The annual skirmishes over R&D funding will be played out this year against an emerging bipartisan concern over innovation and America's continued technological prowess. AAAS has been active on the innovation issue, which has been the subject of a recent National Academies report and a National Summit on Competitiveness hosted by the Department of Commerce in December.

In a 9 December 2005 letter to President Bush, then-AAAS President Gilbert S. Omenn urged the White House and Congress to take steps to improve the climate for innovation in the United States. Omenn, now chairman of the AAAS Board of Directors, cited the broad consensus among business, academic, and labor leaders on the need to strengthen U.S. research as well as the country's "chronic inability to attract enough students into fields of science, technology, engineering, and mathematics."

In a commentary published in the *St. Louis Post-Dispatch* on 16 February as the AAAS Annual Meeting opened, Omenn and AAAS CEO Alan I. Leshner applauded the initiatives offered by Bush and Congress, where at least 11 innovation-related bills have been introduced. But, they added: "We need to pay close attention in the months ahead to possible gaps between these good intentions and actual financial commitments."

With military operations in Iraq and Afghanistan and mounting deficits, Congress faces tough budget choices. But lawmakers can't afford to shortchange the research enterprise or science education, Omenn and Leshner wrote. Even before the modern information revolution, they say, economists concluded that technological innovations account for up to 85% of growth in per capita income in the United States and 50% of overall economic growth.

The United States still accounts for 38 percent of the world's R&D spending. That share has declined only slightly over the past decade, according to Koizumi. But China, among others, has been making a big push. It has risen from 17th to third in world R&D spending since 1992.

"America today remains the world leader in innovation, but our lead is slipping," the AAAS leaders wrote. "We must inspire our children and our communities to look towards the future. We must make the investments that will invigorate research, strengthen science education and nurture innovation in all fields."
–*Earl Lane*

AAAS Council Approves Statements on Censorship, Katrina

Convened during the 2006 Annual Meeting in St. Louis, the Council of the American Association for the Advancement of Science approved two resolutions:

AAAS RESOLUTION ON FREE AND OPEN EXCHANGE

WHEREAS the advance of science depends on the free and open exchange of data and findings among scientists; and

WHEREAS the capacity of members of the public and their representatives in government to understand and effectively address many of the most important policy issues of our time depends on access to the relevant science; and

WHEREAS a substantial fraction of this science is done in governmental agencies or is funded by them; and

WHEREAS censorship, intimidation, or other restriction on the freedom of scientists employed or funded by governmental organizations to communicate their unclassified scientific findings and assessments not only to each other but also to policymakers and to the public is inimical to the advance of science and its appropriate application in the policy domain;

BE IT THEREFORE RESOLVED by the Council of the American Association for the Advancement of Science that such censorship, intimidation, and restriction are inappropriate.

WE APPLAUD in this connection the recent statement of NASA Administrator Mike Griffin that NASA is "committed to open scientific and technical inquiry and dialogue with the public" and that of NOAA Director Conrad Lautenbacher Jr. encouraging NOAA scientists "to speak freely and openly."

— *Approved by the AAAS Council on 19 February 2006*

RESOLUTION FROM THE MEDICAL SCIENCES SECTION

WHEREAS, Hurricane Katrina and the subsequent floods caused unprecedented disruption in research at Tulane University, Dillard University, Louisiana State University, Xavier University, and other New Orleans institutions; and

WHEREAS, the faculty and administration of these institutions are working valiantly to reestablish their research capabilities; and

WHEREAS, specific faculty with federal research grants have been unable to complete experiments and grant proposals in time for renewal applications;

BE IT THEREFORE RESOLVED by the Council that AAAS call upon the federal research agencies to grant an extraordinary extension of previous funding and renewal deadlines, as determined appropriate by the agencies after consultation with the affected institutions.

— *Approved by the AAAS Council on 20 February 2006*

SCIENCE DIPLOMACY

Turekian Named Chief International Officer

Vaughan Turekian, an environmental scientist who has worked at the intersection of science, diplomacy, and public policy, has been appointed the new chief international officer at AAAS.

Turekian comes to AAAS from the U.S. State Department, where he served most recently as special assistant to Paula Dobriansky, undersecretary of state for democracy and global affairs, focusing chiefly on avian flu, climate change, and sustainable development. He assumed the new post on 27 February.

In an interview, Turekian said he sees science as a way to reach out to the world. "Over the coming years," he said, "I would hope to work closely with our membership and the international science community to chart a path forward to help in promoting things like sustainable development, which clearly are global issues and require global action."

A 1993 graduate of Yale University, he received his master's degree from the University of Virginia in 1996 and his Ph.D. from Virginia in 2000. He served for 2 years as a climate expert at the National Academy of Sciences. In September 2002 he became a AAAS Diplomacy Fellow assigned to the State Department, and then was hired by State when the fellowship ended in June 2003.

As special assistant to the undersecretary of state for democracy and global affairs, Turekian worked on an array of issues—technology; climate change, environment, and energy; and health, including the recently launched International Partnership on Pandemic and Avian Influenza.

"AAAS is well-positioned to play a key role in promoting science and developing scientists who will help improve the lives of people on a global scale," he said.

Stem Cells and Their Niches

Kateri A. Moore* and Ihor R. Lemischka

A constellation of intrinsic and extrinsic cellular mechanisms regulates the balance of self-renewal and differentiation in all stem cells. Stem cells, their progeny, and elements of their microenvironment make up an anatomical structure that coordinates normal homeostatic production of functional mature cells. Here we discuss the stem cell niche concept, highlight recent progress, and identify important unanswered questions. We focus on three mammalian stem cell systems where large numbers of mature cells must be continuously produced throughout adult life: intestinal epithelium, epidermal structures, and bone marrow.

What Is a Stem Cell Niche?

Stem cell niches are composed of microenvironmental cells that nurture stem cells and enable them to maintain tissue homeostasis. An appropriate spatiotemporal dialog occurs between stem and niche cells in order to fulfill lifelong demands for differentiated cells. The niche concept was introduced in 1978 (*1*); however, it was largely neglected until *Drosophila* studies provided a stimulus for its resurgence (*2*). Niche cells provide a sheltering environment that sequesters stem cells from differentiation stimuli, apoptotic stimuli, and other stimuli that would challenge stem cell reserves. The niche also safeguards against excessive stem cell production that could lead to cancer. Stem cells must periodically activate to produce progenitor or transit amplifying (TA) cells that are committed to produce mature cell lineages. Thus, maintaining a balance of stem cell quiescence and activity is a hallmark of a functional niche.

The Intestinal Stem Cell Niche

The epithelial villus/crypt structure and its surrounding pericryptal fibroblasts and mesenchyme in the small intestine make up an anatomical unit that generates four cell lineages: absorptive enterocytes and the goblet, enteroendocrine, and Paneth cells of the secretory lineage (Fig. 1A). The crypt is a contiguous pocket of epithelial cells at the base of the villus. Intestinal stem cells (ISCs) and TA cells within the crypt regenerate the entire villus every 3 to 5 days (*3*). Genetic marking shows that crypts are derived from individual or few ISCs and that each villus is the product of cells from several adjacent crypts (*4*). There are four to six ISCs per crypt that are located in a ring about four cell diameters from the crypt bottom. Progeny of activated ISCs migrate upwards to become TA cells. When they reach the top of the crypt, TA cells stop proliferating, differentiate, and assume their appropriate positions within the villus structure. As such, proper cell-fate decisions are organized within the microanatomy of the crypt structure. Asymmetric cell division mediated by oriented mitotic planes, together with defined migratory activities within the overall crypt structure, could produce the correct localization of distinct differentiated cell types. Although asymmetric cell division along the vertical crypt axis is an attractive mechanism, this process has yet to be rigorously demonstrated in the ISC system.

DNA label-retention studies suggest that ISCs are normally quiescent relative to their surrounding cells (*5*). This interpretation assumes symmetric partitioning of the label into both daughter cells after cell division. In contrast, an ''immortal DNA strand'' model proposes that a stem cell retains an initially labeled strand with each division (*6*). Such a mechanism would result in ISC label retention that is independent of proliferation. This issue needs to be clearly resolved and awaits the development of methods including those that allow the prospective isolation of ISCs.

Mesenchymal cells surround the crypt. It is likely that the mesenchymal signals that mediate different cell fates along the vertical crypt axis are spatially organized into distinct domains. The canonical Wnt pathway regulates ISCs (Fig. 1B). This pathway triggers cell-type–specific gene expression programs due to the stabilization and nuclear localization of β-catenin. Mutations in Tcf-4, a transcriptional regulator and partner of nuclear β-catenin, allow essentially normal intestinal development; however, continued proliferation and maintenance of this tissue are severely compromised. Additional studies implicate Wnt signaling in ISC and TA cell proliferation, as well as in intestinal tumorigenesis; however, as is the case in most stem cell systems, it is difficult to say with certainty that a given signaling pathway functions directly in stem cells (*7*).

Genetic experiments have shown that Wnt signals pattern the physical structure of the ISC niche by generating opposing and complementary gradients of Ephrins and their tyrosine kinase receptors, the Eph proteins (*8*). Ephrin/Eph interactions within the crypt control cell migration patterns. A Wnt gradient is predicted by the distribution of nuclear versus cytoplasmic β-catenin along the crypt axis (*9*). A comprehensive study has now shown that Wnt signaling components are expressed by both crypt epithelial cells and surrounding mesenchymal cells, predicting an even broader role for this pathway in normal homeostasis than is indicated by genetic studies (*10*). There is also evidence that Wnt inhibitors such as Dkk3 may be expressed in a graded manner in this tissue, suggesting an intricate quantitative balance between positive and negative regulators of this pathway (*11*).

The bone morphogenetic protein (Bmp) signaling pathway functions as a negative regulator of ISC proliferation, completing a Yin-Yang axis with Wnt. Bmp-4 is expressed in mesenchymal cells adjacent to the ISCs. Conditional deletion of the Bmp receptor 1A (Bmpr1a) in crypt cells results in hyperproliferation and duplication of ISCs, as shown by staining with an ISC-specific marker (*12*). Analysis of adjacent wild-type and mutant crypts shows that Bmp signals repress nuclear β-catenin accumulation. Pten/PI3k/Akt signaling is implicated in the cross talk between Wnt and Bmp. Inhibition of Bmp signaling also results in the generation of new ISCs, ectopic crypts, and precancerous polyps (*13*). Therefore, it appears that an ISC can organize an intact and normal crypt. When crypt structures are first established during development, Hedgehog signals from the intervillar epithelium regulate the underlying mesenchyme in a paracrine manner (*14*). A role for this signaling pathway in the formation of ectopic crypts in adults has not been established.

Periodic activation of ISCs appears to depend on the transient expression of Noggin, an inhibitor of Bmp signaling. Noggin is expressed by ISCs and adjacent mesenchymal cells (*12*). The in vivo dynamics and regulation of Noggin expression need to be defined. Transient Noggin expression may be triggered by an oscillator mechanism within the niche. The Notch pathway can set up oscillating gene-expression patterns during somitogenesis (*15*). Many components of this pathway are expressed in the ISC niche (*7*). Genetic analyses also implicate Notch signaling in the maintenance of undifferentiated crypt cells and in ensuring proper cell-fate outcomes (*16*, *17*). It has also been difficult to ascertain if this pathway is active in the ISC itself, in more committed TA progenitors, or in both cell populations.

Laser capture technology has been used to isolate ISCs for genomic analyses. Various regulatory molecules were identified, including

Department of Molecular Biology, Princeton University, Lewis Thomas Laboratory, Princeton, NJ 08544, USA.

*To whom correspondence should be addressed. E-mail: kamoore@princeton.edu

components of the above signaling pathways (*18*). This type of technology provides an extremely useful tool for capturing other crypt cells for profiling. An analysis of surrounding mesenchyme and pericryptal fibroblasts is lacking in this system and would provide much-needed information.

The Hair Follicle Epidermal Stem Cell Niche

Skin epidermis and its associated structures arise from two stem cell populations within the hair follicle and interfollicular regions. One, in the basal layer of skin, normally gives rise to stratified skin layers. A second, the hair follicle stem cell (HFSC), resides in a region of the outer root sheath called the bulge, and it is responsible for the regeneration of hair and sebaceous glands (*19*). It had been suggested that bulge stem cells are also responsible for the long-term replenishment of the interfollicular epidermis. It is now clear that bulge stem cells are not required for normal epidermal homeostasis, although they can contribute transiently to this tissue in wound healing (*20*, *21*).

The hair follicle structure is complex and multilayered (Fig. 2A). Dermal cells surround and underlie the epidermal cells and are the likely source of many HFSC regulatory signals. Hair follicles possess unique spatial and temporal features. During each hair cycle, follicles undergo temporal structural alterations that bring the HFSCs closer to the dermal papilla. This proximity is necessary for transient HFSC activation, migration to the lower follicle, and the generation of a new hair structure (*22*).

There are differences between hair follicles identified in the pelage and vibrissae; however, the overall principles that govern their function appear to be similar. Vibrissal hair follicles in rodents are large and can be microdissected into segments at different stages of the hair cycle. Whereas HFSC activity was found in the bulge at all hair cycle stages, identical activity was detected in other segments in a stage-dependent manner. Transplantation of microdissected segments under the kidney capsule of hairless mice provided the first demonstration that cells from the bulge could generate a morphologically intact hair follicle (*23*). Lineage tracking experiments in the pelage hair follicles have also demonstrated that the bulge is the origin of cells in the lower follicle (*24*).

The last 2 years have seen an explosion of papers that provide rigorous measures of self-renewal and multipotent differentiation potentials of HFSCs. Experiments from the early 1990s showed that quiescent, label-retaining cells are located preferentially in the bulge region and that they can form large clones in vitro (*22*, *25*). A major advance was the development of two transgenic strategies for the prospective isolation of viable HFSC populations (*24*, *26*). One of these is a variant of label retention as a means to identify quiescent cells. A fluorescent protein marker is introduced into chromatin at a time when all epidermal cells are dividing. The transgene encoding the marker is then turned off, and the fluorescent label is chased out of cells that continue to divide. Nondividing or slowly dividing cells retain the label, and as expected, these cells are in the bulge. These results confirmed that HFSCs are generally quiescent, and they also permit direct functional analysis of HFSCs. This strategy can be combined with other markers such as α6-integrin and CD34 to further subdivide the HFSC-containing population (*26*). A second strategy used the keratin-15 promoter to express fluorescent marker protein in bulge cells. This, together with differential levels of α6-integrin expression, provided substantial enrichment for HFSCs (*24*). Enriched cells were transplanted and robustly produced hair and, to a lesser extent, sebaceous glands and skin epidermis. Genomic profiling was performed with sorted populations in both of these studies and provided the first molecular profiles of HFSCs.

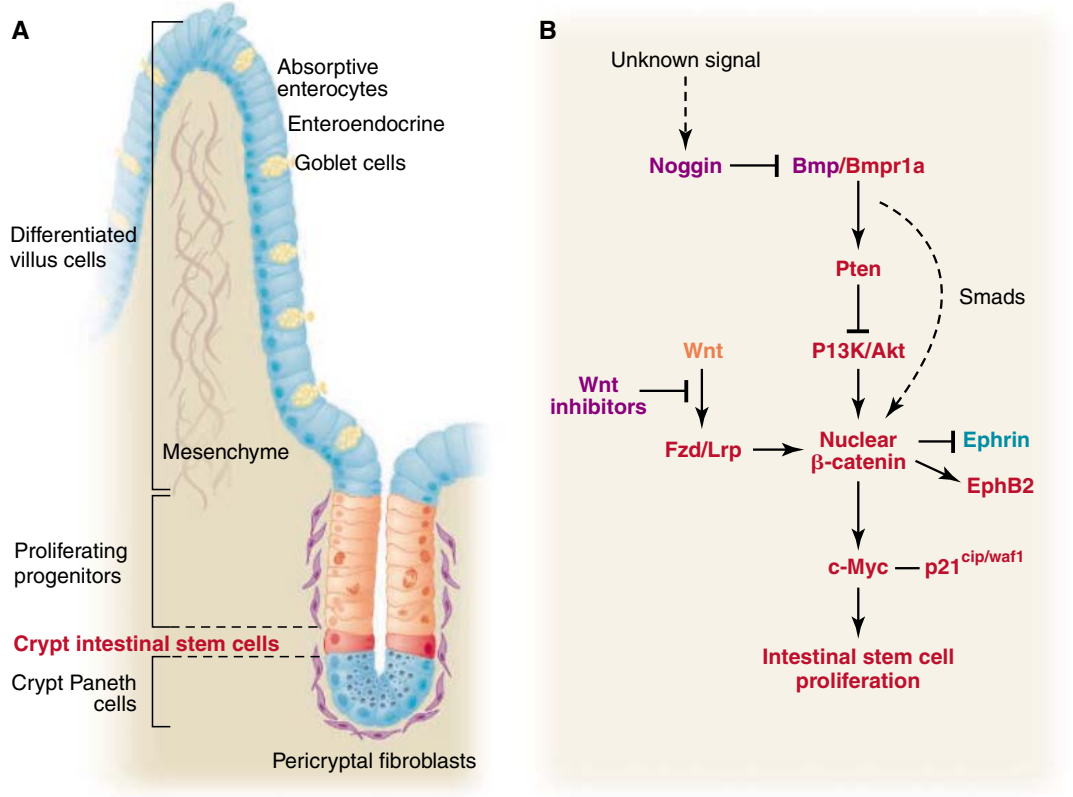

Fig. 1. Stem cells within their niche in the small intestine. (**A**) Schematic diagram of the major types and spatial orientations of cells found within the crypt niche and the villus. (**B**) Interactive signaling pathways that mediate ISC proliferation. Colors represent the cell types sending and receiving the signals as displayed in (A).

Although the aforementioned studies provided valuable prospective definitions for HFSCs, in no case was it directly shown that individual cells can be multipotent, nor was it possible to rigorously measure their self-renewal capacity. Two important studies have addressed these issues (*27*, *28*). In the first study, single bulge HFSCs were purified and shown to self-renew in vitro to produce long-term proliferating clones. Transplantation of clonally expanded cells yielded new morphologically intact hair follicles. Molecular analyses were also performed. Collectively, the molecular analyses of enriched HFSC populations provide suggestions

as to relevant regulatory pathways. Among the identified genes are components of several signaling pathways, adhesion and extra-cellular matrix proteins, as well as molecules involved in cell-cycle control. These genes provide a rich source for future functional analyses. The second study combined single bulge cell isolation, expansion, genetic marking, and transplantation to demonstrate the multipotentiality of rat vibrissal follicle HFSCs. The expanded cells were transplanted into mouse skin at a time when endogenous pelage follicles were first forming, and they contributed to normal intact follicle structures. The transplanted HFSCs could function for at least six to seven hair cycles for over 300 days. Moreover, reisolation and serial transplantation conclusively demonstrated self-renewal abilities (*28*). Serial transplantation first established in the hematopoietic system is the "gold standard" proof of self-renewal.

To date, multipotentiality of single HFSCs has been shown by using cells expanded in vitro; therefore, it may be an acquired property. It remains possible that in situ, individual bulge cells are destined to produce distinct subsets of lineages. Even if in situ, single bulge cells have distinct fates, these may be incompletely "locked in," and thus, the overall differentiation potential may be "expanded" during in vitro culture. An analogous situation can be found in neural development and highlights the complexities inherent in defining stem cells and their immediate progeny as completely deterministic fixed entities (*29*). Freshly isolated bulge cell populations have been used in transplantations (*24*), but not yet as single cells. Such techniques, or an ability to track the progeny of single HFSCs in situ, will be required to accurately assess the multipotential activity of these cells in normal homeostasis. An in situ tracking method has shown that progenitors in the hair follicle contribute to single lineages and possess limited self-renewal potential, suggesting that it may be possible to rigorously measure when and how various lineage potentials are segregated after HFSC activation (*30*).

As mentioned previously, there is little evidence for asymmetric cell division in mammalian stem cell systems. An important study has provided such evidence for basally located cells that generate the skin epidermis during development (*31*). It will be interesting to see if this can be demonstrated in the bulge HFSCs during homeostatic function.

As in the ISC niche, the Wnt pathway is important in the hair follicle system (Fig. 2B). Numerous components of this pathway were identified in molecular profiling studies, and a number of Wnt inhibitors were found. Several transgenic studies demonstrate the role of β-catenin in the skin. A transgenic stabilized form of β-catenin causes de novo follicle morphogenesis and, eventually, skin tumors (*32*). Transient increases in β-catenin levels also accelerate the transition from the resting to the growth phase of the hair cycle (*33*). Additional studies suggest that transient activation of β-catenin in adult epidermis leads to new follicles derived from existing follicles, interfollicular epidermis, and sebaceous glands, but not from HFSCs within the bulge region (*34*, *35*). These authors had previously suggested that distinct stem cell pools exist in interfollicular epidermis, sebaceous glands, and hair follicles (*36*).

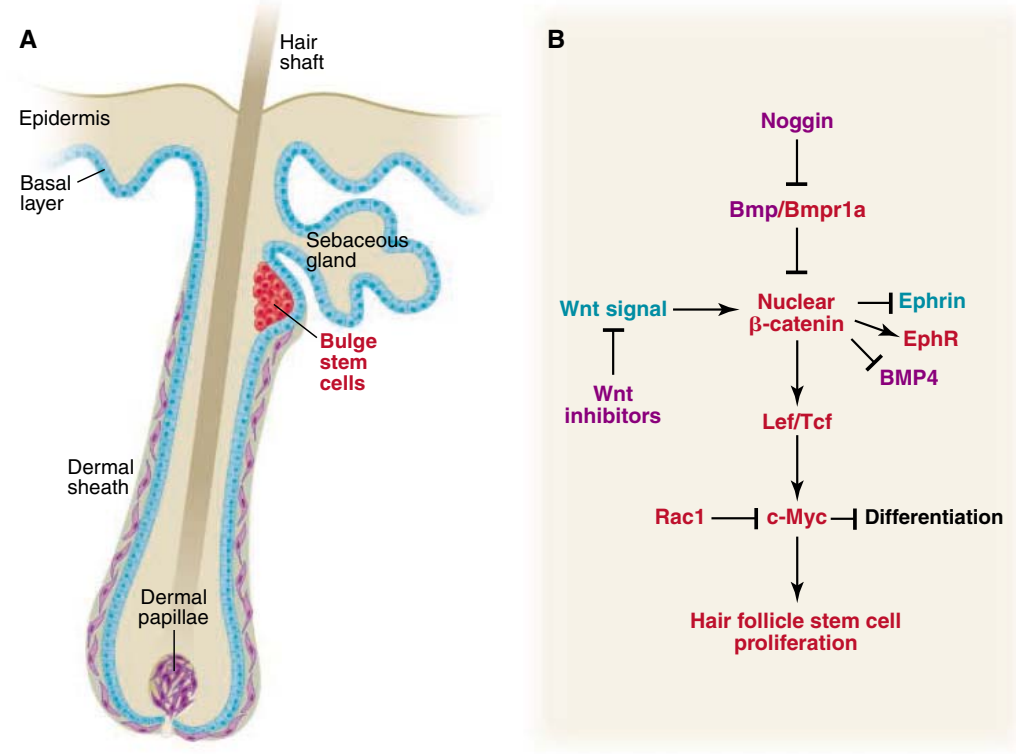

Fig. 2. Stem cells within their niche in the hair follicle. (**A**) Schematic diagram of the major types and spatial orientations of cells that make up the hair follicle. (**B**) Interactive signaling pathways that mediate HFSC proliferation. Colors correspond to the cell types that mediate the interactive signaling leading to the proliferation and differentiation of the hair follicle cell types as displayed in (A).

Bmp signaling is also crucial in the HFSC system. Conditional ablation of Bmpr1a results in hair follicle defects (*37*, *38*). Moreover, mice lacking the Bmp inhibitor Noggin show defects in the function of the canonical Wnt pathway (*39*). Mesenchymal cells produce Noggin in this system (*40*), potentially establishing one way in which these cells can activate the HFSCs. Both activation of the Wnt pathway and inhibition of the Bmp pathway appear to be necessary for functional β-catenin/Lef1 transcriptional complexes. The collective evidence suggests that integration of the Bmp and Wnt signaling pathways occurs in a manner similar to the ISC system.

An emerging theme is the implementation of the same signaling pathways in distinct stem cell systems. This is perhaps not surprising given the limited number of such pathways in all of biology. Nonetheless, it is critically important to identify precisely the actual cells affected by a given signaling pathway. In the hair follicle, Wnt signaling has been shown to affect all phases of stem cell regulation, from quiescence and identity to proliferation and terminal differentiation (*41*). Subtly elevated levels of transgenic stabilized β-catenin cause precocious activation of HFSCs without an increase in their overall numbers. Activated HFSCs return to quiescence in the in vivo niche. Moreover, conditional ablation of β-catenin results in the failure to maintain intact follicles with quiescent HFSCs (*42*). Taken together with other data documenting roles for this pathway in regulating differentiation, a model is proposed where a gradient of Wnt signaling acts on different developmental

stages of the hair follicle system. How quantitative differences in the levels of signaling are interpreted to yield distinct cell-fate outcomes is an unanswered question of fundamental importance.

Other intriguing insights about HFSC regulation are emerging. For example, overexpression of the catalytic component of telomerase promotes HFSC-activating transitions resulting in robust hair growth (*43*, *44*). This occurs through a mechanism that does not involve the synthesis of telomeres. In addition, the deletion of Rac1, which normally negatively regulates c-Myc, stimulates proliferation and terminal differentiation of HFSC and interfollicular stem cells (*45*). Clearly, there will be a need to integrate these observations with the more traditionally studied signaling pathways discussed above.

The Hematopoietic Stem Cell Niche in the Bone Marrow

Bone marrow (BM) hematopoietic stem cells (HSCs) are the best characterized stem cell population. Single HSCs are multipotent, highly self-renewing, and cycle with slow kinetics. Ironically, little in situ information is available to define the anatomical and structural relationships of stem cells, their progeny, and microenvironmental cells. In the ISC and HFSC systems, such information provides the framework for understanding the patterning of fate decisions and the flow of regulatory information. Bone and marrow are intrinsically linked with HSCs, and their primitive progeny are located proximal to the endosteal surface of trabecular bone (Fig. 3A) (*46*). Studies have shown that osteoblast (OB) cells are required for this localization. Genetically engineered increases in OB numbers lead to elevated HSC numbers without changes in committed progenitor populations. In one case, OB numbers were increased after conditional ablation of Bmpr1a (*47*). Bmpr1a is not expressed in HSCs, and Bmp signaling was shown to act cell-autonomously in OB cells. This may contrast with the ISC and HFSC systems and needs further investigation. In a second transgenic study, OB numbers were increased via an activated parathyroid hormone–related protein receptor (PPR) expressed specifically in these cells (*48*). Similar increases in HSC numbers were also observed.

The Bmpr1a and PPR studies provide mechanistic insights into OB-mediated HSC expansion. The Bmpr1a studies identified a specific subset of N-cadherin–expressing OBs that form an N-cadherin/β-catenin adherens complex with HSCs, perhaps mediating the attachment or adhesion of HSCs within their niche. N-cadherin is negatively regulated by c-Myc in differentiating HSCs, perhaps promoting displacement from the endosteum (*49*). In the PPR studies, Notch signaling was implicated, because the Notch ligand Jagged 1 was highly expressed in OBs and Notch activated in HSCs. Wnt protein was previously shown to promote HSC proliferation (*50*, *51*), and now, an additional study has shown that Notch and Wnt inputs are integrated by HSCs. Specifically, Notch signaling appears to inhibit differentiation programs that accompany Wnt-induced proliferation (*52*). However, genetic ablation studies suggest that at least some aspects of these pathways may be dispensable for in vivo HSC function (*53*, *54*). Unfortunately, none of the above studies addressed HSC self-renewal rigorously by long-term reconstitution and serial transplantation. Therefore, the exact roles of Wnt and Notch signaling will require further analysis. A recent study demonstrated that the inhibition of glycogen synthase kinase–3 (GSK-3) activity enhances HSC progenitor activity and maintains but does not expand the stem cell pool (*55*). The GSK-3 inhibitor was shown to modulate Wnt, Notch, and Hedgehog signaling specifically in primitive HSCs. Direct roles for these pathways in self-renewal were not demonstrated; however, roles in stem cell maintenance with an expansion of progenitors are supported by the data. A plausible explanation for maintenance of HSC levels by these signaling pathways could lie in controlling asymmetric cell division. Other mediators of HSC self-renewal have been identified; such as p21 (*56*), p18 (*57*), and bmi-1 (*58*); but how these are controlled by extrinsic signals from the niche has not been determined. Nevertheless, and although different in details, the overall integration of positive and negative stimuli by HSCs is similar to that of ISCs and HFSCs (Fig. 3B).

In transgenic mice where OB cells have been ablated, the marrow is aplastic and extensive extra-medullary hematopoiesis occurs (*59*). This raises questions about the existence of HSC niches in other tissues. HSCs can, in fact, be found in tissues that have no OBs (*60*). Thus, although BM HSC niches are at least in part composed of OBs, other cell types may also provide this function. The contribution of other cellular elements, such as stromal cells or perivascular cells, is yet to be defined. It is has been shown that HSCs can be recruited to a "vascular niche" in the BM (*61*). Such vascular structures could serve as components of extramedullary niches. One intriguing study has demonstrated that HSCs express a calcium-sensing receptor. Stem cells lacking this receptor fail to localize to the endosteal niche and do not function normally after transplantation (*62*). This study highlights the importance of the ionic mineral content of the bone itself and of the bone-derived matrix in the lodgment and retention of HSCs within the endosteal niche.

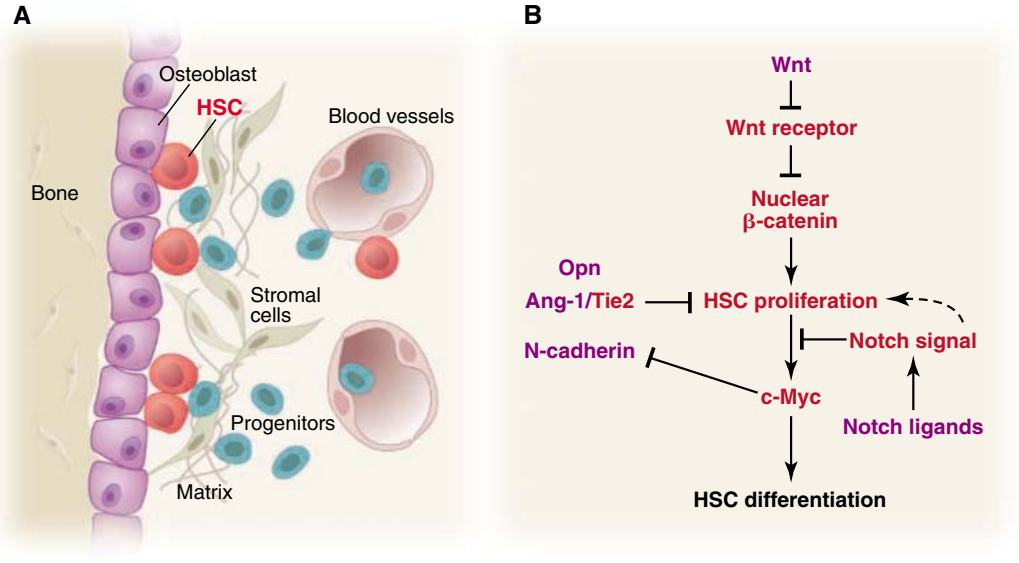

Fig. 3. Stem cells within their niche in the bone marrow. (**A**) Schematic diagram of hematopoietic and niche cellular components in the bone marrow. The exact spatial relationships are not well defined. (**B**) Candidate extrinsic signaling pathways that regulate proliferation and differentiation of HSCs. The colors represent the potential cellular elements that send and receive signals as in (A).

Differential expression of three members of the signaling lymphocyte activation molecule (SLAM) cell-surface receptor family have been used to distinguish HSCs from more committed progenitors in situ (*63*). Vascular and endosteal HSC locations were observed. The existence of multiple types of HSC niches begs the question of potential niche-dependent differences in cell fate. Do niches away from the endosteum contain activated HSCs fated to differentiate? Can HSCs traverse among different niche environments? Indeed, parabiotic experiments suggest that HSCs circulate and return to marrow (*64*).

A major challenge is to define accurately the precise cellular components and anatomical structure of the HSC niche. There are only 10,000 to 20,000 HSCs per mouse, suggesting a limiting number of true niches that can support these cells. In addition, transduction of homeobox genes into HSCs can result in dramatic in vitro expansion (*65*). Yet after transplantation of the cultured cells, normal HSC numbers are restored in vivo. Proper HSC localization within a true niche may impose quiescence and thus limit supra-physiological expansion. Alternatively, the available "space" for HSCs within a niche may be limited.

In the ISC and HFSC systems, more committed TA progenitor cells have been localized within the niche. In the hematopoietic system, such populations have been prospectively identified using cell-surface markers (*66*); however, very little is known about their anatomical relationships to the HSCs. If the utility of the SLAM markers is confirmed by other investigators, perhaps these and other markers from numerous genomic profiling efforts will determine if quiescent and activated HSCs, as well as distinct progenitor cells, occupy specific locations within a niche. If so, then a correlated distribution of microenvironmental signals might be expected. In the HFSC system, one study has indeed shown that progenitors committed to different lineages occupy unique positions adjacent to the dermal papilla microenvironment (*30*). Given the circulatory activity of HSCs, a similar analysis will be more difficult. In contrast to the geographical confines of the ISC and HFSC systems, the emerging picture of the HSC niche must allow for the mobile and fluid nature of this tissue.

Relating mechanisms to functional roles in HSC niches is a key area of investigation. Tie2 (receptor)/angiopoietin-1 (Ang-1, ligand) signaling regulates HSC anchorage and quiescence (*67*). Ang-1–expressing OBs and Tie2-expressing, label-retaining HSCs colocalize. The matrix glycoprotein osteopontin (Opn) expressed by endosteal OBs is a negative regulator of HSC proliferation (*68*, *69*). These and other studies (*61*) provide direct evidence for the involvement of matrix components in HSC regulation and further emphasize the importance of regulating anchorage and quiescence as essential features of niche function.

A mechanism for HSC protection within the niche has been identified. Mice with a truncation mutation in the ataxia telangiectasia mutated (ATM) gene have progressive marrow failure due to an HSC defect (*70*). ATM activates a cell-cycle checkpoint that senses DNA damage, telomeric instability, and oxidative stress. Reactive oxygen species (ROS) are elevated in mutant HSCs, and antioxidant treatment rescues their defects. Overexpression studies of candidate mediators implicate the $p16^{INK4a}$ Rb pathway in HSC dysfunction. ATM mutant mice are likely to be intolerant to radiation, precluding their use as recipients of wild-type HSCs. Nevertheless, because the mice are hematologically deficient, transplantation without conditioning may show if the HSC-depleted niches in these mice can support wild-type stem cells. This may provide insights into possible roles for ATM within the microenvironment. Bone is a very low–oxygen tension environment, and mesenchymal progenitors generate OBs more efficiently in such conditions (*71*). Perhaps a normal function of the marrow HSC niche is to provide an environment of low oxygen tension that would inhibit exposure to ROS. Other reports have indicated the importance of low oxygen tension in the maintenance of hematopoietic and neural crest stem cell populations (*72*). The ATM pathway has also been implicated in radioprotective mechanisms that are directed to the ISCs (*73*). It is therefore possible that this pathway may play an essential protective role in all stem cell niches.

Global gene-expression profiles of quiescent and activated HSCs, as well as more committed progenitor populations, have been described (*74*). Numerous members of signaling and other regulatory pathways are present in these molecular signatures. In addition, a comprehensive genomic analysis of an HSC-supportive microenvironmental cell type has been performed (*75*). It is likely that valuable further insights into HSC regulation will emerge.

If Niches Were Wishes

A stem cell niche is an interactive structural unit, organized to facilitate cell-fate decisions in a proper spatiotemporal manner. Key signaling and molecular cross-talk events are patterned to occur in the right place at the right time. Among these three mammalian systems, certain themes emerge: (i) Anatomical organization, best defined for ISC and HFSC niches, coordinates stem cell function in space and time. (ii) Both positive and negative signaling are integrated. The Bmp/Wnt axis represents one such example. (iii) Intercellular signaling pathways are shared.

Challenges for the future include the following: (i) The development of equivalent definitions and assay systems for all three stem cell systems. For example, in the HFSC and HSC systems, prospective isolation and transplantation assays are available, whereas these do not yet exist for ISCs. The distinction between true stem cells and TA cells needs to be clarified and made uniform in all three systems. In addition, it will be necessary to ask if this and other commitment decisions are "hard and fast" or reversible. The reversibility of early commitment events mediated by the niche has been shown in the *Drosophila* germ line (*76*, *77*). A recent study in the hematopoietic system showed that constitutively active β-catenin, expressed in committed progenitors, results in a "reacquisition" of some stem cell properties (*78*). (ii) A more comprehensive analysis of niche signaling pathways. There are suggestions that other pathways, such as Hedgehog signaling, are important. Comprehensive molecular analyses of directly isolated microenvironmental cells would provide their signaling repertoire. This type of study has been performed with hair follicle dermal papillae and surrounding cell types to investigate the mesenchymal-epithelial cross talk (*79*). Molecules such as Noggin and other components of the Bmp signaling pathway are preferentially expressed in the papillae, further supporting its role as a key signaling center for the HFSC. However, numerous other molecules, such as Wnt proteins and their inhibitors, are also expressed, precluding a coherent picture of orchestrated biological functions. The development and application of more quantitative techniques to analyze the dynamics of signaling pathways at the single cell level may provide further insights. (iii) The development of in vitro systems that accurately recapitulate the in vivo functions of niches. Ultimately, it will be necessary to reconstruct these from defined cellular and molecular components. This will allow a definition of asymmetric division, as well as the intricate macromolecular aspects of multicellular interactions within niches. (iv) The development of effective real-time imaging technologies to analyze stem cell behavior in vitro and niche function in vivo. (v) The description of macromolecular assemblies at the interfaces of cells within the niche. In immunology, such assemblies are called "immunological synapses," and they integrate intercellular signaling. (vi) Elucidation of how signals in the niche are coupled to processes such as cell-cycle regulation and distinct transcriptional programs in a cell-type specific manner. (vii) Elucidation of how niches are altered in situations of stress or pathology. Finally, we suggest that a proper understanding of dysregulated stem cells in cancer requires not just a description of intrinsic processes but also a functional analysis of intact cancer stem cell niches. Indeed, the ability of a tumor cell to orchestrate the establishment of a favorable niche for metastasis has now emerged (*80*).

References and Notes

1. R. Schofield, *Blood Cells* **4**, 7 (1978).
2. H. Lin, *Nat. Rev. Genet.* **3**, 931 (2002).
3. C. S. Potten, M. Loeffler, *Development* **110**, 1001 (1990).
4. J. I. Gordon, G. H. Schmidt, K. A. Roth, *FASEB J.* **6**, 3039 (1992).
5. C. Booth, C. S. Potten, *J. Clin. Invest.* **105**, 1493 (2000).
6. C. S. Potten, G. Owen, D. Booth, *J. Cell Sci.* **115**, 2381 (2002).
7. F. Radtke, H. Clevers, *Science* **307**, 1904 (2005).
8. E. Batlle *et al.*, *Cell* **111**, 251 (2002).
9. M. van de Wetering *et al.*, *Cell* **111**, 241 (2002).
10. A. Gregorieff *et al.*, *Gastroenterology* **129**, 626 (2005).
11. T. Byun *et al.*, *J. Clin. Pathol.* **58**, 515 (2005).
12. X. C. He *et al.*, *Nat. Genet.* **36**, 1117 (2004).
13. A. P. Haramis *et al.*, *Science* **303**, 1684 (2004).
14. B. B. Madison *et al.*, *Development* **132**, 279 (2005).
15. F. Giudicelli, J. Lewis, *Curr. Opin. Genet. Dev.* **14**, 407 (2004).
16. S. Fre *et al.*, *Nature* **435**, 964 (2005).
17. J. H. van Es *et al.*, *Nature* **435**, 959 (2005).
18. T. S. Stappenbeck, J. C. Mills, J. I. Gordon, *Proc. Natl. Acad. Sci. U.S.A.* **100**, 1004 (2003).
19. L. Alonso, E. Fuchs, *Proc. Natl. Acad. Sci. U.S.A.* **100** (suppl. 1), 11830 (2003).
20. M. Ito *et al.*, *Nat. Med.* **11**, 1351 (2005).
21. V. Levy, C. Lindon, B. D. Harfe, B. A. Morgan, *Dev. Cell* **9**, 855 (2005).
22. G. Cotsarelis, T. T. Sun, R. M. Lavker, *Cell* **61**, 1329 (1990).
23. H. Oshima, A. Rochat, C. Kedzia, K. Kobayashi, Y. Barrandon, *Cell* **104**, 233 (2001).
24. R. J. Morris *et al.*, *Nat. Biotechnol.* **22**, 411 (2004).
25. R. J. Morris, C. S. Potten, *Cell Prolif.* **27**, 279 (1994).
26. T. Tumbar *et al.*, *Science* **303**, 359 (2004).
27. C. Blanpain, W. E. Lowry, A. Geoghegan, L. Polak, E. Fuchs, *Cell* **118**, 635 (2004).
28. S. Claudinot, M. Nicolas, H. Oshima, A. Rochat, Y. Barrandon, *Proc. Natl. Acad. Sci. U.S.A.* **102**, 14677 (2005).
29. N. M. Joseph, S. J. Morrison, *Dev. Cell* **9**, 173 (2005).
30. E. Legue, J. F. Nicolas, *Development* **132**, 4143 (2005).
31. T. Lechler, E. Fuchs, *Nature* **437**, 275 (2005).
32. U. Gat, R. DasGupta, L. Degenstein, E. Fuchs, *Cell* **95**, 605 (1998).
33. D. Van Mater, F. T. Kolligs, A. A. Dlugosz, E. R. Fearon, *Genes Dev.* **17**, 1219 (2003).
34. C. Lo Celso, D. M. Prowse, F. M. Watt, *Development* **131**, 1787 (2004).
35. V. Silva-Vargas *et al.*, *Dev. Cell* **9**, 121 (2005).
36. K. M. Braun *et al.*, *Development* **130**, 5241 (2003).
37. K. Kobielak, H. A. Pasolli, L. Alonso, L. Polak, E. Fuchs, *J. Cell Biol.* **163**, 609 (2003).
38. T. Andl *et al.*, *Development* **131**, 2257 (2004).
39. C. Jamora, R. DasGupta, P. Kocieniewski, E. Fuchs, *Nature* **422**, 317 (2003).
40. V. A. Botchkarev *et al.*, *Nat. Cell Biol.* **1**, 158 (1999).
41. W. E. Lowry *et al.*, *Genes Dev.* **19**, 1596 (2005).
42. J. Huelsken, R. Vogel, B. Erdmann, G. Cotsarelis, W. Birchmeier, *Cell* **105**, 533 (2001).
43. I. Flores, M. L. Cayuela, M. A. Blasco, *Science* **309**, 1253 (2005).
44. K. Y. Sarin *et al.*, *Nature* **436**, 1048 (2005).
45. S. A. Benitah, M. Frye, M. Glogauer, F. M. Watt, *Science* **309**, 933 (2005).
46. R. S. Taichman, *Blood* **105**, 2631 (2004).
47. J. Zhang *et al.*, *Nature* **425**, 836 (2003).
48. L. M. Calvi *et al.*, *Nature* **425**, 841 (2003).
49. A. Wilson *et al.*, *Genes Dev.* **18**, 2747 (2004).
50. T. Reya *et al.*, *Nature* **423**, 409 (2003).
51. K. Willert *et al.*, *Nature* **423**, 448 (2003).
52. A. W. Duncan *et al.*, *Nat. Immunol.* **6**, 314 (2005).
53. M. Cobas *et al.*, *J. Exp. Med.* **199**, 221 (2004).
54. S. J. Mancini *et al.*, *Blood* **105**, 2340 (2005).
55. J. J. Trowbridge, A. Xenocostas, R. T. Moon, M. Bhatia, *Nat. Med.* **12**, 89 (2006).
56. T. Cheng *et al.*, *Science* **287**, 1804 (2000).
57. Y. Yuan, H. Shen, D. S. Franklin, D. T. Scadden, T. Cheng, *Nat. Cell Biol.* **6**, 436 (2004).
58. I. K. Park *et al.*, *Nature* **423**, 302 (2003).
59. D. Visnjic *et al.*, *Blood* **103**, 3258 (2004).
60. H. Taniguchi, T. Toyoshima, K. Fukao, H. Nakauchi, *Nat. Med.* **2**, 198 (1996).
61. B. Heissig *et al.*, *Cell* **109**, 625 (2002).
62. G. B. Adams *et al.*, *Nature* **439**, 599 (2006).
63. M. J. Kiel, O. H. Yilmaz, T. Iwashita, C. Terhorst, S. J. Morrison, *Cell* **121**, 1109 (2005).
64. D. E. Wright, A. J. Wagers, A. P. Gulati, F. L. Johnson, I. L. Weissman, *Science* **294**, 1933 (2001).
65. J. Antonchuk, G. Sauvageau, R. K. Humphries, *Cell* **109**, 39 (2002).
66. M. Kondo *et al.*, *Annu. Rev. Immunol.* **21**, 759 (2003).
67. F. Arai *et al.*, *Cell* **118**, 149 (2004).
68. S. K. Nilsson *et al.*, *Blood* **106**, 1232 (2005).
69. S. Stier *et al.*, *J. Exp. Med.* **201**, 1781 (2005).
70. K. Ito *et al.*, *Nature* **431**, 997 (2004).
71. D. P. Lennon, J. M. Edmison, A. I. Caplan, *J. Cell. Physiol.* **187**, 345 (2001).
72. S. J. Morrison *et al.*, *J. Neurosci.* **20**, 7370 (2000).
73. H. J. Ch'ang *et al.*, *Nat. Med.* **11**, 484 (2005).
74. C. E. Eckfeldt, E. M. Mendenhall, C. M. Verfaillie, *Nat. Rev. Mol. Cell Biol.* **6**, 726 (2005).
75. J. A. Hackney *et al.*, *Proc. Natl. Acad. Sci. U.S.A.* **99**, 13061 (2002).
76. C. Brawley, E. Matunis, *Science* **304**, 1331 (2004).
77. T. Kai, A. Spradling, *Proc. Natl. Acad. Sci. U.S.A.* **100**, 4633 (2003).
78. Y. Baba, K. P. Garrett, P. W. Kincade, *Immunity* **23**, 599 (2005).
79. M. Rendl, L. Lewis, E. Fuchs, *PLoS Biol.* **3**, e331 (2005).
80. R. N. Kaplan *et al.*, *Nature* **438**, 820 (2005).

81. K.A.M. and I.R.L. are supported by grants from the National Heart, Lung, and Blood Institute and the National Institute of Diabetes and Digestive and Kidney Diseases of the NIH.

10.1126/science.1110542

How Fast Was Wild Wheat Domesticated?

Ken-ichi Tanno[1] and George Willcox[2]*

The earliest cereal gathering has been dated to 19,000 years before the present (yr B.P.) (*1*) in the Near East. The origins of agriculture have been dated to between 10,500 and 9500 yr B.P. for the region of southeastern Turkey and northern Syria (*2*), where wild wheats [einkorn, *Triticum boeoticum* Boiss and emmer, *T. dicoccoides* (Körn) Aschers and Graebner] still grow today. Wild cereals with dehiscent ears shatter at maturity into dispersal units called spikelets, identifiable by their smooth abscission scars (Fig. 1, A to C). The first domestic cereals arose from mutants, which have indehiscent ears with spikelets that do not shatter but separate when threshed, identifiable by jagged scars (Fig. 1, D and E).

The earliest indehiscent domestic wheat has been recognized in archaeological levels dated to ~9250 yr B.P. How long was wild wheat cultivated before this date? Estimates vary from less than 200 (*3*) to at least several hundred years (*4*). We examined 9844 ancient charred spikelets from four archaeological sites located in northern Syria and southeastern Turkey dating between 10,200 and 6500 yr B.P. to evaluate how quickly domestic wheat emerged. Most of the specimens were damaged by fire or when the wheat was threshed, but 804 were identifiable. The earliest site, which was dated to 10,200 yr B.P., produced no definite domestic spikelets; however, on the three younger sites, domestic spikelets increased progressively. The number of terminal spikelets also increased. In wild populations, terminal spikelets fall first, because the ear disarticulates from the top down; so with increasing indehiscence, terminal spikelets become more frequent (*5*). An independent study of barley—which was domesticated in the same way—at two sites near Damascus (*6*) demonstrated that 30% of the spikelets that were dated to 9300 to 8500 yr B.P. were domestic, and by 8500 to 7500 yr B.P., the number increased to 60%. The combined results (Fig. 1F) indicate that indehiscence took over one millennium to become established. Selection for large cereal grains was slow. Measurements taken from ancient grains demonstrate that the size of wheat and barley grains remained essentially the same between 9500 and 6500 yr B.P. (*7*). Grain size depends more on the position on the ear and environmental conditions than on genetic diversity.

If early farmers harvested after the ears began to shatter, indehiscent mutants would be rapidly adopted. But farmers probably harvested before the spikelets fell to avoid loss, so indehiscence was not advantageous. Furthermore, when crops failed, farmers would have had to gather from the wild. These two practices lowered the probability of the rare indehiscent mutant being selected. Fast artificial selection, as opposed to slow natural selection, was improbable, because domestic traits such as indehiscence and lack of dormancy are not readily visible. Cultivation of wild cereals between 10,500 and 9250 yr B.P. has been posited on the basis of finds of field weeds (*8*) and because many gathered plants were abandoned in favor of wheat and barley, which on some sites were found outside their natural habitats. These findings were not compatible with rapid domestication. We argue that wild cereals could have been cultivated for over one millennium before the emergence of domestic varieties. Domestication was a series of events occurring at different places over thousands of years, during which wild wheat persisted in cultivated fields (it still occurs today as a weed in Turkey). Our data require consolidation, but combined with the data for barley, they support a gradualist domestication model, suggesting that we should examine the possibility that agriculture arose soon after humans adopted a sedentary existence in the early villages of the Near East (*5*).

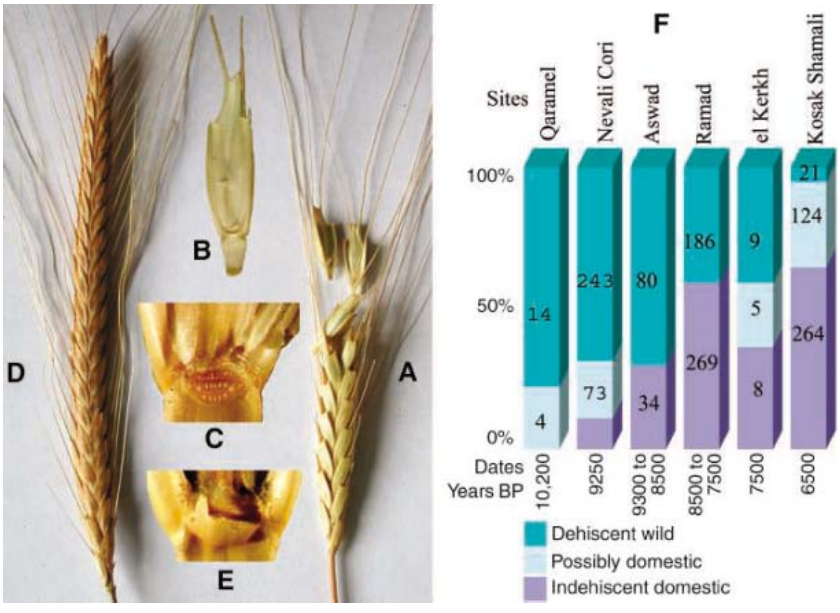

Fig. 1. Modern examples of dehiscent wild einkorn wheat ear (**A**) and spikelet (**B**). Detail of spikelet with smooth wild abscission scar (**C**), indehiscent domestic ear (**D**), and detail of spikelet with jagged break (**E**) are shown. The bar chart (**F**) gives relative frequencies of subfossil finds with the absolute figures. Records from Aswad and Ramad (*6*) are of barley; the other four sites are of wheat. For full data of both studies, see table S1.

References and Notes

1. All dates are in noncalibrated ^{14}C years before the present.
2. S. Lev-Yadun, A. Gopher, S. Abbo, *Science* **288**, 1602 (2000).
3. G. Hillman, S. Davies, *J. World Prehistory* **4**, 157 (1990).
4. M. Kislev, *Isr. J. Plant Sci.* **50**, 85 (2002).
5. The full set of data and references for the sites are available as supporting material on *Science* Online.
6. W. van Zeist, J. H. Bakker-Heeres, *Palaeohistoria* **24**, 165 (1985).
7. G. Willcox, *J. Archaeol. Sci.* **31**, 145 (2004).
8. G. Hillman, R. Hedges, A. Moore, S. Colledge, P. Pettitt, *Holocene* **11**, 383 (2001).

9. We thank R. Pasternack for making available samples from Nevali Cori. This work was partly supported by the European Commission (contract ICA3-CT-2002-10022).

Supporting Online Material

www.sciencemag.org/cgi/content/full/311/5769/1886/DC1
Table S1
References

5 January 2006; accepted 6 March 2006
10.1126/science.1124635

[1]Research Institute for Humanity and Nature, Takashima 335, Kamigyo, 602-0878 Kyoto, Japan. [2]National Centre for Scientific Research (CNRS), Unité Mixte de Recherche 5133, Jalès, Berrias 07460, France.

*To whom correspondence should be addressed. E-mail: george.willcox@mom.fr

A Mitotic Lamin B Matrix Induced by RanGTP Required for Spindle Assembly

Ming-Ying Tsai,[1] Shusheng Wang,[1] Jill M. Heidinger,[1,2] Dale K. Shumaker,[3] Stephen A. Adam,[3] Robert D. Goldman,[3] Yixian Zheng[1,2]*

Mitotic spindle morphogenesis is a series of highly coordinated movements that lead to chromosome segregation and cytokinesis. We report that the intermediate filament protein lamin B, a component of the interphase nuclear lamina, functions in spindle assembly. Lamin B assembled into a matrix-like network in mitosis through a process that depended on the presence of the guanosine triphosphate–bound form of the small guanosine triphosphatase Ran. Depletion of lamin B resulted in defects in spindle assembly. Dominant negative mutant lamin B proteins that disrupt lamin B assembly in interphase nuclei also disrupted spindle assembly in mitosis. Furthermore, lamin B was essential for the formation of the mitotic matrix that tethers a number of spindle assembly factors. We propose that lamin B is a structural component of the long-sought-after spindle matrix that promotes microtubule assembly and organization in mitosis.

Mitotic spindle assembly and chromosome segregation are dynamic processes requiring the coordinated activities of microtubules (MT), MT-based motors, MT-binding proteins, and chromosomes (*1*). It was proposed decades ago that a static scaffold (spindle matrix) might tether spindle assembly factors (SAF) and support the assembly and force production of spindle microtubules (*2*, *3*). However, the molecular nature of the spindle matrix remains elusive.

Much progress in understanding spindle morphogenesis and chromosome segregation has come from genetic screens that identified mutated genes causing cell cycle arrests, mitosis-specific defects, or both, in vivo. Such genetic analysis has led to the identification and characterization of SAFs that have specific mitotic functions. However, genetic analyses could overlook mitotic regulators that also have important functions in interphase. For example, the mitotic role of the guanosine triphosphatase (GTPase) Ran, a protein with well-established function in interphase nuclear trafficking (*4*), was overlooked by genetic studies. Genetic studies could not distinguish between a direct role for Ran in mitosis or an indirect one due to a failure in interphase nuclear trafficking (*5*–*7*). It is now understood that RanGTPase uses similar principles to regulate nuclear functions in interphase and spindle assembly in mitosis (*8*–*11*).

Such dual functions of the Ran system in interphase and mitosis could have more profound implications. From an evolutionary perspective, RanGTPase appears to have branched off relatively early from the related GTPases (*12*, *13*). This may have coincided with the coevolution of the mitotic spindle apparatus and the interphase nucleus in eukaryotes (*13*). We reasoned that such coevolving relationships could also lead to sharing of components that regulate both the interphase nucleus and the mitotic spindle apparatus and that such multifunctional components might be missed in genetic screens.

In addition to chromatin, the interphase nucleus contains the nuclear membrane with associated nuclear pore complexes and the nuclear lamina. The major components of the nuclear lamina are the type V intermediate filament proteins called lamins. The lamins are grouped into A and B types on the basis of their

[1]Department of Embryology, Carnegie Institution of Washington and Howard Hughes Medical Institute, Baltimore, MD 21218, USA. [2]Department of Biology, Johns Hopkins University, Baltimore, MD 21218, USA. [3]Department of Cell and Molecular Biology, Northwestern University Feinberg School of Medicine, Chicago, IL 60611, USA.

*To whom correspondence should be addressed. E-mail: zheng@ciwemb.edu

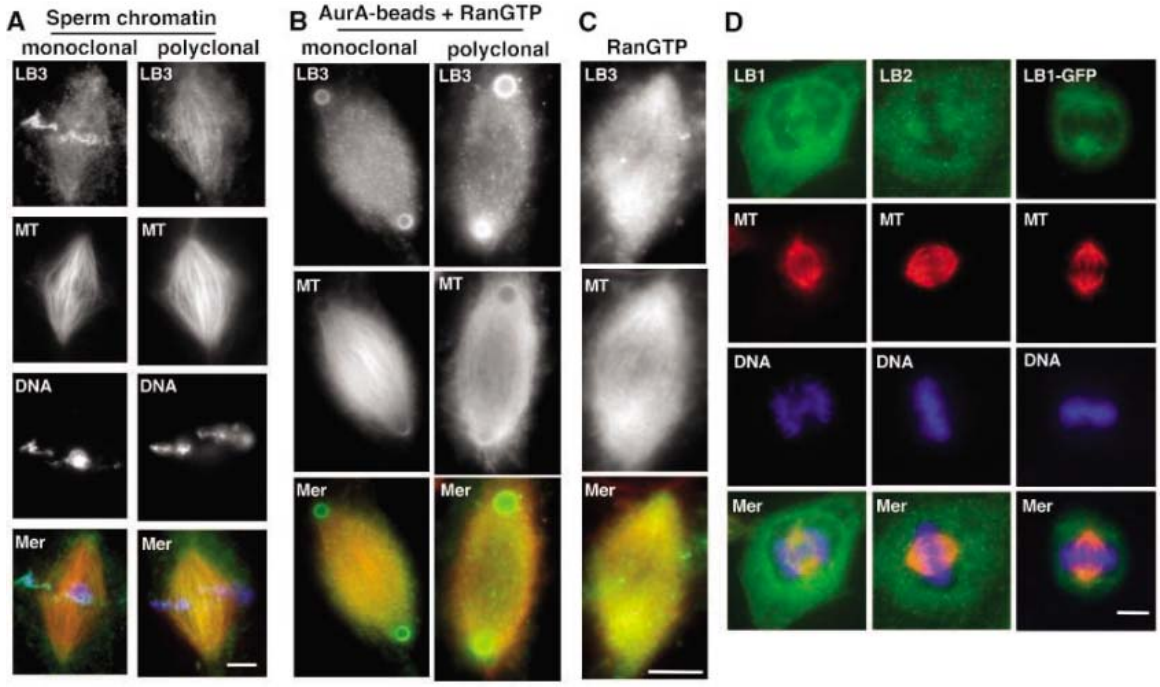

Fig. 1. Association of lamin B with mitotic spindles assembled in *Xenopus* egg extracts and HeLa cells. (**A**) *Xenopus* lamin B detected by either monoclonal or polyclonal (full-length LB3 protein as antigen) LB3 antibody (green). The monoclonal antibody also recognizes the sperm-specific LB4. MTs were labeled with rhodamin tubulin (red). DNA was labeled with 4′,6′-diamidino-2-phenylindole (DAPI, blue). (**B** and **C**) Spindles induced by AurA beads and RanGTP (B) or RanGTP alone (C). LB3 was detected with monoclonal (B) or polyclonal antibodies [antigens are either a peptide corresponding to LB3 (B) or full-length LB3 protein (C), green]. (**D**) Mitotic spindles as detected by antibodies to LB1 or LB2 or green fluorescent protein (GFP)–tagged LB1 in HeLa cells. Spindle MTs were detected with tubulin antibody (red). Scales: white bars, 10 μm; magnetic beads, 2.8 μm.

biochemical properties (*14*). Lamin B proteins are ubiquitously expressed in metazoans and are essential for cell viability (*15*). The A-type lamins are not essential for cell viability, are developmentally regulated, and are expressed primarily in differentiated cells (*16*). Lamins are important for nuclear functions, including nuclear envelope assembly (*17*, *18*), nuclear size and shape, DNA replication (*19*), and RNA polymerase II–driven gene expression (*20*, *21*). They also provide mechanical support for the maintenance of the structural integrity of the nucleus and anchorage and organization sites for interphase chromatin (*16*).

Consistent with the idea that the interphase nuclear components may be used to regulate mitosis, specific nucleoporins are localized to kinetochores, where they regulate the interaction between MTs and kinetochores in mitosis (*22*–*24*). Moreover, down-regulation of the single lamin gene in *Caenorhabditis elegans* leads to cell division defects and eventual cell death (*25*). Because a fraction of lamin B associates with spindles in mitosis in mammalian cells (*19*, *26*–*28*), we used in vivo and in vitro assays to study the mitotic function of lamin B. We show that lamin B is required for spindle assembly and propose that lamin B is a structural component of a spindle-associated matrix that tethers various spindle assembly factors.

Association of lamin B with mitotic spindles. We tested whether the major lamin B isoform in *Xenopus* eggs, lamin B3 (LB3) (*29*), was associated with mitotic spindles assembled in extracts made from the cytostatic-factor-arrested *Xenopus* eggs (M-phase egg extracts). Mitotic spindles were assembled in extracts to which we added *Xenopus* sperm chromatin, RanGTP (RanL43E and RanQ69L both have point mutations in the effector domain that mimic the GTP-bound state) (*30*, *31*), or RanGTP plus magnetic beads coated with protein kinase Aurora A (AurA beads) (*32*). AurA beads function as microtubule organizing centers (MTOC) in the presence of RanGTP to stimulate assembly of both MT asters and spindles, whereas beads coated with the catalytically inactive AurA (AurA-AA) fail to do so (*33*). Immunofluorescence using antibodies to LB3 (*34*, *35*) showed that LB3 was associated with spindles and the peripheral region surrounding the spindle (Fig. 1, A to C) (*32*). Little LB3 staining could be detected in areas devoid of MT structures. Immunofluorescence staining of HeLa cells showed that a fraction of the human lamin B, LB1 and LB2 (*36*), was associated with spindles in mitosis (Fig. 1D). Moreover, a fraction of an LB1–green fluorescence fusion protein expressed in HeLa cells was also associated with mitotic spindles (*32*) (Fig. 1D).

Requirement of lamin B for spindle assembly. To determine whether LB has a role in spindle assembly, we reduced expression of either LB1 or LB2 in HeLa cells by small interfering RNA (siRNA) (*32*) (Fig. 2A). Depletion of either isoform caused an increase in spindle defects (Fig. 2, A to C). Typical mitotic defects included unfocused spindle poles (as judged by localization of γ-tubulin) or poor spindle morphology with mild to severe lack of chromosome congression (Fig. 2C). Consistent with the spindle defects, live imag-

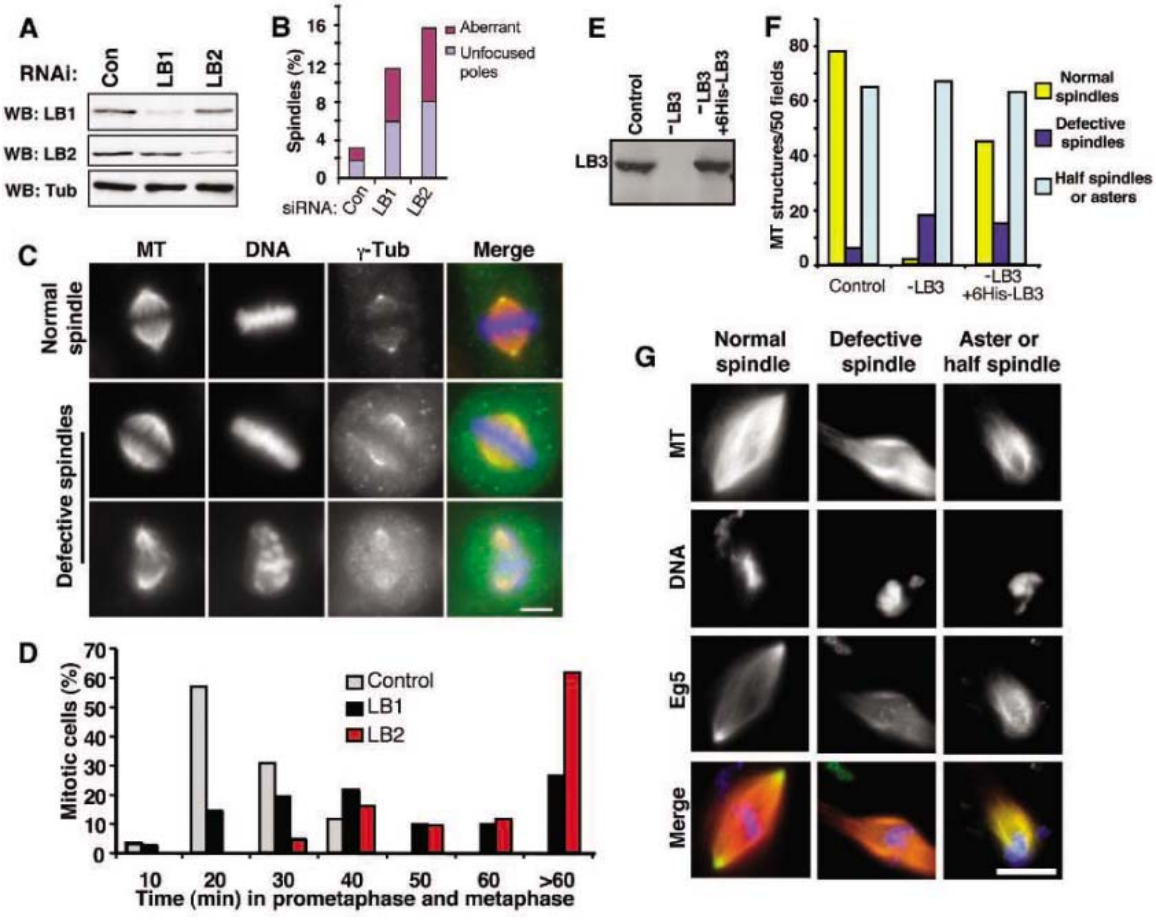

Fig. 2. Requirement of lamin B for proper spindle assembly and function in mitosis. (**A**) Immunoblotting to detect LB1, LB2, or tubulin in HeLa cells treated with control or LB siRNAs. (**B**) Quantification of spindle defects in control or LB siRNA-treated cells. At least 100 mitotic cells were analyzed for each siRNA treatment. Shown are representative quantifications of at least six independent experiments with two different siRNA sequences. (**C**) Examples of normal and defective spindles (unfocused spindle poles or abnormal spindle lacking chromosome congression) in (B) stained with antibodies to γ-tubulin (green) and α-tubulin (red). Defective spindles are from HeLa cells treated with LB siRNAs. (**D**) Effect of depletion of LB on the timing of chromosome alignment and segregation. Control or LB siRNA-treated HeLa cells were imaged. The elapsed time from chromosome congression (the appearance of chromosomal bar) to chromosome separation (splitting of the bar into two) (see fig. S1) in 50 to 100 mitotic cells was analyzed for each siRNA treatment. (**E**) Immunodepletion and add-back of LB3. Rabbit polyclonal or mouse monoclonal antibody to LB3 was used for immunodepletion. 6His-LB3 was added back to the LB3-depleted egg extracts to a final concentration of 0.2 μM. Rabbit or mouse nonimmunized immunoglobulin G was used as a control. (**F**) Quantification of MT structures in 50 random fields. (**G**) Examples of different MT structures (red) immunostained with Eg5 antibodies (green). DNA was stained with DAPI (blue). The defective spindle, aster, or half-spindle shown is from LB3-depleted egg extracts. Scale bars, 10 μm.

ing revealed that LB siRNA-treated cells spent a longer time in prometaphase and metaphase as compared with controls (Fig. 2D and fig. S1). Thus, spindle assembly and function appear to require an appropriate amount of both LB1 and LB2.

Because LB has an important function in the interphase nucleus, the spindle defects observed above could be an indirect effect of perturbing interphase nuclear functions. To determine whether LB has a direct role in spindle assembly, we used M-phase egg extracts. *Xenopus* LB3 was immunodepleted from the M-phase extracts with polyclonal or monoclonal antibodies (*32*) (Fig. 2E). Depleting LB3 by either antibody resulted in severe disruption of spindle assembly, whereas adding back the bacterially expressed and purified 6His-LB3 partially rescued spindle assembly (Fig. 2, F and G) (*32*). Therefore, LB appears to have a mitosis-specific function in spindle assembly.

Assembly of lamin B–containing matrix on mitotic spindles induced by RanGTP. Purified soluble LB3 neither bound to MTs assembled from purified tubulin nor promoted MT assembly in vitro (*32*) (fig. S2). As an intermediate filament protein, LB might regulate SAFs as a polymer or as a soluble protein to promote spindle assembly. We therefore made spindles in egg extracts with either sperm chromatin or AurA beads plus RanGTP, or AurA beads plus 5% dimethylsulfoxide (DMSO), which stimulates assembly of MT asters but not spindles (Fig. 3, A and B) (*30*, *37*). In some experiments, the in vitro–assembled spindles and asters were treated with nocodazole to depolymerize MTs (*32*). Asters were present in extracts containing AurA beads plus DMSO, but these asters were not associated with AurA beads (Fig. 3B). After depolymerization of MTs with nocodazole, the LB3 antibody revealed a fibrillar-granular matrix surrounding more than 90% of sperm chromatin or AurA beads with RanGTP (Fig. 3, A and B, and fig. S3A). In the reaction containing AurA beads and DMSO, few LB3 matrices were found after the addition of nocodazole, and these matrices did not associate with the AurA-beads (Fig. 3B). The fibrillar-granular appearance (fig. S3A) suggests that the matrix might contain membranes. Indeed, the lipid dye (CM-DiI) stained the spindles (fig. S3B) and the matrix (fig. S3C), and Triton X100 treatment completely disrupted the matrix (fig. S3D).

We also assembled spindles on AurA beads with RanGTP, initiated MT depolymerization with nocodazole, and then examined LB3 matrices at various time points. LB3 matrices appeared at all stages of MT disassembly (Fig. 3C). However, the SAF TPX2 (*38*), which has a similar dynamic behavior to that of tubulin (*39*), disappeared as MTs were disassembled in these reactions (Fig. 3C). Thus, LB3 appears to associate with MTs as part of a matrix structure in mitosis.

To study whether MT polymerization is necessary for the formation of the LB3 matrix, we assembled LB3 matrix in the absence of MT polymerization. As a control, spindle MTs assembled in the absence of nocodazole were subsequently depolymerized with nocodazole. LB3 matrices assembled around AurA beads in the presence of RanGTP whether MTs were allowed to polymerize or not (Fig. 3D). However, if MTs were allowed to polymerize, a higher percentage of AurA beads was associated with the matrix. Moreover, the matrix assembled with MTs usually surrounded the AurA beads completely, whereas the matrix assembled in the absence of MTs usually partially surrounded the beads. In the absence of RanGTP, little LB3 matrix was formed (Fig. 3D). Therefore, RanGTP, but not MTs, appears to be required for the assembly of LB3 matrix around the AurA beads.

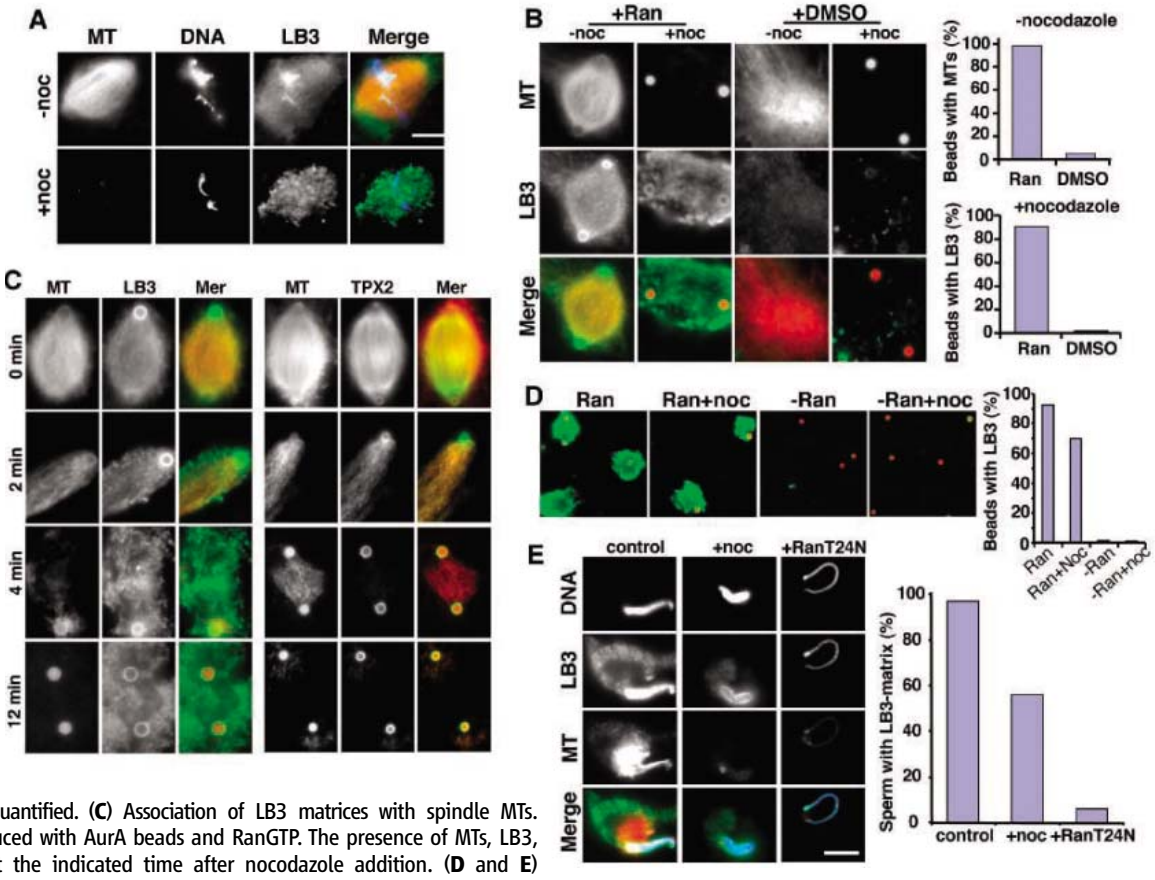

Fig. 3. Requirement of RanGTP for assembly of LB3 matrices. (**A**) Association of LB3 matrices with sperm chromatin. Spindle assembly was induced with *Xenopus* sperm chromatin, and spindle MTs were subsequently depolymerized using nocodazole. MTs (red), LB3 matrix (green), and chromatin (blue) were labeled with rhodamine-tubulin, LB3 monoclonal antibody, and DAPI, respectively. (**B**) Association of LB3 matrices with AurA beads in the presence of RanGTP. MT assembly was induced with AurA beads and RanGTP or AurA beads and DMSO, and MTs were subsequently depolymerized with nocodazole. The percentages of AurA beads that were associated with MTs (red) or LB3 matrix (green) under different conditions were quantified. (**C**) Association of LB3 matrices with spindle MTs. Spindle assembly was induced with AurA beads and RanGTP. The presence of MTs, LB3, or TPX2 was examined at the indicated time after nocodazole addition. (**D** and **E**) Requirement of RanGTP but not MT polymerization for assembly of LB3 matrices around AurA beads (D) or sperm chromatin (E). AurA beads (D) were incubated with egg extracts with or without RanGTP in the presence or absence of nocodazole. Images show AurA beads (red) and LB3 matrix (green). Results were quantified as above. Sperm chromatin (E) was incubated with M-phase egg extracts in the presence or absence of nocodazole or RanT24N for 5 min. MT (red), LB3 (green), and chromatin (blue). Scales: white bars, 10 μm; magnetic beads, 2.8 μm.

We also examined the requirement of RanGTP and MTs for the assembly of LB3 matrices around sperm chromatin. We inhibited RanGTP production on the sperm chromatin with RanT24N (a dominant negative Ran mutant). More than 90% of the sperm chromatin was associated with an LB3 matrix assembled during a 5-min incubation (Fig. 3E). MTs and LB3 matrix formed quickly, but the two structures did not always associate with one another, and often the formation of the LB3 matrix appeared to precede that of MTs (Fig. 3E and fig. S4). When MT assembly was inhibited by nocodazole, the matrix was still assembled around more than half of the sperm, but these matrices were smaller than those assembled in the presence of MTs (Fig. 3E). RanT24N almost completely inhibited the assembly of LB3 matrix around the sperm chromatin (Fig. 3E).

Retention of SAFs by the lamin B matrix after MT disassembly. Two SAFs, NuMA and Eg5, are proposed to be either components of the putative spindles matrix or tethered to the spindle matrix (*40*, *41*). Poly(ADP-ribose) (PAR) also appears to be part of a static scaffold for proper spindle assembly (*39*). To test whether the LB3 matrix is part of the putative spindle matrix that tethers SAFs, we used sperm chromatin or AurA beads with RanGTP to induce spindle assembly. After MT disassembly, a number of SAFs [PAR, NuMA, Eg5, and XMAP215 (a SAF that promotes MT assembly)] remained associated with a matrix (Fig. 4A). Both LB3-containing matrices and SAF-containing matrices exhibited similar associations with AurA beads, and the majority of the matrices contained one or two beads (Fig. 4B). Many matrices that associated with two beads resembled spindles in size and shape (Fig. 4A). However, few TPX2-containing matrices remained after MT disassembly. Double immunofluorescence analyses of matrices assembled in the absence of MTs revealed the presence of both LB3 and SAFs in the same matrices (Fig. 4C). Matrices assembled in the absence of MTs were mostly associated with single AurA beads (Fig. 4C).

To determine whether LB3 is a structural component of the observed matrices containing SAFs, we immunodepleted LB3 from M-phase extracts and used sperm or AurA beads with

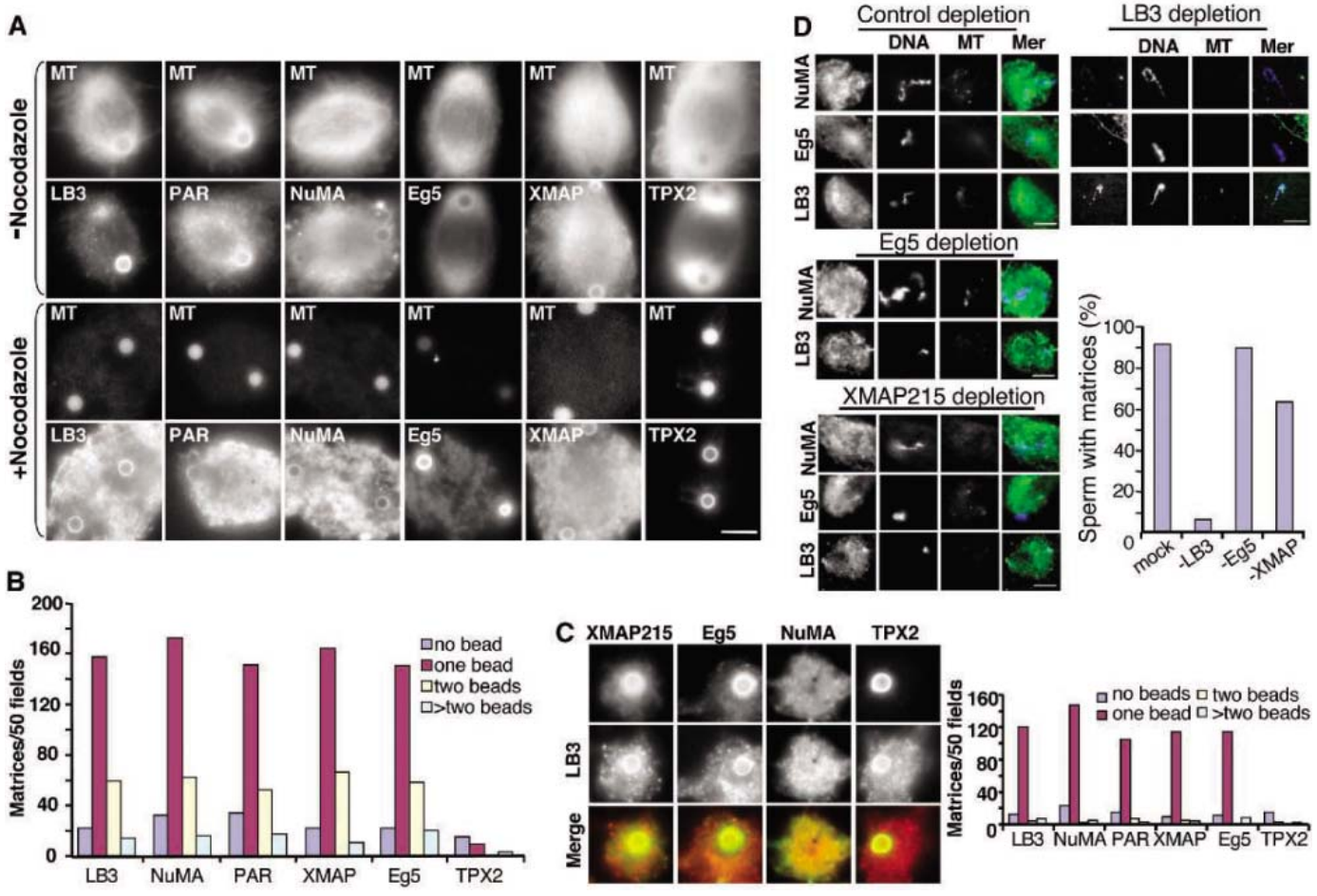

Fig. 4. Requirement of LB3 for the assembly of LB3 matrices that contain SAFs. (**A**) Similarity of LB3 matrices and SAF matrices. Spindle assembly was induced with AurA beads and RanGTP. After MT depolymerization, the remaining structures were immunostained with antibodies to LB3, PAR, NuMA, Eg5, XMAP215, or TPX2. Rhodamine tubulin was used to label MTs. (**B**) Quantification of LB3 or SAF matrices in 50 random fields from (A) that were associated with 0, 1, 2, or more than 2 beads. (**C**) Presence of SAF in LB3 matrices. LB3 matrices were assembled with AurA beads and RanGTP in the absence of MT assembly and double immunostained for SAFs (XMAP215, Eg5, or NuMA in green) and LB3 (red). The graph shows the quantification of LB3, NuMA, PAR, XMAP215, Eg5, and TPX2 positive matrices associated with 0, 1, 2, or more than 2 AurA beads in 50 random fields. (**D**) Requirement of LB3 for the assembly of matrices containing Eg5 and NuMA. Egg extracts were first immunodepleted of LB3, Eg5, or XMAP215 with their respective antibodies and then incubated with sperm chromatin. After depolymerization of MTs, the sperm chromatin was stained with DAPI (blue) and antibodies to LB3, Eg5, or NuMA (green). Rhodamine-tubulin was used to label MTs (red). The percentage of sperm chromatin with associated matrices that contain LB3, Eg5, or NuMA were quantified. When either Eg5 or XMAP215 was depleted from the egg extracts, associations of NuMA, Eg5 (XMAP215 depletion), or LB3 with sperm chromatin as matrices were similar. However, when LB3 was depleted, neither LB3 nor NuMA and Eg5 associated with sperm chromatin as matrices. Shown is a typical graph quantifying the association of LB3 matrix with sperm chromatin. Scales: white bars, 10 μm; magnetic beads, 2.8 μm.

RanGTP to stimulate matrix assembly. Depletion of LB3 inhibited the assembly of matrix structures containing LB3, NuMA, or Eg5 (Fig. 4D), as well as XMAP215 and PAR (*42*). However, depletion of either Eg5 or XMAP215 still allowed assembly of LB3 matrices that contained other SAFs (Fig. 4D). Therefore, lamin B appeared to be required for the assembly of a spindle-associated matrix that contains a number of SAFs. The LB3 matrix induced by RanGTP could be the long-sought-after spindle matrix that tethers SAFs to support spindle assembly.

The assembly of the LB3 matrix required RanGTP but not MTs (Fig. 3). RanGTP stimulates spindle assembly in *Xenopus* egg extracts by causing the release of bound SAFs from importin α and β (*8*–*10*). The C-terminal domain of LB3 contains a nuclear localization signal (NLS) (*36*) that bound to bacterially expressed importin α in vitro (fig. S5A). In M-phase extracts, LB3 interacted with importin α and β, and this interaction was disrupted in the presence of RanGTP (fig. S5B). To determine a potential role for importin α and β in the maintenance of the LB3 matrix, spindles assembled in the egg extracts were diluted by a factor of 100 in extract buffer in the presence of nocodazole and purified importin α and β. Because RanGTP concentration is reduced by dilution, it would not be sufficient to sequester the added importin α and β. We found that importin α and β severely disrupted LB3 matrices containing SAFs (fig. S5C) (*32*). The addition of more RanGTP along with importins prevented the disruption (fig. S5C). This suggests that one function of RanGTP in stimulating the assembly of the LB3 matrix in mitosis might be to displace LB3 from importin α and β.

Stimulation of MT assembly by the isolated LB3 matrix. The presence of SAFs in the LB3 matrix could promote polymerization and organization of MTs during spindle assembly. We developed a procedure to biochemically enrich the matrix. Because AurA beads remained associated with spindles and matrices, we could recover the beads from the egg extracts with a magnet (*32*). Structures retrieved from M-phase extracts were treated with nocodazole to depolymerize MTs, and the remaining matrices were washed (*32*) (Fig. 5A). The matrices could alternatively be released from the AurA beads by repeated pipetting, and the released matrices and AurA beads were separately analyzed. Immunoblotting showed that the released matrices contained LB3, NuMA, PAR, Eg5, and XMAP215 but lacked detectable TPX2 and tubulin (Fig. 5, A to D). We have also identified Eg5 as a component of the purified matrix by peptide mass fingerprinting (*42*). These LB3 matrices nucleated MTs in vitro when incubated with pure tubulin. The matrix-nucleated MT arrays were tethered to the matrices, and no MTs were assembled in the absence of the matrices (Fig. 5, E and F). When LB3 matrices were assembled in egg extracts from which the SAF XMAP215 was immunodepleted, these matrices were unable to promote MT assembly (Fig. 5, E and F). This suggests that the LB3 matrices could promote spindle assembly by tethering SAFs.

The requirement for proper assembly of the LB3 matrix in spindle formation. Immunodepletion of LB3 from M-phase egg extracts severely disrupted spindle assembly and pre-

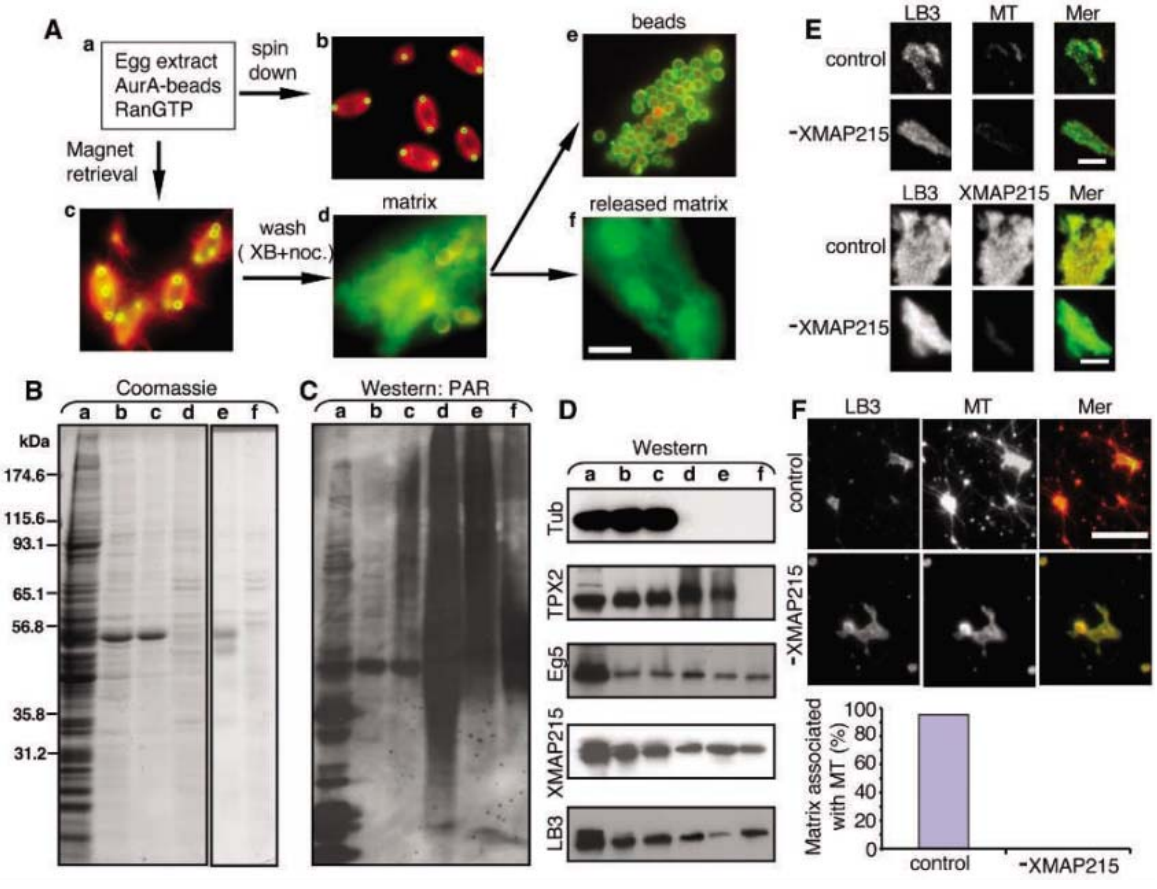

Fig. 5. Isolated LB3 matrices nucleate MT assembly. (**A**) Isolation of LB3 matrix. AurA beads and RanGTP were used to induce spindle assembly in egg extracts (a). Spindles were separated from the egg extracts either by centrifugation through a glycerol cushion onto coverslips (b) or by retrieval with a magnet (c). The magnet-retrieved spindles were washed with buffer containing nocodazole. LB3 matrices were retained on the beads (d). To separate the LB3 matrices from the beads, the sample was pipetted repeatedly. Beads (e) were then retrieved with a magnet, leaving LB3 matrices (f) in the supernatant. Scale bar, 10 μm. (**B**) Commassie blue staining of the samples described in (A). 1 μl of egg extracts, or the equivalent of 5, 30, 120, 600, or 600 μl of extract was loaded in lanes a, b, c, d, e, or f, respectively. (**C**) Western blotting of the samples in (A) with antibody to PAR. Similar amounts of materials were loaded as in (B), except in lanes e and f, where only the equivalent of 120 μl of the extracts was loaded in each lane. (**D**) Western blotting of the samples in (B) with antibody to tubulin, TPX2, Eg5, XMAP215, or LB3. (**E**) Isolation of LB3 matrices from mock-depleted or XMAP215-depleted egg extracts. Top, isolated LB3 matrices (green) with little tubulin (red). Bottom, isolated LB3 matrices (green) from the XMAP215-depleted egg extracts without XMAP215 (red). Scale bars, 5 μm. (**F**) MT assembly induced by isolated LB3 matrices. The LB3 matrices isolated as described in (E) were used in MT assembly assays with pure tubulin. LB3 matrices, green; MTs, red. The graph at the bottom shows the quantification of matrices that nucleated MTs. Scale bar, 10 μm.

vented the assembly of LB3 matrices containing SAFs (Fig. 2, E to G, and Fig. 4D). Lamins assemble into polymers of various organizations, which is important for nuclear assembly and function. To determine whether lamin assembly is required for the formation of mitotic LB3 matrix and spindle assembly, we used three LB3 mutants [ΔNLB3, LB3T, or LB3T(–)nls] that have dominant negative effects on the assembly and organization of nuclear lamina and proper nuclear structure and function (*17*–*19*). Both the N and C termini of LB3 (583 amino acids in length) are required for the polymerization of lamins in vitro (*18*, *36*). These mutant lamins disassemble lamin structures in fully assembled nuclei in vivo and prevent nuclear assembly on sperm chromatin in *Xenopus* interphase egg extracts (*17*–*19*, *36*). The ΔNLB3 mutant lacks the N-terminal 32 amino acids of LB3. LB3T contains the C-terminal 200 amino acids of LB3, and LB3T(–)nls is made from LB3T by mutating the NLS (*32*). Wild-type and mutant LB3 proteins were expressed and purified from bacteria as 6His fusions (Fig. 6A) (*32*).

All three mutant LB3 proteins disrupted spindle assembly in extracts incubated with sperm chromatin or with AurA beads with RanGTP, whereas neither buffer alone nor wild-type LB3 affected spindle assembly (Fig. 6, B and C) (*32*). Localization of SAFs on MT structures was abnormal in the presence of all mutant LB3 proteins. Eg5 and XMAP215 localized to the spindles in the presence of wild-type LB3, but the two SAFs formed aggregates outside the MTs in the presence of LB3 mutants (fig. S6). LB3 mutants may perturb the organization of LB3 matrices, which may in turn disrupt the interaction between the SAFs and MTs. Indeed, we found that all three LB3 mutants disrupted the assembly of the LB3 matrix that is normally associated with either sperm chromatin or AurA beads (Fig. 6D). Thus, proper assembly of the LB3 matrix appears to be required to organize and localize SAFs on spindles in mitosis.

Discussion. Our studies demonstrate that RanGTP regulates the assembly of an LB3 matrix in M-phase *Xenopus* egg extracts. Moreover, similar to MT aster and spindle assembly, the assembly of LB3 matrix is sensitive to increased amounts of importin α and β. Therefore, RanGTP might activate the assembly of the LB3 matrix by displacing importin α and β from proteins that are required for the formation of the matrix.

We propose that *Xenopus* LB3 is one such protein regulated by RanGTP during matrix assembly. LB3 contains an NLS at its C terminus, which has an essential role in the assembly of LB into higher order structures in vitro and the nuclear lamina in vivo (*17*–*19*, *36*). Importin α bound to the NLS in the C-terminal domain of LB3 (fig. S5A), and in the egg extracts, the interaction of LB3 with importin α and β was sensitive to RanGTP (fig. S5B). The release of importins from LB3 by RanGTP may make the C-terminal domain accessible for its assembly into the LB3 matrix.

The assembly of the LB3 matrix did not require MT polymerization. However, LB3 matrices assembled around AurA beads or sperm chromatin in the absence of MTs were smaller (Figs. 3 and 4). This suggests a reciprocal regulatory mechanism; with the LB matrix regulating MT assembly and organization and the MTs in turn regulating the assembly of the LB matrix. Such a reciprocal regulatory mechanism could be mediated by the SAFs that interact with both MTs and the LB matrix (Fig. 7). We have not detected specific interactions between LB3 and any of the SAFs by coimmunoprecipitation from M-phase egg extracts, but SAFs could interact with other proteins on the LB3 matrices.

Immunodepletion of LB3 or addition of truncated LB3 proteins with dominant negative activity that prevents lamin polymerization prevented the assembly of LB3 matrices containing any of the SAFs (Figs. 4 and 5). Thus, we propose that LB3 is a necessary structural component of the mitotic spindle.

The role of nuclear structural proteins such as intermediate filament proteins in mitosis may not be limited to human cells and *Xenopus* egg extracts. Like all other intermediate filament proteins, nuclear lamins assemble into higher order structures through the interactions of their highly alpha-helical central rod domains as well as their non–alpha-helical N- and C-terminal domains (*36*). Although lamins exist only in metazoans, coiled-coil proteins that can self-assemble are also found in the nucleus of plants and fungi. Some of these latter proteins may form nuclear structures similar to lamins (*43*–*47*). These nuclear proteins might become

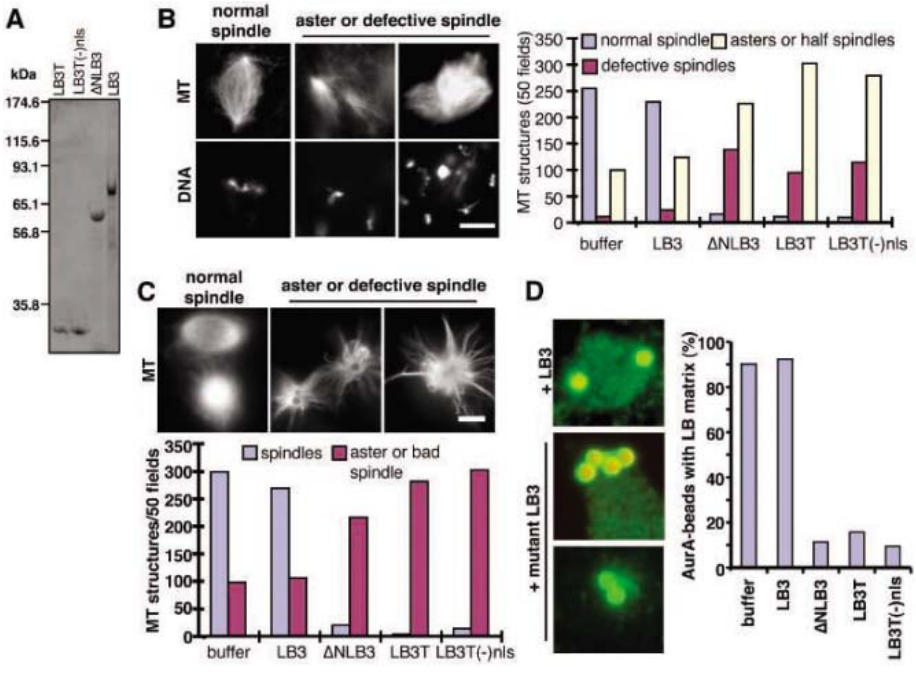

Fig. 6. Effects of mutant LB3 proteins to disrupt mitotic spindles and LB3 matrices. (**A**) Purified LB3 and mutant LB3 proteins were analyzed by SDS–polyacrylamide gel electrophoresis and Coomassie blue staining. (**B**) Effects of mutant LB3 to disrupt spindle assembly induced by *Xenopus* sperm chromatin. Examples of normal and defective spindles or MT asters are shown. The graph shows the quantification of different MT structures under the indicated conditions. (**C**) Effects of mutant LB3 proteins to disrupt spindle assembly induced by AurA beads and RanGTP. Examples of normal and defective spindles as well as MT asters are shown. The graph at the bottom shows the quantification of different MT structures under the indicated conditions. (**D**) Effects of mutant LB3 proteins to disrupt the assembly of LB3 matrices around AurA beads. Spindle assembly was induced with AurA beads plus RanGTP in the presence of buffer, wild-type, or mutant LB3. MTs were depolymerized, and LB3 matrices were detected using LB3 antibody. Examples of beads with associated LB3 matrices are shown. The graph on the right shows the quantification of AurA beads associated with LB3 matrices under the indicated conditions. Scales: white bar, 10 μm; magnetic beads, 2.8 μm.

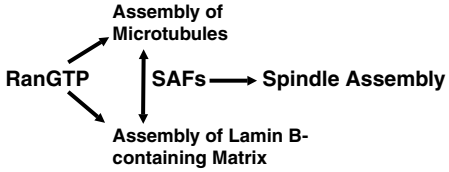

Fig. 7. Model for the mechanism of RanGTP-mediated spindle assembly. RanGTP independently stimulates assembly of MTs and lamin B–containing matrix, which reciprocally regulate each other and SAFs, leading to spindle assembly.

part of the spindle matrix in mitosis. Indeed, the yeast nuclear protein FIN1p contains coiled-coil domains and associates with spindles during mitosis (*46*). Furthermore, purified FIN1p self-assembles into 10-nm filaments resembling the cytoskeletal intermediate filaments formed in vitro (*46*).

In interphase nuclei of vertebrate cells, LB is concentrated at the nuclear lamina and is also distributed throughout the nucleoplasm. During interphase, the lamins interact with a wide range of nuclear proteins to regulate many nuclear functions as well as nuclear structural integrity. At the onset of mitosis, lamins are phosphorylated by Cdk1, which leads to the disassembly of nuclear lamina (*48*, *49*). The prevailing idea is that the disassembled LB is dispersed throughout the cytoplasm during mitosis. However, a fraction of LB is associated with the mitotic spindle and/or mitotic chromosomes (*19*, *26–28*). Our studies suggest that LB might perform functions analogous to those of the nuclear lamina to regulate spindle integrity and chromosome organization in mitosis.

References and Notes

1. J. M. Scholey, I. Brust-Mascher, A. Mogilner, *Nature* **422**, 746 (2003).
2. J. M. Scholey, G. C. Rogers, D. J. Sharp, *J. Cell Biol.* **154**, 261 (2001).
3. K. M. Johansen, J. Johansen, *Cell Cycle* **1**, 312 (2002).
4. K. Weis, *Curr. Opin. Cell Biol.* **14**, 328 (2002).
5. D. Kirkpatrick, F. Solomon, *Genetics* **137**, 381 (1994).
6. I. I. Ouspenski *et al.*, *J. Biol. Chem.* **270**, 1975 (1995).
7. I. I. Ouspenski, *Exp. Cell Res.* **244**, 171 (1998).
8. C. Wiese *et al.*, *Science* **291**, 653 (2001).
9. O. J. Gruss *et al.*, *Cell* **104**, 83 (2001).
10. M. V. Nachury *et al.*, *Cell* **104**, 95 (2001).
11. Y. Zheng, *Annu. Rev. Cell Dev. Biol.* **20**, 867 (2004).
12. D. D. Leipe, Y. I. Wolf, E. V. Koonin, L. Aravind, *J. Mol. Biol.* **317**, 41 (2002).
13. G. Jekely, *Bioessays* **25**, 1129 (2003).
14. H. Herrmann, U. Aebi, *Annu. Rev. Biochem.* **73**, 749 (2004).
15. R. D. Goldman, Y. Gruenbaum, R. D. Moir, D. K. Shumaker, T. P. Spann, *Genes Dev.* **16**, 533 (2002).
16. Y. Gruenbaum, A. Margalit, R. D. Goldman, D. K. Shumaker, K. L. Wilson, *Nat. Rev. Mol. Cell Biol.* **6**, 21 (2005).
17. R. I. Lopez-Soler, R. D. Moir, T. P. Spann, R. Stick, R. D. Goldman, *J. Cell Biol.* **154**, 61 (2001).
18. D. K. Shumaker *et al.*, *Proc. Natl. Acad. Sci. U.S.A.* **102**, 15494 (2005).
19. R. D. Moir, T. P. Spann, H. Herrmann, R. D. Goldman, *J. Cell Biol.* **149**, 1179 (2000).
20. T. P. Spann, A. E. Goldman, C. Wang, S. Huang, R. D. Goldman, *J. Cell Biol.* **156**, 603 (2002).
21. C. J. Hutchison, *Nat. Rev. Mol. Cell Biol.* **3**, 848 (2002).
22. D. Salina, P. Enarson, J. B. Rattner, B. Burke, *J. Cell Biol.* **162**, 991 (2003).
23. J. Joseph, S. T. Liu, S. A. Jablonski, T. J. Yen, M. Dasso, *Curr. Biol.* **14**, 611 (2004).
24. I. Loiodice *et al.*, *Mol. Biol. Cell* **15**, 3333 (2004).
25. J. Liu *et al.*, *Mol. Biol. Cell* **11**, 3937 (2000).
26. S. D. Georgatos, A. Pyrpasopoulou, P. A. Theodoropoulos, *J. Cell Sci.* **110**, 2129 (1997).
27. C. Maison, A. Pyrpasopoulou, P. A. Theodoropoulos, S. D. Georgatos, *EMBO J.* **16**, 4839 (1997).
28. J. Beaudouin, D. Gerlich, N. Daigle, R. Eils, J. Ellenberg, *Cell* **108**, 83 (2002).
29. D. Lourim, A. Kempf, G. Krohne, *J. Cell Sci.* **109**, 1775 (1996).
30. A. Wilde, Y. Zheng, *Science* **284**, 1359 (1999).
31. M.-Y. Tsai *et al.*, *Nat. Cell Biol.* **5**, 242 (2003).
32. Materials and methods are available as supporting material on *Science* Online.
33. M.-Y. Tsai, Y. Zheng, *Curr. Biol.* **15**, 2156 (2005).
34. R. Stick, *EMBO J.* **7**, 3189 (1988).
35. I. Firmback-Kraft, R. Stick, *J. Cell Biol.* **129**, 17 (1995).
36. R. D. Goldman, G. Yosef, R. D. Moir, D. K. Shumaker, T. P. Spann, *Genes Dev.* **16**, 533 (2002).
37. A. Wilde *et al.*, *Nat. Cell Biol.* **3**, 221 (2001).
38. T. Wittmann, M. Wilm, E. Karsenti, I. Vernos, *J. Cell Biol.* **149**, 1405 (2000).
39. P. Chang, M. K. Jacobson, T. J. Mitchison, *Nature* **432**, 645 (2004).
40. T. M. Kapoor, T. J. Mitchison, *J. Cell Biol.* **154**, 1125 (2001).
41. O. Kisurina-Evgenieva *et al.*, *J. Cell Sci.* **117**, 6391 (2004).
42. M. Y. Tsai *et al.*, unpublished observations.
43. C. Mirzayan, C. S. Copeland, M. Snyder, *J. Cell Biol.* **116**, 1319 (1992).
44. K. Masuda *et al.*, *Exp. Cell Res.* **232**, 173 (1997).
45. F. Gindullis, A. Rose, S. Patel, I. Meier, *BMC Genomics* **3**, 9 (2002).
46. M. J. van Hemert *et al.*, *Proc. Natl. Acad. Sci. U.S.A.* **99**, 5390 (2002).
47. B. J. Mans, V. Anantharaman, L. Aravind, E. V. Koonin, *Cell Cycle* **3**, 1612 (2004).
48. M. Peter, J. Nakagawa, M. Doree, J. C. Jabbe, E. A. Nigg, *Cell* **61**, 591 (1990).
49. B. Luscher, L. Brizuela, D. Beach, R. N. Eisenman, *EMBO J.* **10**, 865 (1991).

50. We thank O. Martin for technical support; R. Stick, J. Ellenberg, and A. Merdes for constructs and antibodies; M. Guo for critical reading of the manuscript; and A. Falick (HHMI) for mass spectroscopy analyses. Supported by Howard Hughes Medical Institute and National Institute of General Medical Sciences (GM56312) (Y.Z.) and by National Cancer Institute (CA31760-24) and an Ellison Medical Research Foundation Senior Scholar Award (R.D.G.).

Supporting Online Material

www.sciencemag.org/cgi/content/full/1122771/DC1
Materials and Methods
Figs. S1 to S6
References

18 November 2005; accepted 6 March 2006
Published online 16 March 2006;
10.1126/science.1122771
Include this information when citing this paper.

Cenozoic Plant Diversity in the Neotropics

Carlos Jaramillo,[1] Milton J. Rueda,[2] Germán Mora[3]

Several mechanisms have been proposed to explain the high levels of plant diversity in the Neotropics today, but little is known about diversification patterns of Neotropical floras through geological time. Here, we present the longest time series compiled for palynological plant diversity of the Neotropics (15 stratigraphic sections, 1530 samples, 1411 morphospecies, and 287,736 occurrences) from the Paleocene to the early Miocene (65 to 20 million years ago) in central Colombia and western Venezuela. The record shows a low-diversity Paleocene flora, a significantly more diverse early to middle Eocene flora exceeding Holocene levels, and a decline in diversity at the end of the Eocene and early Oligocene. A good correlation between diversity fluctuations and changes in global temperature was found, suggesting that tropical climate change may be directly driving the observed diversity pattern. Alternatively, the good correspondence may result from the control that climate exerts on the area available for tropical plants to grow.

The tropics of South America hold the highest plant diversity in the world (*1*). However, the origin of this diversity remains elusive. Many mechanisms have been proposed to explain it (*2–4*), which range from a long history of low rates of extinction and high rates of origination (*5*) to recent diversification during Pleistocene glacial-interglacial times (*6*). In particular, the latter mechanism [the "refugia" model (*6*)] is highly controversial and has ambiguous paleobotanical support (*7–11*). Despite the need for paleobotanical data to test Pleistocene and earlier models of diversification, the fossil record is deficient (*12–14*). Here, we present a high-resolution pollen and spore diversity record from the Paleogene to early Neogene in the Neotropics that shows that plant diversity in the tropics is variable through time and correlates with long-term global climatic changes.

The composite section. We analyzed the pollen and spore content from 15 stratigraphic sections in central Colombia and western Venezuela, spanning an area of 180,000 km^2 [Fig. 1; table S1; (*15*)]. The study encompassed 1530 palynological samples, recording 287,736 individual occurrences and 1411 morphospecies, 411 of which are still unnamed (*15*). The sections, as a whole, contain sediments that accumulated in fluvial to coastal plain settings between the Campanian and the middle Miocene [a range of 66 million years (My), from 82 to 16 million years ago (Ma)].

[1]Center for Tropical Paleoecology and Archeology, Smithsonian Tropical Research Institute, Unit 0948, Army Post Office AA 34002–0948, USA. [2]Paleoflora-Colombian Petroleum Institute, Kilometer 7 via Piedecuesta, Bucaramanga, Colombia. [3]Department of Geological and Atmospheric Sciences, Iowa State University, IA 50011, USA.

*To whom correspondence should be addressed. E-mail: jaramilloc@si.edu

Samples from all sections were combined in a single composite section by the method of graphic correlation (*15*, *16*). Each part of the composite section contains information from at least five different sections located across the entire study area. This procedure reduces the chance that differences in areas sampled influence apparent changes in taxonomic diversity over time, an effect commonly observed in continental-scale paleodiversity analyses (*17*).

The dating of the composite section was done by using foraminifera calibration points (*18*, *19*), stable carbon isotope ($\delta^{13}C$) stratigraphy (*15*), and key biostratigraphic datums (*15*). We assumed a linear sedimentation rate between these points in the composite section to transfer the stratigraphic position of each sample from meters to geologic time. It is reasonable to assume linearity, because the composite does not have major stratigraphic breaks and because diversity values are not affected by this assumption.

The composite section spans 66 My (*15*). The mean gap-sample resolution is 0.043 My; 95% of the samples are less than 0.150 My apart, and the longest sample gap is 0.586 My. Edge effects (*20*) artificially increase the number of first appearance datums (FADs) at the oldest end of a section and the number of last appearance datums (LADs) at the youngest end of a section. We estimated the edge effect by performing a piecewise regression (*15*, *21*). All data at both extremes of the composite that had evidence of an edge effect were eliminated from the analysis (the oldest 17.4 My and the youngest 3.3 My), which restricted the composite section from the base of the Paleocene (65.5 My) to the earliest Miocene (20 My). All species with single occurrences (39% of all species) were eliminated from the analysis. Last, the range-through method (*22*) was used to decrease the bias produced by changes in facies and depositional environments within the composite section. Six Holocene sediment cores with palynological data from lowland tropical forests of Colombia (*23*) were combined to produce a diversity benchmark to compare the Paleogene–early Neogene record with Holocene palynofloras (*15*). Because the pollen taxonomic resolution bias in both data sets is similar, their palynological diversity values are comparable. The six cores span an area similar to the area covered by our study, about 250,000 km^2. Samples from each of the cores were reduced to a single sample to replicate the time condensation that a rock sample may have. All of the core samples were combined to have a single composite sample that is comparable to a single data point in the long-term record shown here. This analysis yielded 321 pollen and spore morphotypes (*15*). A rarefaction analysis was also conducted to compare within-sample diversity between the Holocene palynofloras and the Eocene and early Miocene floras (*15*).

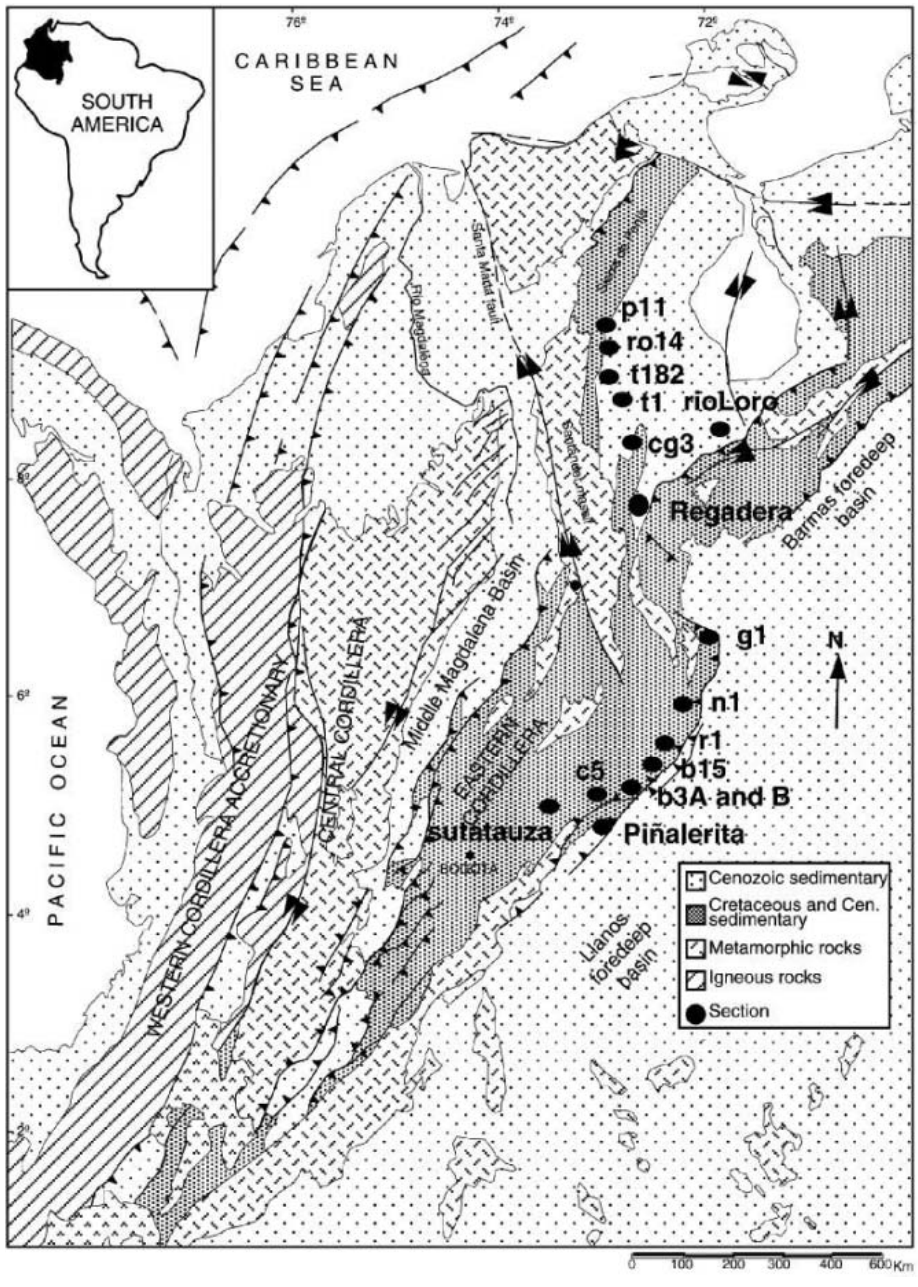

Fig. 1. Geographical location of the studied sections. Map modified after (*45*).

Standing diversity. The pattern of standing diversity (defined in the original sense of number of species) shows low floral diversity during the early Paleocene, followed by a slight increase at the beginning of the late Paleocene and by a subsequent drop in diversity at the end of the late Paleocene (Fig. 2A). Our composite record shows that a steady and fast increase in diversity occurred during the early Eocene, with a peak during the middle Eocene. This increase in Eocene diversity has already been suggested for subtropical South America, Africa, and India, although long-term records have not been yet published (*21*, *24*, *25*). Our record also shows a decline in diversity starting by the late middle Eocene with a steady drop until the early Oligocene. A similar drop has also been suggested for Southeast Asia during this time (*24*). Our record also indicates a relatively stable diversity during the Oligocene, followed by a slight decline during the Oligocene-Miocene transition (Fig. 2A).

Changes in floral composition were assessed using both a detrended correspondence analysis and an agglomerative cluster analysis (Fig. 2, B and C). Both methods show three significantly different floras: a Paleocene low-diversity flora, an early to early late Eocene high-diversity flora, and a mid-diversity late Eocene to early Miocene flora.

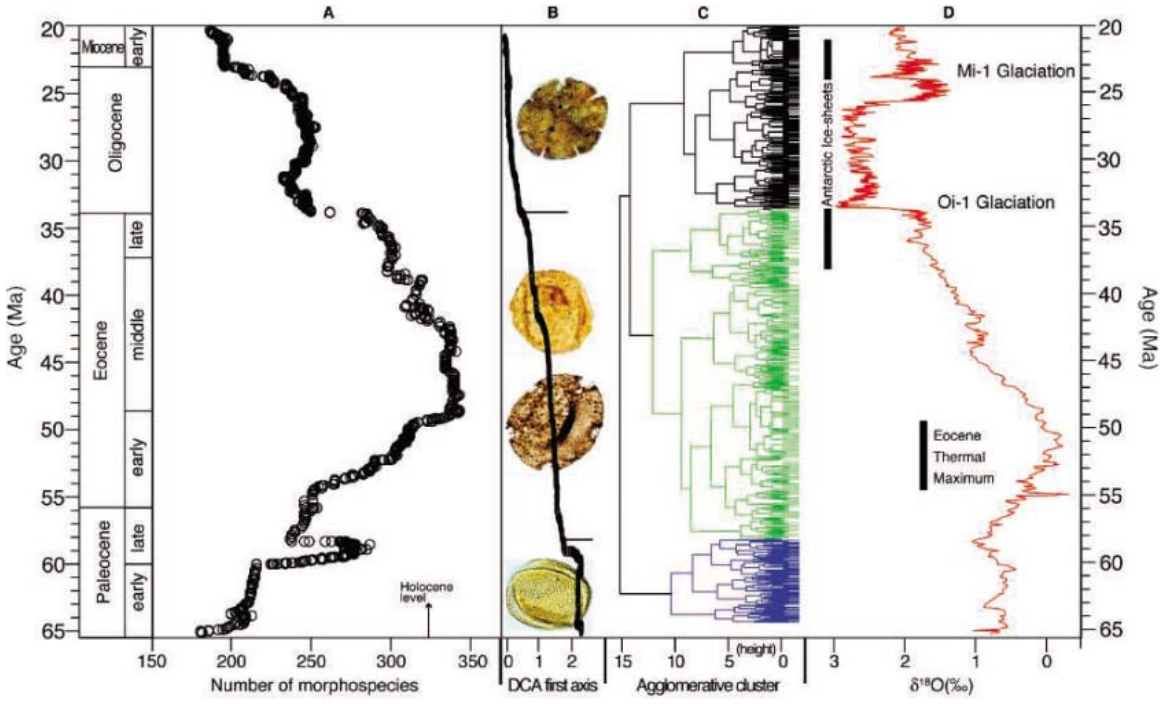

Fig. 2. Changes in palynofloral diversity and composition during the early to middle Cenozoic (*15*). (**A**) Pollen and spore standing diversity calculated by using the range-through method (*15*) and eliminating single-occurrence species. A Holocene composite palynological sample (*15*) of 321 species is drawn as a benchmark. Notice that diversity steadily increases during the early Eocene and gradually decreases during the late middle Eocene to early Oligocene, with a large drop at the Eocene-Oligocene boundary. (**B**) First axis of a detrended correspondence analysis (*15*) that explains 45.9% of the total variance in species composition along the stratigraphic profile. Paleocene palynofloras are clearly different from Eocene to Miocene palynofloras. Characteristic pollen species of each flora are shown: *Proxapertites cursus* for the Paleocene, *Nothofagidites huertasii* and *Echitriporites trianguliformis orbicularis* for the Eocene, and *Jandufouria seamrogiformis* for the Oligocene to early Miocene. (**C**) Agglomerative cluster analysis (*15*), showing three distinct palynofloras: Paleocene, Eocene, and Oligocene to early Miocene. (**D**) Global oxygen isotope curve for the Cenozoic (*27*). Raw data were smoothed using a five-point running average. There is correspondence between the general trend of the diversity curve and the global oxygen isotope curve that is a proxy for average global temperature (*27*).

Origination and extinction rates. Rates of origination and extinction were calculated by using the per capita rates of Foote (*15*, *20*) (Fig. 3). The rate of extinction is stable through time with an increase over background levels during the Eocene-Oligocene transition (Fig. 3A). Although the rate of origination gradually decreased over time (Fig. 3B), an increase over background levels occurred during the early Eocene (Fig. 3B). A high rate of both origination and extinction is apparent at the late Paleocene (Fig. 3, A and B). In fact, many of the species that originated at the beginning of the late Paleocene became extinct by the end of the Paleocene. There is also a major floral turnover at the end of the late Paleocene (Fig. 2, B and C). This interval needs further investigation to establish whether this extinction was gradual, or if it, in fact, dates from the short-lived Paleocene-Eocene thermal maximum and represents a rapid turnover as seen in North American mammals (*26*).

Standing diversity and global temperature. There is a correspondence between the global temperature curve for the Cenozoic (*27*) and the diversity pattern shown here [Fig. 2, A and D, first-differencing correlation of diversity versus $\delta^{18}O$, Spearman rho of –0.508; $P < 0.023$ (*15*)]. The increasing temperature trend from the early Paleocene to the early Eocene thermal maximum is paralleled, although slightly offset, by an increase in floral diversity. The subsequent long drop in temperature (*27*) between the late middle Eocene and the early Oligocene is also paralleled by a similar drop in diversity, with a larger drop in both temperature and diversity at the Eocene-Oligocene boundary (Fig. 2). This correspondence between diversity patterns and global temperature suggests a causal relationship. However, climate change at the tropics per se may not explain the differences seen here, because there is no strong evidence indicating that climate in the lowland tropics changed significantly during the Paleogene. The few available data of Cenozoic climate in the lowlands of the Neotropics indicate that temperature and precipitation may have been similar to modern values (*28*–*32*). However, these results are controversial, because the marine record seems to show a warming of the Tropics (*33*). The floral record also mimics recently estimated atmospheric CO_2 concentrations, which appear to be coupled with global temperature during the Paleogene (*34*). A gradual decrease in the partial pressure of atmospheric carbon dioxide (pCO_2) from the middle Eocene to the late Oligocene was identified from stable carbon isotope values of di-unsaturated alkenones from deep-sea cores (*34*). However, the pCO_2 proxies, based on plant stomatal indices, indicate that atmospheric CO_2 concentrations were near present-day levels during the Eocene (*35*). This conflicting evidence precludes a better understanding of the role of CO_2 on the pattern shown here.

Species-area effect. An alternative explanation to climate change in the Neotropics driving diversification and extinction is a species-area effect. This idea has been proposed before (*36*), but it has received little attention (*37*). During the early and middle Eocene, there was a major global warming event that allowed tropical lineages to expand well into the modern temperate areas (*24*, *25*, *27*). High-diversity forests existed in the early Eocene of northern Patagonia (*12*, *38*), which was located near the southern tip of the tropical belt during the Eocene (*12*). This increase in the area with tropical-like climate could be the main factor enhancing the increase in local diversity in the Neotropics during the Eocene. Larger regions can support more species, which enhance both regional and local diversity (*2*, *35*, *39*) by reducing the risk of extinction and increasing niche opportunities (*2*). In contrast, a cooling event in the late Eocene to early Oligocene reduced tropical areas drastically and, thus, drove local extinction in the Neotropics. A recent analysis of biome

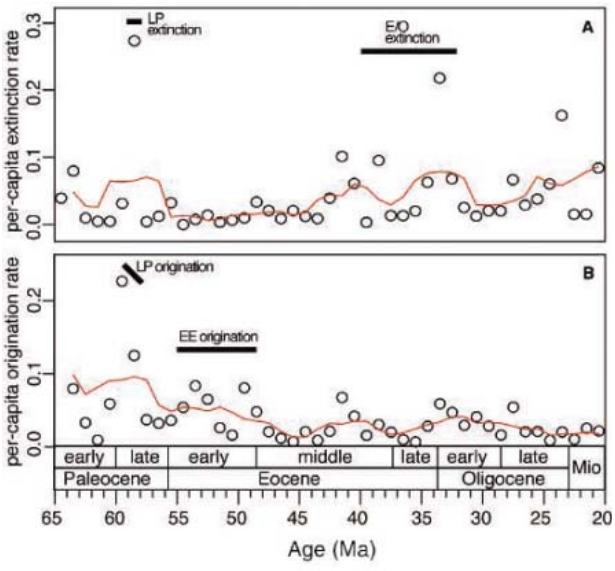

Fig. 3. Per capita rates of origination and extinction (*15*, *20*). (**A**) Per capita extinction rate per million years shows a stable long-term pattern, which increases over background levels during the late Paleocene and the Eocene-Oligocene transition. Raw data were smoothed using a five-point running mean (red line). (**B**) Per-capita origination rate per million years shows a slow, long-term decrease in the rate of origination over time. The rate also increases during the late Paleocene and the early Eocene. Raw data were smoothed using a five-point running mean (red line). LP, late Paleocene; EE, early Eocene; E/O, Eocene-Oligocene.

size integrated over time and diversity also found a primary role for changes in biome area over time in determining current species richness (*37*).

Comparisons with Holocene diversity. Holocene palynological diversity values (Fig. 2A) are lower than early to middle Eocene diversity values, but higher than either Oligocene-Miocene or Paleocene palynofloras (220 to 260 morphospecies). Rarefaction analysis of within-sample diversity also shows the same pattern (*15*). Eocene floras are significantly more diverse than Holocene floras (*t* test, $P < 0.0005$, mean of 44 versus 36 species per sample), and the Early Miocene is less diverse than the Holocene (*t* test, $P < 0.0005$; mean of 30 versus 36 species per sample). This comparison suggests that diversity increased again at some time between the Miocene and the Pleistocene to reach Holocene levels. This increase in diversity could be related to two factors: the 12 to 14 My middle Miocene climate optimum (*27*) that extended tropical areas to midlatitudes or the 5.5 to 3.7 My Andean uplift (*40*, *41*). Although there are now insufficient paleobotanical data to test these two hypotheses, the Andes uplift hypothesis (*40*) seems more likely. There was a long-term cooling phase after the middle Miocene optimum that would have decreased tropical areas and, therefore, would have decreased diversity. On the contrary, the Andes uplift is a more recent event, and a great deal of evidence suggests that it increased speciation: Diversity of Neotropical plants and birds is concentrated along the Andes foothills (*40*, *42*); many Gondwanan families are more speciose near the Andes (*40*); and a radiation of some taxa, such as *Inga,* is inferred as occurring between 10 and 3 My (*43*). High plant-species diversity has also been found to be associated with mountain building, such as the Laramide Front Range during the early Paleocene (*44*). However, a detailed record of Neogene diversity changes in the Neotropics, as the one compiled here for the Paleogene, is needed to test this hypothesis.

The overall pattern shows that plant diversity in the Neotropics has fluctuated greatly through time, as it is sensitive to global temperature. Temperature or precipitation change in the tropics may explain the pattern. An alternative hypothesis involves the control of global climate change on the area available for tropical ecosystems, which could, in turn, affect origination and extinction rates. If the size of forested areas does indeed control levels of local species diversity, conserving isolated pockets of tropical rainforest may not be sufficient to prevent high rates of extinction in the long run.

References and Notes

1. W. W. Thomas, *Biodivers. Conserv.* **8**, 1007 (1999).
2. E. G. Leigh *et al.*, *Biotropica* **36**, 447 (2004).
3. C. Moritz, J. L. Patton, C. J. Schneider, T. B. Smith, *Annu. Rev. Ecol. Syst.* **31**, 533 (2000).
4. K. J. Gaston, *Nature* **405**, 220 (2000).
5. G. L. Stebbins, *Flowering Plants: Evolution Above the Species Level* (Harvard Univ. Press, Cambridge, MA, 1974).
6. J. Haffer, *Science* **165**, 131 (1969).
7. M. B. Bush, M. R. Silman, D. H. Urrego, *Science* **303**, 827 (2004).
8. P. A. Colinvaux, P. E. de Oliveira, *Palaeogeogr. Palaeoclimatol. Palaeoecol.* **166**, 51 (2001).
9. H. Hooghiemstra, T. Van der Hammen, *Earth Sci. Rev.* **44**, 147 (1998).
10. T. P. Kastner, M. A. Goñi, *Geology* **31**, 291 (2003).
11. B. W. Nelson, C. A. Ferreira, M. F. da Silva, M. L. Kawasaki, *Nature* **345**, 714 (1990).
12. P. Wilf *et al.*, *Am. Nat.* **165**, 634 (2005).
13. R. J. Burnham, A. Graham, *Ann. Mo. Bot. Gard.* **86**, 546 (1999).
14. C. Hoorn, *Palaeogeogr. Palaeoclimatol. Palaeoecol.* **109**, 1 (1994).
15. Supporting methods and analysis are available on *Science* Online.
16. V. E. Edwards, *Palaios* **4**, 127 (1989).
17. A. D. Barnosky, M. A. Carrasco, E. W. Davis, *PLoS Biol.* **3**, e266 (2005).
18. J. H. Germeraad, C. A. Hopping, J. Muller, *Rev. Palaeobot. Palynol.* **6**, 189 (1968).
19. J. Muller, E. Di Giacomo, A. W. Van Erve, *Am. Assoc. Stratig. Palynol. Contrib. Ser.* **19**, 7 (1987).
20. M. Foote, in *Deep Time: Paleobiology's Perspective*, D. H. Erwin, S. L. Wing, Eds. (The Paleontological Society, Lawrence, KS, 2000), vol. 26, pp. 74–102.
21. C. A. Jaramillo, *Paleobiology* **28**, 222 (2002).
22. D. Boltovskoy, *J. Paleontol.* **62**, 157 (1988).
23. J. C. Berrio, *Late Glacial and Holocene Vegetation and Climatic Change in Lowland Colombia* (Univ. of Amsterdam, Amsterdam, 2002).
24. R. J. Morley, *Origin and Evolution of Tropical Rain Forests* (Wiley, New York, 2000), p. 362.
25. E. J. Romero, in *Biological Relationships Between Africa and South America*, P. Goldblatt, Ed. (Yale Univ. Press, New Haven, 1993), pp. 62–85.
26. W. C. Clyde, P. D. Gingerich, *Geology* **26**, 1011 (1998).
27. J. Zachos, M. Pagani, L. Sloan, E. Thomas, K. Billups, *Science* **292**, 686 (2001).
28. A. Graham, *Am. J. Bot.* **81**, 301 (1994).
29. B. J. MacFadden, P. Higgins, *Oecologia* **140**, 169 (2004).
30. A. Tripati *et al.*, *Paleoceanography* **18,** 10.1029/2003PA000937 (2003).
31. S. Wing, F. Herrera, C. Jaramillo, paper presented at the International Organization of Paleobotany, Seventh Quadrennial Conference, Bariloche, Argentina, 21 to 26 March 2004.
32. R. J. G. Kaandorp *et al.*, *Palaeogeogr. Palaeoclimatol. Palaeoecol.* **221**, 1 (2005).
33. P. N. Pearson *et al.*, *Nature* **413**, 481 (2001).
34. M. Pagani, J. C. Zachos, K. H. Freeman, B. Tipple, S. Bohaty, *Science* **309**, 600 (2005).
35. D. L. Royer *et al.*, *Science* **292**, 2310 (2001).
36. M. L. Rosenzweig, *Species Diversity in Space and Time* (Cambridge Univ. Press, Cambridge, ed. 3, 1995).
37. P. V. Fine, R. H. Ree, R. J. Burnham, paper presented at "Frontiers in Tropical Biology and Conservation," Annual Meeting of the Association of Tropical Biology and Conservation, Uberlândia, Brazil, 24 to 28 July 2005.
38. P. Wilf *et al.*, *Science* **300**, 122 (2003).
39. R. E. Ricklefs, D. Schluter, in *Species Diversity in Ecological Communities: Historical and Geographical Perspectives*, R. E. Ricklefs, D. Schluter, Eds. (Univ. of Chicago Press, Chicago, 1993), pp. 350–363.
40. A. H. Gentry, *Ann. Mo. Bot. Gard.* **69**, 557 (1982).
41. T. Van der Hammen, J. Werner, H. Dommelen, *Rev. Palaeobot. Palynol.* **16**, 1 (1973).
42. C. Rahbek, G. R. Graves, *Proc. Natl. Acad. Sci. U.S.A.* **98**, 4534 (2001).
43. J. E. Richardson, R. T. Pennington, T. D. Pennington, P. M. Hollingsworth, *Science* **293**, 2242 (2000).
44. K. R. Johnson, B. Ellis, *Science* **296**, 2379 (2002).
45. C. A. Dengo, M. C. Covey, *AAPG Bull.* **77**, 1315 (1993).

46. Supported by the Colombian Petroleum Institute, the Smithsonian Paleobiology Endowment Fund, the Fondo para la Investigacion de Ciencia y Tecnología Banco de la Republica de Colombia, and Carbones del Cerrejón. P. Fine, J. Wright, C. Dick, A. O'Dea, and three anonymous reviewers contributed useful critiques. Thanks to the Biostratigraphic Team at the Colombian Petroleum Institute. R. Condit helped with the R code used in the analysis. Special thanks to M. I. Barreto for her continuous support and source of ideas.

Supporting Online Material

www.sciencemag.org/cgi/content/full/311/5769/1893/DC1
Materials and Methods
Figs. S1 and S2
Tables S1 to S6
References and Notes

14 October 2005; accepted 20 February 2006

Deformation and Slip Along the Sunda Megathrust in the Great 2005 Nias-Simeulue Earthquake

Richard W. Briggs,[1*] Kerry Sieh,[1] Aron J. Meltzner,[1] Danny Natawidjaja,[2] John Galetzka,[1] Bambang Suwargadi,[2] Ya-ju Hsu,[1] Mark Simons,[1] Nugroho Hananto,[2] Imam Suprihanto,[3] Dudi Prayudi,[2] Jean-Philippe Avouac,[1] Linette Prawirodirdjo,[4] Yehuda Bock[4]

Seismic rupture produced spectacular tectonic deformation above a 400-kilometer strip of the Sunda megathrust, offshore northern Sumatra, in March 2005. Measurements from coral microatolls and Global Positioning System stations reveal trench-parallel belts of uplift up to 3 meters high on the outer-arc islands above the rupture and a 1-meter-deep subsidence trough farther from the trench. Surface deformation reflects more than 11 meters of fault slip under the islands and a pronounced lessening of slip trenchward. A saddle in megathrust slip separates the northwestern edge of the 2005 rupture from the great 2004 Sumatra-Andaman rupture. The southeastern edge abuts a predominantly aseismic section of the megathrust near the equator.

A giant megathrust earthquake is the rare expression of the most dramatic moment of a subduction zone's life cycle—the culmination of centuries of strain accumulation across a convergent plate boundary. Robust seismic signals around the globe allow estimation of the gross nature of the event, but the details of rupture are usually obscure due to a lack of geodetic measurements directly above or nearby.

The great [moment magnitude (M_w) = 9.2] Sumatra-Andaman earthquake of December 2004 (Fig. 1) was unusual for a subduction megathrust event in that geodetic measurements of coseismic motions were available from islands directly above the rupture (*1*). These near-field data enabled a detailed investigation of the source of the earthquake. Even so, near-field Global Positioning System (GPS) geodetic measurements were sparse. Furthermore, they were collected in survey mode, with long periods between measurements that led to ambiguities in separating pre-, co-, and postseismic motions.

The great (M_w = 8.7) Nias-Simeulue earthquake, 3 months later and immediately to the south (Fig. 1), presents a substantially better opportunity to constrain rupture processes. Several continuously recording GPS (CGPS) stations had just been established directly above or immediately adjacent to the rupture (*2*). Moreover, the presence of a tropical archipelago above the rupture enabled the use of coral microatolls to measure coseismic uplift and submergence. The resulting rich set of measurements allows us to construct one of the most detailed and accurate maps of deformation obtained for a subduction megathrust earthquake.

Methods. Most of our measurements come from massive corals of the genus *Porites*. Because these are sensitive natural recorders of lowest tide levels (*3*–*5*), they are ideal natural instruments for measuring emergence or submergence relative to a tidal datum. Massive *Porites* coral heads grow radially upward and outward until they reach an elevation that exposes their highest corallites to the atmosphere during lowest tides. This subaerial exposure kills the uppermost corallites in the colony, thus restricting future upward growth. Hence the coral heads provide an opportunity to measure the difference between the highest level of survival (HLS) formed just before and that formed just after a large uplift event (*4*, *6*) and even to extract interseismic histories of vertical deformation (*7*, *8*).

When coseismic uplift occurs, those portions of the microatoll colony raised above lowest tides die. But if lower parts of the coral head are still below lowest tides, its uppermost living tissues demarcate a new, post-earthquake HLS (*4*) (Figs. 2A and 3A). Most of our uplift measurements are derived from the difference between pre- and post-earthquake HLS, often on the same coral head. Where corals rose during both the 2004 and 2005 earthquakes, we can differentiate between the two uplifts (Figs. 2A and 3B).

At locations where uplift was greater than the height of the coral heads and at sites that experienced subsidence (Fig. 2, B and C), we record the elevation difference between the coral's pre-earthquake HLS and average water level at the site at the time of our coral measurement. We then use a numerical tidal model to obtain an estimate of the lowest annual low tide expected at each survey site relative to the water level at the time of measurement. Our tidal calculations are based on harmonic tidal

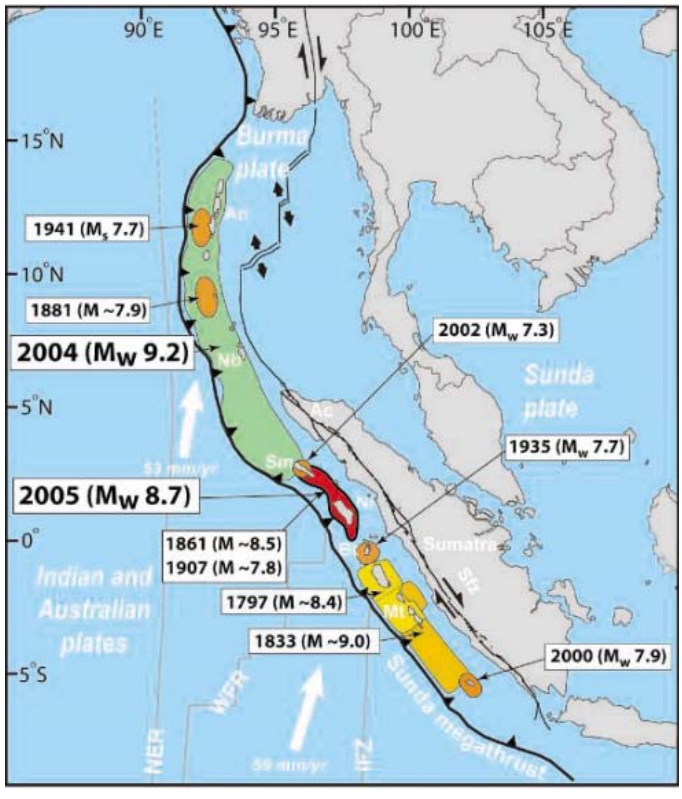

Fig. 1. Regional map of the 28 March 2005 rupture and previous large ruptures of the Sunda megathrust. The 2005 rupture occurred in a 400-km gap between great ruptures in 2004 and 1797. Islands above the rupture allowed detailed measurement of coseismic deformation with corals and GPS. An, Andaman islands; Nb, Nicobar islands; Ac, Aceh province; Ni, Nias island; Sm, Simeulue island; Bt, Batu islands; Mt, Mentawai islands; Sfz, Sumatran fault zone; NER, Ninety East ridge; WFR, Wharton fossil ridge; IFZ, Investigator fracture zone. Previous earthquake locations and magnitudes are from (*1*, *8*, *35*, *36*). Indian and Australian plate motions relative to Sunda are from (*37*) and faults are generalized from (*24*, *38*).

[1]Tectonics Observatory, Division of Geological and Planetary Sciences, California Institute of Technology, Pasadena, CA 91125, USA. [2]Research Center for Geotechnology, Indonesian Institute of Sciences, Bandung, Indonesia. [3]Jl. Mahoni, Blok E, Gang I, No. 13, Rt. 002/015, Kota Jakarta 14270, Indonesia. [4]Cecil H. and Ida M. Green Institute of Geophysics and Planetary Physics, Scripps Institution of Oceanography, University of California San Diego, La Jolla, CA 92093, USA.

*To whom correspondence should be addressed. E-mail: briggs@gps.caltech.edu

constituents extracted from a regional satellite-based model for Indonesia (*9*), using the software package NLOADF (*10*, *11*). The uplift or subsidence value is the difference between the pre-earthquake HLS (old extreme low tide elevation) and the model value of post-earthquake lowest tide. Where we can directly compare post-earthquake HLS and post-earthquake tide elevations, we find that a band of living coral about 4 cm high can survive above the elevation of extreme low tide. Thus, we apply this correction to all measurements that use the tidal model (*12*).

At a few survey sites, coral records are unavailable. There we estimate uplift using geomorphic or cultural features. These measurements often have relatively large uncertainties, but they are still useful in that they offer unambiguous evidence of the direction of land-level change. We also augment our field measurements in a few locations with limits on uplift and subsidence derived from satellite imagery (table S1). Finally, we also use coseismic displacements recorded by CGPS stations of the Sumatran GPS Array (SuGAr) (*2*) and a station (SAMP) operated by the Indonesia National Coordinating Agency for Surveys and Mapping (BAKOSURTANAL). The CGPS data were analyzed (*13*) in 24-hour segments (0- to 24-hour GMT) with data from 10 additional continuous GPS sites on Java, Cocos Islands, Diego Garcia, Singapore, India, Australia, and Guam. These regional network solutions were combined by network adjustment with global GPS network solutions produced routinely at the Scripps Orbit and Permanent Array Center. The resulting 24-hour position time series were fit to estimate three-dimensional coseismic displacements (*13*).

Results. The northern half of Simeulue island, from about 2.5° to 2.9°N, rose during the December 2004 event (Fig. 4A; table S2). Tilts were toward the northeast and southeast, with maximum uplift of 1.45 m on the island's northwestern tip. The uplift of Simeulue constrains tightly the southeastern limit of megathrust rupture during the 2004 earthquake to about 2.5°N (*1*, *11*). The southeastern third of Simeulue subsided in December 2004, but we had little time to document that subsidence in the field before the subsequent March event. We have only a few field measurements from January 2005 and observations from satellite imagery (*11*), as well as the subsidence predicted from an elastic dislocation model of the 2004 rupture (*1*). Rather than apply these largely model-derived corrections to our measurements of March 2005 uplift on southeastern Simeulue, we contour net uplift values for sites that subsided in the 2004 earthquake (Fig. 4B). Moreover, measurements by CGPS show that the postseismic elevation changes by the time of our field survey, 1.5 to 3.2 months after the earthquake, were only rarely more than a few percent of total coseismic motion (fig. S1). Therefore, we have chosen not to include corrections for these relatively small postseismic motions in our depiction of coseismic deformation. Instead, we leave close examination of pre- and post-earthquake deformation to a subsequent manuscript (*14*).

The vertical deformation pattern of March 2005 comprises principally two arc-parallel ridges of uplift on the forearc islands of Nias and Simeulue and a broad subsidence trough between these islands and the mainland coast (Fig. 4B). This pattern—uplift nearer the deformation front and subsidence nearer the arc (fig. S2)—is like that observed after a few other megathrust ruptures, principally in Alaska, Chile, and Japan (*15*–*18*). The asymmetry of the pattern, with maximum uplift (2.9 m) greater than maximum subsidence (1.15 m), is also similar to the patterns in these previous cases. The ridge crests are sharper than the trough. The contours of uplift and subsidence are predominantly arc-parallel, but have a pronounced misalignment near the Banyak Islands, between Nias and Simeulue.

Modeling. We combine our coral observations with coseismic three-component displacements from 16 CGPS stations of the SuGAr network to constrain an elastic dislocation model of coseismic slip on the megathrust (Fig. 5). To construct the model, we assume a 10° dipping

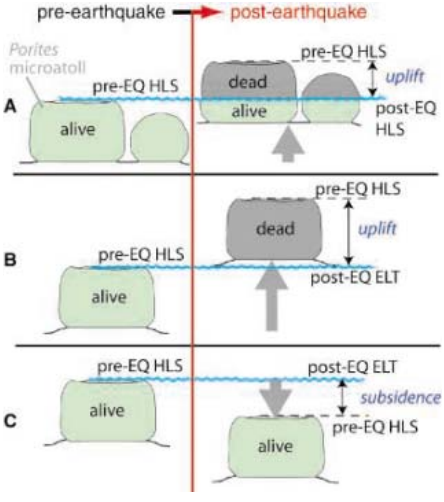

Fig. 2. Three scenarios for measuring vertical deformation using *Porites* coral microatolls. (**A**) Uplift recorded as the difference between pre- and post-earthquake highest level of survival (HLS). (**B**) Uplift as separation between pre-earthquake HLS (pre-EQ HLS) and the model elevation of post-earthquake extreme low tide (post-EQ ELT). (**C**) Subsidence measured upward from pre-earthquake HLS to post-earthquake ELT.

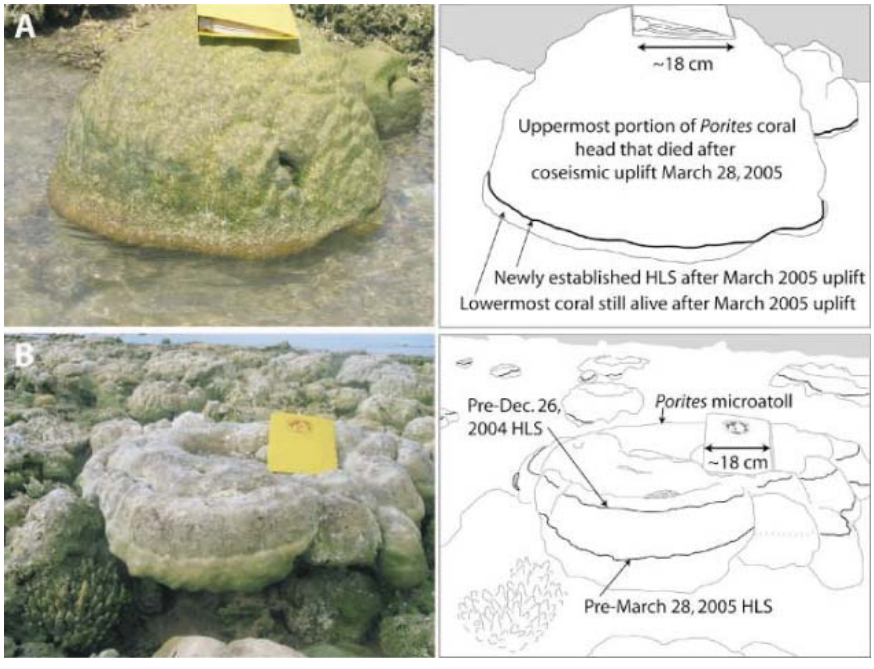

Fig. 3. Photographs and corresponding line drawings of uplifted *Porites* coral heads. (**A**) An uplifted hemispherical *Porites* head that records the new, post-earthquake highest level of survival (HLS) as the top of a thin living strip at its base. The uppermost, exposed portion of the microatoll is dead and covered with algae (site RDJ05-K; table S2). (**B**) A *Porites* microatoll that records multiple uplift events. Uplift of ~11 cm during the December earthquake resulted in the elevation difference between the uppermost living coral before (labeled "Pre-Dec. 26, 2004 HLS") and after ("Pre-March 28, 2005 HLS") the earthquake. The more brightly colored area beneath the pre–28 March 2005 HLS is outward growth during the period between the December and March earthquakes. During the 28 March earthquake the coral was uplifted another ~65 cm, causing the head to be lifted entirely out of the water into a position too high to record post–28 March HLS (site RND05-C; table S2).

fault plane between the deformation front and offshore Sumatra, which conforms roughly to the top of the Wadati-Benioff zone defined by relocated hypocenters from the International Seismological Centre catalog (*19*, *20*). We curve the fault along strike to follow the trench and use a layered elastic structure derived from the crustal model CRUST2.0 (*21*). Models with greater geometrical complexity will not be warranted until the geometry of the megathrust and crustal density structure are better known. Our weighted least-squares approach uses data weights equal to the inverse square root of the data covariance matrix (*22*). We estimate appropriate relative weight between the GPS and coral data in a two-step process. We begin by constructing two independent models that use each data set separately. The final model uses both data sets simultaneously, but with the weight of each data set scaled by the reduced chi-square values inferred from the initial independent models. In this joint inversion, fits to the vertical CGPS and the coral data are generally very good (*22*) (figs. S3 to S7).

Inverting the coral and CGPS data for slip on the megathrust yields a band of high slip that stretches from 3°N to the equator (Fig. 5). The region of high slip comprises two main patches, one northwest and one southeast of the epicenter. Maximum slip near southern Simeulue is about 8 m, whereas under northern Nias it is about 11 m. Most of the moment (95%) is concentrated between depths of about 14 to 35 km. The surface projections of the slip maxima are about 10 km east of the belts of maximum uplift. Slip values are highest at depths of about 25 km and decrease gradually both up-dip and down-dip. The total moment of the rupture is 9.8×10^{21} N-m, nearly identical to the seismological estimate (*23*) and equivalent to $M_w = 8.6$.

Discussion. Our observations have implications for the segmentation of the megathrust and for its long-term behavior. First, we speculate on the importance of the misalignment of the coseismic deformation contours. The bend or tear in the contours between the Banyak islands and Nias (Fig. 4B) separates the two principal rupture patches. It also coincides with a disruption in the bathymetry of the outer-arc ridge, previously interpreted to be a structural tear, possibly the southwestward extension of the Batee fault (fig. S8). This fault offsets forearc geologic features dextrally as much as 90 km (*24*, *25*). We suggest that the misalignment of coseismic deformation contours demarcates a tear in the megathrust between the two principal patches of coseismic rupture. If this break in the megathrust exists, the dip of the megathrust to the northwest (beneath Simeulue) might well be shallower than it is to the southeast (beneath Nias), because the uplift ridge on Simeulue is farther from the trench than the uplift ridge on Nias.

The relationship of coseismic slip on the megathrust to bathymetry, aftershocks, and

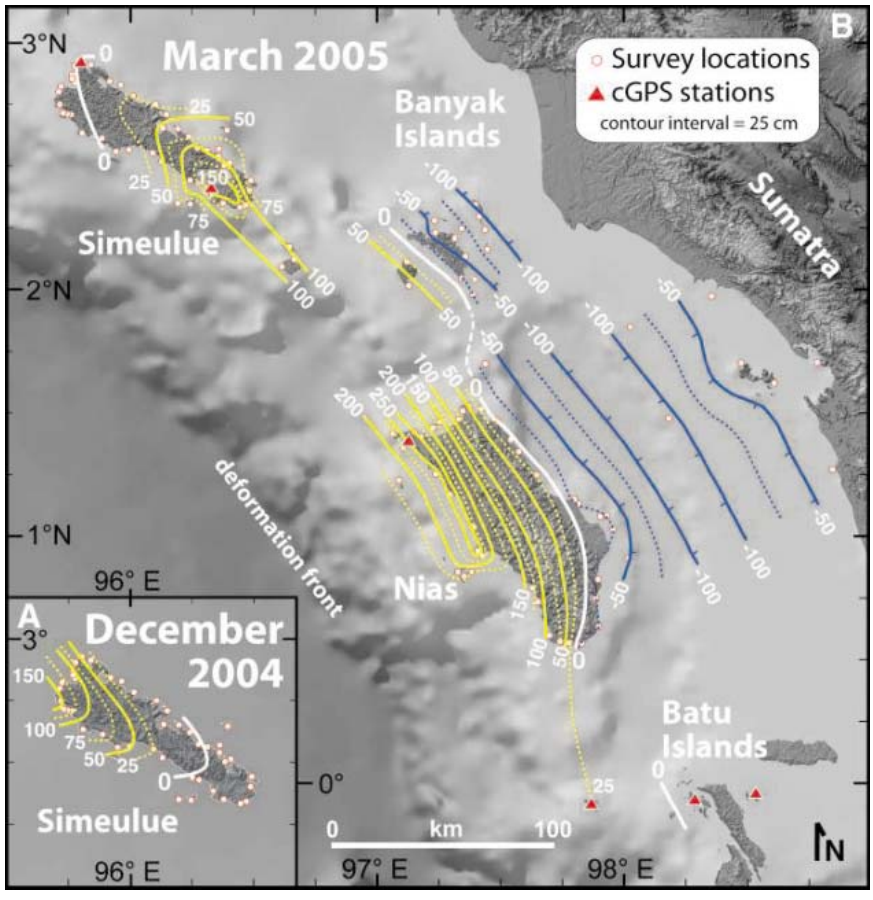

Fig. 4. Contour maps in cm of vertical deformation during the December 2004 (**A**) and March 2005 (**B**) Sunda megathrust ruptures. Yellow contours indicate uplift, blue contours indicate subsidence, and the white contour is the pivot line between domains of uplift and subsidence. Solid contours are at 50-cm interval, and dashed contours are at 25-cm interval. The principal features are two ridges of uplift along the islands of Nias and Simeulue and troughs of subsidence between the islands and the mainland. Shaded relief is from (*39*, *40*).

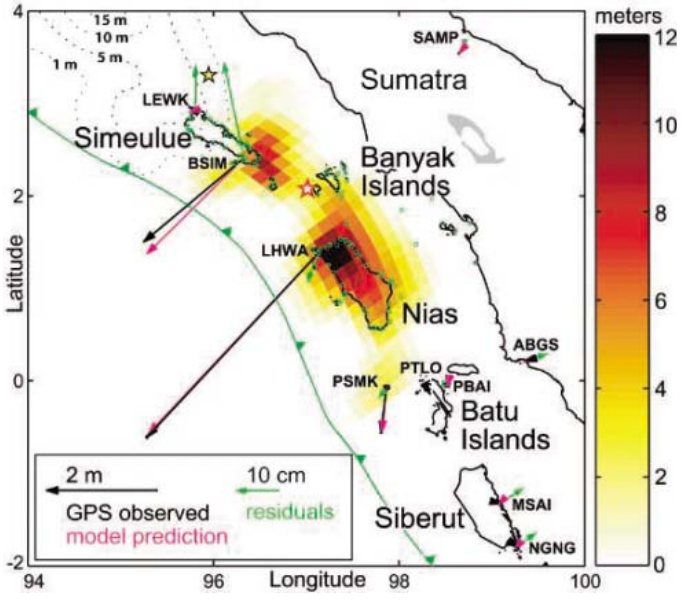

Fig. 5. Map view of model coseismic slip distribution on the 28 March 2005 Nias-Simeulue fault plane. Horizontal displacements from CGPS are in black and model values are in pink. All CGPS sites are from the Sumatran GPS Array (SuGAr), except for site SAMP, which is operated by BAKOSURTANAL. Model residuals are shown as green vectors (note change of scale). Slip reached 8 m under Simeulue and 11 m under Nias. Green circles show locations of uplift measurements. The epicenter of the March 2005 mainshock is shown as a red star, and the green line denotes the position of the Sunda deformation front. Dashed contours show modeled slip for the 2004 Aceh-Andaman rupture from (*1*), and the yellow star denotes the epicenter of the 2004 mainshock.

postseismic slip has implications for the long-term behavior of the megathrust. It is interesting that the two high-slip patches seem to correspond to steep topography rising from the trench (Fig. 4B and fig. S9). Moreover, patches with low slip, between Nias and Simeulue island and under southern Nias island, are coincident with gentler slopes up from the trench. More reliable bathymetry will be necessary to confirm these associations. But if they are indeed correct, high-slip and low-slip patches may be features of the megathrust as long-lived as sea-floor topography. Perhaps the steep slopes have been built above sections of the megathrust with higher friction and the gentle slopes reflect sections of the megathrust with lower friction (*26*).

The coincidence of a dense band of aftershocks (*27*) (fig. S8) with the rapid up-dip decrease in slip just seaward of the islands suggests that stresses imposed by the coseismic rupture were high enough there to induce a concentration of aftershocks on or in the volume surrounding the shallower part of the interface. What prevented the rupture from progressing farther up-dip? Had the shallower part of the megathrust been de-stressed by coseismic rupture in the earlier large historical ruptures of 1907 or 1861? Or does aseismic slip keep the up-dip section de-stressed and unreceptive to the propagation of slip during 2005-like ruptures? Work in progress on postseismic transients recorded by the Sumatran GPS Array (*14*, *28*) addresses these possibilities.

Another interesting aspect of the March 2005 earthquake is the small size of the March 2005 tsunami relative to that of December 2004 (*29*, *30*). Most of the explanation for this difference must lie in a comparison of vertical sea-floor displacements generated during the two earthquakes. First, the length of rupture in March was much less—~400 km versus ~1600 km (*1*). Second, the maximum uplift in March was only about half that in December [2.9 m versus about 5.4 m (*31*)]. And third, the areas of greatest vertical displacement occurred under deep water along much of the December rupture, but on land or under shallow water along all of the March rupture. This third observation supports the calculation of Synolakis and Arcas (*30*), which shows that the presence of islands in the epicentral region substantially lessened the size of the March 2005 tsunami. Finally, the coseismic raising of Nias and Simeulue islands, tens of minutes before the arrival of the 28 March tsunami, would have resulted in a lessening of tsunami height and inundation along the upraised coasts of those islands (*29*, *32*).

It is clear from the cup shape of microatolls on the coasts of Nias and Simeulue that submergence associated with strain accumulation had been prevalent on the forearc in the decades before sudden uplift during the earthquake. This interseismic behavior, abruptly terminated by coseismic uplift, is consistent with slow elastic strain accumulation and abrupt release. Nonetheless, the fact that the pattern of coseismic uplift mimics the topography of the islands (Fig. 4B) suggests that some increment of the coseismic uplift is not elastic and has contributed to building of the outer-arc ridge. Indeed, the presence of well-preserved coral reef terraces tens of meters above sea level on the northern and central coasts of Nias island (*33*) attests to net uplift during the past few tens to hundreds of millennia. The coincidence of the coseismic pivot line with the boundary between long-term erosion (on the west) and deposition (on the east) further supports the argument that the coseismic pattern reflects long-term orogenic processes. The actual relative amounts of permanent and elastic components should be resolvable through a combination of paleogeodetic and neotectonic studies.

The lateral terminations of the March 2005 rupture are particularly interesting. The dense coral measurements on the coasts of Simeulue island allow us to examine the northwestern terminus in particular detail. Uplift during the 2004 earthquake was as high as 1.45 m on the northwestern flank of Simeulue island and tapered toward the southeast to zero (Fig. 4A). Conversely, uplift during the 2005 event was as high as 1.65 m on the southeastern part of the island and tapered toward the northwest nearly to zero (Fig. 4B). Summing uplifts from the two earthquakes reveals a 70-km-long saddle-shaped depression centered on the island (Fig. 6). At the center of this saddle, uplift was only ~0.5 m, at least a meter less than to the northwest and southeast. This implies that slip on the megathrust beneath central Simeulue was appreciably less than it was to the northwest and southeast. The corals also show that uplift associated with the M_w = 7.3 earthquake of 2002 (*34*) was centered squarely in the center of this saddle and had a maximum value of only ~0.2 m, an amount that is inadequate to fill the saddle (Fig. 6).

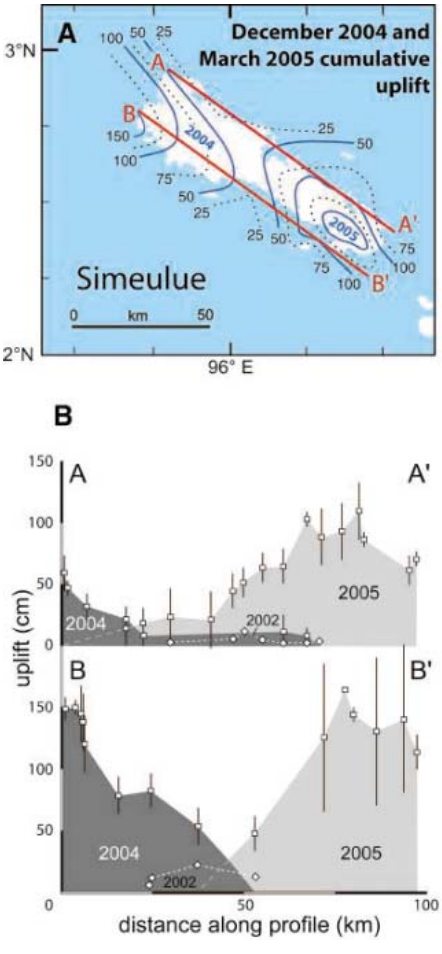

Fig. 6. Contour map of cumulative uplift values (in cm) for the December 2004 and March 2005 ruptures on Simeulue (**A**). Vertical displacement profiles A-A′ and B-B′ (**B**) highlight saddle in displacement between regions of December 2004 and March 2005 uplift. Measurements of uplift associated with the 2002 rupture appear as diamonds.

One plausible interpretation is that the Simeulue saddle reflects a section of the megathrust that commonly slips aseismically or fails in lesser earthquakes. Such a section could serve as an impediment to along-strike propagation of infrequent large ruptures. If slip in the long periods between giant earthquakes occurs largely aseismically and during moderate earthquakes such as occurred in 2002, this 70-km section would be largely unstressed at the time of the giant earthquakes and rupture would be less likely to propagate through. If this were a persistent characteristic of the Simeulue saddle, it would represent a permanent impediment to rupture from the northwest and from the southeast, because it would not accumulate large stresses. Such behavior could be analogous to that documented for the section of the Sunda megathrust at the Equator (*8*). This Batu islands section was flanked on the northwest by the giant ruptures of 1861 and 2005 and on the southeast by the giant earthquake rupture of 1797 (Fig. 1). Throughout at least the past 250 years, the M_w = 7.7 earthquake of 1935 is the largest seismic rupture of the 70-km-long Batu islands patch (*8*). Perhaps slip along the megathrust beneath the Batu islands, and the Simeulue saddle, is predominantly aseismic. The reasons for lateral variations in the mode of failure along the megathrust are unclear; abrupt lateral variations of temperature along the plate interface are improbable, so variations in the mode of slip along strike may instead result from lithologic or pore pressure variations. Another possibility is that structural complexities in the Simeulue saddle and Batu islands patch may have inhibited throughgoing rupture during the 2004 and 2005 giant earthquakes. The slight misalignment of the 2004 and 2005 uplift ridge crests on Simeulue island and the abrupt widening of the island at that misalignment, and the subduction of the Investigator fracture zone beneath the Batu islands zone, support arguments for a structural cause for the

2005 rupture terminations. These might be tears or warps in the megathrust or secondary faults within the slab or within the forearc.

References and Notes

1. C. Subarya *et al.*, *Nature* **440**, 46 (2006).
2. These CGPS data are available (www.tectonics.caltech.edu/sumatra/data.html and sopac.ucsd.edu/projects/sugar.html).
3. T. P. Scoffin, D. R. Stoddart, *Philos. Trans. R. Soc. London Ser. B* **284**, 99 (1978).
4. F. W. Taylor, C. Frohlich, J. Lecolle, M. Strecker, *J. Geophys. Res.* **92**, 4905 (1987).
5. J. Zachariasen, K. Sieh, F. W. Taylor, W. S. Hantoro, *Bull. Seismol. Soc. Am.* **90**, 897 (2000).
6. J. M. Pandolfi, M. M. R. Best, S. P. Murray, *Geology* **22**, 239 (1994).
7. K. Sieh, S. N. Ward, D. Natawidjaja, B. Suwargadi, *Geophys. Res. Lett.* **26**, 3141 (1999).
8. D. H. Natawidjaja *et al.*, *J. Geophys. Res.* **109**, B04306 (2004).
9. G. D. Egbert, S. Y. Erofeeva, *J. Atmos. Oceanic Technol.* **19**, 183 (2002).
10. D. C. Agnew, *J. Geophys. Res.* **102**, 5109 (1997).
11. A. J. Meltzner *et al.*, *J. Geophys. Res.* **111**, B02407 (2006).
12. We use principally a total station and an auto level and stadia rod to obtain field measurements. Total 2σ (95%) uncertainties associated with our coral measurements range from ± 6 to ± 23 cm and take into account variations in HLS, uncertainties in the tide model, survey measurement error, and uncertainties in the lowest low-tide to post-earthquake HLS correction.
13. R. Nikolaidis, thesis, University of California, San Diego (2002).
14. Y.-j. Hsu *et al.*, in preparation.
15. G. Plafker, *Science* **148**, 1675 (1965).
16. G. Plafker, J. C. Savage, *Geol. Soc. Am. Bull.* **81**, 1001 (1970).
17. T. J. Fitch, C. H. Scholz, *J. Geophys. Res.* **76**, 7260 (1971).
18. H. Kanamori, *Annu. Rev. Earth Planet. Sci.* **1**, 213 (1973).
19. E. R. Engdahl, R. van der Hilst, B. Raymond, *Bull. Seismol. Soc. Am.* **88**, 722 (1998).
20. This dip angle is slightly higher than the 7° northeast dipping plane of the Harvard centroid moment tensor solution for the main shock but is consistent with the 10° dip derived from modeling of teleseismic short-period and long-period seismic waveforms as well as normal modes (*23*).
21. C. Bassin, G. Laske, G. Masters, *EOS Trans. AGU* **81**, F897 (2000).
22. In our model we limit slip directions to be up-dip and right-lateral, and we minimize the data misfit and model roughness. The damping parameter between data misfit and model norm is chosen by cross-validation. To weight the GPS and coral data correctly, we first calculated two independent elastic-dislocation models, using each data set separately. The fact that the two solutions yield quite different reduced chi-square values (535 for the CGPS data and 10 for the coral data) suggests that the uncertainties assigned to the two independent data sets do not represent similar confidence levels. As a result, a joint inversion of the two data sets is dominated by the GPS measurements, which have far smaller errors. Thus, the joint inversion largely ignores the coral data, and the resultant slip model is strongly biased by the spatial distribution of the GPS stations. To remedy this bias, our final model is a joint inversion of both data sets with the weight of each data set scaled by the reduced chi-square value from the initial independent models. The rescaling factor between the CGPS data and the coral data is ~7. This procedure preserves the internal consistency of uncertainties assigned to each data set. It assumes that for each data set, real 1σ uncertainties are proportional to the initially assigned uncertainties (meaning that all sources of errors are assumed to be correctly accounted for in the estimated uncertainties). This combination of the two data sets takes appropriate advantage of the accuracy of the GPS measurements and of the dense spatial distribution of the coral measurements. To account for submergence due to the 2004 M_w = 9.2 rupture, our inversion uses a small elastic model–derived correction from Subarya *et al.* (*1*) (column m in table S2) that we apply to 2005 uplift values on southern Simeulue. The chi-square and weighted root-mean-squared values of the best-fit model are equal to 189 and 0.0497 m, respectively [based on 102 (coral) + 16 × 3 (CGPS) = 150 measurements].
23. A. O. Konca *et al.*, *Eos Trans. AGU* **86**, Abstract T31C-03 (2005).
24. D. E. Karig, M. B. Lawrence, G. F. Moore, J. R. Curray, *J. Geol. Soc. London* **137**, 77 (1980).
25. K. Sieh, D. Natawidjaja, *J. Geophys. Res.* **105**, 28,295 (2000).
26. D. Davis, J. Suppe, F. A. Dahlen, *J. Geophys. Res.* **88**, 1153 (1983).
27. Seismicity obtained from the National Earthquake Information Center (http://neic.usgs.gov/neis/epic/).
28. Y. Hsu *et al.*, *Eos Trans. AGU* **86**, Abstract T31C-02 (2005).
29. U.S. Geological Survey, "Notes From the Field…USGS Scientists in Sumatra Studying Recent Tsunamis: Leg 2 Reports, 12 April to 30 April 2005"; available at http://walrus.wr.usgs.gov/news/reports.html (2005).
30. R. A. Kerr, *Science* **308**, 341 (2005).
31. M. Chlieh, personal communication.
32. J. Borrero, B. McAdoo, paper presented at the International Meeting on the Sumatran Earthquake Challenge, Padang, Sumatra, Indonesia, 25 August 2005.
33. H. Th. Verstappen, Geomorphical reconnaissance of Sumatra and adjacent islands (Indonesia), Walters Noordhoff, Groningen (1973).
34. H. R. DeShon, E. R. Engdahl, C. H. Thurber, M. Brudzinski, *Geophys. Res. Lett.* **32**, L24307 (2005).
35. R. Bilham, E. R. Engdahl, N. Feldl, S. P. Satyabala, *Seismol. Res. Lett.* **76**, 299 (2005).
36. K. Sieh *et al.*, *Eos Trans. AGU* **86**, Abstract T31C-05 (2005).
37. L. Prawirodirdjo, Y. Bock, *J. Geophys. Res.* **109**, B08405 (2004).
38. J. R. Curray, *J. Asian Earth Sci.* **25**, 187 (2005).
39. W. H. F. Smith, D. T. Sandwell, *Science* **277**, 5334 (1997).
40. Shuttle Radar Topography Mission (SRTM) data (http://seamless.usgs.gov/).

41. This research was supported by the NSF, the Gordon and Betty Moore Foundation, and the Indonesian International Joint Research Program (RUTI). The National Geographic Channel and The Discovery Channel provided partial helicopter support. The captains and crews of Derazona Helicopters, the Mentawai Indah, the Saraina, and the Sariman Jadi provided expert transportation in the air and on the sea. Thanks to M. Chlieh, M. Tobita, and M. Meiner for helpful discussions and to J. Giberson and S. Healy for assistance with spatial data. Finally, we thank the people in the earthquake-affected region for their hospitality and willingness to share their observations. This is Caltech Tectonics Observatory contribution number 29.

Supporting Online Material

www.sciencemag.org/cgi/content/full/311/5769/1897/DC1
Figs. S1 to S10
Tables S1 and S2
References

14 November 2005; accepted 20 January 2006
10.1126/science.1122602

A Radio Pulsar Spinning at 716 Hz

Jason W. T. Hessels,[1]* Scott M. Ransom,[2] Ingrid H. Stairs,[3] Paulo C. C. Freire,[4] Victoria M. Kaspi,[1] Fernando Camilo[5]

We have discovered a 716-hertz eclipsing binary radio pulsar in the globular cluster Terzan 5 using the Green Bank Telescope. It is the fastest spinning neutron star found to date, breaking the 24-year record held by the 642-hertz pulsar B1937+21. The difficulty in detecting this pulsar, because of its very low flux density and high eclipse fraction (~40% of the orbit), suggests that even faster spinning neutron stars exist. If the pulsar has a mass less than twice the mass of the Sun, then its radius must be constrained by the spin rate to be <16 kilometers. The short period of this pulsar also constrains models that suggest that gravitational radiation, through an *r*-mode (Rossby wave) instability, limits the maximum spin frequency of neutron stars.

The majority of neutron stars are observed to rotate slower than a few times a second; however, those in binary systems can reach spin rates of hundreds of times a second through the transfer of angular momentum from their companion star (*1*, *2*). Some of these neutron stars, termed millisecond pulsars, are persistent radio sources whose emission is modulated at the star's spin frequency. Determining the maximum achievable rotation rate of a neutron star is important for a variety of astrophysical problems, ranging from understanding the behavior of matter at supra-nuclear densities to estimating the importance of neutron stars as gravitational wave sources for current and upcoming gravitational wave detectors. For more than 24 years, the 642-Hz pulsar B1937+21, which is the first millisecond pulsar ever found, has been the fastest spinning neutron star known (*3*). It has been argued that faster ones are exceedingly rare, if they exist at all (*4*).

Per unit mass, globular clusters (GCs) have many more millisecond pulsars than does the Galactic disk. This is due to the extremely high stellar densities in their cores (10^4 to 10^6 pc^{-3}), which promote the creation of binary systems (*5*) where a neutron star is spun-up (or "recycled")

to rotate hundreds of times a second (*1*, *2*). We have searched the massive and dense GC Terzan 5 for millisecond pulsars using the NRAO's (*6*) 100-m Green Bank Telescope (GBT). Our searches have thus far uncovered 30 millisecond pulsars in Terzan 5 (*7*), in addition to the three previously known pulsars in this cluster (*8*–*10*). The discovery of 21 pulsars in Terzan 5 was presented in (*11*). An additional nine pulsars were found in searches of our monitoring observations. Terzan 5 has the largest known population of millisecond pulsars of any GC—roughly one quarter of the entire population of GC millisecond pulsars—and the five fastest rotating pulsars in the Galactic GC system (*7*). Among the newest discoveries in Terzan 5 is PSR J1748–2446ad, a 716-Hz eclipsing binary millisecond pulsar, which is the fastest spinning neutron star ever found.

We discovered PSR J1748–2446ad in 10 November 2004 observations of Terzan 5 and confirmed it in 8 January 2005 observations using the Pulsar Spigot backend (*12*) on the GBT. All observations used the Spigot with 600 MHz of usable bandwidth centered at 1950 MHz, 768 spectral channels, and 81.92-μs sampling. Observations were generally 6 to 7 hours long and taken at roughly monthly intervals starting June 2004. In addition, there was a more closely spaced set of observations in early May 2005.

The discovery observation showed that the pulsar is part of a binary system and is eclipsed by its companion; both of these properties restricted our ability to detect the pulsar in our monitoring sessions. Nonetheless, we have now detected the pulsar in at least 18 of the 30 multihour observations taken thus far (see Fig. 1 for pulse profile). We have derived a reliable orbital ephemeris (Table 1) by initially modeling the pulse phase delays of a few good detections with a simple sine function and then refining the model by fitting pulse times of arrival to a simple Keplerian orbital model with arbitrary pulse phase offsets between observing epochs. This ephemeris allowed us to detect the pulsar in many observations where it was not initially identified through a periodicity search.

The pulsar is in a highly circular 26-hour orbit with a 0.14–solar mass ($M_\odot$) companion, and it is eclipsed for ~40% of its orbit at 2 GHz. Such a large eclipse fraction, corresponding to an eclipse region with physical size ~5 to 6 times the solar radius ($R_\odot$) is extremely rare for such a relatively wide orbit (separation between the pulsar and companion of ~4 to 5 times $R_\odot$). The companion may be a bloated main-sequence star, possibly still filling its Roche Lobe, as has been suggested for PSR J1740–5340, a 35-hour binary millisecond pulsar with a $\geq 0.21 M_\odot$ companion and ~40% eclipse fraction at 1.4 GHz (*13*). The eclipse properties are also similar to those of PSR J1748–2446A, a 1.8-hour binary with a $0.089 M_\odot$ companion, also located in Terzan 5 (*8*). Similar to PSR J1740–5340 and PSR J1748−2446A, there is evidence that the eclipse duration of PSR J1748–2446ad is variable and sometimes lasts longer than 40% of the orbit. On a least two epochs when our ephemeris predicts the pulsar should have been visible for several hours, it was not detected at all. The pulse signal-to-noise ratio is too low to measure variation in the dispersion measure on short timescales. Future observations should allow a phase-coherent timing solution to be derived, which will provide a precise position and observed spin frequency derivative, $\dot{\nu}$. Until then, we have provided an upper limit on $|\dot{\nu}|$ (Table 1).

We have verified that this signal is not harmonically related to any of the other known pulsars in Terzan 5. We have also carefully investigated the possibility that our searches have identified the second harmonic of a 358-Hz pulsar. When we fold the data at 358 Hz, there are two identical peaks [within the resolution and root mean square (RMS) noise level of the Spigot data] separated by 180° in pulse phase. This is what we expect to see if the pulsar signal is folded at half its intrinsic spin frequency, and it strongly suggests that 716 Hz is the true spin frequency of the pulsar. The results of folding the data at other harmonically related spin frequencies are also consistent with the pulsar having a true frequency of 716 Hz. There is also evidence (Fig. 1) for a weak but statistically significant interpulse (extra structure in addition to the main pulse peak) when the data are folded at 716 Hz. This interpulse, if real, is further evidence that the spin frequency is 716 Hz.

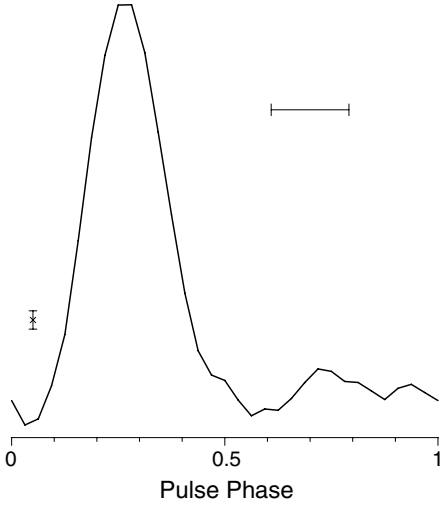

Fig. 1. Master PSR J1748–2446ad pulse profile from the combination of eight GBT Pulsar Spigot observations at 2 GHz with particularly good detections of the pulsar. The cumulative integration time is ~54 hours. There are 32 phase bins across the profile, and the *y* axis plots flux in arbitrary units. The one sigma error bar on the flux is shown in the lower left-hand corner. The effective time resolution of the data, ~300 μs, which accounts for pulse smearing due to channelization of the dispersed data and finite time sampling, is indicated by the horizontal bar. A weak, but statistically significant interpulse is seen at a phase of ~0.75.

Table 1. Measured and derived parameters of PSR J1748–2446ad. All measured spin and orbital parameters were determined with the TEMPO software package (*32*), using arbitrary phase offsets between observing epochs. Given the currently sparsely sampled data, it is impossible to phase connect separate observations. For this reason, we provide only an upper limit on the magnitude of the spin frequency derivative of the pulsar, which incorporates the maximum possible acceleration due to the gravitational potential of Terzan 5 assuming a position close to the cluster center. Likewise, we can currently only place limits on the derived characteristic age, surface magnetic field, and spin-down luminosity. The minimum companion mass is derived assuming a pulsar mass of $1.4 M_\odot$. The dispersion measure was determined by measuring pulse arrival-time delays in the different frequency channels across the 600-MHz observing bandwidth. Numbers in parentheses indicate the error on the last digit. MJD, Modified Julian Day.

Parameter	Value
Rotational parameters	
Pulse period P (s)	0.00139595482(6)
Period derivative $\lvert\dot{P}\rvert$ (s/s)	$\leq 6 \times 10^{-19}$
Pulse frequency ν (Hz)	716.35556(3)
Frequency derivative $\lvert\dot{\nu}\rvert$ (Hz/s)	$\leq 3 \times 10^{-13}$
Epoch (MJD)	53500
Orbital parameters	
Orbital period P_{orb} (days)	1.09443034(6)
Projected semi-major axis x (light-seconds)	1.10280(6)
Time of ascending node T_{ASC} (MJD)	53318.995689(12)
Eccentricity e	<0.0001
Derived quantities	
Companion minimum mass $M_{2,\min}$ ($M_\odot$)	0.14
Dispersion measure DM (pc cm^{-3})	235.6(1)
Flux density at 1950 MHz S_{1950} (mJy)	0.08(2)
Characteristic age τ_c (years)	$\geq 2.5 \times 10^7$
Surface magnetic field B_{surf} (G)	$\leq 1.1 \times 10^9$
Spin-down luminosity $\dot{E}$ (erg/s)	$\leq 1.3 \times 10^{37}$

[1]Department of Physics, McGill University, Montreal, QC H3A 2T8, Canada. [2]National Radio Astronomy Observatory (NRAO), 520 Edgemont Road, Charlottesville, VA 22903, USA. [3]Department of Physics and Astronomy, University of British Columbia, 6224 Agricultural Road, Vancouver, BC V6T 1Z1, Canada. [4]National Astronomy and Ionosphere Center, Arecibo Observatory, HC03 Box 53995, PR 00612, USA. [5]Columbia Astrophysics Laboratory, Columbia University, 550 West 120th Street, New York, NY 10027, USA.

*To whom correspondence should be addressed. E-mail: hessels@physics.mcgill.ca

Lastly, we have simultaneously observed the pulsar using the Green Bank Astronomical Signal Processor (GASP) coherent dedispersion pulsar machine (*14*, *15*), which records only ~⅙ the bandwidth achievable with Spigot but which removes all dispersive smearing due to the ionized interstellar medium, resulting in significantly sharper (i.e., narrower) pulse profiles (*16*). When the GASP data are folded at 358 Hz, two peaks, consistent in shape with each other to within the RMS of the noise, are seen separated by 180° in pulse phase, again indicating that 358 Hz is half of the true spin frequency. We conclude that PSR J1748–2446ad is indeed a 716-Hz pulsar.

The equation of state of matter at supranuclear densities, and thus the mass-radius relation for neutron stars, is unknown. If a star is rotating too rapidly for a given radius, centrifugal forces will cause it to shed mass. Lattimer and Prakash (*17*) derive the following equation, which, independent of the true equation of state, gives the maximum spin frequency for a neutron star with a nonrotating radius R and mass M (assuming this is not close to the maximum mass allowed by the equation of state): $\nu_{max} = 1045(M/M_\odot)^{1/2}(10\ \mathrm{km}/R)^{3/2}$ Hz. Using this, and assuming a mass less than 2 $M_\odot$ [which accommodates all measured neutron star masses (*17*)] we find an upper limit of 16 km on PSR J1748–2446ad's radius. This constraint applies specifically to PSR J1748–2446ad, and slower spinning pulsars could have larger radii. Recently, Li and Steiner (*18*) have derived a radius range of 11.5 to 13.6 km for a 1.4$M_\odot$ neutron star, based on terrestrial laboratory measurements of nuclear matter. For a 1.4$M_\odot$ neutron star, we find an upper limit of 14.4 km, which is in agreement with their result. These radius constraints are more robust than those obtained through observations of neutron star thermal emission, which is faint, difficult to measure, and whose characterization depends on uncertain atmosphere models (*19*). Although in principle a radius measurement could constrain the unknown equation of state of dense matter, PSR J1748–2446ad does not rule out any particular existing models, because the pulsar mass is unknown. It is unlikely that a mass measurement will be achievable through timing of the pulsar, because the orbit is too circular to measure the relativistic advance of the periastron, which would likely be contaminated by classical effects as well. However, once a timing position is available, optical spectroscopy may allow the determination of the mass ratio, as has been done in the case of PSR J1740–5340 in the globular cluster NGC 6397 (*20*). The feasibility of such a measurement will depend on the pulsar not being located in the dense and optically crowded core of the cluster. Fortunately, because PSR J1748–2446ad has a dispersion measure which is ~3 units lower than the ~239–pc cm^{-3} average dispersion measure of the cluster pulsars, it is likely to be located outside of the core.

Although there are selection effects—especially at radio wavelengths—against finding fast, binary pulsars (*21*), we have maintained excellent sensitivity to these by using advanced search techniques (*22*) and data with high time and frequency resolution. For example, these searches blindly detect the 596-Hz binary pulsar PSR J1748–2446O (orbital period P_{orb} ~ 6 hours) at its second and fourth harmonic, which is equivalent to detecting a highly accelerating 1192-Hz pulsar and its second harmonic. Although these searches are clearly sensitive to pulsars faster than 716 Hz, we note that obscuration of the pulsar signal by material blown off the companion by the pulsar wind may play an important role in reducing the chances of detecting such systems (*23*). Of the five fastest known millisecond pulsars (including the two found in the Galactic plane; see Table 2), four are eclipsing, and the fifth, PSR B1937+21, is unusual because unlike ~80% of Galactic plane millisecond pulsars, it has no binary companion. Because rotational energy loss is inversely proportional to the cube of the spin period ($\dot{E} = 4\pi^2 I\dot{P}/P^3$, where $\dot{E}$ is the spin-down luminosity, $\dot{P}$ is the period derivative, and I is the stellar moment of inertia), it is plausible that a large fraction of the fastest binary pulsars are evading detection because their powerful winds are ablating their companions. Some of the ablated material remains in the vicinity of the system and obscures radio pulsations, particularly at lower radio frequencies. Although we have no detections of the pulsar at other frequencies, several other eclipsing pulsars are observed to have longer eclipse durations at lower radio frequencies (*24*). If this is also the case for PSR J1748–2446ad, then the unusually high observing frequency used here (2 GHz, whereas most GC surveys have been conducted at 1.4 GHz or lower) was likely crucial in detecting this pulsar. PSR J1748–2446ad is too weak (the flux density at 1950 MHz is ~0.08 mjansky) to be detectable by the vast majority of Galactic plane surveys, and its high eclipse fraction compounds this problem. This suggests that other even faster spinning pulsars exist, but will require deeper surveys (perhaps at higher observing frequencies to mitigate obscuration of the pulsar signal by intrabinary material) and more concentrated efforts to be detected. In effect, the isolated nature and very large luminosity of PSR B1937+21 make it a unique object, rather than a representative member of the millisecond pulsar population.

Low-mass x-ray binaries (LMXBs) with neutron star members are the likely progenitors of the radio millisecond pulsars. Because the spin-up time for a neutron star to reach >1000 Hz rotation via the accretion of matter in an LMXB is much shorter than the typical LMXB lifetime, one might naïvely expect many millisecond pulsars to be rotating at submillisecond periods. However, given the observed lack of pulsars spinning this fast, gravitational radiation has been proposed as a limiting mechanism, because it could be responsible for carrying away rotational kinetic energy from the star, thus spinning it down. Specifically, gravitational waves may be acting either through an accretion-induced mass quadrupole on the crust (*25*), a large toroidal magnetic field (*26*), or an r-mode (Rossby wave) instability in the stellar core (*27*, *28*).

PSR J1748–2446ad provides interesting constraints on the r-mode possibility. These oscillations are believed to be present in all rotating neutron stars (*29*, *30*). Because of gravitational radiation emission, the r modes become unstable and grow exponentially. The amplitude of the mode continues to grow as angular momentum is radiated away, and the star spins down. However, it is unclear whether the driving of these modes by gravitational waves can overcome viscous damping in the star. Damping depends on the core temperature of the star and its spin rate, as well as several other factors including the thickness of the neutron star crust and how it couples to the core. For a given core temperature, it is possible to derive a critical spin frequency above which the proposed mode is unstable and will cause the star to spin down rapidly. It has been predicted that the critical frequency is <700 Hz for a wide range of core temperature (10^7 to 10^{10} K) and a realistic model of the neutron star crust (*28*). Our discovery of a 716-Hz pulsar indicates that if the r-mode instability limits neutron star spin-up, then either it

Table 2. The 10 fastest spinning known radio pulsars. Data compiled from the Australia Telescope National Facility pulsar database (*33*).

Pulsar	Spin frequency (Hz)	P_b (days)	$M_{2,min}$ ($M_\odot$)	Eclipse fraction	Location
J1748−2446ad	716.358	1.0944	0.14	0.4	Terzan 5
B1937+21	641.931	isolated			Galaxy
B1957+20	622.123	0.3819	0.021	0.1	Galaxy
J1748−2446O	596.435	0.2595	0.035	0.05	Terzan 5
J1748−2446P	578.496	0.3626	0.37	0.4	Terzan 5
J1843−1113	541.812	isolated			Galaxy
J0034−0534	532.714	1.5892	0.14	0	Galaxy
J1748−2446Y	488.243	1.17	0.14	0	Terzan 5
J1748−2446V	482.507	0.5036	0.12	0	Terzan 5
B0021−72J	476.048	0.1206	0.020	0.1*	47 Tucanae

*B0021−72J is eclipsed only at radio frequencies <1 GHz.

must become important only at more rapid spin rates or better modeling of the neutron star crust is required. The current upper limit on the frequency derivative of PSR J1748–2446ad is consistent with those measured for other millisecond pulsars and does not suggest an anomalously rapid spin-down rate. Thus, although there is currently no evidence that PSR J1748–2446ad is spinning down due to gravitational radiation, the possible importance of systems like PSR J1748–2446ad as gravitational wave sources for detectors like the Laser Interferometer Gravitational-Wave Observatory (LIGO) makes improved modeling of neutron star structure and gravitational wave instabilities critically important.

The observed spin frequencies of LMXBs are all less than 620 Hz. The biases that exist at radio wavelengths against finding much faster pulsars do not exist for LMXBs, because x-rays do not suffer from the dispersive effects of the interstellar medium and are less obscured by intrabinary material. This suggests that faster spinning neutron stars in LMXBs should be detectable if they exist. However, transient coherent pulsations are only observed in seven sources, and there may be unidentified sources of bias in the population that are preventing faster pulsations from being detected. Chakrabarty *et al.* (*4*) performed a Bayesian statistical analysis on the spin frequencies of 11 nuclear-powered millisecond pulsars, those for which the spin frequency is known from the detection of burst oscillations, and concluded that the sample is consistent (at the 95% confidence level) with a cutoff ν_{max} = 760 Hz. More recent work by the same authors (*31*), which added 2 pulsars to the sample, has revised this limit to 730 Hz. Based on this result, they conclude that something, possibly gravitational radiation, is limiting the spin frequency of neutron stars. If their statistically derived upper limit is realistic (and therefore some mechanism is limiting neutron star spin-up), then the 716-Hz pulsar presented here is likely an extremely rare object. However, we note that their Bayesian calculation is very sensitive to the neutron star with the slowest spin frequency included in the analysis. In addition, the assumption made by these authors that the pulsar spin rates are uniform in frequency (at least over some range ν_{low} to ν_{high}) would likely not apply to the Terzan 5 pulsars, whose spin period distribution is clearly not uniform (*11*), even accounting for the observational bias against detecting the fastest pulsars. Hence, a recalculation of the maximum spin cutoff using the Terzan 5 sample of pulsars and the same statistical analysis would not be appropriate, although the existence of PSR J1748–2446ad already implies that the cutoff must be higher.

References and Notes

1. M. A. Alpar, A. F. Cheng, M. A. Ruderman, J. Shaham, *Nature* **300**, 728 (1982).
2. V. Radhakrishnan, G. Srinivasan, *Curr. Sci.* **51**, 1096 (1982).
3. D. C. Backer, S. R. Kulkarni, C. Heiles, M. M. Davis, W. M. Goss, *Nature* **300**, 615 (1982).
4. D. Chakrabarty *et al.*, *Nature* **424**, 42 (2003).
5. G. Meylan, D. C. Heggie, *Astron. Astrophys. Rev.* **8**, 1 (1997).
6. The National Radio Astronomy Observatory is a facility of NSF operated under cooperative agreement by Associated Universities, Inc.
7. For an updated list of GC pulsars, see www.naic.edu/~pfreire/GCpsr.html.
8. A. G. Lyne, S. Johnston, R. N. Manchester, L. Staveley-Smith, N. D'Amico, *Nature* **347**, 650 (1990).
9. A. G. Lyne, S. H. Mankelow, J. F. Bell, R. N. Manchester, *Mon. Not. R. Astron. Soc.* **316**, 491 (2000).
10. S. M. Ransom, thesis, Harvard University (2001).
11. S. M. Ransom *et al.*, *Science* **307**, 892 (2005).
12. D. L. Kaplan *et al.*, *Pub. Astron. Soc. Pacific* **117**, 643 (2005).
13. N. D'Amico *et al.*, *Astrophys. J.* **561**, L89 (2001).
14. P. Demorest *et al.*, *Am. Astron. Soc. Meet. Abstr.* **205** (2004).
15. R. D. Ferdman *et al.*, *Am. Astron. Soc. Meet. Abstr.* **205** (2004).
16. The Spigot pulse profile is significantly widened compared with the intrinsic pulse width of the pulsar because the finite number of channels used across the observing bandwidth does not allow for a complete removal of the dispersive effects of the interstellar medium.
17. J. M. Lattimer, M. Prakash, *Science* **304**, 536 (2004).
18. B. Li, A. Steiner, *Nucl. Theor.*, abstract available at http://xxx.lanl.gov/abs/nucl-th/0511064 (2005).
19. V. M. Kaspi, M. S. E. Roberts, A. K. Harding, abstract available at http://xxx.lanl.gov/abs/astro-ph/0402136 (2004).
20. F. R. Ferraro *et al.*, *Astrophys. J.* **584**, L13 (2003).
21. H. M. Johnston, S. R. Kulkarni, *Astrophys. J.* **368**, 504 (1991).
22. S. M. Ransom, S. S. Eikenberry, J. Middleditch, *Astron. J.* **124**, 1788 (2002).
23. M. Tavani, *Astrophys. J.* **379**, L69 (1991).
24. S. M. Ransom *et al.*, *Astrophys. J.* **604**, 328 (2004).
25. L. Bildsten, *Astrophys. J.* **501**, L89 (1998).
26. C. Cutler, *Physi. Rev. D* **66**, 084025 (2002).
27. N. Andersson, K. Kokkotas, B. F. Schutz, *Astrophys. J.* **510**, 846 (1999).
28. Y. Levin, G. Ushomirsky, *Mon. Not. R. Astron. Soc.* **324**, 917 (2001).
29. N. Andersson, *Astrophys. J.* **502**, 708 (1998).
30. J. L. Friedman, S. M. Morsink, *Astrophys. J.* **502**, 714 (1998).
31. D. Chakrabarty, *Astron. Soc. Pac. Conf. Series 328: Binary Radio Pulsars*, F. Rasio, I. Stairs, eds. (2005), p. 279.
32. The software is available at http://pulsar.princeton.edu/tempo.
33. The database is available at www.atnf.csiro.au/research/pulsar/psrcat.

34. We thank R. Ferdman and P. Demorest for help with GASP observations and acknowledge their work, along with that of D. Backer, D. Nice, R. Ramachandran, and J. van Leeuwen, in creating the GASP instrument. We also thank L. Bildsten, P. Arras, and J. Lattimer for very useful discussions. J.W.T.H. is a Natural Sciences and Engineering Research Council of Canada (NSERC) Post Graduate Scholarship–Doctoral fellow and is grateful to the Canada Foundation for Innovation for funding the computing resources used to make this discovery and to P. Mercure for helping to maintain them. I.H.S. holds a NSERC University Faculty Award and is supported by a Discovery grant and University of British Columbia start-up funds. V.M.K. is a Canada Research Chair and is supported by a NSERC Discovery Grant and Steacie Fellowship Supplement, by the Fonds Québécois de la Recherche sur la Nature et les Technologies and Canadian Institute for Advanced Research. F.C. thanks NSF for support. GASP is funded by a NSERC RTI-1 grant to I.H.S. and by NSF grants to D. Backer and D. Nice.

5 December 2005; accepted 6 January 2006
Published online 12 January 2006;
10.1126/science.1123430
Include this information when citing this paper.

A Linear Homocatenated Compound Containing Six Indium Centers

Michael S. Hill,[1]* Peter B. Hitchcock,[2] Ruti Pongtavornpinyo[1]

In contrast to carbon and its heavier congeners, group 13 elements are rarely observed to catenate into linear chains. Here, we find that treatment of indium(I) iodide with a protonated *N*-xylyl β-diketiminate and a strong potassium base in tetrahydrofuran yields a hexa-indium chain. X-ray crystallography revealed one β-diketiminate ligand bound to each indium center with no bridging ligands supporting the five indium-indium single bonds. The terminal indium centers were capped with iodine. Electronic spectroscopy and computations on a model compound offer preliminary support for σ delocalization along the chain.

The capacity of carbon to form single bonds with itself (catenate) is unsurpassed and clearly demonstrated by the structures of the linear *n*-alkanes. Homologs, C_nH_{n+2}, are constructed by addition of tetrahedral (sp^3) carbon centers with no detriment to the stability of the structure with increasing chain length. Although silicon, germanium, tin, and lead also provide sufficient valence orbitals and electrons for the formation analogous extended linear structures, well-defined catenated compounds become increasingly uncommon with greater atomic weight. More diffuse valence orbitals and rising inner shell repulsion result in decreasing homonuclear σ bond enthalpies, D_0, as the group is descended (Table 1) and an increasing tendency to undergo homolytic decomposition (*1*).

For the elements of group 13, the D_0 values are in general some 50 to 60 kJ mol^{-1} lower than those determined for their group 14 neighbors (Table 1). Possession of only three valence electrons also commonly results in the adoption

[1]Department of Chemistry, Imperial College London, Exhibition Road, South Kensington, London SW7 2AZ, UK. [2]Chemistry Laboratory, University of Sussex, Falmer, Brighton, East Sussex BN1 9QJ, UK.

*To whom correspondence should be addressed. E-mail: mike.hill@imperial.ac.uk

Table 1. Comparison of thermochemical single E-E bond dissociation energies, D_0 (kJ mol^{-1}), for the group 13 (B to In) (*20*) and group 14 elements (C to Sn) (*1*).

Group 13	Group 14
B, 293	C, 345
Al, 188	Si, 222
Ga, 113	Ge, 188
In, 100	Sn, 190

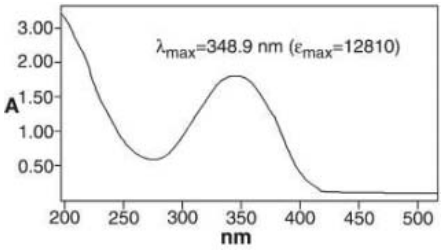

Fig. 2. UV-vis spectrum of compound **5** in hexane at room temperature; ε_{max} is the molar extinction coefficient (dm^3 mol^{-1} cm^{-1}).

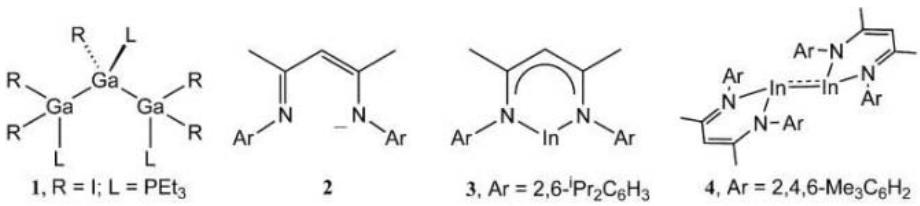

Scheme 1.

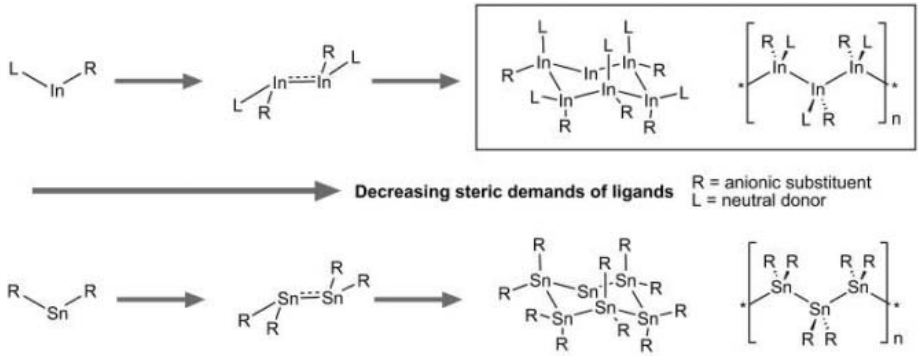

Scheme 2.

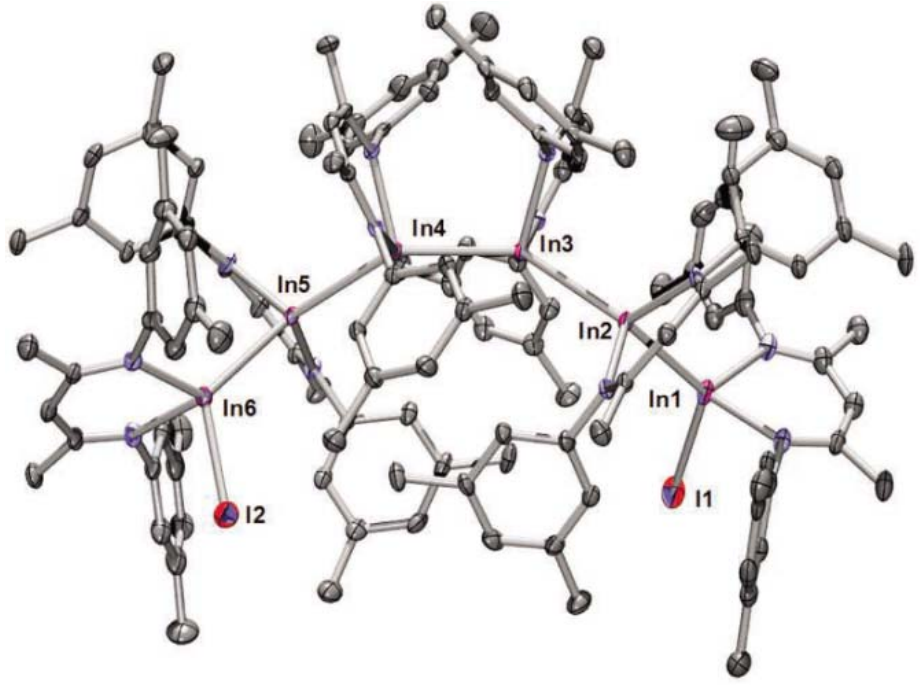

Fig. 1. Oak Ridge Thermal Ellipsoid Plot (ORTEP) (20% ellipsoids) of compound **5**. Key to atom colors: carbon, gray; indium, maroon; nitrogen, blue; and iodine, red.

of aggregated structures and the formation of delocalized cluster molecular orbitals (*2*). Although both these factors mitigate against the routine formation of group 13 catenates, the possibility of extended species was suggested for many years by the existence of molecular dihalides, X_2E-EX_2 (where E is a group 13 element and X is a halide) (*3*, *4*). More recent work has demonstrated that the maintenance of an unsupported two-electron E-E interaction in these compounds is far from unique, and a variety of larger cyclic and halide-bridged structures have also been reported for all the group 13 elements over the past decade (*5*). The observation of more than a single unsupported E-E interaction in a discrete molecule is, however, far from routine. Among the lighter congeners, the only extended open chain complex is the trigallium subhalide $[I_2(PEt_3)GaGaI(PEt_3)Ga(PEt_3)I]$, **1** (Scheme 1) (*6*), and the crystallographically characterized trigonal complex $\{In[In(2,4,6\text{-}^iPr_3C_6H_2)_2]_3\}$ (*7*) is the sole example in indium chemistry. Compound **1** is especially relevant to the current work, because it combines formally anionic iodide (R) and neutral phosphane (L) ligands to enhance the electron count of each four-coordinate gallium center and, as a result, is isoelectronic to the above mentioned group 14 species, i.e., a propane analog.

The β-diketiminate class of anion, **2** (Scheme 1, pictured as a localized iminoamide), attracted our attention because it fulfills similar electronic requirements when bonded to group 13 centers. We have previously reported that the formation of either monomeric, **3** (Scheme 1), or dimeric, **4** (Scheme 1), indium diyls, heavier group 13 analogs of a carbene and an alkene, respectively, is dependent upon the steric demands of the ligand *N*-aryl groups (*8*, *9*). Similar behavior is well established in the valence isolelectronic bis(stannane)diyls, R_2Sn (*10*), when the anionic ligands, R, are bulky. In the case of tin, use of smaller anionic substituents results in the formation of cyclic tin compounds (*11*) (Scheme 2) or, under carefully controlled conditions, linear oligomeric or polymeric materials (*12*–*16*).

With this in mind, we speculated that further reduction of the steric demands of the *N*-aryl substituents of the β-diketiminate ligands of **3** and **4** would likewise result in the formation of oligomeric indium compounds (Scheme 2). This has indeed proved to be the case, and we now report the synthesis of a remarkable catenated hexa-indium complex. Furthermore, we present preliminary evidence that the

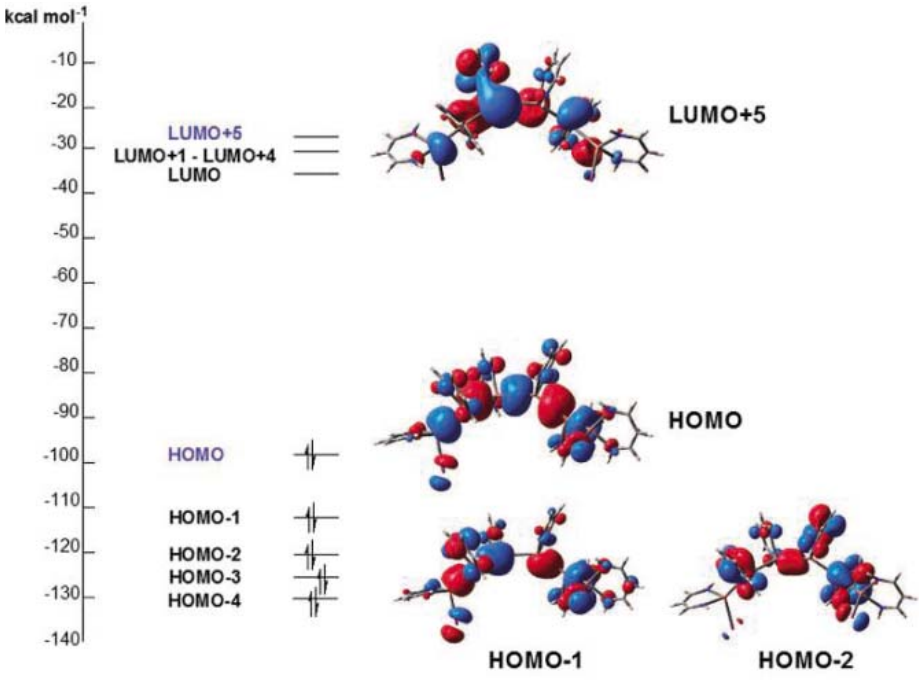

Fig. 3. Molecular orbital analysis (B3LYP/LANDZ) of compound **6**, emphasizing the σ bonding and antibonding orbitals along the In_6 chain.

extended In_6 chain displays behavior consistent with a σ delocalized manifold of molecular orbitals.

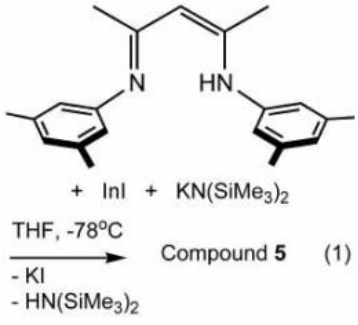

Reaction of *N*-[4-(3,5-dimethylphenylamino) pent-3-en-2-ylidene]-3,5-dimethylbenzenamine with $K[N(SiMe_3)_2]$ and InI (Eq. 1) in tetrahydrofuran (THF) at −78°C produced, upon warming to room temperature, a brown solution together with a heavy gray precipitate. Concurrent deposition of indium metal is a characteristic feature of all our previous successful syntheses of indium-centered diyls (*8*, *9*). Although we have not yet isolated any higher-valent disproportionation products from these reactions, the use of similar salt exchange reactions with monovalent indium halides has previously been observed to result in In(II) or In(III) compounds as the only isolable molecular products (*17*). Removal of the THF solvent, extraction of the solid product with *n*-hexane, and filtration produced a brown solution. Concentration of this filtrate and storage at 5°C produced a mass of red-orange crystals of compound **5**, which were isolated by filtration. In contrast to both **3** and **4**, compound **5**, although air-sensitive, is completely stable to ambient light, and analysis by ^1H and $^{13}C\{^1H\}$ nuclear magnetic resonance (NMR) spectroscopies indicated the presence of multiple β-diketiminate ligand environments.

An x-ray diffraction analysis performed upon a single crystal of **5** obtained from hexane solution revealed a linear structure of six indium centers, each coordinated by a single β-diketiminate ligand (Fig. 1). The indium-indium interactions are completely unsupported by any other bridging unit, and the hexa-indium spine of the molecule appears to comprise a series of five noninteracting two-center two-electron bonds built from pairs of indium sp^3 hybrid orbitals. The four internal indium centers [In(2), In(3), In(4), and In(5)] of compound **5** are coordinated by a single β-diketiminate ligand [the average N-In-N bond angle at In(2) to In(5) is 86.9°] and the distorted tetrahedral metal geometry [average In-In-In bond angle at In(2) to In(5) is 139.4°] is completed by two In-In bonds. Each of these indium atoms, therefore, may be assigned a formal oxidation state of +1. In contrast, the coordination sphere of the terminal indium atoms [In(1) and In(6)] is completed by an additional iodide ligand and consequently may be described as divalent. Evidently, compound **5** is the result of two competing reaction pathways, potassium iodide elimination between the potassium β-diketiminate with indium(I) iodide and simultaneous disproportionation to In(0) and higher-valent indium species. Although the formation of **5** was not foreseen, it has proven to be completely reproducible, and the reaction results in 30 to 40% isolated yield based on InI. As expected from consideration of the formally assigned oxidation states, the terminal In(1)-In(2) and In(5)-In(6) bond lengths (2.8122 ± 0.0010 and 2.8220 ± 0.0010 Å, respectively] are shorter than those of the internal In-In bonds. The In(2)-In(3) (2.8347 ± 0.0009 Å) and In(4)-In(5) (2.8407 ± 0.0008 Å) distances are similar but distinct within the limits of experimental error, whereas the central In(3)-In(4) bond (2.8535 ± 0.0008 Å) is longer than both. Despite this variation, all the In-In bond lengths are within the range previously reported for In(II) complexes containing an In-In single bond, such as those within the alkyl complex $\{In[CH(SiMe_3)_2]_2\}_2$ (2.828 Å) (*18*) and the silyl complex $[In(Si^tBu_3)_2]_2$ (2.922 ± 0.001 Å) (*19*), and are considerably shorter than the In-In distances (3.25 and 3.38 Å) in indium metal (*20*).

The In-N distances display only comparatively minor variations from In(1) to In(6). They are, however, substantially longer on average (average of 2.212 ± 0.008 Å) than those reported for the only other (dinuclear) In(II) β-diketiminate, $\{InCl[N(2,6\text{-}^iPr_2C_6H_3)C(Me)]_2CH\}_2$ (range from 2.1654 ± 0.0012 to 2.1874 ± 0.0012 Å) (*17*). The In(1)-I(1) (2.7980 ± 0.0013 Å) and In(6)-I(2) (2.7802 ± 0.0012 Å) bonds are also lengthened in comparison to those within $\{InI_2[N(2,6\text{-}^iPr_2C_6H_3)C(Me)]_2CH\}$ (2.6050 ± 0.0002 and 2.7008 ± 0.0002 Å), which contains an unambiguous In(III) center (*21*).

A defining feature of catenated compounds of the heavier group 14 elements is the one-dimensional delocalization of σ electron density along the chain (*12*–*16*, *22*). Discrete oligomeric molecules of known chain length have played a prominent role in elucidating the origin of these properties, which are most clearly manifested as moderately intense electronic absorptions assigned to σ-σ* transitions in the ultraviolet-visible (UV-vis) spectra. Irrespective of the supporting ligand groups and chain conformation, this transition has been found to display a characteristic dependence on the number of constituent group 14 atoms in the linear chain, namely a red shift to decreasing energy with increasing chain length, up to a limiting wavelength maximum that is determined by the identity of the constituent element (*22*). For $(R_2Sn)_x$ (where R is an alkyl or aryl) chains containing between five and seven tin atoms, this absorption falls between 320 and 370 nm (*12*). Compound **5** displayed an absorption maximum in hexane at circa 349 nm (Fig. 2). Although it is not yet possible to deconvolute the relative effects of donor ligand identity and chain conformation, this absorption is primary evidence for the existence of analogous delocalization of the indium σ framework. It is likely

that the position of the absorption maximum is dictated by the conformation of the In_6 chain, which describes approximately half a rotation of a screw-like helical progression (fig. S1).

Conformational effects have been widely commented upon in polysilane chemistry (*23*) and it appears likely that the chain conformation of compound **5** is constrained by the steric demands of the *N*-xylyl substituted β-diketiminate supporting ligands. A space-filling representation of compound **5** (fig. S2), illustrates the highly efficient protection of the individual In-In bonds provided by the closely arrayed aryl and methyl ligand susbstituents.

We have undertaken preliminary density functional theory (DFT) analysis (B3LYP/LANDZ) of the model linear In_6 complex $InIL(InL)_4InIL$ [where L is $(HNCH)_2CH$], **6**, constrained to the conformation described by the crystallographic coordinates from the x-ray analysis (*24*). These results provide a qualitative molecular orbital analysis of the bonding along a catenated hexa-indium chain (Fig. 3). The orbitals denoted lowest unoccupied molecular orbital (LUMO) to LUMO+4 are entirely ligand-based, whereas the LUMO+5 is the lowest energy unoccupied virtual orbital involved in In-In σ bonding. Unsurprisingly, the calculated LUMO+5 to highest occupied molecular orbital (HOMO) energy difference for the simplified complex **6** somewhat underestimates the σ-σ* transition energy (389 nm) inferred from the spectroscopic data provided by **5**. More exacting analysis will be required to fully appreciate the effects of differing substituent patterns as well as chain conformation.

References and Notes

1. J. E. Huheey, E. A. Keiter, R. L. Keiter, *Inorganic Chemistry* (Harper, New York, ed. 4, 1995).
2. For a recent review of group 13 cluster chemistry, see H. Schnöckel, *Dalton Trans.* **2005**, 3131 (2005).
3. D. G. Tuck, *Chem. Soc. Rev.* **22**, 270 (1993), and references therein.
4. D. G. Tuck, *Polyhedron* **9**, 377 (1990), and references therein.
5. For a recent comprehensive review of relevant literature, see W. Uhl, *Adv. Organomet. Chem.* **51**, 53 (2004).
6. A. Schnepf, C. Doriat, E. Mülhausen, H. Schnöckel, *Chem. Commun.* **1997**, 2111 (1997).
7. P. J. Brothers *et al.*, *Angew. Chem. Int. Ed. Engl.* **35**, 2355 (1996).
8. M. S. Hill, P. B. Hitchcock, *Chem. Commun.* **2004**, 1818 (2004).
9. M. S. Hill, P. B. Hitchcock, R. Pongtavornpinyo, *Angew. Chem. Int. Ed. Engl.* **44**, 4231 (2005).
10. P. J. Davidson, M. F. Lappert, *J. Chem. Soc. Chem. Commun.* **1973**, 317a (1973).
11. Although Et_2Sn was first reported in 1853 by Frankland, this material was undoubtedly polymeric. For a perspective on the early literature and structural work performed during the 1960s and 1970s, see (*25*).
12. S. Adams, M. Dräger, *Angew. Chem. Int. Ed. Engl.* **26**, 1255 (1987).
13. L. R. Sita, *Organometallics* **11**, 1442 (1992).
14. T. Imori, V. Lu, H. Cai, T. D. Tilley, *J. Am. Chem. Soc.* **117**, 9931 (1995).
15. N. Devylder, M. Hill, K. C. Molloy, G. J. Price, *Chem. Commun.* **1996**, 711 (1996).
16. K. Shibata, C. S. Weinert, L. R. Sita, *Organometallics* **17**, 2241 (1998).
17. M. Stender, P. P. Power, *Polyhedron* **21**, 525 (2002).
18. W. Uhl, M. Layh, W. Hiller, *J. Organomet. Chem.* **368**, 139 (1989).
19. N. Wiberg, K. Amelunxen, K. Nöth, H. Schmidt, H. Schwenk, *Angew. Chem. Int. Ed. Engl.* **35**, 65 (1996).
20. A. J. Downs, *Chemistry of Aluminium, Gallium, Indium, and Thallium* (Chapman, London, 1993).
21. M. Stender *et al.*, *Inorg. Chem.* **40**, 2794 (2001).
22. For a recent review, see I. Manners, *Synthetic Metal-Containing Polymers* (Wiley, Weinheim, 2004).
23. H. A. Fogarty *et al.*, *Pure Appl. Chem.* **75**, 999 (2003).
24. M. J. Frisch *et al.*, Gaussian 03, Revision C.02, Gaussian, Incorporated, Wallingford, CT (2004).
25. W. P. Neumann, in *The Organometallic and Coordination Chemistry of Germaninum, Tin, and Lead*, M. Gielen, P. G. Harrison, Eds. (Freund, Tel Aviv, 1978), p. 71.

26. We thank the Royal Society for funding this work via a University Research Fellowship for M.S.H. Full metrical parameters for the crystal structure of compound **5** are available free of charge from the Cambridge Crystallographic Data Center under reference CCDC 299581.

Supporting Online Material

www.sciencemag.org/cgi/content/full/311/5769/1904/DC1
Materials and Methods
SOM Text
Figs. S1 and S2
Table S1

16 December 2005; accepted 1 March 2006
10.1126/science.1123945

Rotational Coherence and a Sudden Breakdown in Linear Response Seen in Room-Temperature Liquids

Amy C. Moskun,[1]* Askat E. Jailaubekov,[1] Stephen E. Bradforth,[1]† Guohua Tao,[2] Richard M. Stratt[2]†

Highly energized molecules normally are rapidly equilibrated by a solvent; this finding is central to the conventional (linear-response) view of how chemical reactions occur in solution. However, when a reaction initiated by 33-femtosecond deep ultraviolet laser pulses is used to eject highly rotationally excited diatomic molecules into alcohols and water, rotational coherence persists for many rotational periods despite the solvent. Molecular dynamics simulations trace this slow development of molecular-scale friction to a clearly identifiable molecular event: an abrupt liquid-structure change triggered by the rapid rotation. This example shows that molecular relaxation can sometimes switch from linear to nonlinear response.

One of the principal ways in which a solvent facilitates a chemical reaction is by managing the energetics, both by supplying enough energy to surmount activation barriers and by providing channels for excess energy to be dissipated. Given the energies typically involved in chemical bond rearrangement (tens of kcal/mol, or roughly 10^4 K), these are formidable tasks for a solvent armed with no more than ordinary equilibrium (300 K) fluctuations. Nonetheless, as increasingly microscopic studies of solvation and vibrational relaxation have made clear, solvents do fulfill this critical energy management role, and they do so with precisely the rates expected from the solvent's own ability to absorb energy under ordinary equilibrium conditions (*1*).

This idea that excited states relax with rates determined by the solute-solvent system's ordinary energy fluctuations, commonly called linear response theory, is a critical component in the success of transition-state theories of chemical reaction rates in liquids (*2*). Perhaps a surprising consequence of linear response theory is that the details of how a solute's state is prepared—in particular, how much energy is deposited—are not central to determining how quickly a solvent responds. Even though linear response theory is often derived by assuming relatively small displacements from equilibrium (*3*)—an assumption clearly inappropriate for the amounts of energy relevant to most chemical reactions—it seems to hold rather well, a few notable exceptions aside (*4*–*7*). However, three decades of work in the gas phase have explored how the specifics of the forces between atoms involved in isolated chemical reactions determine the final energy partitioning as the reaction moves from the transition state (*8*). Is knowledge of these specifics completely immaterial (*2*) to reaction dynamics in solution?

This dichotomy highlights a principal difference between gas- and solution-phase chemical dynamics: In low-density gases, the natural perspective focuses on discrete collisions between individual molecules, whereas in the condensed phase, a solute's environment is typically treated collectively and its dynamics are

[1]Department of Chemistry, University of Southern California, Los Angeles, CA 90089, USA. [2]Department of Chemistry, Brown University, Providence, RI 02912, USA.

*Present address: Department of Chemistry, University of California, Irvine, CA 92697, USA.

†To whom correspondence should be addressed. E-mail: bradfort@usc.edu (S.E.B.); richard_stratt@brown.edu (R.M.S.)

described in terms of the evolution of chance fluctuations from equilibrium (*1*). Consider the rotational motion of a solute molecule in a liquid. From the collisional viewpoint, the onset of rotational diffusion can be construed in terms of Brownian small-angle reorientation (*9*), where collisions rapidly interrupt and destroy the coherence of an isolated rotor ensemble. This picture implies that there must be some limited time interval over which inertial (gas phase–like) rotation survives, but at normal liquid densities and temperatures this interval usually corresponds to the solute sweeping out no more than a very small angle. This inertial behavior has been observed for solute reorientation in liquids in only a few, rather weakly interacting, cases (*10*–*12*). The usual condensed-phase perspective, by contrast, is that there are no specific events through which the liquid begins to exert its influence; linear response theory dictates that random solvent fluctuations simply extract more and more of the rotor's energy as time goes on.

Consider, then, what happens if a solute is born with extremely high rotational energy. Gas-phase intuition suggests that there may be a much longer period, perhaps more than an entire rotational period, during which entirely gas phase–like dynamics might prevail and the solvent would be unable to disrupt the solute. If so, what does this say about the solvent response in terms of linear response theory? We explore this issue by watching an example of rotational relaxation in a standard chemical environment: liquid water and alcohol solutions. By using a chemical reaction to prepare a high-energy, nonthermal ensemble of rotating diatomic molecules and following the subsequent relaxation on a subpicosecond time scale, we show that neither gas-phase nor liquid-phase intuition is entirely correct. The initial relaxation turns out to proceed just as linear response theory would predict, but the system abruptly reverts to much more gas phase–like dynamics. Such a switch can apparently be attributed directly to specific molecular events occurring in the liquid.

We use ICN photodissociation (*13*, *14*), a chemical reaction in which bond breakage is nearly instantaneous in the gas phase (*15*), leading to a well-characterized, coherent population of highly excited CN rotors with virtually none of the excess energy channeled into CN vibration (*16*, *17*). Although the reaction also has a channel producing cold CN fragments (roughly 60% of the time in the gas phase), the average energy of the hot rotors can be tuned by varying the photoexcitation wavelength, enabling us to generate a controlled and predetermined high-energy distribution of initial rotational states (*18*). In earlier work, Moskun and Bradforth (*19*) were able to show that this reaction also produces rotationally hot CN in room-temperature polar liquids. These results were themselves surprising. The hot rotors apparently act as if they were nearly freely spinning tops, maintaining their rotation plane for tens of rotational periods (several picoseconds). Seeing such gas phase–like behavior in an ordinary room-temperature molecular liquid runs counter to the conventional Brownian small-angle rotational diffusion picture of rotational relaxation, which would have suggested complete randomization of the axis of rotation in well under 1 ps (*9*). Multiple periods of free rotation would also be a striking change from earlier photodissociation studies on I_3^- and HgI_2 in solution, which saw only small-angle ballistic rotation (*20*, *21*).

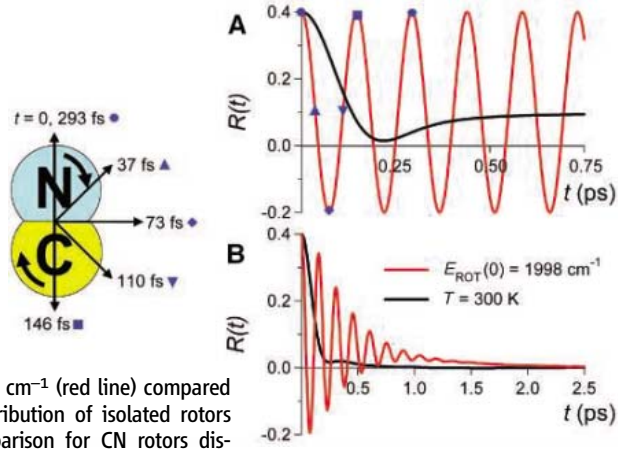

Fig. 1. The connection between transient anisotropy $R(t)$ and the dynamics of molecular reorientation predicted by a classical molecular dynamics simulation. In the experiment reported here, $R(t)$ measures the correlation between the CN bond axis at the instant of photodissociation and the same axis of the CN fragment after elapsed time t. (**A**) Anisotropy evolution of an isolated rotor prepared with a precise rotational energy of 1998 cm^{-1} (red line) compared to that of a 300 K thermal distribution of isolated rotors (black line). (**B**) The same comparison for CN rotors dissolved in 300 K liquid-density (1.344 g/ml) Ar. It is clear from the symbols corresponding to rotations of 0°, 45°, 90°, 135°, 180°, and 360° (as shown at left) that the anisotropy of the single-energy isolated rotor tracks the molecular orientation perfectly, displaying exactly two oscillations for every 360° molecular rotation. Thermal preparation of the rotor evidently destroys too much phase information to carry out such tracking (whether a solvent is present or not), but high-energy rotors can be tracked even in the presence of a solvent; enough of the rotational coherence survives the solvent-induced dephasing for several full rotations to be observable.

These early CN solution experiments, though, were unable to capture the crucial first 200 fs of the dynamics because of insufficient time resolution as well as a strong coherent solvent response near time zero, a response broadened by the thickness of the interrogated liquid film. However, recent advances in ultrashort ultraviolet (UV) pulse generation have allowed us to perform a deep UV-pump/UV-probe experiment with the necessary time resolution. We create photolysis pulses with a wavelength of 233 nm (duration ~33 fs) by four-wave mixing in a rare gas–filled hollow-core fiber, followed by compression using a CaF_2 prism pair (*22*, *23*). Time-delayed 390-nm probe pulses, which monitor the CN product by transient absorption, are selected from a white-light continuum generated in a CaF_2 disk and compressed using a fused-silica prism pair (*18*). We interrogate the ICN solutions in alcohols and water by overlapping linearly polarized pump and probe pulses in a region of a flowing liquid film ~25 μm thick (*24*). The probe beam, polarized 45° relative to the pump, is resolved after the sample into parallel (∥) and perpendicular (⊥) components that are detected simultaneously with two photodiodes (*21*). The rotational relaxation is then tracked by watching the time-dependent anisotropy

$$R(t) = (A_{\parallel} - A_{\perp})/(A_{\parallel} + 2A_{\perp}) \qquad (1)$$

constructed from the two components of the transient probe absorbance $A(t)$.

Although anisotropy does not measure rotational energy relaxation directly, the tendency of rapidly rotating objects to maintain their rotational plane means that the loss of the initial anisotropy is a useful indicator of the loss of rotational energy. The anisotropy function is a vector correlation function and carries additional information about the ensemble motion, including its degree of rotational coherence. In an isotropic environment such as a fluid, the anisotropy is given by

$$R(t) = {}^2/_5\langle P_2[\hat{\Omega}(0) \cdot \hat{\Omega}(t)]\rangle \qquad (2)$$

which measures the angle between the time-0 and time-t transition-dipole vectors $\hat{\Omega}$ averaged over the initial distribution of rotor orientations and angular velocities (P_2 is the standard second-order Legendre polynomial). This same observable has long been used to extract rotational diffusion constants (*9*). However, on an ultrafast time scale, it can be far more informative about the underlying microscopic behavior (Fig. 1).

The anisotropy of free CN rotors prepared with a rotational energy E_{ROT} of precisely 1998 cm^{-1} at time 0 [equivalent to 2875 K of rotational energy and corresponding to rotational quantum number $J \approx 32$, a typical value for ICN photodissociation (*16*)] is compared in Fig.

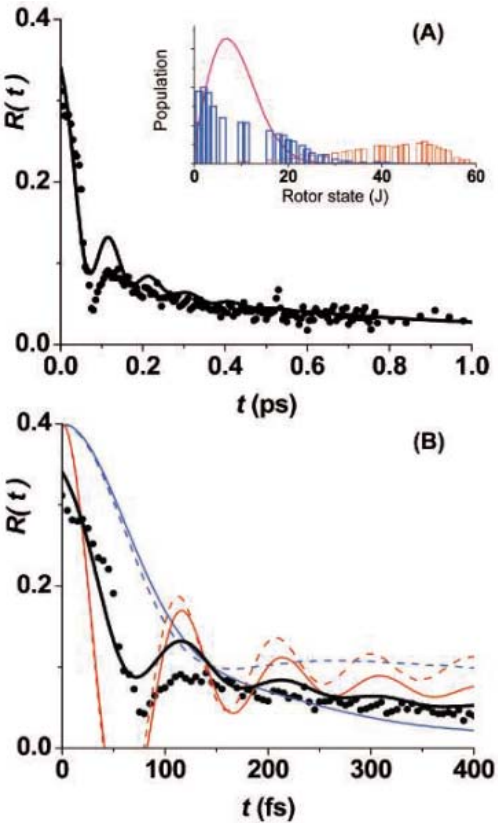

Fig. 2. (**A**) Measured transient pump-probe anisotropy after 233-nm photodissociation of ICN in ethanol (circles). The inset shows the highly non-Boltzmann initial populations of CN fragments in the rotationally hot (red) and cold (blue) channels resulting from this photodissociation in the gas phase (*16*); for comparison, a 300 K thermal rotational distribution is also shown (magenta curve). The gas-phase behavior of the two channels is assumed to carry over to the initial rotor distributions in the condensed phase. (**B**) Molecular dynamics predictions (on an expanded scale) for how each individual channel would contribute in a 300 K, 1.344 g/ml Ar solvent [solid curves; colors as in inset of (A)], contrasted with the behavior of free CN rotors (dashed curves) prepared with the same rotational energy distributions. The black solid curve in both panels is a prediction of the net anisotropy decay this experiment would have produced with a 300 K, liquid-density Ar solvent [calculated as a weighted sum of the solid colored curves corrected for the finite CN lifetime, and convoluted with the experimental response function (*18*)].

1A to the anisotropy for a 300 K equilibrium ensemble. A hypothetical experiment conducted using the perfect rotational coherence of the former (single-energy) ensemble would be able to associate individual points on the $R(t)$ curve with specific angle displacements of the CN radicals. With a thermal (300 K) distribution of rotational energies, by contrast, the anisotropy function would lose most of these oscillations because of the corresponding spread in angular frequencies, although for free rotors there would always be a minimum and the function would tend toward an asymptotic value of 0.1. Given these observations, one might imagine that carrying out the study in a 300 K liquid would remove most of this remaining detail, but as the classical molecular dynamics simulation in liquid-density Ar reveals (Fig.1B), rotational coherence can still be preserved for several rotational periods if the initial rotational energy distribution is sufficiently out of equilibrium with the liquid (*25*).

The simulations reported here were microcanonical, periodic boundary-condition studies conducted by sampling the classical trajectories of a single rigid CN diatomic instantaneously provided with a prescribed rotational kinetic energy in the presence of 106 Ar solvent atoms (*18*). We chose Ar not only for the simplifications it afforded in our subsequent analysis, but because it allowed us to use a high-level ab initio potential surface (*26*) capable of reproducing detailed gas-phase inelastic scattering measurements (*27*). But does this same coherent behavior persist with a more strongly interacting liquid? Our experimental results for 233-nm ICN photodissociation in liquid ethanol (Fig. 2) show that it can. The anisotropy of the CN rotors displays a local minimum at ~80 fs, quickly rises to ~0.1, and then decays over several picoseconds, exhibiting what seem to be weaker oscillations along the way (*28*). Similar results are seen in H_2O and D_2O and in methanol (fig. S5).

The experimental $R(t)$ curves would be expected to differ in a number of ways from the highly idealized oscillatory curve shown in Fig. 1B, but most of these effects are straightforward to characterize. The experiment's finite time resolution is simple to include. More fundamentally, both the hot and cold photodissociation channels produce relatively broad initial distributions of rotational (J) states, but the relevant gas-phase distributions for each channel are known from previous experimental measurement (*16*, *29*) (Fig. 2A, inset). The only important unknown is the liquid-state branching ratio between the two channels. Gas-phase data indicate that the hot channel makes up ~40% of the dissociation yield (*16*), but one might expect a somewhat higher figure for liquid solvents in view of the potential of the liquid to cage the cold photodissociation products (*13*).

Taking these factors into account, we can confirm that the persistent rotational coherence seen in our Ar simulations is the same basic phenomenon observed experimentally in polar solvents. Although CN rotors sampled from the cold-channel distribution undergo a rapid loss of anisotropy in liquid Ar (Fig. 2B, solid blue line), the rotors sampled from the hot-channel distribution retain almost as much coherence in the liquid (solid red line) as they would in the absence of solvent (dashed red line), despite the breadth of these initial distributions. Convolution of the simulation with the 45-fs experimental instrument response function, along with the assumption that liquid-state photodissociation generates an initial ensemble composed of a 60%/40% admixture of the hot and cold gas-phase distributions, yields the anisotropy decay curve (heavy black line) of a hypothetical repetition of this experiment in liquid Ar. The resulting oscillations are somewhat more pronounced in the more weakly interacting solvent than they are in ethanol, but the qualitative features and time scales of the experimental and theoretical curves are otherwise remarkably similar. [Assuming a more gas phase–like 40%/60% branching ratio would lower the amplitude of the predicted oscillations but would not affect their existence or time scales (*18*).]

This level of agreement gives us confidence that our idealized Ar simulations can be used to infer more detailed microscopic information about the development (or more correctly, the lack of development) of rotational friction about a rapidly rotating CN molecule. In simulations, for example, we can directly calculate the energy relaxation function for the actual trajectories

$$S_E(t) = [\overline{E}(t) - \overline{E}(\infty)]/[\overline{E}(0) - \overline{E}(\infty)] \quad (3)$$

where E refers to the rotational kinetic energy and the overbars imply an average over all the initial conditions consistent with the rotor's nonequilibrium preparation. We can then compare the results to the linear-response prediction

$$C_E(t) = [\langle E(0)E(t)\rangle - \langle E\rangle^2]/[\langle E^2\rangle - \langle E\rangle^2] \quad (4)$$

(*1*, *3*), where the angle brackets denote an average over the distribution of molecular velocities and positions that one would find under equilibrium (thermal) conditions.

The results (Fig. 3) show that linear response theory does indeed fail rather dramatically here (*30*): The actual relaxation is considerably slower than the equilibrium rotational energy fluctuations would have predicted, which explains the unexpected level of preservation of rotational coherence. But what is interesting is how this failure occurs. A close inspection of the first 200 fs for a range of different initial rotational energies (Fig. 3, lower panel) reveals that linear response is quantitatively correct for the first 50 to 100 fs—values suspiciously close

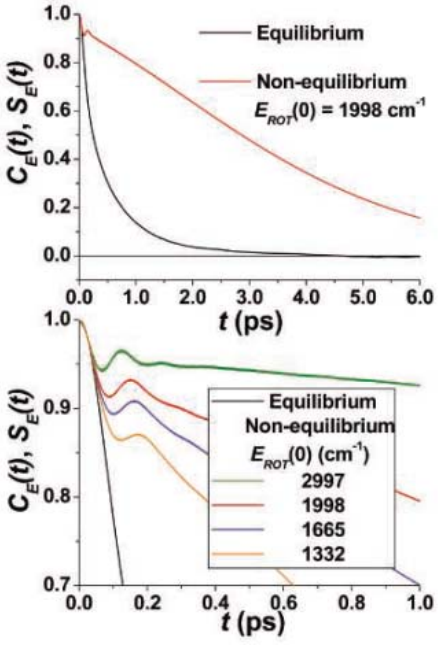

Fig. 3. Molecular dynamics simulation of the breakdown in linear response for hot CN rotors in liquid Ar at 120 K (density 1.344 g/ml). Both panels compare the rotational kinetic energy relaxation functions observed in the actual nonequilibrium simulations $S_E(t)$ (colored lines) with the corresponding linear-response prediction $C_E(t)$ (black line). The nonequilibrium simulations follow the rotational kinetic energy after a CN rotor is given a specific value $E_{ROT}(0)$ at time 0. By contrast, the linear-response curve looks only at the decay of ordinary equilibrium rotational energy fluctuations at the temperature of the liquid (even when extraordinary energies are to be dissipated). (**Top**) The linear-response answer compared with that from a single nonequilibrium calculation over a fairly long time period. (**Bottom**) The subpicosecond dynamics for four successively larger values of $E_{ROT}(0)$. In this panel, it is clear how linear response breaks down only after a well-defined time delay, which becomes increasingly protracted as the initial rotational energy decreases. At these energies, a 90° rotation of an isolated CN rotor would take 60, 73, 80, and 90 fs, respectively.

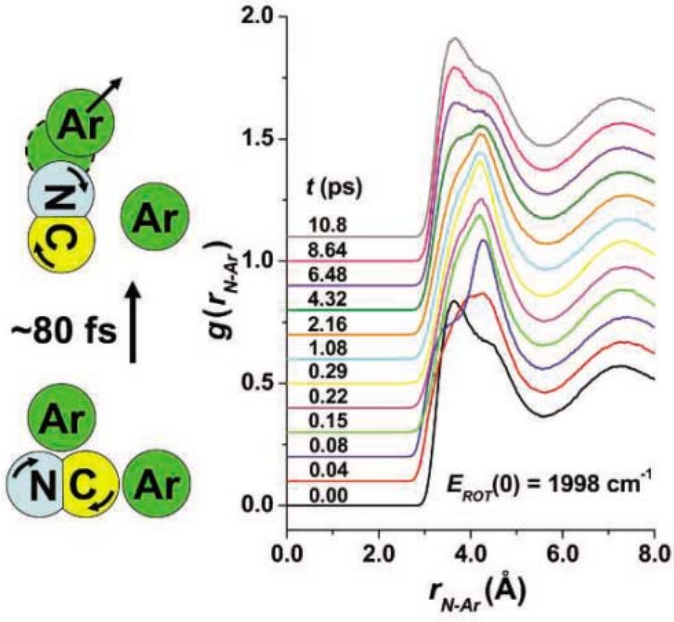

Fig. 4. Liquid-structure changes corresponding to a linear-response breakdown. Shown are molecular dynamics results for the relaxation of a single 1998 cm^{-1} CN rotor dissolved in liquid Ar (under the same conditions reported in Fig. 3). The plot reports the normalized probability densities of N-Ar distances $r_{N\text{-}Ar}$ in the CN-rotor plane (*18*) at the indicated times t after the rotational preparation. Successive curves are translated vertically for ease in viewing. The time-0 curve, in particular, shows the equilibrium structure, an arrangement that is not recovered until 9 to 10 ps later. The principal structural change occurs within 80 fs, the interval (as shown at left) that corresponds to the time needed for a CN to rotate ~90°, forcing a neighboring Ar atom out of the inner solvation shell.

to the 60 to 90 fs that it would take free rotors with these energies to rotate ~90°. Once this amount of molecular reorientation has occurred, though, the solvent evidently begins to function differently and the linear-response predictions begin to fail.

Given the existence of such a well-defined event, it is a simple matter to interrogate our simulations to discover just what the liquid is doing at the critical moment. We plot in Fig. 4 the radial distribution functions for the solvent atoms in the CN rotor plane. By looking at a function of the time elapsed after the rotational excitation, one can see that the liquid structure around the CN solute itself undergoes a relatively sudden change at roughly 80 fs: The loss of the peak at 3.8 Å and the corresponding growth of a peak at 4.5 Å means that a 90° rotation of a CN suffices to push at least some solvent atoms out of the innermost solvent shell. This expulsion of such nearby solvent atoms is what is probably responsible for the sudden diminishment of the local rotational friction. The fact that it then takes on the order of 10 ps for the liquid structure to recover from this first 0.1 ps is surprising, but is nicely consistent with the slow progress of the overall rotational relaxation (*19*).

The presence of a connection between nonlinear response and the evolution of liquid structure has been noted in a number of computer simulation studies of how linear response can fail during solvation (*4*–*6*), although there has never been any direct experimental evidence for such a scenario. In a typical simulation of solvation, the relaxation of the solute-solvent potential energy is monitored after an instantaneous change in the charge distribution of a solute, and linear response theory is found to yield accurate predictions even when solvation energies are greater than 10^4 K (*1*). But in a few cases involving hydrogen-bonding liquids (*4*–*6*) and solute size changes (*5*, *6*), the simulated solvation is noticeably different from predictions based on the solvent's normal equilibrium fluctuations. In each of these instances, it was clear that liquid-structure transformations must have been involved in some way because the liquid's local geometry was different before and after the solvation process. However, in this work, we have observed a discrete molecular event in the solvent, occurring at a specific time, that mediates the failure of linear response.

Our principal experimental result is the time-domain observation of largely free molecular rotation occurring in a strongly interacting room-temperature liquid. The preservation of such free rotation yields valuable clues about the course of energy dissipation in chemical processes. In particular, the observation of coherence tied to the original rotor time scale is direct evidence of a nonlinearly responding solvent. The experiment therefore provides a window into the ultrafast time evolution of not only the solute relaxation but the solvent structure. Moreover, the possibility of controlling the specifics of the preparation of our rotors offers us yet other opportunities, including the chance to learn about some of the key issues germane to solution photochemistry: how a solvent affects the dynamics of an electronic curve crossing and whether cage recombination (*13*, *14*) selects out particular subpopulations of solute states.

References and Notes

1. R. M. Stratt, M. Maroncelli, *J. Phys. Chem.* **100**, 12981 (1996).
2. G. A. Voth, R. M. Hochstrasser, *J. Phys. Chem.* **100**, 13034 (1996).
3. D. Chandler, *Introduction to Modern Statistical Mechanics* (Oxford Univ. Press, New York, 1987), chap. 8.
4. T. Fonseca, B. M. Ladanyi, *J. Phys. Chem.* **95**, 2116 (1991).
5. C. J. Smallwood, W. B. Bosma, R. E. Larsen, B. J. Schwartz, *J. Chem. Phys.* **119**, 11263 (2003).
6. L. Turi, P. Minary, P. J. Rossky, *Chem. Phys. Lett.* **316**, 465 (2000).
7. P. L. Geissler, D. Chandler, *J. Chem. Phys.* **113**, 9759 (2000).
8. R. Schinke, *Photodissociation Dynamics Spectroscopy and Fragmentation of Small Polyatomic Molecules* (Cambridge Univ. Press, Cambridge, 1993).
9. G. R. Fleming, *Chemical Applications of Ultrafast Spectroscopy* (Oxford Univ. Press, New York, 1986), sec. 6.2.

10. S. Grebenev, J. P. Toennies, A. F. Vilesov, *Science* **279**, 2083 (1998).
11. D. G. Taylor, H. L. Strauss, *J. Chem. Phys.* **90**, 768 (1989).
12. Y. Danten, T. Tassaing, M. Besnard, *J. Phys. Chem. A* **104**, 9415 (2000).
13. N. Winter, I. Chorny, J. Vieceli, I. Benjamin, *J. Chem. Phys.* **119**, 2127 (2003).
14. J. Larsen *et al.*, *J. Chem. Phys.* **116**, 7997 (2002).
15. M. Dantus, M. J. Rosker, A. H. Zewail, *J. Chem. Phys.* **89**, 6128 (1988).
16. I. Nadler, D. Mahgerefteh, H. Reisler, C. Wittig, *J. Chem. Phys.* **82**, 3885 (1985).
17. W. P. Marinelli, N. Sivakumar, P. L. Houston, *J. Phys. Chem.* **88**, 6685 (1984).
18. See supporting material on *Science* Online.
19. A. C. Moskun, S. E. Bradforth, *J. Chem. Phys.* **119**, 4500 (2003).
20. H. Bursing, P. Vohringer, *Phys. Chem. Chem. Phys.* **2**, 73 (2000).
21. T. Kuhne, P. Vohringer, *J. Phys. Chem. A* **102**, 4177 (1998).
22. A. E. Jailaubekov, S. E. Bradforth, *Appl. Phys. Lett.* **87**, 021107 (2005).
23. C. G. Durfee III, S. Backus, M. M. Murnane, H. C. Kapteyn, *Opt. Lett.* **22**, 1565 (1997).
24. M. J. Tauber, R. A. Mathies, X. Chen, S. E. Bradforth, *Rev. Sci. Instrum.* **74**, 4958 (2003).
25. Quantum mechanical features of the rotational dynamics are probably not a major concern in the analysis of our experiments: For CN rotors produced in the rotationally hot channel, the average initial rotational kinetic energy is on the order of 4700 K (15 times the 300 K thermal energy of the solvent), whereas the spacing of rotational energy levels corresponds to only 230 K. We therefore use the phrase "rotational coherence" to refer only to classical coherence, not to coherence in the quantum mechanical phase.
26. M. H. Alexander, X. Yang, P. J. Dagdigian, A. Berning, H. J. Werner, *J. Chem. Phys.* **112**, 781 (2000).
27. X. Yang, P. J. Dagdigian, M. H. Alexander, *J. Chem. Phys.* **112**, 4474 (2000).
28. The oscillatory behavior of the early signal is characteristic of coherent free rotation of hot CN, validating the assumption that the dissociation reaction is impulsive with respect to solvent motions.
29. Because of solvent shifts, the data reported for gas-phase photodissociation at 266 nm correspond to our liquid-state photolysis at 233 nm. See (*13*, *19*).
30. Although very similar nonlinear-response behavior is seen in our 300 K liquid-density supercritical Ar simulations, we report in Figs. 3 and 4 the results for the normal 120 K liquid.
31. We thank P. Pieniazek, A. Krylov, I. Benajmin, and M. Alexander for helpful discussions. Work at USC is supported by NSF grant CHE-0311814 and by the David and Lucile Packard Foundation, and at Brown by NSF grants CHE-0131114, CHE-0212823, and CHE-0518169.

Supporting Online Material

www.sciencemag.org/cgi/content/full/311/5769/1907/DC1
Materials and Methods
Figs. S1 to S7
References

12 December 2005; accepted 21 February 2006
10.1126/science.1123738

High-Performance High-T_c Superconducting Wires

S. Kang,[1] A. Goyal,[1]* J. Li,[1] A. A. Gapud,[1]† P. M. Martin,[1] L. Heatherly,[1] J. R. Thompson,[1,2] D. K. Christen,[1] F. A. List,[1] M. Paranthaman,[1] D. F. Lee[1]

We demonstrated short segments of a superconducting wire that meets or exceeds performance requirements for many large-scale applications of high-temperature superconducting materials, especially those requiring a high supercurrent and/or a high engineering critical current density in applied magnetic fields. The performance requirements for these varied applications were met in 3-micrometer-thick $YBa_2Cu_3O_{7-\delta}$ films epitaxially grown via pulsed laser ablation on rolling assisted biaxially textured substrates. Enhancements of the critical current in self-field as well as excellent retention of this current in high applied magnetic fields were achieved in the thick films via incorporation of a periodic array of extended columnar defects, composed of self-aligned nanodots of nonsuperconducting material extending through the entire thickness of the film. These columnar defects are highly effective in pinning the superconducting vortices or flux lines, thereby resulting in the substantially enhanced performance of this wire.

Second-generation high-temperature superconducting (HTS) wires or coated conductors (also known as 2G wires) based on $REBa_2Cu_3O_{7-\delta}$ (RE, rare earth) films have important potential for use in large-scale civilian and military applications (*1*–*3*). For many of these potential applications, large critical currents in high applied magnetic fields are required. This is especially so for electric power applications of HTS materials as well as for military applications. For example, the underground transmission cable application requires critical current per unit width, I_c, greater than 300 A/cm in self-field; for military applications, an I_c greater than 100 A/cm and an engineering critical current density, J_E, greater than 15 kA/cm^2 at 65 K in an operating field of 3 T are required; and for rotating machinery such as motors and generators, a J_E of 30 to 40 kA/cm^2 at 55 to 65 K in operating fields of 3 to 5 T is required.

Coated conductors consist of a flexible substrate (a metallic template with several buffer layers) and an epitaxial superconducting layer (*1*). The goal is to have a biaxially textured superconducting layer so that few if any high-angle, weakly conducting grain boundaries are present. Three techniques for producing biaxial texture in the substrate have been developed: ion beam–assisted deposition (IBAD) of biaxialy textured buffers on polycrystalline alloy substrates (*1*, *4*), epitaxial deposition of buffer multilayers on rolling assisted biaxially textured substrates (RABiTS) (*1*, *5*), and inclined substrate deposition of buffers on polycrystalline alloy substrates (*1*, *6*). For epitaxial HTS films on such textured substrates, the intergranular critical current density is substantially improved because of the elimination of weakly linked, high-angle grain boundaries. However, for practical application of HTS materials, the in-field performance, or the intragranular critical current density, also needs to be enhanced further. It is also essential to increase the overall current-carrying capacity of the coated conductors. The simplest approach is to increase the thickness of the superconductor. However, gradual deterioration of the critical current density occurs with increasing superconductor thickness. For films deposited by in situ techniques such as pulsed laser deposition (PLD), as the superconducting layer becomes thicker, a dead layer that provides no contribution to the current carrying ability forms after a critical thickness of ~1.5 μm (*7*). This has been attributed to roughening of the film with increase in thickness. A solution to this roughness problem was found by fabricating multilayered films with $YBa_2Cu_3O_{7-\delta}$ (YBCO) layers less than 1.5 μm thick alternating with intervening CeO_2 interlayers (*7*). Although there was no dead layer formation in these multilayer films, a single layer is still desirable because of the processing complexity in multilayer growth. We have overcome this problem by manipulation of deposition conditions and substrate characteristics and have demonstrated growth of a 6.4-μm-thick single-layer YBCO film on RABiTS without the formation of any dead layer (*8*, *9*). However, for both the multilayered films and the single-layer-thick films without a dead layer, further improvement in the in-field transport properties is needed to meet the performance requirements for a range of applications. This can be accomplished by improving the flux pinning by introducing appropriate defects into the films.

It is known that defects within superconducting materials can pin the magnetic flux lines, so that large currents can flow through the materials in the presence of high applied magnetic fields. However, in order for the defects to be effective in pinning the flux, their size, density, and geometry need to be appropriately controlled. Defects such as oxygen vacancies, twin boundaries (*10*), and dislocations (*11*, *12*) form naturally inside films and act as pinning centers.

[1]Oak Ridge National Laboratory, Oak Ridge, TN 37831, USA. [2]Department of Physics, University of Tennessee, Knoxville, TN 37996, USA.

*To whom correspondence should be addressed. E-mail: goyala@ornl.gov

†Present address: Department of Physics, University of South Alabama, ILB 103, Mobile, AL 36688, USA.

However, the density and/or pinning potential of these naturally formed defects is not high enough to meet the performance requirements for the various applications in question. To increase the density of defects for effective pinning, there have been extensive studies on introducing artificial pinning defects such as columnar defects via heavy-ion irradiation (*13*), periodic arrays of submicrometer holes (*14*), or magnetic particles and/or nanoparticles (*15*, *16*). Among these, linear defects such as the columnar defects produced via heavy-ion irradiation have proved to be the most effective. This approach, however, is not practical for scale-up because it is not only too expensive but can render the metallic substrate radioactive. A promising approach that simulated the defect structures formed by heavy-ion irradiation was the incorporation of periodic columnar defects composed of self-aligned nanodots and nanorods of $BaZrO_3$ (BZO) into the YBCO film (*17*, *18*), resulting in enhancement of the transport J_c. As compared to YBCO films without the incorporation of self-assembled nanodots and nanorods, an improvement in J_c by a factor of ~5 in the field range from 0.4 to 1.5 T at 77 K, and an improvement of over a factor of 6 beyond 7 T, were obtained. Similar results have also been partially reproduced in 0.25- to 0.3-μm-thick films on IBAD substrates (*19*), indicating the general viability of this approach. However, in all of these previous studies, the films were relatively thin (0.2 to 0.3 μm), and it was completely unclear whether it would be possible to propagate such defects through the substantially thicker films required to enable practical applications.

Here we report large enhancements of critical currents and of J_E in self-field as well as excellent retention of this current in high applied magnetic fields. This result was obtained by fabricating thick YBCO films without any dead layer, as well as by the incorporation of extended columnar defects composed of self-aligned nanodots of BZO during growth of the film. Our films were prepared using pulsed laser deposition on RABiTS (see supporting online material).

Figure 1 shows field-dependent I_c versus applied field at 77 K with the magnetic field parallel to the YBCO *c* axis (*H*//*c*) for a 3.0-μm-thick YBCO plus 2 volume % BZO film on RABiTS. The I_c decrease is only a factor of 4.3 at 1.5 T. The self-field I_c of this film was 389 A, and the corresponding self-field J_c was 1.3 MA/cm^2. The exponent α in the relation $J_c \sim H^{-\alpha}$ was determined to be 0.34 for this sample as compared to the typical value of 0.5 for pure YBCO films, indicating strong pinning for *H*//*c* for the BZO-doped film. The inset shows the angular dependence of I_c at 77 K and 1 T, with the field always in the maximum Lorentz force configuration. Part of the variation of I_c with field orientation or angle is expected because of the electronic mass anisotropy of YBCO. However, the dominant peak for *H*//*c* indicates that there is strong vortex pinning by *c* axis–correlated defects in this film.

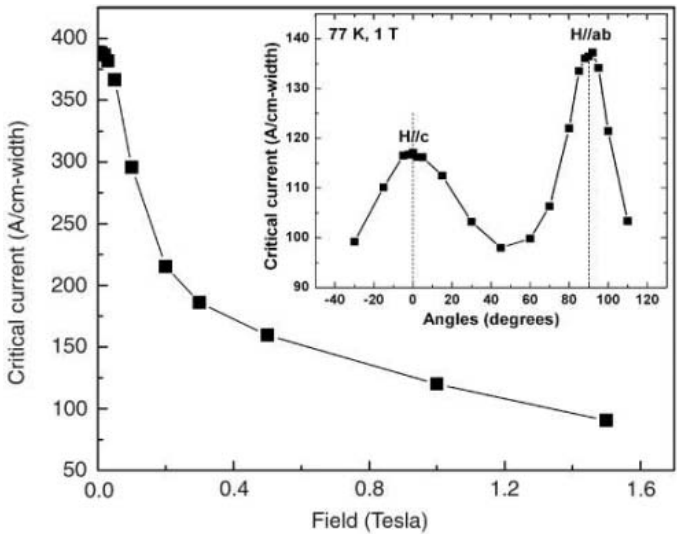

Fig. 1. I_c versus applied magnetic field for a film of YBCO plus 2 volume % BZO grown epitaxially on RABiTS. The inset shows the angular dependence of I_c at 77 K and 1 T.

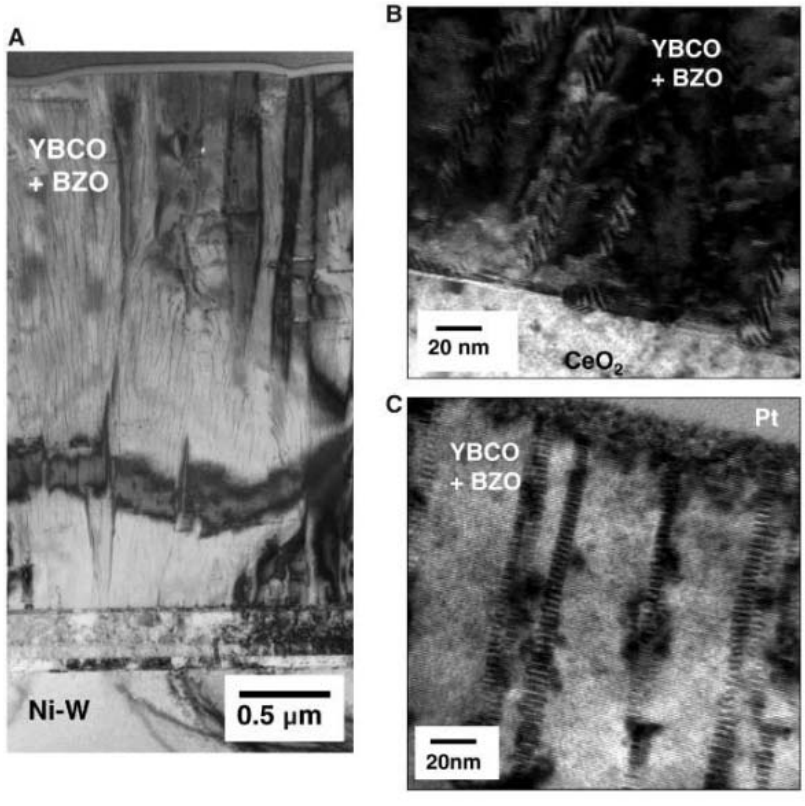

Fig. 2. Cross-section TEM micrographs of a 3.0-μm-thick YBCO film with BZO nanodots grown epitaxially on RABiTS. (**A**) Low-magnification image showing the entire cross-section of the film. The contrast from BZO nanodots aligned along the *c* direction of YBCO can be seen. (**B**) Higher-magnification TEM image showing the nucleation of BZO nanodots at the film/buffer interface. (**C**) Higher-magnification TEM image showing that the columns of self-aligned BZO nanodots extend to the top of the YBCO layer.

In the cross-section transmission electron microscopy (TEM) images (Fig. 2) of 3-μm-thick YBCO film grown epitaxially on RABiTS with the configuration Ni-3 at % W (50 μm)/Y_2O_3 (65 nm)/YSZ (185 nm)/CeO_2 (30 nm), extended columns of BZO nanodots aligned along the crystallographic *c* axis of YBCO, the growth direction of the film, can be seen. As in the 0.2-μm-thick YBCO films reported by us previously (*17*, *18*), self-aligned BZO nanodots were observed through the entire cross-section of the 3-μm-thick YBCO film. Extended BZO nanodots were formed from the bottom of the

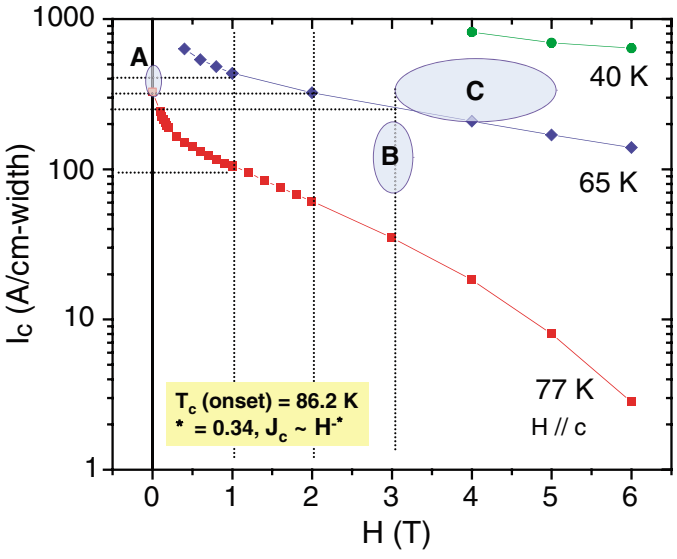

Fig. 3. Field-dependent critical currents at higher applied magnetic fields at three different measurement temperatures: 77, 65, and 40 K. Industry's wire performance requirements for some key applications are shown by shaded elliptical regions as follows: A, underground transmission power cable applications require $I_c \geq 300$ A/cm in a self-field at 70 to 77 K. B, military applications require an $I_c \geq 100$ A/cm and a $J_E \geq 15$ kA/cm^2 at 3 T and 65 K. C, for large-scale rotating machinery such as commercial motors and generators, $J_E \sim 20$ to 30 kA/cm^2 at 3 to 5 T and 55 to 65 K is required. The transport properties of single-layer, 3-μm-thick, YBCO plus 2 volume % BZO film on RABiTS with a periodic array of one-dimensional nanostructures meet the performance requirements for these applications.

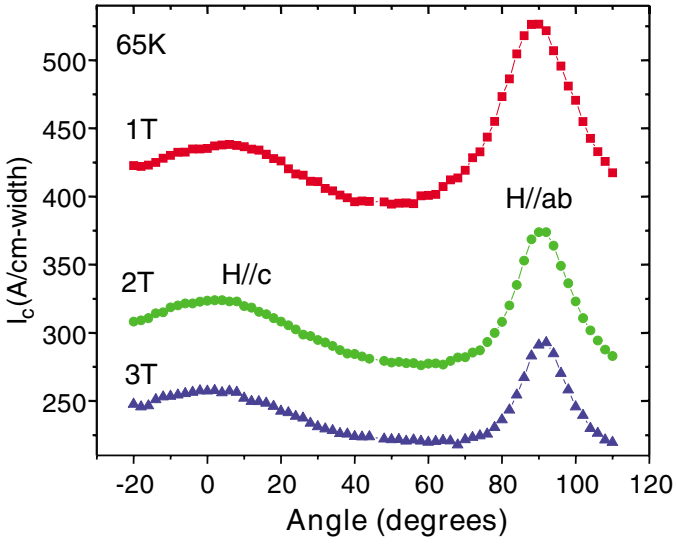

Fig. 4. Critical current per unit width versus angle of applied magnetic field at 65 K and with applied magnetic fields of 1, 2, and 3 T. The applied field was always in the maximum Lorentz force configuration. At 65 K and 1 T, the current per unit width is ~400 A/cm for all angles or applied field orientation. At 65 K and 3 T, the current per unit width is greater than 200 A/cm for all angles or applied field orientation. At 65 K and 3 T, the calculated J_E is 40,740 A/cm^2 without considering a stabilizer and 21,154 A/cm^2 assuming a 50-μm-thick stabilizer at the angle corresponding to the lowest I_c.

YBCO layer (Fig. 2B) to the top of the YBCO layer (Fig. 2C). These self-aligned columns of BZO nanodots form to minimize energy or strain in the growing film stemming from the large lattice mismatch between YBCO and BZO of ~9% (*17*, *18*). Using high-resolution EM in plan view, we have previously shown that for 0.2-μm-thick films on RABiTS, four misfit edge dislocations exist around each BZO nanodot (*17*, *18*). Subsequent nanodots align vertically, so that these misfit dislocations are also aligned, thereby minimizing the misfit strain in the film. These aligned misfit dislocations form ideal extended flux-pinning centers (*17*, *18*). This periodic array of columnar defects is highly effective in pinning superconducting vortices or flux lines, thereby resulting in the substantially enhanced performance of the 2G wire in high applied magnetic fields, as shown in Figs. 3 and 4.

Figure 3 shows I_c versus H for $H//c$ at higher fields and at measurement temperatures of 77, 65, and 40 K. The sample used for these measurements was the same BZO-doped sample for which data are shown in Fig. 1. Because of the limitations on the maximum measuring current, the 5-mm-wide sample was patterned into a 0.2-mm-wide bridge. The self-field I_c is somewhat reduced from that shown in Fig. 1 because of sample handling (mounting and unmounting in one measurement system and remounting in another system) as well as possible damage by the laser scribing used to pattern the bridge on the sample. Nevertheless, at 77 K and low field, I_c is still over 300 A/cm-width, which is suitable for power cable applications. At 65 K and 3 T, I_c is over ~250 A/cm-width, which is well above the threshold values of ~100 A/cm-width for military applications, such as supermagnets for electric ship propulsion systems and magnetic energy storage. At 65 K and 3 T, the J_E for $H//c$ is 46 kA/cm^2. For practical applications, a stabilizer layer comprising a material with high electrical conductivity, such as Cu with a thickness of about 50 μm, will be required to protect the superconductor in case of local loss of superconductivity. If one assumes that a 50-μm-thick stabilizer layer will be deposited on top of the YBCO layer, the J_E for $H//c$ is calculated to be 24.5 kA/cm^2, which is still well over the required 15 kA/cm^2. For large-scale rotating machinery such as motors and generators, a J_E of 20 to 30 kA/cm^2 in the operating temperature range of 55 to 65 K in applied fields of 3 to 5 T is required. The operating temperature range of 55 to 65 K is needed for widespread applications, because this is a temperature regime accessible by present cryocooler technology. Figure 3 shows that at 65 K, the J_E corresponds to 46, 37, and 33 kA/cm^2 without the stabilizer in applied fields of 3, 4, and 5 T, which is clearly above the range needed for application at 65 K. At lower temperatures, for example at 55 K, the J_E is expected to be much higher than the values at 65 K. At 40 K, extrapolated I_c is over 1000 A/cm-width in applied fields of 3.5 T. At 40 K and 4 T, the J_E is 148 kA/cm^2.

Figure 4 shows the angular dependence of I_c at 65 K at applied magnetic fields of 1, 2, and 3 T. The three angular-dependent I_c curves show similar features, indicating that similar pinning mechanisms are operational at these temperatures. At 65 K and 1 T, an I_c of ~ 400 A/cm for all field orientations was obtained. At 3 T, an I_c of ~200 A/cm for all field orientations was obtained. J_E at 65 K and 3 T is calculated to be over ~40 kA/cm^2 at all applied field orientations without consideration of a stabilizer, and to be 21 kA/cm^2 assuming a 50-μm-thick stabilizer, which is still well over the required value of 15 kA/cm^2.

We have successfully engineered defect structures within the HTS film and obtained transport properties exceeding the HTS industry's wire performance requirements for a range of applications. These results are important because they demonstrate the feasibility of fabricating HTS wires that have the performance required to revolutionize the electric power industry as well as applications in the military, medicine, transportation, and high-energy physics.

References and Notes

1. *Second Generation HTS Conductors*, A. Goyal, Ed. (Kluwer Academic, Netherlands, 2004).
2. *New Superconductivity Market Survey 2000–2010* [Consortium for European Companies Determined

to Use Superconductivity (CONECTUS), June 2004] (http://superconductors.org/conectus.pdf).
3. W. V. Hassenzahl *et al.*, *Proc. IEEE* **92**, 1655 (2004).
4. J. R. Groves *et al.*, *Phys. C* **382**, 43 (2002).
5. A. Goyal *et al.*, *Appl. Phys. Lett.* **69**, 1795 (1996).
6. M. Bauer, R. Semerad, H. Kinder, *IEEE Trans. Appl. Supercond.* **9**, 1502 (1999).
7. Q. Xia *et al.*, *Appl. Phys. Lett.* **80**, 1601 (2002).
8. S. Kang *et al.*, *J. Am. Ceram. Soc* **88**, 2677 (2005).
9. K. J. Leonard *et al.*, *J. Mater. Res.* **18**, 1723 (2003).
10. I. Maggio-Aprile *et al.*, *Nature* **390**, 487 (1997).
11. C. Gerber *et al.*, *Nature* **390**, 279 (1991).
12. B. Dam *et al.*, *Nature* **399**, 439 (1999).
13. L. Civale *et al.*, *Phys. Rev. Lett.* **67**, 648 (1991).
14. A. Castellanos *et al.*, *Appl. Phys. Lett.* **71**, 962 (1997).
15. T. Haugan *et al.*, *J. Mater. Res.* **18**, 2618 (2003).
16. J. L. Macmanus-Driscoll *et al.*, *Nat. Mater.* **3**, 439 (2004).
17. A. Goyal *et al.*, paper presented at the 2004 Annual Peer Review of the U.S. Superconductivity Program for Electric Systems, Washington, DC, 27 to 29 July 2004 (www.energetics.com/meetings/supercon04/pdfs/presentations/f_rabits_strategic_talk_ffy04_final.pdf).
18. A. Goyal *et al.*, *Supercond. Sci. Technol.* **18**, 1533 (2005).
19. Y. Yamada *et al.*, *Appl. Phys. Lett.* **87**, 132502 (2005).
20. A. Goyal thanks Q. Jia at Los Alamos National Laboratory for useful discussions pertaining to pulsed laser deposition of YBCO. S. Kang, J. Li, and A. A. Gapud thank Oak Ridge Associated Universities for a postdoctoral fellowship. The research was sponsored by the U.S. Department of Energy, Office of Electricity Delivery and Energy Reliability–Superconductivity Program, under contract DE-AC05-00OR22725 with UT-Battelle, LLC managing contractor for Oak Ridge National Laboratory.

Supporting Online Material
www.sciencemag.org/cgi/content/full/311/5769/1911/DC1
SOM Text

11 January 2006; accepted 2 March 2006
10.1126/science.1124872

Significant Warming of the Antarctic Winter Troposphere

J. Turner,* T. A. Lachlan-Cope, S. Colwell, G. J. Marshall, W. M. Connolley

We report an undocumented major warming of the Antarctic winter troposphere that is larger than any previously identified regional tropospheric warming on Earth. This result has come to light through an analysis of recently digitized and rigorously quality controlled Antarctic radiosonde observations. The data show that regional midtropospheric temperatures have increased at a statistically significant rate of 0.5° to 0.7°Celsius per decade over the past 30 years. Analysis of the time series of radiosonde temperatures indicates that the data are temporally homogeneous. The available data do not allow us to unambiguously assign a cause to the tropospheric warming at this stage.

Meteorological observations from the Antarctic research stations provide the most accurate data to investigate long-term climate change across the continent. Many of the surface records extend back to the International Geophysical Year of 1957 to 1958. These records indicate that the western side of the Antarctic Peninsula has experienced the largest measured annual near-surface warming (0.55°C per decade at Faraday/Vernadsky station) on Earth over the past 50 years (*1*). However, there have been few statistically significant temperature changes at the surface across the rest of the continent (*2*, *3*), and some studies have suggested a slight cooling in recent decades (*4*). This is in contrast to a mean near-surface warming across the Earth of 0.11°C per decade during the past 50 years (*5*).

Although there have been several investigations concerned with surface temperature change across the Antarctic (*6*–*8*), there have not been any comparable investigations of changes at upper levels, because many of the radiosonde observations were not available. Recently, many of the important radiosonde records have been digitized and intensively quality controlled in a project funded by the Scientific Committee on Antarctic Research (*9*). In particular, the Russian radiosonde observations are now available (www.antarctica.ac.uk/met/READER/). This represents a considerable increase in the coverage and completeness over the Antarctic component of previous global radiosonde compilations (*10*–*12*).

A summary of the annual and seasonal temperature trends at the 500-hPa level for the period from 1971 to 2003 is presented in Fig. 1A. We have concentrated on nine stations (most of which are in East Antarctica) that have reasonably complete records for this period; only five of these stations were included in the Angell studies of global upper air temperature trends (*10*, *11*). In this study, a monthly mean temperature was only computed if at least 30% of the daily ascents were available. Only 8% of the monthly means (*9*) were missing across the records of the nine stations, allowing reliable temperature trends to be computed. Figure 1A shows that there have been statistically significant increases in seasonal temperature at many of the stations across the continent, both in the coastal region, where most of the stations are located, and at Amundsen-Scott station at the South Pole.

We examined the mean vertical profile of the temperature trends for winter for the nine stations (Fig. 1B), because this is the season of maximum warming across most of the continent (compare with Fig. 1A). Warming has occurred throughout the troposphere, with the maximum increase in temperature in the midtroposphere (400 to 600 hPa). The mean winter trend for the nine stations from 1971 to 2003 was a 0.5°C increase per decade at the surface and a 0.70°C increase per decade in the midtroposphere. In the stratosphere, there has been cooling between 200 and 50 hPa, and the largest decrease in temperature was –0.16°C per decade at 100 hPa. The standard deviation (SD) of the station trends is large at the surface (Fig. 1B) because the pattern of change at this level is variable across the continent, and in the stratosphere because the impact of the Antarctic ozone hole has varied around the continent. However, the SD values are small in the midtroposphere, indicating that a fairly uniform warming has occurred across the Antarctic at this level.

The Angell analysis of global radiosonde data (*10*, *11*) considered changes over the layer from 850 to 300 hPa. For the period from 1971 to 2003, there was an annual global warming trend of 0.11°C per decade; the largest trend of 0.15°C per decade was during the Austral winter. The annual trend for the Southern Hemisphere was 0.07°C, and the greatest change took place during the winter when the trend was 0.10°C per decade. Within the Southern Hemisphere winter, the trends vary strongly by latitude: Equatorward of 60°S, the trend is 0.06°C per decade (*13*), whereas the data from the nine Antarctic stations analyzed in this paper have a mean temperature trend of 0.43°C per decade for 850 to 300 hPa. Thus, the trend for the Southern Hemisphere is dominated by the changes that have taken place across the Antarctic.

The 40-year European Centre for Medium-Range Weather Forecasts (ECMWF) reanalysis data set (ERA-40) (www.ecmwf.int/research/era) provides an extremely valuable means of examining spatial variability of atmospheric parameters and change in recent decades. Although ERA-40 begins in 1957, there are problems with the quality of the high-latitude fields before 1979 (*14*, *15*). Therefore, we compared the 500-hPa temperature trends in ERA-40 (Fig. 2) with equivalent values from the radiosonde data for the period from 1979 to 2001 (the last full year of the reanalysis). The general pattern of the ERA-40 temperature trends is in broad agreement with the trends from the radiosonde data. However, ERA-40 has larger warming trends than the in situ data, except over the Antarctic Peninsula. For example,

British Antarctic Survey, Natural Environment Research Council, Cambridge CB3 0ET, UK.

*To whom correspondence should be addressed. E-mail: j.turner@bas.ac.uk

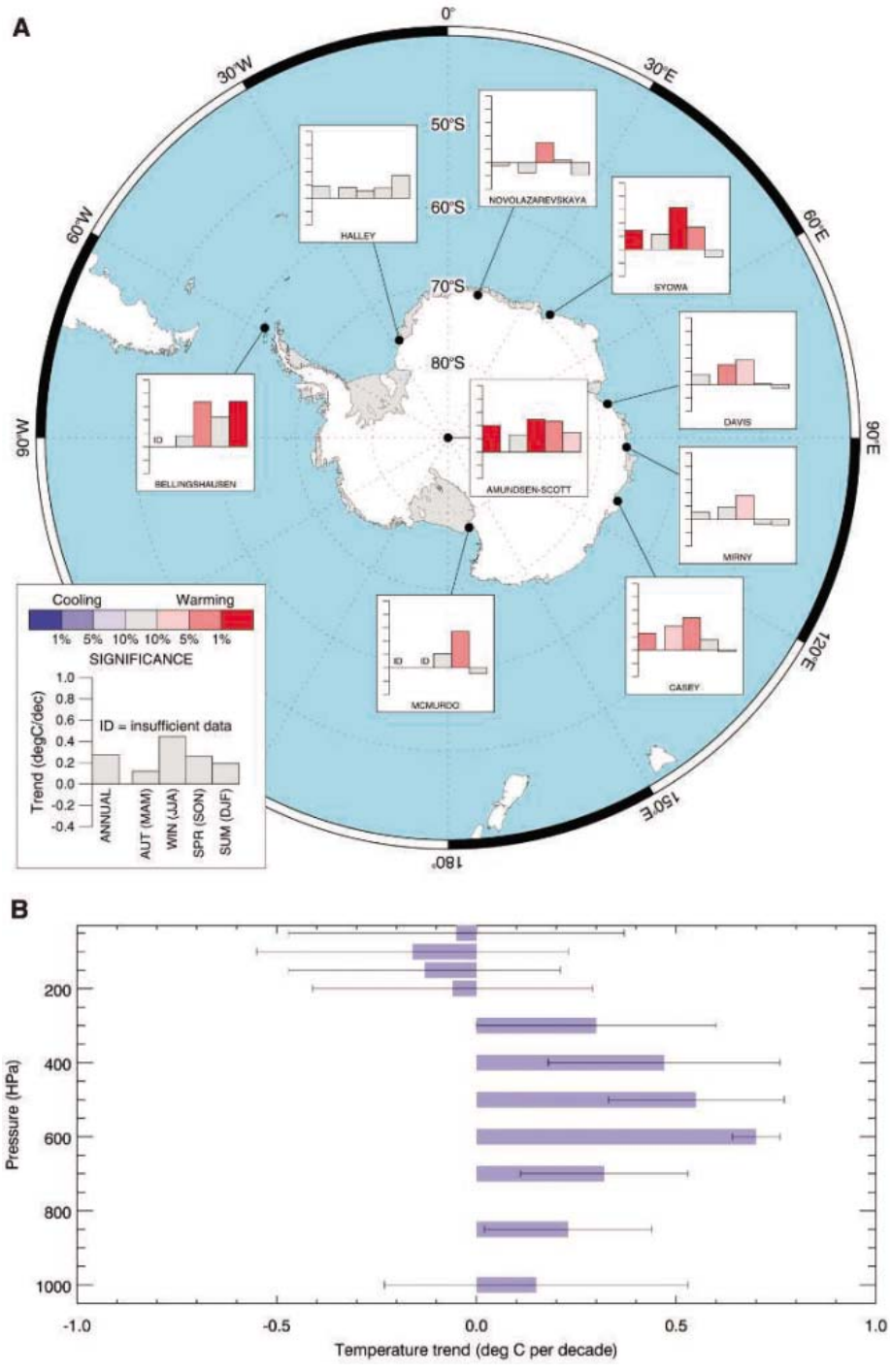

Fig. 1. (**A**) Annual and seasonal 500-hPa temperature trends (°C per decade) from 1971 to 2003 for nine radiosonde stations with long records. The shading indicates the statistical significance. ID indicates that less than 80% of annual/seasonal data were available. (**B**) The mean vertical profile of winter temperature trends and the SD (°C per decade for 1971 to 2003) at standard atmospheric levels for nine Antarctic radiosonde stations.

from 1979 to 2001, winter season 500-hPa temperature trends for Syowa and Casey were 0.92° and 0.73°C per decade, respectively, but Fig. 2 shows that ERA-40 had trends of more than 1°C per decade for this period. Figure 2 indicates that the midtropospheric winter warming observed in the radiosonde data encompasses the whole continent and much of the Southern Ocean. Notably, the largest warming trend in Fig. 2 is located over West Antarctica where there are no radiosonde records to confirm this feature.

The observed winter temperature trends at 850 to 300 hPa for the period from 1979 to 2001 were also compared with comparable trends from the satellite Microwave Sounder Unit measurements (*16*). Although the satellite data showed areas of warming (up to 1°C per decade), it also showed areas of cooling not seen in the radiosonde data nor in the ERA-40 fields. There is, however, evidence (*17*) that the satellite product may not be reliable around Antarctica in the winter because of the effects of the sea ice. Therefore, we did not use these products to interpret the radiosonde trends.

The major source of uncertainty in radiosonde temperatures and trends in their time series is the radiation correction (*18*), which is applied because of radiative effects on the temperature sensor. However, here we focused principally on winter season tropospheric data, when the radiative correction is small. This is because at the latitudes of Antarctica, the Sun is close to or below the horizon in winter. Assessments of radiosonde temperature biases resulting from radiation errors (*19*) suggest that any such errors are much smaller than those needed to give the trends we observed in the Antarctic data.

The trends presented in Fig. 1 were derived from data collected by a number of different national programs, and they used a variety of radiosonde types, so it is unlikely that changes of equipment or observing practice were responsible for an artificial Antarctic-wide temperature trend. Also, we examined the available metadata for changes of radiosonde type, given that instrumental changes can result in jumps in the record (*20*), and found no evidence of discontinuities at these times. We also performed an objective test for discontinuities in the time series of 500-hPa temperatures using the method of Lund and Reeves (*21*), which tests for both jumps and changes in trend. In all cases, the test results indicated no significant discontinuities. Therefore, we are confident that the observed trends are not a result of instrumental changes. Figure 3 shows the 500-hPa winter temperatures from the nine stations and their mean, which reveals a gradual increase in temperatures for all of the stations. However, there is considerable interannual variability in the data.

Changes in the heat budget of the Antarctic may be ascribed to a number of processes. Our data set of daily ascents allows us to examine the changes in the advection of energy into the region or modifications to the radiation regime. Alterations to the poleward flux of heat were investigated by computing the horizontal thermal advection ($-V_g \nabla_p T$, where V_g is the geostrophic wind and $\nabla_p T$ is the horizontal gradient of temperature) from the radiosonde ascents at the coastal stations (*22*). For the period from 1971 to 2003, there was no evidence of a greater horizontal flux of heat into the Antarctic; indeed, during the winter season there was a very small trend toward a slightly reduced poleward heat flux at a number of the stations.

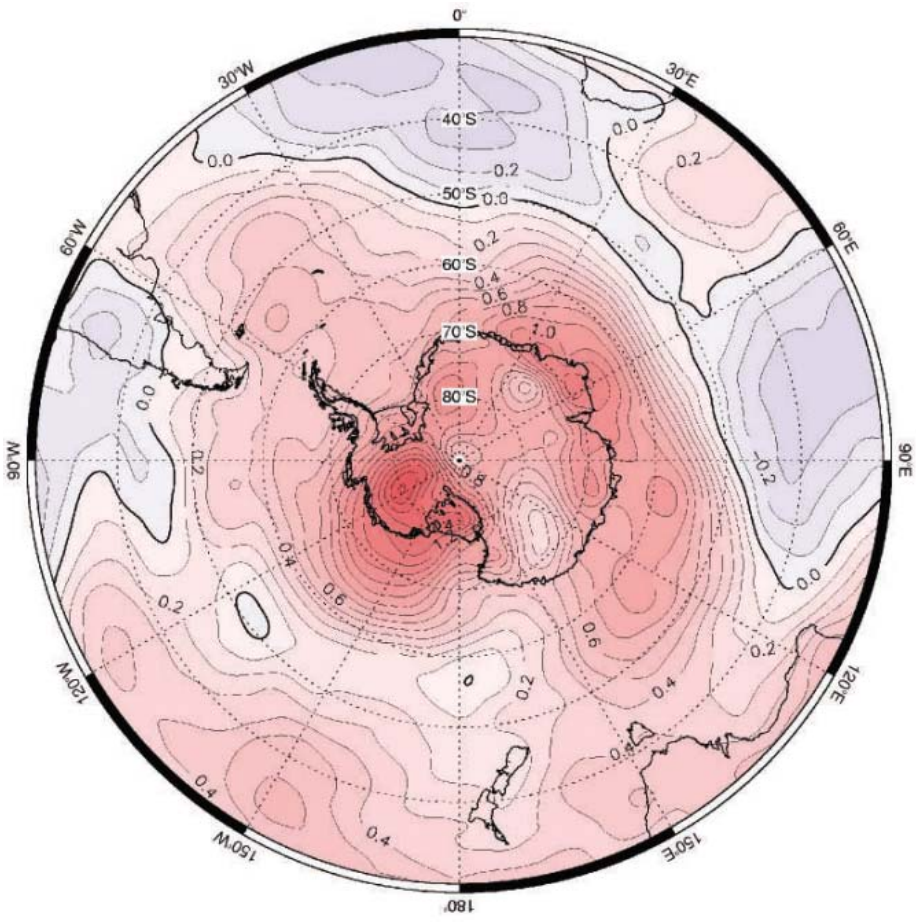

Fig. 2. Trends (°C per decade) in the winter season 500-hPa temperatures from 1979 to 2001 from the ECMWF reanalysis.

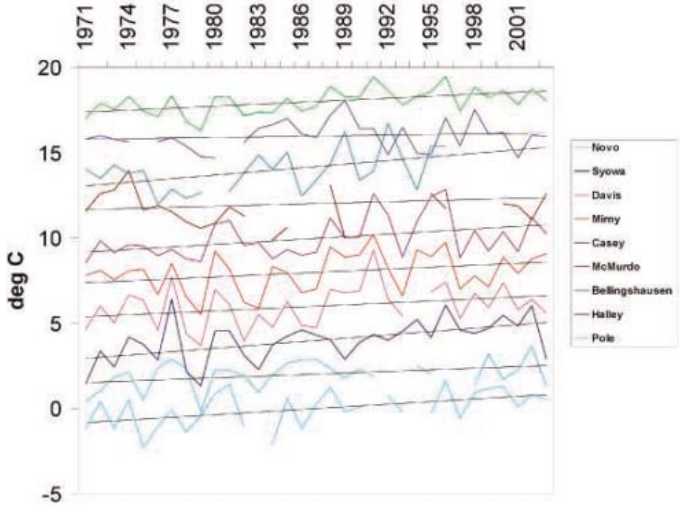

Fig. 3. Time series of winter 500-hPa temperature anomalies (°C) from 1971 to 2003 for the nine stations, along with the mean. Linear regression lines have been added. The data have been offset as follows: South Pole (+0°C), Novolazarevskaja (+2°C), Syowa (+4°C), Davis (+6°C), Mirny (+8°C), Casey (+10°C), McMurdo (+12°C), Bellingshausen (+14°C), Halley (+16°C), and the mean (+18°C).

Vertical velocity changes over Antarctica can modify the temperature regime by means of enhanced subsidence and adiabatic heating. Detecting changes in vertical velocity is extremely difficult, so we have investigated variability in the flow in the high-latitude circulation cell by means of variations in the katabatic outflow from the continent, which is a major feature of East Antarctica. Analysis of the meridional component of the surface winds from the nine stations suggests that there has been no significant change in the katabatic flow and therefore the circulation cell over the past 30 years. Although no relevant circulation changes can be found with the use of the above diagnostic techniques, it is possible that changes below the detection threshold could have contributed to the observed warming.

General circulation models (GCMs) are a very powerful tool for investigating the mechanisms responsible for changes in the Earth system, and climate model runs spanning the instrumental period were examined to see if they reproduced the large warming during the winter. We examined output from a four-member ensemble of the Hadley Centre coupled atmosphere-ocean GCM (HadCM3) (*23*), which was run from 1880 to 1999 forced with realistic greenhouse gases, aerosols, volcanic aerosols, and solar variability. For the period from 1970 to 1999, the four members of the ensemble showed a large variability in the Antarctic tropospheric temperature trends, indicating the difficulty of reproducing climate change across the region. However, on average, the runs had a maximum warming in the midtroposphere, although the winter season trends were only ~0.2°C per decade. Although the trends in the model runs are smaller than in the observations, they are not statistically significantly different.

The available observations and current state of climate models do not allow us to unambiguously assign a cause to the tropospheric warming. The lack of a clear change to the atmospheric circulation suggests in situ effects, such as changes in cloud amount or particle size, and increases in the greenhouse gas concentration may well be playing a part. The temperature changes observed in the radiosonde data of a warming troposphere and cooling stratosphere are what would be expected as a result of increasing greenhouse gases. However, because the climate model runs we examined did not reproduce the observed high-latitude changes, we are unable to attribute these changes to increasing greenhouse gas levels at this time. The lack of a similar warming trend at the surface, the evidence that much of the ocean around the Antarctic is sea ice covered in winter, and the midtropospheric warming observed at the South Pole together make it unlikely that the ocean is playing a major role. The observation of significant tropospheric warming at southern high latitudes, decoupled from a similar surface change, is therefore very important for those investigating natural climate variability and the possible impact of increasing greenhouse gases.

References and Notes

1. J. C. King, J. Turner, G. J. Marshall, W. M. Connolley, T. A. Lachlan-Cope, in *Antarctic Peninsula Climate Variability: A Historical and Paleoenvironmental Perspective,* vol. 79 of *Antarctic Research Series*, E. Domack, A. Burnett, P. Convey, M. Kirby, R. Bindschadler, Eds. (American Geophysical Union, Washington, DC, 2003), pp. 17–30.
2. J. Turner *et al.*, *Int. J. Climatol.* **25**, 279 (2005).

3. J. C. Comiso, *J. Clim.* **13**, 1674 (2000).
4. P. T. Doran *et al.*, *Nature* **415**, 517 (2002).
5. The mean near-surface warming was computed from the Climate Research Unit, University of East Anglia, UK database of in situ surface meteorological observations (see www.cru.uea.ac.uk/ftpdata/tavegl2v.dat).
6. J. Turner, J. C. King, T. A. Lachlan-Cope, P. D. Jones, *Nature* **418**, 291 (2002).
7. S. C. B. Raper, T. M. L. Wigley, P. R. Mayes, P. D. Jones, M. J. Salinger, *Mon. Weather Rev.* **112**, 1341 (1984).
8. T. H. Jacka, W. F. Budd, *Ann. Glaciol.* **27**, 553 (1998).
9. J. Turner *et al.*, *J. Clim.* **17**, 2890 (2004).
10. J. K. Angell, *Geophys. Res. Lett.* **26**, 2761 (1999).
11. J. K. Angell, in *Trends Online: A Compendium of Data on Global Change* (Carbon Dioxide Information Analysis Center, Oak Ridge National Laboratory, U.S. Department of Energy, Oak Ridge, TN, 2005); (http://cdiac.esd.ornl.gov/trends/temp/angell/angell.html).
12. P. W. Thorne *et al.*, *J. Geophys. Res.* **110**, 10.1029/2004JD005753 (2005).
13. Angell gives temperature trends for various latitude bands (*10*, *11*) but not a value for 0° to 60°S. Therefore, we calculated it from his values for 0° to 90°S (0.10) and 60° to 90°S (0.29) using the area weighting of 1/6 for 60 to 90°S that Angell uses: 0-60_trend = [0.1 − 1/6 × (0.29)]/5/6, giving a value of 0.06.
14. G. J. Marshall, *J. Clim.* **16**, 4134 (2003).
15. D. H. Bromwich, R. L. Fogt, *J. Clim.* **17**, 4603 (2004).
16. We used the updated version 5.2 of the Temperature of the Lower Troposphere product of the Microwave Sounder Unit in (*24*).
17. R. E. Swanson, *Geophys. Res. Lett.* **30**, 2040 (2003).
18. S. J. Sherwood, J. Lanzante, C. Meyer, *Science* **309**, 1556 (2005).
19. J. K. Luers, R. E. Eskridge, *J. Clim.* **11**, 1002 (1998).
20. D. J. Gaffen, *J. Geophys. Res.* **99**, 3667 (1994).
21. R. Lund, J. Reeves, *J. Clim.* **15**, 2547 (2002).
22. H. B. Bluestein, *Observations and Theory of Weather Systems,* vol. 2 of *Synoptic-Dynamic Meteorology in Midlatitudes* (Oxford Univ. Press, Oxford, 1993).
23. C. Gordon *et al.*, *Clim. Dyn.* **16**, 147 (2000).
24. R. W. Spencer, J. R. Christy, *J. Clim.* **5**, 858 (1992).
25. We are grateful to the Scientific Committee on Antarctic Research for funding the digitization of the Russian radiosonde data.

21 October 2005; accepted 24 February 2006
10.1126/science.1121652

Changes in Surface Water Supply Across Africa with Predicted Climate Change

Maarten de Wit* and Jacek Stankiewicz

Across Africa, perennial drainage density as a function of mean annual rainfall defines three regimes separated by threshold values of precipitation. This nonlinear response of drainage to rainfall will most seriously affect regions in the intermediate, unstable regime. A 10% decrease in precipitation in regions on the upper regime boundary (1000 millimeters per year) would reduce drainage by 17%, whereas in regions receiving 500 millimeters per year, such a drop would cut 50% of surface drainage. By using predicted precipitation changes, we calculate that a decrease in perennial drainage will significantly affect present surface water access across 25% of Africa by the end of this century.

Water is essential to human survival, and changes in its supply from overland flow can potentially have devastating implications, particularly in Africa, where much of the population relies on local rivers for water. Future climate change poses one of the greatest threats to poverty eradication on this continent, and related changes in surface water supply will exacerbate this threat (*1*). To predict future supply, it is necessary to understand how the drainage relates to biological, geological, and atmospheric parameters. These form a highly complex system, but simpler relationships can be identified within it, in particular relating drainage to precipitation. Even this relationship is nonlinear (*2*, *3*). Our detailed analysis of the African river systems identifies three climatic regimes. Areas receiving a low rainfall have virtually no perennial drainage. Above a threshold rainfall, there exists an intermediate range in which the drainage density increases with increasing rainfall. This regime can be termed "unstable": A change in climate would directly result in a change in surface water supply. This relationship is not indefinite; in high-rainfall areas other factors, like vegetation, begin to play a role, and a slight decrease in drainage density with increasing rainfall is observed. Here, we quantify how a moderate but variable change in precipitation across Africa by the second part of this century, as predicted by an ensemble of global climate-change models, would directly affect African countries, 75% of which fall at least partially into the unstable intermediate rainfall regime.

Our studies make use of AEON's Africa Database (*4*). This geographic information system (GIS) database includes all rivers and lakes in Africa (Fig. 1), manually digitized from topographic maps of individual countries on the basis of their own cadastral databases (figs. S1 to S4). The average stream separation (ratio of land area to total stream length) of the set is 15 km. This corresponds to about 2 million km of digitized rivers. Streams were checked against the 90-m SRTM (Shuttle Radar Topography Mission) digital elevation model (DEM) and were found to be within 300 m from valleys seen on the DEM. This uncertainty is two orders of magnitude less than the resolution of the database. All streams have also been classified as either perennial or nonperennial (as defined on local cadastral maps), and all river networks were ordered according to the Horton-Strahler ordering scheme (*5*). The database also includes climatic conditions over the African continent, such as seasonal rainfall and temperatures (*6*).

To understand the relationship between rainfall and drainage in Africa, we did a continental scale analysis by subdividing Africa into square blocks of 1000 km across [giving areas of 1,000,000 km^2; smaller areas near the coast were combined into bigger blocks (Fig. 1 inset)]. For each of the 37 blocks, we computed the mean annual precipitation as well as the perennial drainage density. This latter quantity is the total perennial stream length per unit area. The exact value of the total length, and thus of the density, depends on the resolution of the map from which the streams were obtained. There are also many finer points of what exactly constitutes a stream (*2*, *4*, *7*). For this reason, it is meaningless to compare density values from different studies on other continents, for example, unless the same resolution and standardized parameters are used. It is also important that these parameters are constant throughout the analysis; otherwise density variations could be observed where none really exist. The plot of perennial density as a function of mean annual precipitation is shown in Fig. 2A. A similar regional analysis was done for southern Africa (south of the Zambezi river, Fig. 1). Here, 24 blocks 500 km across were used (figs. S1 and S2), and the observed results are shown in Fig. 2B.

From the plots in Fig. 2, perennial drainage density as a function of mean annual rainfall consists of regimes separated by threshold values of precipitation. Areas receiving less than 400 mm year^{-1} have almost no perennial drainage (*8*). Above this threshold of ~400 mm year^{-1}, the perennial drainage density initially increases with increasing precipitation, but this does not go on indefinitely. The next threshold is defined statistically at ~1000 mm year^{-1} (*9*).

We therefore propose a model for the relationship between mean annual precipitation and perennial drainage that comprises three scaling regimes separated by two thresholds. Areas receiving less than 400 mm year^{-1} have no perennial drainage, unless they are mountainous regions conducive to runoff (*8*). Above that threshold, density increases linearly with increasing precipitation until another threshold of ~1000 mm year^{-1} is reached. Above that value, the density decreases slightly with increasing rainfall (*8*). We do not know whether there is

Africa Earth Observatory Network (AEON) and Department of Geological Sciences, University of Cape Town, Rondebosch 7701, South Africa.

*To whom correspondence should be addressed. E-mail: maarten@cigces.uct.ac.za

another threshold and a fourth regime for even higher rainfall, but the three-regime model covers the precipitation range of Africa adequately. Some implications of the model summarized in Fig. 2 are shown in Fig. 3A, whereas Fig. 3B shows the distribution of the three rainfall regimes across Africa. The dry regime (marked in red) covers the largest area (41% of the continent), but the intermediate regime (marked in yellow; ~25% of Africa) is of most interest here, because this is where changes to precipitation would result in serious changes in drainage supply. Two densely populated regions are of particular concern. First, southern Africa is in a very disturbing situation. Most of it falls into the unstable regime, and large sections of the arid regime receive their only water from the Orange River, with its sources in the unstable areas. Second, most of East Africa is also in the intermediate range, as are large sections of the upper Nile.

With our model, we now attempt a prediction of the perennial water supply across Africa by the end of this century. That human impact is a major driving force behind the climate changes in the last century is accepted by most scientists [see, for example, (*1*, *10*–*12*)]. Global warming due to anthropogenic emission of greenhouse gasses has received more attention from scientists than can be referenced here. In a recent presentation (*13*), Anthony Nyong said that Africa risks bearing the brunt of this climate change unless urgent action is taken now. He estimated that by year 2050 rainfall in sub-Saharan Africa could drop by 10%, leading to major water shortages. A 10% decrease in precipitation in regions on the intermediate regime's upper boundary (1000 mm year^{-1}) would reduce drainage by 17%, whereas in regions receiving 500 to 600 mm year^{-1} such a drop would cut 50 to 30%, respectively, of surface drainage (Fig. 3A). However, a uniform climate change on a continental scale is clearly a gross simplification, and we use a more detailed future rainfall estimate across Africa as summarized below.

We first make use of the results of the climate change assessment project for Africa by the Climate System Analysis Group (CSAG) based in Cape Town, South Africa (*14*). This group uses results from six global circulation models (GCMs) to assess the projected changes in mean annual rainfall across Africa for the past three decades of the 21st century and to downscale these to regional scales of relevance (*15*, *16*). The GCM simulations span the 20th century with use of specified anthropogenic forcing and continue through the 21st century by using the special reports on emission scenarios (SRES) of increasing greenhouse gas emissions (*17*). Detailed discussion of the configuration of each model simulation is beyond our scope, and the interested reader is referred to the research groups responsible for each model (*14*, *18*–*24*). We follow the example of the CSAG by using the average forecast of these models for Africa and the range covered by the models as a measure of uncertainty. In addition, we compare these forecasts to a composite ensemble of African precipitation models for the period 2070 to 2099, derived from 21 fully coupled ocean-atmosphere GCMs listed by the Intergovernmental Panel on Climate Change (IPCC) (*24*–*26*).

One input parameter used in all the models that will be mentioned is the anthropogenic

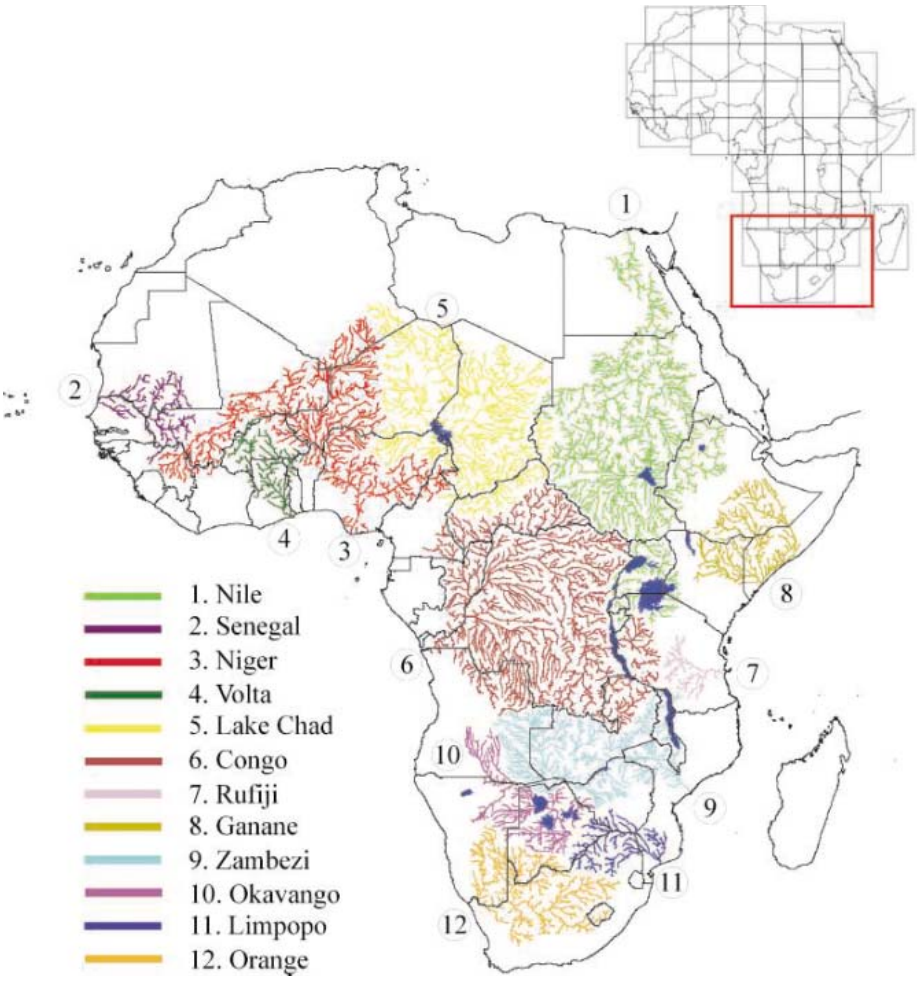

Fig. 1. Major river basins in Africa, selected from the AEON Africa Database. This is not the full resolution of the database. More detailed examples can be viewed in figs. S1 to S4. (**Inset**) 37 Africa-wide blocks (black lines) used to study the relationship between rainfall and drainage. Red block marks southern Africa, which was subdivided into 24 blocks (figs. S1 and S2).

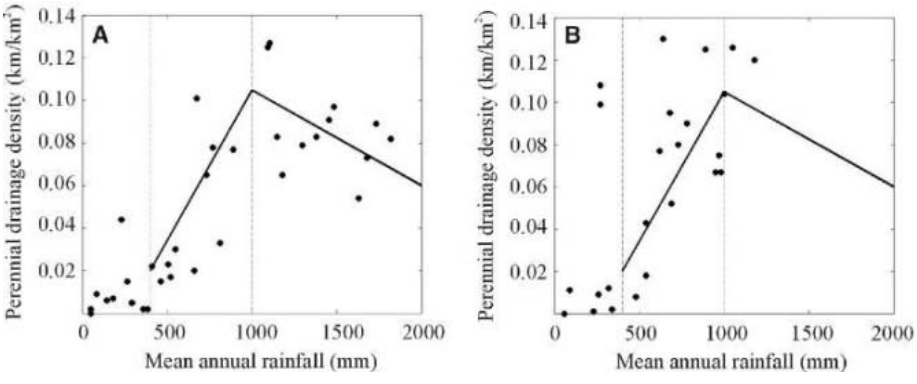

Fig. 2. Perennial drainage density as a function of mean annual rainfall, measured for individual blocks for the whole of Africa (**A**) and southern Africa (**B**). Dashed vertical lines show thresholds of 400 and 1000 mm year^{-1}. Black lines show best linear fits of the combined data sets inside the intermediate and high rainfall regimes (*9*).

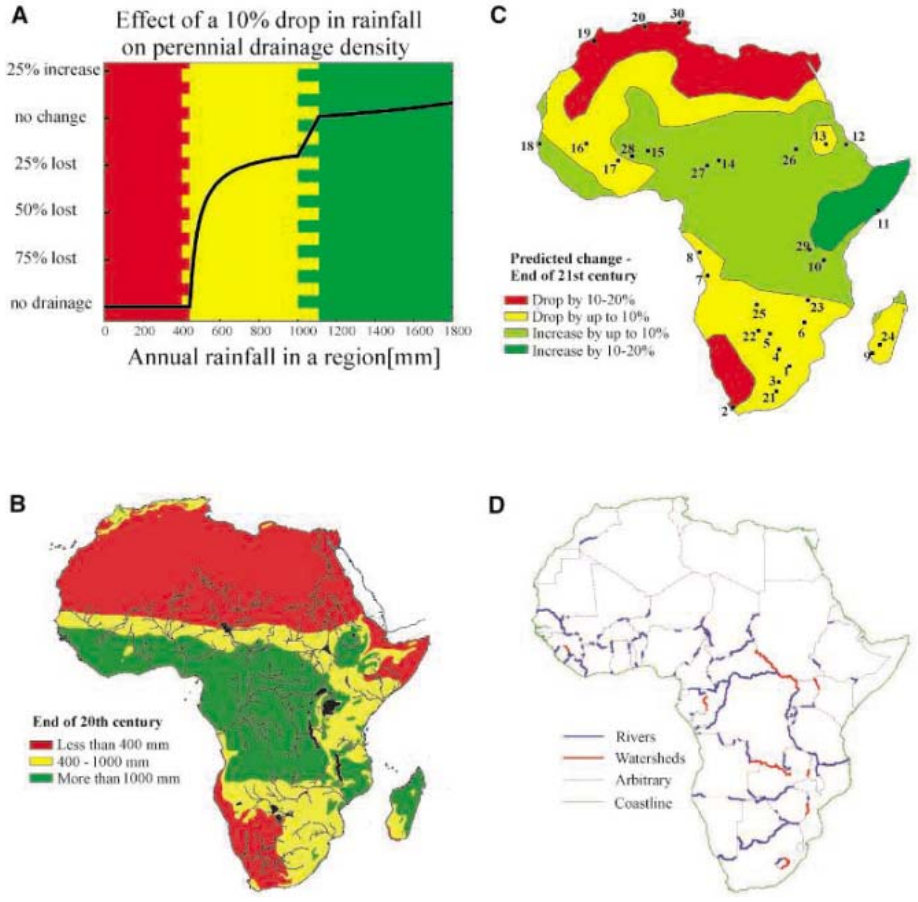

Fig. 3. (**A**) Graph showing the implications of our rainfall–perennial drainage density model. Black curve shows what change in perennial drainage would occur in a region if annual precipitation dropped by 10%. This curve is a function of the annual drainage in the region before the change. The three colors correspond to the three rainfall regimes, distribution of which is shown in (**B**). The two zippers show rainfall ranges where a 10% drop resulted in crossing a threshold. Regions receiving between 401 and 444 mm year^{-1} would drop under 400 (from yellow to red in our color scheme), and those receiving between 1001 and 1111 mm year^{-1} would go from the green to the yellow. One of the consequences of the observed relationship between rainfall and drainage is that a small change in precipitation in a region in the intermediate, unstable regime can cause substantial changes in the perennial water supply. If, for example, in a region receiving 600 mm year^{-1} of rain, the precipitation decreases to 550 mm year^{-1} (a change of less than 10%), perennial drainage will be cut by 25%, wheras a change from 500 mm year^{-1} to 450 mm year^{-1} would cut the drainage by half. (**B**) Present rainfall regimes in Africa. Dry areas (receiving not more than 400 mm year^{-1}) are marked in red. These areas make up 44% of the continent's total area (three countries in Africa fall entirely in this region: Egypt, Djibouti, and Saharawi). The intermediate regime (not more than 1000 mm year^{-1}) is marked in yellow (25% of area; affecting at least partially 75% of all African countries), and the high rainfall areas are marked in green (31%). Only the major rivers and lakes have been superimposed on the figure. Not all of these rivers are perennial. (**C**) Simplified map of Africa showing expected change in precipitation by the end of the 21st century on the basis of the composite of 21 leading fully coupled GCMs adapted by the IPCC for forecasting purposes (*14*, *24*). Here, 10% change contours have been used to simplify the figure; the original models are considerably more detailed. Numbers 1 to 30 are selected positions throughout Africa where we have calculated the expected changes in perennial drainage density (Table 1). Points 1 to 20 correspond to urban areas, whereas 21 to 30 represent rural areas. (**D**) International borders in Africa. Of all inland boundaries, rivers form 33% (blue), with another 6% made up by watersheds (red). These river-related borders apply to 39 of the 48 (i.e., 81%) countries on Africa's mainland. Arbitrary inland borders are shown in gray stipples, and the coastline in green.

CO_2 input into the atmosphere to trace its long-term effect on climate change. Depending on how this changes over the years, each model produces different scenarios depending on the time-integrated greenhouse gas emissions (*17*, *24*, *25*). Here, we concentrate on a relatively optimistic model that includes the assumption of a timely and effective development of nonfossil energy supply (the B1 marker scenario, normalized to the historically observed precipitation in Africa for the 20-year period from 1979 to 1998) (*24*, *25*). On the basis of the above model, the mean expected changes in large-scale precipitation across Africa in the last quarter of the 21st century are shown in Fig. 3C.

For further analyses, 30 selected urban and rural areas in Africa lying in the unstable regime are located on Fig. 3C and listed in Table 1. Two-thirds of the data are derived from cities or towns, because rainfall data are less reliable in rural Africa and because city or town data provide reasonable proxies to large surrounding rural regions. The table shows what percentage of today's perennial drainage the area will have after a specific change in precipitation. Four scenarios are considered: decrease by 10% and 20% and increase by the same amounts. The expected scenario (Fig. 3C) is marked with an asterisk, and some are briefly highlighted below.

Most of southern Africa (including southern Madagascar) lies in either the unstable or the dry regime (Fig. 3B), and much of this region is projected to experience significant losses of what little drainage it does have (Fig. 3C). Areas near Cape Town will likely suffer most, losing more than half their perennial supply. This means there will be no relief for this drought-stricken region (*27*). In addition, the eastern and northern section of the subregion are projected to experience strong to moderate decreases in their water supply. Any such loss in eastern South Africa would affect the upper reaches of the Orange River, whose lower reaches are one of few perennial water supplies in southwestern Africa. The interior of this region is very dry, but the Orange River, with its sources in the east, winds its way through the arid region. This is a major river, with a mean annual discharge of over 11,000 km^3, making it the fifth largest river in Africa and one of the 50 largest ones globally (*28*). However, there were at least five instances between 1862 and 1912 (before any damming schemes) of this river running dry (*29*). In 1903 the river stopped flowing for 2 months, showing that even one of the continent's biggest rivers cannot be truly called perennial. Today, western South Africa is experiencing its biggest drought in over 100 years (*27*), and water shortages in central South Africa in late 2004 led to almost no water being released from the dams on the Orange River. This caused the lower reaches of this river, where it forms the border of Namibia, to reach a very low level.

East Africa's future looks better, with increases of drainage density to be expected, because parts of the region may expect an increase in rainfall that could even put it into the wet regime. However, although Somalia's supply (Mogadishu) could go up by a factor of 10, this may not significantly increase its drainage density (e.g., 10 times very little does not necessarily translate to floods), and this may also stretch the limits of interpreting the spatial detail of the GCM results.

Table 1. Percentages of perennial drainage that will remain following a given change in precipitation. Rainfall values (in mm year^{-1}) obtained from (*32*) for cities 1 to 20 and from the CSAG (*14*) station data archive for rural districts 21 to 30. The potential scenario for each locality at the end of this century, based on climate change models discussed in the text, is marked with an asterisk.

No.	City	Country	Rainfall	During	10% Drop	20% Drop	10% Rise	20% Rise
1	Johannesburg	South Africa	723	1951–1990	78%*	55%	122%	145%
2	Cape Town	South Africa	612	1837–1989	71%	42%*	129%	158%
3	Bloemfontein	South Africa	557	1903–1990	65%*	29%	135%	171%
4	Gaborone	Botswana	526	1922–1988	58%*	17%	142%	183%
5	Maun	Botswana	465	1921–1989	28%*	0%	172%	243%
6	Harare	Zimbabwe	830	1890–1989	81%*	61%	119%	139%
7	Catete-Sede	Angola	606	1918–1972	71%*	41%	129%	159%
8	Cabinda	Angola	798	1913–1980	80%*	60%	120%	140%
9	Tulear	Madagascar	420	1951–1990	0%*	0%	310%	520%
10	Dodoma	Tanzania	551	1922–1989	64%	27%	136%*	173%
11	Mogadisu	Somalia	409	1911–1990	0%	0%	554%	1009%*
12	Adi Ugri	Eritrea	642	1899–1976	73%	47%	127%*	153%
13	Gedaref	Sudan	626	1903–1990	72%*	45%	128%	155%
14	Ndjamena	Chad	570	1904–1990	66%	33%	134%*	167%
15	Niamey	Niger	556	1905–1990	64%	29%	136%*	171%
16	Mourdiah	Mali	529	1930–1985	59%*	18%	141%	182%
17	Ouagadougou	Burkina Faso	814	1902–1990	80%*	61%	120%	139%
18	Dakar	Senegal	505	1897–1990	52%	4%	148%*	196%
19	Rabat	Morocco	538	1930–1989	61%	22%*	139%	178%
20	Algiers	Algeria	660	1870–1973	75%	49%*	125%	151%
				Rural districts				
21	Zastron	South Africa	570	1979–2000	66%*	33%	134%	167%
22	Okavango	Botswana	460	1973–2003	23%*	0%	177%	253%
23	Chipata	E. Zambia	840	1979–2000	81%*	62%	119%	136%
24	Isalo-Ihosy	Madagascar	870	1979–2000	81%*	63%	119%	125%
25	Western	W. Zambia	730	1979–2000	78%*	56%	122%	144%
26	S. Kordofan	Sudan	460	1979–2000	23%	0%	177%*	253%
27	Marona	Cameroon	680	1979–2000	76%	51%	124%*	149%
28	Foda Ngourma	Burkina Faso	830	1979–2000	81%	61%	119%*	140%
29	Northwest	Tanzania	670	1979–2000	75%	50%	125%*	150%
30	Jendouba	Tunisia	440	1979–2000	0%	0%*	210%	320%

A third major unstable area, visible in Fig. 3B, is the east-west band stretching from Senegal to Sudan, separating the dry Sahara from wet Central Africa. This band might look unsubstantial, but it crosses a number of important water bodies, such as the Sudd swamps in the Nile Basin, Lake Chad (which has now shrunk to 10% of its size in 1963), and the Niger River on either side of its inland delta (*30*). The predicted evolution of the southern boundary of the Sahara in west Africa appears complex: The desert's limit should move northward in Chad and Niger, but farther west (Burkina Faso and Mali) the desert will continue to spread south. Although this relies on the finer spatial details of the GCMs, none of the IPCC models predicts enough rainfall change to suggest perennial river networks in the Sahara this century or to have any direct effect on Central and West Africa in the wet regime.

Although water storage and management systems in most large cities can be reengineered to cope with most changes in runoff regimes, the results of this study provide African states with an opportunity to focus adaptation responses on those rural areas where the risk of loss of perennial water is high and more likely to create scarcity. But water can also be a source of international conflict. River channels and basin watersheds frequently demarcate international boundaries; in Africa they make up almost 40% of these borders (Fig. 3D). Furthermore, all major African rivers traverse international boundaries. To what extent reduced flow in major rivers reflects direct changes in rainfall-runoff discharge and groundwater flow, rather than reduced perennial drainage as suggested here, requires further study. However, our results indicate that future access to water, especially in rural areas that depend on low-order streams for surface supply, needs to be seriously addressed by countries that share river basins and that the ability to estimate the future water supply, like this study does, is an essential requirement for water basin management throughout the African continent.

References and Notes

1. World Bank *et al., Poverty and Climate Change: Reducing the Vulnerability of the Poor Through Adaptation* (World Bank, Washington, DC, 2003) (http://lnweb18.worldbank.org/ESSD/envext.nsf/46ByDocName/KeyThemesVulnerabilityandAdaptationPovertyandClimateChange).
2. K. J. Gregory, in *Geomorphology and Climate*, E. Derbyshire, Ed. (Wiley, New York, 1976), pp. 289–315.
3. G. E. Moglen, E. A. B. Eltahir, R. L. Bras, *Water Resour. Res.* **34**, 855 (1998).
4. J. M. Stankiewicz, M. J. de Wit, *Geophys. Geochem. Geosyst.* **6**, 10.1029/2005GC000928 (2005).
5. A. N. Strachler, *Eos* **38**, 913 (1957).
6. D. R. Legates, C. J. Willmot, *Int. J. Climatol.* **10**, 111 (1990).
7. D. R. Montgomery, W. E. Dietrich, *Nature* **336**, 232 (1988).
8. Exceptions to this rule are found in mountainous areas, which are conducive to runoff. This factor accounts for the anomalous point showing perennial density of 0.44 km^{-1} at a rainfall of just over 200 mm year^{-1} in Fig. 2A. This point represents the western section of southern Africa. In the south of the block are steep mountain ranges, collectively known as the Cape Fold Belt. The majority of the rainfall in this area is concentrated in these mountains, which causes a number of perennial rivers to form on the southern extremity of Africa. This anomaly can also be seen in Fig. 2B: Two points give perennial density near 0.1 km^{-1} despite receiving just over 200 mm year^{-1}.
9. The precipitation threshold was moved between 600 and 1400 mm year^{-1}, and points combined from both data sets (Fig. 2) were separated by it into two subsets. Correlation coefficients for each subset were computed. The average of the two correlation coefficients is highest when the precipitation threshold was just over 1000 mm year^{-1}. The individual coefficient is 61.7% for regions receiving between 400 and 1000 mm year^{-1} and an inverse correlation of 59.2% for regions receiving above 1000 mm year^{-1}. Both these correlations can be stated with a confidence of 99%. An identical result was obtained using

GraphPad Prism 4 developed by GraphPad Software (*31*). The inverse correlation in the high rainfall regime is probably the result of dense vegetative growth entering the relationship. We do not know how far this wet regime extends; using the regression computed in this study it would intercept the rainfall axis (i.e., the point of no perennial drainage) at 3200 mm year^{-1}, almost twice as much precipitation as our wettest data point.
10. IPCC, *Climate Change 2001,* J. T. Houghton *et al.*, Eds. (Cambridge Univ. Press, Cambridge, 2001).
11. H. von Storch *et al.*, *Science* **306**, 679 (2004).
12. D. A. Stainforth *et al.*, *Nature* **433**, 403 (2005).
13. A. Nyong, abstract in *Impacts of Climate Change in the Tropics: The African Experience. Avoiding Dangerous Climate Change* (Meterological Office, Exeter, UK, 2005) (www.stabilisation2005.com).
14. CSAG, *Assessments of Impacts and Adaptations to Climate Change: Africa Climate Change Scenarios, Volume 1* (2002) (www.csag.uct.ac.za).
15. B. C. Hewitson, R. G. Crane, *Int. J. Climatol.,* in press.
16. B. Hewitson, personal communications.
17. IPCC, *2000: Special Report of the Intergovernmental Panel on Climate Change,* N. Nakicenovic, R. Swart, Eds. (Cambridge Univ. Press, Cambridge, 2000), p. 570.
18. Canadian Center for Climate Modelling and Analysis (CCCMA), model CGCM2 (www.cccma.bc.ec.gc.ca/data/cgcm2/cgcm2.shtml).
19. Commonwealth Scientific and Industrial Research Organisation (CSIRO), model Mk-2 (http://cera-www.dkrz.de/IPCC_DDC/IS92a/CSIRO/csirogcm.html).
20. Max Planck Institute for Meteorology, model ECHAM4 (www.mpimet.mpg.de/en/extra/models/echam/echam4_description.php).
21. Hadley Centre, global climate model HADCM3 (www.met-office.gov.uk/research/hadleycentre/models/HadCM3.html).
22. National Center for Atmospheric Research (NCAR), Climate System Model (CSM).
23. NCAR, Parallel Climate System Model (PCSM).
24. Model outputs for IPCC AR4 (2005) are available (https://esg.llnl.gov:8443/home/publicHomePage.do).
25. IPCC, *Special Report on Emissions Scenarios* (*SRES*) (www.grida.no/climate/ipcc/emission/098.htm).
26. A notable degree of convergence has emerged over the last decade between all of these models, both for Africa as a whole, and at large regional scales such as for southern Africa (*15*, *16*, *24*, *25*). Although individual models may disagree in specific geographic locations, in terms of area averages the multimodel mean is a good indication of the consensus change. As with all GCM simulations, care must be taken against overinterpreting fine scale information; the skill (especially with precipitation) lies in the area aggregate of the data.
27. R. Mathieu, Y. Richard, *Geophys. Res. Lett.* **32**, 10.1029/2005GL022436 (2005).
28. J. M. Bremner, J. Rogers, J. P. Willis, *Trans. R. Soc. S. Afr.* **47**, 247 (1990).
29. W. van Warmelo, *S. Afr. Irrigation* **1**, 244 (1922).
30. A decrease in precipitation, and the resulting decrease in water supply, anywhere along this band would be absolutely disastrous not just to the population in the band. Africa's two largest deltas, the Nile and the Niger, receive a substantial amount of their drainage from this unstable regime. The Nile drains 11 different countries that depend on it in varying degrees. With increasing populations and decreasing water supply, conflicts over shared water are inevitable. The fact that most models predict an increase in rainfall in East Africa does not decrease the seriousness of this problem, and, if the some of the GCMs turn out to be the correct forecast [e.g., (*20*)], the entire Nile basin, including the Sudd swamps, will be very seriously affected.
31. GraphPad Prism 4, GraphPad Software (www.curvefit.com).
32. World Climate (www.worldclimate.com).
33. Our Africa research is funded by the Africa Exploration Unit of De Beers. We thank M.C.J. de Wit of the Africa Exploration Unit for providing us with African river and climate data; D. Rothman and D. Turcotte for their interest in our African River basin analyses and for sharing their expertise on river networks, F. Cotterill for stimulating our interests in watersheds of sub-Saharan Africa, and J. Rogers for sharing knowledge on the Orange River. We have benefited in particular from discussions with B. Hewitson, who also made available to us the results of the CSAG and facilitated early access to the IPCC data bank of global climate models. We acknowledge the international modelling groups for providing their data for analysis, the Program for Climate Model Diagnosis and Intercomparison (PCMDI) for collecting and archiving the model data, the Joint Scientific Committee (JSC) of the Climate Variability (CliVar) Scientific Steering Group on Coupled Modelling (WGCM) and their Coupled Model Intercomparison Project (CMIP) and the Climate Simulation Panel for organizing the model data analysis activity, and the IPCC WG1 TSU for technical support. The IPCC Data Archive at Lawrence Livermore National Laboratory is supported by the Office of Science, U.S. Department of Energy. We thank B. Hewitson for reviewing this paper. This is AEON contribution 002.

Supporting Online Material

www.sciencemag.org/cgi/content/full/1119929/DC1
Materials and Methods
Figs. S1 to S4

8 September 2005; accepted 21 February 2006
Published online 2 March 2006;
10.1126/science.1119929
Include this information when citing this paper.

Kaposi's Sarcoma–Associated Herpesvirus Fusion-Entry Receptor: Cystine Transporter xCT

Johnan A. R. Kaleeba and Edward A. Berger*

Kaposi's sarcoma–associated herpesvirus (KSHV, human herpesvirus 8) is the causative agent of Kaposi's sarcoma and other lymphoproliferative syndromes often associated with HIV/AIDS. Functional complementary DNA selection for a receptor mediating KSHV cell fusion identified xCT, the 12-transmembrane light chain of the human cystine/glutamate exchange transporter system x_c^-. Expression of recombinant xCT rendered otherwise not susceptible target cells permissive for both KSHV cell fusion and virion entry. Antibodies against xCT blocked KSHV fusion and entry with naturally permissive target cells. KSHV target cell permissiveness correlated closely with endogenous expression of xCT messenger RNA and protein in diverse human and nonhuman cell types.

KSHV is etiologically linked to Kaposi's sarcoma and other lymphoproliferative syndromes that occur more frequently in immunocompromised individuals, including those with HIV/AIDS (*1*). Entry of herpesviruses into host cells generally occurs via attachment to the cell surface, followed by direct fusion between the virion and target cell plasma membranes; alternative routes involving receptor-mediated endocytosis have been reported in some cases (*2*). KSHV can infect a broad range of adherent cell types of different species and tissue lineages in vitro, which indicates broad distribution of the host cell components associated with virus entry; however, the outcome is almost always latency rather than productive infection (*3*). Cells expressing recombinant KSHV glycoproteins undergo cell fusion (*4*); this provides support for a direct fusion entry mechanism. Consistent with these infectivity and fusion studies, we have found that a wide range of cell types from diverse tissues and species are permissive for KSHV glycoprotein–mediated cell fusion and virion entry (*5*); we hypothesized that these processes require a specific KSHV fusion-entry receptor(s) on the target cell surface, distinct from molecules previously implicated in the attachment and entry process.

For KSHV receptor identification, we adapted a vaccinia-based cell fusion assay in which "effector" cells expressing surface viral glycoprotein(s) (and infected with a recombinant vaccinia virus encoding bacteriophage T7 RNA polymerase) were mixed with "target" cells expressing the relevant surface receptor(s) (and containing the *Escherichia coli LacZ* gene linked to the T7 promoter, introduced by plasmid transfection or recombinant vaccinia virus infection); β-galactosidase (β-gal) activity provides a quantitative measure of cell fusion (*6*). Our functional strategy for KSHV receptor identification (*7*) made no assumptions about the specific viral or cellular molecules involved but, instead, relied on the notion that a receptor-encoding cDNA within a library derived from a fusion-permissive cell line would confer fusion susceptibility to an otherwise nonpermissive target cell; use of a selectable reporter would enable enrichment of the fused cells containing the desired cDNA. As KSHV nonpermissive fusion targets, F515 or NIH 3T3 murine fibroblasts were transfected with plasmid pJK7-T7Beacon containing the T7 promoter linked to a tripartite reporter cassette encoding surface epitope tags from influenza virus hemagglutinin (HA) and Myc, plus cytoplasmic enhanced green fluorescence protein (EGFP) (fig. S1A). The targets were also infected with Mel-dT2 (fig. S1B), a

Laboratory of Viral Diseases, National Institute of Allergy and Infectious Diseases (NIAID), National Institutes of Health, Bethesda, MD 20892, USA.

*To whom correspondence should be addressed. E-mail: edward_berger@nih.gov

library of recombinant vaccinia viruses (*8*) containing cDNAs from the Mel 1700 human melanoma cell line, a highly permissive KSHV fusion target (*5*). As effectors, the KSHV chronically infected BCBL-1 cell line was preactivated with 12-*O*-tetradecanoyl-13-phorbol acetate (TPA) to induce KSHV glycoprotein expression, then infected with vaccinia MVA/T7 pol. Preliminary analyses confirmed the functionality of the reporter plasmid, as well as the presence of putative KSHV receptor–encoding cDNAs within the Mel-dT2 library (fig. S2A). The receptor cDNA identification procedure (*7*) involved successive selection rounds to enrich for fused cells; at each step, the associated vaccinia viruses were amplified and used for the next round. With three selection rounds (HA/Myc magnetic immunobeads, ring harvesting of EGFP-positive foci, HA/Myc immunobeads), the vaccinia viruses were increasingly enriched for fusion-promoting activity (fig. S2B). Individual vaccinia clones from the final round were plaque-purified, and several were tested in the KSHV cell fusion assay. Clones that scored positive all contained cDNA inserts with the identical nucleotide sequence, whereas those that scored negative contained other cDNA sequences.

The fusion-conferring cDNA sequence encoded human xCT [gene name SLC7A11; EMBL/GenBank accession numbers AB026891 (*9*) and AJ277882 (*10*)], the 501–amino acid light chain of transport system x_c^- that mediates uptake of extracellular L-cystine coupled to efflux of L-glutamate. The x_c^- system is a member of the family of heterodimeric amino acid transporters (HATS); each contains a distinct nonglycosylated light chain that determines substrate selectivity, linked by an extracellular disulfide bond to the 4F2hc heavy chain (a component of the 4F2 antigen, also designated CD98), a ubiquitous multifunctional type II glycoprotein (*11*). Like other HAT light chains, xCT is predicted to have 12-transmembrane domain (TMD) helices and cytoplasmic N and C termini (fig. S3).

The ability of recombinant xCT to confer KSHV permissiveness to nonsusceptible targets ("gain-of-function") was tested in the KSHV cell fusion assay (*5*, *7*), which enabled analysis of KSHV glycoprotein function independent of other virus components. Transiently expressed xCT rendered NIH 3T3 targets highly permissive for fusion with effectors expressing transfected KSHV glycoproteins (Fig. 1A); in addition, stably expressed xCT converted BHK-21 and K-562 cells into efficient KSHV fusion targets and also significantly enhanced the moderate target cell activity of HeLa cells (Fig. 1B). The gain-of-function criteria were extended to the KSHV virion entry assay (*5*, *7*) with the use of recombinant virus rKSHV.219 containing the EGFP gene linked to a constitutive cellular promoter (*12*). This method enabled analysis of viral glycoprotein function in the context of infectious virions, independent of KSHV gene expression. Whereas negligible virion entry occurred with parental BHK-21 and K-562 targets, the corresponding xCT stable transfectants supported significant entry, indicated by increased EGFP-positive cells (Fig. 1C). Complementary "loss-of-function" experiments were performed with target cells naturally permissive for KSHV fusion and entry (*5*) by examining the effects of rabbit antisera against synthetic peptides (*7*) derived from predicted antigenic regions of xCT, with topological arrangements based on the 12-TMD model (fig. S3). KSHV cell fusion with BS-C-1 (African Green Monkey kidney cell) targets (Fig. 2A) was inhibited in a dose-dependent fashion by antisera against two putative extracellular regions of xCT (peptides P66-77 and P218-232), but not by antisera against two putative intracellular regions (peptides P25-40 and P97-109); surprisingly, dose-dependent inhibition was also observed with antiserum against peptide P255-270 derived from a putative short intracellular region of xCT [discussed in the legend to (fig. S3)]. In all cases, the corresponding preimmune sera were without effect. KSHV virion entry into Vero (African Green Monkey kidney) cells (Fig. 2, B and C) was strongly inhibited by antisera against putative extracellular peptides P66-77 and P218-232, but not intracellular peptide P97-109; as observed for cell fusion, antisera against peptide P255-270 also blocked KSHV virion entry. Consistent results were obtained with other naturally permissive target cells: KSHV fusion with human PCI-13 (head-and-neck squamous cell carcinoma) and Mel-1700 (melanoma) targets was inhibited by antisera against P255-270 (Fig. 2D) and P218-232; KSHV virion entry into RD (muscle spindle rhabdosarcoma) cells was also blocked by antisera against P66-77, P218-232, and P255-270. Thus, xCT is the predominant mediator of KSHV fusion and entry permissiveness for all five cell lines tested from different species and tissue lineages.

xCT mRNA is found in many human tissues and cell lines (*10*). Reverse transcription polymerase chain reaction (RT-PCR) and flow cytometry analyses (*7*) of diverse human cell types indicated that KSHV fusion permissiveness correlated with xCT expression. Thus, xCT mRNA was detected in all fusion-positive cell lines, at especially high levels in the strongest targets (fusion activities >300: Mel-1700, U-87, and PCI-13); by contrast, xCT mRNA was barely detectable in the weak targets (fusion activities <5: CA-46, Ramos, BJAB, KG-1, HSB-2, Huh-7, and K562) (Fig. 3A). Similarly, xCT protein levels varied widely among the cells examined (Fig. 3B) and correlated closely with the corresponding KSHV fusion activities (Fig. 3C).

Transporter proteins containing multiple TMDs (including 12-TMDs) function as receptors for several δ- and γ-retroviruses (*13*); xCT represents an example of the use of this class of

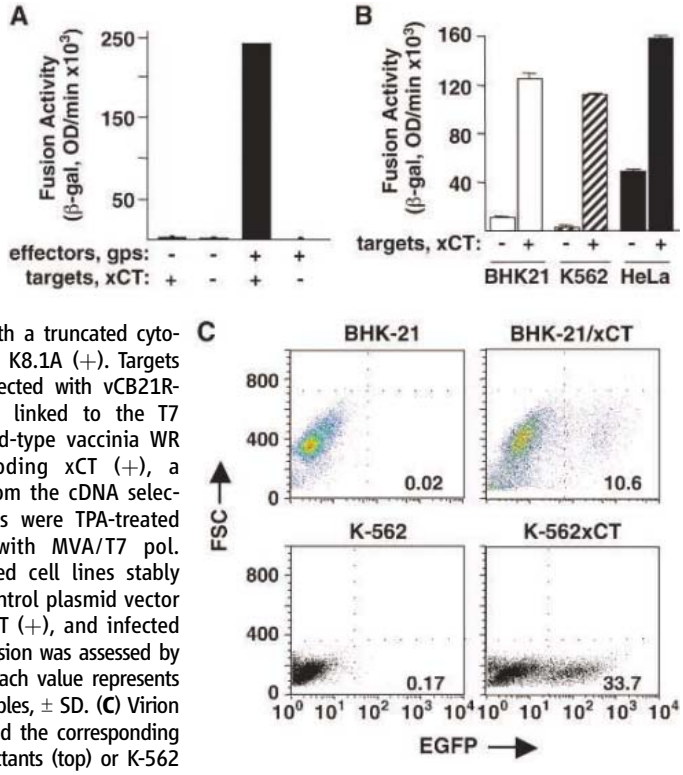

Fig. 1. Permissiveness for KSHV glycoprotein–mediated cell fusion and virion entry conferred by recombinant xCT. (**A**) Fusion effectors were F-515 cells infected with MVA/T7 pol and transfected with either control plasmid vector (–) or a mixture of four plasmids encoding KSHV glycoproteins (gps) gB^{Δ} (gB with a truncated cytoplasmic tail), gH, gL, and K8.1A (+). Targets were NIH 3T3 cells coinfected with vCB21R-*LacZ* (*E. coli LacZ* gene linked to the T7 promoter) and either wild-type vaccinia WR (–) or vJK-Mel.10 encoding xCT (+), a vaccinia clone derived from the cDNA selection. (**B**) Fusion effectors were TPA-treated BCBL-1 cells infected with MVA/T7 pol. Targets were the indicated cell lines stably transfected with either control plasmid vector pCDNA3.1 (–) or pJK9-xCT (+), and infected with vCB21R-*LacZ*. Cell fusion was assessed by measuring β-gal activity; each value represents the mean of duplicate samples, ± SD. (**C**) Virion entry into BHK-21 cells and the corresponding BHK-21/xCT stable transfectants (top) or K-562 cells and the corresponding K-562/xCT stable transfectants (bottom) was analyzed by flow cytometry at day 7 post infection with recombinant rKSHV.219; the numbers within each panel represent $EGFP^+$ cells as a percentage of the total number of cells counted.

molecules by a herpesvirus. Although we demonstrated that xCT functions as a major KSHV fusion-entry receptor in a wide array of human and nonhuman cells from diverse tissue lineages, our findings do not exclude the possible involvement of an alternative molecule (or molecules) for some other targets, nor do they refute previous findings that KSHV enters some cell types by an endocytic pathway (*14*). Indeed, the potential for the same virus to use alternate receptors and entry mechanisms in a host cell–dependent fashion is a growing theme in the herpesvirus field (*2*). Our findings of insignificant KSHV target cell activity among human B cell lines, coupled with the low xCT mRNA levels in these cells, is consistent with, and may explain, a previous report demonstrating the failure of several B cell lines to support the early steps of KSHV infection (*3*). Furthermore, by using RT-PCR, we did not detect xCT mRNA in human CD19$^+$ primary B cells isolated from fresh peripheral blood mononuclear cells. These results remain puzzling because KSHV can infect cultured primary B cells and is also associated with

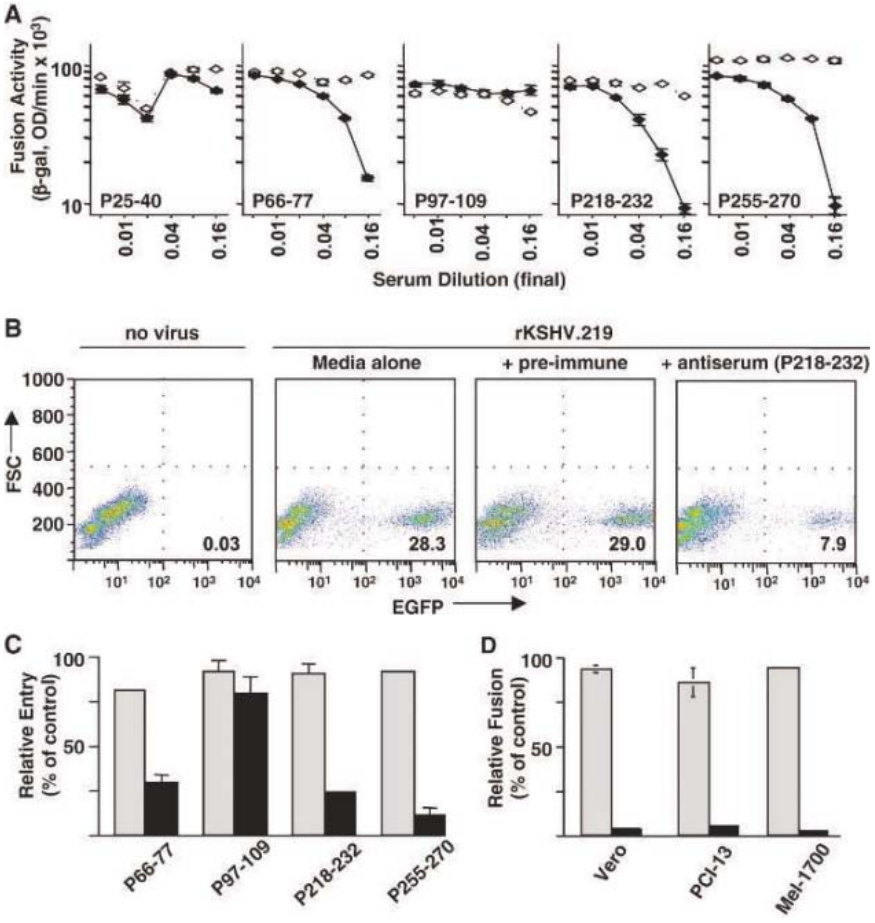

Fig. 2. Effects of xCT peptide antisera on target cells naturally permissive for KSHV cell fusion and virion entry. (**A**) Cell fusion. Assays were performed with TPA-treated BCBL-1 effectors and BS-C-1 targets pretreated with preimmune or immune sera against xCT-derived synthetic peptides: P25-40 (KAL-1), P66-77 (KAL-3), P97-109 (KAL-5), P218-232 (KAL-7), and P255-270 (KAL-10). The final antisera dilutions during the fusion reactions are indicated. Each value represents the mean of β-gal activity from duplicate samples, ± SD. (**B**) Virion entry. Vero cells were preincubated with media alone or with preimmune or immune sera (KAL-7) against peptide P218-232, then infected with recombinant rKSHV.219 and cultured in the continued presence of sera (1:4 final dilution). Virus entry was assayed by flow cytometry at day 3 post infection; numbers within each panel represent the percentage of EGFP-expressing cells. Uninfected Vero cells served as a background control. (**C**) Virion entry into Vero cells was assayed in the presence of a 1:4 final dilution of rabbit antisera against xCT-based synthetic peptides (black bars) or the corresponding preimmune sera (gray bars). Relative entry represents the percentage of EGFP$^+$ cells (at day 3 post infection) in antisera-treated cultures compared with untreated controls. Each value represents the mean of duplicate results for the two rabbit sera against each peptide, ± SD. (**D**) Cell fusion assays with the indicated target cells were performed as described in (A), in the presence of a 1:4 dilution of KAL-10 antiserum against P255-270 (black bars) or the corresponding preimmune serum (gray bars). Each value represents the mean of duplicate samples, ± SD.

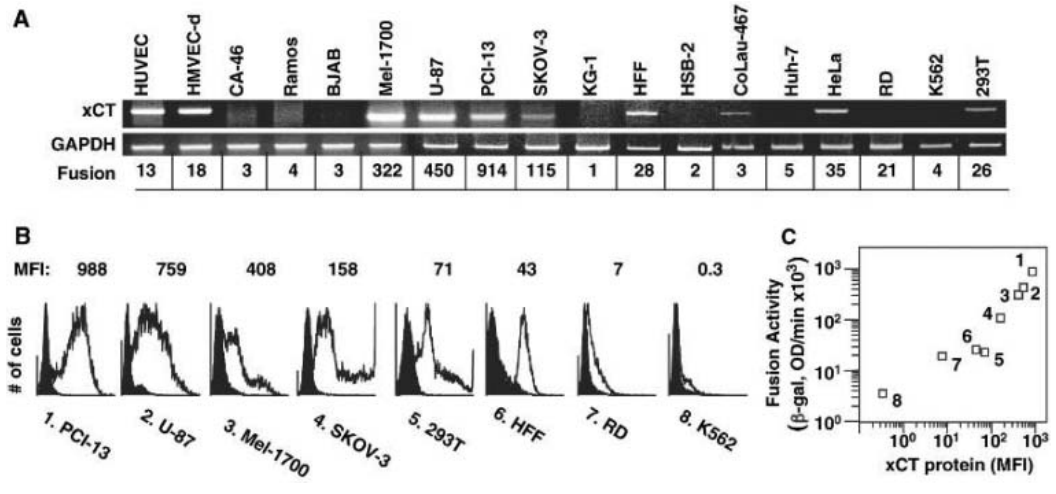

Fig. 3. Correlation of endogenous xCT expression with fusion permissiveness of diverse human target cells. (**A**) xCT mRNA. RT-PCR of xCT mRNA [515-base pair (bp) product] was performed by using total RNA isolated from log-phase cultures of the indicated human cell lines; parallel amplifications of mRNA for glyceraldehyde-3-phosphate dehydrogenase (GAPDH; 357-bp product) were used as internal controls for sample loading. Below each cell line are the corresponding fusion activities [β-gal, optical density (O.D.)/min × 10^3] from assays with TPA-activated BCBL-1 effectors. (**B**) xCT protein. The indicated cell lines were fixed in 4% paraformaldehyde, permeabilized with 0.1% Triton X-100, and stained with KAL-1 antiserum against xCT peptide P25-40 (open histograms) or the corresponding preimmune serum (black histograms). Numbers indicate MFI for xCT. (**C**) Correlation between endogenous xCT protein expression and fusion permissiveness among different targets, numbered as in (B).

B cell neoplasms in infected people (*1*). Therefore, more in-depth studies are required to unravel the various factors that influence the relation between xCT regulation and KSHV entry into cells of the B lymphocyte lineage.

The receptor function of xCT suggests new perspectives on the role of other cell surface molecules previously implicated in KSHV entry, particularly heparan sulfate (*15*, *16*) and integrin α3β1 (*17*). Sulfated proteoglycans and integrins play critical roles in enhancing attachment and internalization of diverse viruses (*18*–*20*); furthermore, accumulating evidence points to complex signaling pathways triggered by KSHV interaction with integrin α3β1 (*17*, *21*). Coupled with the recent observation (*22*) that 4F2hc forms multimeric complexes containing HAT light chains (including xCT) plus β1 integrins (including α3β1), our findings suggest a possible interplay between integrin signaling events and xCT-mediated KSHV entry.

By mediating cystine uptake, a rate-limiting step for glutathione (GSH) biosynthesis, the x_c^- system plays a central role in maintaining intracellular GSH levels during oxidative stress. xCT is up-regulated in response to GSH depletion, e.g., on exposure to reactive oxygen species (ROS) (*23*, *24*). Redox conditions also have substantial influences during KSHV infection, because hypoxia can induce lytic replication in chronically infected cell lines by activating hypoxia response elements in key lytic-phase genes (*25*). Moreover, it has been reported that KSHV induces ROS production in cultured endothelial cells and that ROS exposure results in enhanced virus entry (*26*). In light of these complex virus-host interactions, the identification of xCT as a KSHV receptor suggests novel pathogenic mechanisms whereby the virus might induce or exploit physiologic responses (i.e., ROS production and xCT up-regulation) that favor its own reactivation and dissemination. It is also noteworthy that intracellular GSH levels are progressively depleted during the course of HIV disease (*27*), at least in part because of HIV Tat-mediated down-regulation of GSH biosynthesis (*28*) and regeneration (*29*), plus enhancement of extracellular GSH hydrolysis (*30*). These concerted activities presumably contribute to the recently described Tat stimulation of xCT expression (*30*), as well as KSHV entry and infectivity (*31*). Thus, beyond the obvious consequences of immunosuppression, HIV coinfection might foster clinically aggressive HIV/AIDS-associated Kaposi's sarcoma by the additional mechanism of KSHV receptor up-regulation.

References and Notes

1. D. Bubman, E. Cesarman, *Hematol. Oncol. Clin. North Am.* **17**, 717 (2003).
2. P. G. Spear, R. Longnecker, *J. Virol.* **77**, 10179 (2003).
3. J. T. Bechtel, Y. Y. Liang, J. Hvidding, D. Ganem, *J. Virol.* **77**, 6474 (2003).
4. P. E. Pertel, *J. Virol.* **76**, 4390 (2002).
5. J. A. R. Kaleeba, E. A. Berger, unpublished data.
6. B. Dey *et al*., in *Current Protocols in Immunology*, Unit 12-10, Suppl. 54, J. E. Coligan, A. M. Kruisbeck, D. M. Margulies, E. M. Shevach, W. Strober, Eds., (Wiley, New York, 2003), pp. 12.10.1–12.10.20.
7. Materials and methods are available as supporting material on *Science* Online.
8. E. S. Smith, S. Shi, M. Zauderer, *Methods Mol. Biol.* **269**, 65 (2004).
9. H. Sato, M. Tamba, K. Kuriyama-Matsumura, S. Okuno, S. Bannai, *Antioxid. Redox Signal.* **2**, 665 (2000).
10. M. T. Bassi *et al.*, *Pflugers Arch.* **442**, 286 (2001).
11. F. Verrey *et al.*, *Pflugers Arch.* **447**, 532 (2004).
12. J. Vieira, P. M. O'Hearn, *Virology* **325**, 225 (2004).
13. C. S. Tailor, D. Lavillette, M. Marin, D. Kabat, *Curr. Top. Microbiol. Immunol.* **281**, 29 (2003).
14. S. M. Akula *et al.*, *J. Virol.* **77**, 7978 (2003).
15. S. M. Akula, F. Z. Wang, J. Vieira, B. Chandran, *Virology* **282**, 245 (2001).
16. A. Birkmann *et al.*, *J. Virol.* **75**, 11583 (2001).
17. S. M. Akula, N. P. Pramod, F. Z. Wang, B. Chandran, *Cell* **108**, 407 (2002).
18. K. Triantafilou, Y. Takada, M. Triantafilou, *Crit. Rev. Immunol.* **21**, 311 (2001).
19. D. Shukla, P. G. Spear, *J. Clin. Invest.* **108**, 503 (2001).
20. J. Liu, S. C. Thorp, *Med. Res. Rev.* **22**, 1 (2002).
21. P. P. Naranett *et al.*, *J. Virol.* **77**, 1524 (2003).
22. T. V. Kolesnikova, B. A. Minnion, F. Berditchvski, M. E. Hemler, *BMC Biochem.* **2**, 10 (2001).
23. H. Sasaki *et al.*, *J. Biol. Chem.* **277**, 44765 (2002).
24. W. Qiang *et al.*, *J. Virol.* **78**, 11926 (2004).
25. M. Haque, D. A. Davis, V. Wang, I. Widmer, R. Yarchoan, *J. Virol.* **77**, 6761 (2003).
26. J. F. Wang, X. F. Zhang, B. Chandran, J. E. Groopman, *Blood* (ASH Annu. Meet. Abstr.) **104**, abstr. 605 (2004).
27. L. A. Herzenberg *et al.*, *Proc. Natl. Acad. Sci. U.S.A.* **94**, 1967 (1997).
28. J. Choi *et al.*, *J. Biol. Chem.* **275**, 3693 (2000).
29. S. R. Opalenik, Q. Ding, S. R. Mallery, J. A. Thompson, *Arch. Biochem. Biophys.* **351**, 17 (1998).
30. C. C. Bridges *et al.*, *Invest. Ophthalmol. Vis. Sci.* **45**, 2906 (2004).
31. Y. Aoki, G. Tosato, *Blood* **104**, 810 (2004).

32. This research was supported in part by the Intramural Research Program of NIAID, NIH, and by the NIH Intramural AIDS Targeted Antiviral Program. P. Kennedy and R. Ganesan provided outstanding technical assistance. We thank M. Zauderer and E. Smith for generous donation of the Mel-dT2 cDNA library, J. Vieira for providing Vero-219 cells harboring recombinant virus rKSHV.219, and B. Moss for helpful discussions.

Supporting Online Material

www.sciencemag.org/cgi/content/full/311/5769/1921/DC1
Materials and Methods
Figs. S1 to S3
References

3 October 2005; accepted 3 March 2006
10.1126/science.1120878

Selective Stimulation of T Cell Subsets with Antibody-Cytokine Immune Complexes

Onur Boyman,[1] Marek Kovar,[1] Mark P. Rubinstein,[1] Charles D. Surh,[1] Jonathan Sprent[1,2]*

Interleukin-2 (IL-2), which is a growth factor for T lymphocytes, can also sometimes be inhibitory. Thus, the proliferation of CD8$^+$ T cells in vivo is increased after the injection of a monoclonal antibody that is specific for IL-2 (IL-2 mAb), perhaps reflecting the removal of IL-2–dependent CD4$^+$ T regulatory cells (T regs). Instead, we show here that IL-2 mAb augments the proliferation of CD8$^+$ cells in mice simply by increasing the biological activity of preexisting IL-2 through the formation of immune complexes. When coupled with recombinant IL-2, some IL-2/IL-2 mAb complexes cause massive (>100-fold) expansion of CD8$^+$ cells in vivo, whereas others selectively stimulate CD4$^+$ T regs. Thus, different cytokine-antibody complexes can be used to selectively boost or inhibit the immune response.

Contact with certain cytokines, notably interleukin-2 (IL-2) and IL-15, maintains the survival of T cells, especially CD8$^+$ T cells (*1*–*5*). The responsiveness to these two cytokines is controlled largely by a shared dimeric receptor composed of a β chain (CD122) and a common γ chain (*2*, *6*, *7*). CD122 expression is especially high on many "memory" CD8$^+$ cells primed against defined antigens and also on a naturally occurring population of CD8$^+$ cells with a similar phenotype. These latter, CD122$^{high(hi)}$, memory-phenotype (MP) CD8$^+$ cells proliferate in response to IL-2 or IL-15 in vitro (*1*, *8*), and IL-15 controls their survival and intermittent proliferation (turnover) in vivo (*4*).

Steady-state levels of IL-2 in vivo are normally too low to stimulate MP CD8$^+$ cells but are vital for the survival of CD4$^+$ T regulatory cells (T regs) (*9*, *10*). These latter cells are characterized by strong constitutive expression of IL-2Rα (CD25), which enables the cells to express a high-affinity trimeric αβγ receptor (IL-2Rαβγ) and thereby use low levels of IL-2. Reflecting their dependency on IL-2, CD4$^+$ T regs disappear after the injection of IL-2 mAb (*11*, *12*). However, such treatment surprisingly accentuates the turnover of MP CD8$^+$ cells (*3*, *13*). This effect of IL-2 mAb may indicate that CD4$^+$ T regs have a direct inhibitory influence on MP CD8$^+$ cell turnover (*11*) or that

[1]Department of Immunology, IMM4, The Scripps Research Institute, 10550 North Torrey Pines Road, La Jolla, CA 92037, USA. [2]Garvan Institute of Medical Research, 384 Victoria Street, Darlinghurst, NSW 2010, Australia.

*To whom correspondence should be addressed. E-mail: j.sprent@garvan.org.au

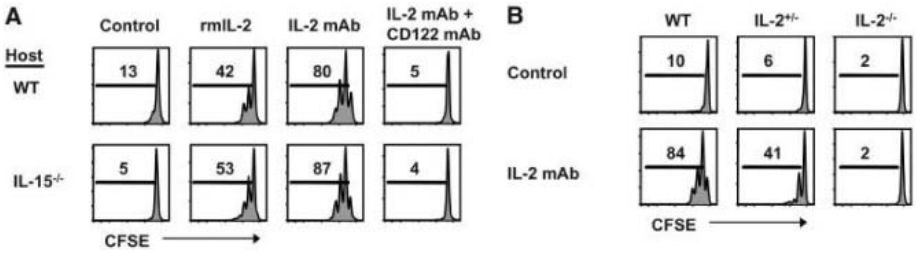

Fig. 1. Stimulation of MP CD8$^+$ cells in vivo by IL-2 or IL-2 mAb. CFSE-labeled purified Thy1.1 MP (CD44^{hi} and CD122^{hi}) CD8$^+$ T cells were transferred intravenously (iv) to (**A**) wild-type (WT) or IL-15$^{-/-}$ mice, which then received daily intraperitoneal (ip) injections of phosphate-buffered saline (PBS) (control), rmIL-2, S4B6 IL-2 mAb, or IL-2 mAb plus CD122 mAb, or to (**B**) WT, IL-2$^{+/-}$, or IL-2$^{-/-}$ mice, followed by daily injections of S4B6 IL-2 mAb or control mAb. Donor cells were analyzed on day 7 by flow cytometry. Numbers represent percentages of divided (CFSE^{lo}) donor Thy1.1$^+$ CD8$^+$ cells. All data in this and the following figures represent at least two separate experiments.

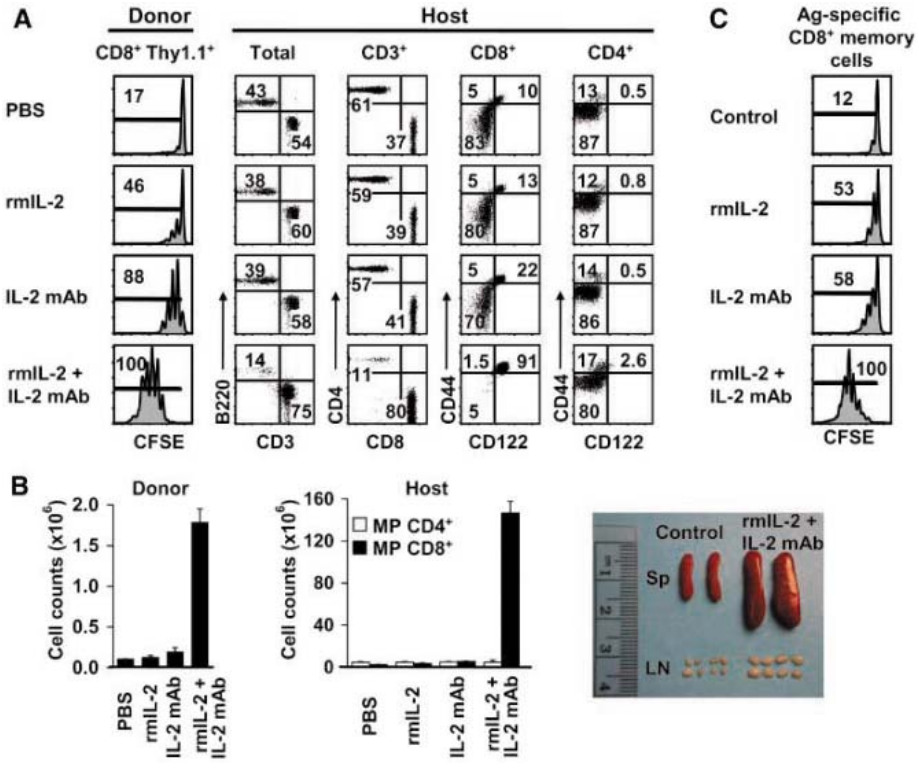

Fig. 2. Marked selective expansion of MP and Ag-specific memory CD8$^+$ T cells in vivo by a combination of IL-2 and IL-2 mAb. (**A**) CFSE-labeled MP CD8$^+$ T cells were transferred to B6 mice, followed by daily ip injections of PBS, rmIL-2, S4B6 IL-2 mAb, or rmIL-2 plus IL-2 mAb. Donor and host cells from LNs were examined for the markers shown on day 7. Comparable results were obtained for spleen cells. (**B**) Total spleen and LN cell numbers of donor and host CD44^{hi} T cells from mice in (A) (+SD, two mice per group). A photograph of two representative spleens and LNs from the injected mice is shown at the right. (**C**) CFSE-labeled Ag lymphocytic choriomeningitis virus–specific memory CD8$^+$ T cells were transferred to B6 mice, followed by daily injections as described above. Donor cells were analyzed on day 7 by flow cytometry. Numbers indicate percentages of divided (CFSE^{lo}) cells in the left column of (A) and in (C).

IL-2 suppresses the synthesis of a putative novel cytokine that stimulates via CD122 (*13*).

The paradox, therefore, is that the turnover of MP CD8$^+$ cells in vivo can be increased by injecting either IL-2 or IL-2 mAb (Fig. 1) (*14*). For IL-2, the proliferation of CD8$^+$ cells in vivo—which is measured by dilution of the dye carboxy-fluorescein diacetate succinimidyl ester (CFSE) (Fig. 1, A and B) or by the incorporation of bromodeoxyuridine (BrdU) (fig. S1)—was prominent after the injection of recombinant mouse IL-2 (rmIL-2) and was largely restricted to MP CD8$^+$ cells, both for host and adoptively transferred, purified CD8$^+$ cells. In contrast, stimulation of naïve T cells, as defined by low expression of CD122 and CD44, was minimal (fig. S1). Confirming previous findings (*3*, *13*), even greater proliferation occurred after the injection of IL-2 mAb, specifically by the anti-mouse IL-2 mAb S4B6 (Fig. 1 and fig. S1). This effect was also seen in IL-15$^{-/-}$ hosts and was blocked by CD122 mAb (Fig. 1A), confirming that the effector cytokine for proliferation is not IL-15 but nevertheless stimulates via CD122 (*3*, *13*).

The unexpected finding was that the stimulation of MP CD8$^+$ cells by IL-2 mAb on adoptive transfer was abolished in IL-2$^{-/-}$ hosts and considerably reduced in IL-2$^{+/-}$ hosts (Fig. 1B). This finding implies that despite its reported neutralizing function in vitro (*15*), S4B6 mAb functions in vivo by increasing the biological activity of preexisting IL-2, perhaps through the formation of immune complexes. To assess this possibility, we used a regime of daily injections of IL-2 and IL-2 mAb in mice. The resulting proliferation of adoptively transferred and host MP CD8$^+$ cells was dramatically enhanced over that seen with single IL-2 or IL-2 mAb administration (Fig. 2A) and led to a very large (>100-fold) increase in the total numbers of MP CD8$^+$ cells in the spleen and lymph nodes (LN) on day 7, with marked enlargement of these organs (Fig. 2B). The combined regime of IL-2 and IL-2 mAb also caused a marked (20- to 30-fold) increase in total numbers of another CD122^{hi} population, namely natural killer (NK) (CD3$^-$, NK1.1$^+$, and DX5$^+$) cells (*16*), but had minimal effects on other cells, including MP CD44^{hi} CD4$^+$ cells and B220$^+$ B cells (Fig. 2, A and B). The proliferation of transferred naïve CD8$^+$ cells was relatively low, suggesting that the IL-2/IL-2 mAb combination was acting largely on preexisting CD122^{hi} cells rather than on naïve CD122^{lo} precursors (fig. S2A). Proliferation was independent of IL-15 because comparable data occurred with transfer of MP CD8$^+$ cells to IL-15$^{-/-}$ hosts (fig. S2B). There was also a strong stimulation of primed virus-specific CD8$^+$ cells (Fig. 2C), indicating that the proliferation of CD122^{hi} CD8$^+$ cells applied to defined antigen (Ag)-specific memory cells as well as to MP cells. For the latter, proliferation did not lead to CD25 up-regulation and was unimpaired with CD25$^{-/-}$ MP CD8$^+$ cells, indicating that stimulation occurred only via IL-2Rβγ (CD122) and not by IL-2Rαβγ (fig. S3).

Near-optimal expansion of CD122^{hi} CD8$^+$ cells occurred with daily injections of a premixed 2:1 molar ratio of IL-2 to IL-2 mAb for 1 week (fig. S4A, arrow, and fig. S4B). At this ratio, even a single injection of IL-2/IL-2 mAb complex caused considerable expansion of CD122^{hi} CD8$^+$ cells (fig. S4C). Based on the results of injecting IL-2/IL-2 mAb complexes at various times before T cell transfer, the biological half-life of IL-2/IL-2 mAb complexes was determined to be relatively short, i.e., <4 hours (fig. S4D).

In addition to S4B6, we also observed equivalent proliferation with the injection of the following: anti-mouse IL-2 mAb JES6-5H4 (JES6-5) plus rmIL-2 (Fig. 3A), and an anti-human IL-2 mAb (MAB602) plus recombinant human IL-2 (rhIL-2) (Fig. 3B). When complexed with IL-2, each of these three mAbs (S4B6, JES6-5, and MAB602) caused marked

expansion of CD122^{hi} CD8^{+} cells on adoptive transfer (Fig. 3, A and B) and strong and selective expansion of host CD122^{hi} cells, including both MP CD8^{+} cells and NK cells (*16*).

The results with a third anti-mouse IL-2 mAb, JES6-1A12 (JES6-1), were quite different (Fig. 3A). IL-2/JES6-1 complexes caused lower proliferation of CD122^{hi} CD8^{+} cells than IL-2 alone, indicating that JES6-1 blocked the in vivo response to IL-2. However, JES6-1 plus IL-2 injection led to mild proliferation of a different IL-2–responsive population, namely CD25^{+} CD4^{+} cells (Fig. 3, C and D). These cells were predominantly Foxp3^{+} and thus resembled T regs. Expansion of these cells was also seen with injection of the other IL-2 mAbs, although this effect was dwarfed by the huge expansion of CD122^{hi} CD8^{+} cells (Fig. 3E).

The above results suggested that S4B6 and related mAbs may bind to a different site on IL-2 than JES6-1 does. IL-2/IL-2 mAb sandwich enzyme-linked immunosorbent assays (ELISAs) provided direct support for this possibility (fig. S5). Similar to its function in vivo, JES6-1 totally blocked the response of both normal and CD25$^{-/-}$ MP CD8^{+} cells to IL-2 in vitro via CD122 (IL-2Rβγ) (Fig. 4, A and B). However, as for CD4^{+} CD25^{+} T regs in vivo, JES6-1/IL-2 complexes were able to induce weak but significant in vitro stimulation of cells expressing high-affinity IL-2Rαβγ, namely CD25^{+} CD3-activated naïve CD8^{+} cells (fig. S6); these cells were very sensitive to IL-2 and were easily inhibited by CD25 mAb. Thus, JES6-1 mAb apparently binds to an IL-2 site that is crucial for interaction with CD122 but less crucial for binding to CD25 (IL-2Rαβγ). In contrast, S4B6 failed to inhibit (or enhance) the response of MP CD8^{+} cells to IL-2 in vitro (Fig. 4, A and B) but strongly inhibited the IL-2 response of CD3-activated CD8^{+} cells (fig. S6). Hence, S4B6 binds to an IL-2 site that partly occludes binding to CD25 but does not impede binding to CD122. When not complexed with exogenous IL-2, a mixture of JES6-1 and S4B6 mAbs caused near abolition of T cell proliferation in vivo, both for MP CD8^{+} cells and for T regs (fig. S7), further suggesting that S4B6 and JES6-1 recognize different sites on IL-2.

Why IL-2/IL-2 mAb complexes are so potent in vivo is unclear. It was reported previously that binding to antibody can increase the half-life of IL-2 (and also IL-4 and IL-6) in vivo; but, other than inducing a mild increase in NK cell–mediated tumor rejection, the effects of IL-2/IL-2 mAb complexes on T cells were not mentioned (*17*–*20*). For the marked expansion of CD122^{hi} MP CD8^{+} cells reported here, F(ab′)$_2$ mAb fragments were much less stimulatory than intact mAb (fig. S8), suggesting that the complexes became bound to cells via the mAb Fc region. Such presentation may be unusually efficient and explain why IL-2/IL-2 mAb complexes are far more stimulatory in vivo than in vitro.

The stimulatory effects of IL-2/IL-2 mAb complexes also applied to complexes of IL-4 and IL-4 mAb (Fig. 4C) and IL-7 and IL-7 mAb (*16*). Thus, the proliferation of CD8^{+} cells was much higher after injection of these cytokine/mAb complexes than with cytokine or mAb alone.

For S4B6 and related antibodies, injecting IL-2/IL-2 mAb complexes might be clinically useful for tumor immunotherapy and for expanding T cell numbers after bone marrow (BM) transplantation. In support of this latter idea, irradiated mice given unseparated BM cells and then a course of IL-2/S4B6 injections showed a rapid restoration of mature T cell numbers, especially CD8^{+} cells, as early as 1 week post-transfer (Fig. 4D). Conversely, the expansion of CD4^{+} T regs by IL-2 and JES6-1 or related mAbs could be useful for treating autoimmune disease.

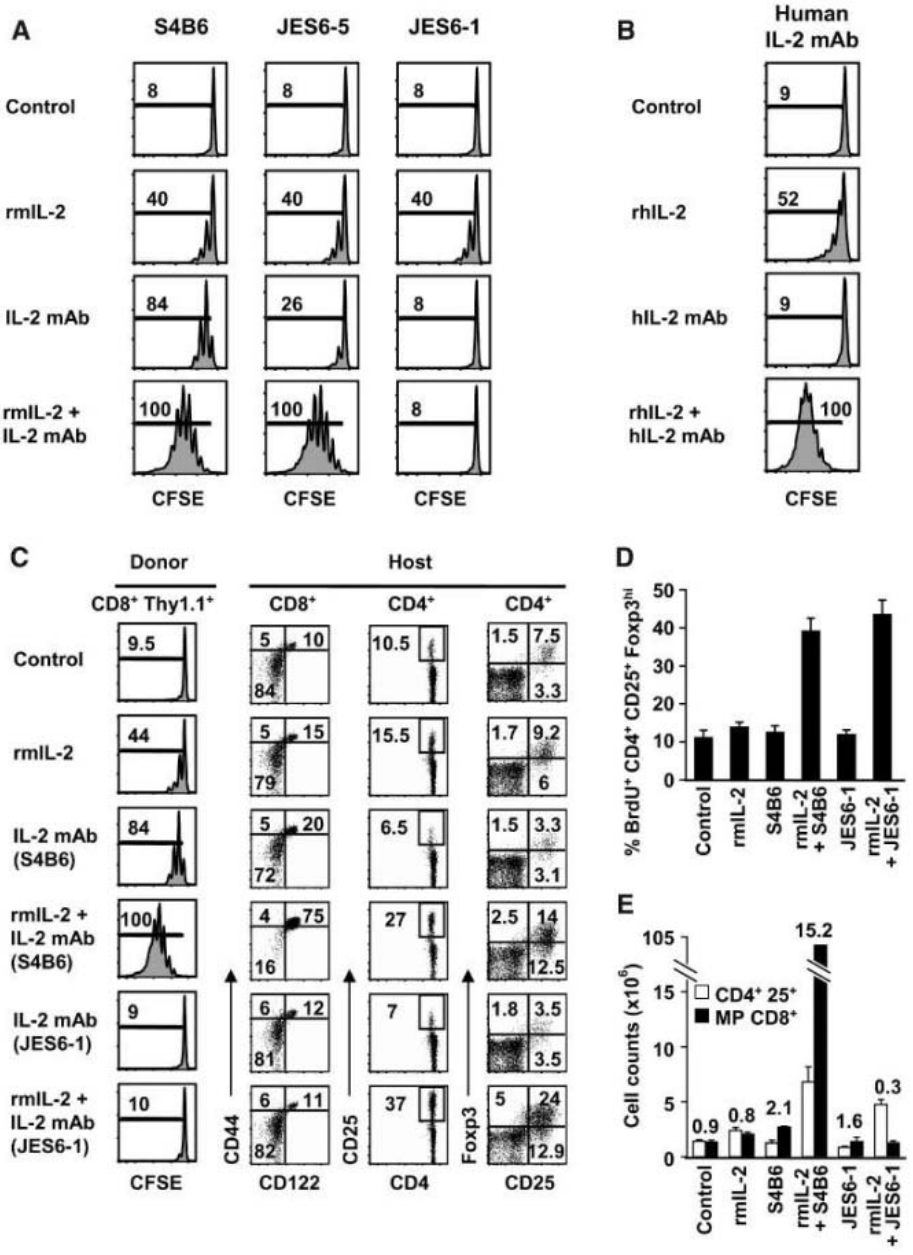

Fig. 3. Selective stimulation of T cell subsets by different IL-2/IL-2 mAb complexes. CFSE-labeled MP CD8^{+} T cells were transferred to B6 mice, followed by (**A** and **B**) daily ip injections of control mAb, IL-2 ([mIL-2 in (A), rhIL-2 in (B)], IL-2 mAb, or IL-2 plus IL-2 mAb as in Fig. 2A. The IL-2 mAbs used were (A) anti-mouse S4B6, JES6-5, or JES6-1, or (B) anti-human MAB602. (**C**) MP CD8^{+} T cells were transferred to B6 mice, followed by daily injections of control mAb, rmIL-2, IL-2 mAb, or rmIL-2 plus IL-2 mAb as above. Donor and host cells from the spleen were examined for the markers shown on day 7. (**D**) Mice treated as in (C) were given BrdU in the drinking water for the last 3 days. Shown are the percentages of CD3^{+} CD4^{+} CD25^{+} Foxp3^{hi} cells that were BrdU^{+} (+SD, 2 mice/group). (**E**) Total cell counts of CD4^{+} CD25^{+} and MP CD8^{+} cells in spleen from mice in (C). The numbers on top of the bars indicate the ratios of MP CD8^{+} to CD4^{+} CD25^{+} cells. Mice were analyzed on day 7 in all panels. Numbers indicate percentages of divided (CFSE^{lo}) cells in (A) to (C), left column.

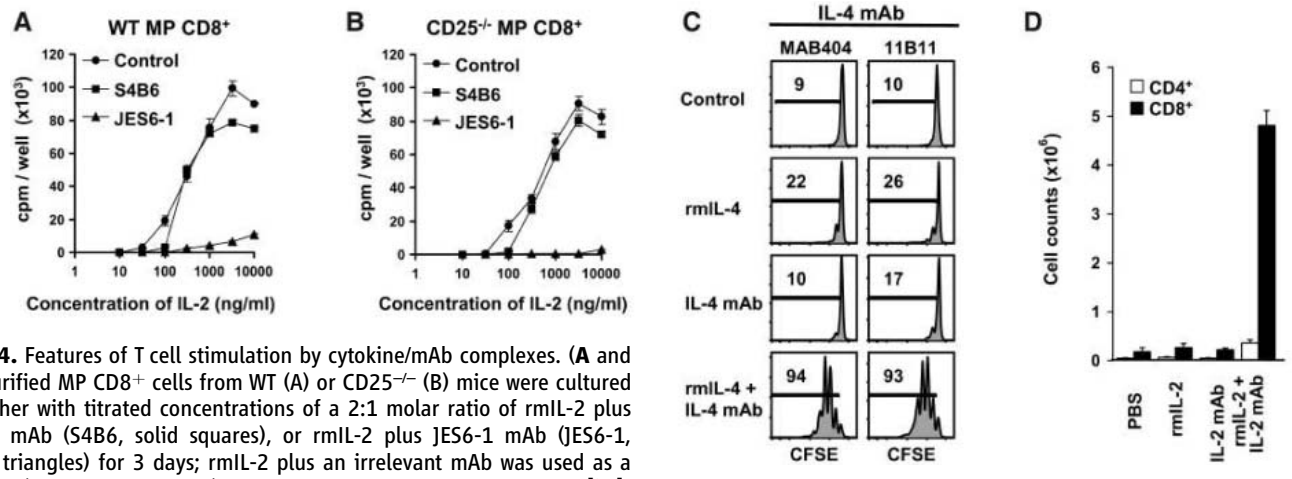

Fig. 4. Features of T cell stimulation by cytokine/mAb complexes. (**A** and **B**) Purified MP CD8$^+$ cells from WT (A) or CD25$^{-/-}$ (B) mice were cultured together with titrated concentrations of a 2:1 molar ratio of rmIL-2 plus S4B6 mAb (S4B6, solid squares), or rmIL-2 plus JES6-1 mAb (JES6-1, solid triangles) for 3 days; rmIL-2 plus an irrelevant mAb was used as a control (control, solid circles). Proliferation was measured by adding [^{3}H]-thymidine for the last 16 hours. (**C**) Purified CFSE-labeled MP CD8$^+$ cells were transferred to B6 mice, which were then given every other day ip injections of control mAb, rmIL-4, IL-4 mAb (MAB404 or 11B11), or rmIL-4 plus IL-4 mAb. Mice were analyzed on day 7. Numbers indicate percentages of divided (CFSE^{lo}) cells. (**D**) B6 mice were irradiated with 1000 centigray (cGy) and injected iv with unseparated versus T cell–depleted B6 BM cells, followed by daily ip injections of PBS, rmIL-2, S4B6 IL-2 mAb, or rmIL-2 plus S4B6 IL-2 mAb. Eight days after adoptive transfer, spleen cells were analyzed by flow cytometry. Shown are mean cell numbers of CD3$^+$ CD4$^+$ and CD3$^+$ CD8$^+$ cells from recipients of unseparated BM (+SD, two mice per group). With injection of T cell–depleted BM, no restoration of T cell numbers occurred (*16*).

References and Notes

1. K. A. Smith, *Science* **240**, 1169 (1988).
2. T. A. Waldmann, *Annu. Rev. Biochem.* **58**, 875 (1989).
3. C. C. Ku, M. Murakami, A. Sakamoto, J. Kappler, P. Marrack, *Science* **288**, 675 (2000).
4. J. Sprent, C. D. Surh, *Annu. Rev. Immunol.* **20**, 551 (2002).
5. K. S. Schluns, L. Lefrancois, *Nat. Rev. Immunol.* **3**, 269 (2003).
6. T. Takeshita *et al.*, *Science* **257**, 379 (1992).
7. Y. Nakamura *et al.*, *Nature* **369**, 330 (1994).
8. X. Zhang, S. Sun, I. Hwang, D. F. Tough, J. Sprent, *Immunity* **8**, 591 (1998).
9. T. R. Malek, A. L. Bayer, *Nat. Rev. Immunol.* **4**, 665 (2004).
10. J. D. Fontenot, A. Y. Rudensky, *Nat. Immunol.* **6**, 331 (2005).
11. M. Murakami, A. Sakamoto, J. Bender, J. Kappler, P. Marrack, *Proc. Natl. Acad. Sci. U.S.A.* **99**, 8832 (2002).
12. R. Setoguchi, S. Hori, T. Takahashi, S. Sakaguchi, *J. Exp. Med.* **201**, 723 (2005).
13. D. Kamimura *et al.*, *J. Immunol.* **173**, 6041 (2004).
14. Materials and methods are available as supporting material on *Science* Online.
15. S. M. Zurawski, T. R. Mosmann, M. Benedik, G. Zurawski, *J. Immunol.* **137**, 3354 (1986).
16. O. Boyman *et al.*, unpublished data.
17. J. Sato *et al.*, *Biotherapy* **6**, 225 (1993).
18. F. D. Finkelman *et al.*, *J. Immunol.* **151**, 1235 (1993).
19. L. P. Courtney, J. L. Phelps, L. M. Karavodin, *Immunopharmacology* **28**, 223 (1994).
20. B. Klein, H. Brailly, *Immunol. Today* **16**, 216 (1995).

21. We thank B. Marchand for typing the manuscript and C. Chahwan, O. Greiner, and V. Martin for helpful discussions. We acknowledge support from the Flow Cytometry and Antibody Core Facility, NIH grants, and the Swiss National Science Foundation and the Novartis Foundation (to O.B.). This is publication no. 17654-IMM from The Scripps Research Institute.

Supporting Online Material

www.sciencemag.org/cgi/content/full/1122927/DC1
Materials and Methods
Figs. S1 to S8
References

22 November 2005; accepted 27 January 2006
Published online 16 February 2006;
10.1126/science.1122927
Include this information when citing this paper.

A Critical Role for the Innate Immune Signaling Molecule IRAK-4 in T Cell Activation

Nobutaka Suzuki,[1] Shinobu Suzuki,[1]* Douglas G. Millar,[2]† Midori Unno,[1] Hiromitsu Hara,[1] Thomas Calzascia,[2] Sho Yamasaki,[1] Tadashi Yokosuka,[1] Nien-Jung Chen,[3] Alisha R. Elford,[2] Jun-ichiro Suzuki,[4]‡ Arata Takeuchi,[1] Christine Mirtsos,[3] Denis Bouchard,[3] Pamela S. Ohashi,[2] Wen-Chen Yeh,[3]§‖ Takashi Saito[1]‖

IRAK-4 is a protein kinase that is pivotal in mediating signals for innate immune responses. Here, we report that IRAK-4 signaling is also essential for eliciting adaptive immune responses. Thus, in the absence of IRAK-4, in vivo T cell responses were significantly impaired. Upon T cell receptor stimulation, IRAK-4 is recruited to T cell lipid rafts, where it induces downstream signals, including protein kinase Cθ activation through the association with Zap70. This signaling pathway was found to be required for optimal activation of nuclear factor κB. Our findings suggest that T cells use this critical regulator of innate immunity for the development of acquired immunity, suggesting that IRAK-4 may be involved in direct signal cross talk between the two systems.

The innate immune system provides a critical front line of protection against infection (*1*, *2*). Among the mediators of innate immunity, the Toll-like receptors (TLRs) are prominent in pathogen recognition, resulting in the activation of transcription factors, mainly nuclear factor κB (NF-κB), through adaptor molecules and downstream kinases (*1*, *2*). Of these kinases, IRAK-4 plays a dominant role, as demonstrated by evidence that IRAK-4–deficient ($^{-/-}$) mice lack the ability to elicit innate immune responses (*3*). These mice fail to eliminate infected bacteria, are resistant to lipopolysaccharide-induced septic shock, and show no response to interleukin-1 (IL-1), IL-18, or most of the TLR ligands. IRAK-4 induces NF-κB activation through a signaling cascade involving MyD88, IRAK-4, and tumor necrosis factor receptor–associated factor 6 (TRAF6).

Vertebrates also develop adaptive immune responses that are initiated by T cell activation after T cell receptor (TCR) engagement by antigen (Ag) peptide–major histocompatibility complexes on Ag-presenting cells (APCs) (*4*). At the molecular level, TCR engagement results in phosphorylation of CD3 chains by the Src-family kinase Lck and recruitment of the Syk-family kinase Zap70 to the TCR complex, followed by the recruitment and phosphorylation of adaptor proteins, including linker of

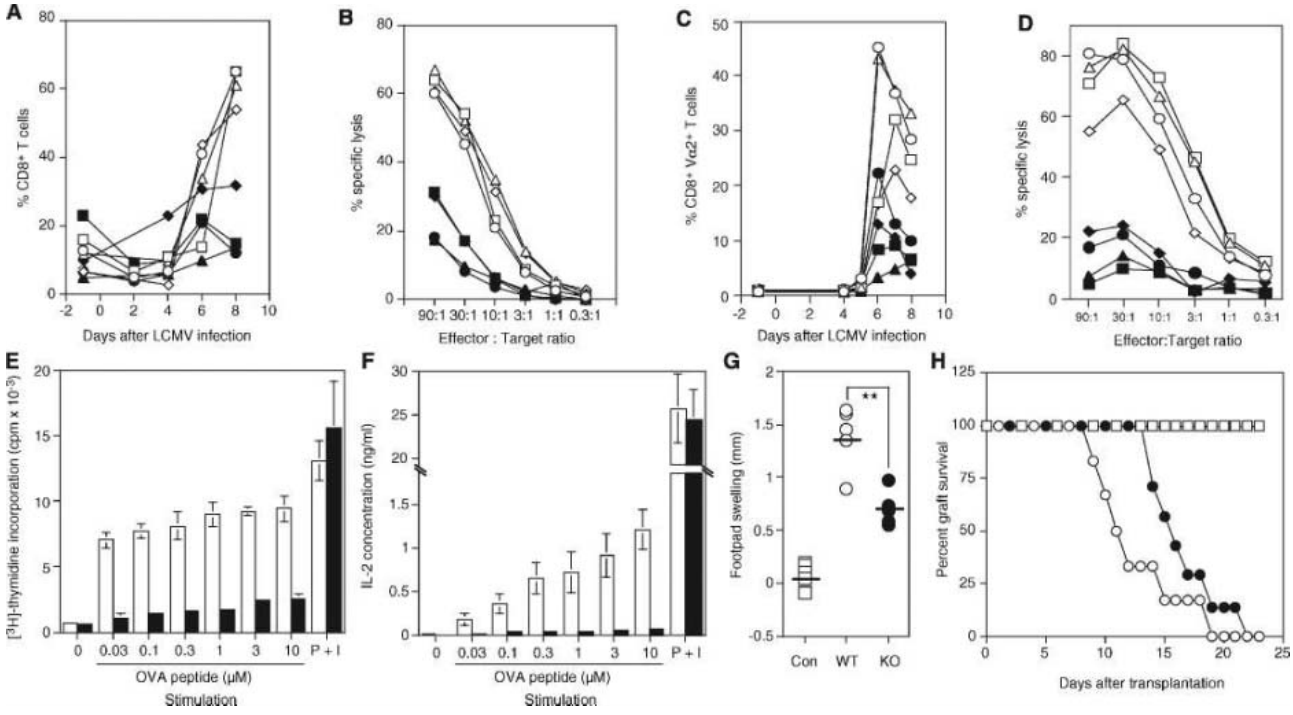

Fig. 1. Impairment of in vivo T cell responses in IRAK-4$^{-/-}$ mice. (**A**) Defective T cell proliferation upon in vivo LCMV infection of IRAK-4$^{-/-}$ mice. Wild-type (open symbols) and IRAK-4$^{-/-}$ (closed symbols) mice were infected with LCMV, and the expansion of CD8^{+} T cells in peripheral blood was monitored by flow cytometry. Each symbol (squares, circles, triangles, and diamonds) represents an individual mouse. (**B**) Severely reduced ex vivo CTL function in LCMV-infected IRAK-4$^{-/-}$ mice. Splenocytes from mice in (A) were assessed 8 days after LCMV infection for cytotoxicity against glycoprotein (gp) 33–pulsed EL4 cells. (**C**) Failure of in vivo expansion of adoptively transferred CD8^{+} T cells from IRAK-4$^{-/-}$ mice. T cells from P14-Tg/wild-type (open symbols) or P14-Tg/IRAK-4$^{-/-}$ (closed symbols) mice were adoptively transferred into C57BL/6 mice, followed by LCMV infection. (**D**) Defective cytotoxicity of adoptively transferred T cells from IRAK-4$^{-/-}$ mice. CD8^{+} T cells from mice in (C) were analyzed for CTL activity against LCMV-peptide MB6 or adenovirus peptide as control. (**E** and **F**) Impaired proliferation (E) and IL-2 production (F) of adoptively transferred CD4^{+} T cells from IRAK-4$^{-/-}$ mice. CD4^{+} T cells from OT-II Tg/wild-type (open bars, ±SD) and OT-II Tg/IRAK-4$^{-/-}$ (solid bars, +SD) mice were adoptively transferred into C57BL/6 mice, followed by immunization with OVA peptide in complete Freund's adjuvant. Splenic CD4^{+} T cells were assessed 10 days later for proliferation upon stimulation with OVA peptide (irradiated splenocytes) or PMA plus ionomycin. IL-2 production was measured by enzyme-linked immunosorbent assay (ELISA). (**G**) Reduced in vivo DTH responses induced by IRAK-4$^{-/-}$ T cells. T cells from wild-type (WT, ○) and IRAK-4$^{-/-}$ (KO, ●) OT-II Tg mice (five mice per group) were adoptively transferred into SCID mice. $OVA_{323-339}$ peptide incomplete Freund's adjuvant (IFA) was injected 7 days later into the left hind footpad of these mice or control mice without T cell transfer (Con, □). IFA was injected into the right footpad as control. Footpad thickness was measured and the magnitude of DTH response was determined as the difference between the right and left footpad thickness. **, $P < 0.01$ in a comparison between wild-type and IRAK-4$^{-/-}$ T cell–transferred mice. (**H**) Delayed skin graft rejection by IRAK-4$^{-/-}$ T cells. T cells from wild-type (○) and IRAK-4$^{-/-}$ (KO, ●) mice (six mice per group) were adoptively transferred into SCID mice. The mice were engrafted 7 days later with skin grafts derived from C57BL/6 mice on the back of these mice or control mice without T cell transfer (Con, □). The graft rejection was scored daily until complete rejection.

[1]Laboratory for Cell Signaling, RIKEN Research Center for Allergy and Immunology, 1-7-22 Suehiro-cho, Tsurumi-ku, Yokohama City, Kanagawa 230-0045, Japan. [2]Institute for Breast Cancer Research, University Health Network, 620 University Avenue, Suite 706, Toronto, Ontario M5G 2C1, Canada. [3]Advanced Medical Discovery Institute, University Health Network and Department of Medical Biophysics, University of Toronto, 620 University Avenue, Suite 706, Toronto, Ontario M5G 2C1, Canada. [4]Department of Molecular Genetics, Chiba University Graduate School of Medicine, 1-8-1 Inohana, Chuo-ku, Chiba City, Chiba 260-8670, Japan.

*Present address: Nihon Schering K. K. Research Center, BMA 3F, 1-5-5, Minatojima-minami-machi, Chuo-ku, Kobe 650-0047, Japan.

†Present address: Faculty of Life Sciences, University of Manchester, C-2259 Michael Smith Building, Oxford Road, Manchester M13 9PT, UK.

‡Present address: Faculty of Pharmacy, Musashino University, 1-1-20 Shin-machi, Nishitokyo-shi, Tokyo 202-8585, Japan.

§Present address: Amgen San Francisco, 1120 Veterans Boulevard, South San Francisco, CA 94080, USA.

‖To whom correspondence should be addressed. E-mail: saito@rcai.riken.jp (T.S.); wyeh@uhnres.utoronto.ca (W.-C.Y.)

activated T cells (LAT) and SH2 domain–containing leukocyte protein of 76 kD (SLP-76), and protein kinase Cθ (PKCθ) (*4*). LAT/SLP-76 induces activation of the transcription factor named nuclear factor of activated T cells (NFAT), whereas PKCθ cooperates with the Carma-1/Bcl10/Mucosa associated lymphoid tissue lymphoma translocation gene 1 (MALT1) (CBM) signal complex (*5*) to culminate in the activation of NF-κB. Although NFAT and NF-κB activation represent hallmarks of the adaptive T cell immune response, signaling pathways for adaptive immunity have also been proposed to share mediators with those for innate immunity (*6*–*8*). In light of the critical role of IRAK-4 in innate immunity, we examined the potential involvement of this kinase in adaptive immunity, specifically in T cell function.

After infection with lymphocytic choriomeningitis virus (LCMV), marked proliferation of CD8^{+} T cells was observed in wild-type but not in IRAK-4$^{-/-}$ mice (Fig. 1A), and IRAK-4$^{-/-}$ mice failed to generate a significant number of LCMV-specific cytotoxic T cells (CTLs) (Fig. 1B). We confirmed that lymphocyte populations in IRAK-4$^{-/-}$ mice appeared to develop normally (fig. S1) despite the normally ubiquitous IRAK-4 expression in wild-type lymphocyte populations (fig. S2). Because IRAK-4$^{-/-}$ mice exhibit impaired dendritic cell (DC) function (*9*), it was important to determine whether this corresponding reduction in T cell responses was the result of an intrinsic defect in T cell immunity or if it resulted from a loss of DC function. To test this, wild-type or IRAK-4$^{-/-}$ TCR Vα2^{+} CD8^{+} T cells from LCMV-specific P14 TCR-transgenic (Tg) mice were adoptively transferred into naïve mice. In contrast to the vigorous expansion of wild-type

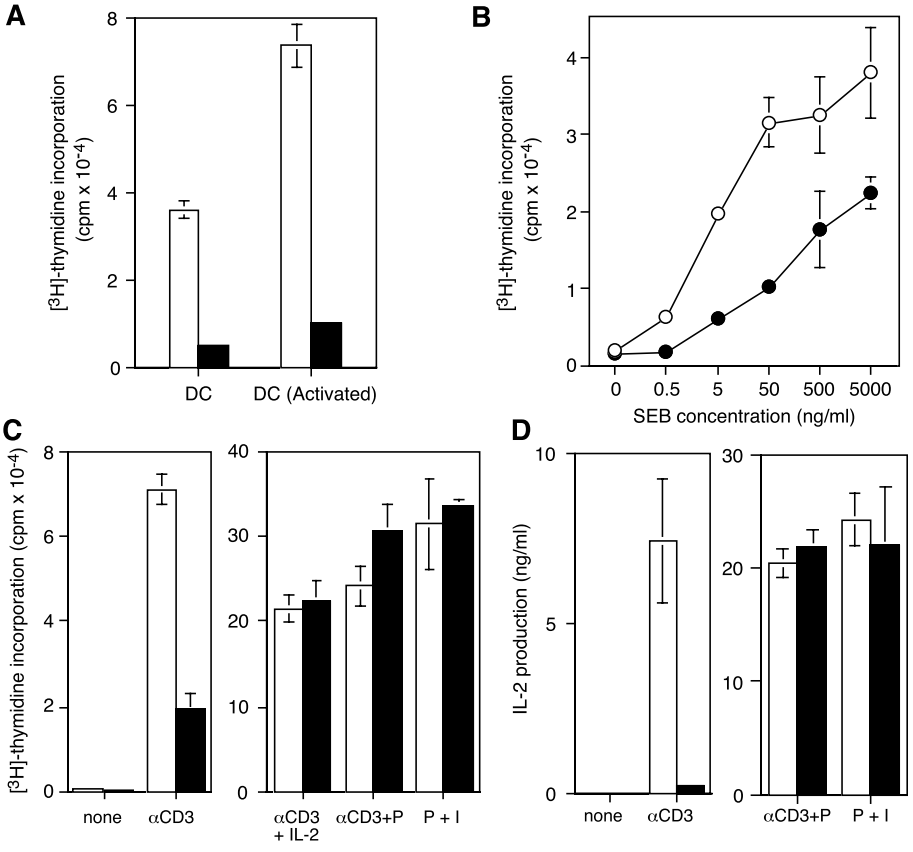

Fig. 2. IRAK-4 is essential for in vitro T cell activation. (**A**) Defective allogenic response by IRAK-4$^{-/-}$ T cells. T cells from C57BL/6 wild-type (open bars, ±SD) or IRAK-4$^{-/-}$ (solid bars, +SD) mice were mixed with bone marrow–derived dendritic cells (BMDCs) from BALB/c mice. (**B**) Reduced superantigen-induced proliferation of IRAK-4$^{-/-}$ T cells. Wild-type (○) or IRAK-4$^{-/-}$ (●) T cells were stimulated with Staphylococcal enterotoxin B (SEB)/APCs. (**C** and **D**) Impaired proliferation (C) and IL-2 production (D) of IRAK-4$^{-/-}$ T cells upon TCR stimulation. Wild-type (open bars, ±SD) or IRAK-4$^{-/-}$ (solid bars, +SD) CD4^{+} T cells were stimulated with αCD3 alone, αCD3 plus IL-2, αCD3 plus PMA (αCD3 + P), and PMA plus ionomycin (P + I). The response of αCD3 plus ionomycin is shown in fig. S5. IL-2 production was measured by ELISA. cpm, counts per minute.

Vα2^{+} CD8^{+} T cells in response to LCMV, the responses in IRAK-4$^{-/-}$ T cells were severely impaired (Fig. 1C). This was reflected by a greatly reduced ex vivo CTL function from these infected mice to LCMV targets (Fig. 1D). Similarly, adoptively transferred CD4^{+} ovalbumin (OVA)–specific T cells from OT-II Tg/IRAK-4$^{-/-}$ mice displayed reduced proliferation and IL-2 production (Fig. 1, E and F). To confirm these results in vivo, T cells from wild-type or IRAK-4$^{-/-}$ OT-II Tg mice were transferred into severe combined immunodeficient (SCID) mice and delayed type hypersensitivity (DTH) responses induced through OVA challenge in the footpad (*10*). IRAK-4$^{-/-}$ recipients showed measurable reduction in DTH response (Fig. 1H). Similarly, in allogenic skin grafting experiments (*11*), SCID mice reconstituted with IRAK-4$^{-/-}$ T cells showed significantly delayed graft rejection (Fig. 1G), which corresponded with reduced in vivo cytotoxic responses against allogenic cells (fig. S3). Collectively, these data are consistent with a central function for IRAK-4 in T cell function in vivo [supporting online material (SOM) text 1].

In vitro, IRAK-4$^{-/-}$ T cells also showed modest responses to allogenic DCs (Fig. 2A) and superantigen Staphylococcal Enterotoxin E (SEE) (Fig. 2B). Consistent with the observed in vivo responses, primary responses of OT-II Tg/IRAK-4$^{-/-}$ T cells to stimulation with OVA peptide–pulsed APCs were also markedly reduced (fig. S4). IRAK-4$^{-/-}$ T cells also exhibited hypoproliferation upon TCR activation when stimulated by an antibody to CD3ε (αCD3), which could be overcome by adding exogenous IL-2 or phorbol 12-myristate 13-acetate (PMA) (Fig. 2C), but not ionomycin (fig. S5). αCD3-induced IL-2 production was also severely affected by the IRAK-4 deficiency, although these T cells could respond normally to stimulation with PMA/ionomycin (Fig. 2D). Consistent with the results of proliferation measured by thymidine incorporation, cell division was inhibited in deficient cells, but could be restored with exogenous IL-2 (fig. S6). The deficiency in T cell stimulation was also apparent by the absence of CD25 and CD69 activation marker expression after TCR induction with αCD3 (fig. S7). In contrast to T cells, IRAK-4$^{-/-}$ B cell proliferation did not appear to be affected by stimulation through surface immunoglobulin M (IgM) or CD40 costimulatory molecules with αIgM or αCD40 antibodies, respectively (fig. S8) (SOM text 2 and fig. S9). These results suggest that IRAK-4 plays an essential role in activating TCR-specific downstream signal transduction pathways.

To understand IRAK-4 function at the biochemical level, TCR proximal signaling was next analyzed. Phosphorylation of CD3ζ, Lck, Zap70, and LAT (Fig. 3A), as well as Ca^{2+} flux (Fig. 3B), were induced normally in IRAK-4$^{-/-}$ T cells (SOM text 3 and fig. S10). Because TCR engagement triggers the activation of two distinct transcription factors, NF-κB and NFAT (*5*), these were next examined. Assays for NFAT activity with the use of luciferase reporter activity and nuclear translocation upon TCR stimulation in IRAK-4$^{-/-}$ T cells showed similar levels of activation to those in wild-type T cells (Fig. 3C). In contrast, IRAK-4$^{-/-}$ T cells showed a clear defect in NF-κB activation upon TCR stimulation (Fig. 3, D to F), with impairment of αCD3-dependent IκB degradation, but no measurable difference upon PMA/ionomycin stimulation (Fig. 3D). Furthermore, NF-κB p65 nuclear translocation, IκBα mRNA induction, and NF-κB p65 binding activity were also impaired in IRAK-4$^{-/-}$ T cells upon αCD3 stimulation (Fig. 3, E and F). These results suggest that IRAK-4 is directly involved in signaling for the activation of NF-κB but not NFAT in T cells.

Lipid rafts represent plasma membrane microdomains that are enriched with key signaling molecules critical for T cell activation, which functions as a scaffold for cell activation (*12*). Similar to other signaling molecules critical for T cell activation, substantial levels of PKCθ and IRAK-4 were detected in the membrane raft fraction upon TCR stimulation (Fig. 4A). The recruitment of these proteins to the immunological synapse (IS) was next analyzed by confocal microscopy, with the use of the Jurkat cell line that expresses Flag-tagged IRAK-4 upon superantigen SEE stimulation. In the absence of SEE, the distribution of lipid rafts, as determined by cholera toxin B (CTx) staining, was homogeneous on the plasma membrane; IRAK-4 and PKCθ were detected primarily in the cytosol (Fig. 4B). Upon SEE stimulation, a large fraction of PKCθ became translocated to the center of IS, and IRAK-4 became recruited peripherally relative to PKCθ (Fig. 4B).

On the basis of the functional demonstration that IRAK-4$^{-/-}$ T cells respond normally to stimulation with combinations of PMA/ionomycin or αCD3 plus PMA, it seems plausible that IRAK-4 may function upstream of PKCθ, because PMA is known to directly activate

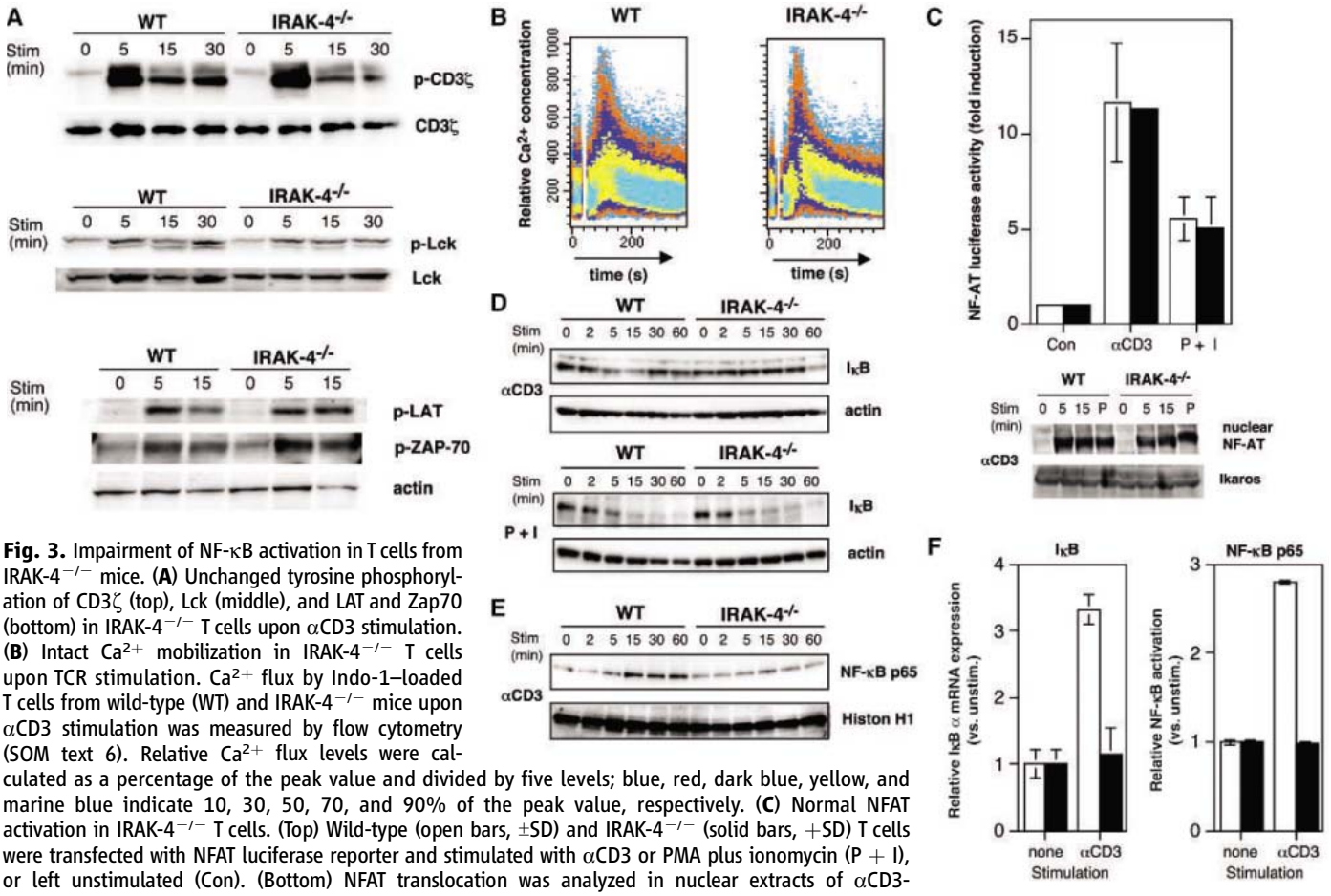

Fig. 3. Impairment of NF-κB activation in T cells from IRAK-4$^{-/-}$ mice. (**A**) Unchanged tyrosine phosphorylation of CD3ζ (top), Lck (middle), and LAT and Zap70 (bottom) in IRAK-4$^{-/-}$ T cells upon αCD3 stimulation. (**B**) Intact Ca^{2+} mobilization in IRAK-4$^{-/-}$ T cells upon TCR stimulation. Ca^{2+} flux by Indo-1–loaded T cells from wild-type (WT) and IRAK-4$^{-/-}$ mice upon αCD3 stimulation was measured by flow cytometry (SOM text 6). Relative Ca^{2+} flux levels were calculated as a percentage of the peak value and divided by five levels; blue, red, dark blue, yellow, and marine blue indicate 10, 30, 50, 70, and 90% of the peak value, respectively. (**C**) Normal NFAT activation in IRAK-4$^{-/-}$ T cells. (Top) Wild-type (open bars, ±SD) and IRAK-4$^{-/-}$ (solid bars, +SD) T cells were transfected with NFAT luciferase reporter and stimulated with αCD3 or PMA plus ionomycin (P + I), or left unstimulated (Con). (Bottom) NFAT translocation was analyzed in nuclear extracts of αCD3-stimulated wild-type and IRAK-4$^{-/-}$ T cells with αNFAT or αIkaros as control. (**D**) Impaired IκB degradation in IRAK-4$^{-/-}$ T cells. Wild-type and IRAK-4$^{-/-}$ T cells were stimulated with αCD3 or PMA plus ionomycin (P + I) (SOM text 7). (**E**) Defective nuclear translocation of NF-κB p65 in IRAK-4$^{-/-}$ T cells. Nuclear extracts from αCD3-stimulated wild-type and IRAK-4$^{-/-}$ T cells were blotted with αNF-κB p65 or αHistone H1 as control. (**F**) Severely reduced IκBα mRNA induction and NF-κB p65 binding activity in IRAK-4$^{-/-}$ T cells. Wild-type (open bars, ±SD) and IRAK-4$^{-/-}$ (solid bars, +SD) T cells were stimulated with αCD3 for 1 hour. IκBα mRNA was analyzed by real-time reverse transcription polymerase chain reaction (left), and NF-κB p65 binding activity was assessed (*17*) (right), compared with unstimulated (none) cells.

PKCθ. Consistent with this possibility, PKCθ phosphorylation was found to be impaired in IRAK-4$^{-/-}$ T cells following TCR stimulation (Fig. 4C). PKCθ accumulates at the center of IS in both wild-type and IRAK-4$^{-/-}$ T cells (Fig. 4D and fig. S12), and the percentages of cells with accumulated PKCθ appeared equivalent in wild-type and IRAK-4$^{-/-}$ T cells (fig. S12), suggesting that IRAK-4 is involved in activation of PKCθ rather than its recruitment into IS.

In further experiments aimed at investigating which molecules upstream of PKCθ might associate with IRAK-4 and recruit it to lipid rafts, we observed that IRAK-4 coprecipitated with Zap70 in IRAK-4–expressing Jurkat cells (Fig. 4E). Because the association was constitutively observed and not inducible, it seems likely that the assembled Zap70–IRAK-4 complex may be recruited to the TCR vicinity upon stimulation. The interaction between IRAK-4 and Zap70 was supported by colocalization of substantial amounts of both proteins in the same area at the periphery of IS upon Ag stimulation (fig. S13). This is also consistent with the recent finding that Zap70 localizes at the periphery rather than at the center of the IS (*13*, *14*).

Our results demonstrate that IRAK-4 plays a key role in TCR-induced T cell activation, in particular through NF-κB activation. Recent studies have identified the CBM signal complex as responsible for TCR-mediated NF-κB activation (*5*). Our data suggest that IRAK-4 may function, through direct or indirect interaction with Zap70, to activate PKCθ, thereby having the potential to activate the CBM complex. In the innate immune response, IRAK-4 activates TRAF6 (*15*). However, because TRAF6 functions downstream of the CBM complex in TCR signaling (*16*), IRAK-4 may not directly activate this adapter in T cell signal cascade. Given that the phosphorylation of Zap70 and LAT and the activation of NFAT remain intact in IRAK-4$^{-/-}$ T cells, IRAK-4 may function as a switch molecule coupling to NF-κB activation in TCR signaling (SOM text 4).

The acquired immune system is highly organized and may have evolved from components of innate immunity (*1*). Because both invertebrates and vertebrates possess innate immune systems as well as NF-κB–related proteins, molecules such as IRAK-4 could have been retained to play key roles in both innate and acquired immunity (*6*–*8*), and our data indicate that IRAK-4 may represent an example of such evolutionary conservation. We suggest that IRAK-4 could have been retained as a central regulator of innate immune responses, with mammals also evolving to harness it as a means of regulating TCR-mediated NF-κB activation (SOM text 5).

References and Notes

1. C. A. Janeway Jr., R. Medzhitov, *Annu. Rev. Immunol.* **20**, 197 (2002).
2. S. Akira, *J. Biol. Chem.* **278**, 38105 (2003).
3. N. Suzuki *et al.*, *Nature* **416**, 750 (2002).
4. L. E. Samelson, *Annu. Rev. Immunol.* **20**, 371 (2002).
5. M. Thome, J. Tschopp, *Trends Immunol.* **24**, 419 (2003).
6. A. I. Chin *et al.*, *Nature* **416**, 190 (2002).
7. K. Kobayashi *et al.*, *Nature* **416**, 194 (2002).

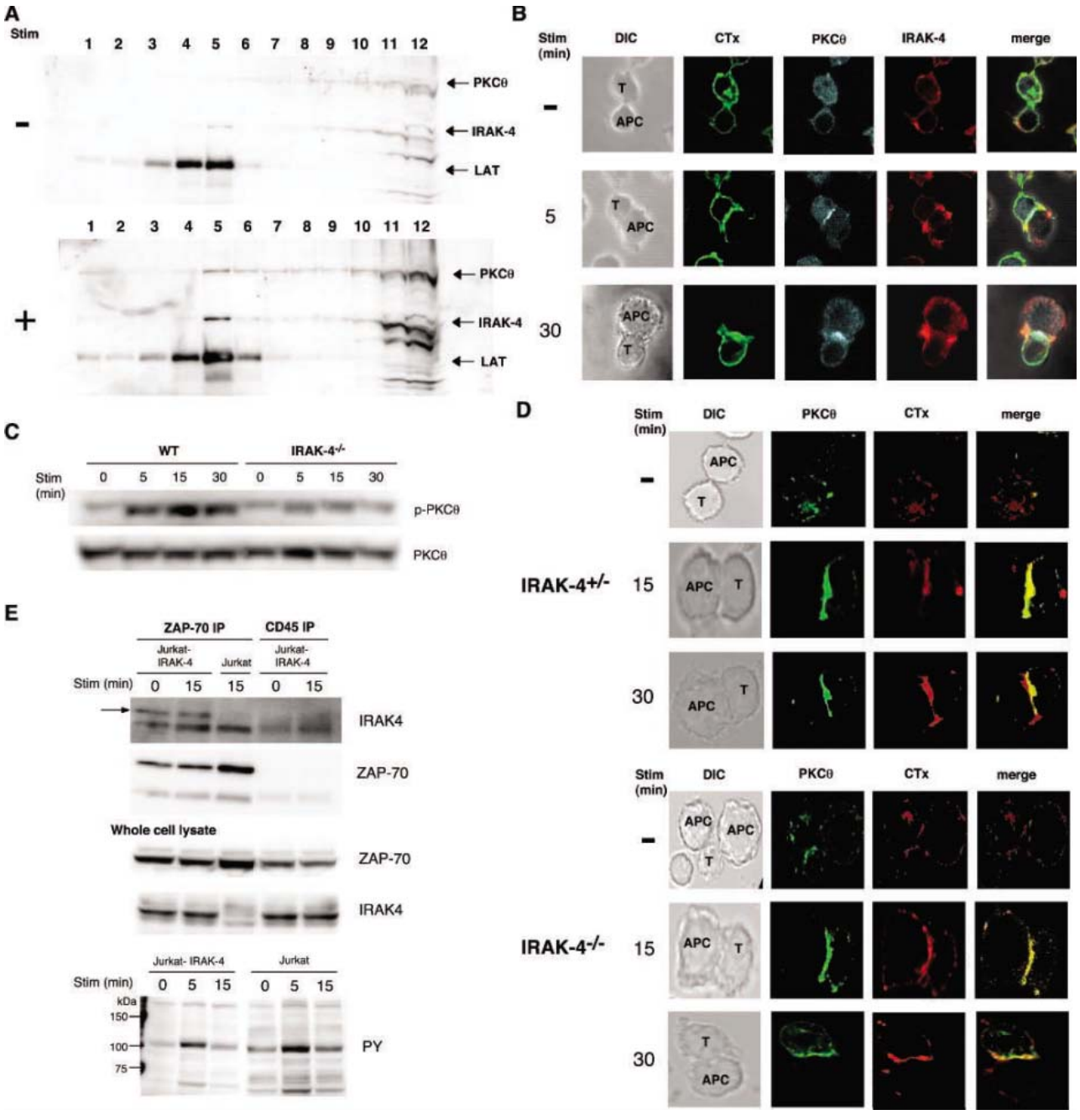

Fig. 4. IRAK-4 functions upstream of PKCθ by interacting with Zap70. (**A**) Localization of IRAK-4 and PKCθ in lipid raft upon TCR stimulation (Stim). Cell lysates of unstimulated (–) or αCD3-stimulated (+) Jurkat were fractionated by sucrose density gradient ultracentrifugation and blotted with each Ab. (**B**) Localization of IRAK-4, PKCθ, and lipid raft upon Ag stimulation. Jurkat cells expressing Flag-tagged IRAK-4 were stimulated with SEE and stained with CTx, αPKCθ, or αFlag (IRAK-4) (SOM text 8). (**C**) Impaired phosphorylation of PKCθ in IRAK-4$^{-/-}$ T cells upon TCR stimulation. Wild-type (WT) and IRAK-4$^{-/-}$ T cells were stimulated with αCD3. Total and phosphorylated PKCθ was blotted. (**D**) Normal recruitment of PKCθ into the central supramolecular activation clusters (c-SMAC) by IRAK-4$^{-/-}$ T cells. CD4^{+} T cells from OT-II Tg/IRAK-4$^{+/-}$ or IRAK-4$^{-/-}$ mice were stimulated with nonpulsed (–) or OVA-pulsed splenic activated B cells and stained with CTx and αPKCθ. Analyses of the *x-z* plane, the fluorescence intensities, and the percentages of T cells with recruitment of lipid raft (CTx) and PKCθ are shown in fig. S10. (**E**) Constitutive interaction between IRAK-4 and Zap70. Jurkat cells or Jurkat cells expressing Flag-tagged IRAK-4 (Jurkat–IRAK-4) were stimulated with αCD3, and cell lysates were immunoprecipitated (IP) with biotin-αZap70 or biotin-αCD45 (control) and avidin-sepharose, followed by blotting with αIRAK-4. Whole-cell lysates were blotted with Abs for IRAK-4, Zap70, and phospho-tyrosine (PY). Arrow indicates Flag-tagged IRAK-4 (SOM text 9).

8. H. Ye *et al.*, *Nature* **418**, 443 (2002).
9. N. Suzuki *et al.*, *J. Immunol.* **171**, 6065 (2003).
10. A. Ohta *et al.*, *J. Immunol. Methods* **209**, 85 (1997).
11. K. Habiro *et al.*, *Transplantation* **76**, 854 (2003).
12. P. W. Janes, S. C. Ley, A. I. Magee, *J. Cell Biol.* **147**, 447 (1999).
13. K. H. Lee *et al.*, *Science* **295**, 1539 (2002).
14. T. Yokosuka *et al.*, *Nat. Immunol.* **6**, 1253 (2005).
15. S. Li, A. Strelow, E. J. Fontana, H. Wesche, *Proc. Natl. Acad. Sci. U.S.A.* **99**, 5567 (2002).
16. L. Sun, L. Deng, C. K. Ea, Z. P. Xia, Z. J. Chen, *Mol. Cell* **14**, 289 (2004).
17. Materials and methods are available as supporting material on *Science* Online.

18. We thank Y. Itoh and K. Ogasawara for in vivo analyses; M. Sakuma, E. Ishikawa, C. Ishihara, and W. Kobayashi for technical support; and H. Yamaguchi for administrative assistance. This work was supported by a Grant-in-Aid for Priority Area Research from the Ministry of Education, Culture, Sports, Science and Technology of Japan (T.S. and N.S.), grants from Kowa Life Science

Foundation, Sumitomo Foundation, Tokyo Biochemical Research Foundation, Uehara Memorial Foundation (N.S.), Boninchi Foundation (T.C.), Terry Fox Foundation from National Cancer Institute of Canada (NCIC) (T.C.), the Canadian Institutes of Health Research (W.-C.Y. and P.S.O.), and a Canadian Network for Vaccines and Immunotherapeutics (CANVAC) Network Centres of Excellence grant (P.S.O.).

Supporting Online Material
www.sciencemag.org/cgi/content/full/311/5769/1927/DC1
Materials and Methods
SOM Text
Figs. S1 to S13
References

23 December 2005; accepted 23 February 2006
10.1126/science.1124256

Genome-Wide Detection of Polymorphisms at Nucleotide Resolution with a Single DNA Microarray

David Gresham,[1,2]* Douglas M. Ruderfer,[1,3] Stephen C. Pratt,[1,3] Joseph Schacherer,[1,3] Maitreya J. Dunham,[1] David Botstein,[1,2] Leonid Kruglyak[1,3]*

A central challenge of genomics is to detect, simply and inexpensively, all differences in sequence among the genomes of individual members of a species. We devised a system to detect all single-nucleotide differences between genomes with the use of data from a single hybridization to a whole-genome DNA microarray. This allowed us to detect a variety of spontaneous single–base pair substitutions, insertions, and deletions, and most (>90%) of the ~30,000 known single-nucleotide polymorphisms between two *Saccharomyces cerevisiae* strains. We applied this approach to elucidate the genetic basis of phenotypic variants and to identify the small number of single–base pair changes accumulated during experimental evolution of yeast.

Despite the ongoing development of DNA sequencing technology (*1*, *2*), it remains technically and financially infeasible for individual laboratories to sequence whole genomes. Moreover, for global comparisons of genomes within species, where one expects a relatively small number of sequence differences throughout the genome, determining the entire sequence is unnecessary. In such cases, it is sufficient to assess the extent and location of sequence variation in a manner analogous to comparative genomic hybridization, which compares copy number changes between closely related genomes at genic resolution (*3*).

DNA microarrays of short oligonucleotides designed to interrogate each base individually (i.e., resequencing arrays) have been applied to the analysis of individual human genes (*4*) and small genomes such as the human mitochondrial (*5*) and the SARS coronavirus (*6*) genomes. However, extension of this approach to whole genomes of most organisms is currently impractical because of the large number of probes required for complete coverage.

An alternative approach uses microarrays that detect mismatches, exploiting the fact that hybridization to a short oligonucleotide is quantitatively sensitive to the number and position of mismatches (*7*). Sequence-level differences are detected, without allele-specific probes, by comparing hybridization intensities of individual features on the microarray [referred to as single-feature polymorphisms (SFPs) (*8*)]. This method has been successfully applied to studies of genetic diversity (*9*–*11*) and gene mapping (*12*–*17*). Until recently, comprehensive detection of single–base pair differences has been limited by probe density across the genome, which is typically a few oligonucleotides per gene. Even complete single-copy coverage of the genome is unlikely to be sufficient for finding all mutations, because statistically detectable decreases in hybridization intensity usually require that a variant nucleotide fall within the central 15 bases of a 25-base probe (*18*).

We used high-density Affymetrix yeast tiling microarrays (YTMs) with overlapping 25-nucleotide oligomers spaced an average of 5 base pairs (bp) apart to provide complete and ~5-fold redundant coverage of the entire *S. cerevisiae* genome. This array design was previously used to discover novel expressed sequences and to precisely map sites of transcription in humans (*19*). This design provides five to seven measurements of a given nucleotide's effect on hybridization efficiency, which we exploited to predict the presence and location of SNPs and deletion breakpoints throughout the entire yeast genome.

Each YTM has ~2.6 million perfect match (PM) probes and ~2.6 million corresponding mismatch (MM) probes. We modeled the decrease in PM probe intensity caused by a single SNP as a function of the SNP's position within the probe, the probe's GC content, the nucleotide sequence surrounding the SNP, and the hybridization intensity obtained using a nonpolymorphic reference (S288C) genome [strain FY3 (*20*)]. To fit the model, we used hybridization data for a training set of nearly 25,000 high-quality SNPs in strain RM11-1a, all identified by direct comparison of the genomic sequences (*20*). The model predicts the intensity of a probe in the presence of a specified SNP (*20*) (figs. S1 and S2) and is used in our algorithm, SNPscanner, which calculates the log of the likelihood ratio (the "prediction signal") for the presence of a SNP at each nucleotide position in the genome using measurements from all probes that cover that site. By scanning the entire genome, we identify SNPs as regions of elevated signal in which the position of the peak value is considered the predicted polymorphic site.

We tested the performance of SNPscanner on a set of 981 high-quality SNPs from RM11-1a that were not included in the training set. We assessed the false-positive rate by using SNPscanner to predict SNPs from an independent hybridization of the reference strain, where no true polymorphisms are expected. At a prediction signal of 1, we detected 915 (93.3%) known SNPs in RM11-1a and called 177 false positives in the reference strain (fig. S3). By increasing the prediction signal to 5 and applying a heuristic filter (*20*), we elim-

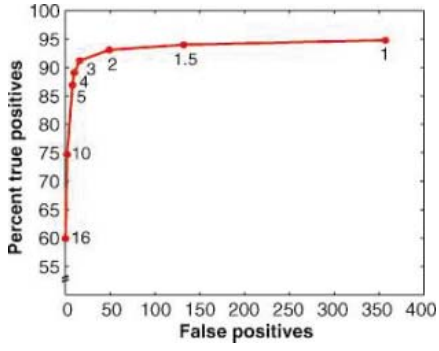

Fig. 1. Nucleotide-level comparison with a genome divergent from the sequenced reference genome. We applied our approach to test how many of 30,303 known SNPs in the yeast strain YJM789 we were able to detect. Numbers on the graph indicate prediction signal thresholds. On the basis of data from a single hybridization experiment, we were able to correctly identify as many as 28,737 SNPs at a prediction signal of 1. At prediction signals of >5, the number of false-positive predictions is reduced to 8 in a test of the reference genome and 86.9% of true positives are still predicted.

[1]Lewis-Sigler Institute for Integrative Genomics, [2]Department of Molecular Biology, [3]Department of Ecology and Evolutionary Biology, Princeton University, Princeton, NJ 08544, USA.

*To whom correspondence should be addressed. E-mail: leonid@genomics.princeton.edu (L.K.); dgresham@genomics.princeton.edu (D.G.)

inated all false positives and retained 77.5% (760) of real SNPs. Analysis of this set of correctly predicted SNPs showed the sequence-confirmed SNP to be within 2 bp of the predicted site 87.1% of the time (*20*).

To test our ability to predict a large number of SNPs, we analyzed the highly diverged sequenced strain YJM789, originally recovered from an AIDS patient (*21*). We selected a set of 30,303 sequence-confirmed SNPs in YJM789 that were isolated from each other by at least 25 bp and were covered by probes on the YTM. Analysis of a single hybridization with SNPscanner yielded 28,737 (94.8%) correctly predicted SNPs at a prediction sig-

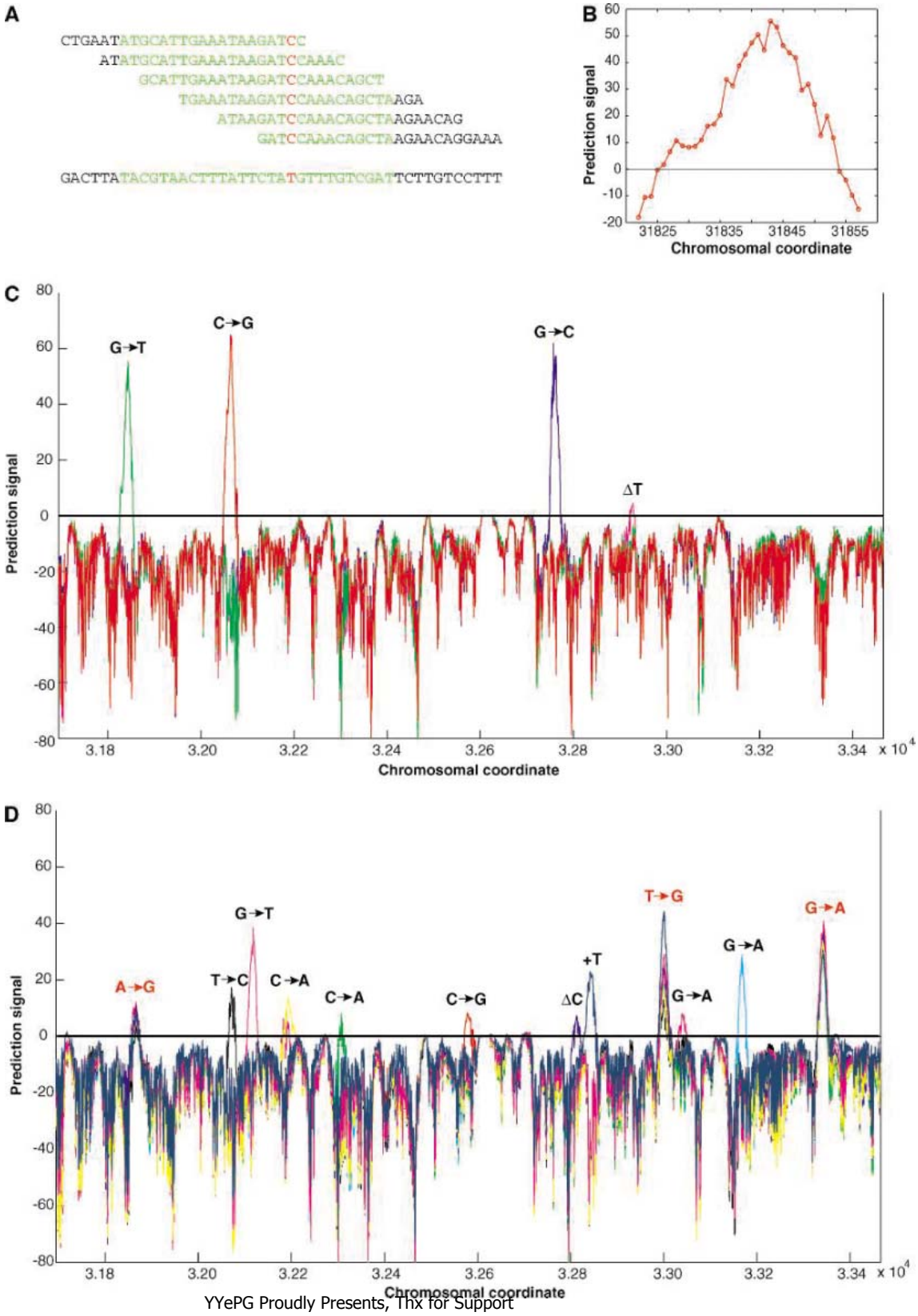

Fig. 2. SNPscanner accurately predicts SNPs in *CAN1* for independent CAN^R mutants. (**A**) Multiple overlapping probes cover each nucleotide. A mutation at the site indicated in red perturbs hybridization of the sample to all probes. (**B**) The decrease in observed hybridization is used to estimate the log of the likelihood ratio of the presence of a polymorphism versus the absence of a polymorphism (the prediction signal). The presence of a SNP typically results in a region of positive prediction signal with a peak defined as the predicted SNP; for the confirmed mutation indicated in red text in (A), the entire sequence in green has a positive prediction signal shown in (B). (**C**) Using this approach, we detected single–base pair substitutions and a 1-bp deletion in four independent spontaneous CAN^R mutants isolated in a reference genome background (each color represents a different experiment). (**D**) SNPscanner accurately predicts mutations and SNPs in a nonreference genome. The results of nine independent CAN^R mutants in the CEN.PK strain background are shown for the entire *CAN1* gene. We confirmed unique nucleotide substitutions for seven of the mutants, as well as a single-base insertion in one mutant and a single-base deletion in another. At common polymorphisms, indicated in red text, the SNPscanner signal is highly reproducible across multiple samples, allowing intrastrain comparisons of nonreference genomes.

nal threshold of 1 (Fig. 1). At a prediction signal threshold of 5, we detected 86.9% of known SNPs and called only eight false positives in a similar analysis of the reference genome. These false positives were readily excluded by our heuristic filter.

To test our ability to detect accurately a very small number of sequence differences that distinguish two genomes, we analyzed spontaneous mutants in the strain FY3. Independent clones from the same archival isolate were grown, and mutants in the *CAN1*, *GAP1*, and *FCY1* genes were selected on plates containing canavanine sulfate, D-serine and D-histidine, or 5-fluorocytosine, respectively (*20*). For each mutant we hybridized total genomic DNA to a single YTM and analyzed the data with SNPscanner (Fig. 2, A and B). In each of four *can1* mutants, we detected a single peak at the *CAN1* locus that fulfilled our prediction criteria for a SNP (Fig. 2C). Amplification and sequencing of the *CAN1* locus identified a single-base substitution in each of three mutants (31844G → T; 32064C → G; 32757G → C) and deletion of a single thymine in a run of four thymines in the fourth (32924ΔT). Although the prediction signal for this deletion was comparatively low, its detection is noteworthy because no insertions or deletions (indels) were included in the set of SNPs used to train the model.

Analysis of DNA from a mutant resistant to D-histidine and D-serine predicted a mutation in *GAP1* (chromosome XI), which we confirmed as a 514919C → G substitution by sequence analysis (fig. S4). Similarly, we accurately predicted a mutation in *FCY1* (chromosome XVI) for a mutant resistant to 5-fluorocytosine (677256C → T; fig. S5). Thus, we were able to detect a variety of single-base changes, including a single-base deletion, at several different loci in the genome and map them to within 2 bp of the verified substitution (table S1).

In addition to the anticipated mutations, our analysis yielded 12 to 414 additional predictions per genome (table S2). We identified two main causes of experimental noise: (i) false positives that fell within repetitive genomic features, such as retrotransposons and telomeres, which we subsequently excluded (table S1); and (ii) manufacturing defects in microarrays, which we computationally removed (*20*) (fig. S6). We ranked the remaining predictions on the basis of signal strength for each mutant and found the expected mutation in the top five predictions for all mutants except the one resulting from an indel (table S1). One SNP prediction (chromosome IV, position 548,350, sequence confirmed as 548348G → C) was common to all samples, suggesting an early mutation event that preceded later experiments (perhaps during single-colony purification from the archived stock culture). Sequence confirmation of high-quality predictions passing our filtering criteria identified additional unique mutations in three of the six spontaneous mutants (table S1). Thus, our algorithm is sufficiently sensitive to detect a small number of base changes that distinguish two genomes with no a priori knowledge of the variants' location. These results indicate that only a small number of mutations (<5) are associated with the generation of spontaneous drug resistance mutants.

We extended our approach to characterize the genome of the unsequenced laboratory yeast strain CEN.PK, commonly used in continuous culture experiments. CEN.PK shares ancestry with the reference strain, S288C, but some genes are absent in CEN.PK (*22*). We obtained a nucleotide-resolution comparison with the reference sequence by analyzing data with SNPscanner from a single hybridization of CEN.PK DNA. CEN.PK has a strikingly mosaic structure, with large portions of the genome sharing essentially complete sequence identity with FY3 interspersed with regions of sequence divergence and large deletions (fig. S7).

We investigated whether we could detect single mutations on a genome-wide scale in a nonreference genome; this was expected to be a more difficult statistical problem (*20*). We selected 10 spontaneous Can^R mutants in the CEN.PK strain background and hybridized genomic DNA to the YTM. SNPscanner predictions correctly identified a mutation in 9 of 10 mutants, as well as three polymorphic sites present in the wild-type CEN.PK background (Fig. 2D). We confirmed the sequences of all *CAN1* mutations and polymorphisms in the 10 Can^R mutants. Whereas seven of the nine detected mutants had base substitutions in *CAN1*, one mutant contained a 1-bp insertion and another had a 1-bp deletion. All mutations were confirmed as lying within 7 bp of the predicted site (table S2).

SNPscanner prediction signals were highly reproducible across multiple experiments. We compared genome-wide SNP predictions for each CEN.PK *can1* mutant to SNP predictions for CEN.PK wild-type DNA and applied our heuristic filter (*20*). This resulted in the prediction of fewer than 100 SNPs genome-wide that were not predicted to exist in wild-type CEN.PK for 9 of 10 mutants (table S2). In most cases, excluding those predictions that fell in repetitive regions further reduced the total number. By using this approach, we retained the identified *can1* mutation for seven of nine mutants. We ranked the remaining predictions and observed that the sequence-confirmed mutation was in the top 10 predictions for all seven mutants. So even in this somewhat more challenging case, our system succeeded in detecting most of the single-nucleotide sequence differences and mapping them within a few nucleotides. Mutations predicted in our

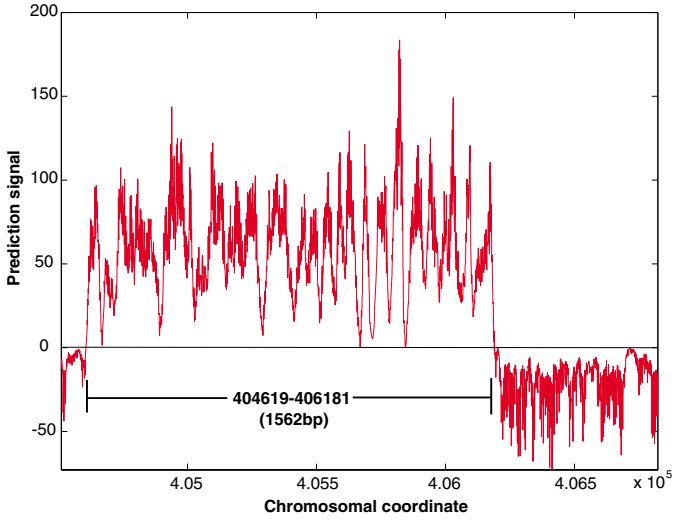

Fig. 3. Genome-wide mutation detection facilitates a genomic approach to genetics. Whole-genome analysis of a strain in which *AMN1* was deleted but that failed to demonstrate the expected nonclumpy phenotype predicted the presence of a 1562-bp deletion (defined by the outermost peak values in prediction signal) in *ACE2* (shown in its entirety). Sequence analysis confirmed the deletion—which spans 1558 bp and is flanked by the nucleotide sequence CTG—and mapped the breakpoints to nucleotides 404,621 to 406,179.

Table 1. Predicted SNPs detected in a yeast strain subjected to experimental evolution.

Strain	Generations under sulfur limitation	Number of SNPscanner predictions	Sequence-confirmed mutation
DBY11130	63	19 unique SNPs	Chromosome IV, 498631C → A in *REG1* (D749Y)
DBY11131	123	6 unique SNPs	Chromosome VII, 858403G → C in *TIM13* (A38P)
DBY11130 and DBY11131	—	12 shared SNPs	—

collection of CEN.PK and FY3 spontaneous mutants corresponded to 9 of the 12 possible base substitutions that resulted in six of the eight possible mismatches between probe and sample. Thus, our method can detect single–base pair indels in addition to virtually all base substitutions.

We sought to apply our genome-wide mutation detection approach to biological questions that had remained refractory to traditional genetic techniques. We complemented a positional cloning project to predict and confirm mutations in *AEP3*, a peripheral mitochondrial inner membrane protein (*23*), that are causative of a growth defect on a nonfermentable carbon source (*20*) (table S3). We also used our method to determine the genetic basis of an unusual phenotype. Deletion of *AMN1* results in upregulation of daughter-specific genes and a nonclumpy growth phenotype (*17*). However, when we deleted *AMN1* in an S288C-like strain (BY4716), we recovered a transformant that displayed low expression of daughter-specific genes and a clumpy phenotype (strain YEF1695). Deletion of *AMN1* in YEF1695 was confirmed by sequence analysis, and independent deletions of *AMN1* in both BY4716 and RM11-1a yielded the expected phenotype, which suggested the presence of a suppressor mutation in YEF1695. Preliminary genetic analysis tended to indicate the presence of an unlinked suppressor mutation. We hybridized genomic DNA from YEF1695 to the YTM. Analysis using SNPscanner confirmed the deletion of *AMN1* (*24*) and identified an additional deletion on chromosome XII (Fig. 3A). The predicted deletion spans ~1.5 kb and includes the majority of the coding region of *ACE*2. Subsequent sequence analysis confirmed that the predicted breakpoints were within 2 bp of the actual sites (Fig. 3).

The deletion of *ACE2* provides a plausible explanation for both aspects of the aberrant phenotype of YEF1695. *ACE2* encodes a transcription factor that is thought to drive the transcription of genes with daughter-specific expression (*25*). Its absence in YEF1695 probably causes a low expression of the daughter cell–specific genes, some of which are required for cell separation after budding (e.g., *CTS1*, which encodes chitinase). Moreover, deletion of *ACE2* alone results in a clumpy phenotype (*26*), and clumpiness segregates with the *ACE2* locus in a cross between YEF1695 and RM11Δ*amn1* (*24*).

Previous studies have shown the occurrence of characteristic gene expression patterns (*27*) and large-scale gene duplication and deletion (*28*) in yeast cultures that are experimentally evolved under a nutrient-limiting condition. However, the extent and nature of nucleotide changes that occur during this process have remained completely unknown. We sought to assess the degree of sequence variation that had accumulated in a strain of yeast subjected to experimental evolution under sulfur limitation in continuous culture. We compared the SNPscanner signals obtained from DNA of the ancestral strain, CEN.PK, to those signals obtained from DNA of two clones from the same population that had undergone experimental evolution under sulfur limitation for 63 (DBY11130) and 123 (DBY11131) generations. We compared our set of predictions to those made for CEN.PK CAN^R mutants to exclude common predictions that were the result of systematic error. SNP predictions that fell within repetitive regions were considered to be unreliable and were excluded from further analysis.

At a prediction signal of >5 we called a small number of predicted SNPs in strains DBY11130 and DBY11131, 12 of which were common to the two strains (Table 1). We confirmed the sequences of single strain-specific mutations found in DBY11130 and DBY11131 (Table 1). The relatively small number of mutations strongly suggests that the events associated with adaptive evolution in chemostats do not involve even transient genome-wide mutagenesis; this number is also consistent with the experience that in yeast, evolved strains are rarely if ever found to have mutator phenotypes (*24*). This is in contrast to studies of *Escherichia coli* grown in batch conditions, in which mutator phenotypes have been observed in numerous independent cultures (*29*). The small number of mutations identified in our experiments means that it will be feasible to comprehensively identify and experimentally verify mutations that are important for adaptation during studies of experimental evolution.

On the basis of a single experimental hybridization, we are able to accurately detect the single-nucleotide changes that distinguish two genomes. Recently, a similar microarray design has been used as a preliminary screen to identify possible mutations in the pathogen *Helicobacter pylori* (*30*). In this method, the initial screen is followed by the manufacture of targeted resequencing microarrays. Our method relies on only a single experiment to derive a statistical measure of the likelihood of a polymorphism at a particular site. Our approach is optimal when direct comparisons are made to the reference strain represented on the microarray. However, we are also able to compare two nonreference genomes and identify the SNPs that distinguish them with only minimal added cost in terms of false negatives and false positives. Although our algorithm is trained on a set of known base substitutions, we found that it also detected single-base deletions and insertions, as well as large deletions with near-nucleotide accuracy in the prediction of breakpoints. Any genomic variation that results in novel sequence (such as inversions or retrotransposon insertions) should, in principle, be detectable by SNPscanner.

We expect that the simplicity and affordability of this method will enable individual laboratory groups to devise and use new and truly comprehensive genomic approaches to Mendelian and complex genetics and to the characterization of mutants obtained through genetic and suppressor screens. In addition, complete knowledge of nucleotide diversity will allow us to address questions regarding the mutagenic effect of phenomena such as aging and recombination on a genome-wide scale. By representing entire genomes of other organisms on oligonucleotide microarrays with a similar redundant design, it is likely that our approach may be extended to higher organisms. Although increased genome complexity presents a challenge, reports of successful SFP-based genotyping in *Arabidopsis* (*12*, *31*), which has a genome of 125 Mb, suggest that genome-wide prediction of all sequence variants may be possible in larger genomes, including those of model organisms such as *Caenorhabditis elegans* and *Drosophila melanogaster*. We analyzed haploid genomes and a single homozygous diploid genome; as with all sequencing technologies, identifying heterozygosity in diploid genomes represents the ultimate challenge.

References and Notes

1. M. Margulies *et al.*, *Nature* **437**, 376 (2005).
2. J. Shendure *et al.*, *Science* **309**, 1728 (2005); published online 4 August 2005 (10.1126/science.1117389).
3. J. R. Pollack *et al.*, *Proc. Natl. Acad. Sci. U.S.A.* **99**, 12963 (2002).
4. J. G. Hacia, L. C. Brody, M. S. Chee, S. P. Fodor, F. S. Collins, *Nat. Genet.* **14**, 441 (1996).
5. A. Maitra *et al.*, *Genome Res.* **14**, 812 (2004).
6. C. W. Wong *et al.*, *Genome Res.* **14**, 398 (2004).
7. U. Maskos, E. M. Southern, *Nucleic Acids Res.* **20**, 1675 (1992).
8. E. A. Winzeler *et al.*, *Science* **281**, 1194 (1998).
9. T. L. Turner, M. W. Hahn, S. V. Nuzhdin, *PLoS Biol.* **3**, e285 (2005).
10. S. K. Volkman *et al.*, *Science* **298**, 216 (2002).
11. E. A. Winzeler *et al.*, *Genetics* **163**, 79 (2003).
12. J. O. Borevitz *et al.*, *Genome Res.* **13**, 513 (2003).
13. R. B. Brem, G. Yvert, R. Clinton, L. Kruglyak, *Science* **296**, 752 (2002); published online 28 March 2002 (10.1126/science.1069516).
14. A. M. Deutschbauer, R. W. Davis, *Nat. Genet.* **37**, 1333 (2005).
15. J. Ronald, R. B. Brem, J. Whittle, L. Kruglyak, *PLoS Genet.* **1**, e25 (2005).
16. L. M. Steinmetz *et al.*, *Nature* **416**, 326 (2002).
17. G. Yvert *et al.*, *Nat. Genet.* **35**, 57 (2003).
18. J. Ronald *et al.*, *Genome Res.* **15**, 284 (2005).
19. J. Cheng *et al.*, *Science* **308**, 1149 (2005); published online 24 March 2005 (10.1126/science.1108625).
20. See supporting material on *Science* Online.
21. Z. Gu *et al.*, *Proc. Natl. Acad. Sci. U.S.A.* **102**, 1092 (2005).
22. P. Daran-Lapujade *et al.*, *FEMS Yeast Res.* **4**, 259 (2003).
23. T. P. Ellis, K. G. Helfenbein, A. Tzagoloff, C. L. Dieckmann, *J. Biol. Chem.* **279**, 15728 (2004).
24. D. Gresham *et al.*, data not shown.
25. A. Colman-Lerner, T. E. Chin, R. Brent, *Cell* **107**, 739 (2001).
26. W. J. Racki, A. M. Becam, F. Nasr, C. J. Herbert, *EMBO J.* **19**, 4524 (2000).
27. T. L. Ferea, D. Botstein, P. O. Brown, R. F. Rosenzweig, *Proc. Natl. Acad. Sci. U.S.A.* **96**, 9721 (1999).
28. M. J. Dunham *et al.*, *Proc. Natl. Acad. Sci. U.S.A.* **99**, 16144 (2002).
29. P. D. Sniegowski, P. J. Gerrish, R. E. Lenski, *Nature* **387**, 703 (1997).
30. T. J. Albert *et al.*, *Nat. Methods* **2**, 951 (2005).

31. S. P. Hazen *et al.*, *Plant Physiol.* **138**, 990 (2005).
32. We thank E. Foss for creation of strain YEF1695, E. Smith for analysis of YEF1695 mapping data, and D. Storton and J. Matese for technical support. Supported by National Institute of General Medical Sciences grant R01 GM046406 and center grant P50 GM071508 (D.B.), NIH grant R37 MH059520 and James S. McDonnell Foundation grant 99-11T (L.K.), and Pew Charitable Trusts award 2000-002558 (S.C.P.). The raw data and software are available at http://genomics-pubs.princeton.edu/SNPscanner/.

Supporting Online Material
www.sciencemag.org/cgi/content/full/1123726/DC1
Materials and Methods
SOM Text
Figs. S1 to S7
Tables S1 to S3
References

12 December 2005; accepted 24 February 2006
Published online 9 March 2006;
10.1126/science.1123726
Include this information when citing this paper.

Rice Domestication by Reducing Shattering

Changbao Li, Ailing Zhou, Tao Sang*

Crop domestication frequently began with the selection of plants that did not naturally shed ripe fruits or seeds. The reduction in grain shattering that led to cereal domestication involved genetic loci of large effect. The molecular basis of this key domestication transition, however, remains unknown. Here we show that human selection of an amino acid substitution in the predicted DNA binding domain encoded by a gene of previously unknown function was primarily responsible for the reduction of grain shattering in rice domestication. The substitution undermined the gene function necessary for the normal development of an abscission layer that controls the separation of a grain from the pedicel.

Cereals, the world's primary food, were domesticated from wild grass species. Because wild grasses naturally shed mature grains, a necessary early step toward cereal domestication was to select plants that could hold on to ripe grains to allow effective field harvest (*1*, *2*) (fig. S1). The selection process might have been mainly unconscious because grains that did not fall as easily had a better chance of being harvested and planted in the following years. Consequently, nonshattering alleles had an increased frequency and eventually replaced the shattering alleles during domestication. The finding that one locus accounted for most phenotypic variance of grain shattering between a cereal crop and its wild progenitor suggested that the domestication process could have been initiated quickly by selection at the locus (*3*–*5*). The molecular genetic basis of the selection, however, has not been characterized.

Rice (*Oryza sativa*) was domesticated from one or both of two closely related species—*O. nivara* and *O. rufipogon*—distributed from southeastern Asia to India (*6*, *7*). Our recent genetic analysis of an F_2 population derived between *O. sativa* ssp. *indica* and the wild annual species *O. nivara* identified three quantitative trait loci (QTL)—*sh3*, *sh4*, and *sh8*—responsible for the reduction of grain shattering in cultivated rice (*5*). Of these QTL, *sh4* explained 69% of phenotypic variance, and the other two explained 6.0% and 3.1% of phenotypic variance. The *sh4* allele of the wild species caused shattering and was dominant.

Department of Plant Biology, Michigan State University, East Lansing, MI 48824, USA.

*To whom correspondence should be addressed. E-mail: sang@msu.edu

Two previous QTL studies using crosses between *O. sativa* ssp. *indica* and the wild perennial species *O. rufipogon* detected four and five shattering QTL (*8*, *9*). Both studies identified a QTL at the same location of *sh4* with either the largest or nearly largest phenotypic effect among the detected QTL. Moreover, genetic analyses between *O. sativa* ssp. *japonica* and *O. rufipogon* and two other closely related wild species *O. glumaepetula* and *O. meridionalis* all found that a single dominant allele from each of the three wild species was responsible for grain shattering (*10*, *11*). This locus, named *Sh3*, was mapped to the same chromosomal location as *sh4*.

Our QTL analysis located *sh4* between simple sequence repeat (SSR) markers RC4-123 and RM280 (*5*), which had a physical distance of about 1360 kb in the *O. sativa* genome (*12*) (Fig. 1A). Because of the large and dominant effect of the *O. nivara* allele, we were able to phenotypically distinguish F_2 individuals that were homozygous recessive (ss) from those that had at least one *O. nivara* allele of *sh4* (ns and nn), regardless of the genotypes at the remaining two QTL of small effect. After evaluating a total of 489 F_2 plants genotyped at the three shattering QTL, we consistently found that plants with the ns and nn genotypes at *sh4* shed all mature grains when hand tapped, whereas plants with the ss genotype at *sh4* did not shed grains or only partially shed mature grains under vigorous hand shaking.

With the reliable phenotyping method available, we grew ~12,000 F_2 seedlings and screened for recombinants between RC4-123 and RM280 (*13*). Plants with the genotype of ss at one marker and ns at the other were selected, and a total of 134 individuals were grown for phenotypic evaluation. By progressively examining SSR and SNP (single-nucleotide polymorphism) markers between RC4-123 and RM280, we finally mapped the mutation responsible for the derivation of nonshattering in cultivated rice to a 1.7-kb region of a gene with a previously unknown function (Fig. 1B and table S1). The gene is predicted to be a transcription factor, and its coding region is physically located between 34,014,305 and 34,012,126 base pairs (bp) on assembly LOC_Os04 g57530 of rice chromosome 4 (The TIGR Rice Genome Annotation Database).

The comparison of the 1.7-kb sequences between the mapping parents revealed seven mutations (Fig. 1C). These include one mutation in the intron: (*a*) a 1-bp substitution; three mutations in the first exon: (*b*) a 15-bp or five–amino acid insertion/deletion, (*c*) a 3-bp or one–amino acid insertion/deletion, and (*d*) a 1-bp or an amino acid substitution; and three mutations 5′ upstream of the start codon: (*e*) a 1-bp substitution at site -55, (*f*) a 3-bp insertion/deletion between sites −343 and −344, and (*g*) an 8-bp insertion/deletion between sites −558 and −559.

To assess the polymorphism and evolutionary direction of these mutations, we sequenced this 1.7-kb region from an additional 14 rice cultivars representing the diversity of *O. sativa* (*14*), 21 accessions of *O. nivara* covering the distributional range of the wild species (*15*), 6 accessions of *O. rufipogon*, and 1 accession of each of the four remaining wild A-genome species (Fig. 1C and table S2). The cultivars were polymorphic for mutation *f*, i.e., some of the cultivars had the same sequence as *O. nivara*. At the remaining six mutation sites, all cultivars shared the same sequences, which were different from those of the *O. nivara* parent.

Surprisingly, three accessions of *O. nivara* had the same sequences as *O. sativa* at these six sites. It was then found that plants grown from these accessions had the nonshattering phenotype. Greenhouse observations indicated that these accessions had additional characteristics of cultivated rice that were not found in *O. nivara*, such as upright tillers, short awns, and/or photoperiod sensitivity. This suggests that the three accessions are weedy rice that has received and fixed the *sh4* allele from cultivars.

The remaining accessions of the wild species with confirmed shattering differed invariably from the cultivars by one mutation, *d*, which was a nucleotide substitution of G for T or an amino acid substitution of

asparagine for lysine in *O. sativa*. At the remaining five mutation sites, sequence polymorphism was found within the wild species (Fig. 1C). That is, some of the wild accessions shared the same sequence with cultivated rice at these sites but had the shattering phenotype. The results thus indicate that the amino acid substitution at site *d* was selected for the development of nonshattering cultivars during rice domestication.

The Blast search of the GenBank for protein sequences identified three predicted genes that are most similar to *sh4*. These include a rice gene (XP_469180) with 32% amino acid sequence identity with *sh4*, and two *Arabidopsis* genes (NP_174416 and NP_181107) with 32% and 29% identity with *sh4*. None of these genes has been functionally characterized. The two *Arabidopsis* genes were predicted to be transcription factors (*16*), and one of them had a cDNA sequence (AAT99796) in the database. The next most similar group of genes was also from rice and *Arabidopsis* but had only 20 to 22% amino acid sequence identity with *sh4*.

Examination of the *sh4* protein, using programs Prosite and PredictNLS, identified a Myb3 DNA binding domain and a nuclear localization signal (Fig. 1D), suggesting that *sh4* is a transcription factor. To test this hypothesis, we fused the gene for a green fluorescent protein (GFP) with *sh4* to make *sh4-GFP*, which was driven by a *Ubi* promoter in the plasmid construct. The construct was introduced into a *japonica* cultivar, Taipei

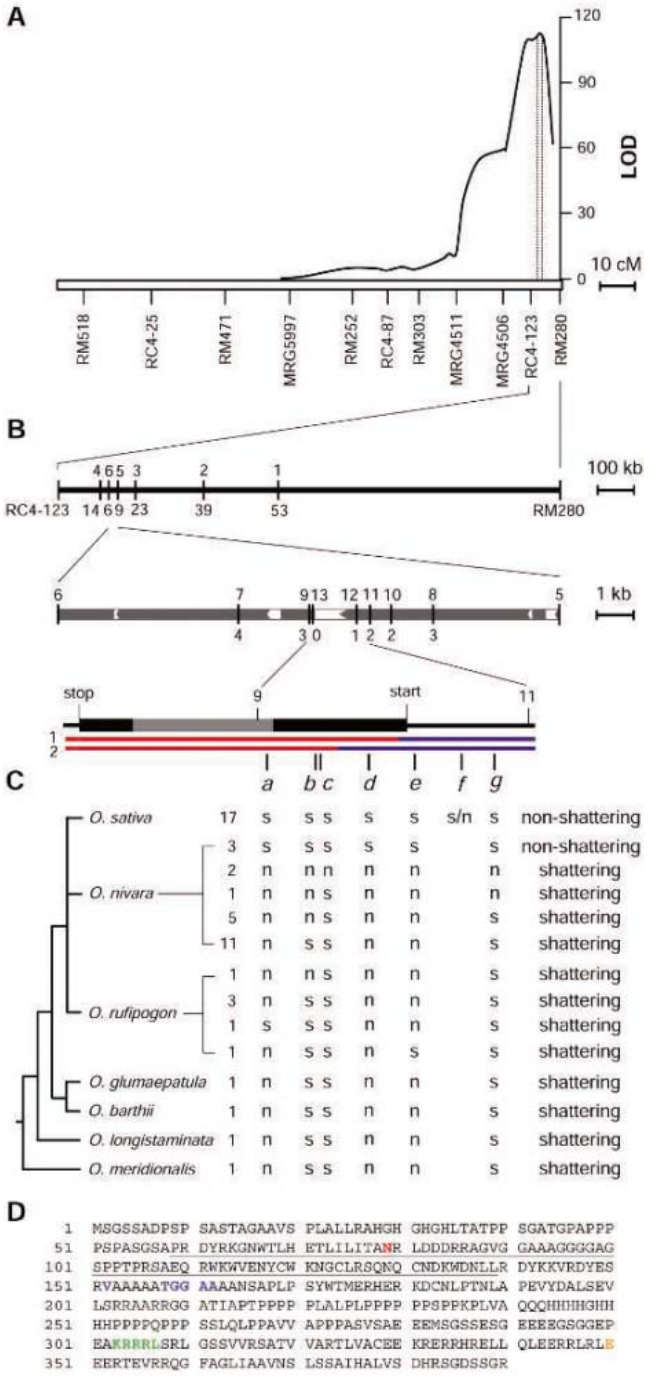

Fig. 1. Molecular cloning of *sh4*. (**A**) Chromosomal location of *sh4* determined by QTL mapping. Dotted lines indicate 1-lod (logarithm of the odds ratio for linkage) supporting interval. (**B**) Fine mapping of *sh4*. Vertical lines indicate SSR and SNP markers. Numbers above lines: markers numbered consecutively according to the order of evaluation; numbers below lines: the number of recombinants left in the chromosomal interval still containing *sh4* after the evaluation of the marker. White horizontal arrows indicate the orientation and size of open reading frames between markers 5 and 6. The mutation responsible for nonshattering was mapped to between markers 9 and 11, in a predicted gene with two exons (black bars) and an intron (gray bar). The start and stop codons of the gene are labeled. Lines below illustrate two constructs made for gene transformation; red and blue represent sequences of *O. nivara* and *O. sativa*, respectively. (**C**) Seven mutations found between the mapping parents are labeled *a* through *g*. Variation at these sites is compared between rice cultivars and wild A-genome species in the phylogenetic context; s and n represent sequences of *O. sativa* and *O. nivara* parents, respectively. The number of accessions of a species with the same combination of sequences is indicated. (**D**) *sh4* protein sequence of *O. sativa*. Mutations between the mapping parents are indicated: red for substitution (mutation *d*; K in *O. nivara*) and blue for insertion/deletion (mutation *b* and *c*; deletion in *O. nivara*). The predicted Myb3 DNA binding domain is underlined. The predicted nuclear localization signal is colored green. The *sh4-GFP* construct for subcellular localization encodes a recombined protein beginning from the sh4 N terminus to the amino acid E (colored orange) followed by GFP. Abbreviations for the amino acid residues are as follows: A, Ala; C, Cys; D, Asp; E, Glu; F, Phe; G, Gly; H, His; I, Ile; K, Lys; L, Leu; M, Met; N, Asn; P, Pro; Q, Gln; R, Arg; S, Ser; T, Thr; V, Val; W, Trp; and Y, Tyr.

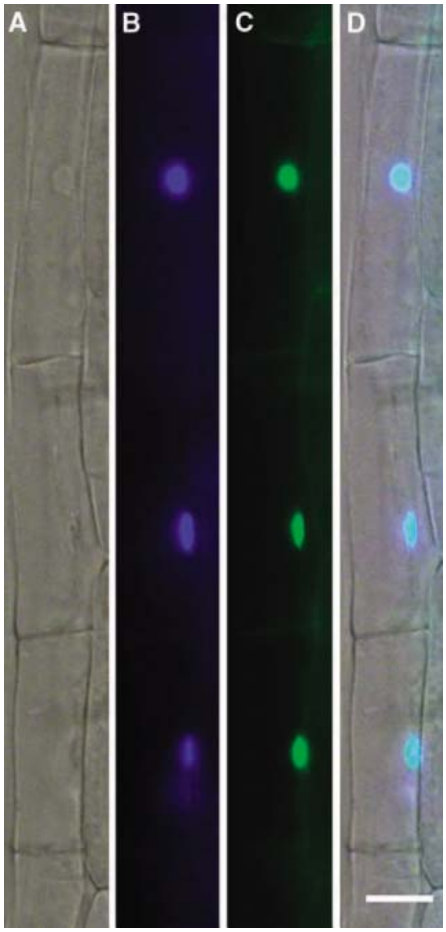

Fig. 2. Subcellular localization of sh4. Roots of rice cultivar Taipei 309 transformed with *Ubi::sh4-GFP* were stained with 4′-6-diamidino-2-phenylindole (DAPI) and observed under various conditions. (**A**) A differential interference contrast image of epidermal cells. (**B**) The same cells showing the DAPI-stained nuclei. (**C**) The same cells showing the nuclear localization of sh4-GFP fluorescence. (**D**) The merged image. Bar, 10 μm.

309, a rice strain tested as suitable for gene transformation (*17*). The nuclear localization of GFP-tagged *sh4* was determined (Fig. 2). This result supports the bioinformatic prediction that *sh4* is a transcription factor.

Reverse transcription–polymerase chain reaction (RT-PCR) detected the expression of *sh4* at the flower and pedicel junction, where mature grains separate from the mother plant (Fig. 3A). Gene expression was not detected in the remaining parts of flowers or pedicels or in the leaves. We amplified, using RT-PCR, the entire coding region of *sh4* cDNA from both mapping parents. The comparison of the cDNA sequences showed that the intron was spliced from the same position as predicted by rice genome annotation.

We conducted real-time PCR to compare the relative levels of *sh4* expression at various stages of flower and seed development in both mapping parents (Fig. 3B). Although there was a trend of increased gene expression as seeds matured, a substantial increase began 12 days after pollination. The expression in *O. sativa* continued to increase on day 18, while the measurement for *O. nivara* was no longer possible due to shattering.

We measured the strength of flower and grain attachment to the pedicel at the corresponding developmental stages. Flowers and grains were pulled away at the interface where a mature grain separates from the pedicel, and the force required was measured. For the first 9 days after pollination, the force was not significantly different between the developmental stages in either species (Fig. 3C). The force began to decrease in both species from day 12. The decline continued at a much faster rate in *O. nivara* than in *O. sativa*. On day 18, shattering prevailed in *O. nivara*, which left few grains to measure. In *O. sativa*, the force measured on day 18 was about half of that required at the earlier stages; it then decreased at a rather slow pace but did not reach the level permitting grain shattering in *O. nivara*.

We conducted rice transformation to confirm the gene function and to test the role of the amino acid substitution. We made two constructs that had the *O. sativa* promoter and recombined coding regions between the mapping parents. The two constructs differed only at the mutation site *d*. Construct 1 contained *O. nivara* sequence from the 3′ nontranslated region to the inclusion of mutation site *d* and *O. sativa* sequence from mutation site *e* to the 5′ regulatory region. Construct 2 contained *O. nivara* sequence from 3′ to the inclusion of mutation site *c* and *O. sativa* sequence from mutation site *d* to the 5′ regulatory region (Fig. 1B). The plasmids were introduced into Taipei 309.

The expression of the introduced constructs in the transgenic plants was verified by RT-PCR identification of the 18-bp deletion of the *O. nivara* sequence at mutation sites *b* and *c*. Transformants expressing construct 1 showed significantly reduced strength of grain attachment to pedicel (Student's *t* test, $P = 0.003$), whereas no significant difference was found between transformants expressing construct 2 and the control (*t* test, $P = 0.5$) (Fig. 3D). The results thus support the finding made from the genetic mapping and sequence comparison that the amino acid substitution at site *d* was primarily responsible for the reduction of grain shattering in rice domestication.

Programmed organ detachment, such as the falling of old leaves, withered floral parts, and ripe fruits, is fundamental to plant function and adaptation and is regulated by an abscission zone at the juncture of the organ and the main body of the plant. The molecular genetic control of the abscission zone development, however, is poorly understood. The study of dicotyledonous plants such as bean, tomato, and *Arabidopsis* showed that an abscission zone encompassed several layers of small, densely cytoplasmic cells. In response to environmental and hormonal signals, the activation of abscission is coupled with cell expansion and secretion of hydrolytic enzymes that break the middle lamella between cell layers in the abscission zone (*18*).

In monocotyledons, including grasses, little is known about the development and function of abscission zones. Genes regulating the developmental processes have not been identified. Here we found that the abscission zone between a rice grain and the pedicel consists of mostly one layer of small, thin-walled cells. *O. nivara* has a complete layer of abscission cells between the grain and the pedicel, which is seen in a longitudinal section as continuous lines of abscission cells between the vascular bundle and the epidermis (Fig. 4A). *O. sativa*, however, has an incomplete abscission layer. In the longitudinal section, the line of abscission cells is discontinuous and completely absent near the vascular bundle, where they are replaced by thicker-walled cells similar to adjacent pedicel cells (Fig. 4, B and C). For both species, these anatomical features were seen in young flowers (flowers ~15 days before opening were examined) and remained similar in mature grains.

Because *japonica* cultivars are generally harder to thresh than *indica* cultivars (*19*),

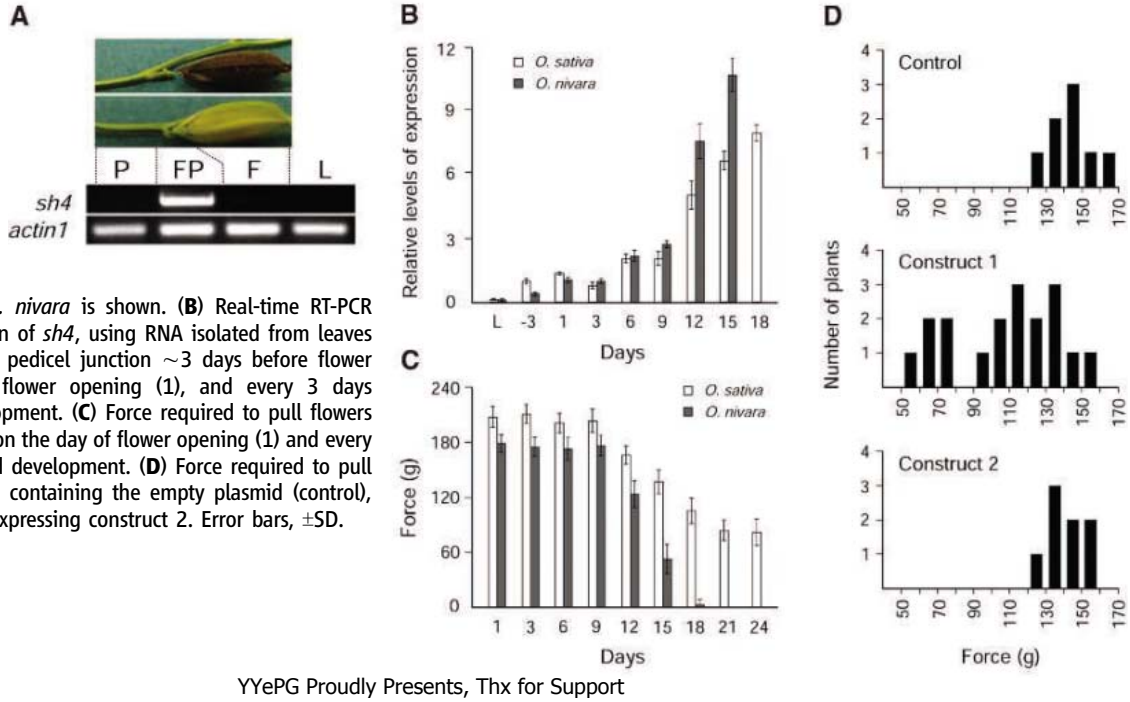

Fig. 3. Expression of *sh4* and flower and grain detachment. (**A**) RT-PCR results, using total RNA isolated from the flower and pedicel junction (FP), from the remaining portions of pedicel (P) and unopened flower (F), and from leaves (L). Above the flower, the separation location of a mature grain from the pedicel of *O. nivara* is shown. (**B**) Real-time RT-PCR estimate of relative expression of *sh4*, using RNA isolated from leaves (L) and the flower/grain and pedicel junction ~3 days before flower opening (−3), the day of flower opening (1), and every 3 days thereafter during seed development. (**C**) Force required to pull flowers or grains away from pedicels on the day of flower opening (1) and every 3 days thereafter during seed development. (**D**) Force required to pull away grains of transformants containing the empty plasmid (control), expressing construct 1, and expressing construct 2. Error bars, ±SD.

Taipei 309 had a stronger grain attachment to the pedicel than the *indica* mapping parent (Fig. 3, C and D). Accordingly, the abscission layer of the *japonica* cultivar showed a higher degree of discontinuity and further retreat from the vascular bundle. The transgenic plants with the strength of grain attachment reduced to less than 100 g had substantially improved abscission layers that were more continuous and extended closer to the vascular bundles (Fig. 4D).

The results indicate that *sh4* plays an important role in the establishment of the abscission layer from the early stage of flower development. The increased expression of *sh4* in the late stage of seed maturation suggests that the gene may also play a role in the activation of the abscission process. One or both of the roles were undermined by the amino acid substitution of asparagine for lysine in cultivated rice.

In the process of rice domestication, human selection was likely to have favored mutations that reduced grain shattering but did not eliminate the formation or function of the abscission layer. In this way, grain loss due to shattering was largely prevented during harvest while a certain level of grain abscission was maintained so that the yield increase was not offset by creating difficulties in threshing. The inverse correlation between the expression level of *sh4* and the strength of grain attachment in *O. sativa* at the late stage of grain maturation seems to suggest that the amino acid substitution did not knock out the gene function in cultivated rice.

The slower pace of increase in the level of *sh4* expressed in *O. sativa* than in *O. nivara* during grain maturation might have been a result of selection in the regulatory region of the gene for a finer adjustment of the shattering/threshing balance during rice cultivation. A comparison of the regulatory sequences of *sh4*, the levels of gene expression, and the phenotypic difference among diverse rice cultivars should provide further insights into the genetic basis of agricultural selection continued through the history of rice cultivation.

Genetic analyses of crop domestication, especially the cloning of domestication-related genes, have shed a light on plant development and evolution. Mutations in regulatory genes were found responsible for drastic morphological modifications during maize and tomato domestication (*20*–*23*). Here we show that the substitution of a neutral for a positively charged amino acid in a predicted DNA binding domain led to a physiological transition key to rice domestication. This is consistent with the finding that positively charged amino acids are critical residues on the surface of DNA binding domains (*24*). The cloning of *sh4* opens opportunities for understanding the developmental pathway of programmed cell separation and seed dispersal in monocotyledonous plants and potentially for optimizing the methods of grain harvest.

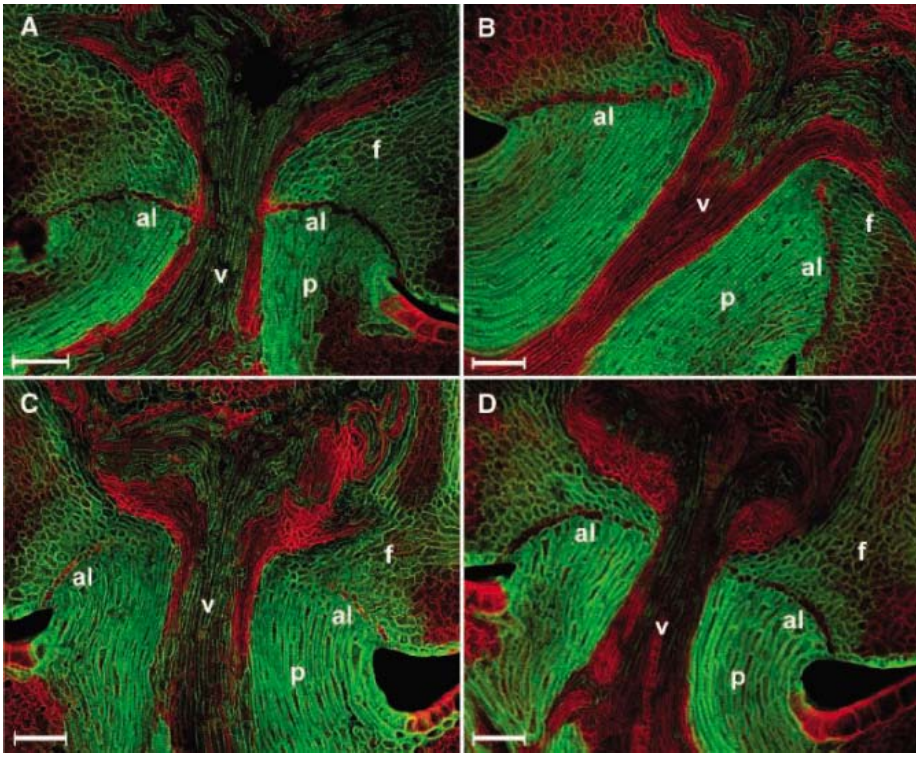

Fig. 4. Fluorescence images of longitudinal section of flower and pedicel junction. (**A**) *O. nivara* mapping parent, with complete abscission layer (al). (**B**) *O. sativa* ssp. *indica* mapping parent, with incomplete abscission layer. (**C**) *O. sativa* ssp. *japonica* Taipei 309, with incomplete abscission layer. (**D**) Transformant of Taipei 309 expressing construct 1, with improved abscission layer. f, flower side; p, pedicel side; v, vascular bundle. Bar, 50 μm.

References and Notes

1. J. R. Harlan, *Crops & Man* (American Society of Agronomy, Madison, WI, 1975).
2. J. F. Hancock, *Plant Evolution and The Origin of Crop Species* (CABI, Cambridge, MA, ed. 2, 2004).
3. V. Poncet *et al.*, *Theor. Appl. Genet.* **100**, 147 (2000).
4. A. H. Paterson, *New Phytol.* **154**, 591 (2002).
5. C.-B. Li, A.-L. Zhou, T. Sang, *New Phytol.* **170**, 185 (2006).
6. H. I. Oka, *Origin of Cultivated Rice* (Japan Scientific Society Press, Tokyo, 1988).
7. S. D. Sharma, S. Tripathy, J. Biswal, in *Rice Breeding and Genetics: Research Priorities and Challenges*, J. S. Nanda, Ed. (Science Publications, Enfield, NH, 2000), pp. 349–369.
8. L. Xiong, K. Liu, K. Dai, C. Xu, Q. Zhang, *Theor. Appl. Genet.* **98**, 243 (1999).
9. H. W. Cai, H. Morishima, *Theor. Appl. Genet.* **100**, 840 (2000).
10. Sobrizal, K. Ikeda, P. L. Sanchez, A. Yoshimura, *Rice Genet. Newslett.* **16**, 74 (1999).
11. Y. S. Nagai *et al.*, *Rice Genet. Newslett.* **19**, 74 (2002).
12. Q. Feng *et al.*, *Nature* **420**, 316 (2002).
13. To screen a large number of seedlings for recombinants, we developed a method of rapid DNA isolation for plants with tough leaves unsuitable for high-throughput protocols (*25*).
14. A. J. Garris, T. H. Tai, J. Coburn, S. Kresovich, S. McCouch, *Genetics* **169**, 1631 (2005).
15. D. A. Vaughan, *The Wild Relatives of Rice: A Genetic Resources Handbook* (International Rice Research Institute, Philippines, 1994).
16. J. L. Riechmann *et al.*, *Science* **290**, 2105 (2000).
17. D. Choi, Y. Lee, H.-T. Cho, H. Kende, *Plant Cell* **15**, 1386 (2003).
18. S. E. Patterson, *Plant Physiol.* **126**, 494 (2001).
19. T. T. Chang, in *Rice: Origin, History, Technology, and Production*, C. W. Smith, R. H. Dilday, Eds. (Wiley, New Jersey, 2003), pp. 3–25.
20. J. Doebley, A. Stec, L. Hubbard, *Nature* **386**, 485 (1997).
21. A. Frary *et al.*, *Science* **289**, 85 (2000).
22. J. Liu, J. Van Eck, B. Cong, T. D. Tanksley, *Proc. Natl. Acad. Sci. U.S.A.* **99**, 13302 (2002).
23. H. Wang *et al.*, *Nature* **436**, 714 (2005).
24. K. Yamasaki *et al.*, *Plant Cell* **17**, 944 (2005).
25. Materials and methods are available as supporting material on *Science* Online.

26. Data have been deposited into GenBank with accession numbers DQ383371 to DQ383414. We thank D. Choi for helping set up rice transformation; S. Owens for suggesting and assisting with confocal microscopy; T. Briggeman for photographing; M. Yano for providing plasmids; J.-P. Hu and J.-L. Fan for helping with the subcellular localization; F. Ewers, N. Gibson, M. Grillo, and W.-X. Zhu for discussion and comments on the manuscript; and S. Ge, B.-R. Lu, and the International Rice Research Institute for providing DNA samples and plant material. The research was supported by the National Science Foundation (USA) and the Rackham Research Endowment Fund.

Supporting Online Material

www.sciencemag.org/cgi/content/full/1123604/DC1
Materials and Methods
Fig. S1
Tables S1 and S2
References

8 December 2005; accepted 28 February 2006
Published online 9 March 2006;
10.1126/science.1123604
Include this information when citing this paper.

Cellulose Synthase–Like *CslF* Genes Mediate the Synthesis of Cell Wall (1,3;1,4)-β-D-Glucans

Rachel A. Burton,[1] Sarah M. Wilson,[2] Maria Hrmova,[1] Andrew J. Harvey,[1] Neil J. Shirley,[1] Anne Medhurst,[2] Bruce A. Stone,[3] Edward J. Newbigin,[2] Antony Bacic,[2] Geoffrey B. Fincher[1]*

A characteristic feature of grasses and commercially important cereals is the presence of (1,3;1,4)-β-D-glucans in their cell walls. We have used comparative genomics to link a major quantitative trait locus for (1,3;1,4)-β-D-glucan content in barley grain to a cluster of cellulose synthase–like *CslF* genes in rice. After insertion of rice *CslF* genes into *Arabidopsis*, we detected (1,3;1,4)-β-D-glucan in walls of transgenic plants using specific monoclonal antibodies and enzymatic analysis. Because wild-type *Arabidopsis* does not contain *CslF* genes or have (1,3;1,4)-β-D-glucans in its walls, these experiments provide direct, gain-of-function evidence for the participation of rice *CslF* genes in (1,3;1,4)-β-D-glucan biosynthesis.

Grasses, which include the common cereals, arguably represent the single most important group of plants for human societies worldwide. Foods prepared from rice (*Oryza sativa*), wheat (*Triticum aestivum*), sorghum (*Sorghum bicolor*), barley (*Hordeum vulgare*), the millets (*Panicum miliaceum* and *Pennisetum americanum*), and sugar cane (*Saccharum officinarum*) account for a high proportion of our daily caloric intake, and numerous forage and fodder grass species support the production of sheep, cattle, and other domesticated livestock. Maize (*Zea mays*) is also used widely for animal feed, and switchgrass (*Panicum virgatum*) and other perennial grasses are showing considerable promise as future biomass energy crops for North America (*1*).

In all cases, the noncellulosic polysaccharides of cell walls in the grasses, which are formally classified in the commelinoid monocotyledon group of land plants (*2*), are crucially linked to the grasses' widespread adoption, utility, and future potential in agricultural practice and energy production. In particular, walls of the grasses contain (1,3;1,4)-β-D-glucans, which are not present in walls of dicotyledons or most other monocotyledonous plants (*2*–*4*). The (1,3;1,4)-β-D-glucans have a structure that is unique in biological systems, insofar as the polysaccharide consists of an unbranched, unsubstituted chain containing a single type of monomeric unit, but with two distinct linkage types that are arranged in a nonrepeating, but nonrandom, fashion (*5*).

The (1,3;1,4)-β-D-glucans are components of dietary fiber that are highly beneficial in the prevention and treatment of serious human health conditions, including colorectal cancer, high serum cholesterol and cardiovascular disease, obesity, and non–insulin-dependent diabetes (*6*, *7*). In contrast, (1,3;1,4)-β-D-glucans have antinutritive effects in monogastric animals, such as pigs and poultry (*7*), and are important in many cereal processing applications, including malting and brewing.

In the work described here, we have identified genes that mediate (1,3;1,4)-β-D-glucan synthesis in the grasses. The first clues to the identity of (1,3;1,4)-β-D-glucan synthase genes came from the discovery of cellulose synthase (*CesA*) genes by Pear *et al*. (*8*). Subsequent analyses of expressed sequence tag libraries and other gene sequence databases indicated that the *CesA* genes were members of a much larger superfamily of genes, which included both the *CesA* genes and the cellulose synthase–like (*Csl*) gene families (*9*–*14*) (fig. S1). Given the chemical similarities between cellulose and (1,3;1,4)-β-D-glucans, it appeared likely that genes encoding (1,3;1,4)-β-D-glucan synthases might be members of one of the *Csl* gene families (*5*).

The *Csl* gene families in most vascular plants are large and have been divided into subgroups, designated *CslA* to *CslH* (*11*) (fig. S1). In *Arabidopsis*, there are at least 30 known *Csl* genes and, in rice, at least 37 (*11*, *15*). In contrast to the *CesA* genes, it has proved difficult to define the functions of the *Csl* genes. Dhugga *et al*. (*16*) first showed that a guar (*Cyamopsis tetragonoloba*) seed (1,4)-β-D-mannan synthase is encoded by a *CslA* gene, and Liepman *et al*. (*17*) recently confirmed that *CslA* family members from rice and *Arabidopsis* also encode (1,4)-β-D-mannan synthases. Thus, of the multiple *Csl* genes in plants, very few have been assigned a biological function.

Here, we have used comparative genomics to identify genes required for (1,3;1,4)-β-D-glucan synthesis in rice. Genetic mapping studies have revealed a high level of synteny, or conservation of genome structure, including gene order (colinearity), in species of the common cereals (*18*). Because (1,3;1,4)-β-D-glucans are central determinants of the malting and brewing qualities of barley, quantitative trait loci (QTLs) of (1,3;1,4)-β-D-glucan contents of ungerminated barley grain have been investigated (*19*). One QTL that has a large effect on (1,3;1,4)-β-D-glucan content in ungerminated grain is located on barley chro-

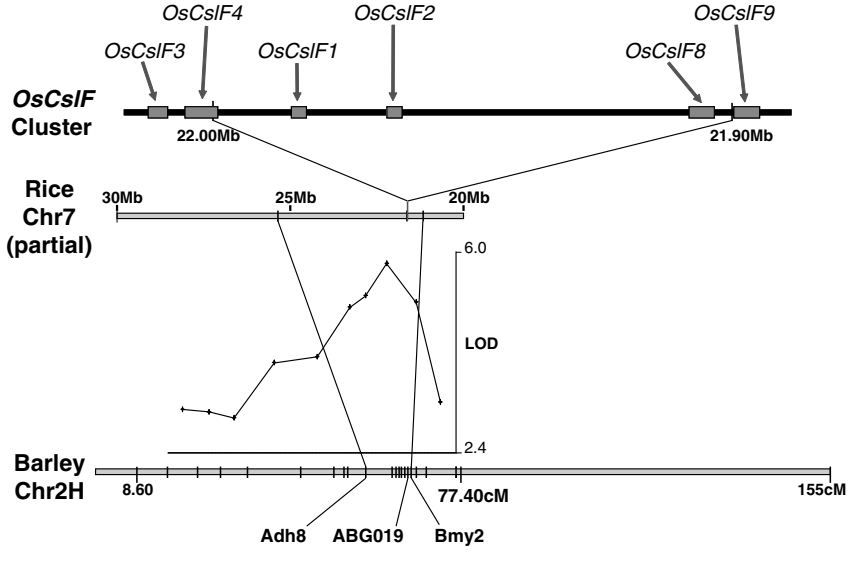

Fig. 1. The *CslF* family was identified as the prime candidate for genes encoding (1,3;1,4)-β-D-glucan synthases. A major QTL for (1,3;1,4)-β-D-glucan content of ungerminated barley grains was identified on barley chromosome 2H by Han *et al*. (*19*) and the logarithm of the likelihood ratio for linkage (lod scores) shown here were derived from that work. Markers flanking the estimated position of the barley chromosome 2H QTL (Adh8, ABG019, and Bmy2), were used to identify a syntenic region of about 3.5 Mb on rice chromosome 7. Examination of the rice genome sequence in this region revealed a group of six *OsCslF* genes, close to the Bmy2 marker; the six genes were clustered within an interval of about 118 kb.

[1]Australian Centre for Plant Functional Genomics; School of Agriculture, Food, and Wine; University of Adelaide, Waite Campus, Glen Osmond, SA 5064, Australia. [2]Australian Centre for Plant Functional Genomics, School of Botany, University of Melbourne, Parkville, VIC 3010, Australia. [3]Department of Biochemistry, La Trobe University, Bundoora, VIC 3086, Australia.

*To whom correspondence should be addressed. E-mail: geoff.fincher@adelaide.edu.au

mosome 2H and is flanked by the Adh8 and ABG019 DNA markers (*19*) (Fig. 1). Because there was no sequence available for the ABG019 marker, we used the sequence of the Bmy2 marker, which is immediately adjacent to the ABG019 marker (*19*) (Fig. 1). Sequences from the Adh8 and Bmy2 markers enabled us to locate a syntenic region of about 3.5 megabases (Mb) on chromosome 7 of rice, in which synteny was confirmed by the presence of more than 10 markers common to both species. Examination of the rice genome sequence corresponding to this region revealed six *Csl* genes clustered in a region of about 118 kilobases (kb) (Fig. 1). The six rice genes are all classified in the *CslF* group and have been designated *OsCslF1*, *OsCslF2*, *OsCslF3*, *OsCslF4*, *OsCslF8*, and *OsCslF9* by Hazen *et al*. (*11*). Besides two truncated *OsCslF* genes that might represent pseudogenes, including the gene designated *OsCslF5* (*11*), five other genes of unknown function and four retrotransposon-like elements were detected in this 118-kb interval of rice chromosome 7. The other *CslF* genes, *OsCslF6* and *OsCslF7*, are located on rice chromosomes 8 and 10, respectively (*20*). We are currently mapping the barley *HvCslF* genes and have so far shown that at least two of the genes map to the region of barley chromosome 2H defined by the (1,3;1,4)-β-D-glucan QTL shown in Fig. 1, close to the Bmy2 marker (*20*).

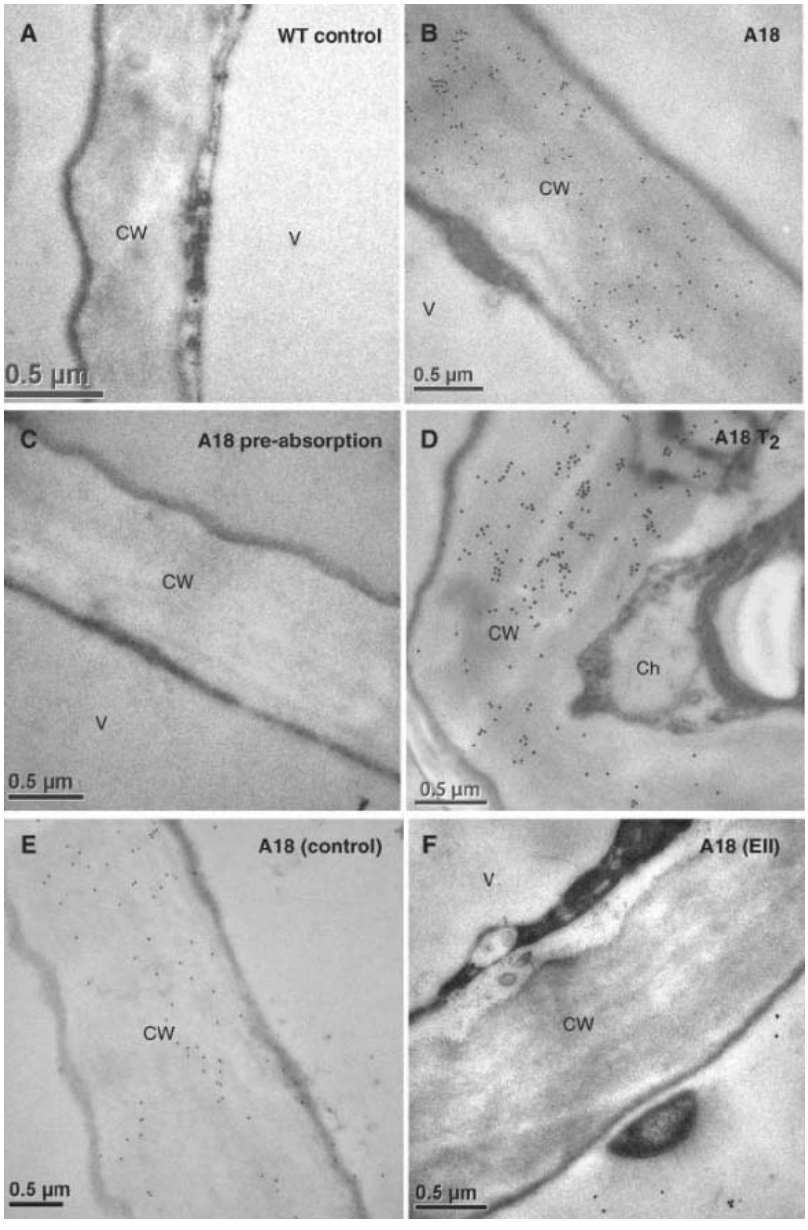

Fig. 2. Immunoelectron microscopy with monoclonal antibodies against barley (1,3;1,4)-β-D-glucan and gold-labeled second stage antibodies show the presence of (1,3;1,4)-β-D-glucan in cell walls of the epidermal layer of leaves from *Arabidopsis* lines transformed with rice *OsCslF* genes. (**A** and **B**) Epidermal walls in leaves from 42-day-old *Arabidopsis* lines confirm the absence of (1,3;1,4)-β-D-glucan in wild-type (WT) *Arabidopsis* controls (A) and the presence of (1,3;1,4)-β-D-glucan in the T_1 A18 line (B). (**C** and **D**) Gold labeling in the walls of A18 plants is not detectable after preincubation of the monoclonal antibody preparation with barley (1,3;1,4)-β-D-glucan (C), whereas the deposition of (1,3;1,4)-β-D-glucan is clearly evident in walls of plants from the T_2 generation of the A18 *Arabidopsis* plant (D). (**E** and **F**) Leaf sections from the transgenic *Arabidopsis* line A18 carrying the rice *OsCslF2* gene were treated before gold labeling with buffer (E) or with barley (1,3;1,4)-β-D-glucan endohydrolase isoenzyme EII (F). The abolition of labeling after the latter treatment confirmed that (1,3;1,4)-β-D-glucan was present in walls of the transgenic *Arabidopsis* lines. CW denotes cell wall, V, vacuole, and Ch, chloroplast.

In this way, comparative genomics enabled us to identify members of the *CslF* group of genes as potential candidate genes for (1,3;1,4)-β-D-glucan synthases in cereals. It is noteworthy that the *CslF* group of genes is found only in monocotyledons (*11*, *13*), consistent with the exclusive occurrence of (1,3;1,4)-β-D-glucans in the cell walls of grasses, cereals, and other members of the Poales (*2*). The possible role of the *CslF* genes in (1,3;1,4)-β-D-glucan synthesis was therefore tested by a gain-of-function approach in transgenic *Arabidopsis* plants. *Arabidopsis* walls contain no (1,3;1,4)-β-D-glucan, and no *CslF* genes are present in the *Arabidopsis* genome (*11*, *21*). Thus, deposition of (1,3;1,4)-β-D-glucan into walls of *Arabidopsis* plants transformed with rice *OsCslF* genes would indicate that the gene products are required for (1,3;1,4)-β-D-glucan synthesis. This approach assumed and depended on the presence and availability in *Arabidopsis* of appropriate donor and acceptor substrates, precursor molecules, activators, intermediates, metal ions, cofactors, or any ancillary enzymes needed for (1,3;1,4)-β-D-glucan synthesis and deposition into the wall.

Accordingly, the full-length open reading frames of *OsCslF2*, *OsCslF4*, and *OsCslF9* cDNAs were amplified from rice (cv. Nippon Bare) RNA preparations using the polymerase chain reaction (PCR), cloned into a binary vector behind the 35*S* promoter (fig. S2), and inserted into *Agrobacterium tumefaciens*, which was used to transform *Arabidopsis* by standard floral dip procedures. In case multiple *OsCslF* genes might be required for (1,3;1,4)-β-D-glucan synthesis, as observed for cellulose biosynthesis (*22*, *23*), transformation was performed not only with single gene constructs, but also with combinations of the *OsCslF* genes. Southern hybridization analyses confirmed the presence of the transgenes, and transcript analyses showed that the 35*S* promoter was driving transcription in selected T_1 and T_2 *Arabidopsis* lines (figs. S5 and S6).

Transgenic *Arabidopsis* lines with high *OsCslF* transcript levels in leaves were chosen for further analysis, specifically with respect to

the deposition of (1,3;1,4)-β-D-glucan in cell walls. In the first instance, immunocytochemical methods based on transmission electron microscopy and a monoclonal antibody raised against (1,3;1,4)-β-D-glucan (*24*) were used to screen for the presence of the polysaccharide in both T_1 and T_2 transgenic *Arabidopsis* lines. The antibody does not bind arabinoxylan, the (1,3)-β-D-glucan, callose, or cellodextrins, and inhibition studies show that it binds very weakly to (1,3;1,4)-β-D-oligoglucosides and xyloglucans, compared with polymeric (1,3;1,4)-β-D-glucan (*24*, *25*). (1,3;1,4)-β-D-Glucan was detected in epidermal cell walls in three of nine T_1 transgenic *Arabidopsis* plants examined, namely, lines A18 (Fig. 2, B and E), A28, and A29 (fig. S7, C and D). Within the epidermal layer, gold labeling in walls was not uniformly distributed. In cells where walls were labeled, the labeling was distributed all around the cell, but was often more intense in the outer periclinal wall of the epidermal cells, adjacent to the cuticle. In control experiments, preincubation of the antibody with (1,3;1,4)-β-D-glucan prevented subsequent antibody binding, so that no gold labeling was observed (*24*) (Fig. 2C). The A18 and A29 lines contained single copies of the *OsCslF2* cDNA, whereas line A28 had two copies of the *OsCslF4* cDNA (fig. S5) (*26*). The *OsCslF* transgenes were isolated by PCR from the three T_1 lines and from the T_2 line of A18 (Fig. 2D), completely sequenced, and shown to have no errors.

Although extensive competition studies have demonstrated that the specificity of the monoclonal antibody against (1,3;1,4)-β-D-glucans is high (*24*), the presence of (1,3;1,4)-β-D-glucans in the walls of transgenic *Arabidopsis* lines was further examined by pretreatment of fixed leaf sections with a specific (1,3;1,4)-β-D-glucan endohydrolase before immunogold labeling (Fig. 2, E and F). Purified barley (1,3;1,4)-β-D-glucan endohydrolase isoenzyme EII (EC 3.2.1.73) was obtained following heterologous expression of the corresponding cDNA in *Escherichia coli* (*27*). When leaf sections of the transgenic *Arabidopsis* line A18 were pre-incubated with the purified enzyme preparations before probing with the specific monoclonal antibodies, gold-labeling was essentially abolished, consistent with the enzymatic removal of (1,3;1,4)-β-D-glucans from walls of these lines (Fig. 2F). In control sections pretreated with buffer, subsequent labeling was unaffected (Fig. 2E). Again, this confirmed that the *Arabidopsis* lines transformed with the *OsCslF2* gene contained (1,3;1,4)-β-D-glucan in their cell walls. We estimate that the (1,3;1,4)-β-D-glucan content of walls in the transgenic *Arabidopsis* lines is considerably less than 0.1% (wt/wt). Trethewey *et al*. (*2*) also concluded that the immunocytological procedure could detect levels of (1,3;1,4)-β-D-glucan corresponding to less than 0.1% of the wall, and noted the high sensitivity of the immunocytological method compared with enzymatic analyses in a survey of (1,3;1,4)-β-D-glucan content of walls in the Poales. Chemical characterization of such small amounts of (1,3;1,4)-β-D-glucan by methylation analysis was not possible against a background of high levels of cellulose and xyloglucans in the *Arabidopsis* walls and of callose in associated plasmodesmata.

The combined QTL, transcript, immunocytochemical, and enzymatic data presented here indicate that *CslF* genes are essential for (1,3;1,4)-β-D-glucan biosynthesis in grasses and cereals. However, the observations do not preclude a requirement for other enzymes, proteins, or cofactors in (1,3;1,4)-β-D-glucan synthesis. The generally low levels of (1,3;1,4)-β-D-glucan in walls of the transformed *Arabidopsis* plants, where *OsCslF* transcript levels were often high, would be consistent with limiting levels of other components that might be required for high-level synthesis of the polysaccharide or its transfer to the cell wall. Similarly, the preferential deposition of the (1,3;1,4)-β-D-glucan in the epidermal layers of the transgenic *Arabidopsis* lines, despite the fact that transgene expression was driven by the constitutive 35*S* promoter, could indicate that the epidermal cells contain ancillary factors that are not abundant in other cells of the leaf.

References and Notes

1. J. S. McLaren, *Trends Biotechnol.* **23**, 339 (2005).
2. J. A. K. Trethewey, L. M. Campbell, P. J. Harris, *Am. J. Bot.* **92**, 1660 (2005).
3. A. Bacic, P. J. Harris, B. A. Stone, in *The Biochemistry of Plants*, vol. 14, J. Priess, Ed. (Academic Press, New York, 1988), pp. 297–371.
4. N. C. Carpita, D. M. Gibeaut, *Plant J.* **3**, 1 (1993).
5. G. B. Fincher, B. A. Stone, in *Encyclopedia of Grain Science*, vol. 1, C. W. Wrigley, H. Corke, C. E. Walker, Eds. (Academic Press, New York, 2004), pp. 206–223.
6. J. T. Braaten *et al.*, *Eur. J. Clin. Nutr.* **48**, 465 (1994).
7. C. S. Brennan, L. J. Cleary, *J. Cereal Sci.* **42**, 1 (2005).
8. J. R. Pear, Y. Kawagoe, W. E. Schreckengost, D. P. Delmer, D. M. Stalker, *Proc. Natl. Acad. Sci. U.S.A.* **93**, 12637 (1996).
9. I. M. Saxena, R. M. Brown Jr., *Cellulose* **4**, 33 (1997).
10. T. A. Richmond, C. R. Somerville, *Plant Physiol.* **124**, 495 (2000).
11. S. P. Hazen, J. S. Scott-Craig, J. D. Walton, *Plant Physiol.* **128**, 336 (2002).
12. P. M. Coutinho, B. Henrissat, in *Recent Advances in Carbohydrate Bioengineering: Carbohydrate-Active Enzymes: An Integrated Database Approach*, H. J. Gilbert, G. Davies, B. Henrissat, B. Svensson, Eds. (The Royal Society of Chemistry, Cambridge, 1999), pp. 3–12.
13. Sequence information related to plant cell wall biosynthesis (http://cellwall.stanford.edu/).
14. Families of carbohydrate-active enzymes (http://www.cazy.org/CAZY/).
15. C. Somerville *et al.*, *Science* **306**, 2206 (2004).
16. K. S. Dhugga *et al.*, *Science* **303**, 363 (2004).
17. A. H. Liepman, C. G. Wilkerson, K. Keegstra, *Proc. Natl. Acad. Sci. U.S.A.* **102**, 2221 (2005).
18. M. D. Gale, K. M. Devos, *Proc. Natl. Acad. Sci. U.S.A.* **95**, 1971 (1998).
19. F. Han *et al.*, *Theor. Appl. Genet.* **91**, 921 (1995).
20. R. A. Burton, A. J. Harvey, G. B. Fincher, unpublished observations.
21. E. Zablackis, J. Huang, B. Muller, A. G. Darvill, P. Albersheim, *Plant Physiol.* **107**, 1129 (1995).
22. N. G. Taylor, S. Laurie, S. R. Turner, *Plant Cell* **12**, 2529 (2000).
23. R. A. Burton, N. J. Shirley, B. J. King, A. J. Harvey, G. B. Fincher, *Plant Physiol.* **134**, 224 (2004).
24. P. J. Meikle, N. J. Hoogenraad, I. Bonig, A. E. Clarke, B. A. Stone, *Plant J.* **5**, 1 (1994).
25. S. M. Wilson, E. J. Newbigin, A. Bacic, unpublished observations.
26. R. A. Burton, G. B. Fincher, unpublished observations.
27. R. J. Stewart, J. N. Varghese, T. P. J. Garrett, P. B. Høj, G. B. Fincher, *Protein Eng.* **14**, 245 (2001).

28. We thank A. Jacobs for providing the transformation vectors; J. Chambers, M. Pallotta, M. Pickering, and J. Rethus for their skilled technical assistance; and M. Doblin, M. Henderson, D. Mather, C. Vergara, and D. Yulia for valuable contributions to various aspects of the work. The work was funded by the Grains Research and Development Corporation, the Australian Research Council, and the state government of South Australia.

Supporting Online Material

www.sciencemag.org/cgi/content/full/311/5769/1940/DC1
Materials and Methods
SOM Text
Figs. S1 to S9
Tables S1 and S2
References

23 November 2005; accepted 31 January 2006
10.1126/science.1122975

Microplate Dispenser

The NanoQuot Microplate Dispenser is an affordable, low-volume liquid-dispensing instrument for the life science research and drug discovery markets. The NanoQuot dispenses volumes down to 0.1 μl precisely and accurately into 96-well, 384-well, and 1536-well microplates. It features an uncomplicated user interface and optional stacker.

BioTek Instruments For information 802-655-4040 www.biotek.com

Automated Extraction of Information from Text

MedScan Reader 1.0 is desktop software that enables automated extraction of information from scientific text. Designed for a broad range of life-science professionals, the software facilitates reading and reduces time spent on literature research. MedScan Reader offers the ability to read and digest thousands of abstracts or documents on the fly, summarize content, and provide an instant snapshot of relevant information. It can process documents on numerous aspects of protein function, biochemistry, cellular physiology, and molecular pathology.

Ariadne Genomics For information 847-644-1557 www.ariadnegenomics.com

Histidine-Tagged Protein Purification

The His SpinTrap is a single-use column designed for efficient purification of histidine-tagged proteins using a standard microcentrifuge. The His SpinTrap allows direct loading of unclarified homogenized cell lysates, without the need for centrifugation or filtration of the sample. The His SpinTrap saves time as it eliminates the need for tedious sample preparation and enables direct protein purification in as little as 10 min per run. By reducing the total purification time, the spin column procedure minimizes the degradation and oxidation of sensitive protein samples and preserves the activity of the target protein.

GE Healthcare For information 732-457-8082 www.gehealthcare.com

Message Booster Kit

The MessageBooster cDNA Synthesis Kit for quantitative polymerase chain reaction (qPCR) improves quantitative reverse transcription-PCR sensitivity of low-abundance transcripts from as little as 1 cell. A MessageBooster reaction amplifies the poly(A) RNA in total RNA from 1 to 50 cells and then converts the amplified RNA to complementary DNA that is ready for qPCR. The process makes use of a linear RNA amplification process that maintains the gene expression profile of the sample.

Epicentre Biotechnologies For information 800-284-8474 www.EpiBio.com

Methods Development Microplate

Two new versions are available of the Microlute 96-well solid-phase extraction (SPE) microplate, which is designed to help accelerate methods development in drug research. The Microlute Methods Development plates offer the user a choice of 8 or 12 different phases and sorbent volumes (10 to 100 mg). This allows the user to rapidly and simply identify the optimal sorbent and loading for a specific application. Constructed from a single piece of molded high-quality plastic, a Microlute Methods Development plate will not bend or distort because individual solid-phase extraction cartridges do not have to be repeatedly plugged in and out. Each well on the plate has an individual drain spout ensuring 100% sample transfer and zero crossover contamination.

Porvair Sciences For information +44 1932 240255 www.porvair-sciences.com

Protease Inhibitor Cocktails

ProteCease protease inhibitor cocktails contain optimized concentrations of various protease inhibitors, which provide superior inhibition of protease activities during protein purification from a wide selection of species. ProteCease has been developed for large-scale preparative applications and is available in two sizes for 50 ml or 100 ml of lysis buffer. ProteCease is available with EDTA (to inhibit metalloproteases) or without EDTA (to maintain activity of proteins dependent on divalent cations). The EDTA-free ProteCease will not inhibit the purification of proteins with immobilized metal affinity chromatography. The convenient format ensures the delivery of consistent concentrations of protease inhibitors that have high protease inhibition (>90% in mouse pancreas lysate).

G-Biosciences/Genotech For information 800-628-7730 www.GBiosciences.com

Literature

The 2006–2007 Cayman Catalog contains more than 300 new biochemicals, including eicosanoids, nitric oxide reagents, lipids, fatty acids, inhibitors, antibodies, and enzymes. It features assay kits for the measurement of eicosanoids, cyclic nucleotides, cytokines, hormones, nitrate/nitrite, oxidative stress markers, and enzymes. It also features charts, graphs, and gene maps.

Cayman Chemical For information 800-364-9897 www.caymanchem.com

Newly offered instrumentation, apparatus, and laboratory materials of interest to researchers in all disciplines in academic, industrial, and government organizations are featured in this space. Emphasis is given to purpose, chief characteristics, and availability of products and materials. Endorsement by *Science* or AAAS of any products or materials mentioned is not implied. Additional information may be obtained from the manufacturer or supplier by visiting www.science.labvelocity.com on the Web, where you can request that the information be sent to you by e-mail, fax, mail, or telephone.

ScienceCareers.org

Classified Advertising

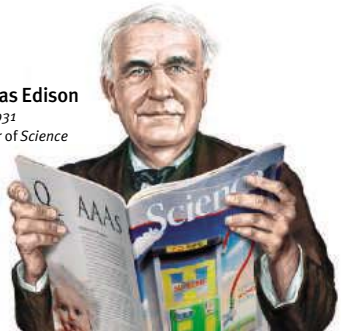

Thomas Edison
1847–1931
Founder of *Science*

For full advertising details, go to **www.sciencecareers.org** and click on **How to Advertise,** or call one of our representatives.

United States & Canada

E-mail: advertise@sciencecareers.org
Fax: 202-289-6742

JILL DOWNING
(CT, DE, DC, FL, GA, MD, ME, MA, NH, NJ, NY, NC, PA, RI, SC, VT, VA)
Phone: 631-580-2445

KRISTINE VON ZEDLITZ
(AK, AZ, CA, CO, HI, ID, IA, KS, MT, NE, NV, NM, ND, OR, SD, TX, UT, WA, WY)
Phone: 415-956-2531

KATHLEEN CLARK
Employment: AR, IL, LA, MN, MO, OK, WI, Canada; Graduate Programs; Meetings & Announcements (U.S., Canada, Caribbean, Central and South America)
Phone: 510-271-8349

EMNET TESFAYE
(Display Ads: AL, IN, KY, MI, MS, OH, TN, WV; Line Ads)
Phone: 202-326-6740

GABRIELLE BOGUSLAWSKI
(U.S. Recruitment Advertising Sales Director)
Phone: 718-491-1607

Europe & International

E-mail: ads@science-int.co.uk
Fax: +44 (0) 1223-326-532

TRACY HOLMES
Phone: +44 (0) 1223-326-525

HELEN MORONEY
Phone: +44 (0) 1223-326-528

CHRISTINA HARRISON
Phone: +44 (0) 1223-326-510

SVITLANA BARNES
Phone: +44 (0) 1223-326-527

JASON HANNAFORD
Phone: +81 (0) 52-789-1860

To subscribe to *Science*:
In U.S./Canada call 202-326-6417 or 1-800-731-4939
In the rest of the world call +44 (0) 1223-326-515

Science makes every effort to screen its ads for offensive and/or discriminatory language in accordance with U.S. and non-U.S. law. Since we are an international journal, you may see ads from non-U.S. countries that request applications from specific demographic groups. Since U.S. law does not apply to other countries we try to accommodate recruiting practices of other countries. However, we encourage our readers to alert us to any ads that they feel are discriminatory or offensive.

ScienceCareers.org
We know science AAAS

Immunology/ Infectious Disease Research Careers

Advertising Supplement

Get the experts behind you.

Be sure to read this special ad supplement devoted to immunology and infectious disease career opportunities in the upcoming **5 May issue of *Science*.**

Find immunology and infectious disease research jobs and other career resources online at **www.sciencecareers.org.**

For advertising information, contact:

U.S. Daryl Anderson, phone: 202-326-6543, e-mail: danderso@aaas.org

Europe and International, Tracy Holmes, phone: +44 (0) 1223 326 500, e-mail: ads@science-int.co.uk

Japan Jason Hannaford, phone: +81 (0) 52 789-1860, e-mail: jhannaford@sciencemag.jp

ScienceCareers.org
We know science AAAS

YYePG Proudly Presents, Thx for Support

Careers in Biotech & Pharma

Changing Courses

Industry offers life scientists multiple opportunities to apply their abilities beyond the bench. Their options include clinical research, regulatory affairs, project management, patent law, and medical communications, all of which require a foundation of basic science. Many firms will help to finance training that permits life scientists to develop the extra skills they need for work outside the lab. BY PETER GWYNNE

Scientists who start their corporate lives in the research laboratory don't have to spend their entire careers at the bench. The pharmaceutical and biotechnology industries, in particular, offer researchers plenty of opportunities to participate in other facets of their companies' enterprises. Such areas as project management, drug development, regulatory affairs, business development, and intellectual property protection demand individuals with strong scientific backgrounds. "There's a spectrum of opportunities, from close-to-the-bench work to the commercial arena," says Matthew Bell, senior director of discovery research at Wyeth. "Supporting scientists who have interests in other, nonresearch-based areas of our organization is extremely valuable for both the employees and the company," adds Lex Van der Ploeg, vice president and basic research site head for Merck Research Laboratories Boston.

Scientists with all levels of training can qualify for work outside the laboratory. Individuals with Bachelor's, Master's, and doctoral degrees, and even postdoctoral experience, can move on to successful careers outside the research arena. The only essential element is the scientific background that permits researchers to bridge the gaps between the lab and the commercial arena. "We consciously do not place degree requirements on internal transfers," says Promega's chief technology officer, Randall Dimond. "They are based only on the perceived capabilities of the individuals." CONTINUED »

Affymetrix
http://www.affymetrix.com

Amgen
http://www.amgen.com

Abbott
http://www.abbott.com

AstraZeneca
http://www.astrazeneca.com

Merck Research Laboratories Boston
http://www.merckboston.com

Promega
http://www.promega.com

Wyeth
http://www.wyeth.com

Careers in Biotech & Pharma

To make a success of careers outside the laboratory, researchers obviously need competencies beyond their scientific expertise. "There's no doubt that cross-disciplinary skills are very, very important in industry," explains Jill Mueller, group vice president for R&D at Abbott. "Scientists with a strong business savvy are very much in demand."

Some of those skills, such as communications ability and an aptitude for leadership, are largely inherent. Scientists can obtain more concrete capabilities through training programs. Many pharmas and biotech firms organize their own courses in such fields as business skills, entrepreneurship, and intellectual property issues. And some will pay for their scientists to attend night school for specific qualifications such as MBA degrees and professional certificates.

MATTHEW BELL

Dual Career Tracks

Companies recognize that not all researchers want to leave the bench for other pursuits. Many firms offer dual career tracks that permit scientists to stay at the bench without sacrificing their chances of corporate prestige and financial advancement. "We've developed a scientific career path that allows scientists to stay at the bench and progressively move through larger responsibilities in science," says Ellen Nichols, associate director for human resources in Amgen's research group. AstraZeneca takes a similar approach. "In many cases, outstanding scientists feel they have to leave the bench if they want to advance their careers," says HR vice president for discovery Jenni Hardy. "We have some of the best and brightest researchers in the world and we place incredible value on their contributions. That's why we established our scientific career ladder which aims to recognize scientific excellence."

Mark Rakic, director of human resources and staffing for Affymetrix, summarizes the basic philosophy of the twin track approach. "We give our scientists the opportunity to stay within the lab if that's their passion," he says. "We tap into their passion for the job whatever it is."

For individuals who want to leave the bench, pharmas and biotech firms offer a wide variety of alternative career paths that start with pursuits closely related to research in the lab and extend to work that's almost entirely on the commercial side. "Project and portfolio management are two common places scientists move to," Bell notes. "Project management gives them the chance to remain in project teams but to be involved in the management and driving of a project; almost all our managers have scientific or medical backgrounds."

Drug development represents another natural avenue for scientists who want to move out of research without going too far away. "The majority of our leaders in drug development are scientists," Mueller says. "We have several vice presidents heading up therapeutic levels and even doing marketing, as well as life cycle management of drugs. Clinical trialing is another option. The majority of our global clinical heads are scientists."

RANDALL DIMOND

Business Benefits

Sales and marketing and related business activity have great appeal for certain researchers. "We have a number of scientists who have moved beyond the lab and are working in our sales organization in field applications. They provide a liaison between the sales person and the customer," Rakic says. "We also have people in our genomics collaboration organization, which gives scientists the opportunity to move into more of a consulting role."

Other aspects of business benefit from the understanding and feel that early work in research imparts. "The nature of business development is that you are still working with the science but looking at opportunities," Bell says. "In business development you really want scientists to evaluate licensing deals, mergers and acquisitions, and other opportunities in the scientific world," Mueller adds. "And scientific acumen is very helpful in the regulatory world."

Some business tasks demand more technical competencies. Intellectual property protection, for example, requires at least some training in patent law and often a law degree. Lawyers with scientific backgrounds can also provide valuable help to business development departments that need to work out the details of licensing deals.

Even further upstream from the basic research lab are commercially focused pursuits such as medical writing and communications. "Here you also need the scientific background," Bell says. "Many practitioners have Ph.D.s or even postdoctoral experience."

Surprisingly, several firms expect scientists who move into sales to possess higher degrees. "Sales relies on people who are facile in their knowledge of the products, as they have to interact with Ph.D.s and postdocs as their customers," Promega's Dimond explains. "So they are usually people with Master's or Ph.D. degrees."

Successful Transitions

Examples of successful transitions abound. Take the career path of Bell, who joined Wyeth as a researcher after earning his Ph.D. in neuroscience. "I got involved in management consulting and then strategy and business planning," he recalls. "We have created a team staffed almost entirely by former scientists with business skills." CONTINUED »

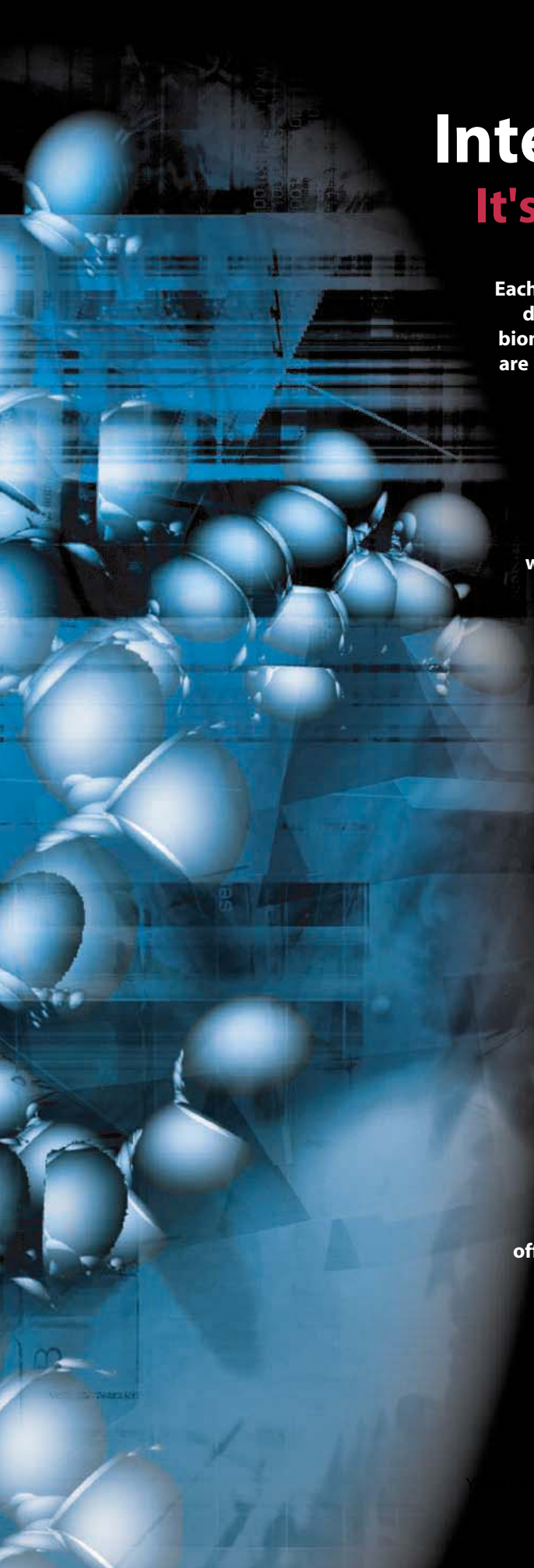

Intellectual Curiosity.

It's Our Organizational DNA.

Each day, Invitrogen puts the vast potential of biology into action, devising technologies used in life science research, commercial biomolecule production, and drug discovery. Our labs and offices are infused with entrepreneurial energy and intellectual curiosity that foster questions and answers that ultimately produce real-world results in more than 70 countries.

We invite you to join us on the greatest adventure of all: the quest for biological understanding.

Our journey to answer science's ultimate question of how life works requires the best and brightest minds from every corner of the globe. Our most profound breakthroughs are the result of thousands of talented employees and their never-ending questions. Without their inquisitive minds, many of the greatest discoveries of the last two decades may never have been realized. Their endless curiosity helped us create products and services that were used in the discovery of the AIDS virus and the sequencing of the human genome, as well as critical advancements in cancer research.

One of your questions could be the key to the very next industry breakthrough.

If you possess a sense of urgency, true intellectual curiosity, and the desire to collaborate with lead scientists in nearly every medical, academic, and private institute, as well as pharmaceutical and diagnostic companies, we want to talk with you.

Stop by Booth #243 at
The BIO 2006 Career Fair
Sunday, April 9th, 11am - 4pm
Hyatt Regency, Chicago.

Invitrogen is an Equal Opportunity Employer and is proud to offer a comprehensive benefits package that leads our industry.

Visit www.invitrogen.com/careers.

Equal Opportunity Employer.

invitrogen™

Careers in Biotech & Pharma


JENNI HARDY

Nichols relates a slightly different story. "I came to Amgen 17 years ago from a clinical background; I was a nurse and I love patient care," she says. "This is a company where you can expand your career after coming in with basic bench experience and go in many career directions."

Merck Research Laboratories Boston offers a similar case. Its head of external scientific affairs, who deals with outside organizations on such issues as licensing and technology transfer, started life as a bench scientist. "There are many other cases like that in the company," Van der Ploeg says. "There are opportunities for basic researchers in many departments across the organization."

The career tracks of two Promega scientists with Master's degrees in biology indicate that departure from the lab can be the first step in a journey without an obvious finishing point. Hired as a bench scientist, Eddie Pahuski moved on to jobs as group leader in food technology, process development manager, and technical operations manager before assuming his present role as vice president of quality assurance and process development. And research scientist Angela Ryan first became a technical services scientist and then transferred to the product management department before becoming marketing manager for clinical diagnostics. Now she is marketing manager for genomics.


JILL MUELLER

Beyond Scientific Excellence

What characteristics do employers seek in scientists whom they want in jobs outside the lab? "Scientific excellence goes without saying," Mueller says. "Vision is also critical. Scientists need to be able to develop a vision for science and business not only today but also for the future. And they need a passion for learning and for teaching others." Nichols outlines two other qualities common to almost every scientist who wants to leave the bench – and even those destined to stay there. "To move into other areas, we need scientists who are very good communicators and team players," she says. "People who want to stay in science also need training in teamwork, leadership, and communications."

Employers generally agree that communications ability represents the most critical characteristic for scientists whom they want to move to jobs outside the lab. "There are no hard and fast rules about the qualities we need," Bell explains. "But you have to have very strong communication skills – communicating with people and presenting your ideas crisply and in a way that's understandable to nonscientists. A lot of scientists are very good at presenting lots of data. It's a slightly different skill to take lots of information and boil it down to its essentials. A scientist who can transition successfully to the business side should be able to do that." Affymetrix's Rakic agrees. "Communication needs to be a high-end skill," he says. "Scientists need to be able to translate scientific jargon into communication that the general public can understand."

Scientists who want to move beyond their own research interests must also learn empathy. "You have to have the ability to take charge of your own tasks while being sensitive to the problems of others, and seeing where you can help solve those problems," Van der Ploeg says. Bell echoes that thought. "We're looking for people who can transition from a lab-based environment in which they're thinking mainly of their own work to someone who can take a broader view," he explains.


ELLEN NICHOLS

Experience Abroad

Experience beyond national shores also serves as a positive indicator for scientists who want to work beyond the bench. "Global experience is effective for scientists moving out of the laboratory," Mueller says. "We look for that in internal candidates and when we hire people outside the company." Such experience, she explains, can include both studying and working abroad. "Having experience in drug discovery overseas is very useful," she continues. "It helps to give individuals cultural sensitivity." Rakic cites an example of a scientist about to gain that type of experience on the job. Having joined Affymetrix after a postdoctoral fellowship, the researcher is moving to Japan to continue work on a project that he started at the basic level in the lab in the United States. "He wanted to move into a different role leveraging different skill sets," Rakic says.

Specific tasks require particular skills. "We place a great emphasis on project leadership and people management," AstraZeneca's Hardy says. "We are a project-driven organization, and individuals who are skilled project managers will find a world of opportunity available to them across R&D and the rest of the company. We also look for scientists who can motivate teams to deliver results and who can create a climate that delivers innovative solutions."

Sales and marketing have their own demands. "A person moving into the marketing or sales environment needs to be very gregarious, to have a different level of interaction skills, and to be able to connect with customers in a different way," Rakic explains.

Companies have their own unique ways of identifying scientists with the talent and the desire to leave the bench. Approaches include monitoring scientists for clues to their nonscientific talents and relying on individuals to inform managers of their interest in life beyond the lab. Managers play key roles. "There is significant career counseling within a manager's portfolio to ensure that every employee is on a steep learning curve, and to see the development of other scientific interests outside the employees' fields," says Merck's Van der Ploeg. CONTINUED »

Careers in Biotech & Pharma


MARK RAKIC

Open Application System

Affymetrix exemplifies the range of possibilities. "We observe scientists' management abilities," he says. "As they grow in the lab they will take on larger projects and will lead research assistants or other scientists. We don't use the title 'manager,' but in fact they are managers. So we observe and monitor them." The company also encourages its scientists to apply for positions outside the laboratory. "We have an open system," Rakic continues. "People can apply for all internal job postings. Scientists who desire to move into other areas have the ability to do so."

Promega also posts its open positions internally. "Anybody who feels ready to make a move and has the right background can apply," Dimond says. "We work on the individual level, but have a couple of things that facilitate moves. We require that supervisors participate in the career planning. And since we're a pretty flat-structure organization that uses a lot of cross-functional teams, R&D scientists working on a new product will typically serve on a team with representatives of marketing, quality assurance, manufacturing, and sales. That gives them a more realistic view of what those people do. Supervisors might give a scientist who wants to move into a specific area a role on the cross-functional team relevant to the task."

Abbott takes a similar approach. "A combination of both managers and individuals makes the decision," Mueller says. "Individual scientists might bring up the idea of other opportunities to their managers. We also target our top talent through various avenues. We think very much out of the box; when we're filling different jobs, we like to think beyond particular disciplines and move people from other groups." Amgen also relies on both managers and scientists to identify new opportunities. "Managers have performance reviews and development discussions with each staffer," Nichols explains. "That's when interest in licensing and development and commerce can be found. If someone expresses interest, the manager may come to me, and I will maybe match the scientist up with a mentor in one of the areas."

Means of Training

The decision to move out of the lab – on the part of scientists and their companies – doesn't necessarily happen quickly. "These things play out over the years," Van der Ploeg says. "They don't come about on short notice. It's important to support, build, and maintain the best possible work force with the people you know."

Whenever it happens, scientists who transfer out of the laboratory need adequate training for their new jobs. That usually involves a mixture of internal instruction and outside courses whose cost the company covers entirely or in part.

Abbott offers several internal programs. "We have a professional development program that hits all disciplines," Mueller says. "People can go through a development rotational opportunity to see how they fit in different tasks. We also have a marketing development program in which we're looking for our commercial leaders and a leadership development for scientists program that has a very heavy curriculum for business and finance."

Promega gives its scientists the chance to learn new skills on the job, as well as in conventional training programs. "Supervisors will put scientists into specific opportunities or give them formal training – internal or external, such as an MBA degree," Dimond says. "If they want additional programs, whether a week-long seminar, a course, or a degree program, Promega will reimburse them if the course is relevant to work they do here."

Many other biotech and pharma firms give scientists part or all of their tuition fees for degree courses. "We offer a robust tuition reimbursement program in some of our U.S. research centers which is highly competitive," AstraZeneca's Hardy says. MBA degrees are particularly popular. "Many scientists choose to take an MBA and use that as a pivot point," Bell says. "If you want to increase your skill set, Wyeth will support you in doing that."


LEX VAN DER PLOEG

Payment for Night School

Usually, firms encourage their scientists to study for their MBAs in night school. "Ours is a partnership in education. Staff members pursue their training in local universities outside working hours, subsidized by Amgen," Nichols says. "Our Boston location puts us in the center of great universities where people can attend classes while successfully managing their daily work and family commitments," Merck's Van der Ploeg adds.

Some companies also pay for scientists to obtain legal qualifications, for future work in intellectual property protection. "We had one scientist in our chemistry group who is now working as a patent agent," Rakic relates. "She had the technical domain experience. We funded her educational pursuit to get a patent certification." Promega currently has a scientist studying for a law degree. "He came from R&D into business development and then into licensing," Dimond says. "We're paying for him to go to law school part time."

Moving out of the lab requires self-confidence and willingness to take risks on the part of scientists and the provision of encouragement and training by corporations. But the rewards for individuals, who can pursue their career interests, and for companies, which gain a cadre of scientifically trained staffers for positions of responsibility, make the costs worthwhile.

A former science editor of Newsweek, *Peter Gwynne (pgwynne767@aol.com) covers science and technology from his base on Cape Cod, Massachusetts, U.S.A.*

New Scientists, Senior scientists and Department Head positions offered at Novo Nordisk China R&D center

Zhongguancun Life Science Park, Beijing, China

Novo Nordisk is a focused healthcare company and a world leader in diabetes care. Novo Nordisk China R&D (NNCR&D) is an integrated part of Novo Nordisk's growing international R&D organization. Building on its extensive expertise in protein expression and purification, NNCR&D actively pursues novel drug target identification and evaluation in the areas of cancer immunology and inflammatory diseases.

NNCR&D has three departments: Molecular Biology, Protein Chemistry and Cell Biology. We are now announcing a number of new scientist positions in these departments and we are seeking for highly motivated colleagues, who plan to advance their career in China. Scientists applying for these positions will take part in the following responsibilities: 1) Expression, purification and analysis of therapeutic proteins like e.g. mAbs produced and optimized at laboratory to pilot scale; 2) Novel drug target identification and evaluation of opportunities in immunotherapy of cancer and inflammation.

The successful candidates must have the following qualifications: 1) Ph.D. in immunology combined with one of the following core technologies: cell biology, biochemistry, molecular biology or protein chemistry; 2) >2 years (Post Doc.) hands-on experience and a good scientific track record within immunology, inflammation and/or cancer research; 3) preferentially industry and/or international experience; 4) independent innovator and at the same time a strong team-player, enjoy problem solving and love the challenge of achieving ambitious goals; 5) excellent communication skills in English, which is the official company language.

Title and compensation will be dependent on the individual candidate's qualifications. For detailed information regarding individual positions, please check the website **www.ebiotrade.com/jobf** or send an inquiry via e-mail to **nncprd@novonordisk.com**

THE ULTIMATE SYMBIOTIC RELATIONSHIP.

Focusing on a common goal. Performing your job accurately so that the next person can do theirs. That's how we work together at ICON Clinical Research. Because at ICON, your personal best is the valuable link we need to achieve quality results.

Working with ICON, you'll share in a unique culture of a large company that emphasizes a warm, friendly environment. This is where career possibilities can become realities... where those who look for challenges, embrace the learning and growth opportunities we offer.

ICON Clinical Research is dedicated to providing the pharmaceutical and biotechnology industries with exceptional clinical research and biometrics services, and we're the first international CRO awarded ISO 9001:2000 quality certification across all divisions and functions.

To continue our legacy of excellence at ICON, GloboMax, a dynamic and innovative Product Development Organization committed to helping pharmaceutical and biotech companies bring products through development from early stage to regulatory approval, is now the Strategic Pharmaceutical Development Division of ICON.

-Clinical Research Associates - all levels, all locations. Experience required.
-Clinical Project Managers - all locations. Experienced required.

Come to ICON and you'll enjoy highly competitive benefits in addition to flexible scheduling, relocation assistance, tuition reimbursement, credit union, health club privileges, and many other exceptional advantages.

To apply, or for more information on our opportunities, please visit us at www.iconclinical.com and CLICK ON EMPLOYMENT OPPORTUNITIES. No agencies, please.

ICON Clinical Research is an Equal Opportunity Employer committed to strength in diversity.

ICON
www.iconclinical.com

ICON. we are the right solution.

Are you looking to work in a global growth company where you can make a real difference? With more than 81,400 associates around the globe in our affiliates in over 140 countries, we share a vision of a better today and tomorrow for patients - a vision that drives our growth and success. Our greatest job satisfaction is knowing that we improve lives, we extend lives, and we save lives - and we do it with increasing precision and efficiency through breakthrough science and innovation.

Research Investigator – Pharmacology

Job ID 7255BR

Novartis Institute for Tropical Diseases, Singapore

Reporting to the Unit Head for Pharmacology, you will be responsible for the *in vitro* and *in vivo* evaluation of novel drug candidates in relevant assays and models in the Tuberculosis & Dengue areas. You will be expected to contribute towards the development of new Tuberculosis and Dengue models and the optimization of existing models, as well as implement conventional *in vitro* and *in vivo* ADME studies. In addition, you will develop efficacy models utilizing non-invasive imaging technologies and expand our repertoire of mechanistic models.

Your Profile:

- PhD in Pharmacology, Biology, Medical or Veterinary Science, with at least 2 years of relevant post-doctoral research or industry experience
- Familiar with modern concepts and technologies of drug discovery, in particular the study of pharmacokinetic and pharmacodynamic parameters
- Hands-on experience in pharmacokinetic profiling of small molecules *in vitro*, and pharmacokinetic studies *in vivo* and infection models with rodents

Postdoctoral Fellow - TB

Job ID 12965BR

Novartis Institute for Tropical Diseases, Singapore

Working with the Research Investigator, you will define and propose the necessary means for research work on drug targets in Mycobacterium tuberculosis. You will remain up-to-date scientifically in your specific field; prepare reports on laboratory activities according to global research standards and present scientific/technical work at internal and external meetings.

Your Profile:

- PhD in Biology, Biochemistry, Molecular Biology, Parasitology or related discipline, preferably with working knowledge of infectious diseases
- Experience in molecular biology and microbiology (BSL-2) desired
- Experience in BSL-3 would be beneficial

To find out more information and to apply, please visit our careers website **www.novartis.com/careers** quoting the relevant job ID.

NOVARTIS

www.novartis.com

UNIVERSITY OF Rhode Island

Vice Provost for Research, Graduate Studies, and Outreach and Dean of the Graduate School

The University of Rhode Island (www.uri.edu) is seeking a Vice Provost and Dean who will provide visionary leadership for its research, graduate, and outreach missions. Reporting directly to the Provost, the Vice Provost is the chief research officer of the University and is responsible for facilitating ongoing academic research, expanding research funding opportunities, developing relationships with government agencies and the private sector, strengthening research infrastructure and nurturing research ideas and initiatives. The Vice Provost will also serve as a leader, advocate and spokesperson for outreach activities at the University, and is responsible for expanding capacity, effectiveness and constituencies of existing programs and identifying and implementing new opportunities for University outreach. As Dean, she/he works closely with college deans and faculty to assist in curricular and resource review of graduate programs, coordinates the development and design of new programs, and serves as an advocate for graduate studies within the mission and goals of the University.

Qualifications for the position include: An earned doctorate with a distinguished record of scholarship and funded research appropriate for appointment as a tenured full professor in an academic department of the university; a clear research vision and an understanding of the mission of a major land grant, sea grant and urban grant research institution; demonstrated commitment to graduate education and outreach; successful administrative and fiscal management experience at the university level; proven leadership ability and outstanding communication skills; strong interpersonal skills; demonstrated ability to organize, coordinate, and supervise support staff; familiarity with university technology transfer and federal regulations governing campus research activities; and a demonstrated commitment to enhancing diversity and equal opportunity for individuals from underrepresented groups.

Visit our website at ***www.uri.edu/human_resources*** for a complete job description.

Review of candidates will begin May 1, 2006 and continue until the position is filled. Applications (including a cover letter, curriculum vitae and the names and contact information for five references) can be submitted in electronic form to **heather@uri.edu** (preferred) or a hard copy can be sent to: **Dr. Jeffrey R. Seemann, Chair of the VP Search Committee, Job Requisition No. SM011352, University of Rhode Island, PO Box G, Kingston, RI 02881-0804.**

Nominations and questions should be directed to: **Dr. Jeffrey R. Seemann at jseemann@uri.edu (Phone: 401-874-2957; Fax: 401-874-4017).**

URI is an AA/EEO employer and values diversity and also is an NSF ADVANCE institutional transformation university, working to advance the careers of women faculty, especially in the science and engineering disciplines.

BIOTECH AND PHARMA

Bioinformatics Researcher

The Emergency Resuscitation Center at the University of Chicago seeks a full-time researcher with an interest in computation biology and bioinformatics. Applicants must have a Ph.D. in bioinformatics with experience in molecular biology research. The ideal candidate will have an advanced knowledge of statistics and experience with pathways, comparative genomics, SNP, or proteomics data.

Please forward CV/Resume and names of three references to:

Dr. Terry Vanden Hoek
University of Chicago
MC5068
5841 South Maryland Ave.
Chicago, IL 60637

or

Email:mretzer@medicine.bsd.uchicago.edu

The University of Chicago is an Affirmative Action/Equal Opportunity Employer.

CAREERS IN BIOTECH AND PHARMA

Opportunities in suburban Philadelphia, PA

Cutting edge science driving the discovery of new medicine.

Driving the success of GlaxoSmithKline - the world's leading pharmaceutical organization - is a continual search for innovation. Apart from a research and development capability that sets the benchmark for our industry, we're committed to recruiting and retaining the best and brightest by providing unequaled individual and career development opportunities within our organization. We currently have the following opportunity available in our state-of-the-art facility, located in King of Prussia, PA.

Manager, Human Target Validation in the Cardiovascular Therapeutic Area

In this challenging role, you will be responsible for assisting the CVU Center of Excellence for Drug Discovery leadership in maximizing the effectiveness of drug discovery and development efforts. By innovative experiments on human samples, you will increase the understanding of the pathophysiological relevance of molecular targets to the disease process. You will also lead the efforts of Ph.D. and non-Ph.D. staff.

Qualifications include a Ph.D., and/or MD and postdoctoral training in Molecular Biology, Pharmacology, Immunology or Cell Biology, with at least 5 years of pharmaceutical industry experience. Strong practical/theoretical knowledge/understanding of human cardiovascular diseases is essential.

For consideration, please visit our website at www.gsk.com/careers. Indicating Req ID: 30293 is essential to search. Principals only, no agencies, please.

GSK is proud to promote an open culture, encouraging people to be themselves and giving their ideas a chance to flourish. GSK is an equal opportunity employer.

Together we can make life better.

gsk GlaxoSmithKline

Featured Employers

Search **ScienceCareers.org** for job postings from these employers. Listings updated three times a week.

Abbott Laboratories
www.abbott.com

Genentech
www.gene.com

Kelly Scientific Resources
www.kellyscientific.com

Novartis Institutes for BioMedical Research
www.nibr.novartis.com

Pfizer Biotechnology, Inc.
www.pfizer.com

Pierce Biotechnology, Inc.
www.piercenet.com

If you would like to be a featured employer, call 202-326-6543.

ScienceCareers.org
We know science AAAS

NATIONAL CANCER INSTITUTE
FOOD & DRUG ADMINISTRATION

RESEARCH & REGULATORY REVIEW FELLOWSHIPS

The National Cancer Institute (NCI) and the Food & Drug Administration (FDA) are providing Research and Regulatory Review Fellowship programs to train a cadre of scientists in research and research-related regulatory review so that they can develop skill sets that bridge the two distinct processes.

The NCI-FDA fellowships offer an unprecedented career opportunity for participating researchers to become uniquely positioned to facilitate the new age of molecular medicine. Fellowships are available in Clinical Oncology Product Research/Review and Cancer Prevention.

Benefits to Researchers

- Mentored research opportunities at NCI and FDA
- Mentored regulatory training and review experience at FDA
- Professional development and leadership preparation
- Skills and experience of value to academia, the pharmaceutical industry, and government agencies

Eligibility Requirements

- M.D. and/or Ph.D., or equivalent doctoral degree
- U.S. citizenship or permanent residency
- Other requirements as specified for each fellowship program.

More Information

Visit the NCI-FDA Research and Regulatory Review Fellowships Web site at ***http://iotftraining.nci.nih.gov*** for additional information on program lengths, eligibility requirements, and curricula. Or contact:

Oncology Product Research / Review Fellowships
CCR Office of Training and Education
CCR Office of the Director
National Cancer Institute
Building 31, Room 4A48
31 Center Drive
Bethesda, MD 20852
Tel: 301-451-9638
Email: wiestj@mail.nih.gov
Web site: http://iotftraining.nci.nih.gov

Cancer Prevention Fellowship
Division of Cancer Prevention
National Cancer Institute
6130 Executive Blvd
EPN, Suite 3109
Bethesda, MD 20892
Tel: 301-496-8640
Email: cpfpcoordinator@mail.nih.gov
Web site: http://cancer.gov/prevention/pob

Postdoctoral, Research and Clinical Fellowships at the National Institutes of Health

www.training.nih.gov/pdopenings

www.training.nih.gov/clinopenings

Train at the bench, the bedside, or both

Office of Intramural Training and Education
Bethesda, Maryland 20892-0240
800.445.8283

MRI Scientist Position

National Institute of Neurological Disorders and Stroke

With nation-wide responsibility for improving the health and well being of all Americans, the Department of Health and Human Services oversees the biomedical research programs of the National Institutes of Health.

The NIH MRI Research Facility (NMRF) in the National Institute of Neurological Disorders and Stroke is seeking an MRI scientist to support the human brain imaging studies conducted by the NIH investigators. NMRF offers state-of–the-art MRI facilities for users throughout the NIH. The NMRF is a part of the NIH In Vivo NMR Center which houses active research programs in brain and cardiac MRI. Four 3T MRI (GE) scanners and a 7T MRI (GE) scanner are available in the NMR Center for human brain research. The successful candidate will have a Ph.D. in a relevant field and interest in application of MRI to study brain function and disorders. Experience in MRI pulse sequence design and programming is required. Knowledge and interest in image processing or MRI hardware is desirable. In addition to collaborative research, the candidate will have the opportunity to initiate new projects that will impact ongoing research. Salary is very competitive and commensurate with education and experience.

Please send a CV and three letters of reference to **Dr. Lalith Talagala, NIH MRI Research Facility, National Institutes of Health, 10 Center Drive, Room B1D69, Bethesda, MD 20892-1060, Email: talagala@nih.gov.**

WWW.NIH.GOV

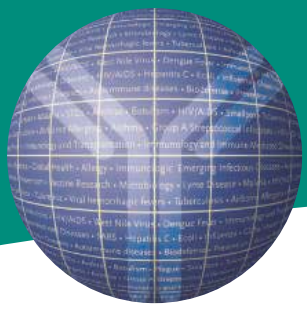

Health Research in a Changing World

Fighting Diseases and Improving Lives

DEPARTMENT OF HEALTH AND HUMAN SERVICES
NATIONAL INSTITUTES OF HEALTH
NATIONAL INSTITUTE OF ALLERGY AND INFECTIOUS DISEASES

Are you ready for an exciting career that could help improve millions of lives around the world?
Then consider joining the scientific and medical forces at NIAID. As part of the Division of Allergy, Immunology, and Transplantation (DAIT) at NIAID, the Asthma, Allergy, and Inflammation Branch (AAIB) is responsible for planning and conducting programs of extramural basic and clinical research aimed at understanding the biology of asthma and allergic diseases. AAIB/DAIT has the following scientific opportunities available:

Program Officer/Medical Officer

As a Program/Medical Officer, the selected candidate will provide leadership and scientific/medical expertise and guidance in the planning, development, implementation and evaluation of basic and clinical research concepts, projects and initiatives to appropriate advisory groups; identify opportunities and problem areas, research gaps and relevant program needs and make recommendations for and facilitate new research efforts, clinical studies, clinical trials or other initiatives; and communicate with grantees/contractors, cooperative group members/representatives and others on policy interpretation, merit review and evaluation processes and procedures, and on decisions, concerns or other issues/matters of a medical/scientific nature. The selected candidate will also oversee and advise on development of clinical trial protocols.

In order to be considered for this position, applicants should have experience in basic and/or clinical research to examine the causes, diagnosis, treatment and prevention of allergic diseases; research on bacteriology, mycology, virology, or research on parasitic and other tropical diseases, or vector biology is required; and the successful candidate must posses a Bachelor's degree, M.D., D.O., or Ph.D. and relevant laboratory research on asthma, allergy, inflammation, or immunology. Experience in clinical trial and/or project management is highly desirable. Only candidates with an M.D. or D.O. degree and current medical licensure are eligible to serve as Medical Officers.

For a complete job announcement and to apply for this position, visit http://usajobs.opm.gov:

Interdisciplinary Vacancy number: NIAID-06-110230
Open: 3/1/06 – 4/28/06
GS-401, 601-13/14 Salary: $77,353 - $118,828
Applications must be submitted to Nolan Jones, Human Resource Specialist, 301-402-0957

Section Chief

As Chief of the Asthma and Inflammation Section of AAIB, the selected candidate will lead an extramural research program with a diverse portfolio of grants and contracts focusing on the immunologic basis, etiology, pathogenesis, and treatment of asthma and inflammatory diseases. The Chief of the section leads a staff of physicians, scientists, and project managers responsible for development and implementation of new initiatives in these areas and the direction and oversight of ongoing research programs through site visits and frequent contact with principal investigators. The selected candidate will also oversee and advise on development of clinical trial protocols.

In order to be considered for this position, applicants should have experience in basic and/or clinical research to examine the causes, diagnosis, treatment and prevention of allergic diseases. Candidates must also have experience in managing complex biomedical research programs, including the development of pre-clinical animal models, human subjects, and/or clinical trials. Experience in the preparation and review of research project grant applications is also necessary. The selected candidate must posses an M.D. or D.O. to be considered for this position.

Salary is commensurate with research experience and accomplishments, and a full package of benefits (including retirement, health, life and long term care insurance, Thrift Savings Plan participation, etc.) is available for this position.

CV, bibliography, and a list of 3 references must be received by April 30, 2006. Application package should be sent to:

Jeryl Wilson
4900 Seminary Road, Suite 1100
Alexandria, VA 22311
1-888-798-4991 ext. 252
For further information, please contact Ms. Wilson by email:
sectionchief@stginternational.com

We are happy to respond to your questions, and you may contact us toll free at 1-888-798-4991 or visit online at: http://healthresearch.niaid.nih.gov/science

DIRECTOR OF RESEARCH
SOUTH CAROLINA COMPREHENSIVE NEUROSCIENCE CENTER

The University of South Carolina School of Medicine invites applications and nominations for a Director of Research in the newly created South Carolina Comprehensive Neuroscience Center. The Director of Research will lead a team of investigators in basic neuroscience discovery and translation of the results into improved patient care. This individual will also facilitate communication and collaboration among basic and clinical neuroscientists in the School of Medicine and the broader neuroscience community at the university and its affiliated institutions.

The purpose of the Comprehensive Neuroscience Center is to provide integrated clinical neuroscience specialty services to treat a variety of neurological disorders and injuries including movement disorders, Alzheimer disease and other dementias, epilepsy, brain and spinal trauma, and stroke. It is also envisioned that the Center will serve as a focus for clinical and translational research in the neurosciences at USC. The clinical faculty of the Center will include neurosurgeons, neurologists, neuropsychiatrists and physiatrists, along with supporting staff. The research faculty will include up to eight scientists conducting studies germane to the clinical services provided by the Center. The Center represents a major investment in clinical and basic neuroscience at USC and complements the recently established statewide Brain Imaging Center of Excellence and other initiatives at the university. The Director of Research will play a major role in developing the Center and will report directly to the Dean of the School in this capacity.

The successful candidate will be appointed as a senior member of the Department of Pharmacology, Physiology and Neuroscience; secondary appointments in clinical or other relevant departments are also possible. The Center will provide generous resources to establish a laboratory and to bring/recruit a team of investigators.

Applicants for the position should have a Ph.D. or M.D. and qualifications for a senior faculty appointment. Individuals with established research programs in stroke, neurodegenerative disorders, movement disorders, chronic pain, epilepsy/seizure disorders, or neuropsychiatric disorders including anxiety, depression and schizophrenia are sought. Candidates should submit a full curriculum vitae and the names and contact information for at least four references. References will not be contacted without the candidate's permission.

Applications should be made online through **http://USCJobs.sc.edu**. Review of applications will begin **June 1, 2006**. Inquiries and nominations may be sent to the search committee chair, **Steven P. Wilson**, at **swilson@gw.med.sc.edu**.

USC is an Affirmative Action/Equal Opportunity Employer.

Tenure Track Faculty Positions
Rush University Medical Center

ASSOCIATE/PROFESSOR and **PROFESSOR** positions are available in the Department of Biochemistry at Rush University Medical Center, Chicago, IL. The successful applicant will join a nationally recognized program in cartilage biology, molecular biology, biochemistry and the pathobiochemistry of osteoarthritis. Applicants should have a Ph.D. or a M.D./Ph.D. in biochemistry or related biological science. The focus will be on research in cell signaling or molecular biology that can be applied to cartilage and the cartilage-bone interface. However, those with interests in related areas are strongly encouraged to apply. The applicant should have experience commensurate with appointments at these academic ranks and evidence of productive research accomplishments. The applicant should have the ability to maintain a rigorous, independent research program funded by external support and be able to contribute to the educational programs in the graduate medical schools. An excellent start up package with new laboratory space is available. Applications will be reviewed upon receipt and accepted until the position is filled.

Please send a letter of interest, statement of research plans, curriculum vitae, and the names of three references to: **Theodore Oegema, Ph.D., Chairman, Department of Biochemistry, Rush University Medical Center, 1735 W. Harrison, Chicago, IL 60612; Ted_Oegema@rush.edu.**

ASSOCIATE/FULL PROFESSOR
IN COGNITIVE NEUROSCIENCE, TENURE TRACK

The City College of New York

The Program in Cognitive Neuroscience of the Department of Psychology at the City College of New York is seeking an outstanding scientist with a strong program of research in Human Cognitive Neuroscience for a full-time, tenure track position at the Associate/Full Professor level to start at the beginning of the Fall 2006 semester.

A doctoral degree in Psychology, Neuroscience, Cognitive Neuroscience or a related field is required. We are particularly interested in candidates employing neuroimaging and electrophysiological techniques to study basic processes of perception, attention, multisensory processing, memory, language or higher cognitive functions. The successful candidate will be expected to maintain an active, externally funded program of research, to publish theoretical and empirical research in top-tier journals, and to be committed to both undergraduate and graduate education.

Salary commensurate with qualifications and experience.

Submit curriculum vitae, selected publications, and a brief statement of research interests and future plans to: **John Foxe, Ph.D., Director of Program in Cognitive Neuroscience, Department of Psychology, The City College of CUNY, 160 Convent Avenue, New York, NY 10031.** At least three letters of reference should be forwarded independently. E-mail: **foxe@nki.rfmh.org**

The City College/CUNY is an EEO/AA/IRCA/ADA Employer.

CITY COLLEGE IS CUNY

California Institute of Technology 1891

PROTEIN LAB DIRECTOR

The Beckman Institute at Caltech is looking for a Director of its Protein Center. The Center's mission is to provide state of the art protein expression, specialty peptide synthesis and protein/peptide purification services to the Caltech research community. The Director will supervise several technicians and take a leadership role in shaping the evolution of the Center, including identifying, importing, optimizing and inventing new technologies. S/he will be invited to conduct a research program related to the Center's mission. Candidates should have a PhD and several years experience with prokaryotic and eukaryotic expression systems and associated protein biochemistry.

Send applications with CV to:
Jay Labinger, Administrator
Beckman Institute
Caltech, 139-74
Pasadena, CA 91125

jal@its.caltech.edu

Caltech is an Affirmative Action, Equal Opportunity Employer.

www.cardiff.ac.uk/jobs

CARDIFF UNIVERSITY
PRIFYSGOL CAERDYDD

Lectureship

Cardiff School of Biosciences

The School of Biosciences, with over 100 academic staff, is one of the largest groups of biological scientists in the UK and a major research strength within the University as a whole. We are therefore seeking to appoint a permanent Lecturer to contribute to our success as a centre of international research and teaching excellence. You should have the potential to achieve grade 4*/3* RAE level, be able to contribute to the School's existing areas of research expertise and ideally have specialist expertise in the area of data analysis/modelling of biological processes and biostatistics.

The School has an outstanding reputation for teaching at all levels and gained 'excellent' in all our submissions to TQA panels, including those for Dentistry and Medicine. You will also be expected to contribute enthusiastically to this aspect of our mission.

The School's research covers the whole range of bioscience with focus in the following areas:

• Biodiversity and Ecological Processes • Connective Tissue Biology • Genetics • Microbiology • Molecular Cell Biology • Neuroscience

Further details regarding these groups can be found at **www.cardiff.ac.uk/biosi/research**

Salary: £24352 - £36959 per annum

Informal enquiries can be made to the Head of School, Professor John Harwood (Harwood@cardiff.ac.uk), to the Joint Heads of Research, Professor Alan Clarke (ClarkeAR@cardiff.ac.uk) and Professor Kevin Fox (FoxKD@cardiff.ac.uk) or to the Head of Teaching, Professor Bernard Moxham (Moxham@cardiff.ac.uk)

Please include full details of publications and research grant income (as relevant) and an indication of your research plans, if appointed. A covering letter of application, setting out personal career aspirations, must be attached.

For an application pack and details of all our vacancies, visit www.cardiff.ac.uk/jobs Alternatively email vacancies@cardiff.ac.uk or telephone + 44 (0) 29 2087 4017 quoting vacancy number 180.

Closing date: 21 April 2006

The Department of Pharmacology and Toxicology, Faculty of Medicine, University of Kuwait invites applications for the following academic positions:

Assistant/Associate Professors in

1. **Neuropharmacology:** Applicants with a PhD or MD degree must be pharmacologists specialized in neuropharmacological research with research publications in internationally recognized indexed and cited journals.
2. **Clinical Pharmacology/Toxicology:** Applicants should have experience in therapeutic drug monitoring and analytical methodology, including GC/LC/MS, in clinical pharmacology and toxicology.

CONDITIONS OF APPOINTMENT: Total monthly salaries will be within the following scales according to qualifications and experience (1 KD = 1.9 St. Pound, US$ 3.3 approximately).

	Professors Min-Max	Associate Min-Max	Assistant Min-Max
Clinical	KD. 2585 – 2745	KD. 2290 – 2450	KD. 2010 – 2170
Non-Clinical	KD. 1670 – 1830	KD. 1320 – 1480	KD. 1030 – 1190

A Social Allowance will be paid in addition to the monthly salary as per the University regulations.

OTHER BENEFITS: Conference attendance. Gratuity. Housing allowance. Free medical treatment in Kuwait. Free annual round-trip air tickets from country of Citizenship or permanent residence for self and family up to three dependent children. Baggage and freight allowance. Education fees for a maximum of three children in Kuwait from elementary through high school. No taxation. Currency is transferable without restriction. 60 days paid annual leave.

METHOD OF APPLICATION: Curriculum vitae which should include the names of 3 referrals; personal particulars; copy of the relevant pages of passport; qualifications with dates, career history, teaching experience, research accomplishments and where appropriate clinical experience should be sent no later than 60 days from the date of this advertisement to:

THE DEAN
(RECRUITMENT OFFICE)
FACULTY OF MEDICINE
KUWAIT UNIVERSITY
P.O. BOX 24923
13110 SAFAT, KUWAIT
FAX: 965 5318454

JOHANN WOLFGANG GOETHE
UNIVERSITÄT
FRANKFURT AM MAIN

The Johann Wolfgang Goethe-University, Department of Life Science, seeks to attract a tenure-track professorship in the institute for Cell Biology and Neuroscience as a

Aventis-Stiftungsprofessur (W2/W3)
for Chemical Biology in Cellular Biochemistry

The position is granted for 6 years.
Candidates should have a research focus in the field of regulation of transcription and translation by small ligands. The candidate should have research experience using cell biology and structural biology. The focus of future research activities should be in signal transduction of proteins or RNA. The aim of the endowed professorship is the strengthening of biological research by a combination of a innovative research field with NMR-spectroscopic expertise.
The candidate will become associate member of the Center for Biomolecular Magnetic Resonance (BMRZ).
The extension of the position will be decided after external evaluation after 5 years.

The employment is based on the Hessisches Hochschulgesetz (HHG), paragraphs 70(6) and 71. Johann Wolfgang Goethe-University seeks to increase the proportion of female staff members in the faculty and therefore urges interested female candidates to apply. In case of equal qualifications preference will be given to disabled applicants.
Applications should be sent within **four weeks** after publication of this advertisement, accompanied by the usual documents (full CV, scientific and occupational career history, lists of publications and lectures, copies of the five most important papers, copies of degree certificates and documents) to **Prof. Dr. Rüdiger Wittig, Dekan des Fachbereichs Biowissenschaften der Johann Wolfgang Goethe-Universität, Postfach 11 19 32, D-60054 Frankfurt am Main, Germany.**
Because of the costs involved, the application papers cannot be sent back. When the process has been completed, the application documents will be destroyed. Further costs regarding your application cannot be refunded.

Hier wird Wissen Wirklichkeit

Assistant Professor of Pathology and Laboratory Medicine for Research in Hemostasis and Thrombosis at the University of North Carolina at Chapel Hill

The Department of Pathology and Laboratory Medicine of The University of North Carolina at Chapel Hill is seeking highly motivated applicants for a tenure track research position at the rank of Assistant Professor. Candidates must hold a Ph.D., M.D., or both. Applicants should have a record of productive research in hemostasis and thrombosis. The principal responsibilities will be to develop a successful research program and to contribute to Departmental teaching of graduate students in Molecular and Cellular Pathology. Competitive candidates will have at least 3 years of relevant post-doctoral research experience and will have demonstrated success at obtaining extramural research funding. Once appointed, the successful candidate is to maintain an extramurally funded, independent research program with a focus on cellular and biochemical mechanisms of hemostasis and thrombosis.

Send a letter of application with a statement of research interests and accomplishments, curriculum vitae, and four names for letters of recommendation to: **David G. Kaufman, Professor and Vice Chair for Research Development, Department of Pathology and Laboratory Medicine, Campus Box #7525, University of North Carolina, Chapel Hill, NC 27599-7525**. See website **http://www.pathology.med.unc.edu/path/** for information about the Department.

The University of North Carolina at Chapel Hill is an Equal Opportunity Employer.

Opportunities in the Department of Structural Biology at the University of Pittsburgh School of Medicine

The University of Pittsburgh School of Medicine has recently established a new Department of Structural Biology with state-of-the-arts facilities in NMR, X-ray crystallography, cryo-electron microscopy as well as extensive biochemical and biophysical instrumentation. The Department is housed in the newly constructed Biomedical Science Tower-3, adjacent to existing and active departments in the School of Medicine and the University of Pittsburgh. We have vigorous ongoing research programs utilizing our expertise in structural studies in high impact research areas. Our extensive technical resources include several NMR instruments ranging in field strength from 14.1 to 21.1 Tesla, two FR-E X-ray generators with four detectors including CCD and image plates, and FEI Polara and Tecnai T20F cryo-electron microscopes. Departmental resources include molecular biology and protein chemistry cores in addition to extensive genomic and proteomics capabilities within the Medical School and the University of Pittsburgh. Both physical proximity and scientific affinities between the Medical School, the University, and Carnegie Mellon University extends the already expansive scope of research being conducted at Pittsburgh. The city of Pittsburgh consistently ranks among the "Best Places to Live in America" and is one of the nation's top 25 arts destinations. The region is home to the Carnegie Museum of Art, Andy Warhol Museum and Pittsburgh Symphony Orchestra.

Post-doctoral opportunities in various disciplines are available immediately for highly motivated and talented researchers with backgrounds or strong interests in experimental structural biology. Further information and links can be found from the Molecular Biophysic's graduate program website at: **http://www.biophysics.pitt.edu/**. Applications should include a CV, a statement of research interests and background, and the names and contact information of three references; these can be submitted to: **Dean Duncan, Department of Structural Biology, University of Pittsburgh, 1050 Biomedical Science Tower 3, 3501 5th Ave., Pittsburgh, PA 15260, USA.; Phone: 412.383.9800; Fax: 412.648.9008; Email: dxd8@pitt.edu.**

The University of Pittsburgh is an Affirmative Action/Equal Opportunity Employer.

Anthony and Lillian Lu Professorship Department of Biological Chemistry University of Michigan Medical School

The Department of Biological Chemistry seeks applications from and nominations of outstanding established investigators for the Anthony and Lillian Lu Endowed Professorship. Areas of emphasis in the Department that we would like to complement with the hiring of a senior investigator are Protein Folding and Processing, Biochemical Signaling or Regulation of Gene Expression. Qualifications include a Ph.D. and/or M.D., a minimum of 8 years of independent research experience and an existing research program of international stature. In addition to maintaining an active research program, the successful candidate will train doctoral students and postdoctoral fellows and participate in classroom teaching activities of the department.

The Department of Biological Chemistry currently has 45 active faculty members and is in the midst of a phase of expansion. There are many opportunities for interactions both within the Department and across the campus. Further information about the Department of Biological Chemistry can be found at **http://www.biochem.med.umich.edu/biochem/**.

Applicants or nominators should submit a curriculum vitae and a one to two page summary highlighting previous research accomplishments and plans for future research to: **Anthony and Lillian Lu Chair Search Committee, c/o Mrs. June Bialecki, 5416 Medical Science I, 1301 E. Catherine St., Department of Biological Chemistry, University of Michigan Medical School, Ann Arbor, MI 48109-0606**. References will not be contacted without the permission of applicants or nominators.

The University is an Affirmative Action/Equal Opportunity Employer.

6 April 2006
San Francisco, CA

UCSF Mission Bay
Community Center
Fisher Banquet Hall
1675 Owen Street
1:00 - 4:30 pm

Science Careers has teamed up with UCSF to deliver an exciting career fair on the new Mission Bay campus of UCSF.

Scientists: Meet with HR representatives of biotech, pharmaceutical, and research organizations who will be exhibiting. Visit ScienceCareers.org and click on Career Fairs on the left side for complete details.

Exhibitors: This fair typically attracts over 800 attendees. To be among the recruiters call Daryl Anderson at 202-326-6543 or visit ScienceCareers.org and click on Exhibit at a Career Fair.

We hope to see you there.

ScienceCareers.org
We know science AAAS

U.S. Department of Health and Human Services
Food and Drug Administration

MICROBIOLOGISTS

The Food and Drug Administration, Center for Drug Evaluation and Research, Division of Special Pathogen and Transplant Products is recruiting Microbiologists to serve as Review Microbiologists to provide scientific and regulatory guidance to sponsors through all phases of drug development, including the review of the activity of the product (*in vitro* and animal studies, clinical microbiology which includes setting of interpretive criteria and the mechanism by which drug exhibits its effect), overall microbiological drug development programs and evaluation of the results.

QUALIFICATIONS: Basic Requirements: Degree: microbiology; or biology, chemistry, or basic medical science that included at least 20 semester hours in microbiology and other subjects related to the study of microorganisms, and 20 semester hours in the physical and mathematical sciences combining course work in organic chemistry or biochemistry, physics, and college algebra, or their equivalent. Candidates for Civil Service or U.S. Commissioned Corps must be U.S. citizens. Permanent U.S. residents may apply for staff fellowship appointments.

HIGHLY DESIRABLE: A doctorate degree with at least two years experience in clinical microbiology and/or immunology. Also desirable is experience in assessment of the mechanisms of actions and resistance to anti-infectives; epidemiology of infectious diseases; work with animal models of infectious diseases; evaluation of clinical/microbial efficacy data from clinical trials; and determining *in vitro* susceptibility test interpretive criteria.

CIVIL SERVICE SALARY: GS-12/13 $65,048 - $100,554

HOW TO APPLY: Submit curriculum vitae with cover letter to source code **# 06-009-1** via e-mail by **May 31, 2006** to: **Employment@cder.fda.gov** or send hard copies to: **U.S. FDA/Center for Drug Evaluation and Research, Office of New Drugs/Program Management Team, Attn: Dwayne Keels, 10903 New Hampshire Ave, Bldg#22, Rm 6445, Silver Spring, MD 20993.** For additional information, please contact the **Office of New Drugs' Program Management Team** at **301-796-0800**.

FDA IS AN EQUAL OPPORTUNITY EMPLOYER WITH A SMOKE FREE ENVIRONMENT.

Tulane University

Wetlands Scientist – Tulane University

The newly formed Division of Earth and Ecological Sciences in the School of Science and Engineering at Tulane University has an opening for a faculty member who is eligible for the rank of full professor. We seek a senior scholar who is an intellectual leader in the broad area of coastal environmental impacts of climate and sea-level change. Fields of interest include hydrology, wetland/riparian ecology, coastal geology, biogeochemistry, ecosystem ecology, coastal oceanography, limnology, paleoecology, paleoclimatology, and remote sensing. We are particularly interested in individuals with a demonstrable cross-disciplinary approach. An outstanding track record reflected by a dynamic, externally funded research program, as well as a proven ability to serve as a team leader and to guide large and diverse collaborative groups, is essential. The successful candidate is expected to play a key role in furthering the research profile of the division. The position includes teaching responsibilities at both the undergraduate and graduate levels.

We will start considering applications by **April 15, 2006**, and the position will remain open until filled. Applications should be sent (email preferred) to: **Dr. Stephen A. Nelson, Department of Earth and Environmental Sciences, Tulane University, 6823 St. Charles Avenue, New Orleans, LA 70118-5698, USA (snelson@tulane.edu)**, and should include a curriculum vitae, statements of research interests and teaching goals, copies of three key publications, and the names and contact information, including email addresses, of at least three referees. Further information can be obtained at **http://www.tulane.edu/~eens/** and **http://www.tulane.edu/~ebio/**.

Tulane University is an Affirmative Action/Equal Opportunity Employer. Women and minorities are encouraged to apply.

NUS National University of Singapore

Department *of* Biological Sciences
Faculty of Science

Faculty Search - Cryo-Electron Microscopist

The Department of Biological Sciences, National University of Singapore (NUS) invites applications for tenure-track faculty positions at Assistant Professorship and Associate Professorship levels with specialization in Cryo-Electron Microscopy.

Established in 1905, NUS has evolved into a quality teaching and research-intensive institution, which is internationally acknowledged as one of the finest universities in the Asia-Pacific. The department is the largest life sciences department in NUS with more than 45 academic staff. The department also leads the campus-wide Structural Biology and Proteomics Research Program. It has established state-of-the-art research facilities for structural biology (including X-ray diffraction, 800 MHz NMR and cryo-electon microscopy facilties) functional genomics, developmental biology and biodiversity. Faculty members can expect competitive salary levels and comparative research support as at the top universities in USA and Europe.

Outstanding individuals with postdoctoral experience and strong commitment to research and teaching are encouraged to send an application (form downloadable from www.dbs.nus.edu.sg), along with curriculum vitae, a brief research plan and names of three external referees to:

Professor Choy-L HEW
Head, Department of Biological Sciences,
National University of Singapore
14 Science Drive 4 Singapore 117543
Republic of Singapore
Fax: (65) 67795671
Email: dbshead@nus.edu.sg

PHYSICIST SCIENTISTS / ENGINEERS

ADVANCED LIGHT SOURCE DIVISION

Lawrence Berkeley National Laboratory (Berkeley Lab) is located in the San Francisco Bay Area on a 200-acre site in the hills above the University of California's Berkeley campus and is managed by the University. A leader in science and engineering research for more than 70 years, Berkeley Lab is the oldest of the U.S. Department of Energy's National Laboratories.

NOTE: These career positions will be hired at either the scientist or staff scientist level, depending on qualifications and experience.

Reporting to the Division Deputy for the Scientific Support Group (SSG) of the Advanced Light Source (ALS) Division, the incumbent functions as an experimental physicist, supporting and planning experiments to meet the SSG's programmatic plans and R&D goals.

018841- Physicist Scientist/Engineer - Working with another beamline scientist, the incumbent will be responsible for the operation, maintenance, and upgrades of ALS beamline 8.0 and its associated endstations. He/she will provide support for the Scientific Support Group experimental program including operation of undulator beamline 8.0.1 and its associated endstations (support of the newly constructed nano science characterization facility and the very productive soft x-ray emission spectrometer).

018842- Physicist Scientist/Engineer - The incumbent will be responsible for development, commissioning, and operation of a new milli eV resolution line (MERLIN, BL 4.0.1) covering an energy range from 8-150eV on an undulator beamline at the ALS, and experimental program involving high-resolution inelastic scattering and angle-resolved photoemission research. Particular focus will be developing a scientific program for the study of strongly correlated electron systems with the use of high-resolution inelastic scattering spectrograph, the MERLIN beamline, and a quasi periodic elliptically polarizing undulator.

Duties: Both candidates will participate in planning and performing forefront research in synchrotron radiation science, with emphasis on the use of photon-in photon-out and photon-in electron-out techniques for studying electronic structures of complex materials. They will handle scheduling of beamline operations, and adherence to environment, safety, and health policies and procedures.

Qualifications: Experience with synchrotron radiation techniques applied to the study of electronic properties of materials is essential, as is knowledge of condensed matter physics and chemistry and a thorough understanding of modern instrumentation techniques applied to these areas. Proven ability to pursue new areas of research in physics involving sophisticated instrumentation including ultra high vacuum, photons, and charged particle detection is necessary. A Ph.D. or equivalent degree in Physics, Chemistry, or Materials Science is required.

Upload your resume online at: **http://jobs.lbl.gov**, select "Search Jobs", and enter **018841** or **018842** in the keyword search field. Enter "Science" as your source. **http://www-als.lbl.gov** EOE

Over 23 million downloads of articles last year. Now that's big.

In 2004 over 23 million HTML and PDF articles were downloaded from *Science* Online. More people than ever are accessing the seminal original research, breaking news, and in-depth special sections published each week in *Science*. So if you want to make a really big impression with your research article or advertising, choose *Science*. Become a member of AAAS at **aaas.org/join**. To advertise, go to **scienceadvertising.org**.

Science

AAAS

Looking for a great science career?

Get the experts behind you.
Visit www.ScienceCareers.org

Your career is too important to leave to chance. So to find the right job or get career advice, turn to the experts. At ScienceCareers.org we know science. And we are committed to helping take your career forward. Our knowledge is firmly founded on the expertise of *Science*, the premier scientific journal, and the long experience of AAAS in advancing science around the world. Put yourself in the picture with the experts in science. Visit www.ScienceCareers.org.

POSITIONS OPEN

BCM
Baylor College of Medicine

FACULTY POSITION
in Cellular/Molecular Neuroscience

The Department of Neuroscience at Baylor College of Medicine is recruiting **ASSISTANT PROFESSORS** on the tenure-track who utilize contemporary tools of molecular and cellular neuroscience to investigate fundamental questions of nervous system function in health, disease, or injury. The successful candidate should have a Ph.D. and or M.D., postdoctoral experience, strong experimental skills, and a record of accomplishment in the application of molecular, imaging, biophysical, or electrophysiological approaches to nervous system function. The Department of Neuroscience is undergoing a major expansion, building on strengths in ion channel function, cellular/molecular imaging, synaptic plasticity, neuronal development, cell signaling, sensory processing, and cognitive/computational neuroscience. The position will provide highly competitive allowances for laboratory support and research program development. Send curriculum vitae and statement of research interests, and have at least three letters of reference sent to: **Michael J. Friedlander, Ph.D., Professor and Chair of Neuroscience, Director of Neuroscience Initiatives, Baylor College of Medicine, One Baylor Plaza, Suite S740A, Houston, TX 77030 (e-mail: friedlan@bcm.edu)** by April 30, 2006. Applications may be submitted electronically or by mail; reference letters must be submitted by mail.

Baylor College of Medicine is an Equal Opportunity/Affirmative Action and Equal Access Employer.

The Virginia Tech-Wake Forest University School of Biomedical Engineering and Sciences (SBES) seeks candidates for a **TENURE TRACK, TEACHING AND RESEARCH FACULTY POSITION,** with degree and expertise in the life sciences. The position is on the Virginia Tech Campus. Primary consideration will be given to applicants with research interests in the cardiovascular system, including expertise in macro biomechanics, tissue and cell science, and/or molecular biology. Computational expertise is desirable, but not necessary. Successful applicants will be expected to develop a strong research program, contribute to our educational goals, and serve the overall mission of the School. In addition to appointment within SBES, the successful applicant will also be appointed to an affiliated department within the College of Veterinary Medicine. The appointment will be for the academic year (nine months). Salary and rank will be commensurate with the candidate's qualifications. Please see full position description and application instructions at **website: http://www.sbes.vt.edu.**

Virginia Tech has a strong commitment to the principle of diversity and, in that spirit, seeks a broad spectrum of candidates including women, minorities, and people with disabilities. Individuals with disabilities desiring accommodations in the application process or needing this material in an alternate format should contact: ***Vanessa McCoy*** *by* ***e-mail: vamccoy@vt.edu*** *or by* ***telephone: 540-231-6505.***

RESEARCH ASSOCIATE/
SPECIAL PROJECTS MANAGER

The University of South Carolina (USC) School of Medicine is recruiting a full-time Research Associate/Special Projects Manager. Responsibilities include grant writing, research project development, and project management related to biomedical sciences. Require a Ph.D. in biomedical sciences with experience in research activities, with preferred experience in grant writing. The search will start immediately and continue until the position is filled. Apply with curriculum vitae and three references to: **Dr. Prakash Nagarkatti, Associate Dean for Basic Sciences, University of South Carolina School of Medicine, Office of the Dean, Columbia, SC 29208** or **e-mail: spresearch@gw.med.sc.edu.** *USC Columbia is an Equal Opportunity Employer/Affirmative Action Employer and encourages applications from women and minorities.*

POSITIONS OPEN

FACULTY POSITION IN THE NEUROSCIENCES
American University of Beirut, Faculty of Medicine and Medical Center, Beirut, Lebanon

There is an opening for a junior/mid-level **NEUROSCIENTIST** with expertise in neurophysiology at the American University of Beirut (AUB), Faculty of Medicine. Individuals with M.D./M.D.-Ph.D../Ph.D. degree(s) are invited to apply. Appointments will be in the Department of Physiology and the Abu-Haidar Neuroscience Institute. This funded position involves teaching of medical/graduate students. Development of individual/collaborative research projects is expected. State-of-the-art laboratories with access to shared core facilities are available. Internal/external sources of funding are available on a competitive basis, including the NIH, NSF, Wellcome Trust, and the Deutsche Forschungsgemeinshaft. The recruitment package consists of an attractive salary, housing and fringe benefits, and relocation expenses. Submit a letter of interest and curriculum vitae to: **Fuad Ziyadeh, M.D., Acting Chairperson of the Department of Physiology, e-mail: fz08@aub.edu.lb,** or to: **Rose-Mary Boustany, M.D, Chairperson of the Abu-Haidar Neuroscience Institute e-mail: rb50@aub.edu.lb.**

AUB is registered with the Department of Education of New York State and accredited by the Middle States Commission on Higher Education. *AUB is a nonprofit institution of higher learning and an Equal Opportunity Employer. Women and Minorities are encouraged to apply.*

FACULTY POSITION
Reproductive Biology
University of Kentucky

The Department of Clinical Sciences is seeking a highly qualified individual for a Tenure-Track faculty position at the **ASSISTANT/ASSOCIATE PROFESSOR** level in reproductive biology. Applicants are required to have a Ph.D., an excellent publication record, and an established record of attracting extramural funding in an area of reproductive biology, including but not limited to uterine biology, immunology, stem cell, genetics, and neuroendocrinology. The Department places special emphasis on faculty-student interaction and we share a fundamental commitment to provide academic excellence. Review of applications will begin on May 15, 2006, and will continue until the position is filled.

Please send letter of inquiry, statement of research interests, curriculum vitae, and three references to: **Jay Ko, Ph.D., Department of Clinical Sciences, University of Kentucky, Room 209G CTW Building, 900 South Limestone, Lexington, Kentucky 40536-0200; e-mail: cko2@uky.edu.**

If offered this position, the successful candidate must pass a required pre-employment drug screen. *The University of Kentucky is an Affirmative Action/Equal Opportunity Employer.*

FACULTY POSITION IN BIOPHYSICS
The Johns Hopkins University

The Thomas C. Jenkins Department of Biophysics is seeking to fill a **TENURED SENIOR FACULTY** position in nuclear magnetic resonance (NMR) spectroscopy, with a strong emphasis on candidates interested in the mechanism of biological regulation. The successful candidate will join our interdepartmental NMR center and use existing instrumentation. Please send by 1 May 2006, a cover letter, curriculum vitae, and brief description of your research plans to: **Faculty Search Committee, T. C. Jenkins Department of Biophysics, Johns Hopkins University, 3400 N. Charles Street, Baltimore, MD 21218-2685; telephone: 410-516-7245.** Following preliminary assessment, promising candidates will be asked to provide letters of reference. *The Johns Hopkins University is an Affirmative Action/Equal Opportunity Employer.*

Science Careers Forum

- How long should it take to get my Ph.D.?
- Academia or industry?
- What will make my resume/cv stand out?
- How do I negotiate a raise?

Connect with Experts

Moderator Dave Jensen
Industry Recruiter

Mr. Jensen has over 20 years of experience in human resource consulting and staffing for the biotechnology and pharmaceuticals industry.

Adviser Bill Lindstaedt
Director,
UCSF Career Center

Mr. Lindstaedt has been providing career related advice to scientists and engineers for nearly 15 years, with a particular emphasis on working with graduate-level trainees in the life sciences.

Adviser Naledi Saul
Assistant Director,
UCSF Career Center

Ms. Saul has 7 years of career counseling with 4 years focused on counseling graduate students and postdocs in the biomedical and health sciences. Her forte is working with scientists pursuing careers in the public health arena.

Adviser Jim Austin
Editor, Science's
Next Wave

Dr. Austin has a Ph.D. in physics and worked in academia before coming on board to write about traditional and nontraditional career paths for scientists.

Visit www.sciencecareers.org and click on Career Forum

ScienceCareers.org
We know science AAAS

YYePG Proudly Presents, Thx for Support

POSITIONS OPEN

The Thermal Biology Institute at Montana State University, Bozeman seeks applicants for two tenure-track positions, one at the **ASSISTANT** or **JUNIOR ASSOCIATE LEVEL** and one at the level of **FULL PROFESSOR,** starting as soon as fall 2006.

We seek individuals who will continue the Institute's reputation for innovation and excellence by maintaining or creating an internationally recognized, externally funded program in thermal biology research in one or more of the following disciplines: microbiology, geochemistry, plant sciences, virology, biochemistry, metabolomics/genomics, environmental/ecological sciences, pre-biotic chemistry, or engineering. The successful applicant for the senior position will participate in shaping the future directions of the Institute and could potentially assume the position of Institute Director. The successful applicants for both positions will receive academic appointments in the College of Agriculture, College of Engineering, or College of Letters and Science, depending on their expertise, and will be expected to teach courses appropriate for their home Department. The successful applicants must have a demonstrated record of achievement or potential for excellence in research and teaching experience appropriate to rank. For complete application instructions, see the vacancy announcement at **website: http://www.montana.edu/jobs/level2/html.**, or contact: **Chair, Thermal Biology Institute Faculty Search, Montana State University, P.O. Box 173142, Bozeman, MT 59717.** Screening of applications will begin June 1, 2006, and continue until the positions are filled. For more information about Montana State University and the Thermal Biology Institute, please browse the applicable links at **websites: http://www.montana.edu** and **www.tbi.montana.edu.** *ADA/Equal Opportunity/Affirmative Action/Veterans Preference.*

SOIL ARTHROPOD ECOLOGY. Department of Entomology, North Carolina State University, tenure-track, eleven-month, **ASSISTANT/ASSOCIATE PROFESSOR FACULTY** position, 80 percent research, 20 percent academic. Develop applied and basic research program on soil arthropods in sustainable agriculture and soil systems. Incumbent expected to obtain extramural funding and collaborate on issues addressing sustainable agriculture and integrated pest management (IPM). Activity in Department undergraduate/graduate teaching program and academic advisement and graduate student training required. Qualifications: Ph.D. in Entomology or related field and experience in soil arthropod ecology, community ecology, and/or arthropod management in sustustainable agriculture systems desirable. Apply online by June 1, 2006. See **website: http://jobs.ncsu.edu** for instructions and required documents. *Affirmative Action/Equal Opportunity Employer. ADA contact:* ***919-515-2746.*** *North Carolina State welcomes all persons without regard to sexual orientation.*

POSTDOCTORAL POSITION available. A Postdoctoral Fellowship in receptor signaling and biochemistry is available through Duke University Medical Center. Expertise in confocal imaging and cell biology is sought. While not required, further experience in biochemical analysis of membrane proteins is considered a plus. Resumes can be sent to: **Dr. D. Schwinn** (**e-mail: schwi001@mc.duke.edu** or **telephone: 919-681-4781**) for consideration.

ASSISTANT or **ASSOCIATE PROFESSOR,** General Mills Land Grant Chair in Cereal Chemistry and Technology, the Department of Food Science and Nutrition, University of Minnesota, seeks candidates for nine-month, tenure-track position. See **website: http://fscn.che.umn.edu/** for details. *The University of Minnesota is an Equal Opportunity Educator and Employer.*

ASSISTANT, ASSOCIATE, OR FULL PROFESSOR
Faculty Position, Stability and Biophysical Chemistry of Macromolecules
University of Colorado at Denver and Health Sciences Center
School of Pharmacy

The Department of Pharmaceutical Sciences is a research-intensive group of faculty focusing their efforts in the areas of molecular toxicology, pharmaceutical biotechnology, biomolecular structure, and experimental therapeutics of anticancer agents. The Department is seeking applicants for up to two tenure-track positions at the level of Assistant, Associate, or Full Professor. Associate Professor and Full Professor positions require an established record of scientific excellence.

Areas of interest are focused on chemical/physical stability of macromolecules and quantitative analyses of macromolecular interactions, broadly defined. Examples include chemical degradation of macromolecules, protein aggregation, thermodynamic analysis of macromolecular structure-function relationships, thermodynamics and kinetics of macromolecular stability, or mechanistic studies of macromolecule-ligand interactions. The successful candidate will contribute to the research and graduate educational programs of the Center for Pharmaceutical Biotechnology and the Department of Pharmaceutical Sciences, including teaching spectroscopy at the graduate level.

Successful candidates will be expected to develop or maintain a successful, extramurally funded research program and contribute to teaching at the professional and graduate levels in the School of Pharmacy. Faculty rank and salary will be dependent upon qualifications and experience. Applicant screening will begin May 1, 2006, and continue until the position is filled. Applicants should send a letter of interest, curriculum vitae, and the names of three references with regular and e-mail addresses, telephone and fax numbers to:

Faculty Search, Biophysical Chemistry
Department of Pharmaceutical Sciences
School of Pharmacy
4200 E. Ninth Avenue, Box C-238
Denver, CO 80262
Fax: 303-315-0274; telephone: 303-315-7732

The University of Colorado is committed to diversity and equality in education and employment.

NATIONAL UNIVERSITY OF SINGAPORE
Department of Chemical and Biomolecular Engineering

The Department of Chemical and Biomolecular Engineering at National University of Singapore invites applications for **TENURE-TRACK FACULTY** positions at all levels. The Department is one of the largest internationally with excellent in-house infrastructure for experimental and computational research. A Ph.D. in chemical engineering or related areas and a strong research record with excellent publications are required. Please refer to **website: http://www.chbe.nus.edu.sg/** for more information on the areas of interest and for application details. Applicants should send full curriculum vitae (including key publications), a detailed research plan, a statement of teaching interest, and a list of names of at least three references to: **Professor Raj Rajagopalan, Head of Department (Attention: Ms. Nancy Chia, e-mail: nancychia@nus.edu.sg).**

POSITION OPENING, ASSISTANT PROFESSOR
Alderson-Broaddus College

Seeking applications for an Assistant Professor/Postdoctoral position to begin summer 2006. Ph.D. in biology or health-related field and cancer research experience required. Twelve-month position with annual renewal. Submit letter of application, curriculum vitae, transcripts, reference list, and statement of teaching/research to: **Human Resources, Biomedical, P.O. Box 2004, Philippi, WV 26416.**

USDA ARS Agricultural Research Service
www.ars.usda.gov

VETERINARY MEDICAL OFFICER
GS-0701-12/13/14/15
Salary Range of $62,291 to $133,850

The United States Department of Agriculture, Agricultural Research Service (USDA/ARS), Arthropod-Borne Animal Diseases Research Laboratory in Laramie, Wyoming, is seeking a permanent, full-time Veterinary Medical Officer to develop research on pathogenic mechanisms, control, and the epizootiologic cycles of arbovirus diseases. Investigates clinical, virological, serological, immunological, and pathological responses of arboviruses from animals to insects to animals (cycle of infection); the isolation and identification of arboviruses from vectors and animals; and the development and implementation of control strategies for Bluetongue, Vesicular Stomatitis, Rift Valley Fever, and other arbovirus diseases of livestock. To have a printed copy of the vacancy announcement mailed to you, call: **Bobbie Bobango, telephone: 307-766-3606,** or access information online at **website: http://www.afm.ars.usda.gov/divisions/hrd/index.html.** Send applications for announcement ARS-X6W-0154 to: **United States Department of Agriculture, Agricultural Research Service, Human Resources Division, Attn: Keli A. Martin, 5601 Sunnyside Avenue, Stop 5106, Beltsville, MD 20705-5106. Fax: 301-504-1535; e-mail: scirecruit@ars.usda.gov.** Applications must be marked ARS-X6W-0154 and postmarked by May 1, 2006. *Citizenship is required.*

USDA/ARS is an Equal Opportunity Employer and Provider.

A **NONTENURE-TRACK FACULTY POSITION** is available at the Albert Einstein College of Medicine to develop high throughput capabilities for the global analysis of protein structure, function, regulation, and integration. There is particular interest in candidates with expertise in the utilization and development of eukaryotic protein expression technologies for the high throughout production of secreted proteins and protein assemblies, or in the application of high throughput approaches for the generation of mouse model systems by targeted gene replacement. The position would be part of a new Integrated Genetics and Systems Biology Initiative and would complement existing strengths in mammalian genetics, microbiology, cancer biology, mechanistic enzymology, and structural genomics. Interested candidates should forward curriculum vitae, a brief one page research plan and the names of three references to: **Dr. Steven C. Almo, Department of Biochemistry, Albert Einstein College of Medicine, 1300 Morris Park Avenue, Bronx, NY 10461; e-mail: almo@aecom.yu.edu.** *Equal Opportunity Employer.*

POSTDOCTORAL POSITION in cellular immunology to study self-antigen processing and presentation in context of T-cell tolerance, autoimmunity, and immune regulation. Experience in tissue culture and handling of rodents essential. Submit curriculum vitae and three letters of reference to: **Kamal D. Moudgil, M.D., Ph.D., Associate Professor, Department of Microbiology and Immunology, 660 W. Redwood Street, HH 323C, University of Maryland School of Medicine, Baltimore, MD 21201. E-mail: kmoud001@umaryland.edu; fax: 410-706-2129.**

STAFF (Manhattan). Perform laboratory procedures for molecular cloning including cDNA library screening, denaturing high-performance liquid chromatography (DHPLC) mutation detection, microsatellite mapping, FP-TDI/Pyrosequencing for single nucleotide polymorphism (SNP) genotyping. Manage research databases on Linux/Solaris system. Master's in biology or related field, plus six months of experience. Send curriculum vitae to: **Ana Ignat, Columbia University, 1150 St. Nicholas Avenue, Room 620, New York, NY 10032.**

SYMPOSIA

COLLEGE OF SCIENCES and MATHEMATICS
AUBURN UNIVERSITY

Frontiers in Nanoscience and Nanotechnology

Presentations will focus on the interdisciplinary nature of the research being conducted in nanosciences leading to developments in nanotechnology.

Featured speakers:
Dr. Paul Barbara – UTexas Austin
Dr. Andrew Hunt – nGimat
Dr. Thomas Mallouk – Penn. State
Dr. Hao Yan – Arizona State
Dr. Peidong Yang – UC Berkeley

Auburn University, Alabama
Tuesday, May 2, 2006
Science Center Auditorium
8 am – 5 pm
www.auburn.edu/cosam/symposium

Registration is free, lunch will be provided to those who register in advance. Email: **Betty Adcock: adcocba@auburn.edu**.

CONFERENCE

YYePG Proudly Present[illegible] for S[illegible]

POSITIONS OPEN

INTERDISCIPLINARY POSTDOCTORAL TRAINING IN CANCER BIOLOGY

The Burnham Institute for Medical Research (BIMR) has Postdoctoral positions available. The Institute is home to an NCI-designated cancer center focusing on basic and translational aspects of cancer research, which offers interdisciplinary training in cancer biology. Training opportunities in cellular signaling, cell death, developmental biology, nanotechnology, bioinformatics, and molecular epidemiology are combined with training in one of our technology centers (i.e. San Diego Center for Chemical Genomics, Center on Proteolytic Pathways, and the Stem Cell Center) that are developing prototypical tools and technologies for drug discovery.

Trainees selected for this program will join a collegial, collaborative environment and work with researchers who embrace an interdisciplinary approach to cancer research.

These positions are open to *U.S. citizens or permanent residents* with an M.D. or Ph.D. and experience in molecular, cellular, or chemical biology. Underrepresented minority candidates are highly encouraged to apply.

To apply: Send a brief statement of research experience and interest, curriculum vitae, and contact information for three references to: **Interdisciplinary Training in Cancer Biology, e-mail: ct32@burnham.org.** See also **website: http://www.burnham.org/ct32.**

BIMR is an Affirmative Action/Equal Opportunity Employer and committed to a diverse workforce.

FACULTY POSITION
Department of Pharmacology
University of Illinois at Chicago

The Department of Pharmacology at the University of Illinois College of Medicine at Chicago is seeking candidates for an **ASSOCIATE PROFESSOR** appointment. This position would be conjoint with the Center for Lung and Vascular Biology as well as other academic departments. Candidates should have a Ph.D. and/or M.D. degree, outstanding publication record in first-tier journals, and a NIH-funded research program in one of the following areas: leukocyte activation mechanisms, inflammation, vascular biology, adhesion molecules, and lung biology. Preference will be given to candidates who have successfully established disease models for research that complements ongoing activities including vascular biology, adhesion of leukocytes and endothelial cells, and G protein signaling in blood and vascular cells. The successful candidate will be offered a highly competitive startup package and new research space. Please send curriculum vitae, statement of research interests/plans, and names of three references to: **Dr. A.B. Malik, Distinguished Professor and Department Head, Department of Pharmacology (MC 868), University of Illinois at Chicago, College of Medicine, 835 S. Wolcott Avenue, Room E403, Chicago, IL 60612.** For fullest consideration, applications should be received by May 1, 2006. *The University of Illinois is an Affirmative Action/Equal Opportunity Employer.*

POSTDOCTORAL/RESEARCH ASSOCIATE positions on molecular and cell biology of neurodegeneration/Alzheimer's disease. Emphasis on function/processing of presenilins (PSs), cadherins and APP, interactions of PSs with PI3K/Akt/GSK signaling, role of PSs in synaptic function and mechanisms by which FAD mutants affect neuronal survival. More information in: **Georgakopoulos et al.,** *Mol. Cell* **4:** 893, 1999; **Baki et al.,** *PNAS* **98:** 2381, 2001; **Marambaud et al.,** *EMBO J.* **21:** 1948, 2002; **Marambaud et al.,** *Cell* **114:** 635, 2003, [commentaries: *Nature* **425:** 565, 2003; *Cell* **114:** 533, 2003]; **Baki et al.,** *EMBO J.* **23:** 2586-2596, 2004; **Georgakopoulos et al.,** *EMBO J* Mar. 2, online, 2006. Contact: **Dr. N. K. Robakis, Mount Sinai School of Medicine, One Gustave Levy Place, New York, NY 10029. E-mail: nikos.robakis@mssm.edu.**

POSTDOCTORAL POSITION
Quantitative Toxicology/Pharmacology

The U.S. Environmental Protection Agency (EPA), National Center for Environmental Assessment in Cincinnati, Ohio, seeks Postdoctoral candidates in computational toxicology and biological modeling for human health risk assessments. Successful candidates will have experience in some of the following areas: toxicology, biochemistry, physiology, pharmacology, statistics, and computer modeling. Specialized education training and/or experience preferred include quantitative structure-activity (e.g., QSAR, SAR) modeling, pharmaco- or toxicokinetic modeling, or physiological or biologically-based dose response modeling. Salary ranges from $50,000 up to $70,000, commensurate with qualification plus benefits. Information on federal positions can be found at **website: http://cfpub.epa.gov/ncea/cfm/recordisplay.cfm?deid=134123 (CINCSAST-010406-01).** For additional information contact **Dorothy Carr** at **telephone: 919-541-4356.** Information on nonfederal positions can be found at **website: http://www.orau.gov/orise/edu/needs/EPA-NCEA-2006-01.pdf.** For additional information please contact **Karen Proffitt** at **telephone: 513-569-7099.**

US EPA is an Equal Opportunity Employer.

ASSISTANT
Department of Pharmacology and Therapeutics
University of Florida

The Department of Pharmacology and Therapetuics invites well-trained, doctorate-level individuals, to apply for a **NONTENURE-TRACK ASSISTANT** faculty position. The successful candidate will determine the neuroprotective and memory enhancing effects of novel nicotinic drugs and nicotinic receptor gene delivery approaches in multiple rodent models. Salary is commensurate with experience. Applicants should apply online at **website: http://jobs.ufl.edu** (position number 00022381), and send their curriculum vitae and three letters of recommendation to: **Dr. Phil Scarpace, Department of Pharmacology and Therapeutics, Box 100267, Gainesville, FL 32610-0267.** Application deadline is May 16, 2006, with an anticipated start date on or after June 12, 2006. *The University of Florida is an Equal Opportunity Institution.*

ACADEMIC FELLOWSHIPS. Opportunities for Postdoctoral training within the University of Maryland Baltimore School of Medicine's Training Program in Cardiac and Vascular Cell Biology. Training areas include: molecular determinants of myocyte function, cell signaling, cytoskeletal functions, extracellular matrix, biophysical modeling, endothelial functions, and biomechanics of tissues and organs. Applicants must have Ph.D. or M.D. *These funded positions are restricted to U.S. citizens and permanent residents.* Please send curriculum vitae, a statement of research interests, and the names of three references to:

Thomas L. Pallone, M.D.
c/o Mrs. Katherine Frankel, Division Manager
Department of Physiology
University of Maryland, Baltimore
School of Medicine
660 West Redwood Street, Suite 511A
Baltimore, MD 21201
E-mail: kfrankel@som.umaryland.edu

POSTDOCTORAL RESEARCH FELLOW sought to study the genetic basis of microcephaly. Requirements include M.D. with significant experience in pediatric neurology including ability to perform clinical analysis of research subjects, gene mapping, and cloning. Salary $70,000 per year. Send resumes to: **Christopher Walsh, M.D., Ph.D., Department of Neurology, Howard Hughes Medical Institute and Beth Israel Deaconess Medical Center, NRB 266, 77 Avenue Louis Pasteur, Boston, MA 02115 (e-mail: walshlab@hotmail.com).**

POSITIONS OPEN

POSTDOCTORAL FELLOWSHIP
Exempt Position 173034
Closes Friday, May 12, 2006, at 4:00 p.m.

The Zoological Society of San Diego is seeking a Postdoctoral Fellow (Ph.D. or D.V.M./Ph.D.) to join the Molecular Diagnostics Laboratory in the Pathology Department. Projects center on discovery and characterization of etiologies and mechanisms of emerging and ongoing infectious and genetic diseases in diverse animal species. A strong background and extensive experience in molecular biology is essential. Experience with human or animal diseases is desirable. This is an Exempt position with a competitive salary, an appointment for two years, and is available as early as May 2006.

Send curriculum vitae and the names of three professional references to: **Human Resources, San Diego Zoo's Wild Animal Park, Attn: PATH 173034, 15500 San Pasqual Valley Road, Escondido, CA 92027-7017. Fax: 760-796-5614. Job Line Information: 760-738-5006.** Additional information at **website: http://www.wildanimalpark.org.**

POSTDOCTORAL POSITION is available to study bioelectrical and biophysical mechanisms in carcinogenesis. Qualified individuals should have a Ph.D. or an M.D./Ph.D. as well as experience in molecular biology and developmental or cell biology. Please send a cover letter, resume or curriculum vitae, and a summary of research interests to: **Carlos Sonnenschein, M.D.** at **e-mail: cschaeberle@gmail.com,** or **fax: 617-636-3971.**

Find out about jobs before you get your issue. Sign up for customized e-mail notification of jobs at **website: http://www.sciencecareers.org** by clicking on Job Alerts. You can also post your resume (open or confidentially) and check how many employers have viewed your resume at your own convenience.

MARKETPLACE

High Resolution Whole Genome Case-Control Association Studies

Now Available to Academic Investigators and Foundations Asking Important Genetic Questions

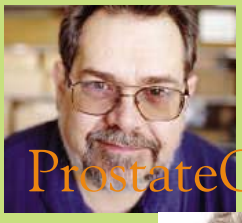

Unprecedented Scale and Resolution

Perlegen scientists and engineers have created – and are now employing – a cost-effective, whole genome scanning approach that enables genetic studies of unprecedented scale and resolution. In case-control association studies, millions of unique SNPs – selected to optimize density, coverage, and reproducibility – are separately analyzed in DNA samples from hundreds of individuals. SNPs found to have statistically significant allele frequency differences between cases and controls are then confirmed by genotyping of the associated SNPs in a separate sample set.

Perlegen Collaborations

In collaborations with many of the world's largest pharmaceutical companies, government agencies, non-profit foundations, and academic researchers, Perlegen works to discover the genetic causes of common diseases as well as genetic markers that predict patient response to drugs. Our comprehensive approach identifies novel biological pathways involved in a complex disease – discoveries that help to focus the ongoing research efforts of scientists in a disease field.

We'd Like to Collaborate with You

If you have access to DNA samples for a well-characterized human phenotype, we'd like to meet with you to discuss writing a collaborative grant proposal or other funding approaches, conducting never before possible genetic research, sharing our data, and publishing results together.

To learn more, contact:

Perlegen Sciences Japan K.K.
Tokyo, Japan

telephone: +81 (0)3 3444-6080
genetics@perlegen.com
www.perlegen.com

Targeting today's drugs. Discovering tomorrow's.™

PERLEGEN SCIENCES